Name:	Tim Kerr
Full title of thesis:	Precipitation distribution in the Lake Pukaki catchment, New Zealand
Degree:	Doctor of philosophy
Year of presentation:	2009
University Department:	Geography
Chief Supervisor:	Ian Owens

Student signature: Date

Chief Supervisor Date

Dean of Postgraduate Studies Date

Librarian Date Received:

Precipitation distribution in the Lake Pukaki Catchment, New Zealand

---

A thesis submitted in fulfilment

of the requirements for the degree

of

Doctor of Philosophy

by

Tim Kerr

Department of Geography

University of Canterbury

2009

Table of contents

Acknowledgements

For top class supervision I must thank Roddy Henderson and Ian Owens.
Meridian Energy Ltd, NIWA, the Tertiary Education Commission and The Department of Geography – University of Canterbury, have provided financial assistance. Without thier support this research would not have occurred.
Humes Pipeline Systems, The Department of Conservation, Mt Hutt Ski Area, The Helicopter Line, Mt Cook Ski Planes and Glacier Explorers have also kindly given assistance through materials or time.
NIWA, Meridian Energy Ltd, Braemar Station, The Department of Conservation and Mt Cook Station have provided permission for access to locations and data.
Too many people to name have assisted in a multitude of ways through the course of this research. I will attempt to name them here and apologise if I have missed anybody; an omission is more an indication of my poor memory than of the lack of desire to acknowledge: Jennifer Purdie, Dinesh Chand, Eddie Stead, Ray Bellringer, Shirley Slatter, Kerry O'Neill, Cam Mulvey, Greg Preston, Julia and Hamish Mackenzie, John Hooker, Bob Munro, Kathy Walter, Elaine Fouhy, Ross Woods, Jim Renwick, John Fenwick, Mauri McSaveney.
Brian Anderson, Dorothea Stumm, Pascal Sirguey, Trevor Chinn, Jordy Hendrikx, Martyn Clark, Wolfgang Rack, Heather Purdie, Andrew Mackintosh, Mike Green, Marwan Katurji, Tim Appelhans, Vaughan Wood and Simon Parsons have all been kind enough to feign interest in my research long enough to have to endure yet another precipitation monologue.
General support from the staff and students of the Department of Geography, University of Canterbury has helped keep equipment maintained, computers backed up and morning tea breaks sociable.
Simon Allen, with whom I have shared an office, has obliged me with an immediate feedback system to any question or comment I make, as well as helping out with field work when all other assistants had retreated.
Grant Singleton put in the hard yards during the field campaign. My health and safety was secure under his watchful eye.
Most importantly, another three years of self absorbed study has been endured by my long suffering partner Clare to whom I am once again indebted

Abstract

Mountain precipitation, as a major component of global ecology and culture, requires diverse observation-based distribution studies to improve process characterisation and so enhance environmental management and understanding. Analysis of data from an array of precipitation gauges within the nationally important, and internationally extreme, mountainous Lake Pukaki catchment in New Zealand has been undertaken in an effort to provide such a study, while also improving local hydrological understanding.

An objective observation based undercatch-corrected 1971-2000 average annual precipitation distribution has been prepared for the mountainous Lake Pukaki catchment, New Zealand. Precipitation records from 58 gauges at 51 sites, augmented with 10 new gauges, were used in preparation of the distribution. The assessed undercatch correction of 17 % across the catchment indicates that mountain hydrological investigations in New Zealand that use precipitation data and yet do not consider undercatch will be in considerable error. The average annual distribution confirms the existence of high precipitation magnitudes and horizontal gradients in the catchment in comparison with other mountain regions around the world. The high magnitude is unusual when its position in the lee of the principal orographic divide is considered indicating rare precipitation distribution processes occur in the region. Consideration of river flows, glacial change and evaporation led to a confirmation of the gauge derived average catchment precipitation.

Precipitation to wind direction relationships identified the predominant westerly wind to be the primary precipitation generating direction with large magnitude events biased towards the northerly direction. All directions from the eastern side of the mountain divide had the lowest frequency and daily precipitation magnitude. Derivation of wind-classed precipitation distributions identified a distinctive south east to north west precipitation gradient for all wind directions, most severe for the north west direction and least severe for the easterly direction. Precipitation extent was greatest for the northerly direction and least for the south south westerly. The wind-classed distributions enable the estimation of daily precipitation likelihood and magnitude at any location in the catchment based on knowledge of the synoptic wind flow direction and precipitation at just one reference site. Improved river flow and

lake inflow estimates resulted from the use of wind classed daily precipitation estimates validating the quality of the wind classed distributions.

From 1939 to 2000 there has been no statistically significant trend in precipitation magnitudes, frequencies, or extremes in the catchment. At Aoraki/Mt Cook village, in the upper catchment, there have been significant increases in magnitude, frequency and extremes associated with the phase change of the Interdecadal Pacific Oscillation (IPO) in 1978. This change can be explained by the increase in strength of westerly winds for the different IPO phases but not by a change in frequency of different wind directions. In the lower catchment the IPO relationship is of an opposite sense to that observed in the upper catchment, indicating that the areas operate under two different climate regimes with different precipitation controls. The significant relationship to the IPO phase indicates that it is more important than climate warming in terms of future precipitation distribution in the Lake Pukaki catchment, and by extension the Southern Alps.

The distributions prepared provide a valuable tool for operational and academic hydrological applications in the region. In addition, they provide a valuable characterisation of the precipitation in a Southern Hemisphere mid-latitude lee to predominant westerlies glacierized mountain catchment. From this standpoint they highlight the contrast to Northern Hemisphere mountain precipitation distributions commonly used in model validation studies, thereby providing an extension of locations with which to refine orographic precipitation process understanding.

List of Figures

List of Tables

List of Symbols and abbreviations

ARPS	Advanced Regional Prediction System
AS	Air Safaris – a company in Tekapo. The abbreviation is used as a suffix to Tekapo as a site name for the precipitation gauge operated on the company's premises
ASTER	Advanced Spaceborne Thermal Emission and Reflectance radiometer – a satellite based remote sensing device
CDNC	Cloud Droplet Number Concentration
COAMPS	Coupled Ocean/Atmosphere Mesoscale Prediction System
CUSUM	CUmulative SUM
DEM	Digital Elevation Model
DSIR	the Department of Scientific and Industrial Research - a former NZ government organisation
ECAN	Environment CANterbury – the regional government authority for the Canterbury region.
EGM96	Earth Geopotential Model 1996
ENSO	El Ninó-Southern Oscillation
EWS	Electronic Weather Station. This is an alternative to the more common Automatic Weather Station. The abbreviation is used as a suffix to Mt Cook as a site name for the NIWA owned automatic rain gauge sited in Aoraki/Mt Cook Village.
GIS	Geographic Information Systems
GR3J	Génie Rural à 3 paramètres Journalier – a rainfall-runoff model
HBV	Hydrologiska Byråns Vattenbalansmodell – a rainfall-runoff model
ICESat	Ice Cloud and land Elevation Satellite
IPO	Interdecadal Pacific Oscillation
LINZ	Land Information New Zealand – a NZ government organisation
MC2	Mesoscale Compressible Community model
MCNP	Mount Cook National Park – the former name of Aoraki/Mt Cook National Park
ME	Model Efficiency
MM5	Mesoscale Model version 5

MWD	Ministry of Works and Development – a former NZ government organisation
NCAR	National Centre for Atmospheric Research – a US research organisation
NCEP	National Centers for Environmental Prediction – a US research organisation
NIWA	National Institute of Water and Atmospheric research
NIWA A	National Institute of Water and Atmospheric research Archives
NIWA CD	National Institute of Water and Atmospheric research Climate Database
NSC	Nash Sutcliffe goodness of fit Criterion
NZMS	New Zealand Meteorological Service
NZMS260	New Zealand Map Service 260 series – the 1:50000 metric topographical map series for New Zealand
PDO	Pacific Decadal Oscillation
RAMS	the Regional Atmospheric Modelling System
SAM	Southern Annular Mode
SMAR	Soil Moisture Accounting and Routing model
SO	Southern Oscillation
SOI	Southern Oscillation Index
SRTM	Shuttle Radar Topography Mission
SWE	Snow Water Equivalent. The depth of water that would result if a column of snow was melted.
THC	Tourist Hotel Corporation. A former government agency. The abbreviation is now used as a suffix to Franz Josef as a site name for the rain gauge that used to be located near the Franz Josef Hotel, which was previously owned by the Tourist Hotel Corporation.
UBC	University of British Columbia
WGS84	World Geodetic System 1984
WRF	Weather Research and Forecasting model
WMO	World Meteorological Organisation
CR	Catch Ratio (in percent) of the observed catch to the true precipitation
Ws	daily average Wind speed in metres per second at the orifice height
U	wind speed

U_w	westerly wind component
U_s	southerly wind component
z_0	roughness length
y	dependent variable
m	slope constant
x	independent variable
c	offset constant
A_f	average measurement period as a fraction of a year
s^2	estimated population variance
i	sample number
N	number of samples
x_i	the residual from the regression line for sample i
$\bar{x}$	mean
$+CL(0.95)$	upper 95 % confidence limit
$-CL(0.95)$	lower 95 % confidence limit
θ	wind direction (from north)
A_c	the calibrated automatic sensor signal,
A_u	uncalibrated automatic sensor signal
M	manual measurement
t	time
p	estimated precipitation at the point of interest
p_{rs}	observed precipitation at the reference site.
P	precipitation,
Q_s	stream flow,
Q_g	ground water flow
ΔS_s	change in solid water storage (ice and snow)
ΔS_l	change in liquid water storage (lakes)
ΔG	change in groundwater storage
E	evapotranspiration
$Q(T)$	flow
V	constant
f	melt factor
f_{min}	minimum melt factor (mm ^{o} C^{-1} d^{-1})
$f_{max,i}$	initial maximum melt factor (mm ^{o} C^{-1} d^{-1})

a	wet/dry day constant
y_c	computed value
y_o	observed value
w_i	weighting of site i and
ρ_i	correlation coefficient at site i.
z	elevation (m)
B	non dimensional blocking number
N	Brunt-Vaisala frequency (s^{-1})
h	height (m)
e_s	saturation vapour pressure in hPa
T	air temperature

1 Introduction

1.1 Mountain precipitation

Precipitation in mountain regions frequently provides the primary source of water to their surrounding region (Barros and Lettenmaier, 1993). This precipitation also affects the environment through erosional, ecological, cryospheric and hydrological effects (Roe and Baker, 2006). Previous observations show that orographic influences on precipitation operate at different scales (Smith, 1979) through a range of different mechanisms (Smith, 2006) leading to location specific magnitudes and distributions. Unfortunately, the underlying influence of mountains on precipitation magnitude and distribution is not well understood (Barry, 1992). This knowledge deficiency is in part attributable to the paucity of observations (Basist et al., 1994). An obvious step to take in improving this deficiency is to measure the precipitation distribution in as many different mountain forms and climate types, as possible.

1.2 Mountain precipitation in the Southern Alps, New Zealand

The interaction of the Southern Alps with the Southern Hemisphere westerly wind belt provides a natural idealised mountain precipitation laboratory. The high frequency of saturated airflow in a perpendicular direction to a long mountain range enables the exploration of precipitation processes in a near-2D environment. The varying cross-mountain profile of the Southern Alps allows investigation of the effect of different mountain heights and widths, while the seasons enable the assessment of temperature impacts. However, the availability of this natural laboratory is not the main driver of precipitation research in the region. It is, instead, the need to know how much mountain precipitation there is, where it is and when it occurs. These questions of primary concern are generally in relation to electricity generation, recreation, agriculture and drinking supplies. Fortunately, the questions are of equal interest to the advancement of mountain precipitation knowledge. If this were not the case, then we would already know the answers to “how much”, “where” and “when”. There are arguably few locations in the Southern Alps of more hydrological significance than the Lake Pukaki catchment. Nationally significant tourism, recreation, agriculture and electricity generation are all reliant in a major way on the precipitation occurring within it. Repeated attempts at characterising the precipitation distribution have been made (see the following “Review of mountain precipitation” chapter, which provides

a review of investigations). The difficulties of access, the harshness of the environment, and the extremes of the climate have hampered these investigations (Anderton, 1975 258). The potential to constrain the previous precipitation estimations by combining all previous observations with new observations provides a clear path to improving on the "where" and "how much" questions. Linking the precipitation distribution to different climate types enables answers to the "when" question at a short term scale. Longer term, "when?" may be done through analysis of temporal trends, trends that are more easily discerned as the length of quality records increases. While the Lake Pukaki catchment precipitation characterisation is undertaken pragmatically to provide application directed outcomes, it is equally of value as an extension of known mountain-precipitation interactions. To this end, the precipitation distribution from this natural laboratory provides a new regime to add to the international mountain precipitation collection.

1.3 Aims and objectives

The aims of this thesis are principally:

- to improve the knowledge of the long term precipitation distribution in the Lake Pukaki catchment,
- to describe the observed climate-to-precipitation distribution relationships,
- to improve daily precipitation distribution estimation in the catchment,
- to independently validate the precipitation distributions,
- to place the distributions in a temporal context and
- to contrast the distributions to those observed in other regions of New Zealand and the world.

1.4 Lake Pukaki catchment

The Lake Pukaki Catchment is situated near the centre of the South Island of New Zealand at 170^{o} 10' E, 43^{o} 48' S (Figure 1-1). The axis of the catchment runs roughly north-south with the north-western boundary on the Main Divide of the Southern Alps and the southern edge in a dry intermontane basin. The catchment area is 1359 km^2 with a length of 79 km and a width of 22 km. The elevation of the catchment averages 1260 m, ranging from the lake level at 524 m up to 3754 m, the height of Aoraki/Mt Cook, the highest peak in New Zealand.

The upper catchment contains 133 glaciers, including New Zealand's 1st, 2nd, 6th and 7th largest glaciers respectively (Chinn, 2001). Lake Pukaki itself covers an area of 168 km^2 (one eighth of the catchment area) and has a maximum depth of 99 m close to its south western shore. It was originally formed behind a terminal moraine (Wallace, 2001) and has twice been raised, (1952 and 1976) for flood control and improved storage for hydro electric generation (Sheridan, 1995).

The climate of the catchment is primarily influenced by its position adjacent and east of the main divide of the Southern Alps, which themselves lie astride the Southern Hemisphere westerly wind belt in a maritime setting. High precipitation created by spill over from the west dominates the north and western catchment with a reduction in precipitation away from the divide. In contrast, the south and eastern regions of the catchment are characterised by high sunshine hours, and low rainfall (Ryan, 1987). Temperatures vary throughout the catchment according to altitude, with the mountain tops remaining below zero degrees celsius for the majority of the year. Seasonal variation occurs throughout the catchment, though it is more pronounced in the lower eastern portion of the catchment. Snow can fall in the catchment at any time of the year but accumulation of snow from one storm to another is more common in the winter months from April until October. This climate has resulted in seasonal snow and perennial ice being important components of the catchment's environment.

The dominant rock type within the catchment is Permian-Triassic quartzofeldspathic indurated sedimentary rock (commonly known as greywacke) classified as part of the Rakaia terrane, itself a member of the Torlesse composite terrane, with overlying postglacial alluvium (Cox and Barrell, 2007; Suggate, 1978). This arrangement is a result of two major processes, uplift and erosion. The uplift is from the Pacific tectonic plate moving up against the Australian plate at the Alpine Fault just 20 km west of the catchment. The uplift is estimated at 10-20 mm per year (Coates, 2002). Erosion transforms the uplifted greywacke into alluvium and spreads it across the lower catchment through primarily fluvial processes and rock avalanching (Whitehouse, 1988). Glaciation's role in erosion has resulted in distinctive landforms throughout the catchment. The southern end of the lake is dammed by a terminal moraine originating from the Tekapo glacial advance with terminal moraines from two earlier advances directly behind indicating the Lake has been in its current position for some time. The lower eastern boundary of the catchment is formed by a medial moraine from when the glaciers of the Lake Pukaki catchment combined with

those of the neighbouring catchment during the major Balmoral advance (Wallace, 2001). The currently existing 133 glaciers (Chinn, 2001) continue to erode the underlying rock, forming characteristic arêtes, horns and cirques. The related over-steepened slopes result in extensive rock fall and formation of large talus slopes with rivers and glaciers transporting debris to lower regions (Whitehouse, 1988). This in turn produces the classic glacial outwash plains of the catchment's river flats.

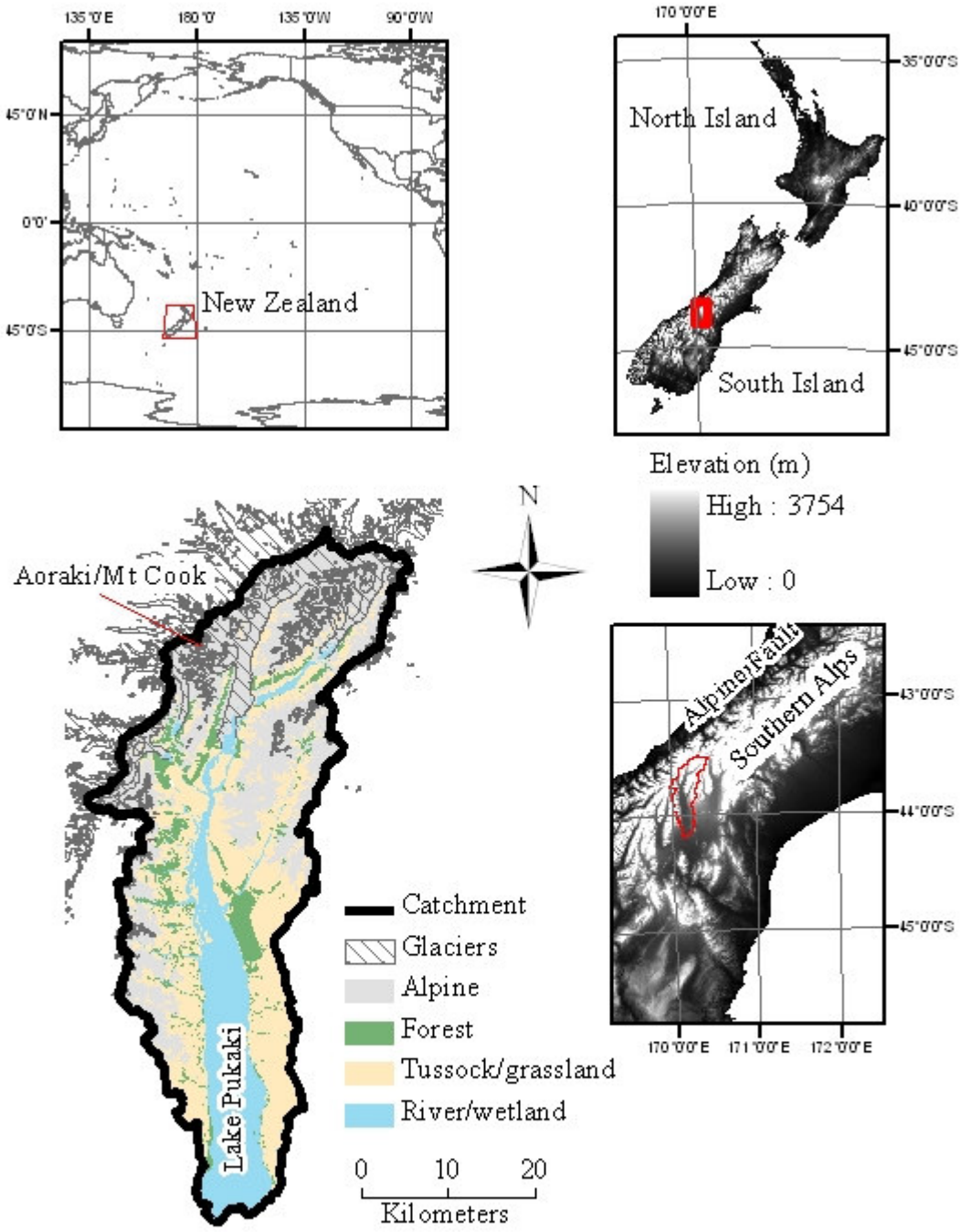

Figure 1-1. Land cover of Lake Pukaki catchment in New Zealand.

The flora and fauna of the Lake Pukaki catchment may be divided into four broad zones based on land cover types:

1. Alpine
2. Forest
3. Tussock/grasslands
4. River/wetland

The Alpine and Tussock/grassland zones are by far the largest, being 38% and 37% of catchment area respectively, followed by the River/wetland zone (18%) and just 7% in the Forest zone. The highest of these, the Alpine zone, has large tracts of non-vegetated cover, herb fields, short grass lands, and sub alpine scrub. Tahr (*Hemitragus jemlahicus),* Chamois (*Rupicapra rupicapra*), Kea (*Nestor notabilis*) and Rock Wren (*Xenicus gilviventris*) frequent these areas. Though much smaller than the alpine regions, the Forest zone is important as a habitat for a variety of native forest birds like the Grey Warbler/ Riroriro (*Greygone flaviventris*) and Kereru/Wood Pigeon (*Hemiphaga novaseelandiae*). Wilding pines (*Pinus spp.*) and forest plantations in the farmed areas are becoming an increasingly large component of the Forest zone, though the fauna is less prolific in these habitats. The Tussock/grassland zone, which includes scrub covered regions as well as the tussock (*Chinacloa spp.* and *Poa spp.)* and grassed farmland, forms the significant portion of the agricultural regions. Sheep, cattle and rabbits are the dominant animals in this zone. Invertebrates, such as grasshoppers, moths and flies, though found throughout the catchment, are particularly common in the Tussock/grassland zone. The remaining River/wetland zone is colonised by rapidly spreading and growing species of vegetation such as Lupin (*Lupinus spp.*), Willow (*Salix spp.*) and Foxglove (*Digitalis purpurea*), the first to take hold after frequent flooding events. These areas are important ecologically to the myriad of birds that make this zone their home including the rare Black Stilt (*Himantopus novaezelandiae*) and Wrybilled Plover (*Anarhynchus frontalis*). Within the water bodies themselves the glacial flour renders the larger rivers and Lake Pukaki itself low in life while the non-glacial and spring fed tributaries thrive.

1.5 Thesis structure

Following this introduction, the "Review of mountain precipitation" chapter is dedicated to reviewing the current state of knowledge of mountain precipitation. This explores methods of precipitation observation, errors of observations, and a variety of

mountain precipitation observation campaigns from around the world including in New Zealand's Southern Alps. From this background, the "Mountain precipitation observations" chapter provides a detailed description of all available precipitation observations made in the Lake Pukaki catchment, including new observations undertaken as part of this research. This leads to the generation of a new 1971-2000 average annual precipitation distribution. This chapter also considers observation error and undercatch, enabling the generation of an undercatch corrected 1971-2000 average annual precipitation distribution. The "Wind dependent precipitation distributions" chapter takes average annual distributions one step further to provide wind-classed precipitation distributions. The chapter also provides a method of using these new distributions to generate improved daily spatial precipitation estimates for the catchment. The chapter "Precipitation validation through flow" describes the use of stream flows and lake inflows to validate the average annual distribution, the wind-classed distributions, and daily distributions generated from them. The "Long term trends of precipitation" then provides an assessment of the temporal variability of precipitation within the catchment. This enables the temporal context within which to place the previously determined and validated precipitation distributions. Finally, in the "Conclusions" chapter, a summary of the research findings, the conclusions that may be drawn from those findings, their implications and a direction for future research is provided.

2 Review of mountain precipitation

2.1 Introduction

The aim of this chapter is to outline the current knowledge in mountain precipitation with particular emphasis on spatial distribution. To do this, the chapter begins by reviewing precipitation observation techniques, focusing on methods applicable to mountain regions where different phases of precipitation are likely. Included is an overview of measurement system limitations and common approaches to overcoming them. Global precipitation data are then used to highlight the disparity in observation density, observation accuracy, and precipitation variability between mountainous and non-mountainous regions. This leads to the description and findings from individual observation campaigns for a selection of sites around the world including a variety of New Zealand mountain precipitation distribution estimates. An explanation of mountain precipitation processes is then provided, concluding with a discussion of the status of current mountain precipitation modelling systems.

2.2 Methods of observing mountain precipitation

2.2.1 Precipitation measurement

Precipitation is known to have been systematically observed during the Babylonian Culture (3000 to 1000 B.C.) in what is now Iraq and documented evidence exists of the use of rain gauges from the 4th century B.C. in India (Biswas, 1967). Such observations were thought to be largely associated with agriculture in lowland populated regions. In contrast, systematic observations in mountain regions did not begin until about 1850 (Barry, 1992). While such observations were initially undertaken to understand the precipitation mechanism, their value in forecasting rainfall, runoff and avalanches soon became apparent.

At the simplest level a precipitation gauge may be any open topped container. For rainfall, the measurement of the volume of water that has fallen into the container divided by the planimetric area of the container opening provides an estimate of the depth of precipitation that has fallen since the container was last emptied. Where the precipitation falls as snow, the snow needs to be melted prior to measuring the volume. For staffed precipitation observation sites this is a standard system, with the

gauge contents measured (and emptied) at fixed intervals (usually daily or shorter). The U.S. 8 inch standard gauge, the Hellmann gauge, the 5 inch copper manual gauge, the Tretyakov gauge and the Nipher gauge are just some of the precipitation gauges used around the world of this type (see Figure 2-1).

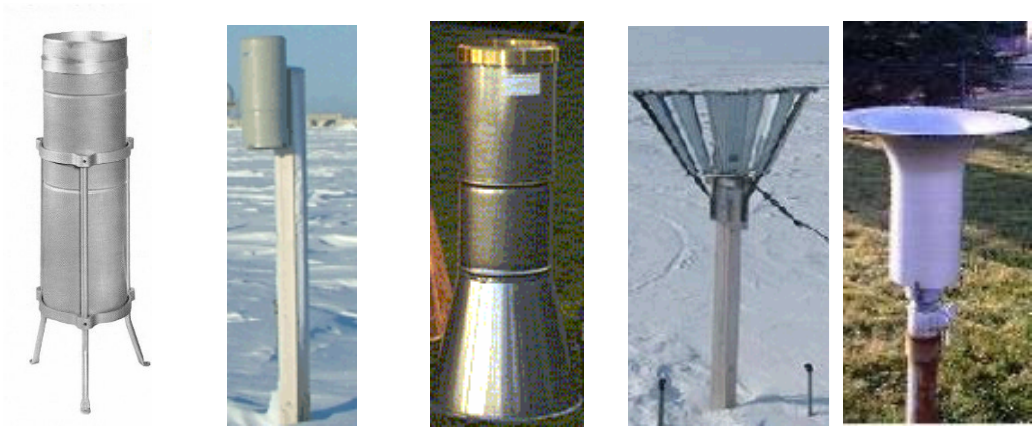

(a) (b) (c) (d) (e)

Figure 2-1. Manual precipitation gauge examples. a) U.S. 8 inch standard gauge (Keefer, 2006), b) Hellmann gauge (Berezovskaya, 2006), c) 5 inch copper gauge (Fenwick, 2008), d) Tretyakov gauge with wind shield (Berezovskaya, 2006), e) Nipher gauge (Environment Canada, 2008).

The depth of a manual precipitation gauge needs to be such that it will not overflow between gauge checks. In areas where gauge inspection is intermittent, the volume of the gauge may need to be much greater than a gauge that is checked daily. Such a large volume gauge is frequently referred to as a storage gauge. The operation of a storage gauge may require two modifications from a standard non-recording gauge. Firstly, a small quantity of oil is required to be added to the gauge to act as an evaporation barrier. Secondly, in locations where frozen precipitation may occur, antifreeze is required so that snow and ice that accumulates within the gauge melts and prevents freezing of gauge contents during cold temperatres. When the accumulated liquid is measured, it is necessary to account for these additives. Examples of two types of storage gauge are shown in Figure 2-2. Note the tapered orifice, allowing the measurement of greater depths of precipitation than the height of the gauge itself.

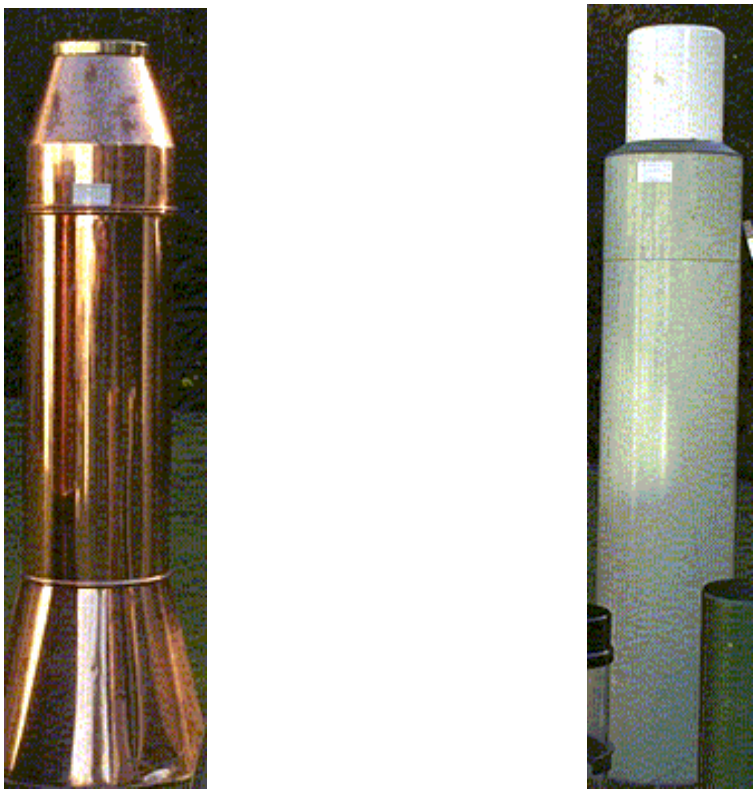

(a) (b)

Figure 2-2. Storage precipitation gauge examples. a) Octapent 50 inch gauge, b) Kainga (NIWA) storage gauge (Fenwick, 2008).

As technology has allowed, automatic measurement systems have been developed enabling high temporal resolution of precipitation measurements. Six automatic systems are in common usage:

1. The tipping bucket rain gauge (see Figure 2-3). A tipping bucket gauge collects a specified volume of water before emptying itself. This specified volume divided by the gauge orifice area is the quantum resolution of the measurement, determining the minimum observable intensity. The number of bucket tips per logging interval provides an assessment of total precipitation during that period. The main advantage of the tipping bucket system is that it does not need emptying. The mechanical requirements of the system mean it cannot measure snowfall, though it will measure the melt of snow that falls into its collecting reservoir. If the reservoir is not overfilled with snow, then an accurate assessment of total precipitation will still be obtained, though the logged time of the precipitation fall will be delayed. One solution to this problem is the use of a heated gauge. This requires considerable power, so is

generally not used in remote regions. A heated gauge will still result in a delayed catch, and during large snow falls may not be able to melt the snow faster than it accumulates, possibly resulting in an under catch. A second solution is to use a separate antifreeze filled reservoir in conjunction with the tipping bucket gauge (see Figure 2-3 b). As precipitation falls into this reservoir, the overflow is gauged by the tipping bucket. Over time the antifreeze becomes more dilute, requiring replacement, and for high precipitation and/or very cold areas, the gauge may require a considerable quantity of antifreeze. This solution also introduces the problem of disposal of the waste diluted antifreeze. Some delay occurs with this system during heavy snow falls as the snow may accumulate faster than it mixes into the antifreeze. Tipping bucket precipitation gauges are an industry standard precipitation measurement device and are a standard automatic precipitation measuring device used in New Zealand, especially in remote and mountain locations.

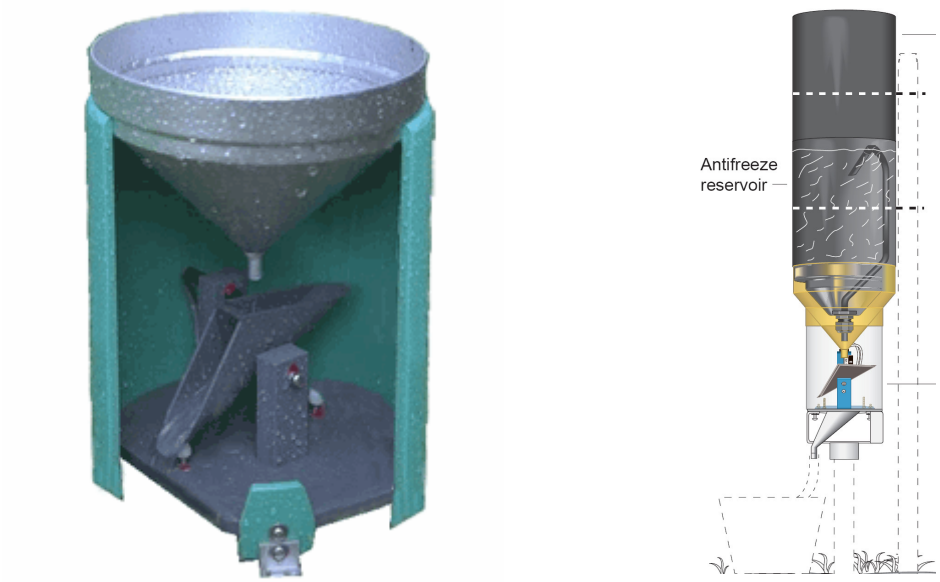

(a) (b)

Figure 2-3. Tipping bucket rain gauge. a) Cut away view of the tipping mechanism (Madgetech, 2008), b) Antifreeze reservoir adaption for snowfall (Campbell Scientific Inc., 2004).

2. Fluid level recorder. Fluid level recorders enable the automatic measurement of the depth of fluid within a gauge. For this reason they work well with

storage gauge systems. Level recording may be done with a number of different systems that may include capacitive, float, or pressure sensors (see Figure 2-4). An automatic siphon may be used to avoid having to manually empty the gauge, though where antifreeze is used this still needs to be added post-emptying. Prior to fully electronic systems, float type recording gauges provided a means of interfacing to mechanical punch tape, or pen chart recording devices. The advent of low power electronic logging systems has enabled low maintenance no-moving-parts sensors (with reduced maintenance) to be utilised.

(a) (b) (c)

Figure 2-4. Examples of three types of level sensors, a) Capacitive level sensor (Sitron, 2006) b) Float sensor (Measurement Resources, 2006), c) Pressure sensor (Global Water, ND)

3. Mass recorder. The mass of the contents of a gauge can be converted to a precipitation depth through knowledge of the dimensions of the gauge orifice. This is a popular system in mountain regions as it works well for both rain and snow without the requirement for the snow to be melted first. As with the fluid level recorders, the gauge still requires emptying and if snow is not melted an automatic siphon will not operate. Mass recording precipitation gauges are an industry standard device and are used extensively in the northern hemisphere in locations where rain and snow occur. Two examples of mass recording precipitation gauges are shown in Figure 2-5.

(a) (b)

Figure 2-5. Mass recording precipitation gauges. a) Fisher and Porter weighing gauge (NWS, 2006), b) Belfort weighing gauge, outer case and internal mechanism (Belfort Instrument, 2008).

4. Flow sensing gauge. A method of measuring precipitation other than through accumulated totals (of mass or volume) is to measure the rate of precipitation. One method of accomplishing this is to use what is effectively a highly sensitive tipping bucket gauge that counts drips of water instead of bucket tips. Precipitation is collected in a funnel and directed to a hollow needle, which drips water through electrodes closing an electrical circuit every time a drop passes through, enabling a count of drips. The funnel and needle dimensions determine the range of intensities able to be observed. A large (small) funnel with a small (large) needle enables very low (high) intensities to be observed. The funnel and needle size combination also controls the maximum intensity limit above which the drips become a constant flow and no record is obtained. Another limitation of the system is with solid precipitation, which can block the funnel and lead to missed measurements, or alternatively delayed measurement until melt occurs, leading to a temporal offset in combination with exaggerated intensities. An advantage of the system is that there are no moving parts. Figure 2-6 shows the detail of the drop mechanism in a flow sensing gauge.

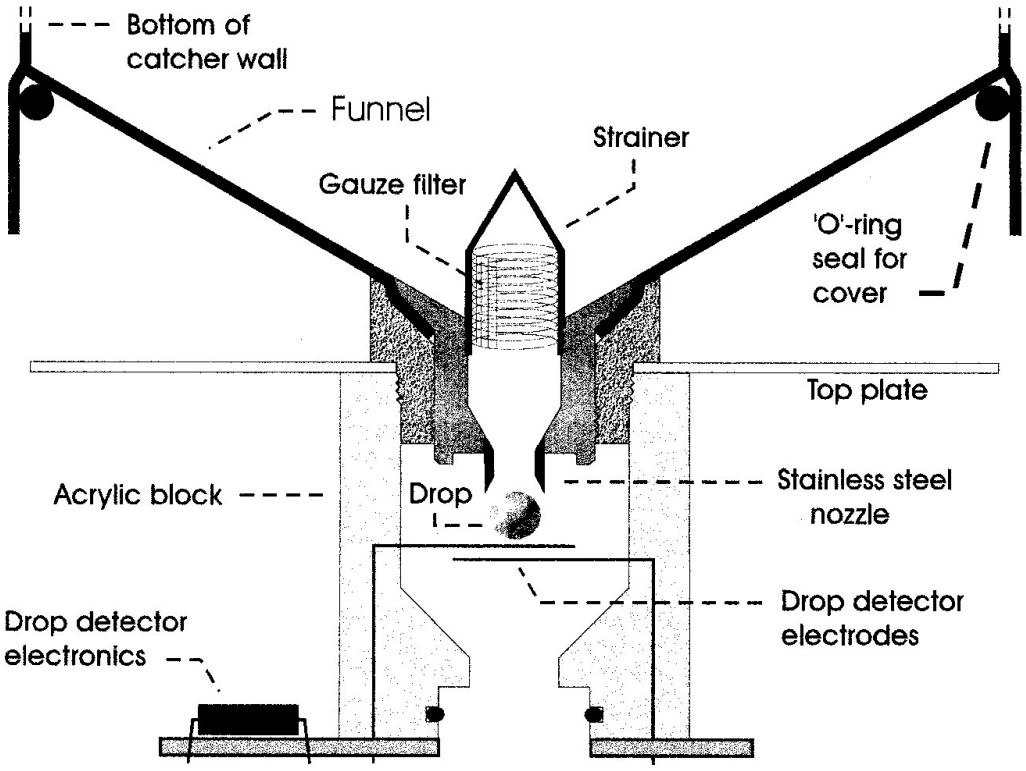

Figure 2-6. Drop creation and measurement mechanism of a flow sensing gauge (Stow et al., 1998).

5. Optical rain gauge. An optical rain gauge measures the attenuation of an optical light source by rain drops as they pass between the light source and a light detector (Figure 2-7). This provides a measure of the intensity of the precipitation. An optical system has the advantage that it does not need to be emptied and it has no moving parts. The disadvantage is that conversion from precipitation intensity to precipitation depth requires knowledge of the phase of the precipitation which the system cannot determine.

Figure 2-7. Optical precipitation gauge (Thies Clima, 2005)

6. Impact sensor. An impact sensor counts the number and size of precipitation particles hitting a surface. The total number and size of the impacts may then be used to infer the precipitation rate. This system has a lower limit on the size of the impact so that currently snow flake detection is not possible. As with the optical gauge, no precipitation is collected and there are no moving parts. An example of an impact sensor is shown in Figure 2-8.

Figure 2-8. Impact sensing gauge (Disdromet Ltd., 2004)

Where only snowfall is required to be monitored, a manual snow course may be utilised. This is simply a series of depth and density measurements of snow across a region of ground. By taking several measurements an assessment of variability is obtained. The use of a snow board provides a similar, but more controlled point manual system. A snow board is nothing more than a moveable flat surface. After snow has accumulated on the surface, depth and density of that snow is measured. After the measurement, the surface is cleared of snow and moved to the same level as the surrounding snow surface. The depth and density of snow enables the depth of the snow water equivalent (SWE) to be calculated which allows the direct comparison of precipitation between solid and liquid precipitation events and sites.
Both a snow course and a snow board are fully manual systems limited by the possibility of melt events occurring since the last snowfall, leading to false total precipitation measurements. Automatic snow measurements track both the build up and reduction of snow. They also have the advantage of determining timing of events and their intensities. There are two commonly used automatic snow measurement

systems, as distinct from total precipitation systems, that have not been considered so far:

1. Snow pillow. A snow pillow is a horizontal fluid filled envelope connected to a pressure sensor. As snow builds up on the envelope, the pressure increases. Knowledge of the area of the envelope enables a depth of snow water equivalent to be established. Potential exists for bridging of the snow pillow by crusts within the snow pack preventing an accurate reading of the total snow mass overlying the snow pillow. The large area of a snow pillow goes some way to alleviate this problem. A snow pillow installation is shown in Figure 2-9.

Figure 2-9. Snow pillow (California DWR, 2008).

2. Sonic ranger. A sonic ranger is a distance measuring device mounted above the snow surface. As snow builds up, the distance to the device is reduced. To convert the depth of snow to a depth of snow water equivalent, an estimate of the density of the snow is required which tends to reduce the accuracy of this system. Sonic rangers have the disadvantage that they return false readings during snow falls or when there is drifting snow. Their simple installation (compared to a snow pillow) makes them a useful option in many circumstances. A diagram representing the operation of a sonic ranger is shown in Figure 2-10.

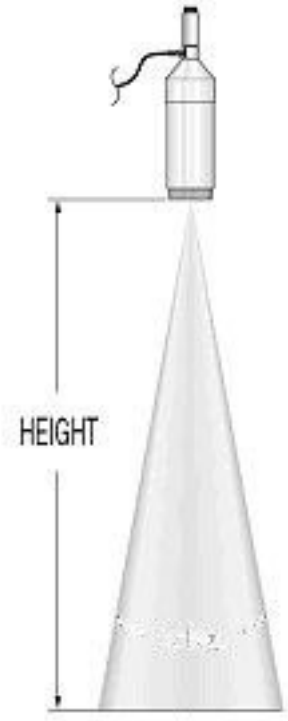

Figure 2-10. Sonic ranger (Campbell Scientific Inc., 2008)

A different style of precipitation measurement is the use of microwave reflectivity in rain radar systems. A rain radar sends out a microwave beam and detects the reflection from liquid and frozen water particles in the beam path. They are used both in ground and satellite based operations and provide precipitation information for large areas at a high resolution. Unfortunately, converting radar reflectance to precipitation quantity is difficult and requires calibration against precipitation gauge data (Gray and Austin, 1993). The line-of-site operation reduces the applicability of ground based systems in highly variable terrain. Satellite based systems still operate in these regions but their reflectance is necessarily from air borne precipitation. This means that they are not always able to distinguish between cloud condensate and what is actually falling to the ground.

Table 2-1 summarises the precipitation gauge types and indicates their suitability for the measurement of rain and snow.

Table 2-1. Precipitation measurement systems.

Measurement Type	Manual or automatic	Rain	Snow	Comments
Tipping bucket gauge	Automatic	Yes	No	Standard automatic rainfall gauge
Heated tipping bucket gauge	Automatic	Yes	Yes	High power usage.
Tipping bucket gauge with antifreeze reservoir	Automatic	Yes	Yes	Requires refilling and waste removal
Collection gauge	Manual/automatic	Yes	Yes	Standard manual gauge
Storage gauge	Manual/automatic	Yes	Yes	Needs evaporation inhibitor, antifreeze and waste removal
Flow sensing gauge	Automatic	Yes	No	No moving parts.
Optical sensor	Automatic	Yes	Yes	Different calibrations are required for rain, hail and snow which can not be distinguished between.
Impact sensor	Automatic	Yes	No	Provides drop size distribution as well as precipitation rate. Different calibrations are required for rain and hail
Snow course	Manual	No	Yes	Provides a spatial variability assessment of accumulated snow. Cannot account for melt.
Snow board	Manual	No	Yes	Simple. Cannot account for melt.
Snow pillow	Automatic	No	Yes	Snow pack may bridge the pillow.
Sonic ranger	Automatic	No	Yes	Requires an estimate of snow density.
Microwave reflectivity	Automatic	Yes	Yes	Provides a spatial distribution. Needs calibration against gauge measurements. Limited to line of sight.

In New Zealand, a range of precipitation measurement systems have been used or are in use. The most commonly used system is the manual collection gauge, generally operated by private individuals on a daily basis, contributing to the National Climate Database administered by the National Institute of Water and Atmospheric Research (NIWA). Many institutions also operate precipitation gauges (e.g. NIWA, Transit New Zealand, universities, NZ Meteorological Service, NZ Fire Service, regional and local council authorities) and these tend to be automatic tipping bucket gauges. Some of these sites have a storage gauge associated with them for use as a check against the automatic measurements. Storage gauges, both manual and automatic and impact gauges have been used for different observation campaigns in the past by various organisations. In the mountains, a heated tipping bucket gauge is operated in the Milford Road area by Transit NZ for avalanche forecasting, an antifreeze reservoir enhanced tipping bucket gauge is operated through the winter at Porter Heights Ski Area in Canterbury, and an Alter Shielded weighing bucket rain gauge is operated at Broken River ski field (Prowse and Owens, 1984), also in Canterbury. Most ski fields throughout the country maintain snow courses and snow boards during the winter for their snow safety systems. A snow pillow and sonic ranger are operating on a permanent basis by Meridian Energy Ltd. at high elevation sites in the upper Lake Pukaki catchment, for hydro-electric inflow forecasting (Halstead et al., 2003). The ability of rain intensity gauges to measure rain duration and rate at a high temporal resolution led them to be used in concert with radar to explore orographic enhancement in the southern North Island mountains (Sanson and Gray, 2002). Lastly, rain radars are operated out of Auckland, New Plymouth, Wellington, Christchurch and Invercargill by the NZ Meteorological Service for forecasting (NZMS, 2008) and for research (e.g. Gray and Austin, 1993) and mobile units have been used for research purposes at various locations around the country (Gray and Seed, 1997; Purdy and Austin, 2003; Purdy et al., 2005).

2.2.2 Precipitation gauge measurement errors

As with any measurement system, there is a limitation to the accuracy of precipitation observations. These errors may be a result of (but not limited to) incorrect calibration, measurement precision, evaporation, splash, wind (inducing undercatch), wetting (Legates and Willmott, 1990) equipment malfunction (Groisman and Legates, 1994),

freezing and drifting (Goodison et al., 1981). The magnitude and relevance of these errors varies, depending on the type of gauge. For instance, the tipping bucket gauge accuracy relies on accurate bucket calibration and efficient mechanical operation with significant sampling errors found for times scales less than 15 minutes (Habib et al., 2001). Mass sensing systems have difficulty detecting low rainfall rates and require correction in these situations (Sevruk and Cvila, 2005). Of the hundreds of publications dedicated to these issues the majority agree that the influence of wind on gauge catch (usually causing under catch) is the single greatest cause of error (Larson and Peck, 1974; Neff, 1977; Tabler et al., 1990). In response to this problem, pit gauges (Koschmieder, 1934) and windshields have been developed (Goodison et al., 1983; Warnick, 1953). Pit gauges work well for liquid precipitation but cannot operate correctly where a build up of snow may occur. In these areas, an elevated gauge orifice is usually used so some sort of wind shield is the most common means of limiting wind induced under catch. Two of the more common wind shield designs are the Alter and Nipher shields (see Figure 2-1). Use of Alter and Nipher windshields around a rain gauge have been shown to increase catch by 2% and 4% respectively for rainfall events, and 45% and 44% for snowfall events (Allis et al., 1963). The Nipher gauge has even been shown to over catch in some circumstances (Goodison, 1978). Use of a wind fence that shelters the entire gauge, not just the orifice was shown to also reduce under catch and led to the development of the Wyoming shield (Rechard and Larson, 1971) effectively a double row of snow fences surrounding the gauge (see Figure 2-11).

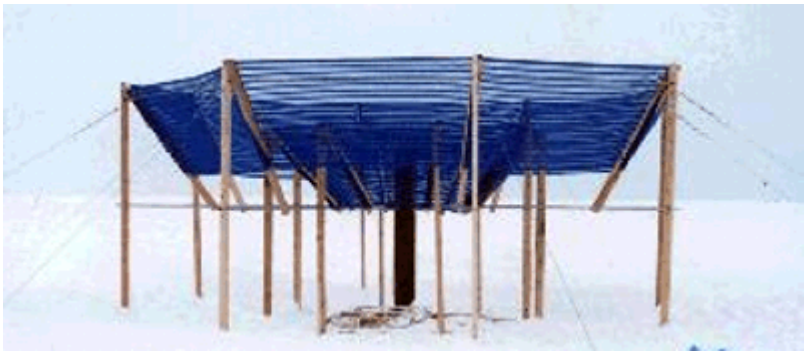

Figure 2-11. Wyoming shield (Berezovskaya, 2006).

While wind shields reduce under catch, they do not remove it completely. The finding that the catch difference between an unshielded and shielded gauge is related to the difference between an unshielded gauge and true precipitation led to a dual

gauge system being developed (Hanson et al., 2004). Comparisons between the Wyoming shield and the dual gauge system have shown little difference during rain events, but for monthly snow fall totals, the dual gauge system out-performed the Wyoming shield (Hanson, 1989; Sturges, 1984, 1986). An alternative to the dual gauge system is to account for under catch using a correction factor. This correction factor may be determined through gauge comparisons, empirical relationships with wind or through water balance assessments (Larson and Peck, 1974). To this end, in 1985 the World Meteorological Organisation recommended that a comparison of solid precipitation measurement systems be undertaken (Goodison et al., 1989). Following from this recommendation, the gauge catch of eight different gauge types were compared resulting in the finding that each gauge caught different amounts of precipitation (Hanson et al., 1999; Yang et al., 1999a). The amount captured varied not only with gauge type and wind shield, but also with wind speed, and precipitation type. The comparisons enabled empirical relationships to be established between wind speed and under catch for each precipitation type and gauge. In this way, measurements using different gauge types may be compared (e.g Yang et al., 1999a) and an improved estimate of true precipitation established (Allerup et al., 1997; Yang et al., 1999b). The limitation of this correction system is that it requires a knowledge of the wind speed and temperature at a site, and this information is often not available. The importance of solid precipitation and wind upon catch error are particularly important in mountain regions where both of these elements are frequently accentuated. Measurements in these areas are therefore particularly susceptible to gauge under catch errors (Legates and DeLiberty, 1993).

2.3 Mountain Precipitation Observations.

2.3.1 Global

Precipitation observations are made throughout the world on a regular basis with global precipitation data sets having been prepared (Beck et al., 2004; Chen et al., 2002; Huffman et al., 1997; e.g. Legates and Willmott, 1990; Mitchell and Jones, 2005; New et al., 2002; Peterson et al., 1993; Willmott and Matsuura, 2001; Xie and Arkin, 1996). These studies have found that the majority of precipitation around the world occurs in the tropics associated with the intertropical convergence zone, the South Pacific convergence zone, and over tropical Africa and South America (Chen et

al., 2002; Huffman et al., 1997). Legates and Willmott (1990) also found that marine west coast regions in the mid-latitudes were centres of high precipitation (Figure 2-12) and that mountainous areas were characterised by greater variability. This greater variability is accentuated by uncertainties in gauge catch error and poor gauge representation (Frei and Schär, 1998). A comparison of global mountain precipitation distribution derived from corrected gauge data with that determined using stream flow information and modelled evapotranspiration estimated the corrected gauge data to still be 20 % below the true precipitation (Adam et al., 2006). These studies highlight that in many coastal maritime mountains (including the Southern Alps) the precipitation is globally significant and that in mountain regions in general there is a need for improved quality and spatial resolution of observations.

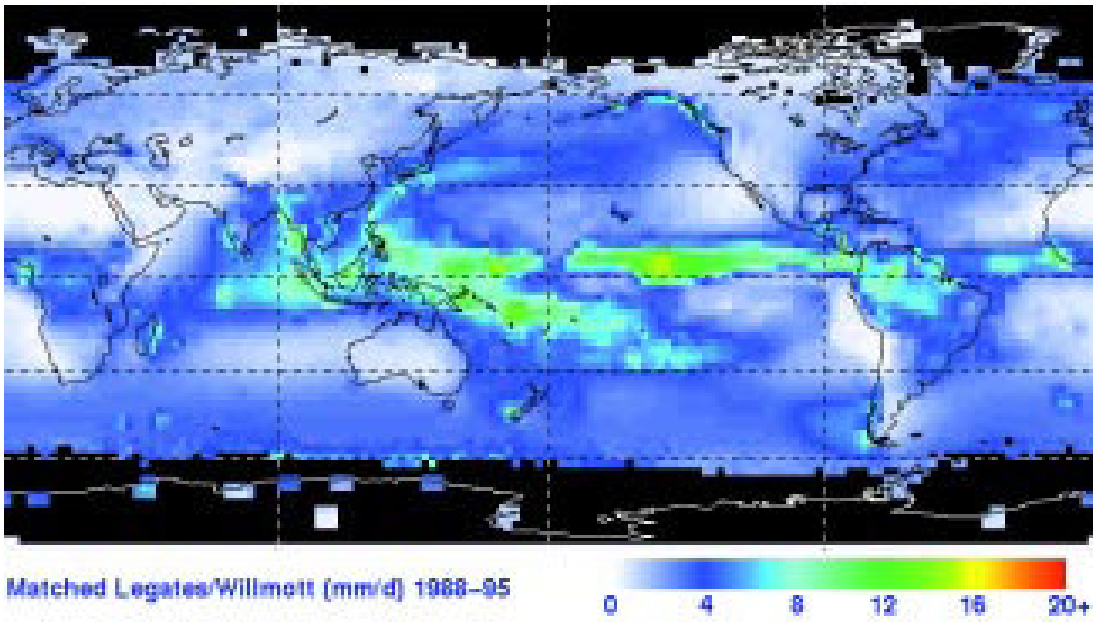

Figure 2-12. Eight year mean daily precipitation derived from the Legates and Willmott (1990) global precipitation distribution, prepared by Huffman et al. (1997).

2.3.2 Regional

Assessments of precipitation distribution at a regional level have been carried out for mountain regions throughout the world. For example, in California (see Figure 2-13 for locations mentioned in the text) the precipitation distribution around the summit of a 1320 m high peak in the Santa Ynez Mountains has been investigated (Hovind, 1965). Fourteen rain gauges were located within 500 m of the summit for the duration of three frontal storms. For each storm the windward gauges consistently caught 50 % of the summit gauge, while the lee gauges always caught more than the summit gauge with the amount varying dependent on wind speed. Nearby, in the San Gabriel

Mountains, the topographic influence on precipitation distribution has been investigated using 11 years of data from 141 gauges (Burns, 1953). Significant relationships were found with elevation, slope and aspect, but no relationship to distance to a windward barrier was determined. A very similar study carried out for the whole of northern California also found elevation, slope and aspect to have significant relationships to precipitation, and in addition, the height of windward barriers within 73 km and the environmental zone a gauge was within were shown to relate to precipitation amounts (Linsley, 1958). Further north, leeward/windward precipitation differences have been investigated for a small hill (less than 100 m high) in the Willamette Valley in Oregon, (James, 1964). For three months, the weekly catch at two gauges, either side of the hill (positioned to be leeward and windward based on the predominant wind direction), was recorded. The leeward gauge consistently caught more (average 110 %) than the windward gauge, with the relationship wind speed dependent. Closer to the coast, and slightly north, the Olympic Peninsula is a mountainous region with routine climate observation sites around the edge of the mountains, but none within the mountains themselves (Rasmussen et al., 2001). To address this lack of information, precipitation on the Blue Glacier within the Olympic Peninsula was observed daily from August 1957 until July 1958. A combination of a standard 8 inch gauge for rain, and a snow board for snow accumulation was used. The observations indicated that 1.475 times the precipitation which occurs at the nearest lowland observation site falls on the glacier, leading to an estimated mean annual precipitation of 4469 mm (Rasmussen et al., 2000). On the south western side of the Olympic Peninsula, ten precipitation gauges have been installed in a 20 km transect across a 900 m ridge. Over three seasons, the ridge top gauges were found to receive 1.33 times the precipitation as the valley floor gauges (Anders et al., 2007; Minder et al., 2008), indicating a strong elevation relationship to precipitation. Carrying on up into British Columbia, a campaign to establish controls on the precipitation distribution in a single catchment has been carried out (Loukas and Quick, 1996). Six weighing gauges, charged with antifreeze, were installed in forest clearings in the upper catchment of the Seymour River. Comparisons between shielded and unshielded gauges and with nearby snow course information showed that the gauge catch was a close approximation to true precipitation. Measurements revealed that there was no precipitation-elevation relationship in the catchment and that the distribution varied both with the time of

year and with the type of precipitation. On the east coast of the continent, the small elevation scales of Connecticut topography have been found to be a primary controller of precipitation distribution in the region (Wilson and Atwater, 1972). Analysis of two years of storm rainfall data from 135 locations found that more rain fell in the hills than the coastal and valley region, that rainfall gradients were closely associated with elevation gradients, and that wind direction modified particular storm precipitation distributions.

In Europe, a lack of mountain precipitation sites in the French Alps led to installation of an intense network of mountain rain gauges in 1986 (Givone and Meignien, 1990). The results showed that the mountain precipitation distribution varied both with topography and meteorological indices with highly complex relationships to observations in nearby non-mountain regions. A more intensive study of precipitation distribution was carried out in a research basin in Switzerland (Sevruk and Nevenic, 1998). Ten years of summer data from 61 gauges in this small 13 km^2 basin were analysed. The gauges were a mix of ground level gauges, elevated daily gauges, and storage gauges. Great care was taken in correcting the gauge catch for wind and wetting loss. The study showed seasonal and elevation relationships to gauge catch, but also demonstrated a difference between windward, valley bottom and leeward sited gauges with the valley bottom gauges having the highest catch. This elevation relationship was further explored for sixty different catchments in Switzerland (Sevruk and Mieglitz, 2002). The relationship between elevation and precipitation varied seasonally and spatially throughout, but no spatial or meteorological patterns could be identified. The precipitation distribution for the entire European Alps has been investigated through interpolation of over 6600 precipitation gauge records (Frei and Schär, 1998). Enhanced precipitation was found to be distributed on the outside primary flanks of the mountains with less precipitation in the interior. This general distribution held throughout the year but with considerable seasonal variation in magnitude at specific locations.

While Britain may not be considered a mountainous region, several investigations of the orographic influence on precipitation have been undertaken there. Precipitation observations in South Wales during stable, constant but strong low level wind situations found that the highest catch was not in the maximum uplift region but further to the lee, providing evidence that precipitation distribution was influenced by advection as well as condensation location (Browning, 1980). Following from this,

when considering precipitation enhancement by topography throughout Wales, Hill (1983) found that this enhancement location was highly dependent on wind direction, and for coastal exposed regions, to wind speed. A similar investigation was carried out for Scotland with precipitation enhancement strongly controlled by slope orientation to the wind, but with peak precipitation, unlike in the events investigated by Browning, often occurring to windward of the orographic barriers (Weston and Roy, 1994).

In Sweden, a two year, summer rainfall measurement campaign was undertaken in the Storsjön and Anjansjön catchments (Niemczynowicz, 1989). Ten tipping bucket rain gauges were installed at a range of elevations from 400 m to 1000 m. The summer rainfall in these catchments was found to vary with elevation on average 9.5 % per 100 m. Additionally, 11.5 % of the precipitation variance was attributable to the distance of measurement sites to the North Sea (the nearest large body of water to windward). Other variations in the precipitation field were attributed in a qualitative manner to local wind variability. This wind-topography-precipitation relationship was investigated at a wider scale for the whole of Sweden by Johansson and Chen (2003). Wind speed, wind direction, topographic slope, distance to the sea (in the windward direction) and the elevation difference to the upwind barrier were all found to be statistically significant variables in determining precipitation. Including this information in an interpolation system, the seasonal distribution of precipitation was improved and the sensitivity to missing precipitation observations reduced (Johansson and Chen, 2005). Further west on the island of Iceland, a smaller scale study utilising a large number of rain gauges has been undertaken (de Vries and Olafsson, 2003). In 2002, thirteen rain gauges were installed along a 30 km transect across the 700 m high Reykjanes mountain ridge, enabling detailed investigation of cross profile precipitation distribution during individual rain events. Rain gauges were installed at ground level, and only rainfall events measured, thus limiting the under catch error. For summer rainfall events, the precipitation near the ridge crest was found to be three to four times greater than at the windward coast, and 5-6 times greater than the lee coast, with temperature and wind speed dependencies.

Two catchments in the western Himalayas, the Beas and Satluj have been the subject of precipitation distribution research (Singh and Kumar, 1997). The precipitation gauges in the Satluj catchment covered an elevation range of over 3000 m.

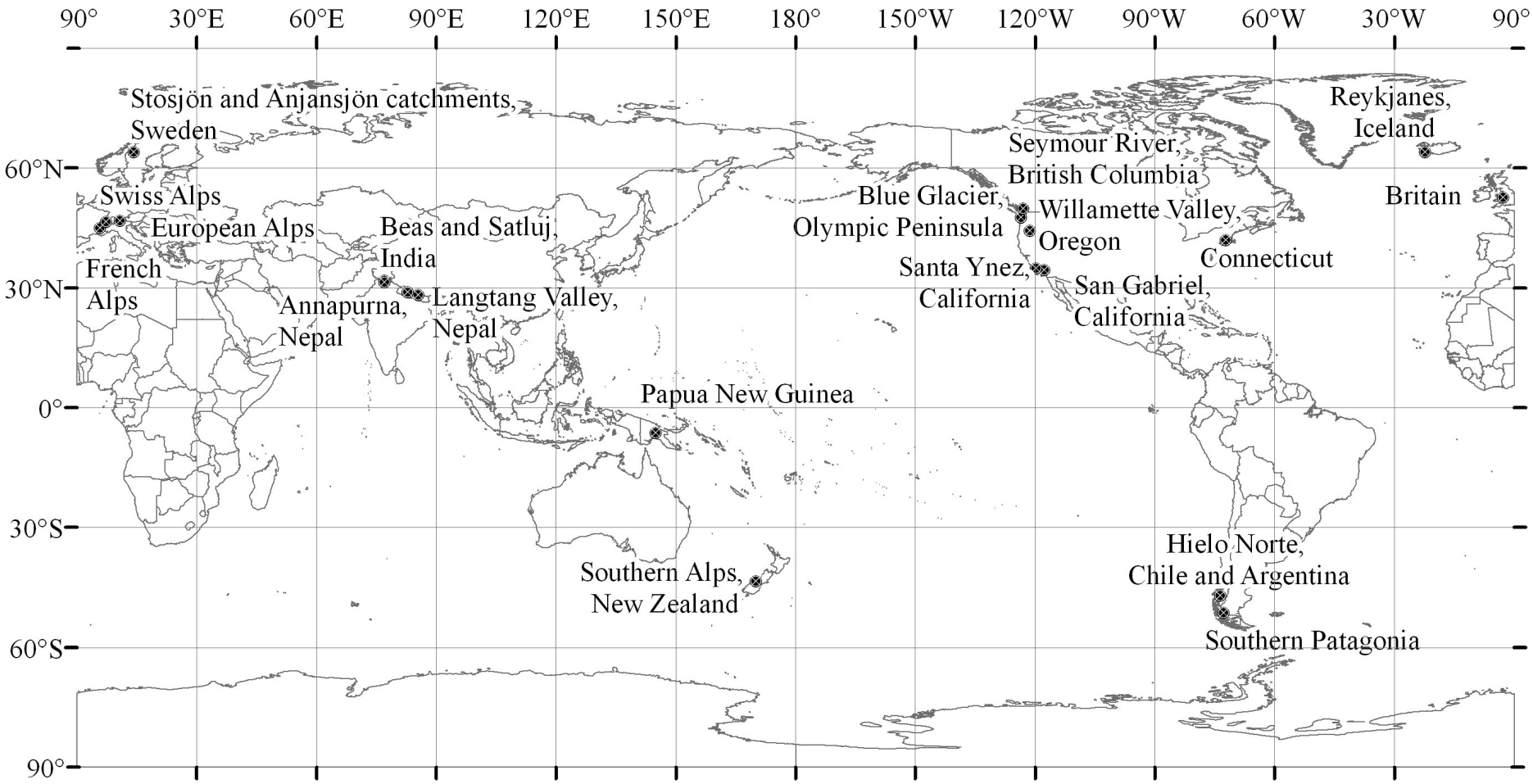

Figure 2-13. Locations mentioned in the text.

In both basins the precipitation was found to increase with elevation for the gauges on the lee (eastern side) of the mountains as a result of increased intensity and, in the case of the Beas Basin, frequency. The elevation relationship held on the windward slopes for the Beas Basin, but not for the Satluj. In all cases the precipitation distribution was strongly dependent on the season with the majority of precipitation occurring during the monsoon season. Overall the windward side of the mountains received more precipitation than the leeward, especially in the Beas Basin with almost twice the precipitation measured on the windward side compared with the leeward.
Still in the Himalaya but over 1000 km away in the Langtang Valley, a similar assessment of precipitation has been carried out (Seko, 1987). Analysis of a year of data from three tipping bucket rain gauges at 3500, 3920 and 5090 m within the valley revealed strongly seasonal precipitation distribution variations. During July and August (monsoon), a small amount of precipitation fell on every day. From September to October (late monsoon) frequency of rain reduced, but individual event quantities increased. Through November to January, precipitation events were few, though very large amounts fell when it did occur. From February to June, the frequency of rain slowly increased, while the event totals again reduced. During the monsoon season the precipitation in the Langtang Valley was less than that measured at the lower elevation Kathmandu site to the south. During winter, this changed, with increased precipitation at the higher elevation sites. The rains during the monsoon season were associated with large convective systems, whereas the winter precipitation was associated with the passage of westerly troughs. More recently, nineteen precipitation gauges were installed across the Annapurna Range of the Himalaya (Putkonen, 2004). A significant difference in distribution was again found between the monsoon season and winter with the later related to elevation and the monsoon season precipitation related to distance to a windward baseline. The monsoon season precipitation provided the largest component of the annual precipitation total with a peak annual precipitation of 5000 mm being observed at the 3000 m site on the windward side of the orographic barrier.
In the mountains of Papua New Guinea, a precipitation profile has been prepared, based on mean annual precipitation records in the vicinity of the 145^{o} E longitude line (Barry, 1978). This profile indicates a peak of 8000 mm on the southern slopes of the mountains, reduced precipitation across the highlands above 2000 m and then a

second smaller precipitation peak on the steep northern slopes. The reliability of the profile is complicated by the severe seasonality and annual variability of the precipitation distribution, as well as the general paucity of high elevation precipitation observation sites. The profile approach to describing cross-mountain precipitation has also been used in southern Patagonia (Schneider et al., 2003). New precipitation observation sites located between two long term weather observation sites enabled a 300 km transect to be established. Measurement difficulties with the tipping bucket gauges at the newer sites from wind induced under catch, vibration induced sensor excitation and lost measurement from snowfall were unable to be accounted for. Nevertheless estimates of annual precipitation of 4400 mm windward of the mountain range, 11000 mm within the mountain range and 500 mm lee of the mountain range were returned. This last transect highlights the extreme variation possible in mountainous areas, variation that would not be possible to estimate from the long term observation sites either side of the mountains. Similarly extreme variation was found across the Hielo Norte (Northern Patagonian Icefield) a remote region of the Southern Andes where few precipitation observations have been made (Inoue et al., 1987). During the summer of 1985-1986 , a series of precipitation measurements were taken using recording and storage gauges (Fujiyoshi et al., 1987). These short term measurements were compared to the record from a nearby low altitude measurement site enabling a four year average of annual precipitation to be estimated. The results indicated that at sea level to windward of the Hielo Norte, 3700 mm falls per year, 13000 mm of water equivalent falls at the top of the west-flowing San Rafael Glacier, just west of the ice divide and 2200 mm at the terminus of the east-flowing Soler Glacier.

Table 2-2 provides an overview of the various observed precipitation distributions and the related controls.

While repeated themes of wind speed, wind direction, season, slope orientation and elevation are apparent as important influences on orographic precipitation throughout the world, the relative importance of any of these factors changes from location to location. In some situations, the precipitation maximum was observed windward of the barrier, sometimes near the crest, sometimes in the lee. Individual storm (or even season) precipitation distributions differed from long term distributions. Even average annual precipitation magnitudes varied considerably from location to location.

Table 2-2. Mountain precipitation distribution measurement campaigns from around the world.

Country/region	Catchment/ area	Precipitation relationships determined	Reference
California	Santa Ynez Mountains	Wind direction, wind speed	(Hovind, 1965)
California	San Gabriel Mountains	Elevation, slope, aspect	(Burns, 1953)
California	Northern California	Elevation, slope, aspect, windward barrier height, environmental zone	(Linsley, 1958)
Oregon	Willamette Valley	Wind direction, wind speed	(James, 1964)
Olympic Peninsula	Blue Glacier	1.45 times the nearest lowland gauge site	(Rasmussen et al., 2000)
British Columbia	Seymour	Season, precipitation type	(Loukas and Quick, 1996)
Connecticut	Connecticut	Elevation, slope, wind direction	(Wilson and Atwater, 1972)
France	French Alps	Topography and meteorology	(Givone and Meignien, 1990)
Switzerland	Research catchment	Season, elevation, slope, wind direction	(Sevruk and Nevenic, 1998)
Switzerland	60 valleys	Variable elevation dependency	(Sevruk and Mieglitz, 2002)
Europe	European Alps	Primary mountain flanks, season	(Frei and Schär, 1998)
Britain		Wind speed and direction	(Browning, 1980; Hill, 1983; Weston and Roy, 1994)
Sweden	Storsjön, Anjansjön	Elevation, distance to the North Sea, local wind	(Niemczynowicz, 1989)
Sweden		Wind speed, wind direction, slope, distance to sea, distance to upwind barrier	(Johansson and Chen, 2003, 2005)
Iceland	Reykjanes	Elevation, wind speed, wind direction, temperature	(de Vries and Olafsson, 2003)
India, Himalaya	Beas, Satluj	Wind direction, elevation of leeward slopes, season	(Singh and Kumar, 1997)
Nepal, Himalaya	Langtang Valley	Season	(Seko, 1987)
Nepal, Himalaya	Annapurna	Season	(Putkonen, 2004)
Papua New Guinea	145^{o}E	Primary mountain flanks, season	(Barry, 1978)
Chile (Patagonia)	53^{o}S	Wind direction, distance to barrier	(Schneider et al., 2003)
Chile, Argentina (Patagonia)		Wind direction, distance to barrier	(Fujiyoshi et al., 1987)

These variations may be explained by the fact that every mountain region is different in its physical shape and global location and so interacts with the atmosphere in its own unique manner. Implications from this assertion are that a generalised understanding of orographic precipitation processes requires observations in a full spectrum of climate/topography types, and that transfer of process understanding from one region or climate type to another must be done with caution.

2.3.3 New Zealand

One of the earliest precipitation distribution estimations for the Southern Alps of New Zealand (see Figure 2-14 for locations within New Zealand) was the 1929 mean annual rainfall map, based on 1891 to 1925 observations (Kidson, 1929). On this map the highest, 200 inch (5080 mm), isohyet runs along the head of the Lake Pukaki catchment, with the 30 inch (762 mm) isohyet in the vicinity of the lake itself. The highest precipitation area is shown to be west of the main divide in the Franz Josef névé region, but straddles the main divide 100 km further north east in the vicinity of Arthurs Pass. Such mean annual precipitation maps have been regularly prepared for the Southern Alps, each with a different estimation of the precipitation distribution in the un-gauged high mountain regions. The mean annual precipitation map based on the 1921-1950 rainfall normals as used by Anderton (1974) estimated most of the Tasman Glacier to receive over 7500 mm. The 1941 to 1970 mean annual precipitation map still had the zone of highest precipitation to the west of the main divide, but this time the maximum precipitation had been raised to 8000 mm (NZMS, 1975a). This map includes text to say that the high precipitation gradient and low number of measurement sites means that in mountainous regions the map cannot provide an accurate estimate of precipitation. Ten years later the 1951 to 1980 precipitation normals enabled yet another mean annual precipitation map to be prepared (NZMS, 1985a). On this map the 600 mm isohyet is shown at the outlet from Lake Pukaki, while the main divide is at 9600 mm. The highest precipitation region in the country is depicted as being just to the west of the main divide near Aoraki/Mt Cook with over 12800 mm of mean annual precipitation.

In an endeavour to improve on the acknowledged lack of observation data in the Southern Alps, an intensive precipitation observation campaign in the Hokitika-Rakaia region was carried out (Griffiths and McSaveney, 1983a).

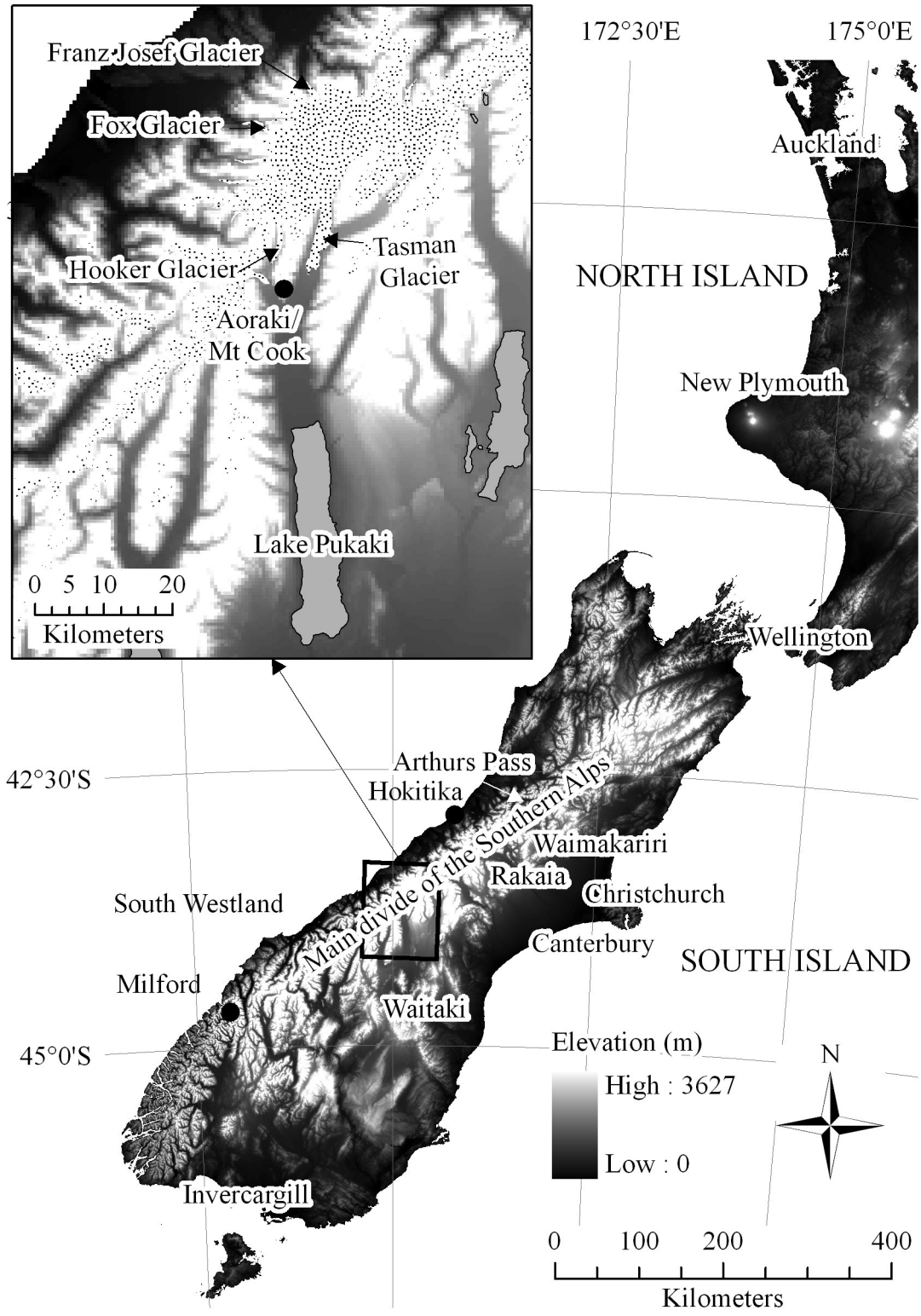

Figure 2-14. New Zealand locations mentioned in the text

This work proved the existence of a very high horizontal precipitation distribution, and very high average annual precipitation at the transect peak, relative to the rest of the world (Figure 2-15). These new data enabled an exponential relationship to be derived between eastern catchment mountain precipitation and the distance to a windward orographic barrier baseline (McSaveney et al., 1978). This was perhaps the first objective mountain precipitation estimation system employed for these catchments. This relationship was verified through analysis of over 50 years of stream runoff measurements (Thompson and Adams, 1979).

In 1993 a coordinated effort to improve knowledge of the interaction of weather and climate with the Southern Alps was undertaken through the multi-agency Southern Alps Experiment (SALPEX) (Wratt et al., 1996). One of the outcomes of this initiative was analysis of storm rainfall data for four different cross mountain transects along the Southern Alps (including the Rakaia-Hokitika transect), finding that the profile shape was similar at each transect, merely differing in magnitude (Henderson and Thompson, 1999). The suggestion was made that the peak precipitation location is related to the position of the base of the windward mountain slope, and that the magnitude was related to the barrier crest elevation. As part of the same experiment, cross mountain profiles were examined throughout the duration of a storm (Sinclair et al., 1997). Interestingly, the profile was not stable, with the maximum precipitation location moving from west of the orographic barrier to lee of the barrier as the storm cycle progressed. This result is important in that it highlighted that annual precipitation distributions do not indicate a constant distribution. In exploration of the processes behind the observed orographic precipitation during the experiment, Revell et al. (2002) identified the importance of flow blocking to precipitation distribution, while, through the use of a vertically pointing radar the occurrence of the seeder-feeder mechanism was clearly identified (Purdy and Austin, 2003; Purdy et al., 2005) (see section 2.4.2 to follow for a description of this process).

Another approach applied was through the use of glacier features (Ruddell, 1995). Instead of using direct observations, Ruddell modelled mean annual precipitation at the long term equilibrium line altitude of glaciers. This resulted in a map of the estimated average annual total precipitation (for the 1961-1990) of the Southern Alps. He estimated 7000 mm of precipitation at the equilibrium line of the Tasman and Hooker Glaciers increasing to 9000 mm at the equilibrium line of glaciers immediately west of the main divide.

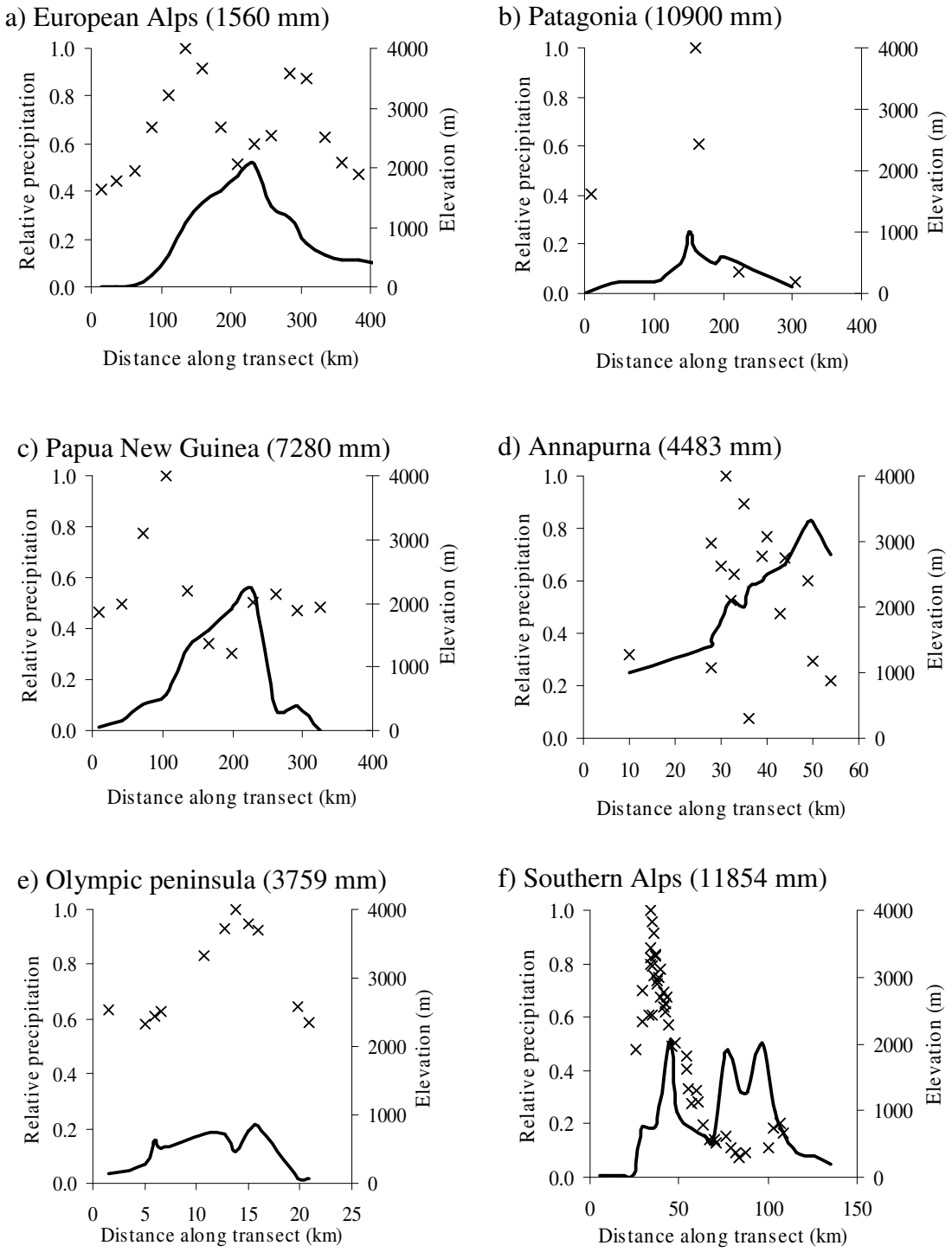

Figure 2-15. A selection of cross mountain precipitation transects from around the world. Precipitation is given as a proportion of the maximum observed across the transect. Elevation scales are standard, but horizontal scales are not. a) European Alps (Weingartner and Pearson, 2001), b) Patagonia (Schneider and Gies, 2004), c) (Barry, 1978), d) Annapurna (Putkonen, 2004), e) Olympic Peninsula (Minder et al., 2008), f) Southern Alps (McSaveney et al., 1978).

At about the same time, Horrell (1990) prepared a map of the mean annual rainfall for the South Westland region of New Zealand using precipitation and stream flow observations. In this map the glaciated regions from Aoraki/Mt Cook Village to Franz

Josef Glacier were omitted as the area was still considered an unknown (Horrell, 2006), though proximal regions along the main divide to the south west were estimated at over 12000 mm.

These long term mean annual precipitation distributions are not immediately applicable to daily or single storm events. In addressing this problem a precipitation map was prepared for the mountains of the Lake Pukaki catchment specifically for north westerly storms (McNulty, n.d.). This map depicts contours of precipitation proportion compared to that which occurs at Aoraki/Mt Cook village. The map was prepared for skiing operations and is still (as of 2007) in use.

Daily precipitation input was also required for a snow storage model for the Waitaki region (Fitzharris and Garr, 1995). This was achieved through using large elevation bands for which a simple elevation-precipitation relationship was applicable. With advances in computer power, downscaling of this model by McAlevey led to the elevation-precipitation relationship no longer being reasonable (McAlevey, 1998). This was overcome by including consideration of the 1951-1980 mean annual precipitation surface when estimating daily rainfall distribution. When tuning this model to the Lake Pukaki catchment, Kerr (2005) removed any elevation consideration, utilising instead an exponential relationship to the distance to the orographic barrier as determined by observations. In approaching the same problem of estimating snow storage for the upper Waitaki Region, Thompson (1997) prepared a map of total annual precipitation, less evaporation, for 1996 (termed effective precipitation). The distribution was tuned to match the catchment runoff resulting in estimates of annual precipitation of up to 15 m. The 1996 water budget was considered by Thompson to be 46% greater than the long term average. The upper estimate of 15 m for 1996 would then relate to a long term average maximum of 10.3 m in the catchment. A mean monthly precipitation surface for New Zealand on a 1 km grid has been prepared based on records from 2202 different gauge sites (Leathwick et al., 1998). A spline interpolation was used, incorporating a topographic sheltering variable, tuned to minimise the error at gauge sites. For the Lake Pukaki catchment the maximum precipitation is 628 mm (7500 mm mean annual) with the maximum precipitation estimated to be near the head of the Fox Glacier at 900 mm (10800 mm mean annual).

Daily gridded (5 km) precipitation maps have been prepared for the period from 1985-2002 based on trivariate (latitude, longitude, elevation) spline interpolation of

observations (Tait and Turner, 2005). The quality of the interpolation in remote regions was found to be poor compared to populated, well gauged areas. To improve the interpolation in these regions a scaling factor was derived through comparison of modelled precipitation totals with the interpolated precipitation during a period where the model output was known to be accurate in at least one region of the Southern Alps. These scaling factors were then applied at a daily level for the entire period. A comparison of the resulting 1985-2002 mean annual precipitation distribution was made with the manually drawn 1951-1980 mean annual precipitation distribution (NZMS, 1985a). The differences were reduced in the Southern Alps, compared to the non-scaled interpolation, but were still 60 % over estimated in the central and eastern regions of the North Island. This discrepancy was considered a result of the model having been tuned to the Southern Alps, and evidently not generally applicable to all remote regions of the country. Trivariate spline interpolation of observations was used again for preparing daily gridded precipitation maps, but this time the third variable used was a mean annual precipitation surface, rather than elevation (Tait et al., 2006). Evaluation of the resulting grids against river flow data found they were better than the previous spline-plus-model method.

As well as estimating the location and magnitude of precipitation in the Southern Alps, there have been many efforts to relate the distribution to the underlying physical processes and climatic conditions. In considering what conditions resulted in north westerly rain in Canterbury, Hill (1961) reviewed two years of rainfall data from observation sites and compared them to mean sea level pressure analysis charts for the region. Under undisturbed north westerly conditions it was found that rain rarely extended to the Canterbury plains, was much reduced in the eastern foothills, and often resulted in only small rain events even to the west of the divide. The situation changes with the passing of a front or trough line within the north westerly airstream. Increased rain is observed to the west of the divide, with periods of heavy rain associated with the passing of the disturbance. Attempts to relate eastward spread of rain to leeside humidity, stability or winds failed to find a correspondence. A similar investigation was later undertaken for the Waimakariri region using a transect of rain gauges installed specifically for the task from 12th July until 28th December 1994 as part of the SALPEX experiment (Chater and Sturman, 1998). Hourly rainfall measurements were used, rather than the daily observations that Hill was limited to. How far to the lee of the divide that rainfall occurred was found to be clearly related

to wind strength, air mass instability and frontal intensity. The quantity of rain that fell to the lee of the divide was most highly related to just wind speed (though including wind speeds at the 850 hPa level) and air mass instability. The single storm analysis by Sinclair et al. (1997) found that the temporal variation in cross mountain precipitation profile was related to stability, wind speed and freezing level. With low wind speeds and high stability, a low level blocking wind flowing along the western foothills of the mountains forms causing the general westerly flow to rise above this blocking wind and precipitation to fall well upwind of the alpine divide. As the wind strength increases and the stability reduces, this blocking wind disintegrates and the vertical ascent of air occurs further downwind, resulting in a precipitation peak moving leeward and some precipitation falling on the lee side of the alpine divide. With a lowering of the freezing level the fall time of the frozen precipitate increases, further increasing lee side precipitation. For this storm, regression analysis determined that wind speed above the freezing level, and a blocking factor (based on low level stability and wind speed) explained 93 % of the variance of the fraction of precipitation falling to the lee of the alpine divide. This work was extended by Wratt et al. (2000) who found that the cross mountain orographic precipitation total variations were well explained by atmospheric humidity, wind velocity, stability and synoptic uplift.

Table 2-3 provides an outline of the various New Zealand located precipitation distributions.

2.4 Precipitation processes

Condensation of atmospheric water vapour into liquid or solid particles followed by transportation of the particles to the earth's surface describes the process of precipitation. In this section the condensation and transport processes are described in turn with specific relation to the mountain environment.

Table 2-3. Distributed precipitation estimates for the Lake Pukaki catchment.

Type	Period	Resolution	Method	Region	Reference
Mean annual	1891-1925	1127 mm (50 inch) contours	Observations and subjective interpolation	South Island	(Kidson, 1929)
Mean annual	1921-1950	2500 mm contours	Observations and subjective interpolation	Lake Pukaki catchment	(Anderton, 1974)
Mean annual	1941-1970	800 mm contours	Observations and subjective interpolation	New Zealand	(NZMS, 1975a)
Mean annual	1951-1980	3200 mm contours	Observations and subjective interpolation	New Zealand	(NZMS, 1985a)
Mean annual	1941 - 1970		Exponential decay east of a maximum precipitation line	Hokitika – Rakaia transect	(Griffiths and McSaveney, 1983a; McSaveney et al., 1978)
Mean annual	1925 - 1977		River flow assessment and subjective interpolation	Southern Alps eastern catchments	(Thompson and Adams, 1979)
Mean annual	1951 - 1980		Observations and subjective interpolation	Southern Alps transects	(Henderson and Thompson, 1999)
Mean annual	1961-1990	1000 mm contours	Model output, observed glacier equilibrium lines and subjective interpolation	Central Southern Alps	(Ruddell, 1995)
Mean annual	1941-1970	1000 mm contours	Observations and river flows with subjective interpolation	South Westland	(Horrell, 1990)
North westerly proportional to a single point	Unknown	2400 mm equivalent contour	Manual	Aoraki/Mt Cook region	(McNulty, n.d.)
Daily		300 m elevation bands	Observations and elevation with objective interpolation	Central southern Alps	(Fitzharris and Garr, 1995)
Daily		1 km	Observations, elevation and an annual average precipitation surface with objective interpolation	South Island	(McAlevey, 1998)
Daily		1 km	Observations and an annual average precipitation surface and objective interpolation	Lake Pukaki Catchment	(Kerr, 2005)
1996 annual	1996	1 km	Observations and river flows with subjective interpolation	Lake Pukaki Catchment	(Thompson, 1997)
Mean monthly		1 km	Observations and topographic shielding and objective interpolation	New Zealand	(Leathwick et al., 1998)
Daily		5 km	Observations and model output and objective interpolation	New Zealand	(Tait and Turner, 2005)
Daily		5 km	Observations and an annual average precipitation surface and objective interpolation	New Zealand	(Tait et al., 2006)
North westerly	1958 - 1959		Observations	Canterbury	(Hill, 1961)
Lee	1994		Observations	Upper Waimakariri valley	(Chater and Sturman, 1998)

2.4.1 Condensate formation

Condensation of water vapour occurs whenever a water molecule has insufficient thermal energy to overcome both intermolecular attractive forces from other molecules and surface tension of the formed condensate. As such, condensation may come about through a change in temperature and pressure, which impact on available energy, or a change in available condensation nuclei (CN), which increases surface tension forces. The normal fluctuations of the atmosphere from earth rotation and solar inputs cause a continual variation in these variables.

There are a number of different atmospheric processes that lead to condensation formation that may or may not involve interaction with the earth's surface and/or mountainous terrain. Frontal and cyclonic systems are two examples requiring no surface interaction to cause condensation. In a frontal system the ascent of warm air masses above cold air masses leads to the warm air mass cooling (through reduced pressure at elevation, and through mixing with the cold air) resulting in condensation. In a cyclonic system condensation occurs as a result of the ascent of the air mass in the reduced pressure leading to reduced energy of water molecules. In contrast, the earth's surface is usually required for convective processes to occur. In this case, the transfer of heat from a surface to the overlying air mass leads to the expansion and decreased pressure of the air mass resulting in buoyancy enabling the air mass to rise to cooler elevations and in turn cause condensation. While all of these mechanisms may occur without the presence of mountains, their presence will generally affect the process. For instance, precipitation has been observed to be enhanced on the windward side of a mountain range and reduced to the lee during the passage of a front (Hobbs et al., 1975). The windward increase was thought to be a result of terrain forced ascent of the low level moist air, whereas the lee reduction was caused by blocking of the same moist flow by the range. Another example is the build up of cyclones in the lee of mountain ranges following the perturbation of the air mass by the mountain range (Funatsu et al., 2004; McGinley, 1982). Convection systems may also be influenced by mountainous terrain. Thermally induced up-valley flows can overcome atmospheric stability resulting in convective cloud and precipitation (Banta, 1990; Braham Jr, 1960), or equally terrain forced vertical flow (of a more general horizontal synoptic flow) may trigger convection (Fuhrer and Schär, 2005; Kirshbaum et al., 2007). Condensation that is brought about by mountains alone follows the

interaction of the mountains on air mass flow. This may come about through convergence of air masses directed horizontally by mountains (Mass, 1981) or more commonly, through the ascent and cooling of an air mass prior to (Revell et al., 2002), during (Houze Jr., 1993) or after passing (Reinking et al., 2000) over that terrain.

2.4.2 Condensate transport

Once formed, individual condensation particles, be they ice or water, are frequently referred to as hydrometeors. This name puts the emphasis on the air suspended state of the condensate, rather than the initial formation, or the final fall out. Indeed, the presence of a hydrometeor provides no guarantee that it will fall to the earth's surface as precipitation. As soon as a hydrometeor is formed, its mass and size dictate its path through the atmosphere. A large mass results in greater gravitational forces, while a large size results in greater advective and frictional forces. Gravitational forces are directed earthward, advective forces follow atmospheric pressure differences (i.e. air mass flow), while friction opposes both these forces. The path of a hydrometeor is therefore largely governed by its mass, its size and the air flow that it is within. None of these are constant.

The processes related to condensation equally involve evaporation. Most commonly, atmospheric temperature increases as elevation reduces. As a hydrometeor falls to lower and warmer elevations it may gain sufficient energy to enable its constituent water molecules to melt (if it is in the solid state) and/or evaporate. This in turn absorbs energy and affects the temperature of the surrounding atmosphere. Such cooling has been found to be large enough to induce drainage air flows that can oppose the general synoptic conditions (Steiner et al., 2003). Equally possible is that a hydrometeor acts as a condensation nucleus itself, enhancing further condensation and so providing a positive feedback to the process. There is also a negative feedback in the system in that the condensation of water releases energy to the surrounding atmosphere which enhances evaporation. Hydrometeors may also interact with each other, sometimes accreting into larger forms, and sometimes breaking apart. This continual change in the mass and volume of a hydrometeor results in a continual change in its fall path. Sometimes its mass is large enough that gravity overcomes upward advective forces, at other times it may not. A modelling study of the Bergeron-Findiesen process (Stickley, 1940) whereby frozen hydrometeors grow at the expanse of liquid hydrometeors because of the vapour differential between the

particle types, provided a good example of this. As ice particle concentration increased, riming (freezing of liquid water on to the ice particles) reduced at the expense of vapour deposition, leading to greater advection down wind of the hydrometeors (Hobbs et al., 1973). The fall path may also transport the hydrometeor into different thermal or pressure zones, again affecting whether they change and/or reach the ground. An example of hydrometeors being advected into a zone of evaporation is frequently encountered in the lee of mountains. Clouds forming on the windward side of mountains following terrain induced uplift will often evaporate on the leeward side as the hydrometeors pass into a warmer and drier zone. The seeder-feeder mechanism (Banta, 1990; Choularton and Perry, 1986; Robichaud and Austin, 1988) is an example of falling hydrometeors enhancing condensation and accretion through a lower condensation zone that would not have otherwise resulted in precipitation reaching the ground.

As well as the hydrometeor path having an impact on its phase, size and whether or not it reaches the ground, it also has an impact on the horizontal location of where it reaches the ground. This last consideration has an important effect on the final distribution of precipitation. Condensation transport can be seen as a complex dynamic relationship between a hydrometeor and its environment.

2.5 Process modelling

Models enable the estimation of precipitation through consideration of other known variables. This is useful for the estimation of precipitation at locations, times or situations where no direct measurements are available, and may be used to discern what processes are likely to influence precipitation in a particular area. The paucity of observations and known high variability in mountainous regions makes modelling particularly desirable for these regions.

A standard method of estimating precipitation in mountainous regions is to use a linear relationship to elevation, with typical values of increasing precipitation with elevation ranging from 0.06 to 0.25 % m^{-1} (Smith, 1979). In such a system the complex and dynamic relationships between atmospheric water vapour and air flow, as described in the previous section, are reduced to a simple and easy to apply relationship. With calibration to observations, such a model can work well for large spatial and temporal scales and is used extensively in operational systems around the world including the Hydrologiska Byråns Vattenbalansmodell (HBV) (Lidén and

Harlin, 2000) and University of British Columbia watershed model (UBC) (Micovic and Quick, 1999) rainfall-runoff models. As a second order model, precipitation may be related to a combination of topographical characteristics (Basist et al., 1994; Daly et al., 1994) utilising well known topographic values (e.g slope, aspect, elevation). The justification for this approach is that precipitation is closely related to airflow. Consideration of slope provides an indication of the vertical motion of air, aspect provides an indication of the direction of that vertical motion, and elevation provides an indication of the saturation of the air mass. A limitation of this approach is that the relationships are scale and location dependent, and are not universally applicable.

A more analytical approach is an upslope model whereby precipitation is equated to the total moisture in a vertical air column that is in excess of total saturation after the column has been lifted by terrain, assuming adiabatic cooling (Smith, 1979, 2003). Such a model requires surface elevation, temperature, pressure, and saturation information to generate precipitation output. The primary precipitation-causing elements of this model are assumed to be terrain forced uplift only. No account of 2^{nd} dimension horizontal air flow, convection, condensation growth or hydrometeor trajectories is taken into account. Even so, this model provides surprisingly useful results in determining general precipitation patterns for certain circumstances. For example, a slightly modified upslope model was used in analysing the precipitation distribution associated with Cyclone Bola which caused damage in the North Island of New Zealand (Sinclair, 1993). Vertical ascent of air was taken as though surface winds followed the terrain in the direction of the wind. A reduction of vertical ascent with elevation above the surface was included, with the formulation of this being a method of tuning the model. It was found that not until a reduction of resolution from 100 km to 10 km was the observed magnitude of the rain able to be modelled. Addition of condensation growth and hydrometeor trajectories to the upslope model enables improved precipitation distribution estimation especially in areas lee of a mountain crest (Roe and Baker, 2006; Sinclair, 1994). Even with these additions, such models still only really consider precipitation related to terrain forced ascent, with no consideration of flow dynamics and convective processes. Models that include all of these processes are commonly known as full physics models. Examples are the Weather Research and Forecasting (WRF) model (Skamarock et al., 2005), Mesoscale Model Version 5 (MM5) (Grell et al., 1995), the Regional Atmospheric Modelling System (RAMS) (Cotton et al., 2003; Pielke et al., 1992), the Mesoscale

Compressible Community (MC2) (Benoit et al., 1997) and the Coupled Ocean/Atmosphere Mesoscale Prediction System (COAMPS) (Hodur, 1997). These models include full vertical and horizontal air flow components allowing for momentum and energy exchange between air mass components. This enables convection and hydrometeor trajectories to be modelled. Condensation and evaporation is accounted for through consideration of air parcel saturation and temperature. Complexities of condensation rates, accretion, deposition, aggregation, hydrometeor splitting, and nucleation are handled to a greater or lesser extent by parameterisations by the models, with these microphysics considerations the subject of ongoing research.

These models have been used to explore process controls on mountain precipitation distribution, and to determine limitations of the models themselves. A good example of modelling revealing processes different to traditional understanding is in the analysis of air parcel trajectories as they pass over a mountain (Smith et al., 2003). Contrary to the expected path of windward rise and lee descent, it was found that air parcels that were lifted on the windward slopes and gained latent heat, continued to rise lee of the mountains. Air parcels that descended to the lee had little latent heat exchange and originated from higher elevations to windward. Another example of the application of modelling to understand process controls has been to discern the influence of a lee side cold air pool on precipitation distribution and air flow (Lee et al., 1989; Zängl, 2005). Modelled outputs were compared for scenarios with and without the cold air pool. Analysis of model results not only showed an extension of lee precipitation but was able to show that this related to the suppression of lee air descent and the associated lee mountain waves.

The use of models enables idealised situations to be represented to explore the effects of individual parameters on precipitation. Such an approach has enabled the influence of mountain size on precipitation fields to be investigated (Barstad et al., 2007; Colle, 2004). The modelling results indicated that increased mountain height increased condensation and precipitation, with the peak precipitation region moving to windward. Reducing the mountain width again increased the condensation, but generally decreased the total precipitation, though not linearly. More significantly, changing the half width had a strong impact on the location of the precipitation with the maximum precipitation band becoming narrower, closer to the ridge crest and with a second lee side precipitation maximum.

An example of verification of the MM5 model and an assessment of its sensitivity to model parameters is that which has been undertaken by Rögnvaldsson et al. (2007). A transect of rain gauges across a mountain range in southern Iceland was used to provide validation data for model runs over the same region. The results showed the ice initialisation and horizontal diffusion methods made little difference on output whereas the resolution, the cloud droplet number concentrations (CDNC) and the initial condition's data origins did make a difference. In all cases, the model runs under-estimated the downstream precipitation. The best simulations were with the finest resolution (2 km) the lowest CDNC number (30) and the National Centers for Environmental Prediction/ National Center for Atmospheric Research (NCEP/NCAR) reanalysis data initialisation. A variety of reasons were suggested for the poor downstream precipitation modelling, including overestimation of descending motion, initialisation data being too dry, or over efficient upstream precipitation. A similar verification of the RAMS model has been carried out against observed precipitation in the Southern Alps of New Zealand (Bormann and Marks, 1999). In this case the inclusion of snow, graupel and aggregation processes was found to improve simulations of high precipitation events especially to the lee of the mountains, though over simulated light rain situations. The very ability of these complex models to incorporate various process options still leaves the need for optimisation and tuning for any application. For instance, a sensitivity analysis of model parameters in simulating a single orographic precipitation event has been undertaken for the MM5 model (Zängl, 2004). Individual components were modified while all others were held constant. Every considered component of the model (cloud microphysics, convection, boundary layer, diffusion, vertical coordinates, initialisation analysis data) was found to affect the precipitation with the most sensitive being the method of temperature and moisture diffusion (either terrain following or horizontal) which could result in a 35% difference in precipitation amount. Such a result highlights the inability of even the most complex models to accurately capture precipitation fields a priori.

It can be seen then, that models provide a useful means of process exploration but, as yet, are unable to determine precipitation distribution without observation calibration and verification.

2.6 Conclusion

Precipitation measurement techniques have been developed in lowland rainfall regions and adapted to mountainous, mixed precipitation regions. Known precipitation measurement limitations are commonly accentuated in mountain areas especially with regard to the effects that higher wind speeds and increased snow fall have on under catch.

Precipitation measurement campaigns from around the world show that distribution varies with scale, location and underlying precipitation process. No universal empirical topographic-precipitation relationship has been determined, though calibrated models based on such relationships are commonly applied to specific regions. Common influences on precipitation distribution as determined through observation campaigns include wind speed, wind direction, elevation, slope and season, though the relative importance is highly variable.

Numerous precipitation distributions for the Lake Pukaki catchment have been prepared with the variety of estimations for the upper catchment reflecting the different interpolation techniques used and evolving state of understanding. Observations and estimates indicate precipitation magnitudes and horizontal gradients approaching the most extreme values found in the world.

A general theory of precipitation requires a full understanding of air flow, moisture availability, condensation, accretion, evaporation and hydrometeor fall dynamics. Interactions between all of these processes produce a formidably complex system. Modern precipitation modelling systems incorporate these processes to a greater or lesser extent. This ranges from simple empirically based elevation-precipitation relationships, through to full physics formulations. The validation of these models against observations has shown that the relative importance of model components is location specific. This is reflected by the incorporation of tuning parameters and selectable precipitation schema.

Both observation and modelling studies identify a limit to mountain precipitation process understanding through a lack of measurement data. This in turn limits the application of what understanding there is. Generally, increased precipitation observations in as wide a variety of regions and resolutions as possible is required to improve process understanding. For specific applications, precipitation observations at a resolution sufficient to capture the variability that is significant to the application

is required. Using the application based local observations to improve on the general process understanding provides a pragmatic and logical approach.

3 Mountain precipitation observations

3.1 Introduction

Precipitation measurements provide the hooks upon which to hang spatial precipitation estimates. The greater the number of measurements, the more constrained such estimates become. The remote nature of the Lake Pukaki catchment has prevented an even or representative distribution of measurement sites, with primary sites necessarily being located in easily accessible locations. In turn, low confidence is given to spatial precipitation distribution estimates in the region. Many people and institutes have set out to improve this situation (e.g. Anderton, 1975; Ruddell, 1995; Wratt et al., 1996), though all available data have seldom (if ever) been considered in unison. Bringing together disparate measurement sets, in itself, is problematic. Different measurement types, different periods of measurement, different duration of measurements all confound the coordination of the records. Such problems are not unknown globally, and much work has been done to enable comparison of data from different sources (e.g. Adler et al., 2001; Rhoades and Salinger, 1993; Yang et al., 1999a). Two primary steps of measurement adjustment are required. Firstly, the establishment of true precipitation values, as opposed to measured precipitation, must be established by accounting for deficiencies of measurement systems. Secondly, calculation of thirty year average annual values, or Normals, must be calculated by allowing for temporal variation in precipitation amounts and defining the period of applicability.

This chapter sets out to establish average annual true precipitation totals for all known precipitation measurement sites within the Lake Pukaki catchment. This is followed by a description of a new set of measurements, taken at sites intended to extend the spatial coverage of the historic data. An account is then provided of the preparation of an average annual precipitation surface for the catchment based on all precipitation site data. Finally the magnitude and variation of this new precipitation distribution is compared to distributions elsewhere in New Zealand and the world.

3.2 The Hermitage precipitation gauge

In 1901, the first rainfall recordings were started in the vicinity of the Aoraki/Mt Cook village (for locations mentioned in the text see Figure 3-1) at the Hermitage

Hotel near what is now the White Horse Campground (Salinger, 1981). The name later allocated to this site within the national climate data base, as administered by the National Institute of Water and Atmospheric Research (NIWA), was "The Hermitage, Mt Cook". The general location of the site was in the middle of the 1.5 km wide Hooker valley surrounded on all sides by mountains rising over 1000 m above the valley floor. Early monthly totals from this gauge are found in the New Zealand Gazette, a government publication (e.g. New Zealand., 1857). Archived daily records from this station held in the national climate database are only available from June 1928 (NIWA, 2008) by which stage the gauge had been moved, with the construction of the new Hermitage Hotel (Wilson, 1968), to a position 1.6 km south, nearer the south west side of the valley and almost 1.2 km down valley. The gauge type was a 5 inch manual copper gauge with the orifice height at 305 mm above the ground. The gauge was placed within a fenced off meteorological instrumentation enclosure. Over time, the vegetation around the enclosure increased so that the enclosure became increasingly sheltered. Prior to the 1st of January 1950, readings were taken at 9:30 am local time (NZMS, 1966) and from then at 9 am. Readings were taken by staff of the Hermitage Hotel up until 1970, and then by staff of the National Park Board. The gauge was replaced with an Octapent storage gauge after the 5 inch gauge overflowed during a large storm on the 5th November 1973. The gauge was eventually removed in 2000. The record from this precipitation gauge site is the longest that exists within the Lake Pukaki catchment and has been used in a wide range of research including climatology (McGowan and Sturman, 1996a; McKerchar et al., 1998; Ryan, 1987; Salinger, 1980), botany (Archer et al., 1973; Wilson, 1976), geology (Cox et al., In preparation; Whitehouse, 1982), glaciology (Purdie and Fitzharris, 1999; Salinger et al., 1983), hydrology (Anderton, 1974; Bowden, 1994; Kerr, 2005) as well as for engineering and land use (McSaveney and Davies, 2005; Skermer et al., 2002). The value of the record is not just in its length but also in the location of the gauge, being one of the few long term gauges sited within the Southern Alps.

3.2.1 Homogeneity

From knowledge of the cause of measurement error, as outlined in the previous chapter, the changes in exposure, positioning, gauge type and operators are likely to have had an effect on the percentage of true catch that the gauge collected through the years. It is important to consider this when preparing long term records.

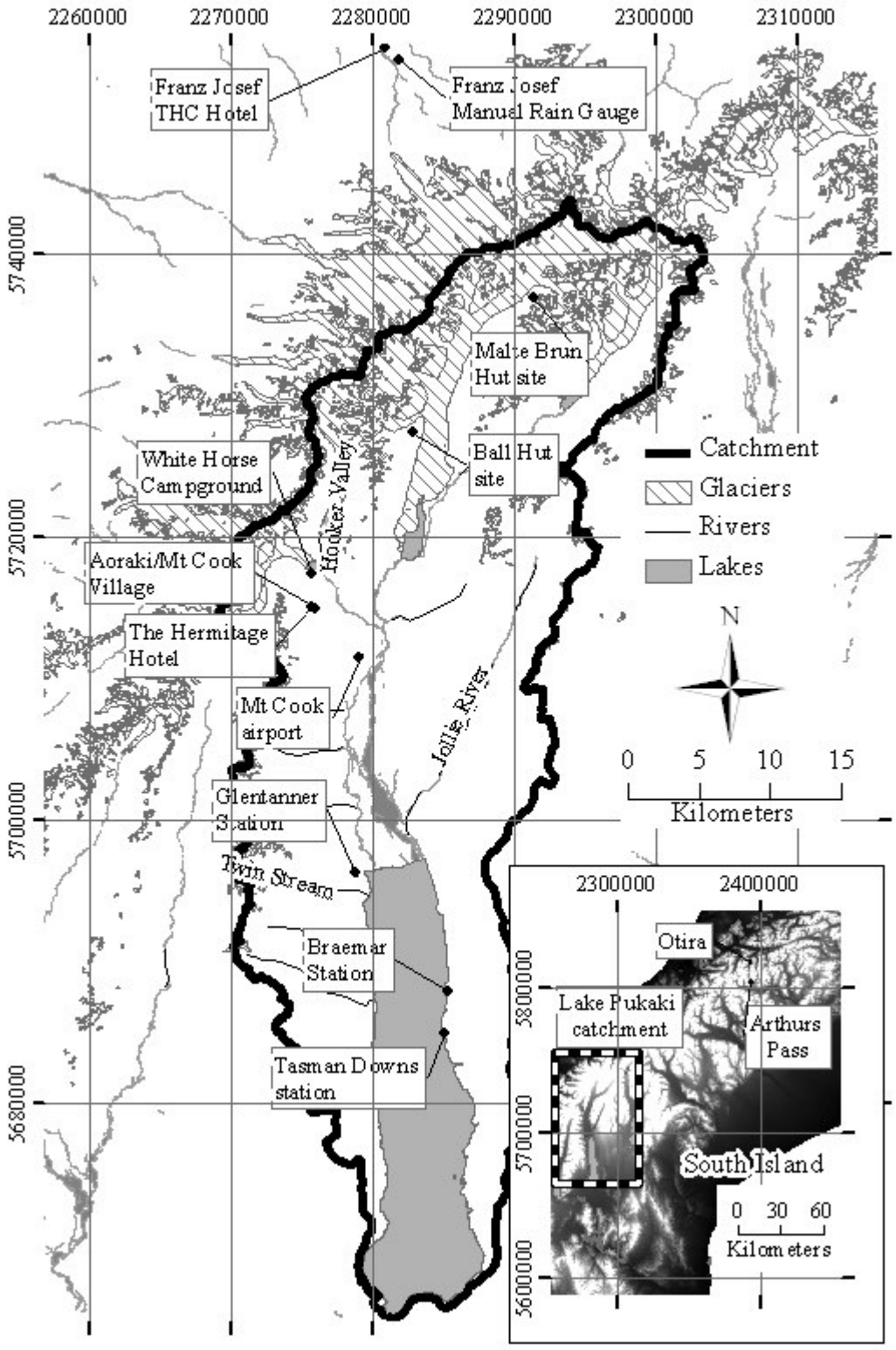

Figure 3-1. Locations of place names mentioned in the text.

A precipitation gauge record unaffected by (or corrected for) these non-climatic influences is considered homogenous. Conversely, the record from a precipitation gauge that has been affected by non-climatic effects may be considered to be inhomogeneous. The level of effect is the homogeneity of the record.

Numerous methods exist for the identification and correction of inhomogeneities as reviewed by Peterson et al. (1998). The inspection of site information and metadata in combination with related observations was found to be preferred to consideration of a single precipitation series in isolation. Subjective analysis of related series for inhomogeneities as used by Rhoades and Salinger (1993) through the visual inspection of parallel CUSUMs enables the incorporation of related series that may otherwise not stand up to the rigours of a more objective, statistical approach. For example the use of stream flow series or other inhomogeneous precipitation series. A drawback of this approach is that the level of change that leads to a noted inhomogeneity is variable and poorly defined. Where the likelihood of inhomogeneity is high, as in a high precipitation gradient location, periods of homogeneous records are shorter, which in turn requires a greater shift for a statistically significant inhomogeneity to be identified. In the Southern Alps region, where related sites are rare, a reference series does not exist, and site changes are frequent, the subjective approach to inhomogeneity identification is considered appropriate.

Identification of site changes that affect the precipitation record may be made through plotting the cumulative sums (CUSUM) of the difference between monthly rainfall totals and the long term monthly mean (Rhoades and Salinger, 1993). On such a CUSUM plot, a change of slope coincident with a known site change provides an indication that the change has had an effect. Figure 3-2 below presents the CUSUM plot for The Hermitage record from 1928 to 2000. The only major slope change to occur during a known site change was for the 1948 site upgrade. The other slope changes observed may be a result of unknown site changes, slow site changes (for instance a change in exposure from nearby vegetation), or climatic variations.

To determine whether precipitation variations are site or climate driven, comparison of a sites CUSUM plot with those obtained from nearby sites in a parallel CUSUM plot may be used. The isolation of The Hermitage from nearby long term gauges that are in a similar climate zone makes it difficult to use this approach. A nearby gauge is at Braemar, but this receives considerably less rainfall than at Aoraki/Mt Cook, just 854 mm for the 1961–1990 normals (Tomlinson and Sansom, 1994), and may be

considered to be in a different climate zone (Salinger, 1979). Franz Josef THC (Tourist Hotel Corporation) is another nearby rain gauge site that receives a similar amount of annual precipitation with 4950 mm for the 1951–1980 rainfall normals (NZMS, 1985b), sited on the western side of the Southern Alps but considered to still be in a similar climate region to The Hermitage (Salinger, 1979). The CUSUM plot for Franz Josef THC is shown below in Figure 3-3. In these CUSUM plots the values have been normalised by dividing by the long term monthly mean. This ensures the vertical scales for each site are relatively the same enabling improved comparisons between sites with different precipitation magnitudes.

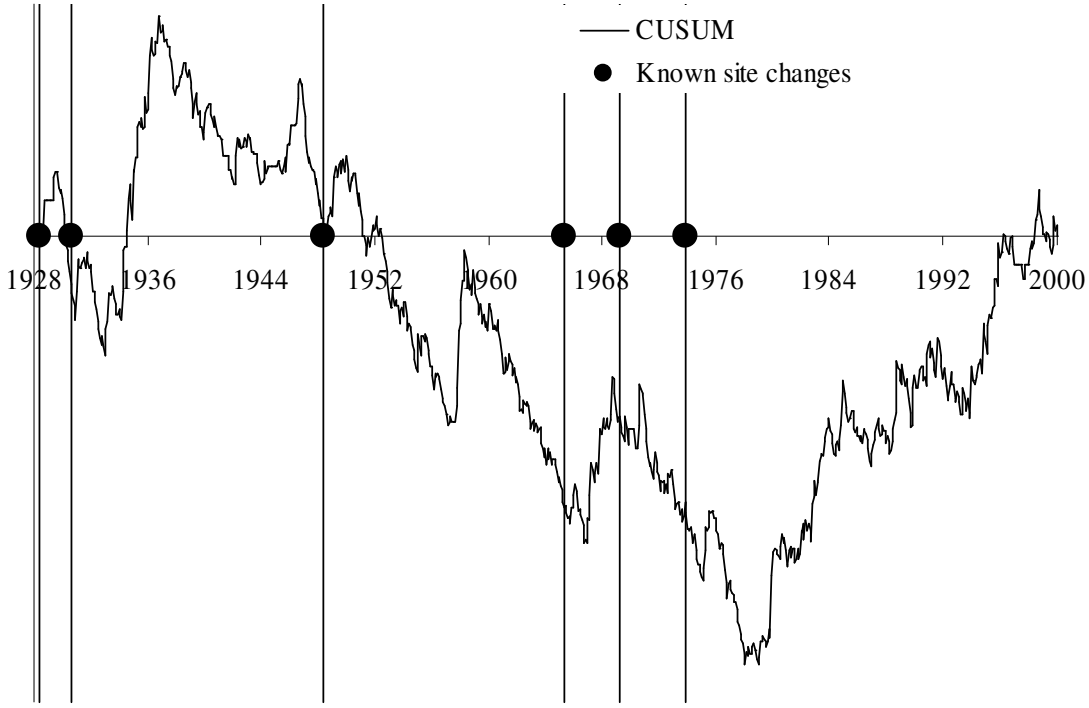

Figure 3-2. CUSUM plot for The Hermitage, Mt Cook rain gauge data. The slope indicates the magnitude of the deviation of the monthly precipitation from the long term mean.

Although the Franz Josef THC gauge operated for a different period and with its own unique site change occurrences and record breaks, CUSUM slope changes similar to that observed for The Hermitage can be seen for 1957, 1958 and a very similar general CUSUM plot shape from 1966 through to the station closure in 1984. This would indicate that the changes observed in The Hermitage record during those periods are indeed climate variations, and not gauge site impacts. A review of South Island lake inflows by McKerchar and Pearson (1997) clearly shows the 1957 and 1958 flow variation at all seven flow records considered, confirming that the changes observed on those years are climatic in origin.

Another comparison site is Otira. This is again on the western side of the main divide, but is much closer to the divide itself. Otira may be considered to be in a similar rainfall climate zone as The Hermitage (Salinger, 1981) even though it is over 150 km to the north east. Similarly, the record from Arthurs Pass, close to Otira but just east of the main divide may be used. The CUSUM plots for Otira and Arthurs Pass are shown in Figure 3-3. The Otira record confirms The Hermitage record is reasonable from 1948 through to 1988, and the Arthurs Pass record confirms that it is reasonable from that point on to 2000. The Arthurs Pass record also has similar changes to The Hermitage between 1937 and 1943, though Otira does not. Both the Otira CUSUM and the Arthurs Pass CUSUM indicates that the two slope changes in 1934 and 1937 in The Hermitage CUSUM trend are likely to be related to site changes. Additionally, a comparison may be made to records of inflow into Lake Pukaki. Lake inflow is effectively a spatial integral of all catchment hydrological processes.

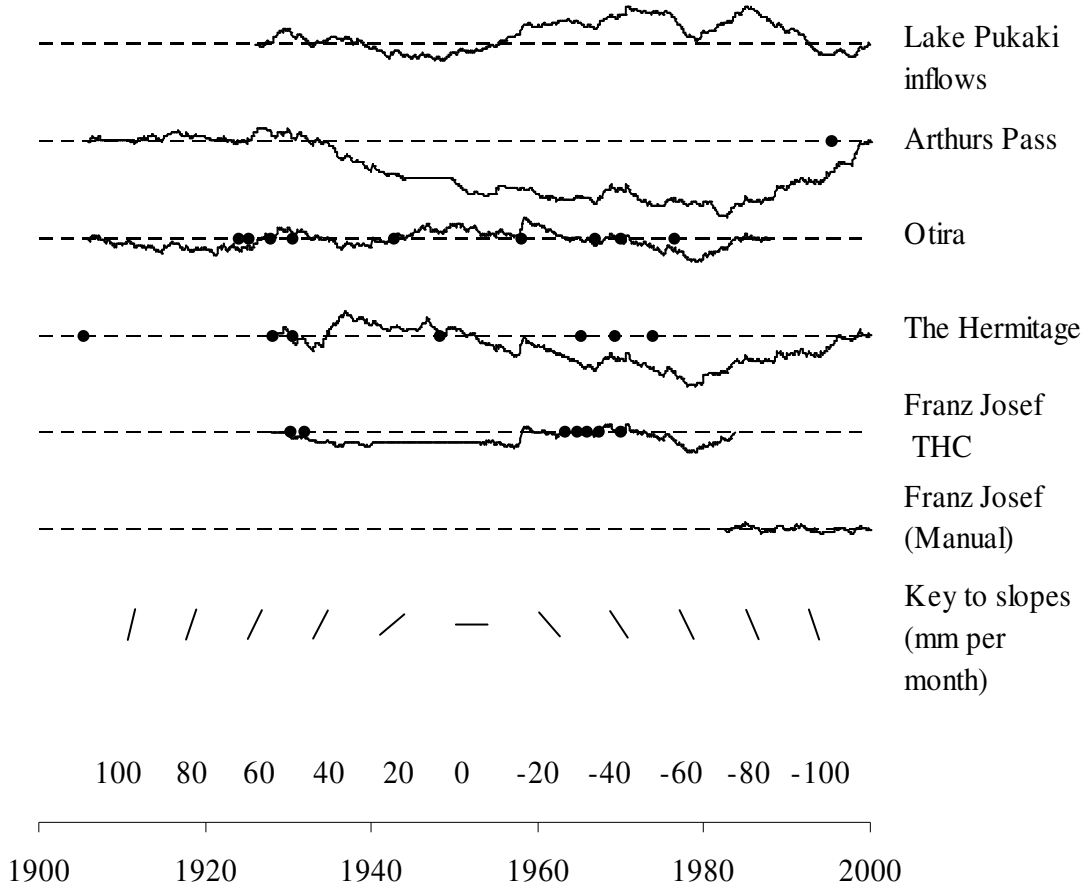

Figure 3-3. CUSUM plots for Lake Pukaki inflows and precipitation at Arthurs Pass, Otira, The Hermitage, Franz Josef THC and Franz Josef (manual). Dots are occurrences of known site changes for the respective sites. The series' slopes indicate the magnitude of how any individual month differs from the long term mean. No data is presented as a 0 (horizontal) slope.

In a location where rainfall is a major contributor to the hydrology, climate variations that affect precipitation are likely to also affect inflow. The monthly CUSUM of the Lake Pukaki inflow is shown in Figure 3-3. The precipitation increase in 1958 and 1968 are observed in the inflow CUSUM, but general reducing trends in precipitation between 1958 and 1967, and again from 1969 to 1976 are not. The glacial nature of the Lake Pukaki catchment means that reduced precipitation may be offset by increased melt which could explain this disparity between precipitation and inflow trends. Overall it seems fair to conclude that The Hermitage had site changes that affected the precipitation observations in 1934, 1937 and 1948. The importance of this analysis can be seen in that such a record variation as that which occurred with the 1934 and 1937 site changes may be misinterpreted as climatic effects as has been done by McGowan and Sturman (e.g. 1996b; 1996c).

Additional graphical analysis of the homogeneity of The Hermitage record may be carried out by plotting the parallel CUSUMs of the logarithm of the ratio of monthly rainfall between The Hermitage and related sites. In this case, changes of slope are related to differences between sites (Rhoades and Salinger, 1993). This is effectively a filter to remove the site common climate signal. Figure 3-4 shows this parallel CUSUM for stations with respect to The Hermitage. Times when there is a common change in slope indicate that The Hermitage site has changed. From these plots, the effect of the site changes in 1934 and 1937 are confirmed. This analysis enables periods of stable records to be selected for use in further analysis minimising the risk of site changes influencing results. In this case the record from 1959 onwards appears to be free of inhomogeneities.

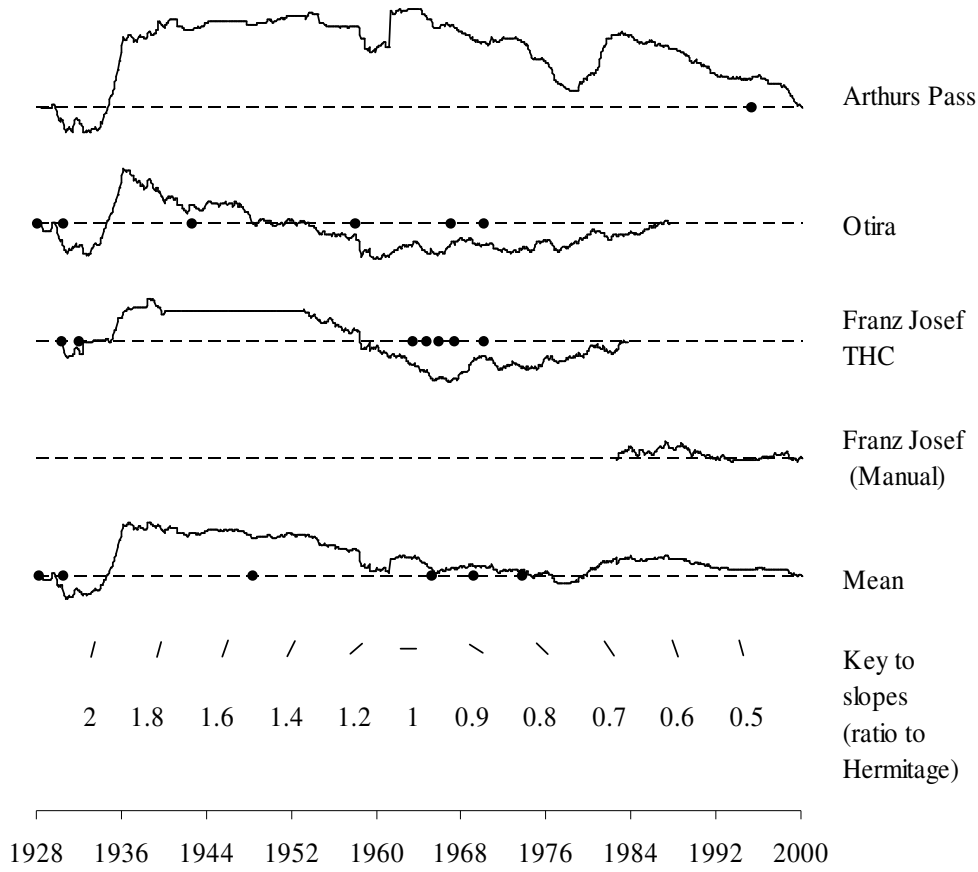

Figure 3-4. CUSUM plot of the log of the ratio of The Hermitage monthly rainfall total, to totals at Arthurs Pass, Otira, Franz Josef THC, Franz Josef Manual, and a mean of the non-zero CUSUMs. Dots indicate known site changes at the respective sites, with The Hermitage site changes shown on the Mean CUSUM. The series' slopes indicate the magnitude of how each site's monthly log of ratio of precipitation to Hermitage precipitation, varies from the long term mean. No data is presented as a unity ratio (horizontal slope).

3.2.2 Undercatch assessment

To enable a precipitation record to be used for more than relative assessments, an evaluation of the catch with respect to true precipitation is required. The wetting loss of a 5 inch copper gauge has been estimated as 0.1 mm per event (Austin, 1939). This leads to a long term (1961-1990) mean annual estimate of 19.6 mm missed catch or 0.5 % of the published mean annual rainfall at The Hermitage for that period (Tomlinson and Sansom, 1994), assuming an average of one rain event per rain day. This error will vary with the number of rain events and with the evaporation rate, itself affected by humidity and temperature, and so is different from site to site. In comparison, the undercatch associated with wind is related to the magnitude of the catch, not the frequency of events. To estimate this error, the empirical formula determined from the World Meteorological Organisation solid precipitation

measurement intercomparison project is used as presented by Yang et al.(1998). The relationship was derived for an unshielded National Weather Service 8 inch gauge, a gauge with a larger orifice than the 5 inch copper rain gauge that was in use at The Hermitage. This will tend to underestimate the undercatch. The empirical relationships are as follows:

Snow

$$CR = \exp(4.606 - 0.157Ws^{1.28}) \quad \textbf{(1)}$$

Mixed Precipitation

$$CR = 100.77 - 8.34Ws \quad \textbf{(2)}$$

Rain

$$CR = \exp(4.605 - 0.062Ws^{0.58}) \quad \textbf{(3)}$$

Where:

CR = catch ratio (in percent) of the observed catch to the true precipitation

Ws = daily average wind speed in metres per second at the orifice height.

Wind speed at The Hermitage is obtained at a mast height of 5 m. A logarithmic wind profile using a roughness length of 0.03 m (Sevruk, 1985) has been used to estimate the wind speed at the orifice height (305 mm) using the following formula:

$$U(h) = U(H)\frac{\ln(h/z_0)}{\ln(H/z_0)} \quad \textbf{(4)}$$

Where:

U(h) is the estimated wind speed (m s^{-1}) at the gauge orifice height, h (m),

U(H) is the observed wind speed (m s^{-1}) at the anemometer height, H (m)

z_0 is the roughness length (m).

The undercatch formula was determined from a limited set of observations with wind speeds below 6.5 m s^{-1}. The relationship for wind speed above this level is unknown. For this reason, 6.5 m s^{-1} (at gauge orifice height) has been set as an upper threshold ensuring the undercatch estimate is conservative.

To determine the phase of the precipitation, the temperature data available at The Hermitage was used. The threshold temperatures used were 0 ^{o}C, below which precipitation is considered to be solid, 0 – 3 ^{o}C, within which precipitation is considered to be mixed solid and liquid, and 3 ^{o}C, above which precipitation is considered to be liquid (Fassnacht, 2004). The temperatures are taken as the average of the daily minimum and maximum.

The assessment is made at a daily level as this is the temporal resolution of the available data. This introduces error into the correction in that rain events are unlikely to be precisely for one complete day. The temperatures and wind speeds used will therefore not be correct for a particular rain event, merely an estimate. Other deficiencies in the system include the variation of wind speeds and precipitation phase within a precipitation event, the variation of the roughness length around the precipitation gauge over time (e.g. through change in grass growth), and turbulence at the gauge site rendering the assumption of logarithmic wind profile incorrect. The significance of these errors reduces as the period of time for which the assessment is made is increased.

The wind information at The Hermitage is available from 1972. From 1972 to 2000 the measured catch is estimated to be 92.6 % of the wind corrected precipitation. This is equivalent to a further 8 % of the measured catch. Applying this factor to the 1961-1990 mean annual precipitation value, results in an estimate of 4529 mm. This may be an over estimation, as the majority of the period for which the undercatch correction was derived was during the positive phase of the Interdecadal Pacific Oscillation (IPO), which as discussed in Chapter 6, is a period of stronger average winds. The estimated undercatch varies little with season as can be seen in Figure 3-5.

The increase in undercatch that would be expected with increased solid precipitation during winter (as seen in Figure 3-6) is offset by the reduced precipitation and the lower winds (also shown in Figure 3-6).

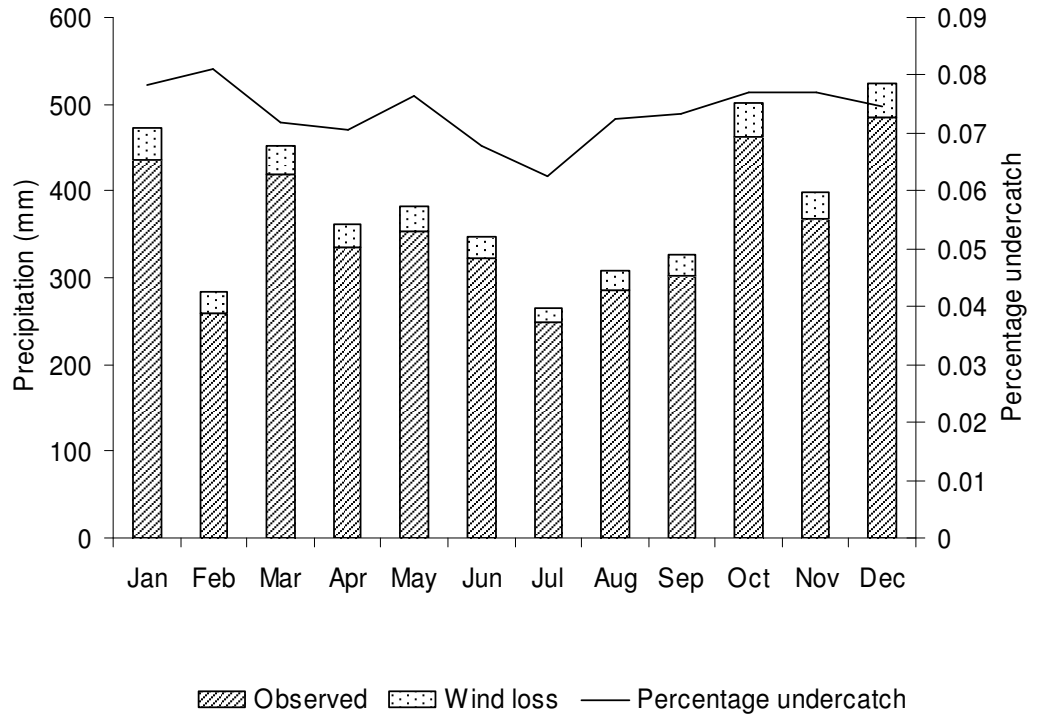

Figure 3-5. Seasonal variation in estimated undercatch on 1972-2000 mean monthly precipitation totals.

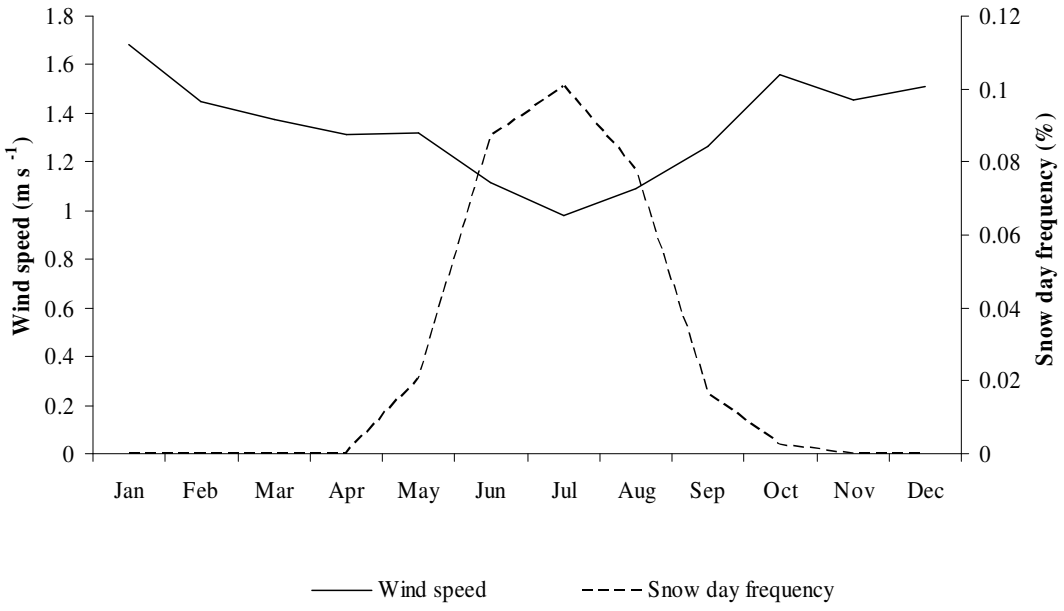

Figure 3-6. Long term (1972-2000) average daily estimated weather conditions on days with precipitation for each month; wind speed and snow day frequency, where a snow day is defined as a day with the average temperature below 0°C.

Undercatch can be seen to be fairly consistent through the year at between 7 and 8 percent. The greatest percentage undercatch occurs in February with the greatest absolute undercatch occurring during the high precipitation months of October-January, and March.

The percentage undercatch assessed for The Hermitage is not large on a global scale as shown in the summary in Table 3-1. Undercatch can be seen to increase significantly as the percentage of snow, the gauge orifice height and the wind speed increases. At The Hermitage these parameters are low with undercatch only slightly larger than at rain-only sites.

3.3 Precipitation gauge observations within the Lake Pukaki Catchment

The Hermitage precipitation observations are far from being the only observations taken in the catchment. This section outlines the various precipitation gauging efforts that have been, and are being carried out in the catchment. The gauges are described in a geographical order starting with the Hooker Valley area, moving down to the junction with the Tasman Valley. From there, the gauges up the Tasman Valley are identified, followed by gauges down the catchment to finish at the Lake Pukaki outlet. The details for each gauge are listed in Table 3-2, indexed to the operating period shown in Figure 3-7 and the location in Figure 3-8.

As described earlier, The Hermitage gauge site ceased to operate in 2000 with new electronic gauges installed at the nearby Department of Conservation climate monitoring enclosure. The regional authority (ECAN) established a tipping bucket gauge at this site in 1989, while NIWA established a second tipping bucket gauge when The Hermitage gauge was closed down in 2000. Moving away from the Aoraki/Mt Cook Village, in 1960 a rain gauge was established at the nearby Hooker Flat. This was augmented in 1962-1963 with three rain gauges at Hooker Hut (one automatic daily logging gauge and two storage gauges) and a storage gauge at Stocking Stream Shelter. The automatic gauge at Hooker Hut was removed in 1966, while reading of the storage gauges continued until 1968. The records from the Hooker Flat gauge finish in 1970.

Table 3-1. Precipitation gauge undercatch estimates. Empty cells indicate the values are unknown.

Location	Gauge type	Orifice height (mm)	Observation period	Min. temp. (^{o} C)	Max. temp. (^{o} C)	% of snow	Wind (m s^{-1})	Annual precip (mm)	catch ratio (%)	Reference
The Hermitage, New Zealand	Unshielded Copper 5" and Octapent	305	1972 - 2000	-3.9	22.8	2	1.3	4354	93	This study
Barrow, Alaska	Wind shielded NWS 8"	1800	1982 - 1983	-15.3	-9.9	75.4	5.4	102.5	68	(Yang et al., 1998)
Kodiak, Alaska	Unshielded NWS 8"	1200	1982 - 1983	3.0	9.1	18.1	5.4	1847	79	(Yang et al., 1998)
Prins Christian Sound, Greenland	Wind shielded Hellmann Gauge	3000	1994 - 1997	-1.5	2.9	48.1	6.8	720.9	74	(Yang et al., 1999b)
Jokioinen, Finland	Shielded Tretyakov	1500	1988 - 1993	-5.8	10.9	22.8	2.8	579.4	81	(Yang et al., 1995)
Reynolds Creek, Idaho	Unshielded Hellmann gauge	3050	1983 - 1986			23.1	2.34	944	81	(Hanson, 1989)
Pullman, Washington	Unshielded NWS 8"	1000	1934 - 1939						91	(Neff, 1977)
Valdai, Russia	Unshielded NWS 8"	900	1966 – 1969 (summer only)				2.8	378.3	96	(Golubev et al., 1992)
Grono, Switzerland	Unshielded Hellmann gauge	1500	1972 - 1978			9	0.3	1536	97	(Sevruk, 1985)
Taita, New Zealand	Unshielded gauge	300	1971 - 1972			0		1083.3	93	(Aldridge, 1976)
Thames, New Zealand	Unshielded Met. Office Mk2	3050	1962 - 1966			0			97	(Green, 1970)

Within a decade (1977) another storage rain gauge had returned to the Hooker Hut site and then in 1980 another was re-established back at the Stocking Stream site. These were monitored by the National Park Board staff until 1983, when they were removed.Down valley at the airport a rain gauge (called Tasman Aero) was in operation between 1974 and 1984 (NIWA, 2008) as part of the climate observations taken to assist airport operations. Unfortunately these gauge records have not been located. Nearby to the airport at the Hooker Rd Bridge a tipping bucket rain gauge was installed in late 1993. This gauge is used operationally to help with hydro-electricity generation planning down valley. This installation came about after the 1992 energy crisis (Fitzharris, 1992) and is part of a wider network in the region. Gauges from the network have measurements telemetered in near real time to the hydro-electricity control centre. At a higher elevation, the Rose Ridge weighing bucket precipitation gauge (established in 2002) is also part of this network. This gauge is supported with two sonic ranger snow depth sensors, and a snow pillow snow mass sensor. In the Tasman Valley a rain gauge was operated at Ball Hut between 1st October 1932 and 31st October 1936. This was at a time when the Ball Hut was a popular destination for tourists and skiers (Wigley, 1979). Records from this gauge are also unavailable. Fortunately, another gauge was installed near this location from 1972 until 1979. This was a recording storage gauge providing daily measurements. This later Ball Hut precipitation gauging was part of glaciological investigations on the Tasman Glacier and included a second precipitation gauge installed at Malte Brun Hut (now removed) (Anderton, 1975) with records from 1967 until 1972. These glaciological investigations were part of a larger programme to understand the hydrology of the region as part of planning for the hydro-electricity generation scheme about to be built (Anderton, 1975). Further glaciological investigations led to short term precipitation gauge installations on the lower Tasman Glacier in 1995 (Purdie and Fitzharris, 1999), at Mueller Hut in 1996 (Neale, 1996) and Tasman Saddle in 2001 (Cutler, 2002). Down valley, the Jollie Catchment and the (Devils) Elbow Stream were selected as research catchments with a large number of storage gauges installed within them. The Jollie Catchment had its first two gauges installed in 1966, a further five gauges in 1970, and three more high elevation gauges, accessed by helicopter, in 1990. Supporting this storage gauge network was a tipping bucket gauge at Jollie Hut which operated from 1972 until the end of 1999.

Table 3-2. Lake Pukaki catchment precipitation gauges. NB. NIWA CD = National institute of water and atmospheric science climate database. NIWA A = NIWA archives.

Name	Map index No.	Type	Agency	Start	Finish	Data source
Tasman Saddle	1	Tipping Bucket	Cutler	19/01/2002	21/02/2002	(Cutler, 2002)
Malte Brun Hut	2	93 day cassella	Ministry of Works	02/06/1967	20/07/1970	NIWA CD
Rose Ridge	3	Tipping bucket	Meridian	17/10/2002	17/10/2007	NIWA
Ball Hut	4	Recording rain gauge	Ministry of Works	23/08/1972	30/01/1979	NIWA CD
Ball Hut	4	Manual 5 inch copper rain gauge	Unknown	01/10/1932	31/10/1936	Not found
Hooker Hut	5	90 day Cassella recording gauge	DSIR	09/02/1962	31/12/1966	NIWA A
Hooker Hut	5	"Milk can" manual storage gauge	DSIR	23/04/1963	18/08/1968	NIWA A
Hooker Hut	5	Octapent manual storage gauge	DSIR	23/04/1963	18/08/1968	NIWA A
Hooker Hut	5	150 mm diameter, PVC Storage gauge	MCNP	20/10/1977	07/11/1983	NIWA A
Tasman Glacier Snout	6	Tipping bucket	Purdie	17/01/1995	20/03/1995	(Purdie, 1996)
Catriona Tarn	7	Storage gauge	DSIR	19/01/1990	06/01/1994	(Halstead, 1994)
Stocking Stream	8	Octapent manual storage gauge	DSIR	23/03/1963	18/08/1968	NIWA A
Stocking Stream	8	150 mm diameter, PVC Storage gauge	MCNP	02/05/1980	11/10/1983	NIWA A
Pinnacle Stm	9	Octapent manual storage gauge	DSIR	11/03/1970	06/01/1994	NIWA CD
Mueller Hut	10	Tipping Bucket	Neale	19/10/1995	22/10/1995	(Neale, 1996)
Littles Hut	11	Octapent manual storage gauge	DSIR	20/06/1966	06/01/1994	NIWA CD
The Hermitage	12	Rain gauge	Tourist Hotel Corporation	02/06/1928	01/03/2000	NIWA CD
Mt Cook EWS	13	Tipping bucket	NIWA	30/03/2000	Current	NIWA CD
Mt Cook ECAN	13	Tipping bucket	ECAN	26/11/1989	Current	ECAN
Hooker Rd Bridge	14	Tipping bucket	Meridian Energy	04/12/1993	Current	NIWA
Hooker Flat	15	Auto weekly rain gauge	Unknown	03/09/1960	01/03/1970	NIWA CD
Tasman Aero	16	Manual 5 inch copper rain gauge	Unknown	01/01/1974	01/04/1984	Not found
Bird Creek Hut	17	Octapent manual storage gauge	DSIR	20/06/1966	06/01/1994	NIWA CD
Mt Kea	18	Octapent manual storage gauge	DSIR	01/01/1970	06/01/1994	(Halstead, 1994)
Pyramid Bluff	19	Octapent manual storage gauge	DSIR	12/02/1970	06/01/1994	NIWA CD
Lower Kea	20	Octapent manual storage gauge	DSIR	06/05/1970	06/01/1994	NIWA CD
Lower	21	Octapent manual	DSIR	06/05/1970	06/01/1994	NIWA CD

Name	Map index No.	Type	Agency	Start	Finish	Data source
Pyramid Waterfall Basin	22	storage gauge Storage gauge	DSIR	19/01/1990	06/01/1994	(Halstead, 1994)
Birch Hill Airstrip	23	Octapent manual storage gauge	Birch Hill Station	01/01/1959	22/11/1991	NIWA CD
Parsons Saddle	24	Storage gauge	DSIR	19/01/1990	06/01/1994	(Halstead, 1994)
Sealey Village	25	Rain gauge	Unknown	04/04/1969	01/05/1972	NIWA CD
Devils Elbow1-7	26-32	Octapent manual storage gauge	DSIR	01/01/1963	01/01/1965	Not found
Golden Gully	33	Octapent manual storage gauge	DSIR	20/06/1966	06/01/1994	NIWA Climate database
Jollie Hut	34	Tipping bucket	DSIR /NIWA	09/08/1972	21/12/1999	NIWA Climate database
Twin Stream	35	Climate station	Grasslands Division of DSIR	01/03/1966	31/12/1969	(Archer, 1970; Archer and Collett, 1970)
Glentanner	36	Rain gauge	Glentanner Station	04/05/1967	01/04/1970	NIWA CD
The Rest	37	Rain gauge	Unknown	02/09/1959	01/04/1976	NIWA CD
Braemar Hut	38	Octapent manual storage gauge	DSIR	27/07/1970	06/01/1994	Not found
Braemar Station	39	Manual 5 inch copper rain gauge	Braemar Station	01/12/1913	Current	NIWA CD
Guide Hill	40	Manual 5 inch copper rain gauge	Tasman Downs Station	03/10/1976	01/03/2000	NIWA CD
Tasman Downs	41	Manual 5 inch copper rain gauge	Tasman Downs Station	03/01/1977	Current	NIWA CD
Lake Pukaki No 1	42	Manual 5 inch copper rain gauge	Unknown	03/11/1952	01/02/1972	NIWA CD
Lake Pukaki, M.W.D.	43	Auto daily rain gauge	Ministry of Works	03/09/1969	31/12/1984	NIWA CD

Gauge data from the Jollie has largely been archived by NIWA, either within their climate database, their archived records, or in retained field books. No data from Braemar Hut, or from any of the the (Devils) Elbow network have been located. The dates of operation of the (Devils) Elbow network are unknown, but snow survey data taken in association with the gauge network indicate the gauges were in operation at least from 1963 until 1965. Nearby to the (Devils) Elbow Stream, the Grasslands division of the DSIR established a precipitation gauge at Twin Stream (Archer, 1970). This operated at least from autumn 1966 through to 1969.

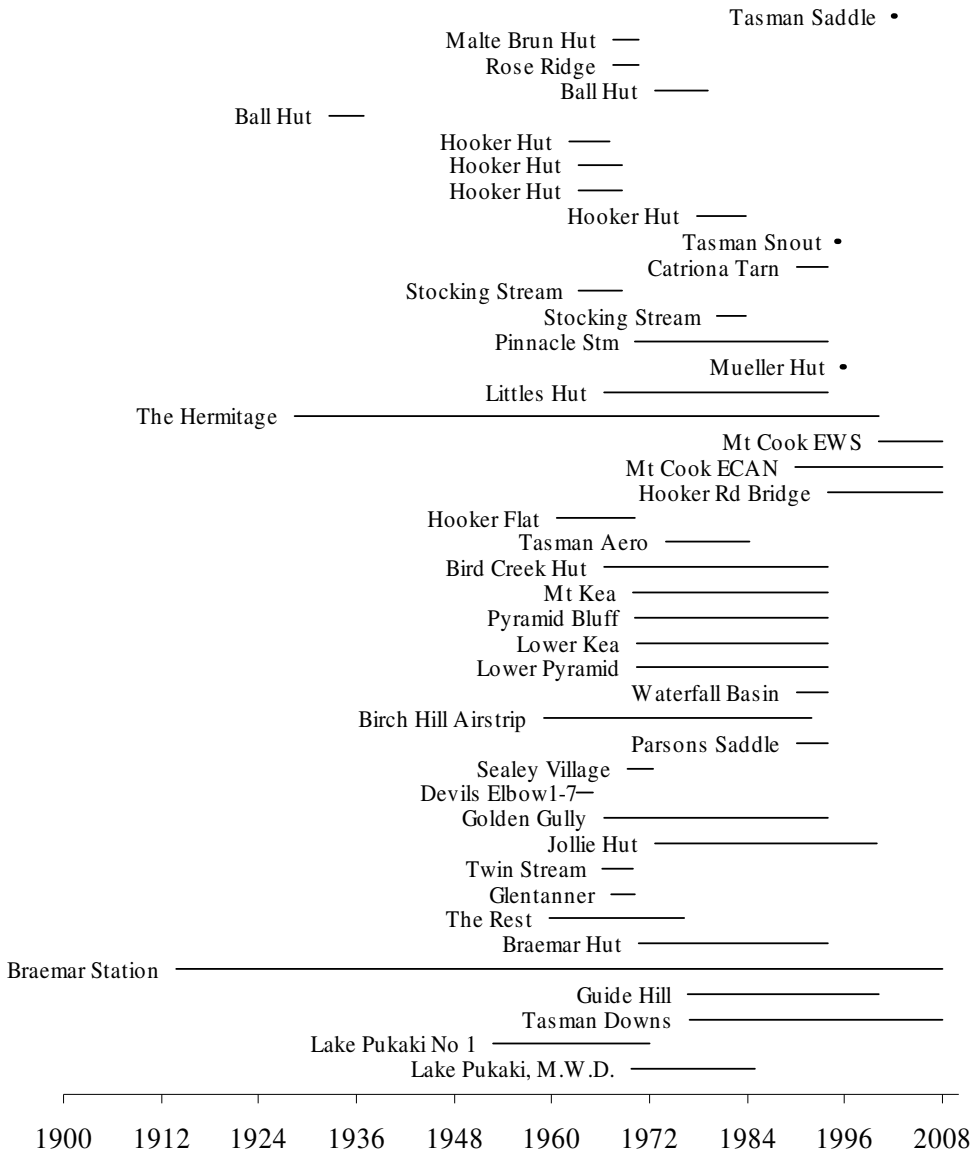

Figure 3-7. Time line of precipitation gauge operation within the Lake Pukaki catchment.

While gauge records have not been found, monthly means for the four year period have been published (Archer, 1970; Archer and Collett, 1970). Additional gauges operated by private individuals have been sited at a variety of locations associated with the different stations in the catchment. These gauges include Birch Hill airstrip, Glentanner, Guide Hill, Braemar and Tasman Downs. Of these sites, the last two are still operating. The NIWA climate data base identifies a further four gauges that operated along the western side of the Lake Pukaki valley. These are Sealey Village, The Rest, Lake Pukaki No. 1. and Lake Pukaki MWD. All of these gauges no longer operate.

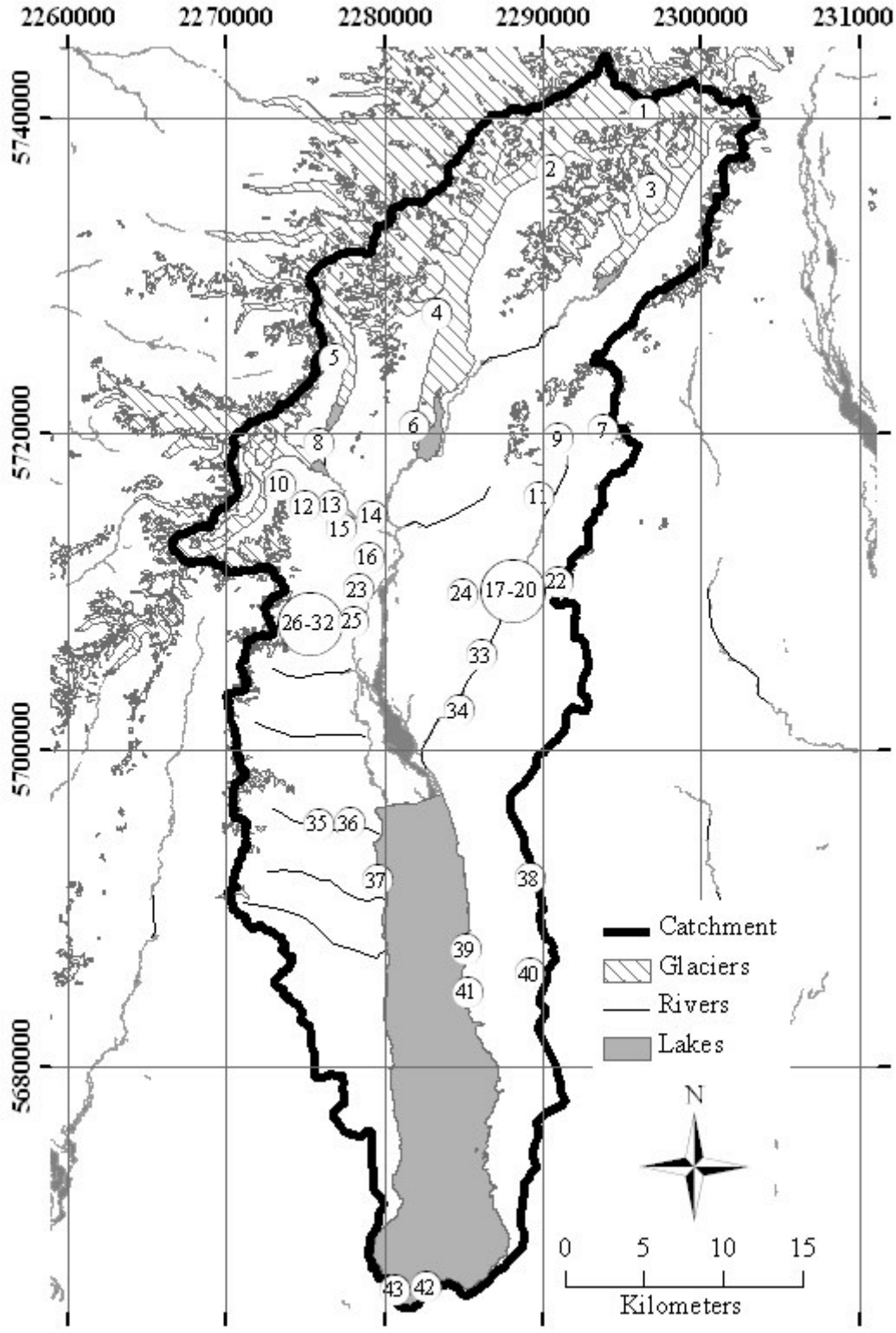

Figure 3-8. Locations of precipitation gauges that have or are operating within the catchment prior to this study. Site references are given in Table 3-2.

3.3.1 Mean annual precipitation

Long term averages of precipitation measurements provide a measure of a location's climate. This in turn can be used for comparison or prediction (Guttman, 1989), comparison to other locations and other time periods, prediction of future conditions for planning and risk assessment. To ensure international compatibility of long term averages the World Meteorological Organisation recommend the use of thirty year average annual precipitation totals, for which they gave the name "rainfall normal" (WMO, 1983). For compatibility the thirty year period starts with the first year of a decade utilising data recorded from throughout the entire thirty year period under consideration.

Thirty year normals have been published for various Lake Pukaki catchment precipitation gauge sites as shown in Table 3-3. Where an entire thirty year record is unavailable, an estimate of the normal may be generated. For example the normals calculated for the 1941-1970 period were allocated a quality rating from 1 to 5. A "1" indicates a complete good quality record from 1941-1970. A "3" indicates a station with an incomplete record and only medium confidence in the estimated normal which is provided to the nearest 10 mm with a recommendation of being of value to the nearest 50 mm. A "5" indicates the station was a storage gauge. For the 1951-1980 period, estimated normals were allocated a quality rating based on the correlation to the reference station used; "1": A complete record with 6 or less months of missing data; "2": $r^2 > 0.9$; "3": $0.8 < r^2 \leq 0.9$; "4": $0.7 < r^2 \leq 0.8$; "5": $0.6 < r^2 \leq 0.7$; "6": $0.5 < r^2 \leq 0.6$.

Table 3-3. Published precipitation normals (mm) for Lake Pukaki Catchment sites.

	Normal period			
Site	1921-1950	1941-1970 (quality)	1951-1980 (quality)	1961-1990
The Hermitage	4387	4071(1)	3985(1)	4194
The Rest			1467(6)	
Lake Pukaki no. 1		640 (3)	627(4)	
Braemar			905(4)	854
Guide Hill				860
Birch Hill Airstrip		2118 (5)		
Hooker Flat		3900 (3)	3877(2)	
Lake Pukaki, MWD			673(5)	
Sources	(NZMS, 1966)	(NZMS, 1973, 1975b)	(NZMS, 1985b)	(Tomlinson and Sansom, 1994)

Following from the homogeneity tests of The Hermitage precipitation record, outlined in section 3.2.1, the thirty year period from 1971-2000 was selected for estimating a set of precipitation normals for all current and historic precipitation gauge sites within the catchment. During the 1971-2000 period there appeared not to be any catch-affecting site changes at The Hermitage which was the most commonly used reference site for estimation of normals at the nearby short term gauge sites. Homogeneity tests were carried out for all daily sites with longer than twenty five years of recording. Parallel normalised CUSUM plots for these sites are shown in Figure 3-9. The Braemar Station CUSUM was divided into two sections to improve comparison with the other sites.

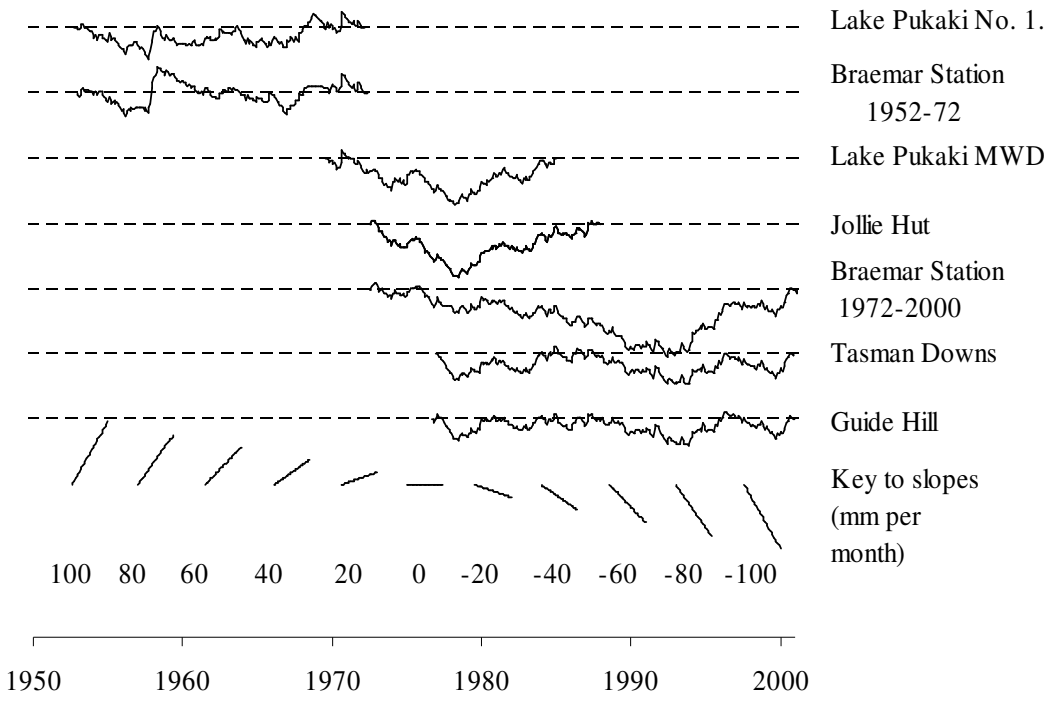

Figure 3-9. Parallel CUSUM plots for precipitation gauge sites in the Lake Pukaki catchment with longer than 20 years of operation. The series' slopes indicate the magnitude of how any individual month differs from the long term mean

Overlapping plots show similar slope changes indicating that site changes have had a limited effect on the record at these sites. The high precipitation and high precipitation gradient at The Hermitage meant that any site change there was likely to make a noticeable effect on the gauge catch. At the sites considered here the amount of

precipitation measured is much smaller, and the general precipitation field is much less variable. This means that any site changes have a limited effect on the gauge catch. This analysis shows that no major inhomogeneities exist in these sites ensuring their suitability for preparation of precipitation normals. Where observations for the complete thirty year period are not available, or exist only outside the thirty year period, an estimation of the climate normal may still be prepared. This is done through consideration of statistical relationships between sites.

Ideally for regression purposes the frequency distribution of the variable of interest is Gaussian. This may be considered the case for annual precipitation totals, but as the period length shortens to monthly, the distribution becomes increasingly skewed (WMO, 1983). An approximation to a normal distribution may be made through using the logarithm of the monthly totals. Figure 3-10 shows that a reasonable approximation to a normally distributed frequency is obtained with the log of monthly precipitation totals at The Hermitage based on 1928 to 1999 data. Such a technique is often applied when statistically analysing monthly precipitation data (e.g. Rhoades and Salinger, 1993; Rodriguez-Puebla et al., 2001). This was the approach used here.

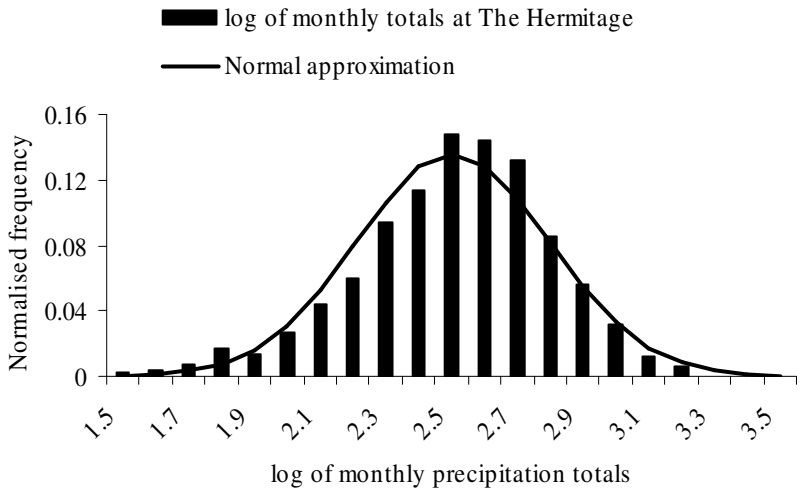

Figure 3-10. Frequency distribution of the log of monthly precipitation totals at The Hermitage from 1929 to 1999.

For stations with monthly totals for at least five years (i.e. five Januaries, five Februaries etc, not necessarily the same five years), a comparison to monthly totals at nearby longer term sites for the same years was made, providing correlation

coefficients for each month type. The nearby site with the highest mean monthly correlation coefficient was identified and regression equations established for each month type between the sites. This enabled the monthly total record to be extended to include those months at the correlated site. This process was repeated until all month totals for the period of interest had been estimated, or there were no further correlated sites from which to extend the record. Once all monthly totals for the period of interest had been obtained, the normal was simply the total rainfall for the period divided by 30. The significance of the correlation between sites depended upon the number of years being compared. The Student's *t* statistic determined that for five samples (years), a correlation coefficient of $r^2 = 0.80$ or better is required for there to be a probability of 0.95 % that the correlation is not random. For this reason only site pairs with five years or more in common, and with r^2 values greater than 0.8 were used to extend a record.

In the case of The Hermitage site, monthly totals exist for 340 of the 360 months from January 1971 through to December 2000. A high average monthly r^2 correlation of 0.93 exists with respect the Mt Cook-ECAN site. This relationship enabled The Hermitage record to be extended by 17 months. This left just three months missing from the Hermitage record. The extended record at The Hermitage now overlapped with the Mt Cook-EWS site with a correlation of $r^2 = 0.95$. This enabled an estimate of one of the three missing months for The Hermitage record to be made. The last two months were estimated from the Hooker Rd Bridge site which had a lower correlation coefficient of $r^2 = 0.92$. This completed the 1971 to 2000 monthly total record for The Hermitage. The same system was used to extend the other precipitation records within the catchment. The sites that had a mean annual average estimated for the 1971 – 2000 period are shown in Table 3-4.

Two of the long term sites did not correlate well to other nearby sites. They were The Rest and Lake Pukaki No. 1. The Rest is an interesting site in that it sometimes correlated highly to The Hermitage site up valley, and sometimes correlated highly with the Braemar site down valley and to the east (Figure 3-11). This may indicate that the correlations are weather-type dependent. The poor correlation to any one site again prevented extension of the site record using the monthly correlation technique.

Table 3-4. Long term precipitation gauge sites and estimated annual average precipitation for 1970 to 2000.

Gauge Site	Estimated Annual average (mm)	Correlated sites used to complete the record	r^2	Number of months
The Hermitage	4346	Mt Cook-ECAN	0.93	17
		Mt Cook-EWS	0.95	1
		Hooker Rd Bridge	0.92	2
Mt Cook-ECAN	4070	Mt Cook-EWS	0.98	1
		The Hermitage	0.95	244
		Hooker Rd Bridge	0.98	2
Mt Cook-EWS	3988	Mt Cook-ECAN	0.98	105
		The Hermitage	0.95	244
		Hooker Rd Bridge	0.98	2
Hooker Rd. Bridge	2776	The Hermitage	0.83	280
Hooker Flat	4232	The Hermitage	0.87	340
Ball Hut	4321	Ball Hut	0.88	290
Jollie Hut	1312	Guide Hill	0.80	14
Braemar	855	Tasman Downs	0.85	9
Guide Hill	887	Braemar	0.83	70
Tasman Downs	882	Guide Hill	0.94	5
Lake Pukaki MWD	649	Tasman Downs	0.79	192

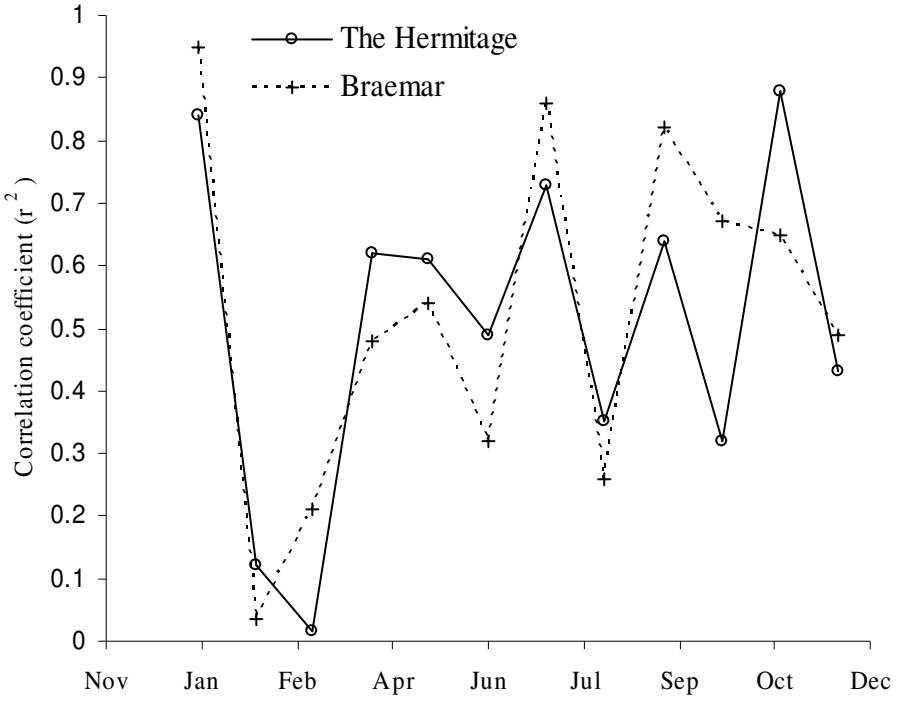

Figure 3-11. Correlation coefficient values for relationship between monthly precipitation totals at The Rest compared to The Hermitage and Braemar, 1959 - 1975.

The Lake Pukaki No. 1 site is very close to the Lake Pukaki MWD site. The period of overlap between the two sites was less than five years (for many months, there were just two years congruent) so was not used for record extension. In this case, it was decided to use the more general correlation of all monthly totals as outlined to follow. For sites with measurement periods of less than 5 years, or that operate as storage gauges, another approach to the monthly total correlation system is needed to determine average annual precipitation. For daily gauge sites with less than five years, the correlation may be determined from all monthly totals, not just the same month for each year as was done previously. This increases the sample size by a factor of twelve enabling a higher significance of correlations to be obtained. The disadvantage of this approach is that any seasonal variation in correlation is lost. For storage gauges, correlations of totals for the measurement periods may be obtained. In either case the number of months (for daily data), or measurement periods (for storage gauges) used to determine the correlation was kept to 5 and above, with r^2 values high enough to maintain the level of significance above 0.95. Again, the log of the measurement period totals, rather than the totals themselves were used.

When a reference site was determined, the equation of the linear relationship between the log totals may be determined along with the average length of the measurement period, as a fraction of a year. An estimate of the log of the precipitation total for the average period length at the site of interest may then be found using:

$$\log(yA_f) = m\log(xA_f) + c \quad \textbf{(5)}$$

Where

y = average precipitation total at the site of interest.

m = the slope of the regression line between measurement period log totals at the site of interest and the reference site.

x = average precipitation total at the reference site.

c = the offset of the regression line.

A_f = the average measurement period as a fraction of a year.

This may then be exponentiated and multiplied by $1/A_f$ to give an average annual precipitation estimate for the site of interest.

The average annual precipitation total (y) may then be established using:

$$y = \frac{10^{m\log(xA_f)+c}}{A_f} \quad \textbf{(6)}$$

Correlations and derived annual average precipitation have been established for many of the short term and storage gauge sites as shown in Table 3-5.

No significant correlation (with any other sites) was found for the Tasman Glacier Snout, Mueller Hut and Tasman Saddle sites. This is largely a result of the short period (less than 2 months) of record from each of these sites.

The record from The Rest did not correlate well to any station when month-of-the-year correlations were used. The same was true for all months. The nearby Glentanner and Twin Stream gauges both correlate well to The Rest, but a thirty year record is not able to be derived from the three stations. In this case the average annual precipitation was determined for the shorter period available for The Rest. In this situation the period for which measurements were available at The Rest are considered as representative of the 1971 to 2000 period. This extension of record loses the interannual variability that the correlation process allows, so has a major impact on the error of the final estimated normal (as shown later).

The Rose Ridge precipitation gauge site presents its own set of difficulties. The elevation of this site (1940 m) ensures that it regularly receives snow falls and freezing conditions. To avoid the possibly of false precipitation records from snow fall, only summer and autumn months were used (December to April) to determine a correlation with another station. This limited the correlation periods to just 15 months. The Mt Cook EWS site was used as the reference site.

Catriona Tarn, Waterfall Basin and Parsons Saddle are high elevation storage gauge sites from the Jollie catchment. Only three years of data has been obtained for these sites, which amounts to just eight measurement periods. No significant correlations were obtained between these sites and any other site. In this case, an average annual precipitation was estimated through determining the ratio of total recorded precipitation at the site of interest to the total recorded precipitation for the same period at nearby sites. This ratio was then applied to the average annual precipitation at the nearby sites, with the average of these values taken as the average annual precipitation value at the site of interest. This method makes the assumption that a correlation does exist between sites, but the small number of measurements prevents the correlation being determined. There is a possibility that the high and seasonally variable undercatch likely at these stations means that even with a longer record period no correlation in fact exists meaning that these values are indicative only.

Table 3-5. Short term and storage precipitation gauge sites and estimated annual average precipitation for 1970 to 2000.

Gauge Site	Est. Annual average (mm)	Correlated sites used to estimate the average annual precipitation	r^2	Slope (m)	Offset (c)	Avge. period (days)	No. of periods
Tasman Saddle		No significant correlation					
Malte Brun Hut	5366	The Hermitage	0.66	0.832	0.145	30	21
Rose Ridge	4674	Mt Cook EWS	0.54	0.6	1.07	30	15
Hooker Hut (95 day Cassella)	6389	The Hermitage	0.86	0.86	0.52	30	55
Hooker Hut (Storage - Milk Can)	6760	The Hermitage	0.93	0.67	1.05	34	24
Hooker Hut (Octapent storage)	6590	The Hermitage	0.91	0.66	1.06	35	25
Hooker Hut (PVC storage)	6738	The Hermitage	0.87	0.83	0.63	29	58
Tasman Glacier Snout		No significant correlation					
Catriona Tarn	2558**	No significant correlation					
Stocking Stream (Oct. storage)	4633	The Hermitage	0.74	0.68	0.9	45	43
Stocking Stream (PVC storage)	4651	The Hermitage	0.87	0.7	0.92	63	12
Pinnacle Stream	2259	Jollie Hut	0.90	0.91	0.46	110	55
Mueller Hut		No significant correlation					
Littles Hut	1887	Jollie Hut	0.94	0.93	0.33	62	112
Tasman Aero		No data	n/a	n/a	n/a	n/a	n/a
Bird Creek Hut	1591	Jollie Hut	0.88	0.85	0.42	46	165
Mt Kea	1955	Lower Kea	0.72	0.90	0.46	107	11
Pyramid Bluff	1945	Jollie Hut	0.93	0.86	0.52	94	67
Lower Kea	1745	Jollie Hut	0.88	0.92	0.34	96	75
Lower Pyramid	1994	Jollie Hut	0.92	0.88	0.48	93	73
	2403**	no significant correlation					
Waterfall Basin							
Birch Hill Airstrip	2118*	No data					
	2300**	no significant correlation					
Parsons Saddle							
Sealey Village	2215	The Hermitage	0.82	0.75	0.35	30	29
Devils Elbow1-7		No data					
Golden Gully	1410	Jollie Hut	0.91	0.948	0.145	44	168
Twin Stream	1401	Glentanner	0.95	1.06	-0.147	31	16
Glentanner	1483	Guide Hill	0.67	0.87	0.47	31	11
The Rest	1107	Lake Pukaki MWD	0.57	0.99	0.25	30	21
Braemar Hut		No data					
Lake Pukaki No. 1	647	Lake Pukaki MWD	0.96	0.94	0.1	30	28

* Estimate from 1941-1970 normals (NZMS, 1975b).

**Estimate based on average of ratios of total observed to total observed at nearby stations

No data have been obtained for Birch Hill Airstrip, Braemar Hut, Tasman Aero or any of the Devils Elbow gauges. A climate normal was published for Birch Hill Airstrip in the 1941 to 1970 climate normals (see Table 3-3) so this has been used as an estimate, but for the other gauges no estimate has been determined.

3.3.2 Average annual precipitation error

The methods used to observe the precipitation and to calculate the 30 year average annual precipitation affect the error of the determined figure. For a site with a complete 30 years of precipitation observations, there is no calculation error, but there is a random error from the precision of the measurement, and systematic errors through undercatch as previously discussed. The measurement precision may be considered to be +/- half the smallest scale division for each observation. For The Hermitage, the smallest scale division is 0.1 mm, so the error of each measurement is taken as 0.05 mm. The maximum possible measurement error for the 5601 non-zero observations taken from 1971 until 2000 is 5601 x 0.05 = 280.05 mm or 0.2 %. As the measurement error may be considered to be random, over many measurements it will largely cancel itself out. For the 5601 observations the total error may be considered normally distributed about 0 with a probability of 2/5601 (0.0004) that the error equals the maximum of 280.05 mm. From the *t* distribution, a 95 % confidence limit to the total error of the 5601 observations is +/-157 mm or just 0.13 %. This means that observation error at The Hermitage may be considered to total zero over the 1971 to 2000 period, with a 95 % probability of being less than 157 mm.

Wetting undercatch was assessed as being 0.5 % and wind induced undercatch as 8 % (see section 3.2.2 above).

Twenty of the months used to prepare The Hermitage 1971 – 2000 normal were derived from correlations to nearby sites. These derived values are an estimate only and so include an error, which in turn affects the overall error of the precipitation normal. It also needs to be remembered that the regression is based on the log of monthly totals, so that the final error confidence limits need to be exponentiated to provide errors in mm of precipitation.

An estimate of the variance of the entire thirty year population of residuals (s^2) from the regression line may be estimated from the variance of the sample of known residuals from which the regression line was created using (Heyworth and Sealy, 1980):

$$s^2 = \frac{\sum_{i=1}^{N} (x_i - \bar{x})^2}{N-1} \quad \textbf{(7)}$$

Where

i = sample number.

N = number of samples.

x_i = the residual from the regression line for sample i.

$\bar{x}$ = mean of the residuals.

The variance of the log of the average month type precipitation (s^2_{amtp}) may be found as follows:

$$s^2_{amtp} = \frac{1}{30^2} \sum_{i=1}^{n} s_i^2 \quad \textbf{(8)}$$

Where

$s_1^2, s_2^2 ..... s_n^2$ are the variances of each estimated log of the monthly total for a specific month type.

Similarly the variance of the estimate of the log of the average month (s^2_{amp}) may be found:

$$s^2_{amp} = \frac{1}{12^2} \sum_{i=1}^{n} s^2_{amtp,i} \quad \textbf{(9)}$$

Where

$s_1^2, s_2^2 ..... s_n^2$ are the variances of each estimated log of the average month type precipitation.

The 95 % upper (+*CL(0.95)*) and lower (-*CL(0.95)*) confidence limits for an average month may then be found by:

$$+CL(0.95) = 10^{\overline{\log(month)} + 2\sqrt{s^2_{amp}}} \quad \textbf{(10)}$$

$$-CL(0.95) = 10^{\overline{\log(month)} - 2\sqrt{s^2_{amp}}} \quad \textbf{(11)}$$

Where

$\overline{log(month)}$ = mean log of monthly precipitation.

The average annual precipitation error may then be found through finding the difference between the confidence limits and the average monthly precipitation, and multiplying by twelve.

As an example, the variances for the twenty estimated months of The Hermitage 1971 – 2000 average annual precipitation are given in Table 3-6.

Table 3-6. variance for estimated log of monthly totals at The Hermitage.

Month	Correlating station	Variance (s_i^2)
Feb 97	Mt Cook-ECAN	0.0007
Mar 97	Mt Cook-ECAN	0.0028
Apr 97	Mt Cook-ECAN	0.00035
May 97	Mt Cook-ECAN	0.0027
Jun 97	Hooker Rd. Bridge	0.001
Aug 97	Mt Cook-ECAN	0.00024
Oct 97	Hooker Rd. Bridge	0.0014
Dec 97	Mt Cook-ECAN	0.0038
Jan 98	Mt Cook-ECAN	0.011
Feb 98	Mt Cook-ECAN	0.0007
Mar 2000	Mt Cook-ECAN	0.0028
Apr 2000	Mt Cook EWS	0.00035
May 2000	Mt Cook-ECAN	0.0027
Jun 2000	Mt Cook-ECAN	0.0140
Jul 2000	Mt Cook-ECAN	0.013
Aug 2000	Mt Cook-ECAN	0.00024
Sep 2000	Mt Cook-ECAN	0.0006
Oct 2000	Mt Cook-ECAN	0.00006
Nov 2000	Mt Cook-ECAN	0.0019
Dec 2000	Mt Cook-ECAN	0.0038

The sum of these variances, divided by one thirtieth squared gives the month-type variance, as shown in Table 3-7. The average annual precipitation variance is then simply the sum of these month-type variances, from which the standard deviation and the 95 % confidence limits can be determined, as also shown in Table 3-7. It is found that for The Hermitage, there is a 95 % probability that the true 1971-2000 average annual precipitation total falls within 4350 +/- 10 mm. While this provides a good indication of the confidence of the determined total, it is based on some assumptions that may not be true. First, is the assumption that the residuals are normally distributed. Figure 3-12 shows a plot of the frequency distribution of the residuals between the log of monthly totals at Braemar Station and the estimated log of monthly totals derived from the correlation between Braemar and Guide Hill. The figure also shows the normal distribution based on the mean and standard deviation of the

residuals. Clearly the residuals are not a perfect fit to the normal distribution, but have a rightward skew. This would result in the estimated errors being less than they actually are. This result may be in part a result of the imperfect conversion of the monthly precipitation totals to a normal distribution by the log transformation (WMO, 1983), and may also be a result of using least squares regression when the independent variable is known to have error (Henderson et al., 2003).

Table 3-7. Probability range of The Hermitage average annual precipitation based on the variance of estimated average month type totals.

Month type	Variance (s^2_{amp})
Jan	12.0×10^{-6}
Feb	1.6×10^{-6}
Mar	6.2×10^{-6}
Apr	0.8×10^{-6}
May	6.0×10^{-6}
Jun	16.7×10^{-6}
Jul	14.4×10^{-6}
Aug	0.5×10^{-6}
Sep	0.7×10^{-6}
Oct	1.6×10^{-6}
Nov	2.1×10^{-6}
Dec	8.4×10^{-6}
Variance of estimated log of monthly precipitation (s^2_{aap})	0.5×10^{-6}
+CL(0.95) of monthly precip	363.3 mm
-CL(0.95) of monthly precip	361.0 mm
Centred monthly precipitation (+/- 95% confidence intervals)	361.7 +/- 0.7mm
Average annual precipitation (+/- 95% confidence intervals)	4340 +/- 10 mm

The second, possibly more important assumption is that the residuals are a random variable. It is likely that relationships between gauge sites vary with long term climate fluctuations (e.g. Interdecadal Pacific Oscillation, El-Nino Southern Oscillation, global warming), so that if one month is estimated low, the likelihood of the next month being estimated low is increased. This means that the random error range is less than if this dependence was accounted for. The random error determined here provides a lower bound of the real error and enables a relative measure of error for each site.

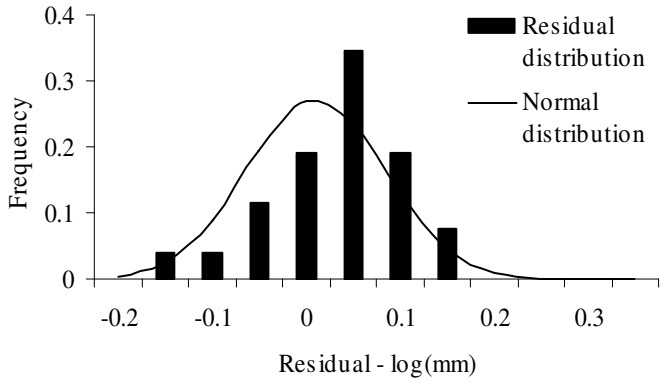

Figure 3-12. Distribution of residuals between a regression of the log of monthly precipitation totals at Braemar against the log of monthly totals at Guide Hill.

For The Hermitage, the estimation of missing months leads to 95 % confidence limits of 10 mm for the average annual precipitation estimate. This low figure reflects the large number of months considered (360), with the majority of them being known and not estimated.

Overall there is a 0.1 % random measurement error, an 8.5 % systematic undercatch offset error and a 0.2 % random correlation error. So the observed average annual precipitation total for The Hermitage site from 1971 to 2000 may be given as 4340 +/- 14 mm. The undercatch corrected average annual precipitation total for The Hermitage site from 1971 to 2000 is estimated as being 4710 +/- 20 mm.

This error should not be confused with a measure of the variability of the annual precipitation total. This value is the standard deviation of the annual totals (which for The Hermitage is 876 mm). It is this value that is important for prediction of annual totals (under the assumption of no climate change). This means that if we assume the annual precipitation totals are normally distributed about the average annual precipitation (Figure 3-13), for any one year in the 1971 to 2000 period there is a 68 % probability that the measured annual precipitation total is between 3400 mm and 5300 mm. Once again this assumes that the variation of a year from the 30 year mean is random, which it is not. So again this is merely indicative.

An assessment of measurement error and undercatch has been prepared for each gauge and is shown in Table 3-8. Measurement error for each manual site was determined in the same way as assessed for The Hermitage above. For automatic sites, the measurement resolution was assessed from the calibration. For the Mt Cook EWS

and Hooker Rd Bridge sites, the gauges are routinely checked and calibrated to be accurate to within 1 tip in 40, or 2.5 % (Halstead, 2008a).

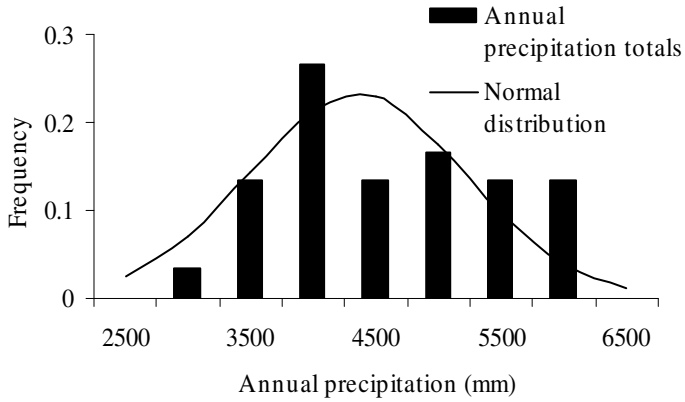

Figure 3-13. Frequency distribution of The Hermitage annual total precipitation between 1971 and 2000.

The calibration is unknown at the other automatic gauges, so a subjective accuracy was applied. The other tipping bucket gauges were given an equivalent 2.5 % accuracy, while the automatic gauges at Hooker Hut, Malte Brun and Ball Hut were allocated an arbitrary 5 % measurement accuracy. The undercatch at the different daily gauges was assessed following section 3.2.2. As before, the wetting undercatch is based on a loss of 0.1 mm per rain event, with, on average, one rain event occurring per rain day. The wind induced undercatch requires wind speed and temperature parameters. These values were taken from either The Hermitage, or the Mt Cook EWS sites, depending on which provided the greatest overlap with precipitation data. In either case the temperature was lapsed to the site elevation using an arbitrary wet adiabatic lapse rate of 0.005 ^{o} m^{-1}, a value determined from comparison of temperature records in the region by Kerr (2005). Orifice heights were assumed to be 300 mm above ground, except for the Ball Hut site, where the gauge frame is still on-site, with the top of the frame 2 m above the ground. The Malte Brun and Hooker Hut daily gauges were likely to have orifice heights above 300 mm, but in both cases their measurement record was outside the period for which wind data was available (from 1972). The daily undercatch parametric approach is not suitable for storage gauges as there is no daily assessment of precipitation. For these sites, undercatch was allocated subjectively based on nearby, or similar sites, accounting for the site elevation, average annual precipitation, and orifice height.

Table 3-8. Measurement, undercatch, random error and annual standard deviation of estimated average annual precipitation totals.

Gauge Site	Measure-ment error (%)	Random error (%)	Wetting (%)	Wind induced under-catch (%)	Estimated observed annual average precipitation (mm)	Estimated true annual average precipitation (mm)
Malte Brun Hut	5.0*	1.7	0.3	16*	5400 +/- 400	6300 +/- 400
Rose Ridge	2.5**	1.0	0.6	16*	4300 +/- 300	5000 +/- 400
Ball Hut	5.0*	1.3	0.3	13.9	4300 +/- 300	4900 +/- 300
Hooker Hut (95 day Cassella)	5.0*	1.1	2.0	14*	6400 +/- 400	7400 +/- 500
Hooker Hut (Storage - Milk Can)	0.2	1.0	4*	14*	6500 +/- 100	7700 +/- 100
Hooker Hut (Octapent storage)	0.2	1.0	4*	14*	6500 +/- 100	7700 +/- 100
Hooker Hut (PVC storage)	0.1	1.4	4*	14*	6900 +/- 100	8100 +/- 200
Catriona Tarn	0.05		3*	12*	2600 +/- 500*	3000 +/- 600*
Stocking Stream (Oct. storage)	0.2	1.6	4*	10*	4800 +/- 100	5500 +/- 100
Stocking Stream (PVC storage)	0.1	1.7	4*	10*	5200 +/- 100	5900 +/- 100
Pinnacle Stream	0.1	1.0	4*	10*	2250 +/- 90	2560 +/- 100
Littles Hut	0.1	1.5	4*	9*	1870 +/- 90	2100 +/- 100
The Hermitage	0.2	0.3	0.4	8.0	4350 +/- 20	4720 +/- 20
Mt Cook-ECAN	2.5*	1.0	0.4	8.3	4000 +/- 200	4400 +/- 200
Mt Cook-EWS	2.5**	0.9	0.5	8.4	4000 +/- 200	4300 +/- 200
Hooker Rd. Bridge	2.5**	1.0	0.6	8.4	2800 +/- 100	3000 +/- 100
Hooker Flat	1.8	1.3	0.4	8*	4200 +/- 200	46000 +/- 200
Bird Creek Hut	0.1	1.8	4*	8*	1620 +/- 80	1810 +/- 90
Mt Kea	0.1	0.7	4*	11*	2000 +/- 100	2300 +/- 100
Pyramid Bluff	0.1	1.0	4*	10*	1960 +/- 80	2240 +/- 90
Lower Kea	0.1	1.1	4*	9*	1760 +/- 70	1990 +/- 80
Lower Pyramid	0.1	1.0	4*	9*	2030 +/- 80	2290 +/- 90
Waterfall Basin	0.05		3*	12*	2400 +/- 500*	2800 +/- 600*
Birch Hill Airstrip	No data		4*	9*	2120 +/- 20	2390 +/- 30
Parsons Saddle	0.05		3*	12*	2300 +/- 500*	2600 +/- 600*
Sealey Village	0.6	1.9	1.1	8.3	2310 +/- 70	2520 +/- 80
Golden Gully	0.1	1.5	4*	8*	1430 +/- 70	1540 +/- 70
Jollie Hut	2.5*	0.5	1.1	6.7	1320 +/- 40	1420 +/- 40
Twin Stream	0.3	0.5	0.7*	8*	1700 +/- 700	1900 +/- 700
Glentanner	0.7	1.7	0.7	8*	1800 +/- 600	1900 +/- 600
The Rest	0.3	44	0.6	6.9	1300 +/- 600	1400 +/- 600
Braemar Station	1.1	0.2	1.0	6.6	860 +/- 10	920 +/- 10
Guide Hill	1.3	0.7	1.4	6.8	890 +/- 30	970 +/- 30
Tasman Downs	1.2	0.5	1.3	6.6	890 +/- 50	960 +/- 50
Lake Pukaki No. 1	1.4	1.5	1.4	6*	650 +/- 90	700 +/- 90
Lake Pukaki MWD	1.5	1.3	1.5	6.3	660 +/- 70	710 +/- 70

***These values have been subjectively estimated.**

****These values are from calibration.**

No evaporation estimate was made, as the standard technique for storage gauges is to add an anti-evaporation oil barrier to gauge contents. This was assumed to have been done for the storage gauges considered.

The random error was determined in the same manner as assessed for The Hermitage above except for The Rest, which had no correlating site. For this site, twice the square root of the sum of the variance for each month-type average was used as the 95 % probability range for the average annual precipitation.

3.4 Precipitation observations from this study

3.4.1 The need for new observations

Previous investigations of the precipitation distribution in the Lake Pukaki catchment describe strong precipitation gradients towards the north west of the catchment. Figure 3-14 showing the NZMS 1951 to 1980 average annual precipitation contours clearly demonstrates this.

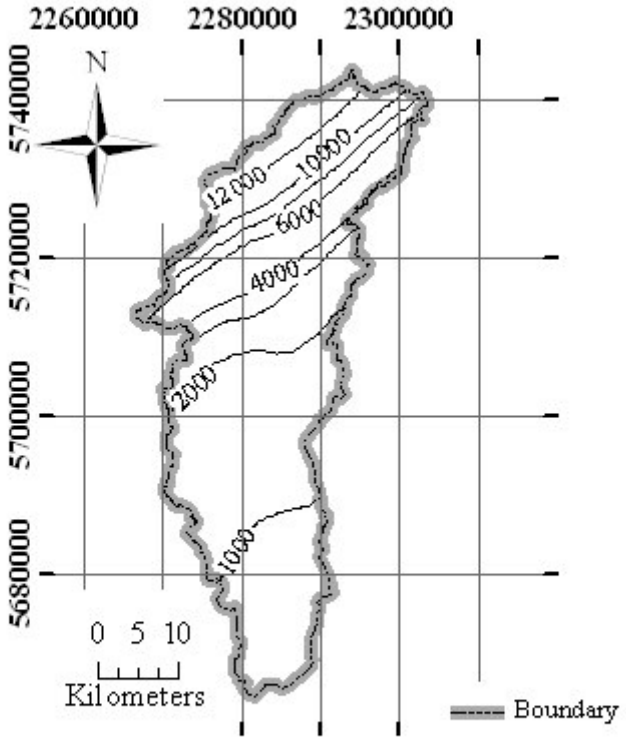

Figure 3-14. NZMS 1951 to 1980 average annual precipitation isohyets (NZMS, 1985a).

Unfortunately the lack of precipitation gauging in these areas makes it difficult to conclude, to any level of error, what the precipitation actually is in these regions.

Figure 3-15 shows estimated 1000 mm precipitation bands from the average annual precipitation surface prepared by Kerr (2005) with the location of gauge sites that are, or have been located within the catchment. The three highest bands (combined into one on the map) have not had any gauges sited within them, while the next three highest have only had one gauge sited within each of them. Lower in the catchment, the area of each precipitation band is larger and so the number of gauges in each band also increases. The diagram is a classic example of the need for higher density gauging in mountainous regions compared to lowland regions, to achieve the same level of precipitation sampling. New gauges were installed to address the sampling imbalance in these mountainous regions.

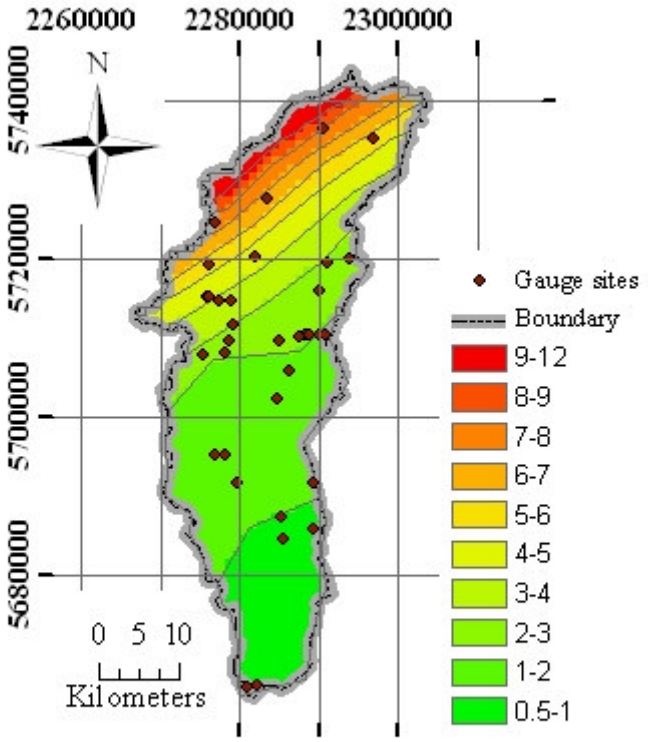

Figure 3-15. Estimated 1 m average annual precipitation bands with sites that have been gauged.

3.4.2 Observation equipment

In determining the type of gauge to be used, consideration of likely precipitation type, quantity, site access, desired temporal resolution and budget needed to be made. Being a largely glacierized region, the ability to measure solid and liquid precipitation was required. Inflow records for Lake Pukaki indicated that some parts of the catchment must be receiving more than the 4300 mm of average annual precipitation

estimated at The Hermitage. Much of the upper catchment is in the Aoraki/Mt Cook National Park and so has restricted vehicular access. These considerations point towards a logging storage gauge. The strong possibility of large swings in temperature during precipitation events with freezing and thawing, possibly in association with strong winds means that the use of a gauge with no moving parts was advisable. The availability of capacitive loggers in conjunction with 2 m high, 150 mm inside diameter stand pipes provided an instrumentation solution. Manual transportation required that wind shielding was not possible. This solution follows that implemented as part of the Rakaia Transect programme (Chinn, 1979; Griffiths and McSaveney, 1983a; McSaveney et al., 1978) except that data loggers were included.

3.4.3 Storage gauges

The storage gauges consisted of 2 m high 150 mm inside diameter PVC stand pipes. An end cap was glued over one end of the pipe, creating a container, with the other open end chamfered to a fine edge. A small (20 mm) hole was made near the open end of the gauge through which the sensing cable of the capacitive water depth sensor and logger was inserted. The body of the logger was fixed to the outside surface of the gauge while the sensor cable exposed to the outside of the gauge was shielded with conduit (as shown in Figure 3-16) to prevent damage by Kea (an alpine parrot).

Figure 3-16. Detail of attachment of data logger to the outside of the precipitation gauge. The sensor cable enters the gauge via the "Kea proof" conduit.

Gauges were prepared for installation on either a glacial or bare ground surface. Those to be installed on bare ground were held upright with three wire guy ropes attached to near the top of the gauge, and to metal stakes driven into the ground at approximately 1.5 m from the base of the gauge with rocks placed around the base of the gauge for additional support (see Figure 3-17). Gauges for installation on a glacial surface were fitted to a wooden cross 4 m x 4 m. The gauge was guyed to this stand, and rocks placed on the stand as shown in Figure 3-18.

Figure 3-17. Precipitation gauge on bare ground showing guy wires and rocks used for support.

Figure 3-18. Glacier located gauge with a wooden cross base.

3.4.4 Site locations

Precipitation gauge locations were selected to be accessible, would not be buried by snow, were free of being damaged by rock, snow or ice avalanches, were unlikely to become crevassed, were representative of the surrounding area, and were distributed across the regions that had not been sampled before. Such sites were identified at a general scale through geographic information system (GIS) analysis, with more precise positioning through manual interrogation of topographic maps, and finally through on-site investigations.

The GIS data used were:

1. Maximum winter snow depth estimate from SnowSim-Pukaki (Kerr, 2005). SnowSim-Pukaki is a degree day snow storage model tuned to the Lake Pukaki catchment. For each 1 km x 1km grid cell within the catchment, the maximum estimated snow depth, in snow water equivalent, of any day between 2000 and 2005 was found. This is shown in Figure 3-19.
2. Slope angle. For each 25 m x 25 m grid square, slope was derived from a 25 m resolution digital elevation model (Barringer, 2003) as shown in Figure 3-20.
3. Current and historic precipitation gauge sites, as shown in Figure 3-8.
4. Average annual precipitation distribution (Kerr, 2005) as shown in Figure 3-21.

Areas with less than 2 m of maximum accumulated snow (so that gauges will not get buried) were intersected with areas with slope angles less than 30^{o} (reduced rock fall, icefall and avalanche risk) as shown in Figure 3-22. A snow depth of 1.2 m s.w.e. was used, which relates to 2 m snow depth for a snow density of 600 kg m^{-3}. This is more dense than would be expected, and so there will still be a chance that a gauge sited in the snow depth marginal regions will be covered. This was a calculated risk in that burial might be for a limited time, yet may allow the sampling of a very high precipitation region. Within the low slope, low snow build up areas, the average annual precipitation surface was classified into precipitation bands (Figure 3-15), and the total precipitation gauge operation time in each band determined. This provided a map of site priority, where poorly gauged bands were a high priority and well gauged bands a low priority as shown in Figure 3-23. It is clear from this analysis that the Mueller, Hooker, Tasman and Murchison valleys were the areas where an opportunity to gauge the higher precipitation regions were most likely. The manual topographic

map interrogation and on-site investigation led to the selection of gauge sites as shown in Figure 3-24. A gauge was sited in the Mt Cook/Aoraki village to enable comparisons against the long term gauges sited there. The site in the Jollie River was in a low priority area but provided a means of extension of the more westerly gauges, enabling northwest-southeast, and west-east transects. The Rudolf and Tasman gauges were at the limit of the "low snow" criteria. Personal experience of winters in the Tasman Valley led to the assumption that the low-snow estimate on the Tasman was too liberal, and worth the risk of siting the gauge there. The Rudolf site enabled the sampling of a higher estimated precipitation region than any other location, and so was also thought to be worth the risk of being covered by snow.

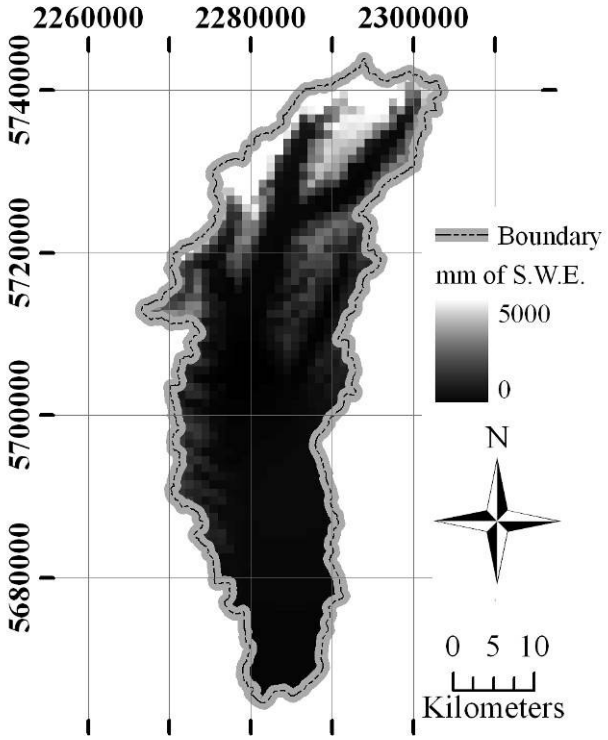

Figure 3-19. Estimated maximum snow depth in mm of snow water equivalent (SWE) derived from the SnowSim-Pukaki snow storage model (Kerr, 2005).

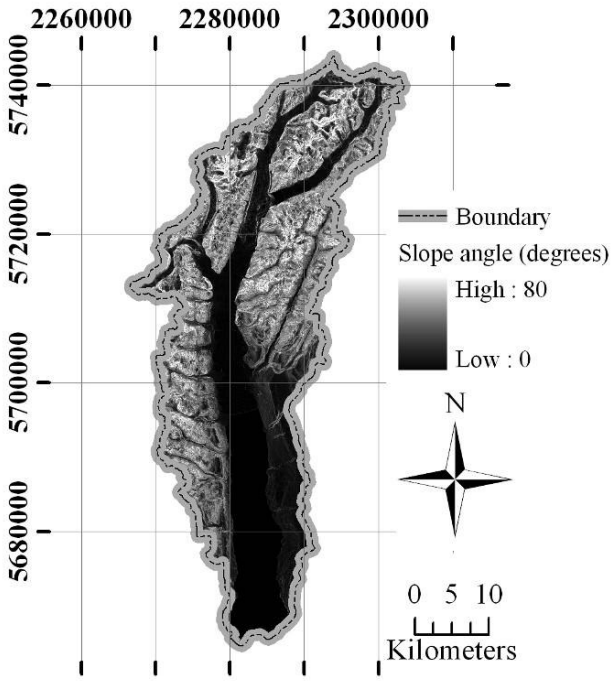

Figure 3-20. Surface slope angle in degrees from horizontal.

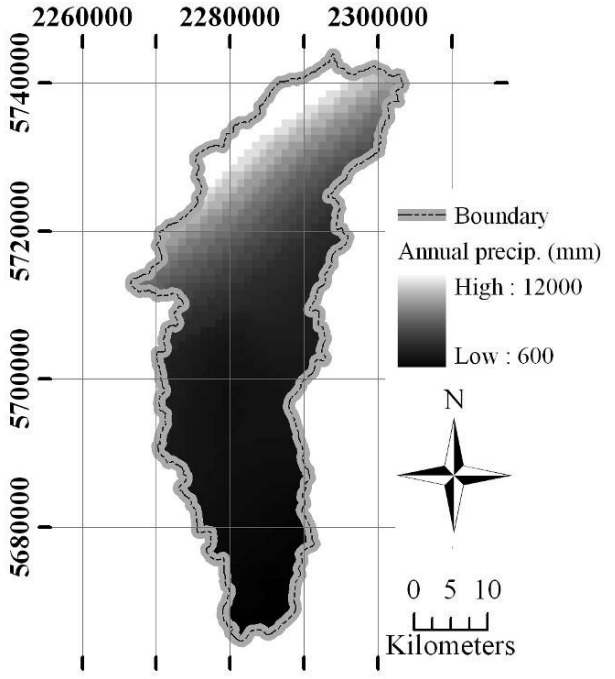

Figure 3-21. Estimated average annual precipitation (mm).

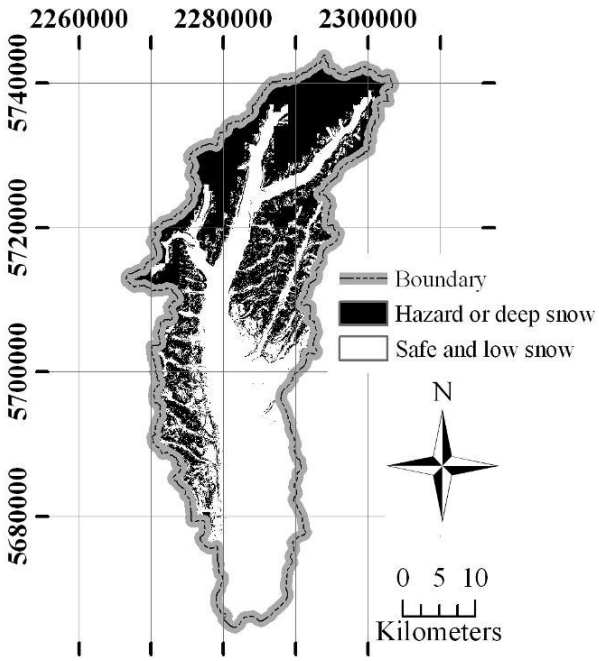

Figure 3-22. Catchment region with surface slope less than 30 degrees above horizontal and has a low likelihood of having a build of snow of more than 2 m of snow during the year.

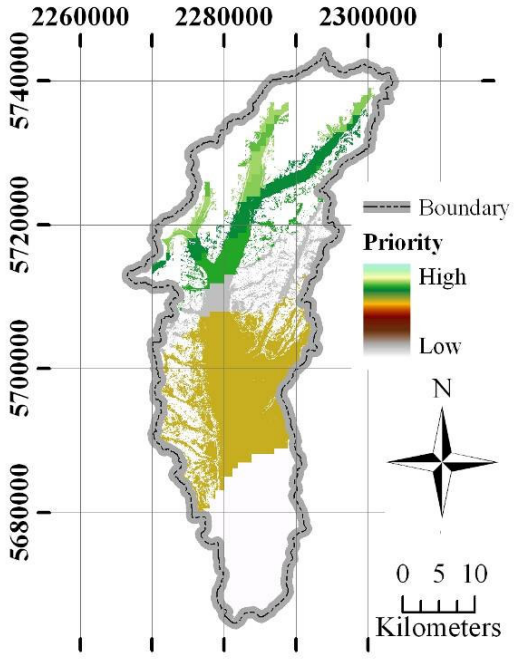

Figure 3-23. Gauge siting priority map.

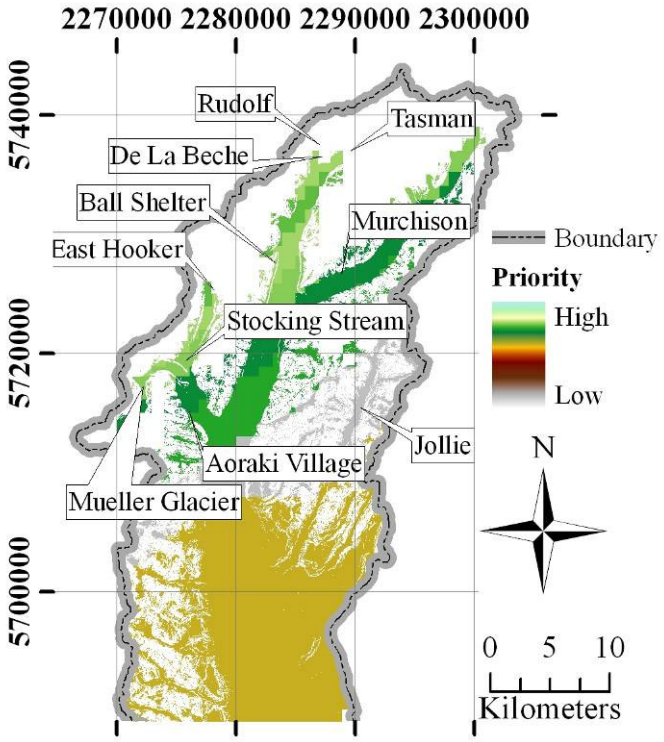

Figure 3-24. New gauge sites installed for this study.

3.4.5 Observation operation

Each gauge was primed with a mix of antifreeze and methylated spirits (McSaveney, 1979). The methylated spirits is required so that the specific weight of the mix is less than water to ensure that it floats to the top of the water column within the gauge. This means that solid precipitation comes into contact with the antifreeze immediately it falls into the gauge. No anti-evaporation oil was added to the gauge as it was found to interfere with the operation of the capacitive sensor. The oil coated the sensor cable creating an intermittent barrier to the water, effectively increasing the width of the capacitor dielectric and hence the observed capacitance.

Most gauges were inspected once a month, but at least once every two months. During an inspection the fluid height was manually measured. This was done through measuring with a metallic tape measure, the distance from the top of the fluid to the highest edge of the gauge. The manual measurement error was considered to be within +/-5 mm. The variation in the height of the top edge of the gauge, the twisting of the tape measure inside the gauge, and the difficulty in judging the precise moment

of tape measure-to-fluid contact led to this error assessment. When the gauge was over half full, the contents were emptied, new antifreeze mix added, and a new manual measurement taken. During each gauge inspection the data logger was downloaded and restarted. The gauge was checked for leaks, both visually, and through checking the manual measurements against the previous measurements. The battery of the data logger was checked and replaced if necessary. The guy wires of the gauge were checked for security and the gauge itself checked to ensure it was still vertical +/- 3 ^{o}. During winter four litres of antifreeze mix was added after a gauge was emptied. During the remainder of the year two litres of antifreeze mix was added. If a leak was found it was repaired as soon as possible. Where the contents of a gauge were frozen, every effort was made to empty the gauge.

3.4.6 Manual measurement results

Manual measurements at the gauges were obtained during inspections. On many occasions no measurement was taken because of leaks, fallen gauge, buried gauge or frozen gauge contents. Appendix 1 outlines the manual measurements taken. The automatically recorded measurements obtained by the capacitive level sensor provided high temporal resolution observations but were considered less accurate than the manual observations over longer periods because of intermittent operation and thermal drift of the associated electronics. Section 5.3 discusses the electronically recorded observations. For the purposes of preparing the annual average precipitation distribution the manual observations were considered the most useful and most accurate.

3.4.7 Average annual precipitation estimation from new manual measurements

The gauges used in this study had manual measurements taken approximately once a month. These measurements provide long term precipitation totals that may be used to establish ratios to correlated reference sites.

In some months some gauges froze or were found to leak, or in one instance dead animals were in the gauge. In these circumstances the manual measurement in question was not used. The manual measurements provide a much longer overall period of precipitation observation compared to the automatically recorded measurements, improving the estimation of ratio to correlated reference sites.

Average annual precipitation estimates were prepared following the method outlined for storage gauges in section 3.3.1 above. In two cases (Murchison and Rudolf) the correlations were not significant at the 0.99 % level. This is likely to be a result of the small number of observations, rather than there not actually being a relationship. The average annual precipitation was still estimated in these instances.

Table 3-9. Manual precipitation measurement derived annual average precipitation for 1970 to 2000.

Gauge Site	Estimated average annual (mm)	Correlated site	r^2	Slope (m)	Offset (c)	Average period length (days)	No.of measure-ment periods
Ball Shelter	3674	Mt Cook EWS	0.97	1.04	-0.15	30	14
De La Beche	9985	Mt Cook EWS	0.91	0.86	0.76	37	10
Jollie	1593	Mt Cook EWS	0.83	1.38	-1.45	53	9
Murchison	2020	Mt Cook EWS	0.75*	1.15	-0.71	59.0	6
Rudolf	*10904*	*Mt Cook EWS*	*0.59**	*0.83*	*0.88*	*38*	*4*
Hooker	9051	Mt Cook EWS	0.86	1.03	0.28	34	13
Mueller	7342	Mt Cook EWS	0.90	1.01	0.24	32	13
Stocking	4974	Mt Cook EWS	0.89	1.08	-0.11	32	15
Aoraki	3438	Mt Cook EWS	0.93	1.01	-0.08	32.6	13
Tasman	4478	Mt Cook EWS	0.86	1.06	-0.09	34	6

*not statistically significant at the 0.99 level

3.4.8 Error and undercatch assessment

The measurement accuracy was determined as +/- 5 mm. This enables a percentage measurement error to be determined for each gauge through the knowledge of the number of measurements taken and the total precipitation measured. An undercatch error that has not been considered up to now is evaporation. Wherever precipitation is retained within a gauge there is potential for evaporation. In this regard, storage gauges are susceptible to this error. The standard procedure is to add a small quantity of oil to the gauge which floats on top of the stored water and acts as an evaporation barrier. It was found that the oil interfered with the operation of the capacitive logger and so was not used for this gauge network. Assessment of evaporation requires a full knowledge of energy inputs, unavailable at the sites. The Village storage gauge is sited in close proximity to the NIWA tipping bucket gauge Mt Cook EWS. A

comparison of gauge catches enables an assessment of the total undercatch of the storage gauge. A comparison of catches for the manual measurement periods is shown in Table 3-10. On average the storage gauge captured 90 % of the precipitation that the tipping bucket gauge measured.

Table 3-10. Precipitation total comparison between Mt Cook EWS 300 mm high tipping bucket gauge, and nearby 2 m high storage gauge.

Period (days)	Period start date	Period end date	Mt Cook EWS (mm)	storage gauge (mm)	Ratio
30	18 January 2006	17 February 2006	75	60	0.8
31	17 February 2006	20 March 2006	203.8	228	1.1
20	20 March 2006	10 April 2006	182.2	230	1.3
37	10 April 2006	18 May 2006	285.4	253	0.9
45	18 May 2006	3 July 2006	486.4	460	0.9
14	3 July 2006	17 July 2006	144.8	118	0.8
30	17 July 2006	17 August 2006	147.6	118	0.8
29	17 August 2006	15 September 2006	255.0	204	0.8
34	15 September 2006	20 October 2006	593.2	520	0.9
42	20 October 2006	1 December 2006	982.2	886	0.9
47	1 December 2006	18 January 2007	380.6	284	0.7
42	18 January 2007	1 March 2007	262.6	157	0.6
32	1 March 2007	3 April 2007	333.4	272	0.8
				Average	0.9

An assessment of wind induced undercatch following the methods set out in section 3.2.2 above determined an undercatch of 12.5 % if the Mt Cook EWS gauge orifice height was at 2 m (compare with 8.4 % for an orifice height of 300 mm). The 90 % ratio of storage gauge catch to tipping bucket gauge catch indicates an 11 % undercatch to bring it in line with the tipping bucket catch. A further 8.4 % must still be added to provide an estimate of the true precipitation. This indicates a 20.4 % undercatch to true precipitation which is much greater than the 12.5 % estimated. This suggests that 7.9 % of the undercatch is a result of evaporation or approximately 300 mm. Without on-site daily temperature, radiation and wind measurements, obtaining an estimate of evaporation and wind-induced undercatch at the other gauge sites is problematic. The simple, conservative approach of applying the undercatch ratio established at the Aoraki/Mt Cook site to all storage gauge sites was used. This simple

ratio method is likely to underestimate the wind induced undercatch at gauge sites in windier, colder and wetter locations, and overestimate the wind induced undercatch at warmer, calmer, drier sites. In contrast, the evaporation error is likely to be underestimated at the dry, warmer sites, and overestimated at the cool, wetter sites. Random error may be determined in the same manner as used in section 3.3.2. These error values are shown in Table 3-11.

Table 3-11. Observation, undercatch and random error of estimated average annual precipitation totals.

Gauge Site	Obs. err. (%)	Rdm. err. (%)	Wet. err. (%)	W., evap. u-catch (%)	Total u-catch (%)	Observed avg. ann. precip. (mm)	Estimated true avg. ann. precip. (mm)
Ball Shelter	0.8	1.3	4	20	24	3900 +/- 300	4800 +/- 300
De La Beche	0.4	1.2	4	20	24	10000 +/- 700	12400 +/- 800
Jollie	1.1	2.8	4	20	24	1700 +/- 200	2100 +/- 200
Murchison	0.7	3.9	4	20	24	2300 +/- 200	2800 +/- 300
*Rudolf**	*0.9*	*0.04*	*4*	*20*	*24*	*12200 +/- 700*	*15200 +/- 900*
Hooker	0.3	1.8	4	20	24	9000 +/- 600	11200 +/- 800
Mueller	0.4	1.1	4	20	24	7000 +/- 500	8700 +/- 600
Stocking	1.0	2.3	4	20	24	5100 +/- 400	6300 +/- 500
Aoraki	0.9	1.3	4	20	24	3500 +/- 300	4300 +/- 300
*Tasman**	*0.7*	*1.4*	*4*	*20*	*24*	*4700 +/- 300*	*5900 +/- 400*

***Indicative only as figures are derived from a non-significant correlation.**

3.5 Daily precipitation data from this study

Ideally the preparation of wind-classed precipitation distributions would utilise precipitation data observed during a specific class. Unfortunately the wind data are limited to 6 hourly estimates, and the majority of precipitation data have a minimum time resolution of one day. This has provided the temporal limit to the analysis. Even at 1 day, many of the precipitation observations used in preparing the average annual precipitation distribution in the previous chapter must be abandoned. This eliminates the 19 storage gauges from the analysis greatly reducing the spatial resolution of observations. The storage gauges installed for this study (see section 4.4) were fitted with recording water level sensors ensuring that they are able to be included in the preparation of wind-classed precipitation distributions.

The level sensor used for this study's precipitation gauges was a capacitance measurement between an insulated length of wire hanging within the gauge and the

gauge contents. The system requires no moving parts and may be completely sealed so is ideal in a harsh environment. As the gauge contents level rises from precipitation, the sensor measures increased capacitance. By priming the standpipe with antifreeze (a monopropylene glycol, ethylene mix (McSaveney, 1979)) snow, hail and graupel are converted to fluid enabling measurement by the sensor. This system provides the basis of a low cost, robust, logging precipitation gauge capable of operating in a very high precipitation region where both solid and liquid precipitation is possible.

Following implementation of this gauge design for the precipitation gauge network, it was found that the sensor signal occasionally decreased, frequently followed by increases. On some occasions this variation was clearly repeating regularly each day. An example of these variations is shown in Figure 3-25.

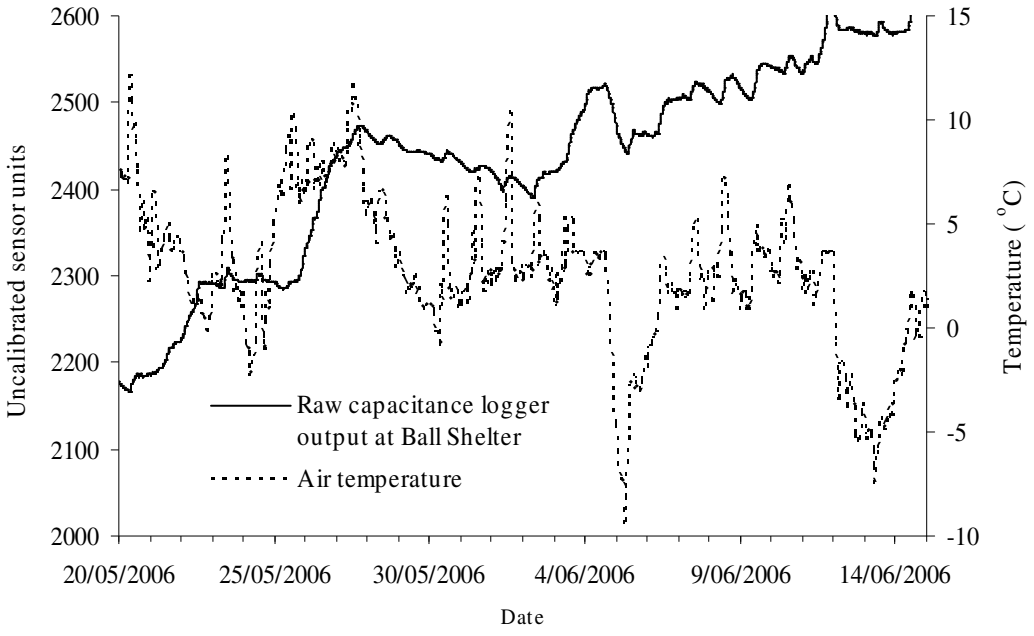

Figure 3-25. Example of sensor signal oscillation (from the Ball Shelter gauge) and associated air temperature. Note that air temperature was estimated by lapsing against elevation from the nearby Rose Ridge climate station.

Upon enquiry to the manufacturer and inspection of the sensor electronics, it was found that the sensor did not have any compensation for the impact of temperature variation on the measured capacitance. The heating up and cooling down of the sensor and electronics was causing the sensor signal to vary. The manufacturer places reliance on the temperature stability in the environment under which the sensor operates for accurate operation. In underground industrial water tanks where the

sensor is commonly used this reliance is justified. The use of capacitive sensors for precipitation gauges on ocean buoys have shown similar temperature sensitivities (Serra et al., 2001) but not to the extent observed here. It is likely that this was one of the first times this particular make and model of sensor had been used in this application. The result of the deficiency is that a system is needed to remove the temperature derived signal from the sensor output, thus leaving the required water level signal.

No temperature measurements were taken on site though they were available from nearby sites. Application of thermodynamic equations to estimate fluid temperature was trialled without success. An alternative subjective approach was then taken that selects sections of the sensor signal that are considered likely to be related to precipitation and discards the remainder. A full explanation of the method is described in the next section.

3.5.1 Method

Periods when the signal varies without an overall increase were identified and removed. The assumption was made that no precipitation occurred during these periods and so the variation was caused by temperature alone. Comparison against a nearby temperature record enabled a method of confirming this assumption by noting the relationship between signal level and temperature (see Figure 3-25).

When an increase in signal level was not associated with a related change in temperature, a precipitation event was considered to have occurred. Removing data points from these variable periods left the signal from precipitation events only, as shown in Figure 3-26.

Following removal of the periods when no precipitation was considered to have occurred, a reduced dataset was obtained. At this point the raw signal was rounded to the nearest multiple of 5. This cleared up a lot of the noise of the signal.

With the “no precipitation” periods removed it was noted that the beginning of the data point at the end of a precipitation event may be at a different level to that at the beginning of the next event. This is likely to be a result of the temperature being different at these two times. To correct for this an offset was applied to all later data as shown in Figure 3-27.

Following adjustment for offset, the data were examined for outliers and small frequency variations. This was done by finding all the data points that were less than their surrounding data points and eliminating them.

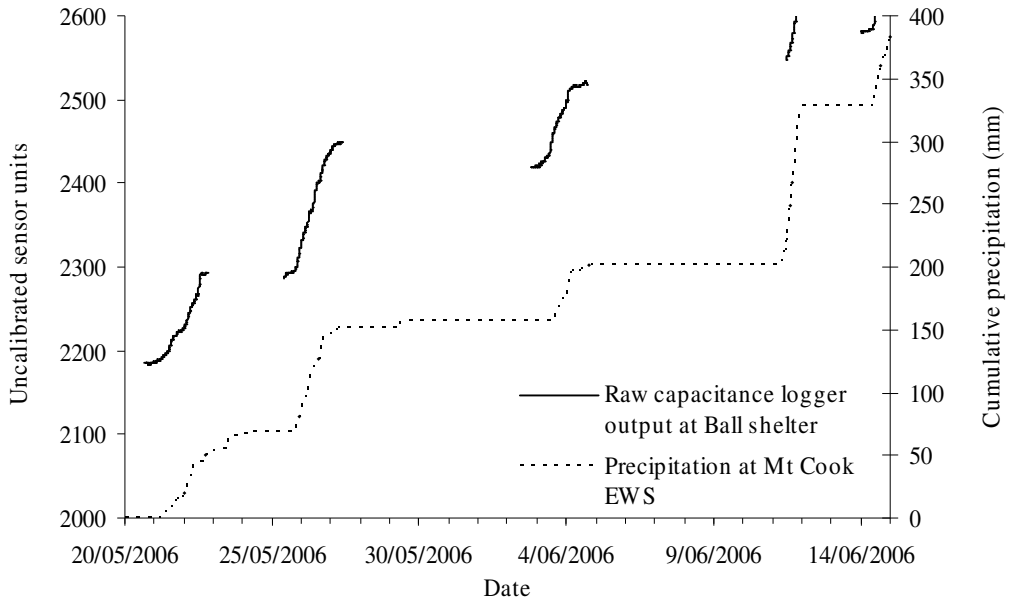

Figure 3-26. Sensor signal with data points removed from periods considered to have received no precipitation. The precipitation record from Mt Cook EWS is shown for comparison.

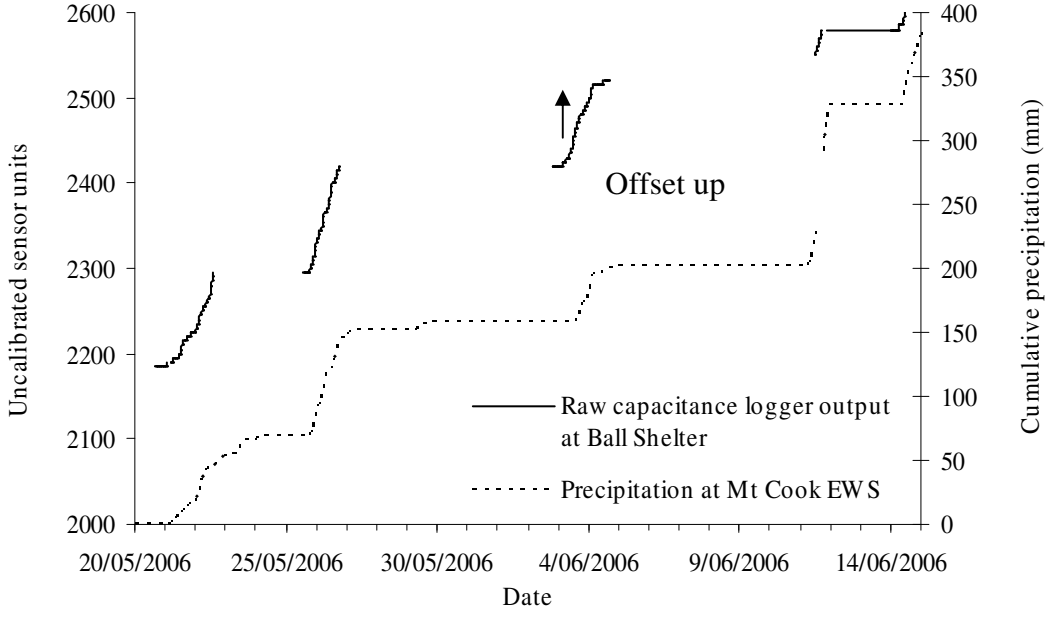

Figure 3-27. Signal following adding an offset prior to 3/6/2006 to bring the end of the no-precipitation period into line with its beginning. The precipitation record from Mt Cook EWS is shown for comparison.

Changes of temperature that occur during precipitation events will affect the signal output, but no reasonable method of correcting for this is possible. Where variations in the sensor signal cannot be reasonably related to temperature or precipitation effects, they have been removed.

While all care and considerations is made in adjusting the signal, there is still potential for the signal to have been incorrectly adjusted which should be considered when using the data for further analysis.

- There can be an overestimation of precipitation (when the temperature increases during precipitation) or an under estimation of precipitation (when the temperature drops during precipitation). This second possibility includes the situation where the signal increase caused by water level increase is exactly matched by the signal level drop caused by a drop in temperature. Under this circumstance not just the magnitude of the event will be misreported, but the event itself may be missed. Comparison of the corrected precipitation data to nearby gauges enabled an assessment of whether events had been missed.
- Small variations in between major events may occur through dew (increasing water level) or from evaporation (decreasing water level). Dew will normally form during rapidly cooling temperatures (e.g. evening). Evaporation will be greatest during hot dry periods. Evaporation is likely to be greater as the water level approaches the rim of the gauge where air turbulence is greater.
- At lower temperatures, freezing fluid will increase the volume of the contents of the gauge and the water level. Similarly if the gauge contents are partially frozen, warming temperatures will cause melt and a reduced volume. The signal relationships to temperature under these conditions are opposite to what would normally occur. It is likely that many of the periods of anomalous sensor operation are related to melting or freezing of the gauge contents.

3.5.2 Calibration

Once the sensor signal has been adjusted for temperature variation, it requires calibration against the manual measurements (see section 4.4) using:

$$A_c = mA_u + c \qquad \textbf{(3-12)}$$

Where:

A_c is the calibrated automatic sensor signal,

A_u is the uncalibrated automatic sensor signal

m is the calibration slope

c is the calibration offset

The calibration slope may be determined from the manual readings:

$$m = \frac{M_t - M_{t-1}}{A_{u,t} - A_{u,t-1}} \quad \textbf{(3-13)}$$

Where:

M is a manual measurement

t is the time step

as can the calibration offset:

$$c = \frac{M_t - mA_{u,t} + M_{t-1} - mA_{u,t-1}}{2} \quad \textbf{(3-14)}$$

The calibration was done for each manual observation period to limit the impact of the seasonal variation of temperature on the sensor output.

A rounding of the calibrated water level to the nearest mm was then applied. This rounding on top of the earlier rounding of the raw signal leads to a resolution of 3 mm. This is taken as the best possible accuracy of the water level signal. The temporal resolution is also reduced to 60 minute intervals during precipitation periods, again a subjective assessment of the best possible accuracy under the circumstances. Figure 3-28 is an example of a calibrated sensor signal.

This correction and calibration against the manual record was carried out for each storage gauge installed as part of this study. This provided eight new daily precipitation observation sites, one extended observation period (Ball Shelter) and one supporting observation period (Aoraki/Mt Cook Village) within the Lake Pukaki catchment.

These data augment the current and historical daily precipitation observations in the catchment enabling the preparation of wind classed precipitation distributions.

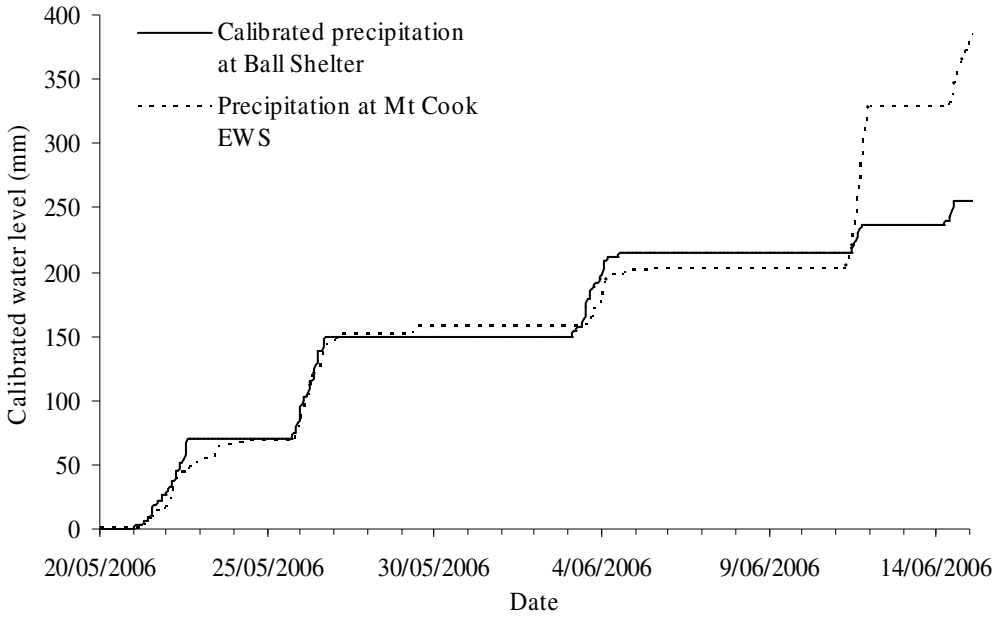

Figure 3-28. An example of calibrated cumulative rainfall measurements (from the Ball Shelter gauge) following subjective signal processing. The precipitation record from Mt Cook EWS is shown for comparison.

3.6 Average annual precipitation map

Production of an average annual precipitation map requires interpolation of precipitation normals from measurement sites to all sites within the region of interest. The average annual precipitation maps produced in New Zealand have used subjective analysis from climate experts to determine the values at non-measured locations. Objective methods of spatial interpolation are commonly available on geographic information systems. Interpolation methods vary considerably requiring the considered selection of an appropriate technique. Two frequently used systems for precipitation map production are spline interpolation and kriging. Spline interpolation generates a constrained surface such that the surface curves are minimised and the difference between the constrained surface and known value sites are minimised. The constraint of the surface may be set to any type of analytical function within a defined spatial area and/or a defined number of sample sites. The smoothness of the output surface and the variation of the surface from known value sites may also be controlled. A type of spline interpolation is used for the interpolation of North American precipitation data by the PRISM system (Daly et al., 1994) and by ANUspline for the production of national daily precipitation maps of New Zealand

(Tait et al., 2006). Spline interpolation treats all points equally so that the error of the interpolation at each measurement point has an equal weight. This method of interpolation works well when there is an even distribution of sample points. Where the spatial distribution of sample points is variable, variability from spatially dense measurement sites may impact heavily on adjacent poorly sampled regions. Kriging is similar to spline interpolation, except that the weighting of influence of measured points on the resulting surface varies. A spatial analysis of all sample points is initially carried out to determine how spatial variability is related to distance between points. This relationship (semivariogram) is then approximated with an analytical formula. When estimating surface values at new points, the weighting of surrounding sample points is related to the estimated sample variance based on the distance to each point. Kriging allows for different spatial variance functions (e.g. exponential, Gaussian, constant) determined either from all sample sites, or from within a specified range of the point of interest. Kriging also allows for spatial trends, which may themselves be analytically described (e.g. linear, exponential) or provided as a related surface (termed co-kriging). Spline interpolation, inverse distance weighting and sample averaging interpolation methods may all be reproduced using kriging. As such, kriging may be seen as an over-arching interpolation method. Until recently the computational expense of kriging outweighed its value as an interpolation technique (Cruetin and Obled, 1982). Kriging is now available as a standard component of GIS applications, with standard computer capability great enough that kriging calculations are no longer limiting. Kriging has been used to prepare an isohyet map for the Lake Pukaki catchment based on the estimated average annual measured precipitation, and for the estimated average annual true precipitation. Ordinary kriging (where the mean of the precipitation field is assumed to be constant but unknown) was applied from within ArcGIS™ 9.2. The output cell size was set to 1000 m with at least 12 sample sites used to interpolate each point. A spherical model of the semivariogram was used with the parameters calculated internally by the application. The output raster was clipped to the catchment and a contour map generated from that raster. The two isohyet maps are shown in Figure 3-29 and Figure 3-30. The estimated true precipitation varies from 710 mm per year in the south eastern corner of the catchment to 13200 mm in the north west of the catchment. The precipitation distribution shows a striking gradient perpendicular to the main divide indicating that

the governing control on the precipitation distribution is related to this major topographic feature. The very high precipitation in the elevated north west is based on the extrapolation of precipitation gradients from low elevation sites to the east. Personal observation of these regions would indicate that this is reasonable, and may even be conservative. The average precipitation for the catchment as determined from these surfaces is 2913 mm and 3396 mm for the estimated measured and true surfaces respectively.

The estimated average annual measured and true precipitation surfaces have been compared to the NZMS 1950-1981 normal map (NZMS, 1985a) and the average annual precipitation map generated for the catchment by Kerr (2005) based on an integration of precipitation measurements and a "distance to the west" function. Difference maps are shown in Figure 3-31. The estimated true surface is greater than the NZMS 1951–1980 and Kerr 2005 surfaces in the southern region of the catchment, but is less in the northern areas. It would be expected to have been greater in all areas, as the other surfaces are derived from measurements without any undercatch assessment.

The difference in the northern region highlights the uncertainty in this high precipitation region. The measured surface matches well to the NZMS 1951-1980 and Kerr 2005 surface in the southern region of the catchment but has an even greater difference in the north. All comparisons show increased precipitation estimation for the middle western region of the catchment compared to the NZMS 1951-80 and Kerr 2005 surfaces. This area is near the Twin Stream, The Rest and Glentanner average annual precipitation totals, values that would not have previously been used.

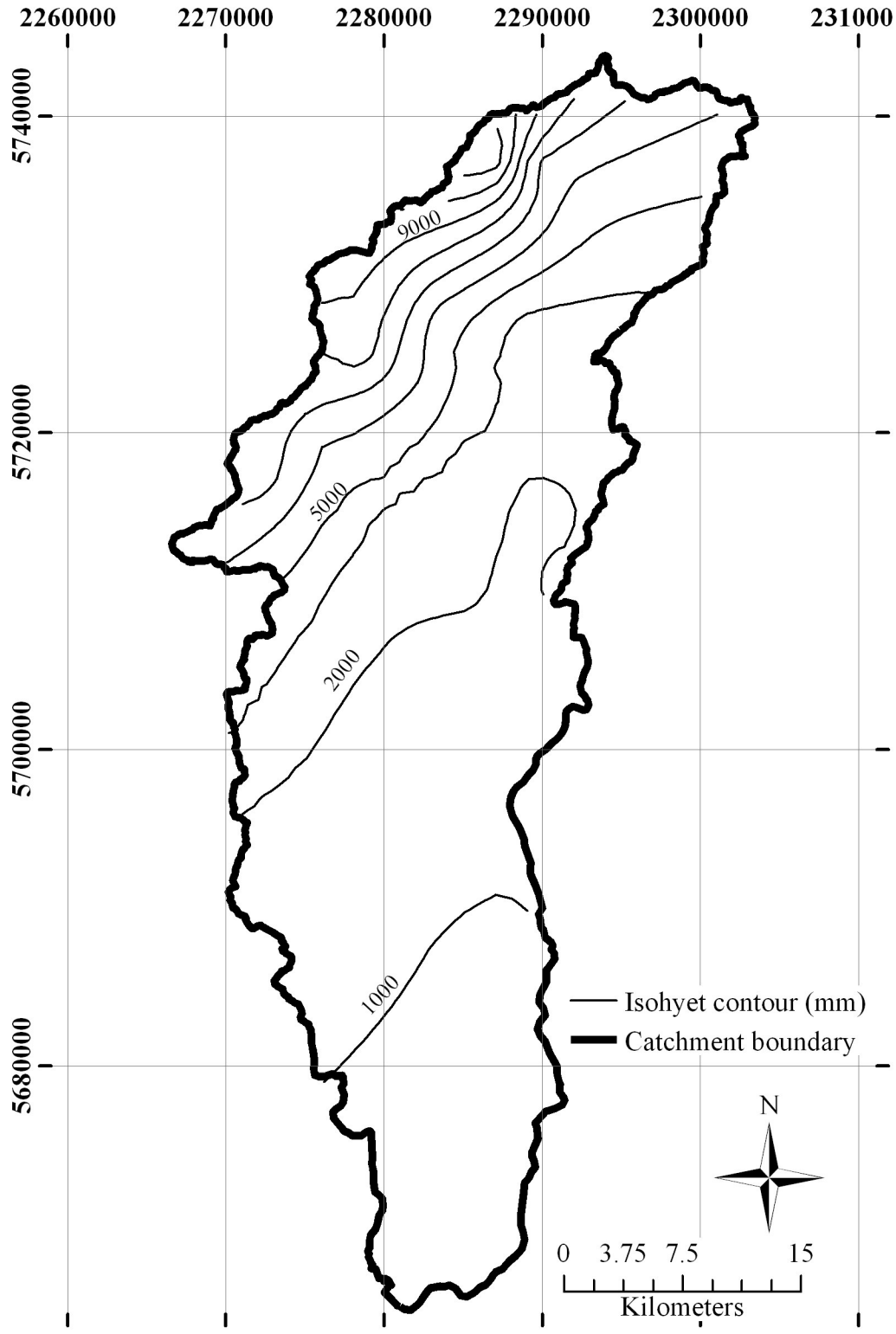

Figure 3-29. Isohyets determined through ordinary kriging of estimated average annual measured precipitation at measurement sites.

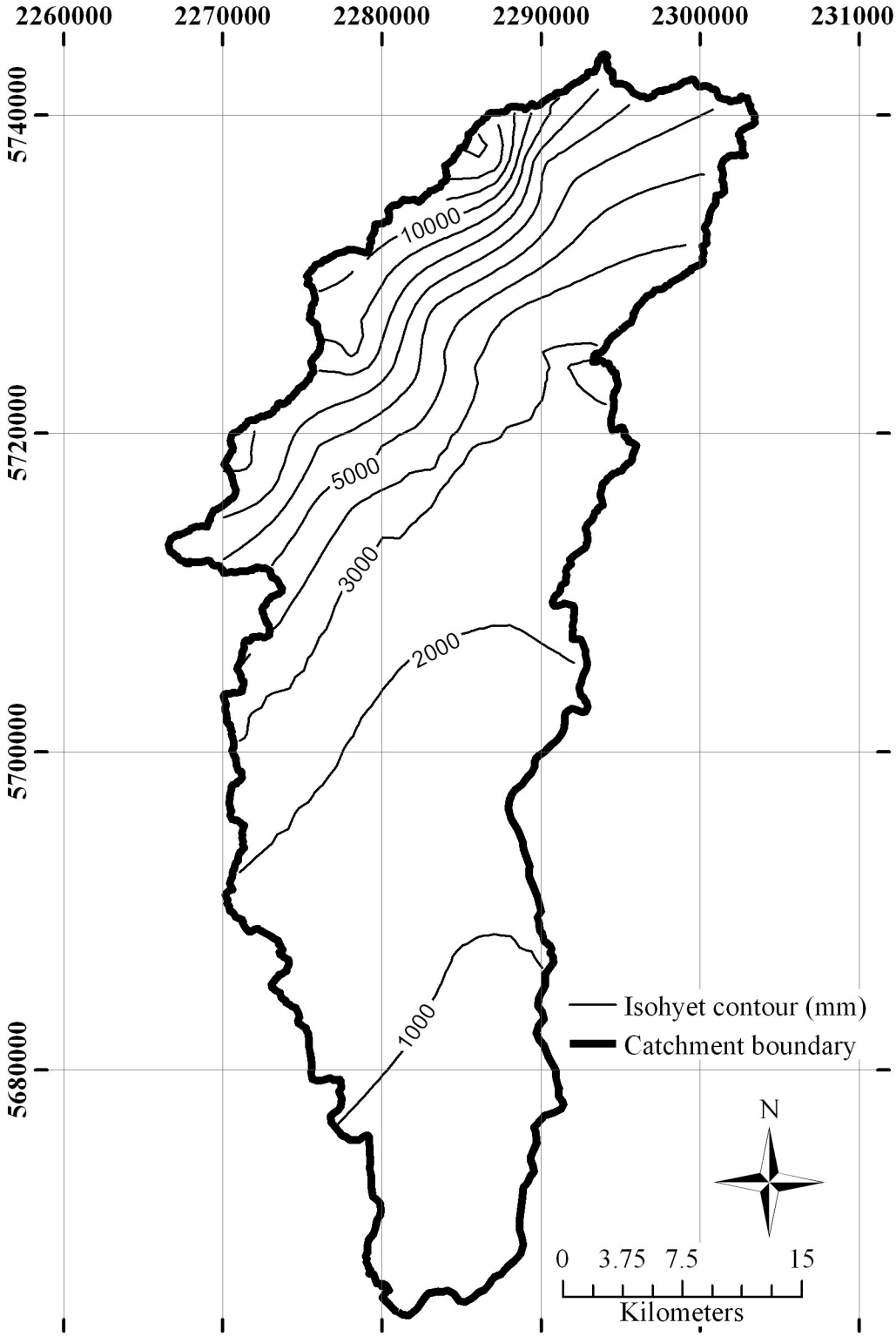

Figure 3-30. Isohyets determined through ordinary kriging of estimated average annual true precipitation at measurement sites.

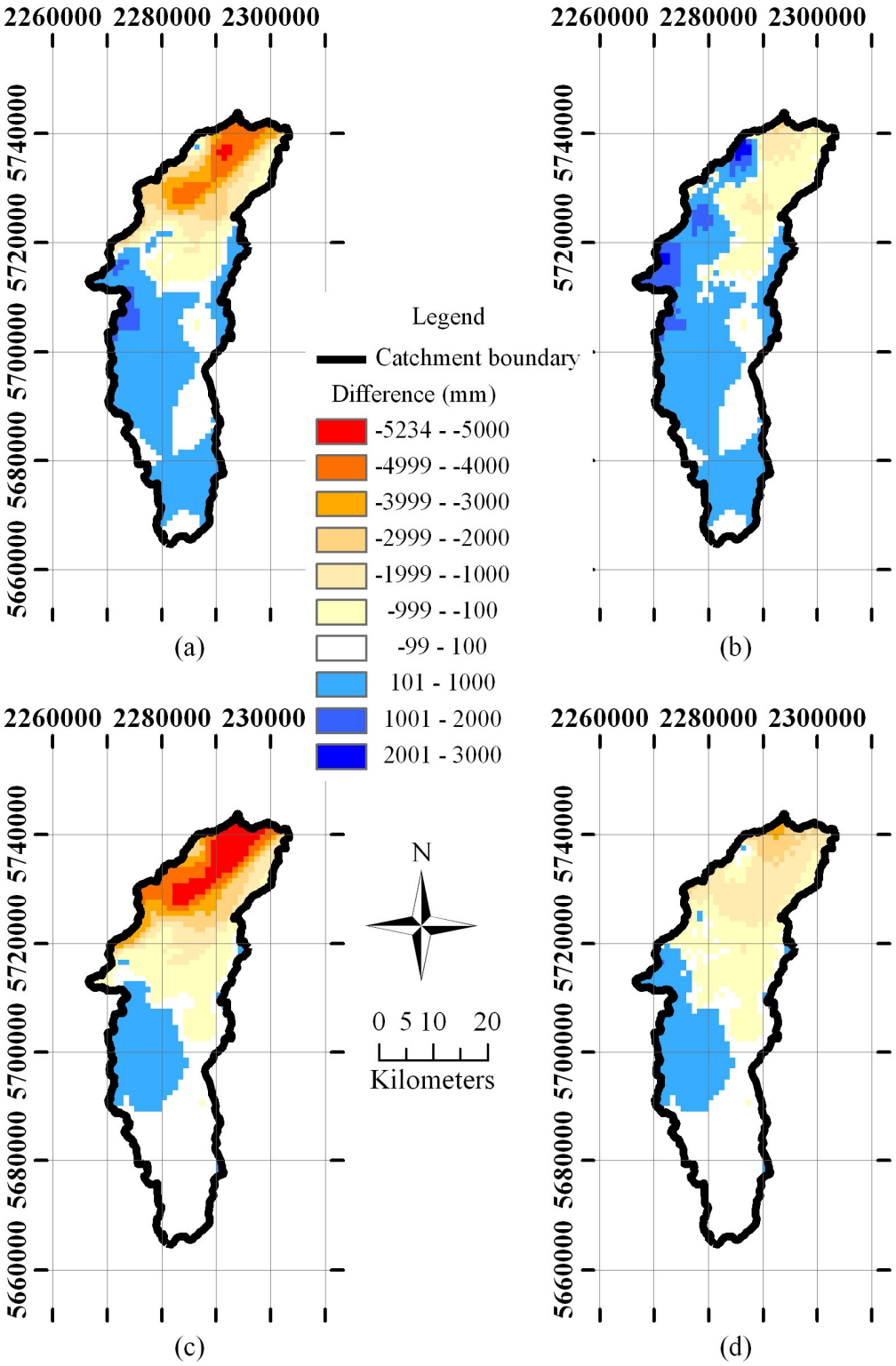

Figure 3-31. Difference maps of estimated average annual precipitation; a) estimated average annual true precipitation less NZMS 1951 - 1980 average annual precipitation surface; b) estimated average annual true precipitation less Kerr 2005 average annual precipitation surface; c) estimated average annual measured precipitation less NZMS 1951 – 1980 average annual precipitation surface; d) estimated average annual measured precipitation less Kerr 2005 average annual precipitation surface (Kerr, 2005; NZMS, 1985a).

3.7 Discussion

The estimated average annual true precipitation in the north west of the catchment indicates the region is an extreme precipitation area. Equivalent precipitation has been observed 80 km to the north east in the Cropp Basin (Griffiths and McSaveney, 1983b) and 200 km to the south west in Milford Sound (Henderson and Thompson, 1999). Both of these locations are considered to be the highest precipitation in their local region, and were both west of the main divide. There is no indication from the data gathered from within the Lake Pukaki catchment as to the location of the cross-mountain precipitation peak. Empirical estimation of the precipitation peak in the region by Griffiths and McSaveney (Griffiths and McSaveney, 1983a) suggested a value of 16 000 mm near the main divide, with the proviso that undercatch and high elevation wind flow were not considered in their analysis. This very high value was based on the main divide near Aoraki/Mt Cook being the first barrier to the predominant westerlies, and it being particularly high (relative to other Southern Alps barriers). In most other regions of the Southern Alps, mountain ridges windward of the main divide act as initial orographic barriers prior to an air mass reaching the main divide. It is also not always the case that the main divide is the highest barrier an air mass will meet as it passes over the Southern Alps. This identifies two characteristics of the Lake Pukaki catchment unique to a leeward catchment; the north west edge of the catchment is very high (relative to New Zealand elevations) and the north west edge of the catchment is the initial orographic barrier to the predominant westerly flow. The precipitation distribution used as input to a glaciological model of the Franz Josef glacier, immediately to the west of the catchment, suggests a precipitation peak considerably to the west of the divide, with the precipitation dropping to the leeward (Anderson, 2004). Such a regime is in line with that which has been observed elsewhere in the Southern Alps (Henderson and Thompson, 1999). The average annual precipitation estimated by Anderson (2004) at the north west edge of the Lake Pukaki Catchment is less than 5000 mm, considerably less than the 10000 mm to 12000 mm estimated here. This discrepancy may be accounted for by the possibility of a dual peak in the cross mountain average annual precipitation in this region, with a second peak close to, or just to the lee of the main divide. Modelling of orographic processes on idealised mountain forms raises the possibility of a dual peak in a precipitation transect with one peak to windward of the orographic barrier and a

second peak close to or even leeward of the orographic barrier (Sarker, 1966; Zängl, 2005, 2008). Such a regime requires a precise combination of topography and atmospheric profile that may occur in the Aoraki/Mt Cook region. A dual peak average annual precipitation transect may also occur through the combination of two different single peak distributions. Analysis of individual storms has found that the cross mountain precipitation peak moves as conditions change (Sinclair et al., 1997), so that it may be that the cross mountain precipitation distribution is bi-modal. Internationally the magnitude of the precipitation and the precipitation gradient are both very high. If measured in Europe, Australia or North America, the De La Beche and Hooker precipitation gauge sites would set new records (WMO, 2008). The estimated average annual precipitation in the north west of the catchment is the equivalent to the highest recorded in Africa and not far short of the highest recorded in Asia and South America (WMO, 2008).

The horizontal precipitation gradient in the north west areas of the catchment are estimated at over 1000 mm km^{-1}. Equivalent gradients are estimated for the central Southern Alps in the NZMS 1951 -1980 surface (NZMS, 1985a), either side of the precipitation peak in the Whitcombe-Rakaia transect (McSaveney et al., 1978) and along the lower Franz Josef Glacier region (10 km to windward of the main divide) (Anderson, 2004). Even higher gradients (~ 1200 mm km^{-1}) are estimated within the Upper Cropp Basin (Griffiths and McSaveney, 1983b). This shows that while the gradients are high, they are not unprecedented, at least within the Southern Alps of New Zealand. The generally lower precipitation of North America and Europe makes these extreme precipitation gradients highly unlikely with precipitation gradients estimated at 316 mm km^{-1} in the Olympic Peninsula (Daly and Taylor, 2000), 350 mm km^{-1} in the Seymour River near Vancouver (Loukas and Quick, 1996) and a maximum of 685 mm km^{-1} in the Swiss Alps from published 1961-1990 precipitation normals (MeteoSwiss, 2005). More extreme precipitation gradients have been observed on the San Rafael Glacier on the windward side of the Northern Patagonian Icefield with 1500 mm km^{-1} (Fujiyoshi et al., 1987) and 2080 mm km^{-1} near the summit of Koolau a leeward mountain range on the island of Oahu in Hawaii (Mink, 1960). As is the case with the precipitation magnitude, the precipitation gradient is globally high, but not extreme.

3.8 Conclusion

Precipitation observations have been recorded for locations throughout the Lake Pukaki Catchment for over a century. The locations, gauge life, gauge type and quality of observations have varied throughout this time. The Hermitage precipitation gauge may be considered the most important site in the catchment as a result of its long life and its position in a relatively high precipitation area. The high horizontal precipitation gradient at the location makes The Hermitage site extremely sensitive to site variations. Homogeneity analysis through comparison to records from other gauges in similar climate regions identifies The Hermitage record for the measurement period of 1948 to 2000 as being free of significant non-climatic variations. Wetting and wind induced undercatch for The Hermitage gauge has been estimated at 8 % of the observed catch. This is slightly more than would be expected at a rain-only gauge, but much less than has been determined for gauges where snow contributes a significant fraction of their catch.

Where available, precipitation records from gauges throughout the catchment have been located. 48 different gauges are known to have existed at forty three different sites. Data have been located for 38 of these gauges. Where possible a 1971 to 2000 precipitation normal has been generated for these sites. This has involved estimation of precipitation for periods when no record is available. This estimation was enabled through significant correlation to nearby sites with records that extended into the missing periods. For daily records correlations were based on monthly totals, for storage gauges, correlations were based on measurement periods. Precipitation normals ranged from 652 mm at the outlet of Lake Pukaki, to 5441 mm half way up the Tasman Glacier. The use of correlations has introduced error into the determined normals. This error has been statistically determined and range from 0.3 % for The Hermitage (which was missing 20 months from the 360 required) to 1.9 % for Sealey Village (which had just 17 of the 360 required). Measurement errors were determined for each site. At manual sites this was based on half the smallest scale division and the number of measurements taken. As such, storage gauges had a lower measurement error (0.05 % to 0.1 %) than daily gauges (0.2 % to 1.5 %). Tipping bucket gauge measurement error was based on the standard calibration check of being within 1 tip in 40 (2.5 %). Estimates of undercatch have been prepared for all sites. This estimate has largely been subjective through the consideration of gauge orifice heights, snow

fraction of the gauge catch, and gauge exposure to wind. Where possible, wind and temperature data at Aoraki/Mt Cook has been used to assist with estimation of wind induced gauge catch at sites with daily data. Values between 6 % (at the Lake Pukaki outlet) through to 16 % (half way up the Tasman Glacier) were estimated. Wetting errors were subjectively estimated based on likely precipitation frequency and depth of the gauge. Values as high as 4 % were estimated for the 2 m high gauges located in the drier regions of the catchment. Total undercatch was estimated as high as 18 % for a 2 m high storage gauge in an area with a significant proportion of frozen precipitation and high total precipitation. The highest error estimate (measurement plus random) was for the site with uncalibrated automatic measurement and no record within the 1971 to 2000 period.

An assessment of available gauge records and a likely precipitation field in the catchment enabled the informed of ten new gauges, with eight in previously poorly gauged precipitation zones. These storage gauges were monitored for over a year with measurements taken every month if possible, but at least every two months. Correlations to permanent gauges enabled estimation of 1971-2000 precipitation normals for eight of the sites. Measurement errors, random errors and undercatch estimates were generated for each site. Three of the sites returned estimated average annual true precipitation (including undercatch estimate) totals in excess of 8000 mm, more than has previously been observed in the catchment confirming the high magnitude estimates that have been made in the past for the catchment.

Two 1971 to 2000 average annual precipitation surfaces have been prepared for the catchment based on all estimated normals. One map is of measurement totals and one is for true totals (which accounts for undercatch). The interpolated surfaces show a strong south-east to north-west trend with the precipitation gradient increasing as the north-west side of the catchment is approached. This is in agreement with previously established average annual precipitation surfaces of the catchment. The high precipitation estimates determined in the north-west of the catchment are in conflict with modelled precipitation immediately to the west of the catchment. This disparity questions the application of a general Southern Alps cross–mountain precipitation profile to the Aoraki/Mt Cook region. A dual peak profile may explain this disparity. The precipitation magnitudes estimated within the catchment are equivalent to high precipitation regions elsewhere in New Zealand and approach the magnitudes determined in notably high precipitation regions of the world. The horizontal

precipitation gradient is also very high. Few high density precipitation gauging networks return similar gradients. Other than in New Zealand, equivalent values have been determined in Hawaii and Patagonia, both notably extreme precipitation locations.

The new gauge measurements have provided extension of a validated precipitation surface for the Lake Pukaki catchment. The measurements and surface confirm the upper catchment as being a high precipitation region with a steep horizontal precipitation gradient away from the orographic barrier. Consideration of undercatch at gauge sites presents a similar precipitation distribution structure within the catchment with proportionally elevated values throughout. In the northwest of the catchment this leads to an estimated extra 2000 mm of precipitation, a significant quantity, even considering the small area it applies to. The estimated true precipitation surface should prove a valuable resource for hydrological and glaciological applications within the catchment.

4 Wind dependent precipitation distribution

4.1 Background

Estimation of the spatial distribution of precipitation is becoming increasingly important as input to hydrological models, and for validation of climate models (Ahrens, 2006; Garen, 1995; Hewitson and Crane, 2005). In addition it is of value directly to land users. In the Lake Pukaki catchment, these include farm labourers, conservation workers, recreationists (including, but not limited to, skiers, climbers, hikers, tourists, mountain bikers, fisher people, hunters), guides for recreational activities, and land managers (for both farm and conservation land). Down valley the hydrological information (river flows, lake levels, soil moisture content) derived from the spatial precipitation data is of value to the same user group as well as to irrigation and hydro-electric managers. This vast network of people use spatial precipitation information in a number of different ways. For some, long term data is required to understand annual and seasonal variations for planning purposes. Other people need to know what precipitation has fallen over the more recent past for flow forecasting, avalanche forecasting, or selection of specific locations to undertake an activity (e.g. where has new snow fallen for skiing).

The rate of change of precipitation fields and the temporal scale of user activities means that spatial estimates for as short a time period as possible are of most value. The daily resolution of the majority of the precipitation gauges in the Lake Pukaki catchment (historic and current) provides a logical limit to this temporal scale.

The aim of this chapter is to provide a method of deriving improved daily spatial precipitation estimates for the Lake Pukaki catchment through the consideration of synoptic wind flow. This is to be done in a manner that may be applied using publicly available historic, near real time, or forecast point precipitation data, thereby being available for all users.

At the simplest level, spatial precipitation estimation in an ungauged region is established through consideration of observed precipitation at a gauged site in combination with a known horizontal precipitation gradient. In areas with low horizontal gradients simple distance weighted averaging may be applied as has been done for Alberta, Canada (Shen et al., 2001) and Denmark (Jansson et al., 2007). In mountain regions, where spatial variability is not well represented by the gauge sites,

such averaging may lead to large errors. For instance in the Lake Pukaki catchment there are no operating gauges between Aoraki/Mt Cook village and Franz Josef. Distance averaging from these two sites means that precipitation estimates at any point between them cannot be greater than that observed at either site. This is clearly not often the case as can be seen from the average annual precipitation distribution derived in the previous chapter. One common approach in mountain regions is to use elevation/precipitation relationships to estimate remote precipitation. Such precipitation lapse rates have been widely used for daily precipitation interpolation around the world. For example Garen (1995) established short period (7 to 28 day) precipitation-elevation relationships from observations and then applied them when preparing daily precipitation fields in the Big Wood River watershed in Idaho, U.S.A. In Norway, Mohr and Tveito (2008) used two precipitation-elevation gradients when preparing daily precipitation maps, one for areas below 1000 m, and one for above 1000 m. Hofierka et al. (2002) take a slightly different approach whereby daily precipitation fields for Switzerland and Slovakia were generated using a spline interpolation which incorporated a spatial precipitation scaling factor derived from elevation. These methods work well where a clear precipitation/elevation relationship exists, but as spatial resolutions decrease below 5 km, such relationships are found to be less robust (Sharples et al., 2005) and for shorter time periods (24 hours or less) the relationships become increasingly variable (Haiden, 2008). Another approach is to use a spatial precipitation scaling factor based not on elevation, but on a long term average precipitation distribution. It is this approach that was considered the most successful for preparation of daily precipitation grids for New Zealand (Tait et al., 2006). Similarly, interpolating precipitation based on the average annual precipitation distribution rather than an elevation gradient was found to improve snow storage estimates in the Lake Pukaki catchment (Kerr, 2005).

Statistically, the error of a population average, as an estimate of a sample average, increases as the sample size reduces. In the same way, the likelihood of a long term average precipitation distribution being representative for time periods less than the period from which they were prepared, decreases as those time periods reduce. This situation may be improved by refining the conditions under which the long term average applies, and using a different long term average for each condition type. Examples of commonly used condition types are seasons, months, climate types, or wind directions. The condition type used depends on availability of condition

information, and the variability of distribution with respect to the condition. In areas with highly seasonal precipitation distribution (e.g. monsoonal, continental or tropical) the use of monthly or seasonal precipitation distributions is likely to be an improvement over annual distributions. For this reason, large scale precipitation distributions are frequently provided at a seasonal and/or monthly level (e.g. Daly et al., 1994; Frei and Schär, 1998). In comparison to the European Alps, the seasonality of New Zealand's Southern Alps precipitation is not as pronounced (Sturman and Wanner, 2001) indicating that derivation of daily precipitation distribution from seasonal or monthly climatological distributions may not be as effective as in Europe. Utilising climate-type precipitation distributions appears more appropriate for the Southern Alps where precipitation predominantly originates from air flow-orography interactions with limited seasonality. Such an approach has proved effective in central Greece (Mamassis and Koutsoyiannis, 1996), Germany (Bardossy and Plate, 1992) and eastern United States (Hay, 1991). Use of synoptic classing was suggested by Tait et al.(2006) as a method of improving the New Zealand national daily precipitation distributions generated through spline interpolation of observations. In New Zealand the Kidson synoptic classifications (Kidson, 2000) provide 12 synoptic classes derived from cluster analysis of 12 hour synoptic analyses from the NCEP/NCAR dataset (Kalnay et al., 1996). Regional precipitation anomalies associated with the three main synoptic groupings identified a statistically significant difference (at the 0.95 level) for just one of the groupings. This effectively reduces the 12 synoptic classes down to two precipitation-relevant classes; those with westerly flow across the South Island, and those without. The climate typing is also limited in application to catchment scale processes in that the types are derived from a much larger region encapsulating the whole of the New Zealand region. This means that spatial positions of the climate types can vary by hundreds of kilometres without affecting the typing, and yet radically change the flow strength and direction over any one individual catchment. From this point of view, considering synoptic wind direction across the location of interest, rather than the general synoptic type provides a more spatially robust indicator of flow. This also provides a closer link to physical precipitation processes. In line with this and with respect to land areas adjacent to oceanic regions, Sweeney and O'Hare (1992) considered wind direction and exposure the principle control on mesoscale precipitation distribution at single day time intervals. Similarly Ndiaye et al. (2008) considered low level flow the most appropriate climate parameter

available from a global climate model for prediction of rainfall in the Sahel region of Africa. Such wind classed precipitation distributions have indeed enabled improved understanding of precipitation processes. Some examples of its application include; improved runoff modelling in Sweden (e.g. Johansson and Chen, 2003, 2005), the identification of areas of orographic influenced precipitation in Scotland (Weston and Roy, 1994), the improved representation of known orographic precipitation effects in The Rhine (Gysi, 1998), improved short-period forecasts for England (Hill, 1983) and improved nowcasting of orographic precipitation in the Italian Alps (Panziera and Germann, 2008). These examples highlight the value of wind classed precipitation distributions in regions where orographic precipitation is important and hence wind direction has a strong effect on the distribution. Following these examples, with the view to provide precipitation distributions applicable at the daily level for operational and academic use, wind classed precipitation distributions have been prepared for the Lake Pukaki catchment.

This chapter begins with an exploration of the relationship between wind direction and observed precipitation within the catchment, leading to a classification of wind directions. The derivation of new daily precipitation data from gauges installed for this study is then described. The wind-classed relationship between precipitation at sites with available daily data (including those gauges installed for this study) and three reference sites is then investigated. Next, a description of the preparation of precipitation fields from these relationships is provided. Lastly, an explanation of the use of these fields to provide an estimation of the precipitation at any site in the catchment, or the entire catchment, given the synoptic wind direction and precipitation at one or all of the reference sites, is given.

4.2 The classification of Wind directions based on precipitation

Wind direction for the region was obtained from the NCEP/NCAR reanalysis data (Kalnay et al., 1996). Wind observations taken at Aoraki/ Mt Cook Village were not used as the valley bottom location is unlikely to be representative of the synoptic conditions. The NCEP/NCAR data provides estimates of a variety of climate variables at 2.5^{o} intervals throughout the world. The variables are generated by a global climate model that has been constrained by climate observations. The NCEP/NCAR data

starts in 1948 and continues through to present time. The reanalysis data is provided at six hour intervals and at 17 different pressure levels. Two of the variables generated are wind speeds flowing parallel to the lines of latitude (zonal) and wind speeds flowing parallel to the lines of longitude (meridional). A positive zonal wind speed indicates a westerly wind (blowing from the west). A positive meridional wind indicates a southerly wind (blowing from the south). These wind vectors enable the wind direction (θ) to be determined through trigonometry:

$$U_s, U_w > 0 \quad \Rightarrow \theta = 180 + \tan^{-1}\frac{U_w}{U_s} \qquad \textbf{4-1}$$

$$U_s, U_w < 0 \quad \Rightarrow \theta = -\tan^{-1}\frac{U_w}{U_s}$$

$$U_s < 0 < U_w \Rightarrow \theta = 360 - \tan^{-1}\frac{U_w}{-U_s}$$

$$U_s > 0 > U_w \Rightarrow \theta = 180 - \tan^{-1}\frac{-U_w}{U_s}$$

Where

U_w = westerly wind component,

U_s = southerly wind component.

The 850 hPa pressure wind variables were used which relates to an elevation of approximately 1460 m. This elevation will vary with different climate types as the sea level pressure, the air temperature and the air density change. For example with a sea level pressure of 1020 hPa, sea level temperature of 20 ^{o}C and a lapse rate of -0.005 ^{O}C m^{-1} the 850 hPa level will be at 1550 m, whereas for a sea level pressure of 980 hPa, sea level temperature of 5 ^{o}C and a temperature lapse rate of -0.0065 ^{o}C m^{-1} the 850 hPa level will be at just 1150 m. In analysis of Southern Alps precipitation, low level blocking flows during a single storm have been found to be restricted below the 850 hPa level (Sinclair et al., 1997) and over an entire year were largely restricted to below 1000 m (McCauley and Sturman, 1999). This indicates that 850 hPa winds are high enough to be indicative of the general synoptic flow, but low enough to represent the air mass that interacts with the mountain barrier.

Average daily zonal and meridional winds are available as standard NCEP/NCAR analysis products. Their dates were advanced by one day to convert from midnight-midnight UTC to midday-midday NZST with the date stamp allocated from the

second midday. In this way the wind data are date stamped at the end of the period of interest in a similar manner to precipitation data. It should be noted that precipitation data is recorded for the 24 hours prior to 9 am (or 8 am for manual stations in summer) of the date stamp, whereas the wind data is for the 24 hours prior to midday of the date stamp, three (or four) hours later than the precipitation period.

Values for the 170°E 42.5°S grid point (100 km north of the catchment) and 170°E 45°S (100 km to the south) were obtained (see Figure 4-1 for locations). Wind directions were taken as the average of the two points when they were within 30° of each other. When they were not within 30° a null wind direction was allocated to the day. Conditions when the two grid points have a greater than 30° discrepancy indicate non-uniform flow over the Southern Alps, generally associated with a centre of high or low pressure.

For the 1971 to 2000 period, the relative frequency of days with 850 hPa NCEP/NCAR wind from each 10° wind direction is shown in the wind rose diagram Figure 4-2 a. This clearly shows the predominance of winds from the westerly quarter, with the highest frequency wind direction from 230° to 300°. The frequencies of 10° wind directions on rain days at The Hermitage, Jollie Hut and Braemar Station are shown on the same figure (b – d). Only observation days with non-zero recorded precipitation were considered. At each site the rain-day wind frequencies are slightly more northerly than for all days. For the station rose diagrams, daily precipitation magnitude is shown by the colour of the petals. These show that as well as an increased frequency, the more northerly wind directions have increased precipitation magnitudes. This is likely to be a combination of increased moisture from the warmer northerly flows, and a more perpendicular flow to the primary orographic barrier, increasing uplift rates and reducing the distance between the catchment and the uplift zones to windward. The wind speed does not show an increase towards the north for all days, indicating that it is not related to the increased precipitation. These diagrams also show the much greater magnitude of precipitation that is observed at The Hermitage compared to Jollie Hut and Braemar Station for the north westerly wind directions, but not for the south south westerly directions. Note that the precision of the observations at Braemar Station prevents the identification of sub millimetre precipitation events.

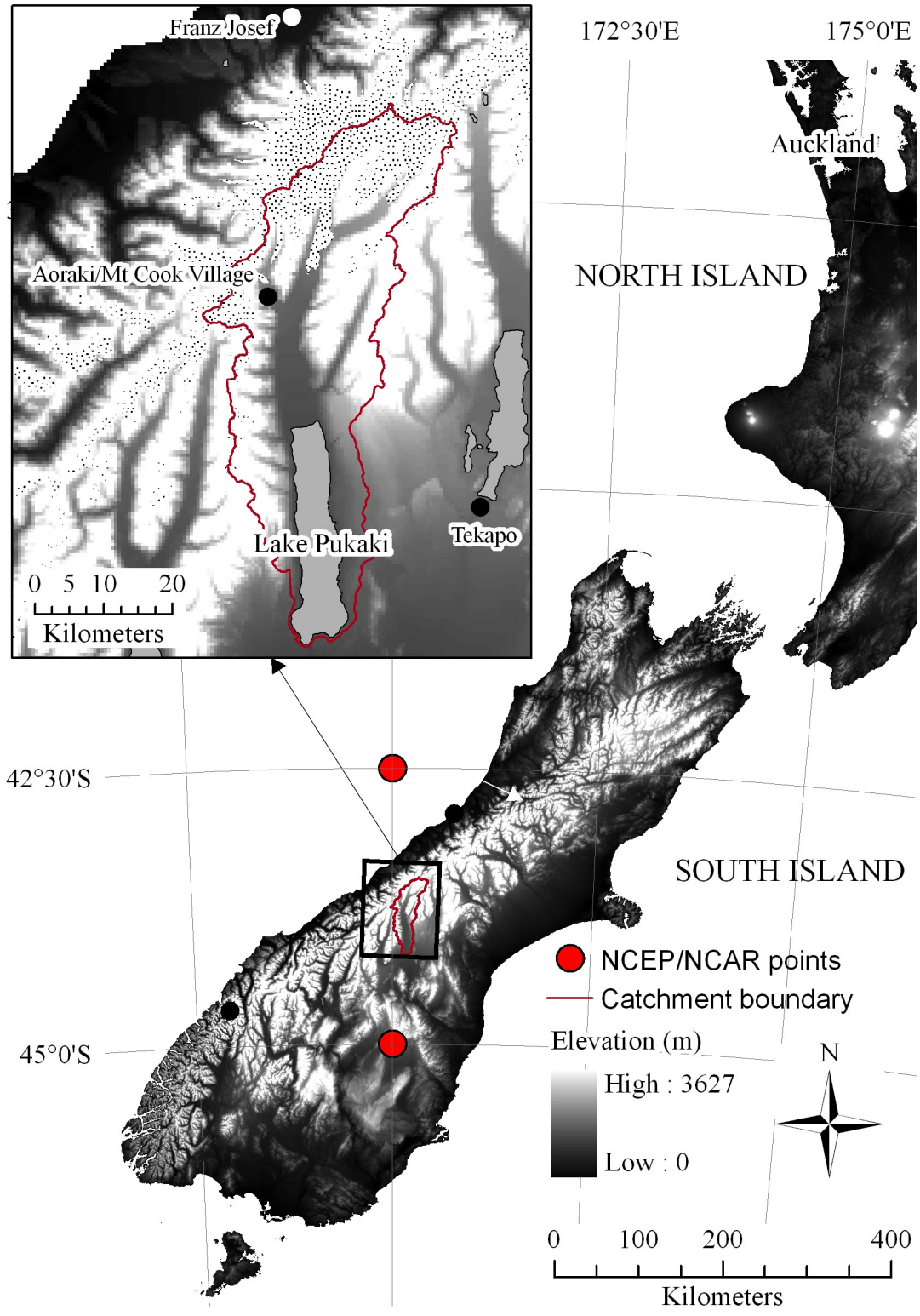

Figure 4-1. Location of NCEP/NCAR reanalysis sample points used in the wind direction class analysis.

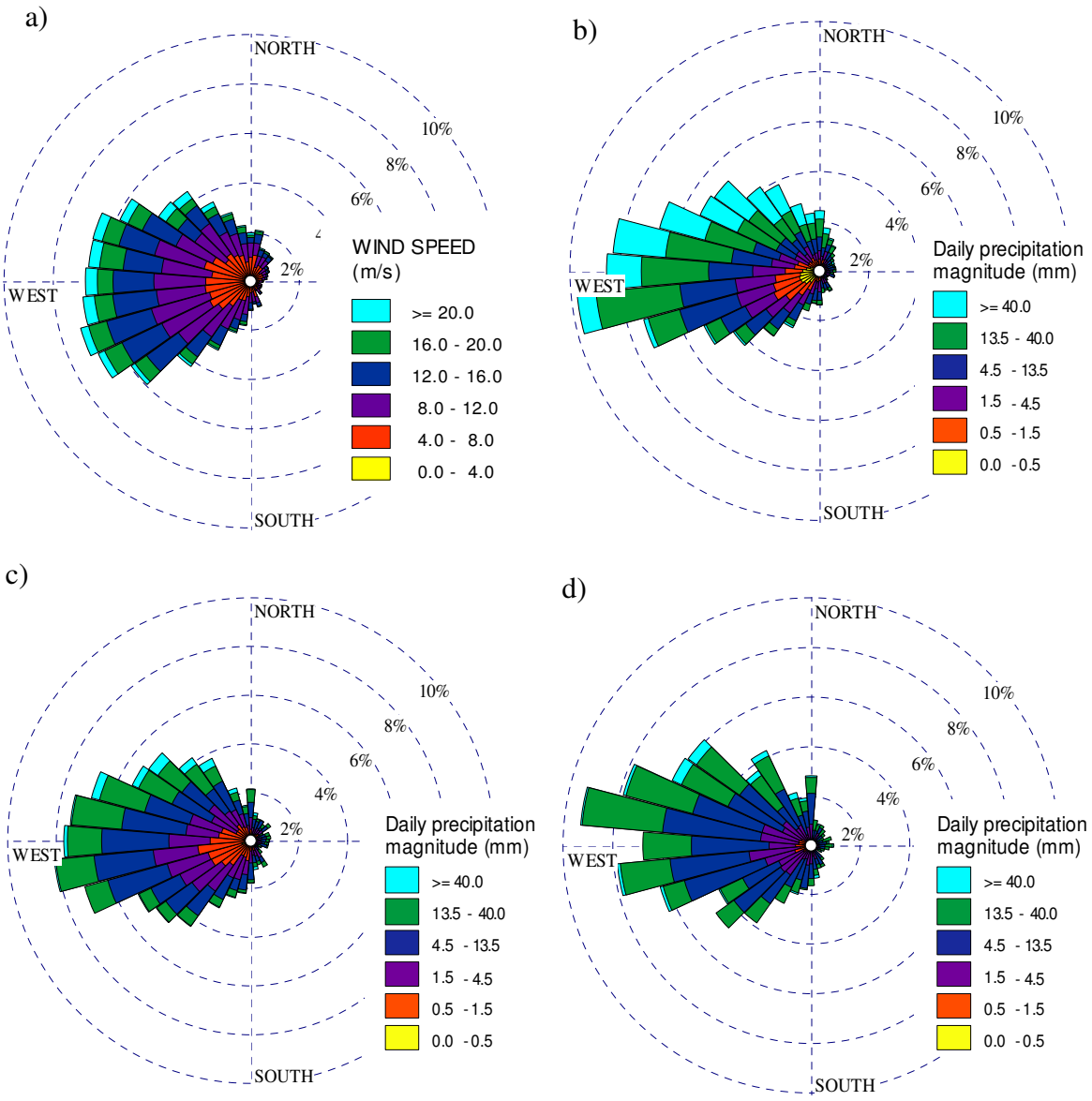

Figure 4-2. Relative frequency of 10° wind classes for the NCEP/NCAR 850 hPa wind direction for a) all days, and for rain days at b) The Hermitage, c) Jollie Hut, d) Braemar Station sites.

This analysis demonstrates the importance of wind direction on precipitation in the catchment. Precipitation frequency, magnitude and between-site precipitation relationships are all shown to be affected by the direction of the wind.

4.2.1 Cluster analysis of wind direction

It is clear from visual analysis of Figure 4-2 that there are some wind bands that have similar precipitation characteristics. Ideally, the different wind bands may be classed into groups that reflect these characteristics. A subjective analysis based on visual interpretation of The Hermitage precipitation-based wind rose diagram (Figure 4-2 b)

may lead to a division of wind into a high (255^{o} to 15^{o}) and low (15^{o} to 255^{o}) precipitation sectors, or alternatively into frequent (245^{o} to 295^{o}) and infrequent (295^{o} to 245^{o}) precipitation sectors. Assessment of each of the other sites may produce their own particular wind direction divisions. To enable an objective combined-site assessment of similar precipitation-affecting wind directions, a cluster analysis approach was undertaken. This was carried out using the computer application Statistica 7.1 by StatSoft™.

Initially, the median precipitation magnitude was determined for each 10^{o} wind class and site. The median was used instead of the average because of the non-normal distribution of precipitation at the daily level. The three-band centred mean of these medians was then allocated to each band. For example the 355^{o} to 5^{o} band was allocated the mean of the medians for the 345^{o} to 355^{o}, 355^{o} to 5^{o} and 5^{o} to 15^{o} bands. This was done to ensure clusters are weighted towards neighbouring bands to overcome the discretisation of the parameters into wind bands, when in reality wind direction is a continuum. The log of these mean values was then found. This was done to reduce the dominating effect of the high precipitation magnitude wind directions. Each site's values were then normalised by dividing by the site maximum. This was done to prevent The Hermitage values dominating the clustering. In this way each wind band had three parameters, one for each of the long term precipitation sites. These may be represented in three dimensional space as a point cloud. The clustering algorithm then determines a linkage tree based on the euclidean distance between clusters. At the first step, the euclidean distance between all points and all other points is found. The two points that are closest are combined as a cluster, with their linkage distance determined by their euclidean separation. The distance between this cluster and all other points is then found. This distance is determined as the average of the distance between each of the in-cluster points and other points. The next shortest linkage distance is found, and the second cluster is formed (or a third point is added to the original cluster). As new clusters are generated, their distance to other clusters is determined as the average of the distance between all between-cluster pairs. This process is repeated until there is one single cluster incorporating all points. The combining of points into clusters and the distance between clusters may be graphically represented through a linkage tree as shown in Figure 4-3. At the top level the clustering identifies a similar split as subjectively determined above. It has one

cluster for winds from 270° to 10° (north west sector) and the rest in the other cluster (east and south). The east and south cluster is divided at the next level to those bands either side of the northwest sector (10° to 20° and 260° to 270°), and a south and east group (20° to 260°).

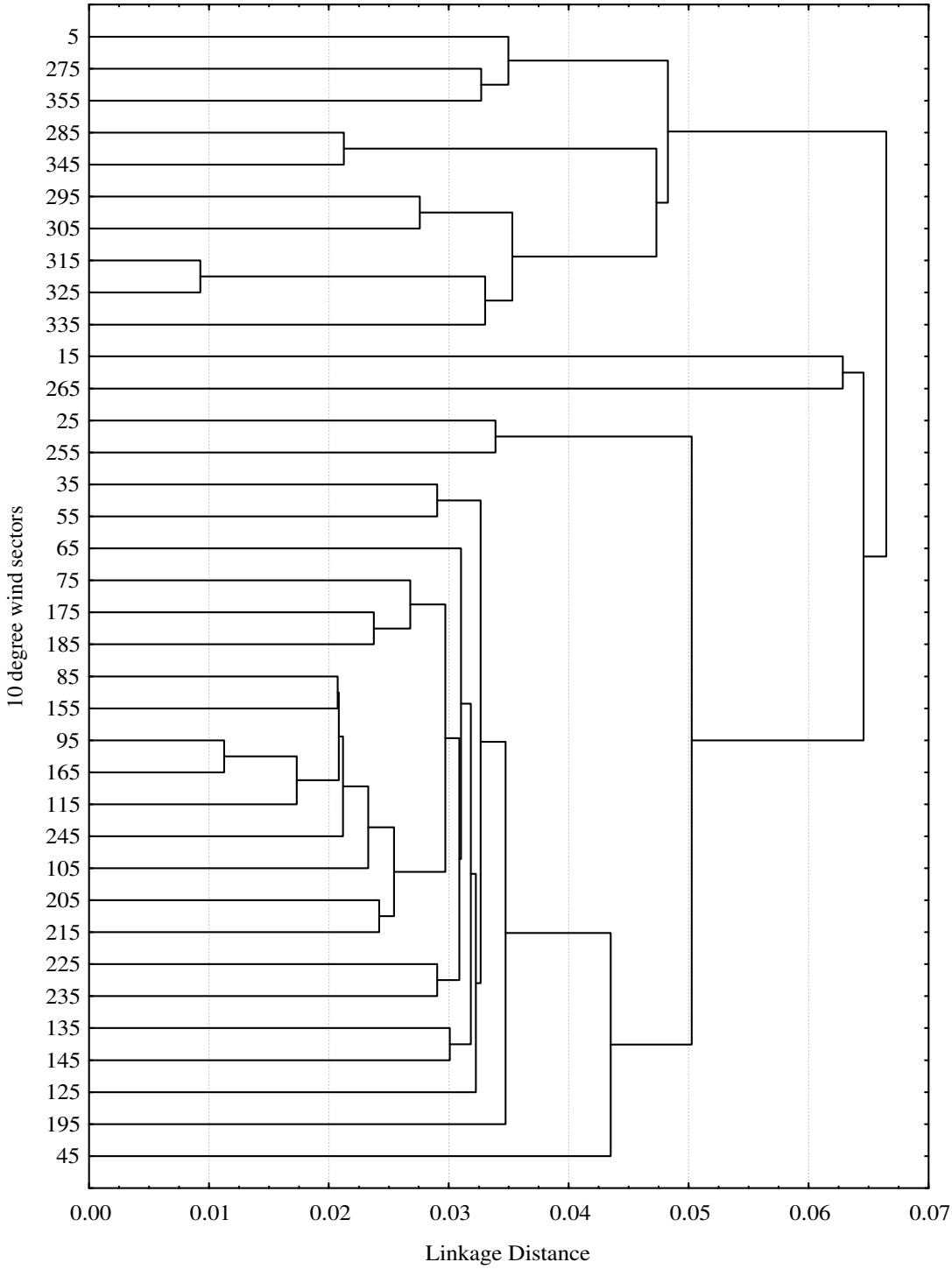

Figure 4-3. Linkage tree of three sector average median magnitudes from The Hermitage, Jollie Hut and Braemar Station. Linkage distance provides a relative measurement of how close each linked cluster is.

This south and east group has no further clear sector divisions with a central grouping of both east (60^o to 120^o) and south (150^o to 220^o) sectors intermingled and small single or paired clusters on the periphery of this. Through consideration of these clustering results in combination with the orientation of both the principal orographic barrier and the main catchment valley, five wind classes of continuous sectors were selected. The directions and their descriptive parameters are shown in Table 4-1. These wind sectors provide the basis for wind direction specific precipitation distributions.

Table 4-1. Rain parameters for different wind classes at The Hermitage.

Wind class	Direction	Relative frequency for all days	Relative frequency for rain days	Proportion of all rain	50 percentile of daily rain magnitudes (mm)
North west	270 to 340	0.28	0.40	0.67	21.6
North	340 to 10	0.05	0.07	0.10	18.9
East	10 to 200	0.14	0.13	0.05	3.00
South south west	200 to 250	0.20	0.13	0.03	2.00
South west	250 to 270	0.11	0.12	0.07	6.50
Unclassed	n/a	0.22	0.15	0.08	5.00

4.3 Wind classed precipitation

Daily rainfall data (24 hour accumulated rainfall prior to 9 am local time on the day of observation) were obtained from the twenty six historic and current gauge sites distributed across the catchment, including the eight new sites from this study. Figure 4-4 shows the location of the different sites used with site details in Table 4-2.
For each wind class the correlations between observed daily precipitation at catchment precipitation gauge sites and three reference sites were determined. The reference sites used were Mt Cook EWS (EWS stands for electronic weather station), Tekapo EWS and Franz Josef EWS. These stations have publicly available daily precipitation data at near real time (next day or better). These reference sites were used so that the wind-classed precipitation distributions may be used operationally by any interested party. Other nearby operational gauges are either not publicly available (Rose Ridge, Hooker Rd Bridge), or file data manually (Braemar, Guide Hill, Tasman Downs) leading to a delay of weeks to months before it becomes publicly available. Mt Cook-ECAN (ECAN stands for Environment Canterbury, the regional

government) data is also available publicly, and could have been used as an alternative to the Mt Cook EWS data. The Tekapo EWS site was used even though it is outside the catchment, as it returned better correlations to the southern catchment gauge sites in comparison to Mt Cook EWS. The Franz Josef EWS site was used as it provides a better relationship to precipitation occurrence in the upper catchment.

Table 4-2. Lake Pukaki catchment daily recording precipitation gauges.

Name	Map No.	Type	Agency	Start	Finish	Data source
Malte Brun Hut	1	90 day Cassella recording gauge	MoW	02/06/1967	20/07/1970	NIWA CliDB
Rose Ridge	2	Tipping bucket	Meridian	17/10/2002	17/10/2007	NIWA
Ball Hut	4	Recording rain gauge	MoW	23/08/1972	30/01/1979	NIWA CliDB
Hooker Hut	5	90 day Cassella recording gauge	DSIR	09/02/1962	31/12/1966	NIWA Archives
The Hermitage	12	Rain gauge	THC	02/06/1928	01/03/2000	NIWA CliDB
Mt Cook EWS	13	Tipping bucket	NIWA	30/03/2000	Current	NIWA CliDB
Mt Cook ECAN	13	Tipping bucket	ECAN	26/11/1989	Current	ECAN
Hooker Rd Bridge	14	Tipping bucket	Meridian	04/12/1993	Current	NIWA
Hooker Flat	15	Auto weekly rain gauge	Unknown	03/09/1960	01/03/1970	NIWA CliDB
Sealey Village	25	Rain gauge	Unknown	04/04/1969	01/05/1972	NIWA CliDB
Jollie Hut	34	Tipping bucket	NIWA	09/08/1972	21/12/1999	NIWA CliDB
Glentanner	36	Rain gauge	Glentanner	04/05/1967	01/04/1970	NIWA CliDB
The Rest	37	Rain gauge	Unknown	02/09/1959	01/04/1976	NIWA CliDB
Braemar Station	39	Manual 5 inch copper rain gauge	Braemar	01/12/1913	Current	NIWA CliDB
Guide Hill	40	Manual 5 inch copper rain gauge	Tasman Downs	03/10/1976	01/03/2000	NIWA CliDB
Tasman Downs	41	Manual 5 inch copper rain gauge	Tasman Downs	03/01/1977	Current	NIWA CliDB
Lake Pukaki No 1	42	Manual 5 inch copper rain gauge	Unknown	03/11/1952	01/02/1972	NIWA CliDB
Lake Pukaki, M.W.D.	43	Auto daily rain gauge	MoW	03/09/1969	31/12/1984	NIWA CliDB
Tasman Glacier	K1	Logging storage gauge	Kerr	01/04/2006	01/04/2007	This study
Rudolf Glacier	K2	Logging storage gauge	Kerr	01/04/2006	01/04/2007	This study
De La Beche	K3	Logging storage gauge	Kerr	01/04/2006	01/04/2007	This study
Ball Shelter	K4	Logging storage gauge	Kerr	01/04/2006	01/04/2007	This study
Murchison	K5	Logging storage gauge	Kerr	01/04/2006	01/04/2007	This study
East Hooker	K6	Logging storage gauge	Kerr	01/04/2006	01/04/2007	This study
Stocking Stream	K7	Logging storage gauge	Kerr	01/04/2006	01/04/2007	This study
Mueller Glacier	K8	Logging storage gauge	Kerr	01/04/2006	01/04/2007	This study
Jollie Stream	K9	Logging storage gauge	Kerr	01/04/2006	01/04/2007	This study

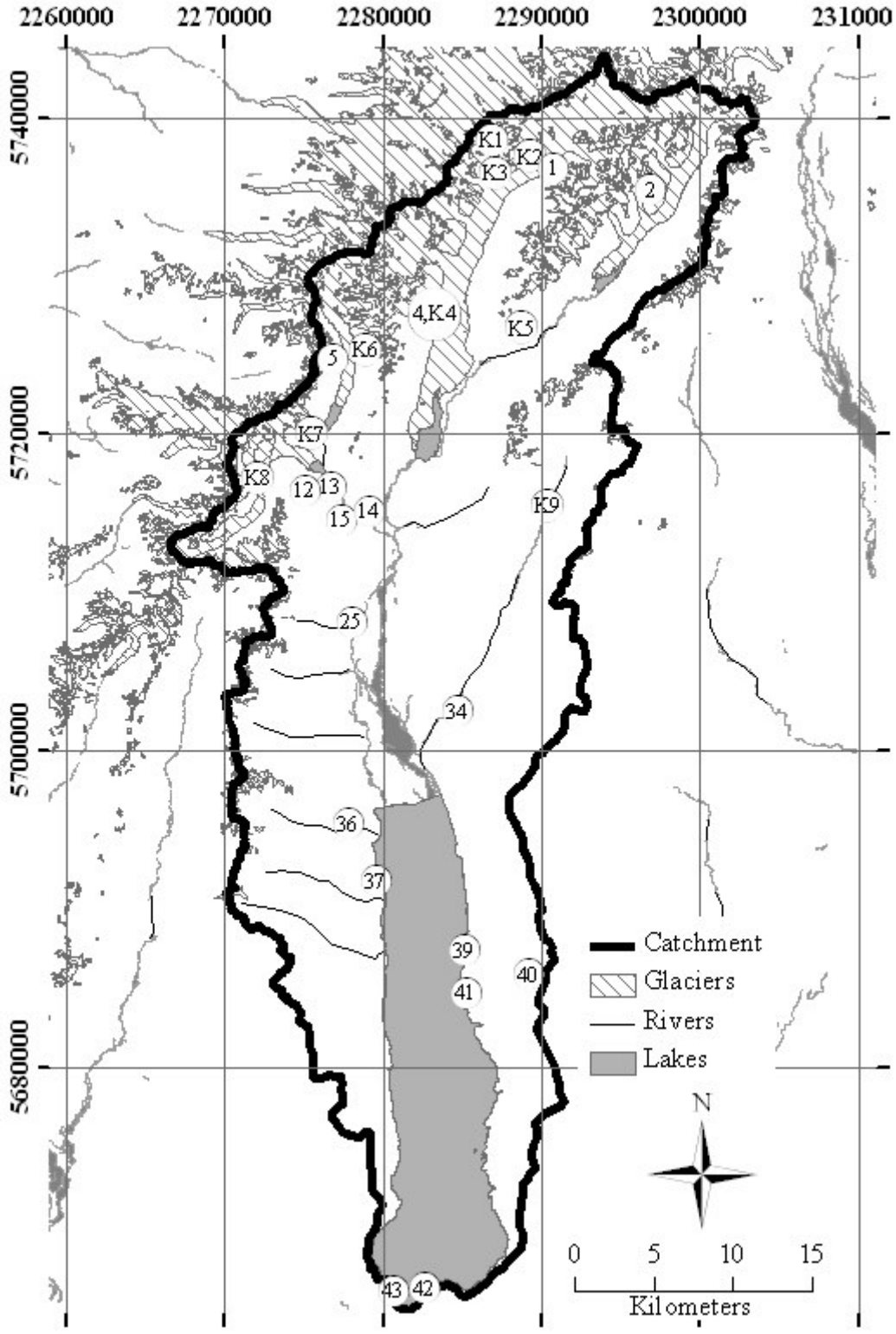

Figure 4-4. Locations of daily recording precipitation gauges. Site details are in Table 4-2.

Correlations between the reference sites and all other sites were determined for days when precipitation was observed at both. As with the monthly data analysed in the previous chapter, correlations were based on the log of daily precipitation totals at each site. The log transformation changes the frequency distribution from being strongly skewed, to an approximation of the normal distribution, required for the regression analysis. Figure 4-5 shows the daily Hermitage data frequency distributions after log transformation for three of the wind classes, together with the normal distribution based on the mean and standard deviation of the log data. Note that the gap in the log distributions at the low end is a function of the resolution of the observations.

One was added to each day's total precipitation so that sub-millimetre precipitation values converged on zero. For sites with a significant correlation at the 0.99 level, a regression line, forced through zero, was established. The gradient of this line provides a ratio of the log of the precipitation at a site of interest with respect the reference site when precipitation occurs at both sites.

For those sites that were not operating in parallel with the reference sites, ratios were established to sites nearby to the reference sites. For Mt Cook EWS this was The Hermitage site, for Tekapo EWS, this was Tekapo AS (AS stands for Air Safaris, the name of the company on whose land the weather station is sited), for Franz Josef EWS, this was Franz Josef manual, and Franz Josef THC. The Mt Cook-ECAN site operated for a time that overlapped both The Hermitage and Mt Cook-EWS. Using relationships between these three sites for the different wind classes, all established proportions to The Hermitage were able to be corrected to Mt Cook EWS. In the same way, relationships between Franz Josef THC, Franz Josef Manual and Franz Josef EWS enabled all Franz Josef relationships to be corrected to Franz Josef EWS. The low precipitation and precipitation gradient at Tekapo means the magnitude correction is less critical at this site. Correlations to Tekapo AS were taken as being the same as with Tekapo EWS.

For each site, wind-sector and reference site combination, the number of days of observations used for the regression, the ratio of the logs of precipitation, the correlation coefficients and the likelihood of precipitation were determined. The likelihood of precipitation was the proportion of the reference site precipitation days for which precipitation occurred at the site of interest.

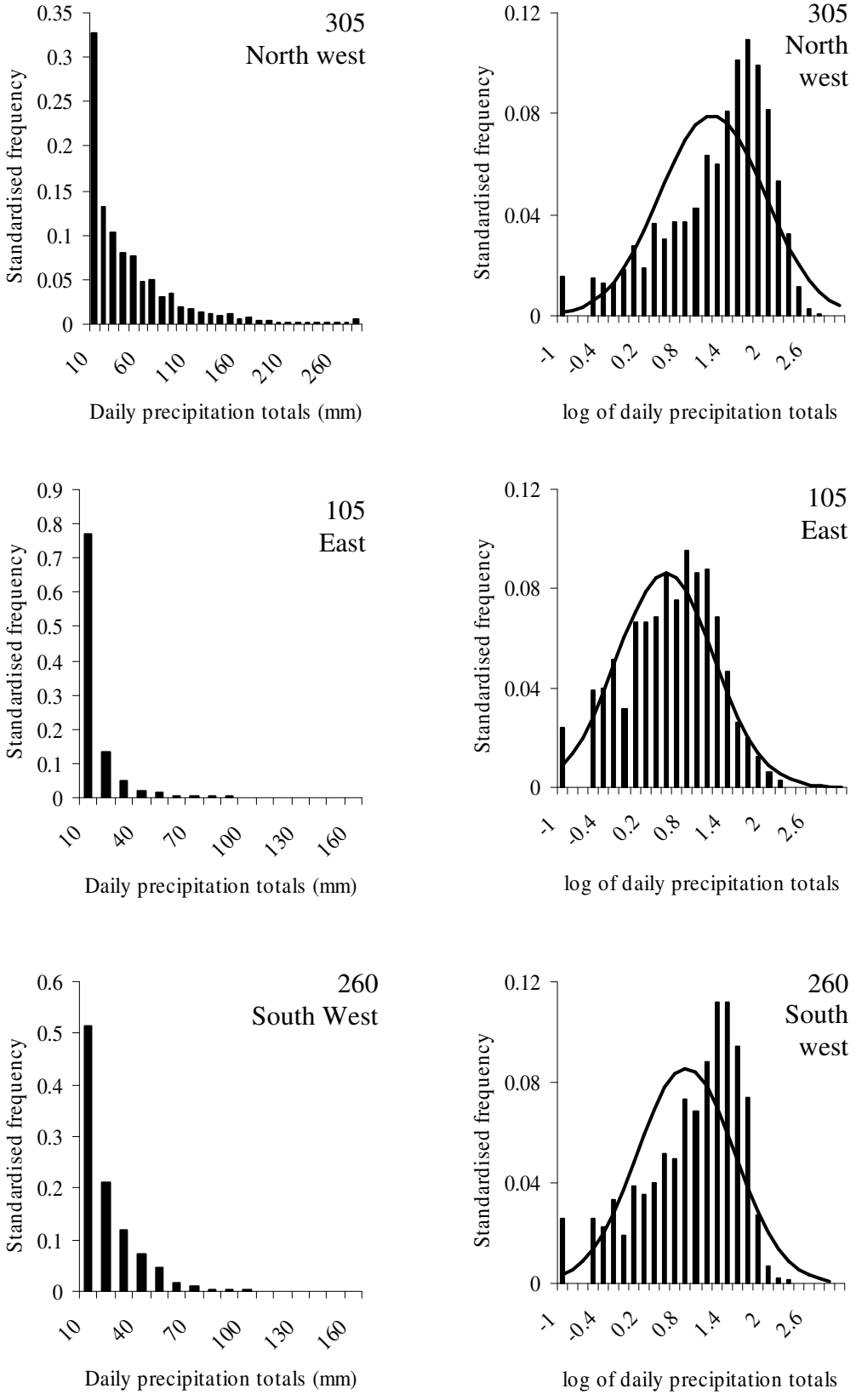

Figure 4-5. Standardised frequency distribution daily precipitation totals (left side), and of the log of daily precipitation totals at The Hermitage for three different wind classes, together with the normal distribution based on the mean and standard deviation of the log of the precipitation totals (right side).

Scatter plots and regression lines for each of these site pairs are shown in Appendix 2, together with tables of the number of observation days used in each regression.
For each reference site and wind class the ratios, correlation coefficients and likelihood of precipitation values were interpolated across the catchment using ordinary kriging with a spherical semivariogram with a nugget of 1 km, a partial sill of 30 km, and a major range of 60 km. This means that sites within 1000 m of each other have equal weighting, the weighting of stations decreases out to 30 km, then is at a constant low level out to 60 km beyond which stations have no influence. The kriging used a variable search radius of 12 sites and an output resolution of 1 km. Only sites that had a correlation significant at the 0.99 level, and five or more observations were used in the interpolation. Contours were prepared from the ratio interpolations at 0.05 intervals. A polynomial smoothing algorithm with a 10 km base was then applied to the contour lines to remove high frequency variations that are difficult to defend given the sparse sampling sites. Figure 4-6 to Figure 4-8 show plots of the ratio contours and likelihood of precipitation fields for each wind direction for Aoraki/Mt Cook, Tekapo and Franz Josef reference sites respectively.
The wind classed precipitation maps enable a comparative assessment of the precipitation distributions with regard to likelihood of precipitation, and precipitation gradients.

4.3.1 Likelihood of precipitation

The likelihood of precipitation fields show clear differences between the Tekapo fields, and the Franz Josef and Aoraki/Mt Cook Village fields. For the Tekapo reference site, given precipitation there the likelihood of precipitation at all other sites in the catchment is reasonably high, meaning that precipitation seldom falls at Tekapo without falling throughout the catchment. For the Franz Josef and Aoraki/Mt Cook Village reference sites, the likelihood of precipitation in the south of the catchment can be relatively low, meaning that it is not uncommon for precipitation to be occurring at Franz Josef or Aoraki/Mt Cook village, while there is no precipitation around the lake. For the south west and south south west wind directions, much of the catchment can be precipitation free when precipitation is observed at Franz Josef.

Reference site location

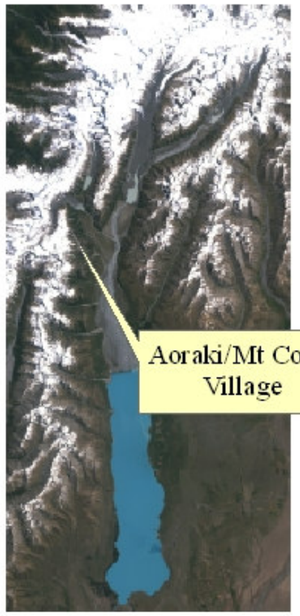

Landsat 7 ETM+ Image
Band 1 : Blue
Band 2 : Green
Band 3 : Red
Image obtained 31 December 2002
Image sourced from the
Global Land Cover Facility (GLCF)
http://www.landcover.org

To estimate the precipitation at a site:
1/ determine the precipitation, *p*, at Aoraki/Mt Cook Village,
2/ determine the synoptic wind direction,
3/ locate the site of interest on the relevant wind-classed map,
4/ determine the likelihood of precipitation from the background colour,
5/ determine the precipitation ratio constant, *c*, from the contours,
6/ estimate the precipitation using:

$$10^{c(\log p+1)} - 1$$

Precipitation ratio contour

Likelihood of precipitation

High : 1.0

Low : 0.3

0 12.5 25 50

Kilometers

North westerly

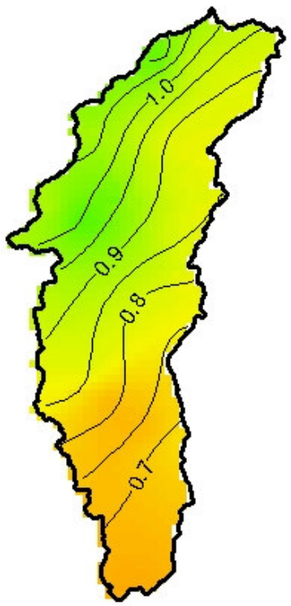

Northerly

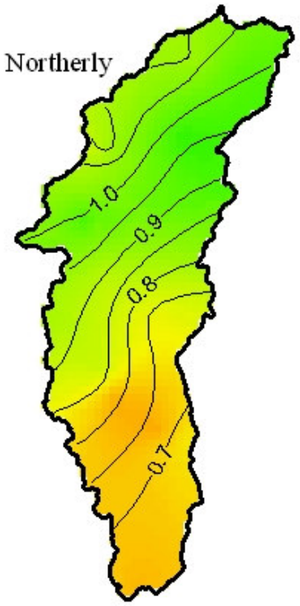

South westerly

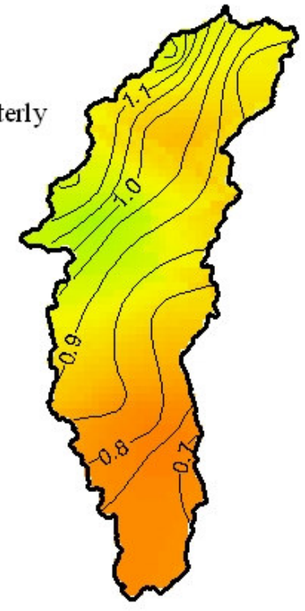

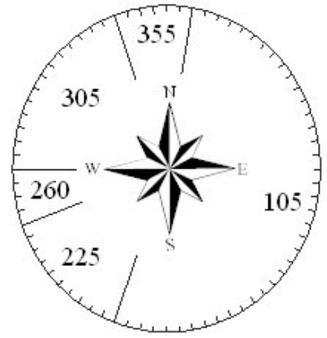

Easterly

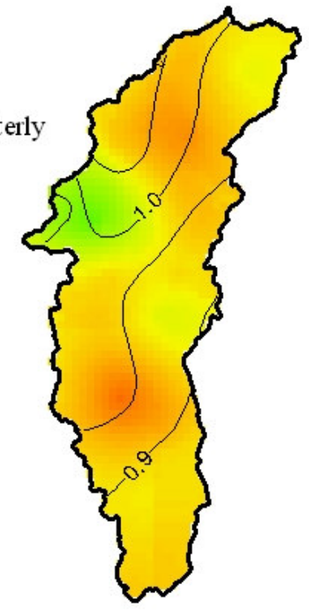

South south westerly

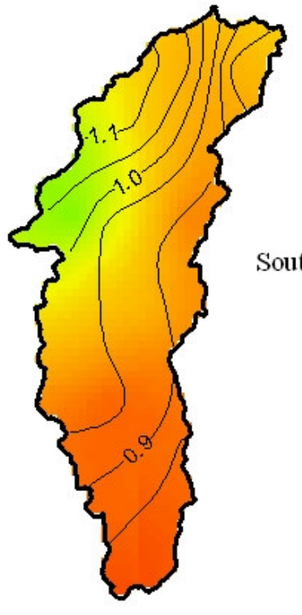

Figure 4-6. Precipitation distribution in the Lake Pukaki catchment for different wind direction classes. Contours represent the ratio of the logs of precipitation with respect to Aoraki/Mt Cook Village on precipitation days. Colour backgrounds indicate the likelihood of precipitation days given that precipitation is occurring at Aoraki/Mt Cook Village.

Reference site location

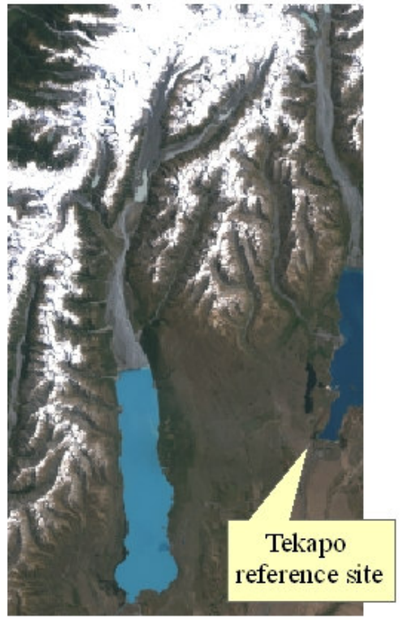

Landsat 7 ETM+ Image
Band 1 : Blue
Band 2 : Green
Band 3 : Red
Image obtained 31 December 2002
Image sourced from the
Global Land Cover Facility (GLCF)
http://www.landcover.org

To estimate the precipitation at a site:
1/ determine the precipitation, *p*, at Aoraki/Mt Cook Village,
2/ determine the synoptic wind direction,
3/ locate the site of interest on the relevant wind-classed map,
4/ determine the likelihood of precipitation from the background colour,
5/ determine the precipitation ratio constant, *c*, from the contours,
6/ estimate the precipitation using:

$$10^{c(\log p+1)} - 1$$

Precipitation contour

Likelihood of precipitation

High : 1

Low : 0.3

0 12.5 25 50

Kilometers

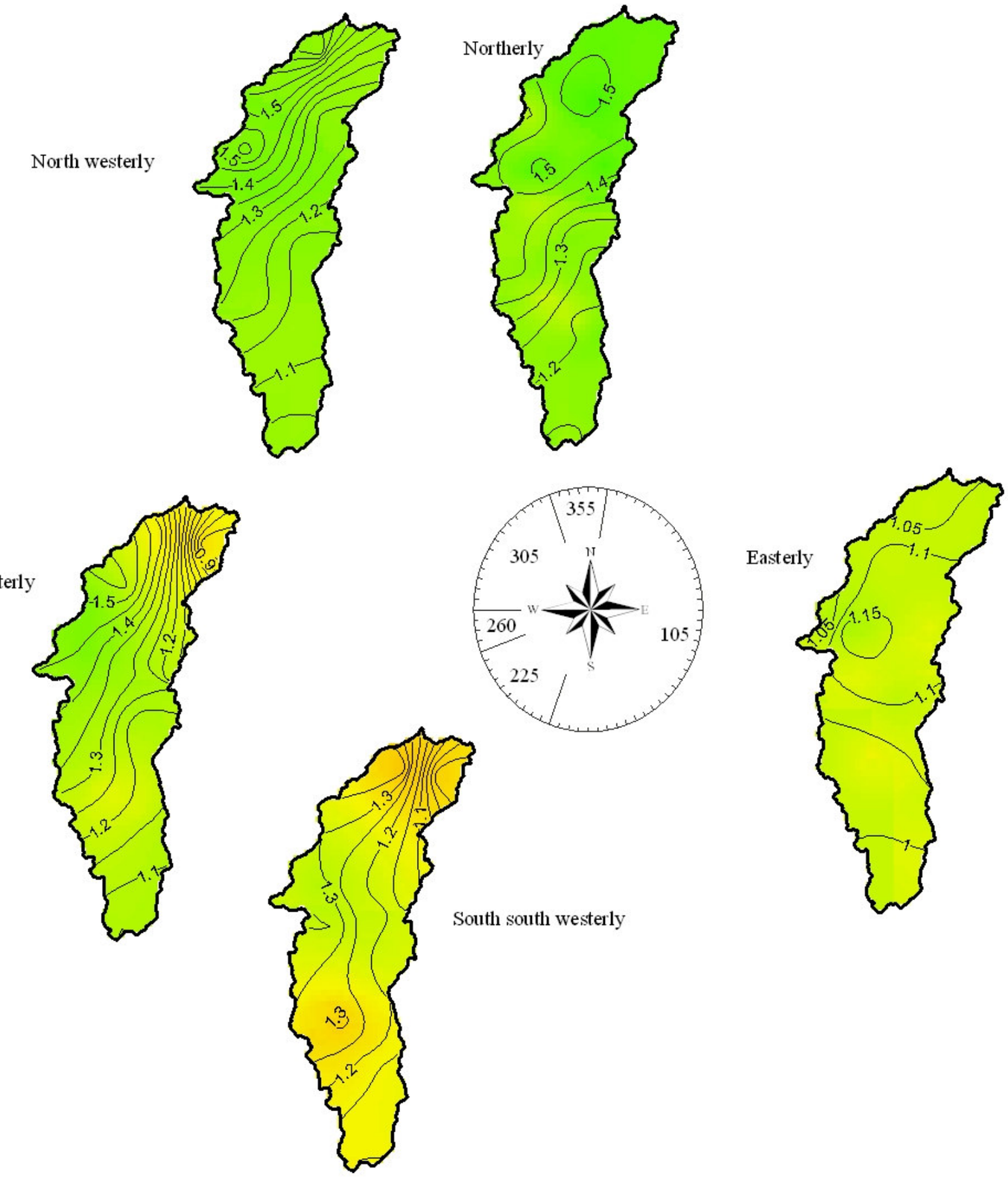

Figure 4-7. Precipitation distribution in the Lake Pukaki catchment for different wind direction classes. Contours represent the ratio of the logs of precipitation with respect to Tekapo on precipitation days. Colour backgrounds indicate the likelihood of precipitation days given that precipitation is occurring at Tekapo.

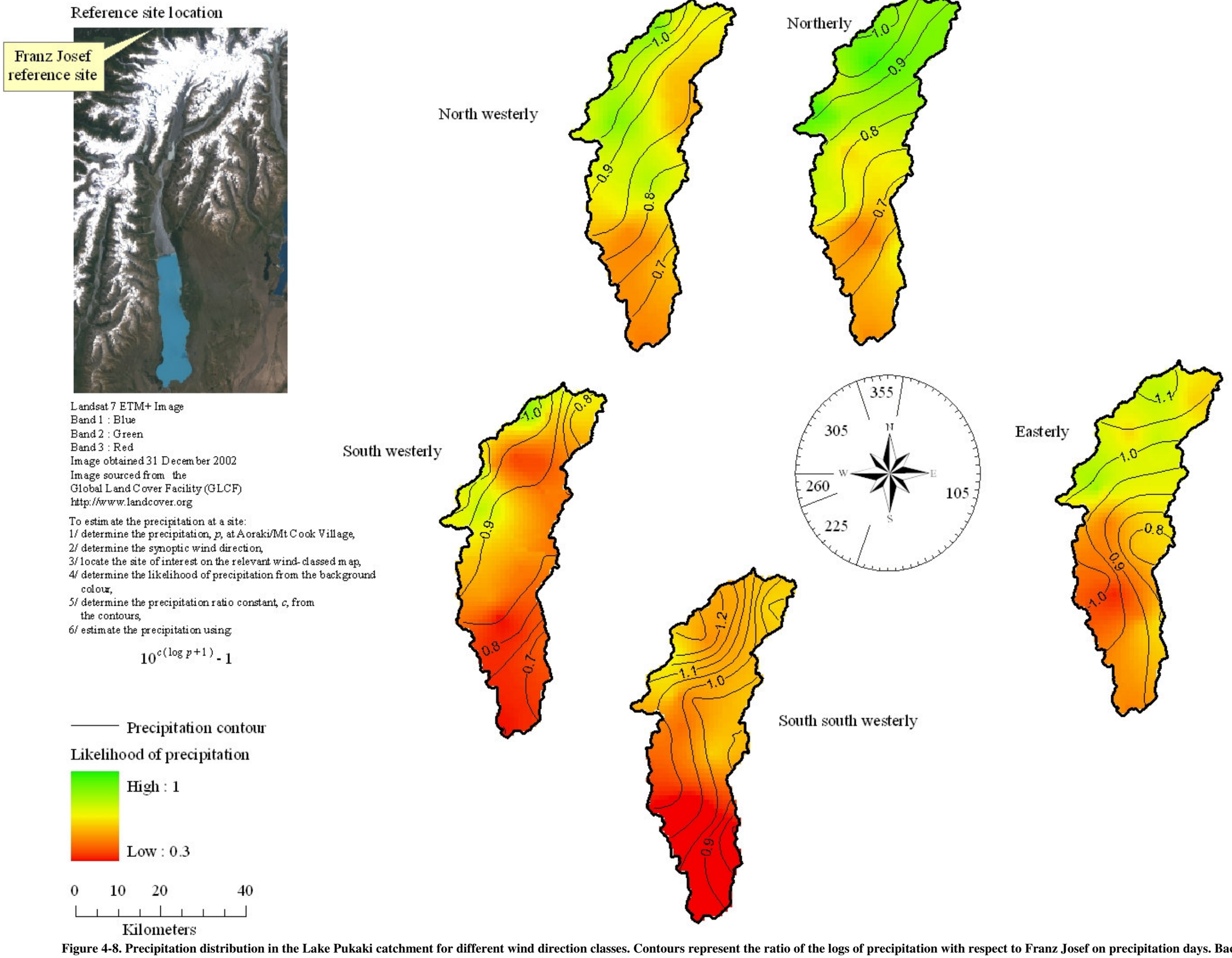

Figure 4-8. Precipitation distribution in the Lake Pukaki catchment for different wind direction classes. Contours represent the ratio of the logs of precipitation with respect to Franz Josef on precipitation days. Backgrounds indicate the likelihood of precipitation days given that precipitation is occurring at Franz Josef.

4.3.2 Precipitation gradients

The precipitation gradients are generally north west to south east in all situations. This may be in part attributable to the 24 hour limit on the precipitation observations. The very high frequency of westerly wind with respect to all other wind directions means that the likelihood of westerly precipitation occurring on any one day, including those classed to a different wind direction, is reasonably high. On these days the precipitation observed is biased to the westerly precipitation, leading to all of the wind-classed precipitation distributions also becoming biased. Even with this effect, the easterly wind–direction class is quite distinct from the westerly and northerly precipitation distributions with lower gradient magnitudes and less defined gradient direction. For this wind class the use of the wind-classed precipitation, as opposed to the all-direction average annual precipitation distribution will lead to the greatest improvement for estimating daily precipitation fields. More subtle differences exist between the precipitation gradients of the westerly and northerly precipitation distributions. As would be expected, the orientation of the precipitation gradients are slightly different for each wind-direction, though not as distinct as the wind directions themselves. This may indicate the influence of the barrier orientation on the precipitation distribution as well as the cross-class influence of the more frequent westerly precipitation events as discussed previously. The lack of observations leads to interpolation artefacts in some situations. For instance the observations from the isolated Rose Ridge site in the north east of the catchment leads to a very high precipitation gradient in that region for the south west and south south west precipitation distributions related to the Tekapo reference site. Without further sites in the region it is not possible to determine how accurate this gradient is. This highlights the limitations in estimating precipitation fields at a scale smaller than the observation site density.

4.3.3 Precipitation estimation

The precipitation distributions determined here enable daily precipitation estimates to be established for any point in the Lake Pukaki catchment, given the synoptic wind direction and the observed precipitation from at least one reference site.
This may be done by selecting the distribution that relates to the synoptic wind direction and reference site of choice. The likelihood of precipitation may be

determined from the "likelihood of precipitation" fields. The precipitation magnitude factor can be established from the precipitation contours. The estimated precipitation (p) at the selected point may then be established using the following formula:

$$p = 10^{c \log(p_{rs}+1)} - 1 \qquad \textbf{4-2}$$

Where

c = precipitation magnitude factor

p_{rs} = observed precipitation at the reference site.

Where precipitation is observed at more than one reference site, a scaling raster may be prepared to alter the relationship grid to match the extra observations. This can be done by establishing, for each observation site, the ratio of estimated precipitation to observed precipitation. Interpolating these values provides the scaling raster. The estimated precipitation field may then be multiplied by the scaling raster to provide an improved estimation. This is in effect a method of assimilating extra observations into the estimations.

4.4 Discussion

Investigations of wind classed precipitation distributions for England found that precipitation in maritime wind exposed regions during onshore synoptic winds was up to 3.5 times that expected from the average annual precipitation. For areas in the lee of hills, precipitation was commonly just half of that expected from the average annual precipitation (Hill, 1983). The variance from the average annual precipitation was closely related to the frequency of the different wind classes, and the precipitation magnitude associated with them. A similar situation is found for the Lake Pukaki catchment, where the average annual precipitation distribution is similar to the high magnitude, high frequency north westerly precipitation distribution, but quite distinct from the low frequency, low magnitude easterly distribution. In Scotland, the wind classed precipitation distributions show increased precipitation on the windward coast (Weston and Roy, 1994). In the Lake Pukaki catchment, the highest precipitation in all cases was in the north west of the catchment. This may be a case of different scales not being directly comparable, but may also reflect the dominance of the relatively higher mountains (relative to windward barriers) in the north west of the catchment enhancing orographic precipitation in all wind classes. In Sweden, with a mountain range axis running along its western border in an orientation similar to the Southern

Alps the opposing east and west wind directions result in significantly different precipitation distributions, both in magnitude and extent. The easterly wind distribution shows widespread precipitation of a reasonable magnitude, whereas the westerly distribution has high precipitation in the western mountains dropping rapidly to the lee (Johansson and Chen, 2003). To a limited extent the same is observed in the Lake Pukaki Catchment. The north westerly wind class has high precipitation in the north west with the notably high horizontal precipitation gradient to the south east. The easterly distribution shows a much less pronounced horizontal gradient, with much higher precipitation in the lower catchment relative to the upper catchment. In the north of the European Alps the climatologically frequent north west classed precipitation distributions show a strong similarity with each other and to the average annual precipitation distribution while the north east distribution is distinctly different (Zängl et al., 2008). A very similar situation is observed for the Lake Pukaki catchment with the climatologically rare easterly wind-class precipitation distribution quite different from the westerly-classed distributions, and from the average annual distribution. These comparisons indicate that the features of the Lake Pukaki wind classed precipitation distributions are not uncommon in other global locations where precipitation is largely controlled by orographic uplift. This should not be surprising as one of the justifications for using this approach was the close physical link between air flow-orography relationships and precipitation.

4.5 Conclusions

Different synoptic wind directions have a marked effect on the magnitude and frequency of precipitation in the Lake Pukaki catchment. The direction which most frequently occurs is between 250 and 300 degrees. This highlights the importance of the location of the catchment within the Southern Hemisphere westerly wind belt on the region's climate. The Tasman Sea to the north west of New Zealand and the Southern Ocean to the south west ensure that for any westerly air flow there is ample opportunity for the lower atmosphere to become saturated prior to reaching New Zealand. It is of no surprise then, that as well as being the most frequent wind direction, the west and north west directions result in the most precipitation, both annually, and on a per day basis for sites in the upper catchment. The increased proportion of precipitation from the more northerly wind directions may reflect the increased moisture contained in the warmer air from this direction, but also reflects

the south west to north east orientation of the mountain range, so that for winds perpendicular to the mountain range orientation there is a reduced distance between the catchment and the primary uplift regions.

Statistical classification of 10^{o} wind bands based on daily precipitation magnitudes and precipitation day frequencies at three long term gauge sites across the catchment has led to five wind classes; Northerly, easterly, south south westerly, south westerly and north westerly. The dominance of westerly classes highlights the importance of this general direction on the precipitation in the catchment. For each wind class, daily relative magnitudes (relative to a reference site) of precipitation at all available gauge sites have been determined for days when precipitation was observed at both sites. The reference sites used were Aoraki/Mt Cook Village, Tekapo and Franz Josef. In addition, the likelihood of precipitation at any site given precipitation at the reference site has been determined. Relative magnitudes and likelihoods of precipitation have been interpolated across the catchment for each wind class and reference site. The resulting distributions show a general north west to south east precipitation gradient across the catchment. North westerly class shows the greatest horizontal precipitation gradient which increased in the upper catchment as the precipitation extent increases south eastward to encompass Tekapo. The northerly precipitation extent is generally more widespread including the upper eastern quadrant of the catchment with greater relative magnitudes to the south. Except for northerly and north westerly wind classes, precipitation observation at Aoraki/Mt Cook village and at Franz Josef is a poor indicator of precipitation being observed in the catchment. Conversely, precipitation observed at Tekapo is a good indication that precipitation occurred throughout the catchment, except for the south south westerly wind class. The relationships determined enable an estimate of precipitation distribution to be established for the Lake Pukaki catchment given the observed precipitation at Aoraki/Mt Cook, Tekapo or Franz Josef and the synoptic wind direction. A limitation of the use of the distribution maps is the inability to determine precipitation extent or the precipitation field during non classed synoptic wind conditions.

The wind classed precipitation distributions determined here enable spatial precipitation estimations on days that have wind direction differing from the average. Through utilising reference sites with publicly available data these distributions enable operational daily catchment-wide precipitation estimates. The combination of distributions from the different reference sites provides an indication of precipitation

extent and extends estimates to include days with precipitation at any one of the sites. The relationship of precipitation to synoptic air flow enables potential assessment of likely precipitation changes given air mass circulation changes (e.g. ENSO, IPO).

5 Precipitation validation through flow

5.1 Introduction

Water balance models are traditionally used for assessment of hydrological variables in different catchments (e.g. Xu and Singh, 1998). The water balance equation may be arranged to solve for the precipitation (P) variable:

$$P = Q_s + Q_g + \Delta S_s + \Delta S_l + \Delta G + E \quad \textbf{(5-1)}$$

Where

Q_s = stream flow,

Q_g = ground water flow,

ΔS_s = change in solid water storage (ice and snow),

ΔS_l = change in liquid water storage (lakes),

ΔG = change in groundwater storage,

E = evapotranspiration.

If all other water balance components are established, area averaged precipitation may be estimated without using precipitation gauges. This approach led to the discovery of enhanced precipitation over Lake Victoria in Africa (Nicholson et al., 2000) after land based gauge observations did not match that derived from a water balance assessment of the lake levels. Such a water balance approach to precipitation estimation provides a means to validate gauge derived precipitation estimates. This has been done for two mountainous catchments in Japan (Tani, 1996) providing confidence in the accuracy of the elevation/precipitation relationship that had previously been established. While this method of precipitation validation is not a common application of the water balance equation, it is useful where gauge density is too low to use the more popular cross validation approach (Daly, 2006). For example in south east British Columbia and south west Alberta a lack of validating gauge sites led to the use of a water balance for evaluating different Canadian precipitation interpolation systems in those regions (Milewska et al., 2005). The system has also been used on a global scale to assess and correct gridded precipitation products (Adam et al., 2006). In New Zealand precipitation distribution has frequently been determined from water balance assessments. Thompson and Adams (1979) found through consideration of stream flows and catchment areas that as the proximity to the headwaters of the South Island's east coast rivers increased, there was an exponential increase in the area

averaged precipitation . When preparing a map of the annual rainfall in South Westland, Horrel (1990) utilised stream flow based precipitation estimations in many regions where no precipitation observations had been made. Water balance validation of model derived precipitation estimates was used by Thompson et al. (1997) in the lower North Island of New Zealand enabling them to attach error values to their precipitation estimates. In a similar manner Tait et al. (2006) used flow data to evaluate their trivariate spline interpolated precipitation fields, uncovering a 75 % underestimation of precipitation in the Southern Alps. This led to the use of an annual average precipitation surface, rather than the original elevation surface as the third interpolation variable, reducing the precipitation to runoff discrepancy. For the Lake Pukaki catchment, with few precipitation gauges, the water balance approach provides an ideal method of validating the gauge-derived average annual precipitation distribution.

Flow models are effectively high temporal resolution water balance models. In the same way that long term precipitation estimates may be validated using the water balance approach, so too can daily precipitation field estimations be validated through flow model output. The simplicity of the water balance equation (5-1) belies the complexity of the relationship between stream flow and precipitation, a complexity that varies at and with spatial and temporal scales (Eder et al., 2003) and also ensures that direct flow-to-precipitation comparison is difficult at the daily level. Instead, estimated daily flow derived from daily precipitation may be compared to observed flow. Where a change in the method of daily precipitation estimation is made, the value of this change may be assessed through the change in the quality of the modelled stream flow. If the wind-classed precipitation distributions presented in the previous chapter are to be of any value, then they must provide improved daily precipitation estimates over those that are achieved using the average annual precipitation distribution. Comparison of flow estimates with and without the wind-classed precipitation estimates therefore enables a measure of the quality of the wind-classed precipitation distributions.

In this chapter, the water balance components for the Lake Pukaki catchment and two sub catchments are assessed to provide a validation of the previously determined average annual precipitation distributions. Once this is done, flow event volumes are estimated for the three catchments for available records between 1970 and 2000. This leads to the exploration of relationships of flow event frequency and magnitude with

synoptic wind direction. These results are compared to those obtained in the previous chapter for precipitation. Finally an assessment of the quality of the wind-classed precipitation fields is made using modelled flows.

5.1.1 Catchment flow regimes

Within the Lake Pukaki catchment there are two river stage gauges: one at the Ball Hut Rd Bridge on the Hooker River and one in the lower Jollie Stream (Figure 5-1). Stage heights are converted to river flow through the use of rating curves which are determined intermittently using stream section profiles and flow rate observations. Supplementing these stream flow estimates are the Lake Pukaki inflow estimates derived from lake level observations. The lake level is monitored within a stilling chamber near the outlet of the lake at its southern end (Figure 5-1). Conversion of lake level to lake inflows is done through consideration of lake area, shoreline topography, canal inflows and outflows, and lake outflow. The derived lake inflows are the inflows that would occur without the inclusion of the canal inflows that are redirected into Lake Pukaki from the adjacent catchment.

Flow indices provide a simple means of comparison of flow regimes. Following Duncan and Woods (2004), Table 5-1 provides flow indices for the three flow sites. All three catchments have nationally high mean specific flows and mean specific 7-day low flows (Duncan, 1987; Pearson, 1995). Through consideration of low flows throughout New Zealand, Hutchinson (1990) allocated the inland region of the South Island, east of the main divide but bordering the mountains, to be in a single low-flow class. This class was characterised by high low-flows with respect to rainfall. This characteristic was attributed to the effect that snow storage, regular strong rainfall and high ground water storage in valley floors had on the river flows. Of the three flow sites, only the Jollie has a similar flow to precipitation ratio as Hutchinson's eastern-mountain class, and the Jollie does have snowfall, frequent rainfall, and a relatively large gravel valley floor. The Hooker and Lake Pukaki low flow indices are more in line with Hutchinson's West Coast class. While the Hooker and Lake Pukaki catchments both have snow fall and frequent rain, it may be that the relative size of their ground water storage with respect to the catchment's mean precipitation is not large enough to keep the low flows at a high level. The Hooker's specific mean annual flood flow is in the highest category of Duncan (1987) which is expected when the mean annual precipitation is considered, but is less than the highest values

determined by McKerchar and Pearson (1989) for other wet mountain regions of New Zealand. This highlights the moderating effect of the glacierization on flood flows (Fountain and Tangborn, 1985). The average number of times a year the Lake Pukaki inflows exceed its median flow by a factor of 3 is just below the median value determined for 62 New Zealand rivers considered by Clausen and Biggs (2000). This too is not unexpected for a generally wet catchment. The seasonal variation in flows for the three gauge sites is shown in Figure 5-2 to 4. The winter low flows and summer high flows are clearly evident. This regime is typical of snow fed catchments (Duncan and Woods, 2004). The low flows occur when the proportion of precipitation falling as snow is the highest, when there is no snow melt, and when precipitation is at a seasonal low. The high flows occur when there is a maximum of snow and ice melt and maximum precipitation. Characteristic of a heavily glacierized catchment, the high flows for the Hooker are in late summer associated with maximum melt water production and possibly the delay of spring meltwater within englacial storage (Fountain and Tangborn, 1985). The high proportion of glaciers in the catchment (42 % of the area) ensures that melt water is not limited by available snow and ice to melt, but just by available energy to melt. In the Jollie, the flow maximum occurs in November coincident with the maximum available snow to melt. This earlier peak may be explained by the proportion of perennial ice cover being much smaller (3 %) in the Jollie compared to that within the Hooker. The entire Lake Pukaki catchment has its flow peak in January, between the months for the Jollie and the Hooker, reflecting the percentage of glacierization being between that of the other two catchments (15 %). Globally the flow regimes fit into an early spring/moderate spring flow class common to temperate regions with seasonal snow melt (Haines et al., 1988). The flow peaks with respect to mean flows are not large when compared to values returned for Australia, South Africa, Europe and the United States, though the 7-day minimum for the catchment is much higher than the mean for these regions (Poff et al., 2006). The mean specific flows are globally high, with the New Zealand region in general equivalent to other high precipitation regions of the world such as the tropical western Pacific, the southern Amazon basin, the highlands of the Indian sub-continent and the Andes (Dettinger and Diaz, 2000).

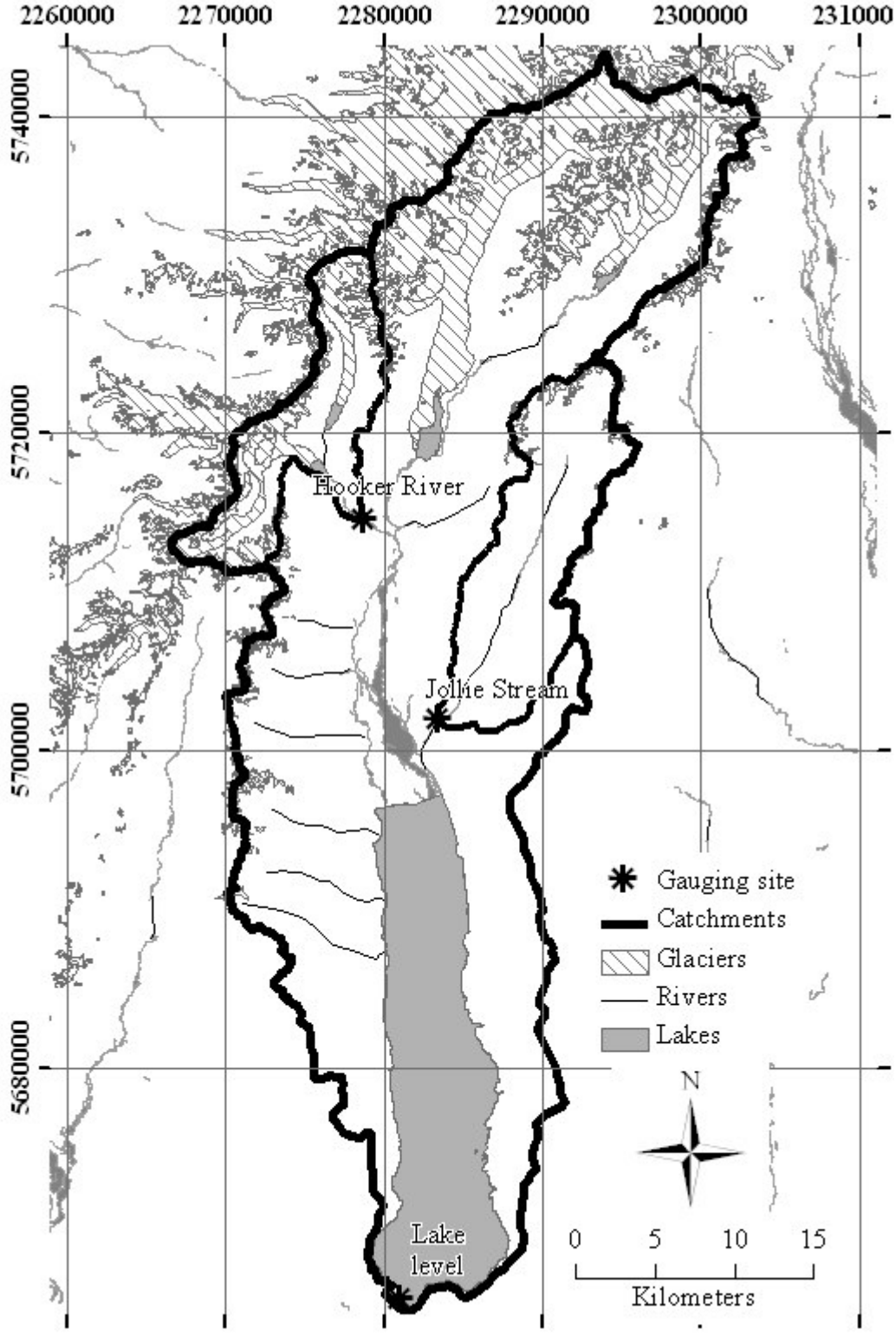

Figure 5-1. River flow and lake level gauging sites within the Lake Pukaki catchment. Solid black line delineates the catchment boundary for the Hooker, Jollie and Lake Pukaki catchments.

Table 5-1. Flow indices for the three sites within the Lake Pukaki catchment (data source NIWA).

Index	Units	Lake Pukaki (1971-2000)	Hooker (1995 – 2000)	Jollie (1971-2000)
Mean flow	$m^3 s^{-1}$	133	25	8.2
Mean flow	mm per year	3083	7540	1860
Mean specific flow	$l s^{-1} km^{-2}$	90	239	66
Mean annual 7 day low flow	$m^3 s^{-1}$	17.8	4.0	3.1
Mean annual 7 day low flow	mm over 7 days	7.9	23.5	13.5
Mean specific 7-day low flow	$l s^{-1} km^{-2}$	13	38.8	22.3
Mean annual flood	$m^3 s^{-1}$	1033	377.6	69.0
Mean annual flood	mm per day	66	313.7	42.9
Mean specific annual flood	$l s^{-1} km^{-2}$	760	3631.1	496
Mean number of flood events per year greater than three times the median flow		9	13.5	7.3

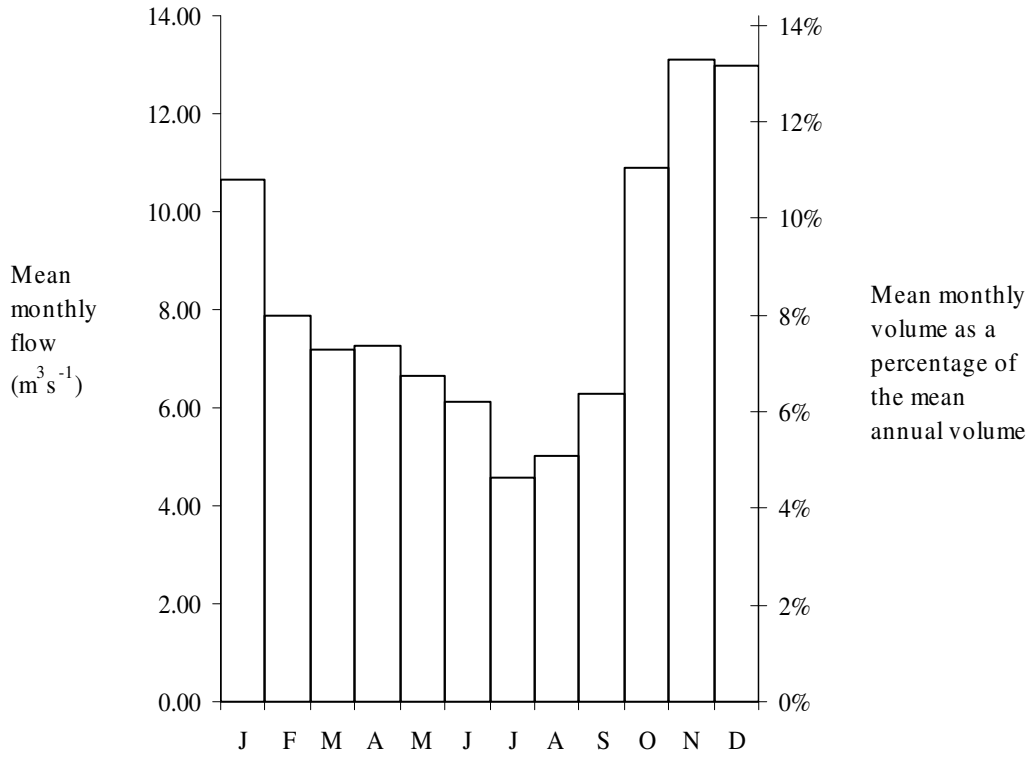

Figure 5-2. Seasonal flow regime of the Jollie (data source NIWA).

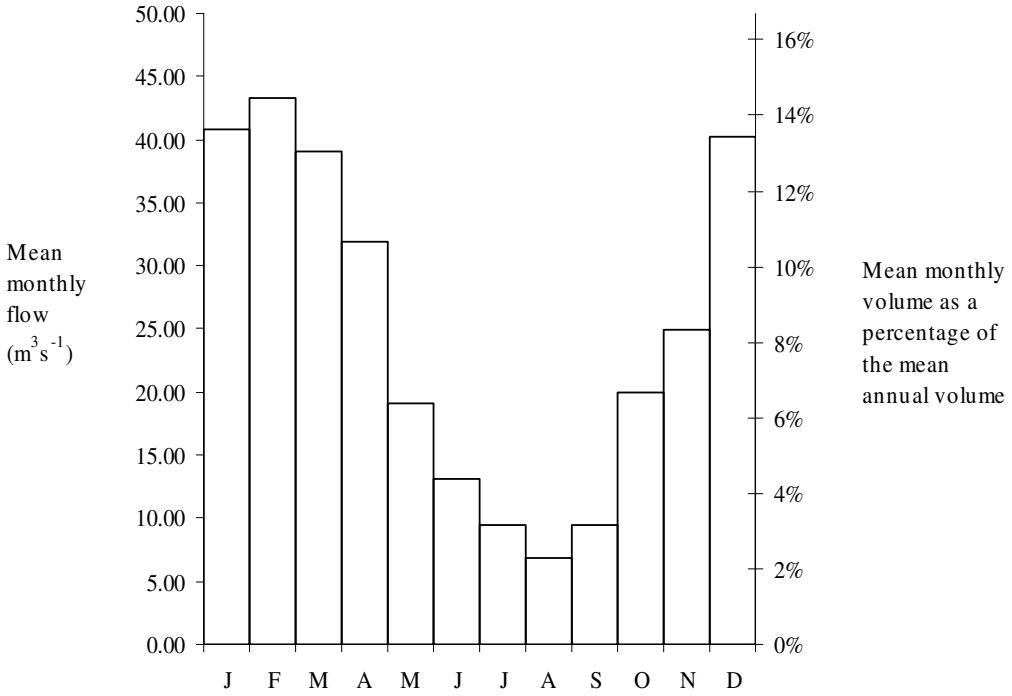

Figure 5-3. Seasonal flow regime of the Hooker (data source NIWA).

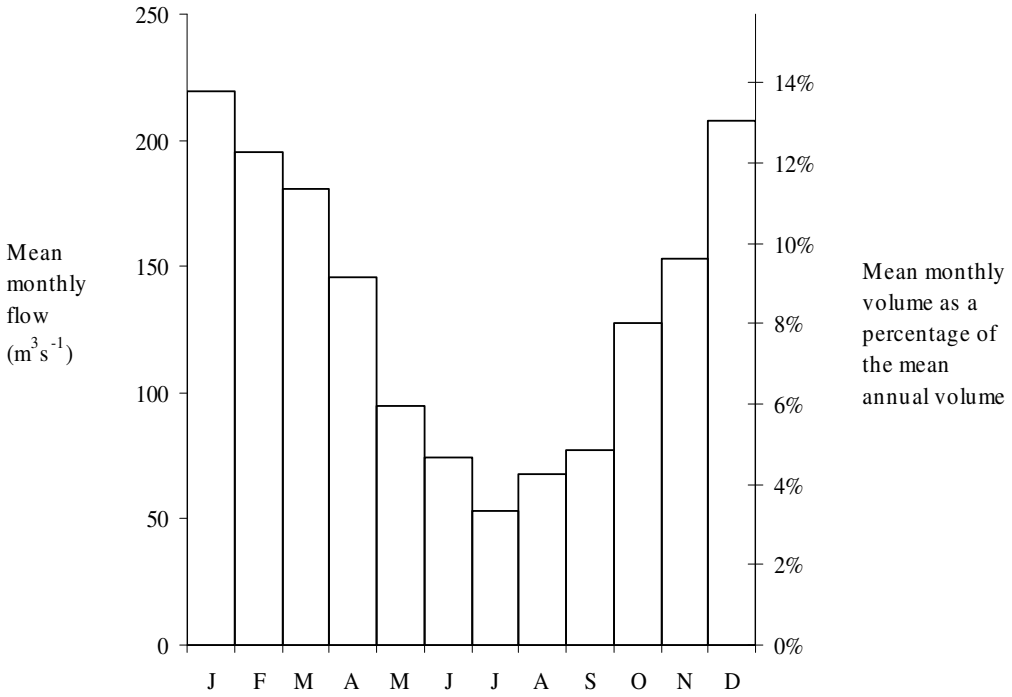

Figure 5-4. Seasonal flow regime of the Lake Pukaki catchment (data source NIWA).

5.2 Catchment precipitation determined from the water balance

A thirty year consideration of the water balance equation provides a method of determining average annual precipitation. To do this, estimates of the average annual stream/lake (in)flows, the groundwater flow, the change in ice storage, change in lake storage, change in ground water storage and average annual evapotranspiration need to be made. Average annual flows may be determined from the flow record. Ground water flows are unknown, though the lower Tasman River, Lake Pukaki and regions to the east and south are located within the Mackenzie Basin groundwater zone (Brown and Weeber, 2002). McKerchar et al. (1996) considered that the fine glacial sediment found in the major catchment tributaries and in Lake Pukaki would block potential groundwater flow paths and thereby greatly restrict any groundwater leakage from the catchment. For this reason, groundwater flows are considered negligible relative to surface water flows. Change in ice storage may be determined through comparison of glacier elevations before and after the thirty year period. In a similar manner, change in lake storage may be determined through comparison of lake areas at the beginning and end of the thirty year period, and through depth measurements/estimates of any new lake areas. The change in groundwater storage may be estimated as being zero through the assumption that there is no long term trend of wetting or drying of the catchment. Evapotranspiration may be determined from spatial estimates of available water, available energy and land cover. Each of these water balance components are considered below.

5.2.1 Average annual flows

Average flow rate into Lake Pukaki for the 1971-2000 period is 133 $m^3 s^{-1}$. This is just 9 $m^3 s^{-1}$ greater than that value determined by McKerchar and Pearson (1997) who used 1927 to 1992 data. A mean flow of 133 $m^3 s^{-1}$ relates to an average depth of water over the catchment of 3082 mm per year. For the Jollie catchment, the average flow rate was 8.2 $m^3 s^{-1}$ (or 1860 mm) For the Hooker River it was 24.86 $m^3 s^{-1}$ (7540 mm), but this was not for the entire 1971 to 2000 period as records are predominantly from 1994 to 2000. Stream flow errors are kept within 8 % through comparison of flow rates before and after rating curve changes and through manual gaugings (Halstead, 2008b). If all possible sources of error are considered, errors of high flows

may be much greater than this (McMillan et al., 2008) and have been estimated to be as high as 27 % for river flow estimates during unsteady high flow (Montenari, 2004). The error for the lake inflows is difficult to ascertain as they are determined from lake level measurements, lake bed and shore elevations and canal inflows, each of which have their own unknown error component. A subjective estimate of the error of 8 % has been applied. Figure 5-5 shows the annual average flow rate for the Hooker River, the Jollie Stream, and into Lake Pukaki, from 1971 to 2000 (Hooker River flow gaugings began in mid 1994). The much greater flow rate into the Lake compared to the Hooker River and Jollie Stream is clearly evident. This is a reflection of the different catchment sizes: 1359 km^2 for Lake Pukaki compared with just 104 km^2 and 139 km^2 for the Hooker River and Jollie Stream catchments respectively. Figure 5-6 shows the mean runoff per unit area. This shows that the catchment above the Hooker River gauging site receives more than double the water per unit area than the Lake Pukaki catchment average, and that the Jollie Stream catchment receives just two thirds.

Comparison of the variation in mean runoff per unit area of the Lake Pukaki catchment with that found for the Jollie Stream indicates that the two regions operate under similar but not identical hydrological regimes. This is more clearly shown in Figure 5-7 where the flow rates have been normalised by dividing by the long term average. In 1974 and 1989 the Jollie Stream flow is much lower than the average, whereas this is not the case for the entire catchment. Similarly for 1983, 2000 and 2002 the Jollie flows are significantly higher than the average, but are close to average for the Lake Pukaki catchment as a whole. The Hooker river flows, on the other hand, follow the Lake Pukaki inflows more closely, at least for the few years both sites were recording as shown in Figure 5-8. This would indicate that a hydrological characteristic common to the Hooker and Lake Pukaki catchments is different in the Jollie catchment. This characteristic may be the climate regime, with the Jollie, being further from the western orographic boundary, receiving less westerly derived precipitation than the Hooker and the Lake Pukaki catchment in general. Another characteristic differential is the glacierization, as represented by percentage of ice covered area. The greater relative glacierization in the Hooker and Lake Pukaki catchments could conceivably enable higher flow rates in a hot dry year, conditions that would cause low flows in the Jollie. Conversely, a year of high flows in the Jollie

may follow a winter of high snow accumulation, conditions that may lead to increased glacierization rather than flows in the Hooker and Lake Pukaki catchments.

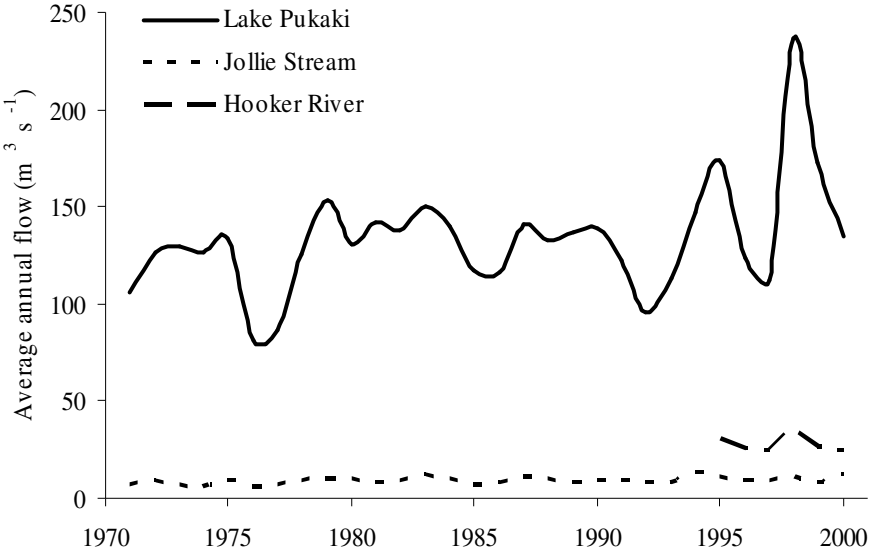

Figure 5-5. 1971 to 2000 average annual flow rate into Lake Pukaki and for Jollie Stream and Hooker River.

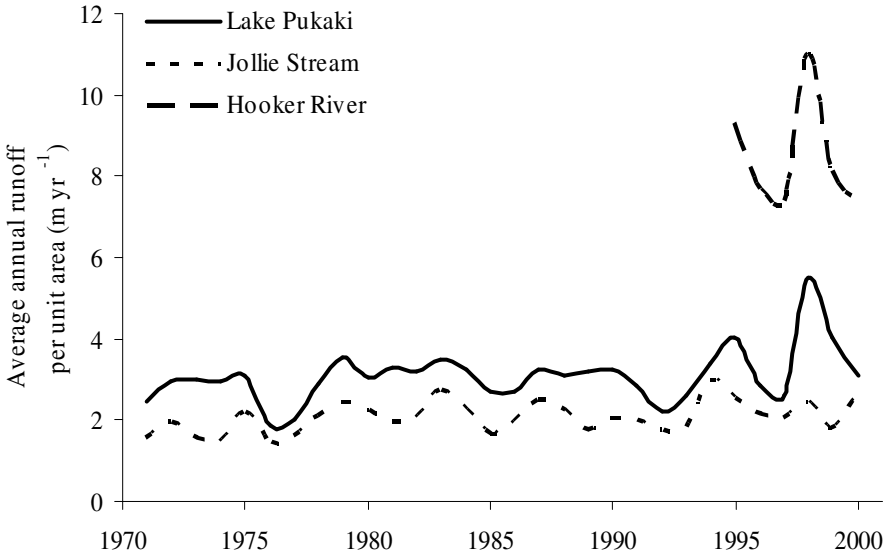

Figure 5-6. 1971 to 2000 average annual runoff per unit area for Lake Pukaki, Jollie Stream and Hooker River.

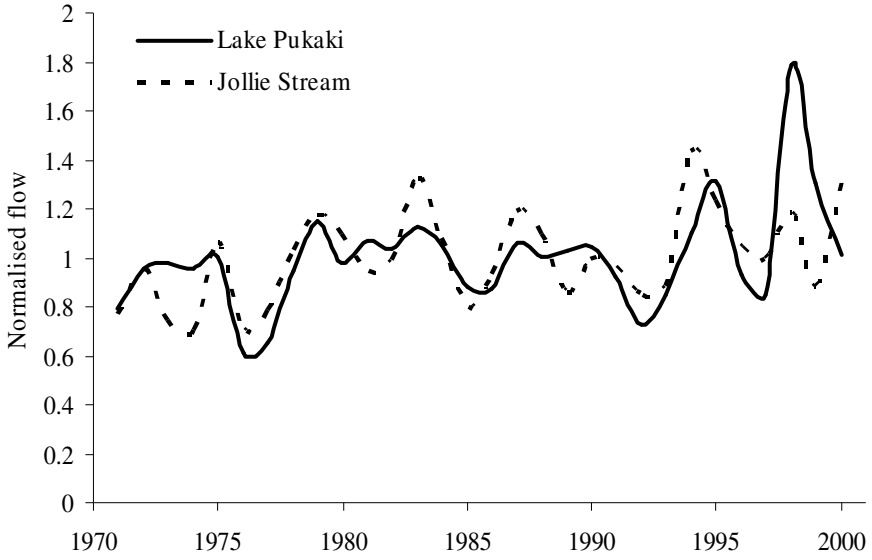

Figure 5-7. Normalised flow into Lake Pukaki, and down Jollie Stream.

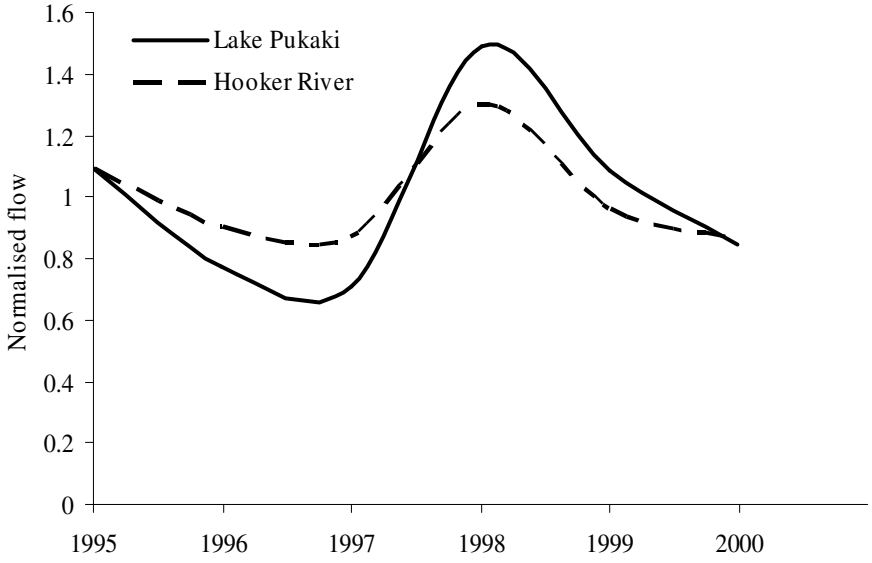

Figure 5-8. Normalised flow into Lake Pukaki, and down the Hooker River.

5.2.2 Change in frozen water storage

Change in frozen water storage in the Lake Pukaki catchment is closely tied to the change in liquid water storage. The retreat of the larger valley glaciers has resulted in the formation of pro-glacial lakes. This has occurred at the snouts of the Tasman, Hooker, Mueller and Murchison glaciers. From a water balance point of view, this means that space that was occupied by ice (with a density of approximately 900 kg m^{-3}) is replaced by water (1000 kg m^{-3}). The down wasting of the glaciers to pro-glacial lake level decreases the water storage in the catchment, but the replacement of ice with liquid water increases the water storage. An estimate of the down wasting and retreat of glaciers to lake levels from 1986 to 2000 may be ascertained through the comparison of the elevations shown in the New Zealand Map Service 260 Series (NZMS260) map sheets for the region (derived from 1986 aerial photographs), digitized by Landcare (Barringer, 2003), and the elevations determined from the Shuttle Radar Topography Mission from 2000 (Farr et al., 2007). Comparison of bare land elevations (i.e. not ice or lake) between the elevation sets enables an estimate of error. Lake and ice regions for 1986 were taken from the digital NZMS260 layers. 2000 lake areas were derived from ASTER satellite imagery using automatic classification techniques devised by Allen et al. (2008). The differences between the elevation models over this non-ice, non-lake area have a mean of -1.9 m (the –ve sign indicates the SRTM DEM is higher than the NZMS260 DEM) with a standard deviation of 12 m. The -1.9 m systematic error is partly a result of the two elevation models using different vertical projections. The NZMS260 DEM has an International 1924 ellipsoid vertical projection corrected to the New Zealand geodetic datum 1949, whereas the SRTM DEM is aligned with the WGS84 ellipsoid, corrected with the EGM96 geoid model. The NZMS260 DEM is a close approximation to New Zealand height above mean sea level elevations through the alignment with the local datum. The EGM96 geoid model provides a global correction of the WGS84 ellipsoid to local gravitational anomalies. Land Information New Zealand (LINZ) have generated a local geoid NZGEOID05 for correcting WGS84 ellipsoid to NZ mean sea level elevations (LINZ, 2007). Within the Lake Pukaki catchment the EGM06 geoid model correction of the WGS84 ellipsoid is in error with respect to the NZGEOID05 by an average of 3.4 m. This partly explains the systematic error observed between elevation data. The high standard deviation is a result of the limitations of SRTM in

steep regions with similar errors returned elsewhere in the world. For instance a mean error of -2.3 m with a standard deviation of 20 m was found in the Swiss Alps against a 1991 air photo derived DEM (Kääb, 2005). Comparisons against ICESat showed an increase of mean error from -0.6 to -4.8 m in the western US when the comparison areas changed from gentle to rugged relief (Carabajal and Harding, 2005). Elevation related biases of -7 m per 1000 m were found in the Mont Blanc region of the Swiss Alps (Berthier et al., 2006). Possible explanations of systematic offsets may be the reduced signal to noise ratio and hence greater error on aspects facing away from the space shuttle, or slight misregistration of the two elevation models leading to vertical errors (Stozzi et al., 2003). Certainly the difference-image highlights aspect variation (Figure 5-9) and the large relatively flat areas in the central part of the catchment return difference values close to the catchment mean indicating that one or both of these errors is present. The greatest mean difference occurs for aspects from 310^{o} to 315^{o} at 13.8 m. For a 45^{o} slope this could be caused by a 13 m horizontal misregistration, well within the combination of quoted horizontal errors for the NZMS260 and SRTM. Another limitation of the SRTM elevation data is the large areas where the topography and or land cover prevented the radar from returning a coherent elevation. In these areas topographic shading may prevent some surfaces from being in the line of site of the shuttle or the coherent elevation changes on the source interferogram cannot be traced back to a known reference elevation (Stueffer et al., 2007). Unfortunately these "holes" are found in the steeper glaciated regions requiring estimates of glacier change in these areas to be inferred from similar nearby observed areas. The approach taken was to average snow and ice elevation differences for the areas available in each catchment, and then apply these means to total snow and ice areas within each catchment. The very large inter annual variation in snow accumulation in the glacial nevés combined with the known SRTM deficiencies in steep terrain has led to a subjective estimate of error of 80 % for the Lake Pukaki and Hooker catchments, and 100 % for the Jollie catchment. The ice lost within each catchment determined from the 1986 to 2000 comparison is given in Table 5-2.
The 1971-2000 ice loss has been taken as twice the 1986-2000 estimate. The validity of this is difficult to defend as prior to 1978 the glaciers in the region were in strong negative mass balance, but post 1978 were largely in positive mass balance (Kerr and Owens, 2008). The relative importance of the annual ice loss is small in comparison to the flow component of the water balance, so the doubling of the 1986-2000

estimates of ice loss to give a 1971-2000 estimate is unlikely to affect the final result significantly.

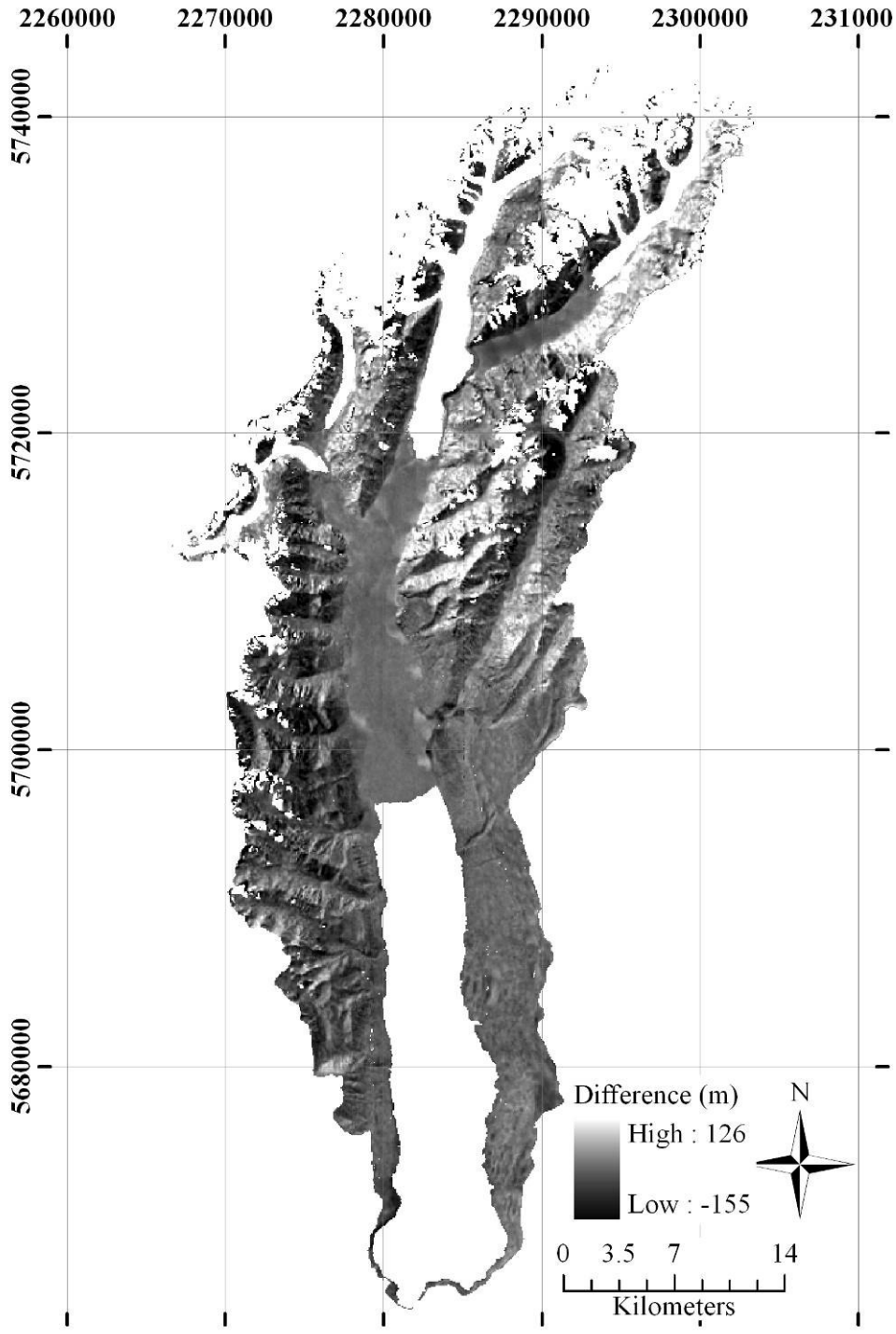

Figure 5-9. Difference image after subtracting the SRTM elevations values from the NZMS260 map series elevation values in areas that are not lakes or glacier.

Estimates of ice storage change for the catchment have previously been determined as 6% of annual flows in 1996 (Purdie and Fitzharris, 1999). This is considerably larger than the values given here as this estimate disregards the effect of the growth of the pro-glacial lakes. In terms of water balance the rapid change in several of the region's glacier termini has merely led to a phase change in the stored water.

Table 5-2. Average elevation change for snow and ice regions from 1986 to 2000, not including below pro-glacial lake level.

Catchment	Lake Pukaki	Hooker	Jollie
Average change in elevation over ice free and lake free areas (m)	-1.96	1.08	-1.7
Average change in elevation over snow and ice areas (m)	4.2	4.9	-12
Total average snow and ice elevation change (m)	6.2	3.8	-13.7
Total snow and ice volume change (x 106 m3)	1290	160	-38
Average annual snow storage change (mm)	61	100	-18

5.2.3 Change in liquid water storage

To determine the change in water storage resulting from the growth of pro-glacial lakes, an estimate of the lake volumes is required. Lake depths for the Tasman, Hooker and Mueller lakes were determined in 2002 (Röhl, 2005). The lake depths in 2000 were estimated by applying the average 2002 depths to the 2000 lake areas. No depths have been taken of the Murchison Lake so a subjective estimate was made based on the size of the lake and consideration of the depths of the other terminus lakes in the catchment. The error of these estimates has been subjectively allocated as 30 %. The minor contribution that the lakes have to the water balance means that the error of their estimation has little effect on the final result. The change in pro-glacial lake volume for each lake is given in Table 5-3 with their influence on the respective catchments given in Table 5-4

Table 5-3. Change in pro-glacial lake volume from 1986 to 2000.

Lake	Tasman	Hooker	Mueller	Murchison
Change in area (x 10^3 m^2)	1200	400	370	630
Average depth (m)	75	65	9	40
Change in volume (x 10^6 m^3)	90	26	3.33	25.2

No alteration in the change in liquid storage was made to provide a 1971-2000 estimate, as prior to 1986 the pro-glacial lakes in the catchment were relatively small

(Hochstein et al., 1998; Kirkbride and Warren, 1999), and their effect on the long term water balance is well within error of the flow and evapotranspiration components.

Table 5-4. Change in water storage from growth of pro-glacial lakes.

Catchment Lakes	Lake Pukaki Tasman Hooker Murchison Mueller	Hooker River Hooker Mueller
Total volume change (x 10^6 m^3)	14.453	2.933
Average annual lake storage change (mm)	1	2

5.2.4 Evapotranspiration

Evapotranspiration for the Lake Pukaki catchment has been estimated by several authors: 440 mm a^{-1} (Anderton, 1974) and 522 mm a^{-1} by Fitzharris and Garr (1995), whereas McKerchar and Pearson (1997) suggest 700 mm a^{-1} for areas with greater than 800mm a^{-1} rain and negligible ground water loss. Woods et al. (2006) compared three different methods of preparing an actual evapotranspiration climate surface for New Zealand. They concluded that using an empirically based ratio of calculated potential evapotranspiration to precipitation provided the best result. In a similar manner, a New Zealand map of the monthly mean ratio of rainfall to potential evapotranspiration has been prepared by Landcare Research as part of their national climate surface products (Leathwick et al., 2003; Leathwick et al., 1998). By using the rainfall surface prepared as part of the same group of products, a grid of evapotranspiration may be derived. A Lake Pukaki catchment evapotranspiration estimate was selected as being half way between the limits of previous estimates, with an error that encompasses the full range: 550 ± 200 mm a^{-1}. For the sub catchments, the Landcare values were adopted with the same percentage error as determined for the whole Lake Pukaki catchment. That is, for the Hooker catchment, 400 ± 120 mm a^{-1} and 440 ± 130 mm a^{-1} for the Jollie catchment.

5.2.5 Precipitation

Table 5-5 combines the various components of the water balance for each catchment providing an estimation of catchment precipitation. The error for each value is given to one significant figure, and the values are set to the same precision as their errors.

A comparison of the water balance determined precipitation and precipitation gauge determined precipitation for each catchment is given in Table 5-6. All three water balance based estimates are in agreement with the gauge based estimates. In each case the water-balance estimate is slightly higher than the gauge-based estimate.
This indicates that either the undercatch estimation is too conservative, the interpolation of the precipitation fields is incorrect, or that the flow ratings are in error. It is likely that each of these possibilities is true to a greater or lesser extent and to some degree they are taken into account by the error estimates.

Table 5-5. Catchment estimated 1971-2000 average annual water balance components with the derived precipitation. All values are in mm of water depth.

Catchment	Lake Pukaki	Hooker	Jollie
Precipitation	3600 ± 500	7700 ± 900	2300 ± 300
Surface flow	3100 ± 200	7500 ± 600	1900 ± 200
Ground flow	0	0	0
ΔS_i	-100 ± 100	-200 ± 200	40± 40
ΔS_l	1.0 ± 0.3	2.0 ± 0.6	
ΔG	0	0	0
E	600 ± 200	400 ± 100	400 ± 100

Table 5-6. Comparison of gauge estimated and water balance estimated average annual precipitation.

Catchment	Lake Pukaki	Hooker River	Jollie Stream
Precipitation gauging (mm)	3397	7154	2237
Water balance (mm)	3600 ± 500	7700 ± 900	2300 ± 300

5.3 Storm flows

In an alpine catchment there are two sources of water flow, liquid precipitation and ice melt (which includes snow melt). When unconfined, these water sources flow to adjacent areas of lower elevation if they exist. When confined, they flow to adjacent locations of lower pressure. On a hill slope, this is generally a combination of over the surface, into or out of the soil/ground and through the soil/ground. Streams are simply surface expressions of this water flow, though it is more common to think of them as surface flows in semi-permanent flow channels. The flow rate over/through a medium is dependent on the properties of the medium and is regulated by flow conductivity for sub surface water, or flow friction for surface water. It is this control on flow rate that leads to a delay between water input to a catchment and flow out of a catchment.

What is more, it is the spatial diversity of water inputs and catchment flow rates that ensure the outflow is more than a simple temporal transformation of the water input flow. Generally, stream flows consist of base flow and event flow. The base flow originates from the low flow rate from ground water discharge. Event flows occur following a precipitation or melt event. An increase in catchment water volume results in increased surface and ground water flows, then a decline back to base flows once the precipitation or melt event has finished. An example of precipitation events with associated flow events is given in Figure 5-10. This simplistic view of water input to flow relationship may be confounded by input events occurring in isolated locations throughout a catchment, by input rates varying during a storm, by snow pack and glacier effects, and by input events occurring prior to the complete outflow of the previous storm.

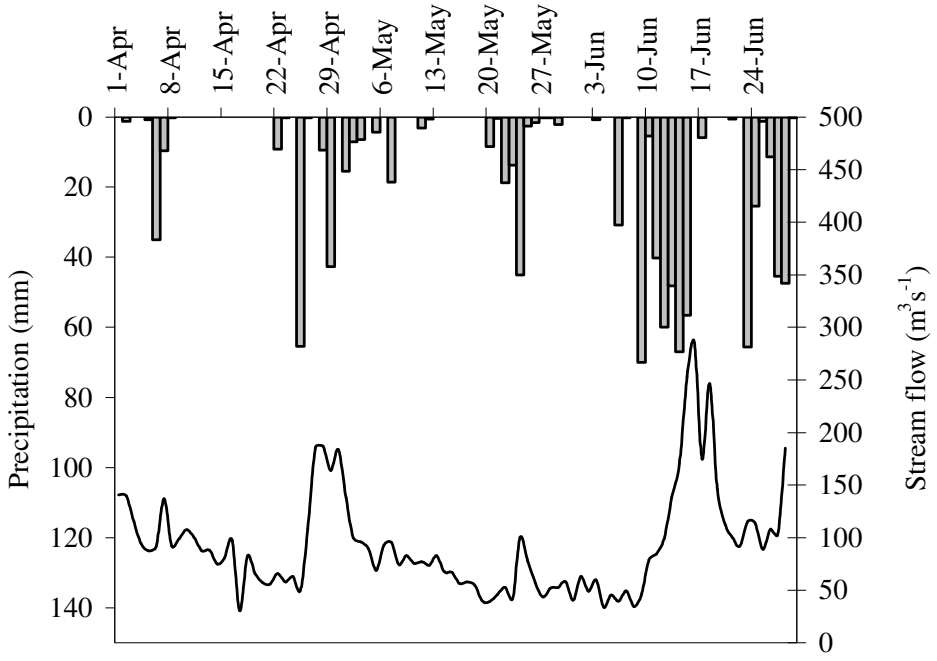

Figure 5-10. Precipitation at Mt Cook EWS (bar plots) and Lake Pukaki inflow (line plot) during 2002.

For this reason comparison of outflow with water inputs is complex. In this study, the interest is in comparing single flow events with single climate events as a means of verifying precipitation to climate relationships. To do this, that component of the stream flow that may be reasonably related to a single precipitation event is identified in the hydrograph. While such hydrograph separation is a field of research in itself (e.g. Kirchner, 2008) and unambiguous separation is not currently possible (e.g. Weiler et al., 2003), simple event flow volume determination may provide the level of

separation required for this application. This has been done by selecting individual flow peaks and extrapolating their recession curves down to the base flow (Figure 5-11). The integral of each flow event with extrapolated recession, less the base flow, less any concurrent recession flows (from previous peaks) provides the flow volume associated with the related precipitation event.

Several steps must be taken to determine this volume:

- Estimation of base flows,
- Identification of storm flow onsets,
- Extrapolation of recession flows.

The methods used to complete each of these steps, together with their combination to generate storm volumes, are outlined in the following sections.

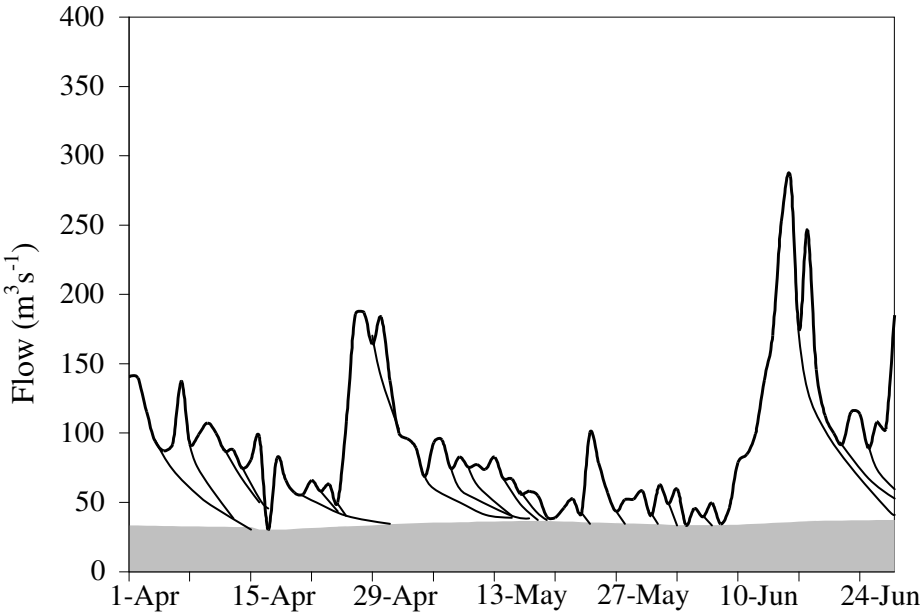

Figure 5-11. Lake Pukaki inflow hydrograph divided into individual flow events. Base flow is shaded grey.

5.3.1 Base flows

The interpretation of base flows is subjective with various approaches taken (Ibbitt et al., 2004). In this study, base flows have been taken as the 31 day running average of the 31 day minimum flows. This ensures that the event flow is always above the base flow, and smooth enough to not include any single flow events. The base flows during 2002-3 snow year (where a snow year is taken as being from 1st April to 31st March)

for the Lake Pukaki catchment, is shown in Figure 5-12. A clear seasonal cycle may be seen relating to the snow and ice melt cycle.

5.3.2 Storm flow onset

The onset of flow events is identifiable as a flow rate change-point from decreasing flow to increasing flow. A flow event is considered to begin when the current flow rate is less than the immediately prior and subsequent flow rate.

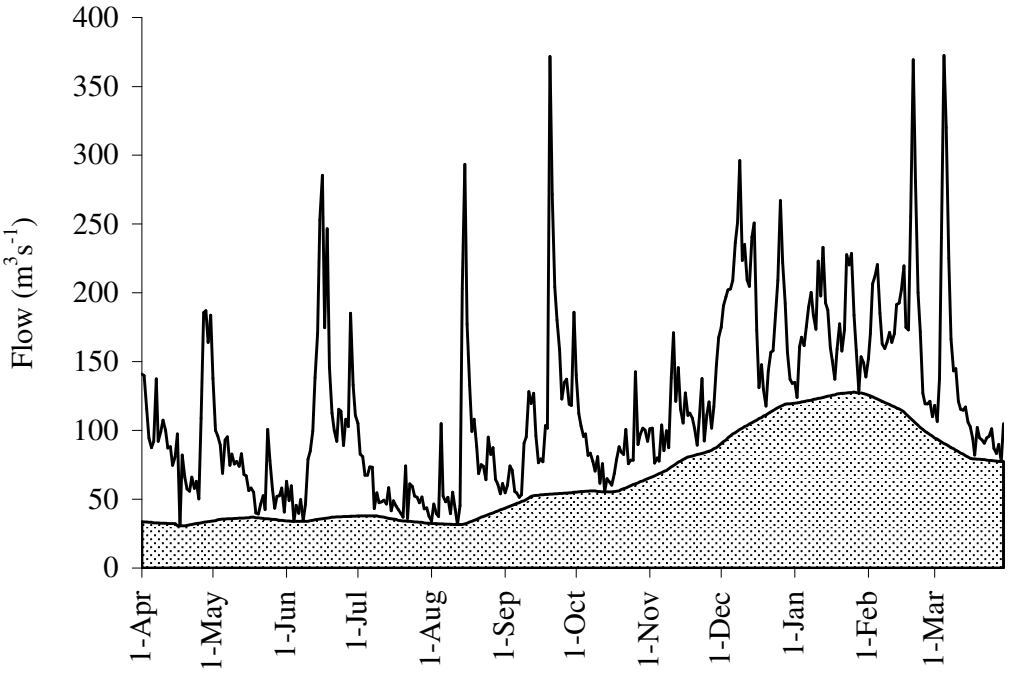

Figure 5-12. Observed mean daily flows into Lake Pukaki catchment during 2002-3 with base flow shaded.

5.3.3 Recession flow

After the peak of a flow event the observed flow matches the event recession flow until either the base flow rate is reached, or another flow event occurs. For locations with regular rainfall and snow melt the recession flow may be characterised by the following formula (Thompson, 2002):

$$Q(T) = \frac{Q(T_p)}{1 + \frac{(T - T_p)Q(T_p)}{V}} \quad \textbf{(5-2)}$$

Where:

$Q(T)$ = flow at time T (m^3s^{-1})

$Q(T_p)$ = flow peak at time T_p (m^3s^{-1}).

V = constant (m^3).

The constant V is catchment dependent and may be thought of as an index of the storage volume of the catchment. A low V results in a rapid recession while a high V leads to a slow recession. Figure 5-13 shows the recession curves for an 80 $m^3 s^{-1}$ flow peak with different V values. Optimised V values have been determined for each catchment through comparison of the resultant curve to observed flow under different recession flows. For Lake Pukaki inflows a value of 13.8 x 10^6 m^3 was returned, while for the Hooker and Jollie flows, 13.0 x 10^6 m^3 and 8.6 x 10^6 m^3 respectively were found. Event recession flows were extrapolated to below the observed flow hydrograph by applying the recession flow formula (with the appropriate V constant) and offsetting it to match the observed flow prior to the subsequent event. In this way, each flow event has its own particular hydrograph from onset through to the recession flow matching the base flow, or previous recession flow.

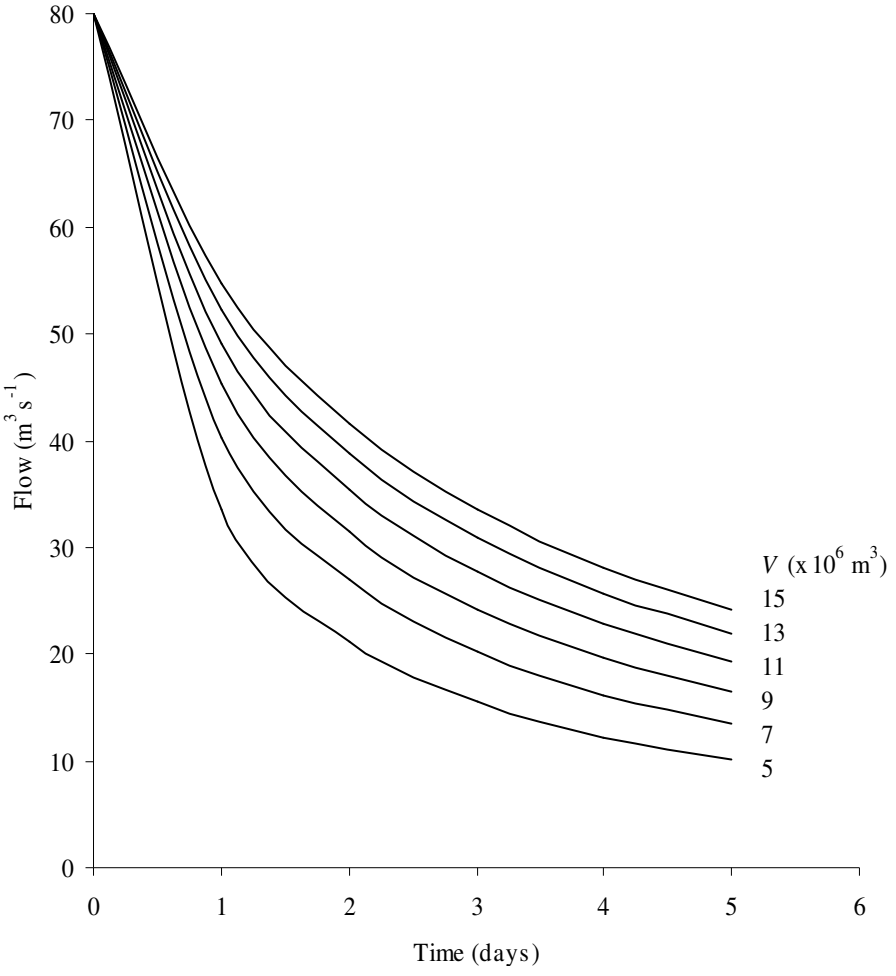

Figure 5-13. Recession curves for an 80m^3s^{-1} flow peak with varying recession parameters, *V*.

5.3.4 Flow event volumes

With individual event hydrographs established, the event flow for each day may be determined by subtracting the base flow, and any prior event recession flow from the event flow. This flow rate may (in $m^3 s^{-1}$) then be converted to a volume (m^3) by multiplying by 24 x 60 x 60 (the number of seconds in a day). The total event volume may then be established by summing the event volumes for each day of the event. An example of event volumes estimated for Lake Pukaki inflows is shown in Figure 5-14.

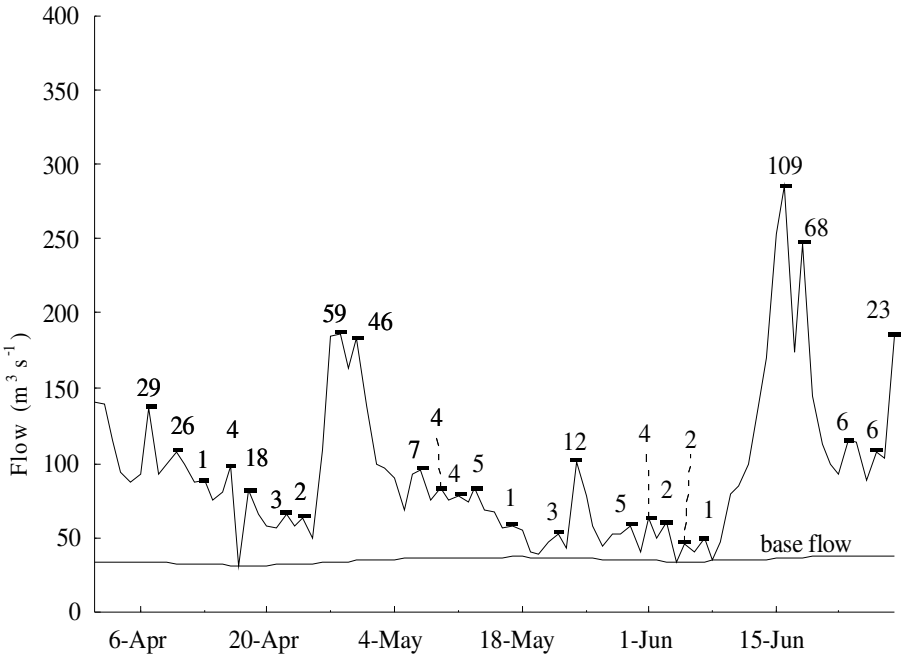

Figure 5-14. Flow event volumes (in $x10^6$ m^3) for Lake Pukaki inflows in 2002.

These volumes may then be used to explore relationships between event magnitudes and synoptic wind directions. For the Jollie catchment, the frequency distribution of flow peaks (with single day rise times) for different wind directions on the day of the rise are shown in Figure 5-15. The predominant wind directions related to flow events is west to north west. Very few flow events were observed after days with east or south east wind directions. The north west events have a higher magnitude than the westerly events, though generally there is a wide spread of magnitudes for all event directions. The flow event relationship is very similar to that found for the precipitation record from Jollie Hut, The Hermitage and Braemar Station as shown in the previous chapter. The wind direction relationship to flow events for the Hooker is shown in Figure 5-16. A similar pattern to the Jollie is seen. West to north west winds predominate, with a slight increase in magnitude for the more northern directions.

Unusually, direct westerly events are not well represented. This was related to the much smaller number of events sampled (as a result of a shorter record) and the bin classes used. A similar result could be obtained by restricting the Jollie flows to the 1994-2000 period. The lower frequency southern and eastern events exhibit a reduced magnitude relative to the westerly events. The wind direction to flow event relationship for the entire catchment is shown in Figure 5-17. This wind rose shows a distinct swing to the south west compared to that for the Jollie and Hooker. Magnitudes are varied in all wind directions with no direction obviously different to the others. The shift to the south may be an artefact of the delay between precipitation and inflow, but analysis of the wind direction on the day before the rise day returned a similar wind rose to that shown for the rise day. What is more likely is that with the larger catchment, the transformation of precipitation to flow is less linear than for the smaller sub-catchments. This means that days prior to a flow peak are simply a sample of all days, with no bias to the precipitation bearing wind that initiated the flow. This would explain why the wind frequencies are very similar to that returned for all days as shown in the previous chapter.

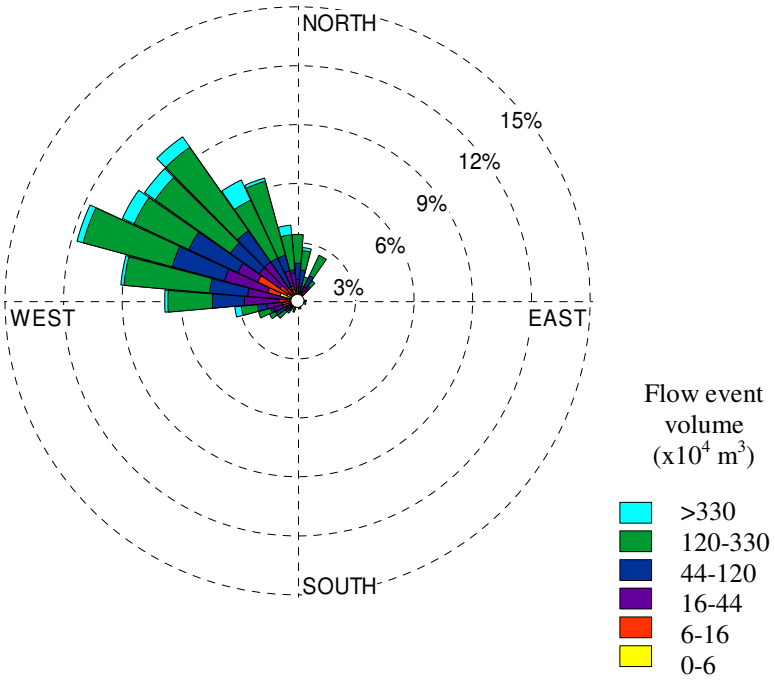

Figure 5-15. Windrose plot for NCEP-NCAR 850 hPa wind on days immediately prior to an observed flow peak at the Jollie stream gauge. Rings give the frequency of each sector's wind direction. Colours give a break down of the flow magnitudes in x10^4 m^3. Only flow peaks with a single day rise time were used. Flow data was from 1971 to 2000.

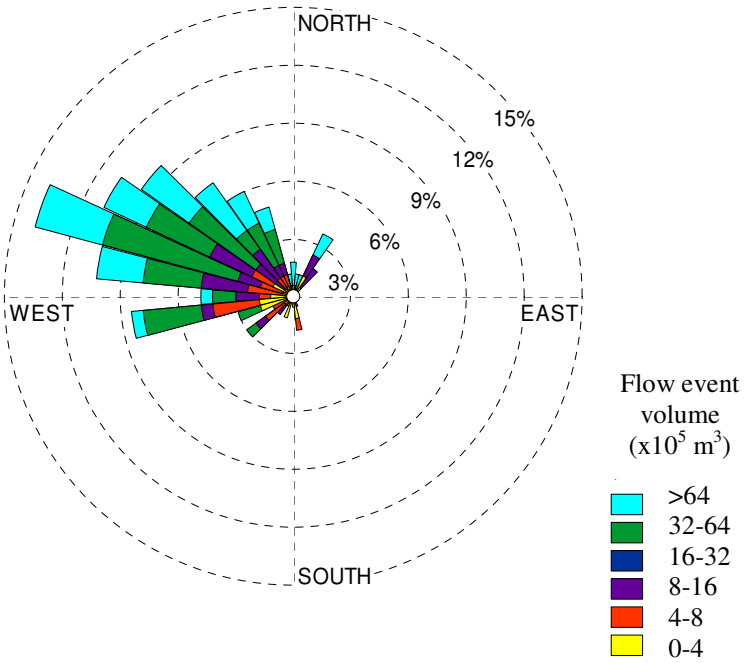

Figure 5-16. Windrose plot for NCEP-NCAR 850 hPa wind on days immediately prior to an observed flow peak at the Hooker stream gauge. Rings give the frequency of each sector's wind direction. Colours give a break down of the flow magnitudes in x10^5 m^3. Only flow peaks with a single day rise time were used. Flow data was from 1971 to 2000.

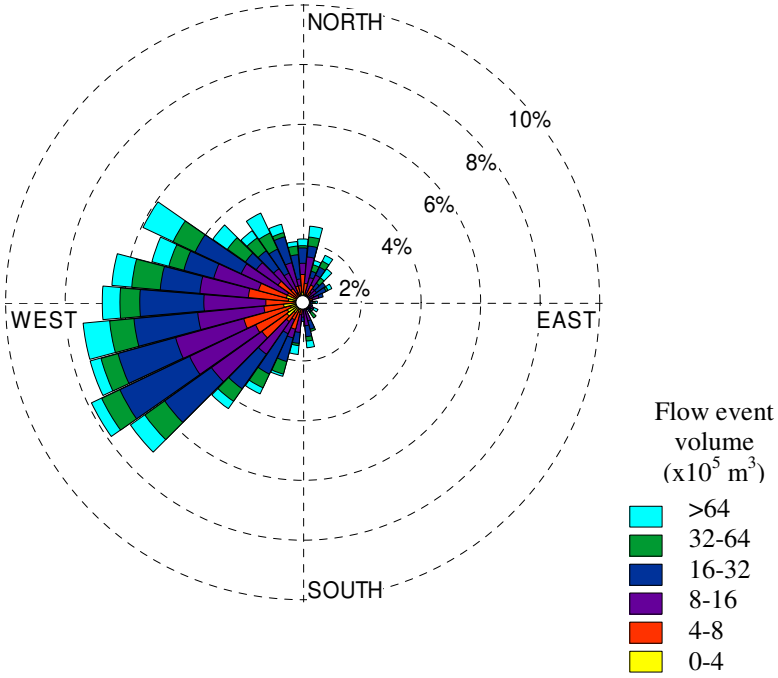

Figure 5-17. Windrose plot for NCEP-NCAR 850 hPa wind on days immediately prior to an observed flow peak in the Lake Pukaki inflows. Rings give the percentage frequency of each wind direction. Colours give a break down of the flow magnitudes in x 10^6 m^3. Only flow peaks with a single day rise time were used. Flow data was from 1971 to 2000.

The flow event magnitudes enable a comparison to the related precipitation events. This may enable a validation of estimated precipitation distributions. Flow events with a single day rise time were classed according to the NCEP/NCAR wind direction classes as used in the previous chapter. The 50 percentile flow volume was determined which was divided by the area of the catchment to provide a flow measure in depth that may be compared to catchment precipitation depths. The 50 percentile catchment precipitation for each wind class was determined by multiplying the mean catchment precipitation ratio to Mt Cook, by the 50 percentile Mt Cook precipitation. These values are shown in Table 5-7. For the Jollie catchment the estimated precipitation is always equal to or more than the estimated flow which may be accounted for by evapotranspiration being a significant relative term in this catchment. In the Hooker catchment the hydrologically significant wind classes north west, north and south west show greater flow than is estimated from precipitation. This is likely to be a result of the contribution of melt to flows in this highly glacierized catchment (Flowers, 2008) as under these synoptic conditions snowmelt is known to increase significantly in New Zealand's Southern Alps (Neale and Fitzharris, 1997; Prowse and Owens, 1982). For the entire Lake Pukaki catchment, there is a poor correlation between the flow and precipitation observations. The size of the catchment with the related non-linear relationship between precipitation and inflow is likely to cause this.

Table 5-7. Comparison of wind classed catchment average water input (in mm depth) derived from flow and precipitation observations.

	NW	N	E	SSW	SW
Jollie Catchment					
Flow	5.0	5.7	3.2	2.2	3.1
Precipitation	8.7	6.0	3.2	2.6	5.2
Hooker Catchment					
Flow	28.6	57.0	4.6	3.0	17.0
Precipitation	23.3	22.6	5.0	4.0	8.8
Lake Pukaki Catchment					
Flow	8.8	8.4	7.3	8.4	8.2
Precipitation	13.1	13.1	3.3	3.0	5.8

Direct comparison of flow event volumes and gauged precipitation is limited in three major ways.

1. Flow event volumes are a spatial integral of a catchment's liquid water inputs. In an area where the spatial precipitation distribution is non-constant the likelihood of a single point precipitation measurement being representative of the entire catchment is low. This was clearly demonstrated in the United Kingdom's Lee catchment where the ability to capture the spatial variability of the precipitation was found to be the dominant effect on the quality of the modelled stream flow (Segond et al., 2007).
2. Catchment liquid water inputs may be derived from melt water, not precipitation, and precipitation may fall as snow, thereby not contributing to catchment liquid water inputs (Verbunt et al., 2003).
3. Flow events may be considered a delayed signal of catchment water inputs, with the delay dependent on land cover, soil and rock type, slope, aspect and distance to the liquid water inputs (Gurtz et al., 1999).

These limitations were confirmed through a comparison of flow event volumes for each catchment with gauged precipitation at The Hermitage. The precipitation and flow volumes were log transformed to improve the normality assumption of their frequency distributions, required for regression. Correlations were either generally poor with $r < 0.5$ or not significant at the 0.99 level.

Table 5-8. Correlations between flow event volumes and precipitation at The Hermitage and jollie Hut

	NW		N		E		SSW		SW	
Site	**r**	**No. of days**	**r**	**No. of days**	**r**	**No. of days**	**r**	**No. of days**	**r**	**No. of days**
The Hermitage										
Jollie Stream	0.41	662	0.35	117	0.18	82	0.20	35	0.09	70
Hooker River	0.38	188	0.41	28	0.5	16	0.23	8	0.23	21
Lake Pukaki catchment	0.28	609	0.15	109	0.13	142	0.14	135	0.15	132

This presents a difficulty in using flows to validate the wind-classed precipitation distributions.

The approach that has been taken here is to test whether the use of the wind-classed precipitation distributions for determining daily precipitation fields leads to improved catchment flow estimates, compared with not using the wind-classed distributions. In this way a relative measure of the wind classed precipitation distributions is gained. The flow estimates are derived through the temporal averaging and optimised delay of the daily catchment liquid water output of a simple degree-day snow storage model, SnowSim-Pukaki.

5.4 SnowSim-Pukaki

Physically based hydrological modelling is problematic through the limitation of underlying equations and the spatial and temporal heterogeneity of flow processes (Beven, 1989). Empirical approaches enable the reduction of model complexity, thereby limiting the possibility of the tuning of model parameters compensateing for each other. In an assessment of hydrological modelling complexity Jakeman (1992) found that no improvement in model output was gained when more than four parameters were used. At the simplest level water input may be transformed to runoff through a delay and time averaging transformation (2 parameter model). Such a model is considered a benchmark with which to compare more complex models (Schaefli and Gupta, 2007). In a glacierized catchment, water input is a combination of liquid precipitation and melt water. These dual inputs may be assessed through consideration of precipitation in conjunction with temperature. In situations where the temperature is near to or below the melting point, precipitation may be considered to be solid and does not contribute to stream flows. When the temperature is above the melting point, any accumulated snow and ice will undergo melt, augmenting stream flows. Such considerations are incorporated into the snow storage model SnowSim (Fitzharris and Garr, 1995) which was prepared specifically for the Southern Alps eastern hydro catchments. A generalised New Zealand version was later prepared by McAlevey (1998) and a Lake Pukaki catchment specific version, SnowSim-Pukaki, prepared by Kerr (2005). This model will be used to generate catchment melt water and liquid precipitation estimates. These estimates will then be compared to the flow hydrograph as 14 day running averages with an optimised lag. Model efficiency assessments with and without the wind-classed precipitation distributions then provide a measure of the value of their quality.

5.4.1 Model operation

SnowSim-Pukaki uses temperature and precipitation observations as inputs, interpolates spatial temperature and precipitation fields and then determines the change in snow accumulation through the consideration of the temperature and precipitation at each location. Snow accumulates where the temperature is below a fixed temperature threshold. Snow melts when the temperature is above a fixed

threshold, at a rate related to the temperature, the length of time since the last snow fall, and the time of year. This is given by:

$$f = f_{\min} + \frac{f_{\max} - f_{\min}}{e^{(2.5-0.2at)} + 1} \quad \textbf{(5-3)}$$

Where:

f = melt factor,

f_{min} = minimum melt factor (mm ^{o} C^{-1} d^{-1}),

$f_{max} = f_{max,i}$ for days 1 to 250 (where day 1 is April 1st),

$f_{max,i}$ +1 for days 250 to 280 (Dec 6th to Jan 6th),

$f_{max,i}$ + 2 for days 280 to 300 (Jan 6th to Jan 26th),

$f_{max,i}$ + 4 for days 300 + (Jan 26th to Mar 31st),

$f_{max,i}$ = initial maximum melt factor (mm ^{o} C^{-1} d^{-1}),

a = 1 for a dry day, 2 for a wet day,

t = time in days, since the last snow fall.

Temperature is interpolated across the catchment in the following manner:

- observed temperatures are converted to a standard elevation using a fixed lapse rate,
- the standard-elevation-temperatures are interpolated using an inverse distance weighted algorithm to all grid locations,
- all grid location temperatures are converted back to their appropriate location elevation (as determined by a DEM) using the standard lapse rate.

The default precipitation interpolation occurs in a similar manner. For each available observation, the fraction of the average annual precipitation at that site is found. These fractions are interpolated across the catchment, with the resulting grid multiplied by an average annual precipitation surface.

The model operates on a daily time step over a 1000 m resolution grid that encompasses the Lake Pukaki catchment. Precipitation and temperature data are taken from all available observation sites within 60 km of the catchment. The model includes the following tuneable parameters:

- Snow/rain temperature threshold
- Minimum melt factor

- Initial maximum melt factor

These parameters are optimised through comparison of 14 day running average modelled catchment free water (liquid precipitation and melt water) to 14 day running average observed lake inflows over a calibration period. The 14 day running means enable a direct comparison of catchment liquid water to inflows without the need of a flow model.

The lack of an ice-melt component has been identified as a shortcoming of the SnowSim-Pukaki model in the past (Kerr, 2005) so it has been modified to include one as follows. Ice melt was estimated using the melt/temperature formulae derived empirically by Kirkbride from observations on the Tasman Glacier (Kirkbride, 1995):

$$\begin{aligned} For\ z = 960\ m \quad & y = 6.03e^{0.191x} \\ For\ z = 1360\ m \quad & y = 3.035e^{0.216x} \end{aligned} \qquad \textbf{(5-4)}$$

Where:

z = elevation (m)

y = ablation (mm day^{-1})

x = arithmetic mean of the daily maximum and minimum temperatures (^{o} C).

The melt at 960 m and 1360 m is determined for each day and each grid point using the interpolated temperature grid lapsed to the two reference elevations. Melt at the grid point's actual elevation is derived through the assumption that the change in ablation with respect to elevation is constant. Ice melt is determined for only those areas of glacial ice (as derived from the digital NZMS 260 map series ice layer) with no snow cover. Snow cover is a model derived output taken to be all grid points with more than 5 mm of accumulated snow. Areas of moraine covered ice, also derived from the digital NZMS 260 series, are allocated a melt reduction factor of 0.68 as determined by Kirkbride (1995).

A new precipitation interpolation method using the wind-classed precipitation distributions was implemented as follows:

A check for a valid NCEP/NCAR wind class the day of interest is made. If precipitation was observed at Mt Cook EWS, and a valid NCEP/NCAR wind class was given, then a precipitation field was derived using equation 5.5. If other observations were available (including zero measurements), they were assimilated into the precipitation estimation. This was done by finding the ratio of observation to estimated precipitation for each observation site. A scaling grid was prepared from an

interpolation of these observation-to-estimation ratios. The scaling grid was multiplied by the original precipitation estimation grid to provide an observation-corrected estimated precipitation distribution. When no precipitation was observed at Mt Cook EWS, but there was at Franz Josef EWS, then the same procedure was applied except using the Franz Josef grids. If no precipitation was observed at either Mt Cook EWS or Franz Josef EWS, but was at Tekapo EWS, then the Tekapo grids were used. If no precipitation was observed, no observation was available or no valid NCEP/NCAR wind class occurred, then the default precipitation interpolation system using the average annual precipitation surface was used. A flow diagram of the process outline is provided in Figure 5-18.

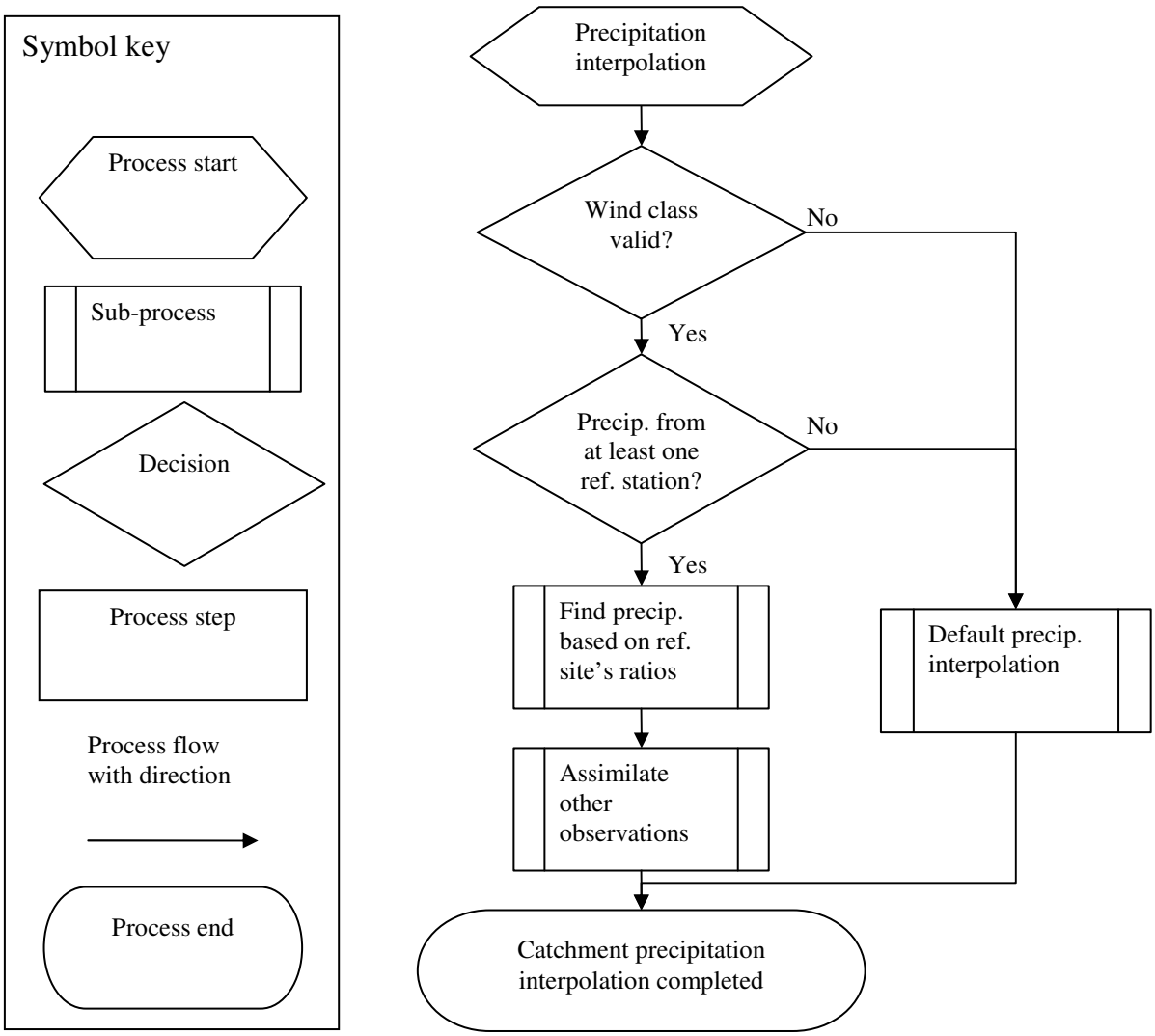

Figure 5-18. Flow diagram describing the selection of precipitation interpolation process.

5.4.2 Model tuning

Tuning of the model, and assessment of model quality is carried out using the Nash-Sutcliffe criterion (NSC) (Nash and Sutcliffe, 1970). This is frequently used in hydrology for model evaluation (Krause et al., 2005) and was selected by the World Meteorological Organisation (WMO) as one of the numerical criteria for validation of snow storage models (WMO, 1986). The NSC criterion provides an indication of how much better the computed daily inflows are compared to the observed average. A value of 1 indicates a perfect model. A value less than 0, indicates the model is worse than using a constant equal to the average. The NSC criterion is given by:

$$NSC = 1 - \frac{\sum (y_c - y_o)^2}{\sum (y_o - \bar{y}_o)^2} \quad \textbf{(5-5)}$$

Where:

y_c = computed value,

y_o = observed value.

Tuning SnowSim-Pukaki for each catchment is carried out through the comparison of catchment liquid water model output with stream flow or lake inflow. 14 day averages are used to account for the integrative properties of stream flow, as well as a constant delay and offset parameter to account for flow and catchment storage processes. The model was applied as a precipitation validation tool requiring relative output measures that can be reasonably attributed to the differing precipitation inputs. For this reason model simplicity is required, limiting the possibility of improved output being a result of changes in model parameterisations unrelated to precipitation input. The model was tuned by optimising the NSC criterion (equation 5.5) for the 14 day averages over the April 1st 2002 to 31st March 2003 period. For lake inflows, an NSC of 0.78 was returned, for the Hooker flows, 0.82 and for the Jollie, 0.58. These values were an improvement for each catchment over those returned using the original precipitation estimation system. Table 5-9 shows the optimised model parameters for each catchment with and without the wind-classed precipitation system.

Table 5-9. NSC criteria and optimised parameters for tuned SnowSim-Pukaki output with and without wind classed precipitation distribution for 2002-3.

	Lake Pukaki		Hooker		Jollie	
	Wind classed precip	No wind classed precip.	Wind classed precip	No wind classed precip.	Wind classed precip	No wind classed precip.
NSC	0.78	0.63	0.82	0.72	0.58	0.57
Parameter						
Offset ($m^3 s^{-1}$)	18	-2	4	0	1	0
Delay (days)	4	4	4	3	5	5
Snow-rain threshold (^oC)	2.5	2.5	2.5	2.5	2.5	2.5
Minimum melt factor (mm $^oC^{-1}$ day^{-1})	1.5	2.0	2	3	1	2
Initial maximum melt factor (mm $^oC^{-1}$ day^{-1})	1.5	0.5	1	0	3	2.5

A measure of the change in model efficiency (ΔME) after inclusion of the wind-classed precipitation may be made by relating the improvement of the model to the improvement required to give a perfect model (Nash and Sutcliffe, 1970) and is given by:

$$\Delta ME = \frac{NSC_2 - NSC_1}{1 - NSC_1} \quad \textbf{(5-6)}$$

Where:

NSC_2 is the NSC score for the altered model and

NSC_1 is the NSC score for the model without alterations.

The ΔME returned for the Lake Pukaki, Hooker and Jollie catchments for the 2002-2003 snow year are 41 %, 36 % and 2 % respectively. This indicates that for each catchment, use of the wind-classed precipitation distributions led to an improvement in model performance. A comparison of observed and modelled hydrographs for the Lake Pukaki, Hooker and Jollie catchments is given in Figure 5-19, Figure 5-20 and Figure 5-21. The large variation in NSC values between the Hooker and Jollie catchments is a reflection of their different precipitation occurrence frequencies. When precipitation is observed at Aoraki/Mt Cook, there is generally a high likelihood that precipitation is also occurring across the Hooker catchment, especially for the more common north westerly events. In the Jollie catchment, occurrence of precipitation is less likely. The occurrence of precipitation will more often be in error in the Jollie catchment than the Hooker catchment. This can be seen clearly in Figure 5-22. Examples of events that are modelled but are not observed in the flow hydrograph occur in April, July and January as shown in Figure 5-21.

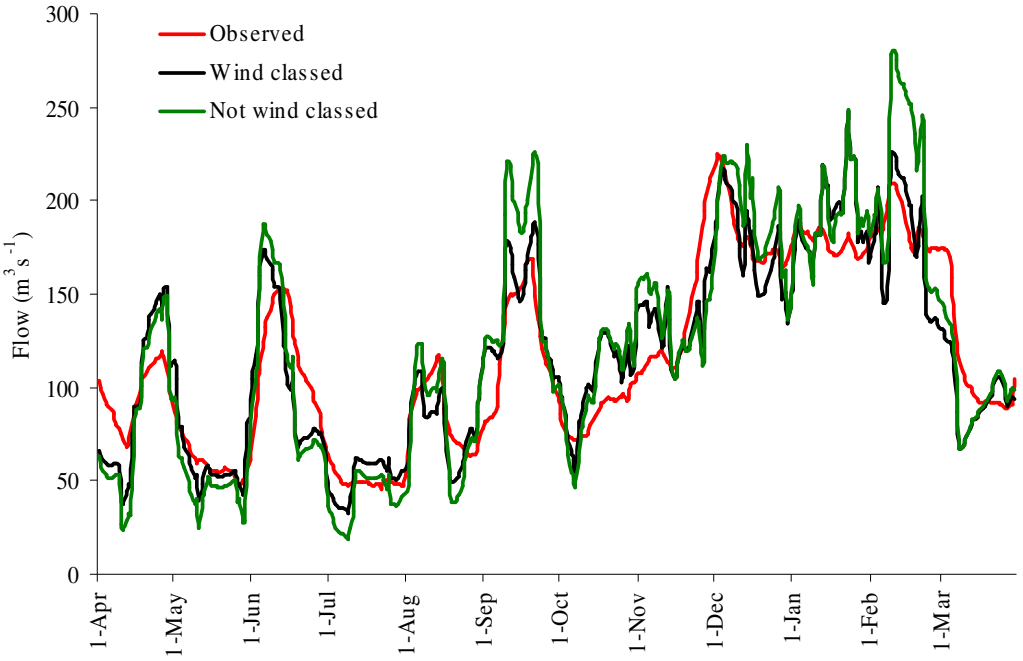

Figure 5-19. Lake Pukaki fourteen day running mean inflows as observed and SnowSim-Pukaki output with and without the daily wind classed precipitation distribution for 2002-3.

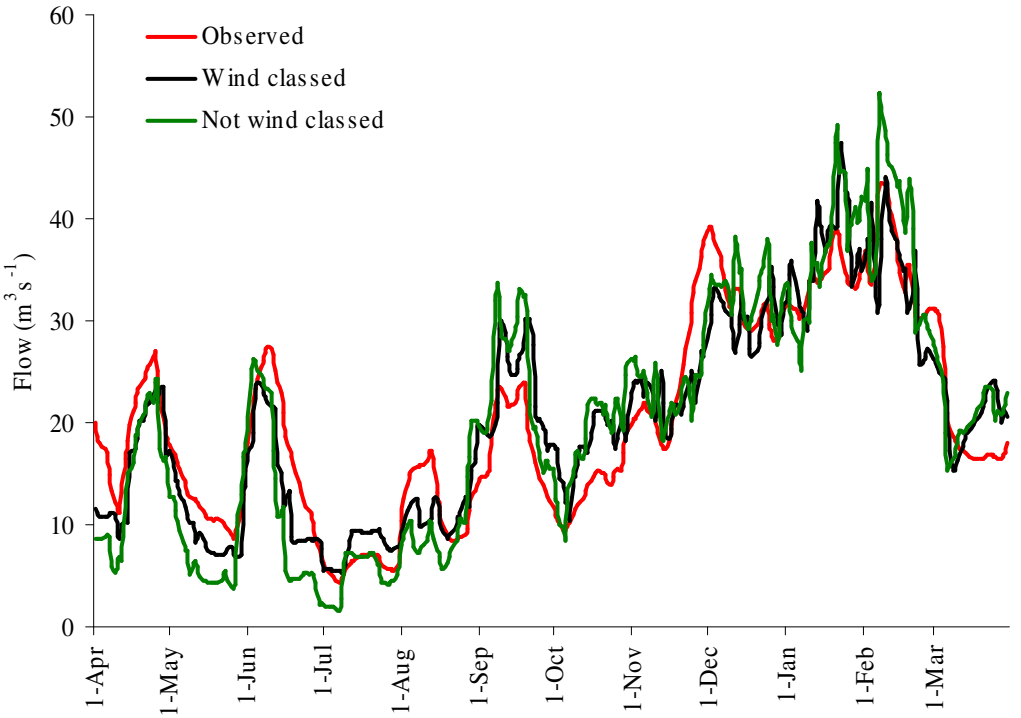

Figure 5-20. Hooker fourteen day running mean flows as observed and SnowSim-Pukaki output with and without the daily wind classed precipitation distribution for 2002-3.

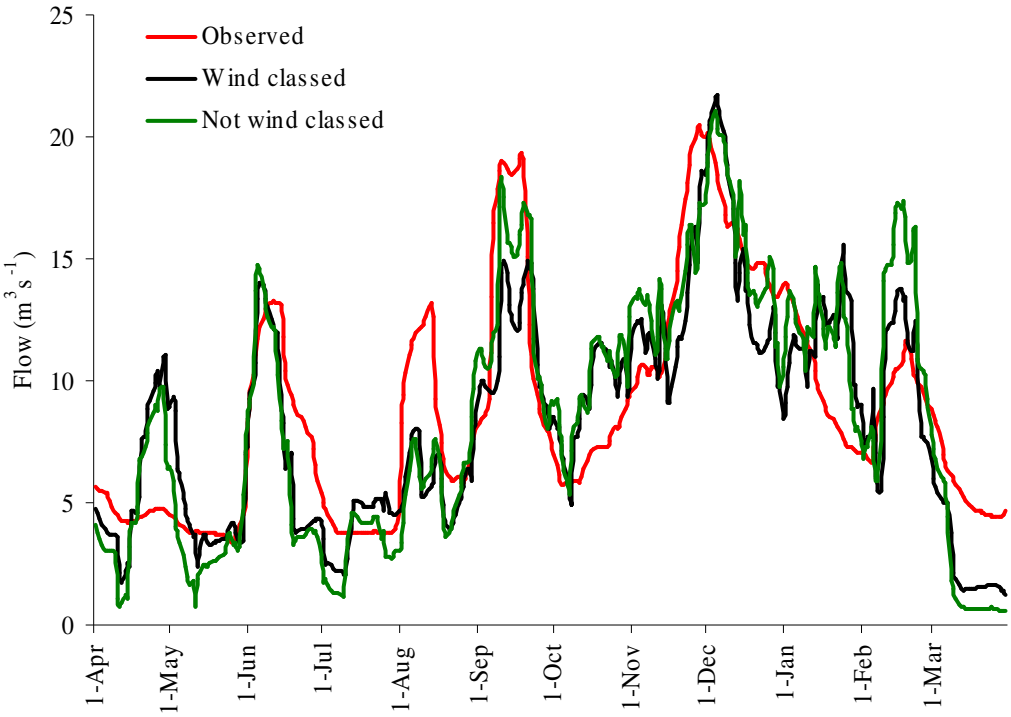

Figure 5-21. Jollie fourteen day running mean flows as observed and SnowSim-Pukaki output with and without the daily wind classed precipitation distribution for 2002-3.

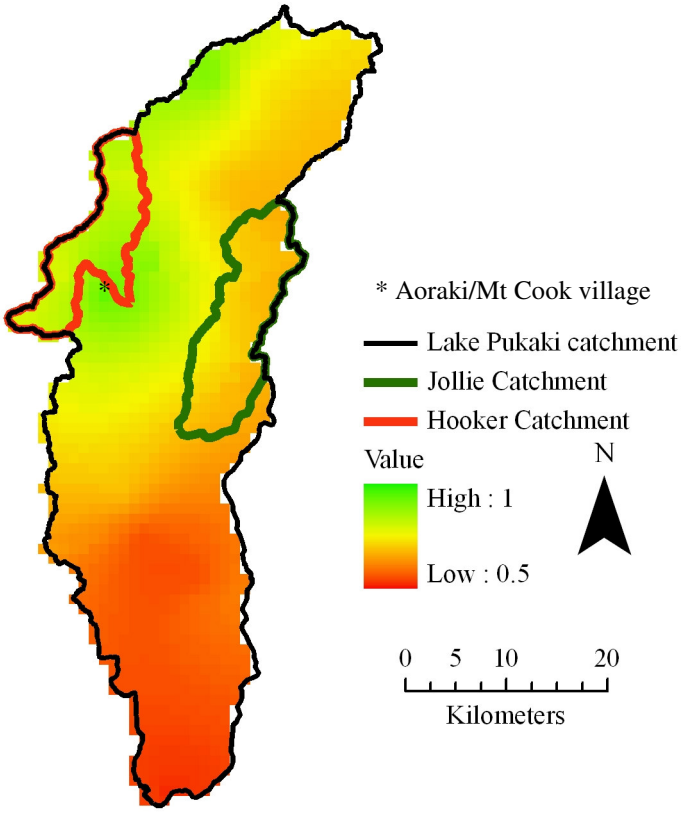

Figure 5-22. Map of the likelihood of daily precipitation with respect to precipitation being observed at Aoraki/Mt Cook Village. This highlights the increased likelihood of precipitation in the Hooker catchment compared to the Jollie catchment.

To further test the validity of the wind-classed precipitation distributions for daily precipitation estimation, the SnowSim-Pukaki model was run for the extended 2000 to 2005 period. The wind classed precipitation provided a general improvement in model output beyond the calibration period for the Jollie (41 %) and Lake Pukaki (33 %) catchments, but a decline for the Hooker (-28 %). In all cases the model efficiency for the Jollie was the least with NSC values of just 0.59 and 0.31 for wind-classed and not wind-classed model options respectively. The Hooker catchment verification results are also counter to the calibration results with the no-wind-classed-precipitation model returning the higher NSC value of 0.8. Observation of the modelled and observed hydrographs (see Appendix 3) indicate the high flow events are when the wind classed precipitation model underperforms, particularly for the major flow events in December 2001 and January 2002 both of which occurred in the 2001-2002 snow year. Excluding this year, the wind-classed precipitation distributions led to an improved model efficiency of 12.5 %. This indicates that it was the mismodelling of the two major flow events that reduced the model efficiency for the entire validation period. From comparison of the monthly maximum daily flows for the calibration and verification periods as shown in Figure 5-23 it appears that high flows were under represented in the calibration period. There is also the possibility that the flow observations are in error during these high flow events, as it is precisely these conditions that lead to the greatest error (Montenari, 2004).

For all three catchments the model tuning resulted in different model parameters. This indicates that to some degree the model tuning is compensating for the different precipitation interpolation methods. The decrease in model efficiency between the calibration and verification periods also indicates that the model has been over tuned to the calibration year. Certainly the results for the Hooker and Jollie indicate the calibration year poorly represented the variations observed during the verification years. Care should be taken in interpreting the results as indicative of the influence of the wind-classed-precipitation system as opposed to the confounding influence of the different model tuning parameters.

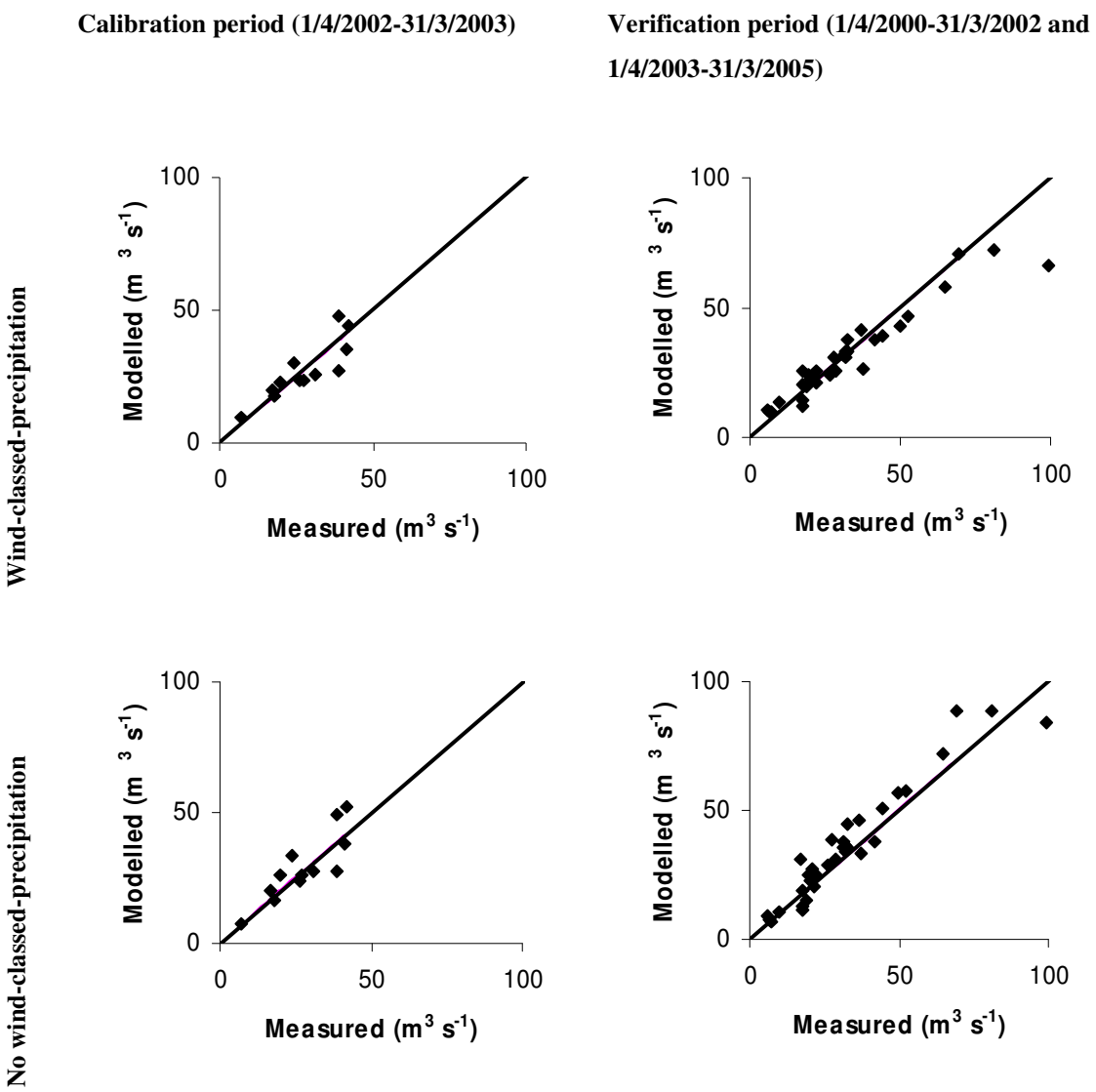

Figure 5-23. Scatter plots of modelled versus observed monthly maximum daily Hooker flows.

5.5 Discussion

The Nash-Sutcliffe change in model efficiency criterion provides a means of comparison of SnowSim-Pukaki model gain with improvements of other models. For example the addition of a percolation function to the GR3J stream flow model returned a 7.5% general improvement (Perrin et al., 2003). An inclusion of parameterisation of infiltration of water into soil led to a 25.6 % improvement of the Soil Moisture Accounting and Routing (SMAR) model (Tan and O'Connor, 1996). A general upgrade of the HBV model, which included a new precipitation interpolation scheme, returned an average improvement over 7 different catchments of 19% (Lindström et al., 1997). While these are average values for a variety of catchments,

and so are not directly comparable to the single catchment application of SnowSim-Pukaki, they do indicate that the model output improvement of 33 % for the Lake Pukaki catchment gained through inclusion of wind direction based precipitation fields is reasonable.

It is likely that part of this improvement is to do with the consideration of likelihood of precipitation occurrence for the wind-classed distributions. When using the average annual precipitation distributions for daily precipitation distribution estimation there is an assumption of precipitation occurrence across the entire region, except at locations where zero precipitation was observed. The wind-classed system restricted precipitation to only those regions where historic synoptic classed observations had shown that precipitation was likely. This combination of considering the synoptic condition and the limits of the precipitation field has also been approached by Hewitson and Crane (2005), with subjectively assessed improvements in spatial precipitation for South Africa returned.

5.6 Conclusion

Water balance estimates of the 1971-2000 annual average precipitation for the Lake Pukaki catchment, the Jollie Catchment, and the Hooker Catchment are 3500 mm, 7700 mm and 2300 mm. These values are within error of the precipitation gauge based distributions thereby confirming their validity. This confirms the high precipitation estimated for the north western regions of the Lake Pukaki catchment, and indicates that if anything, the gauge-based precipitation estimates are conservative. Analysis of storm flow event relationships to the synoptic wind direction on the day immediately prior to the event shows a distribution very similar to that found for precipitation. Variations can be attributed to the impact of evapotranspiration and melt water on flows.

The snow storage model SnowSim-Pukaki provided improved fortnightly averaged catchment liquid water estimates when wind-classed precipitation distributions were used in generating the models precipitation fields. This result provides weight to the value of using wind-classed precipitation fields for the entire catchment, and indicates the generalised wind-class based precipitation fields derived in the previous chapter have a degree of accuracy. An improvement was also returned for the Jollie catchment, but not for the Hooker catchment. This would suggest that in the high precipitation regions, during high precipitation events, the average annual

precipitation surface (derived from all available precipitation measurements) is a better descriptor of the precipitation field than the wind-classed precipitation field (derived from limited daily precipitation observations).

The Nash Sutcliffe change in model efficiency criterion returned a value of 33 % for the application of SnowSim-Pukaki to the entire catchment using the wind-classed precipitation distributions. This level of improvement validates the quality of the wind-classed distributions and shows they are an improvement over using the average annual precipitation distribution.

6 Long term trends of climate and precipitation

6.1 Introduction

The relevance of a climatology to any period of time, other than that used to establish it, is dependent on the rate of change of the climate, and where the climatology sits within temporal climate variations. Climate varies across the full spectrum of temporal scales (Figure 6-1). These changes are in response to external forcings (e.g. solar activity, earth orbit variations) and to earth system feedbacks (e.g. snow cover variation, ocean currents), none of which are fully understood. In combination, all forcings and system feedbacks lead to complex temporal variations in climate.

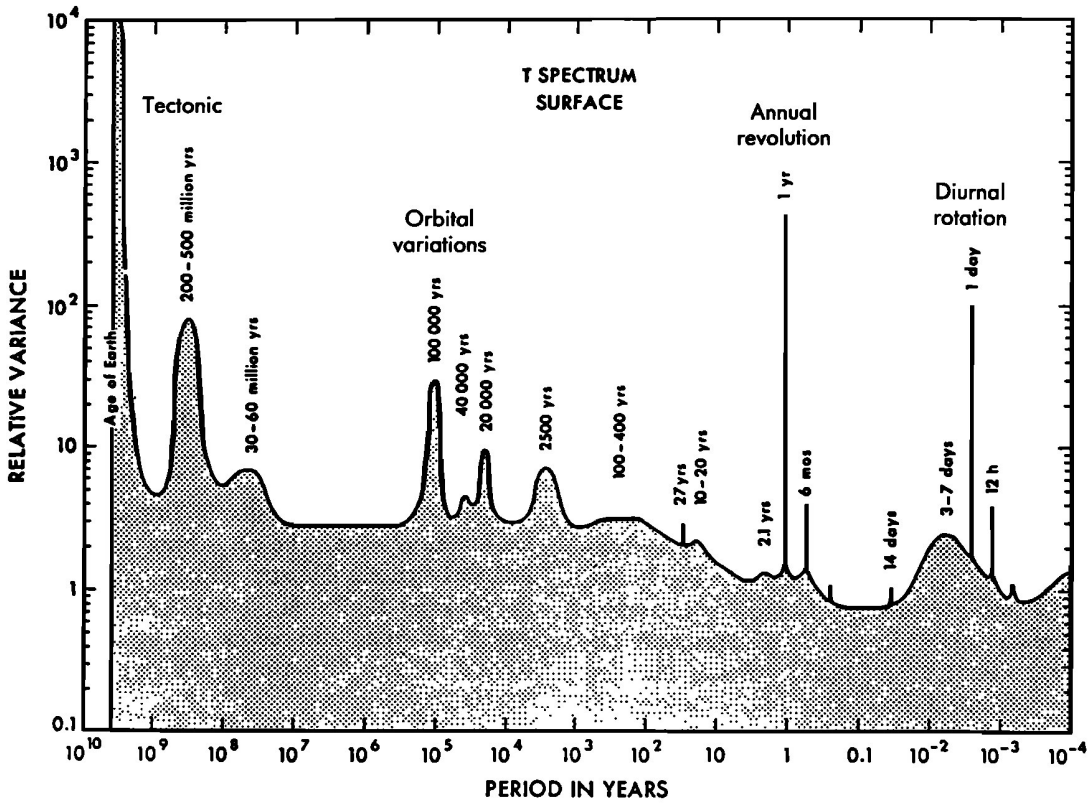

Figure 6-1. Climate period spectrum with peaks and tentative causes (Berger, 1988 p. 626).

Non-cyclical climatic variations of a random nature are also observed and may be considered a reflection of the complexity of all these climate processes. Establishment of climate trends and cycles requires distinguishing them from the random variations. With respect to a precipitation climatology based around a thirty year average, trends and cycles of a decadal scale or greater are of interest. A brief review of the literature

below indicates there are two such climate variabilities, the first is a long term trend associated with global climate warming, the second is a multidecadal climate variation associated with the Interdecadal Pacific Oscillation.

A warming trend in temperature of 0.7 ^{o}C over the 1899 to 1993 period has been identified in both sea surface temperatures around New Zealand and land based observations within New Zealand (Folland and Salinger, 1995) with most of that warming (0.5 ^{o}C) observed between the 1940s and 1950s (Salinger et al., 1995). This change in temperature increases the water holding capacity of the atmosphere thereby increasing the water available for precipitation. This link has been used to explain the modelled global increase in precipitation associated with increased greenhouse gases (Buishand and Brandsma, 1999) and as a direct driver of regional climate change studies (e.g. Schär et al., 1996). Climate models provide an indication of general trends in large scale precipitation fields but are currently not able to provide definite forecasts for specific mountain regions (Schär and Frei, 2005). Recourse to observations and their discernible trends is therefore required to provide an indication of the links between precipitation variability and global climate warming.

In New Zealand, a trend in precipitation has been determined for the 1930-2004 period (Griffiths, 2006). This study found significant (at the 0.95 level) decreasing trends in precipitation frequency and magnitude in the north east of the North Island, and increasing trends for stations in the south west of both islands though not at Aoraki/ Mt Cook. These spatially consistent trends were attributed to circulation changes, and particularly to a strengthening of westerly flow. The relationship to circulation is consistent with that observed by other New Zealand studies (Lorrey et al., 2007; Salinger et al., 1995, 2001; Salinger and Mullan, 1999), though in these cases, no trends were found. Instead of a trend, they identified a shift in precipitation magnitude in 1945 and 1978 associated with the Interdecadal Pacific Oscillation (IPO). The IPO is an index of a multi-decadal variation in Pacific region sea surface temperatures (Salinger et al., 2001). Several indices exist that are largely equivalent to the IPO (Power et al., 1999) and are all based on principal component analysis of Pacific sea surface temperatures. These include the Pacific Decadal Oscillation (PDO) derived from North Pacific sea surface anomalies (Mantua and Hare, 2002). For the twentieth century, the IPO has changed phase in 1912, 1924, 1944, 1977 and 2000 as shown in Figure 6-2. Relationships between the IPO and precipitation is not uncommon with coastal central Alaskan precipitation found to be associated with the

PDO (Simpson et al., 2002), Australian precipitation relationships to ENSO modulated by the IPO (Power et al., 1999), and North American wintertime precipitation correlated to the PDO (Mantua et al., 1997).

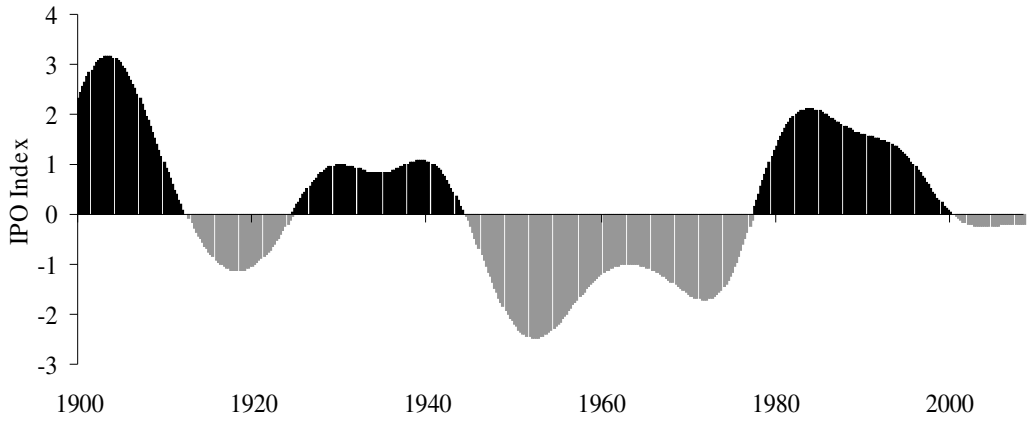

Figure 6-2. IPO index (Folland, 2008)

The IPO has been shown to affect the strength of the Southern Oscillation, with the +ve IPO phase enhancing it and the –ve IPO diminishing it (Salinger et al., 2001). The Southern Oscillation is a two to three year shift in atmospheric mass from the South Pacific sub-tropical high to the Indonesian equatorial low, closely associated with the El Nino/La Nina sea surface temperature variations (Rasmusson and Carpenter, 1982), and well indexed by the difference in pressure between Darwin and Tahiti (Chen, 1982). This Southern Oscillation Index (SOI) has been shown to relate to circulation changes in New Zealand, and thereby to precipitation and temperature variation (Gordon, 1986). It is this modulation of the Southern Oscillation by the IPO which is used to explain the shifts in sea level pressure, temperature and precipitation observed in the South Pacific (Salinger et al., 2001) and glacier mass balance regimes in the Southern Alps (Fitzharris et al., 2007). In addition to the Southern Oscillation, another sub decadal climate variation known to impact on New Zealand climate is the Southern Annular Mode (SAM) (Clare et al., 2002; Ummenhofer and England, 2007). The SAM describes the main pattern of variation of sea level pressures from the climatological mean for the Southern Hemisphere mid to high latitudes (Baldwin, 2001). The SAM is circumpolar in form (hence the Annular) with the positive (negative) phase having anomalously low (high) pressure over Antarctica and

anomalously high (low) pressures in the 40-55^{o} latitudes. Several indices have been derived to describe the SAM (Marshall, 2003) with daily indices showing variations at the weekly scale (Renwick and Thompson, 2006) and with a general trend towards the positive mode particularly since the mid 1970s (Marshall, 2003). Like the Interdecadal Pacific Oscillation, the SAM is an index of observed variability of unclear origins that describes definite spatial connections. Unlike the Interdecadal Pacific Oscillation the SAM has no clear periodicity (Renwick and Thompson, 2006). In terms of the precipitation normals determined for the Lake Pukaki catchment, it is the long term cycles and trends that are of interest rather than the shorter term ENSO and SAM variabilities which over the thirty year period are largely averaged out.

It is under this background of long term warming trends, IPO phase based climate shifts related to SO modulation, in combination with effectively random variability, that the Lake Pukaki precipitation record is explored.

Within the catchment, long term precipitation records are limited to those obtained at The Hermitage and at Braemar Station. These two sites provide the basis for temporal variation assessment. Investigation of long term trends in precipitation frequency, magnitude and extremes is carried out first. Then the impact of different IPO phases on precipitation frequency, magnitude and extremes is explored. Following from the established relationships between wind classes and precipitation (see chapter 5), the long term trends, and IPO shifts, of wind-class frequency and strength are investigated. Previously identified wind-class to precipitation relationships are then combined with observed wind-class temporal variations to assess whether circulation changes can explain the observed precipitation changes.

6.2 Precipitation trends

6.2.1 Quality of records

Systematic observations of precipitation at Aoraki/Mt Cook Village (see Figure 6-3 for locations) have been taken since 1901 (Salinger, 1981). The observations were initially recorded as monthly totals, later daily, then most recently for every 15 minutes. As was discussed in chapter 3, the exact location of the observations, the exposure of the precipitation gauge, and the method of observation have all changed through time. All these changes impact on the observed precipitation totals so must be accounted for when using the record to discern climatological trends.

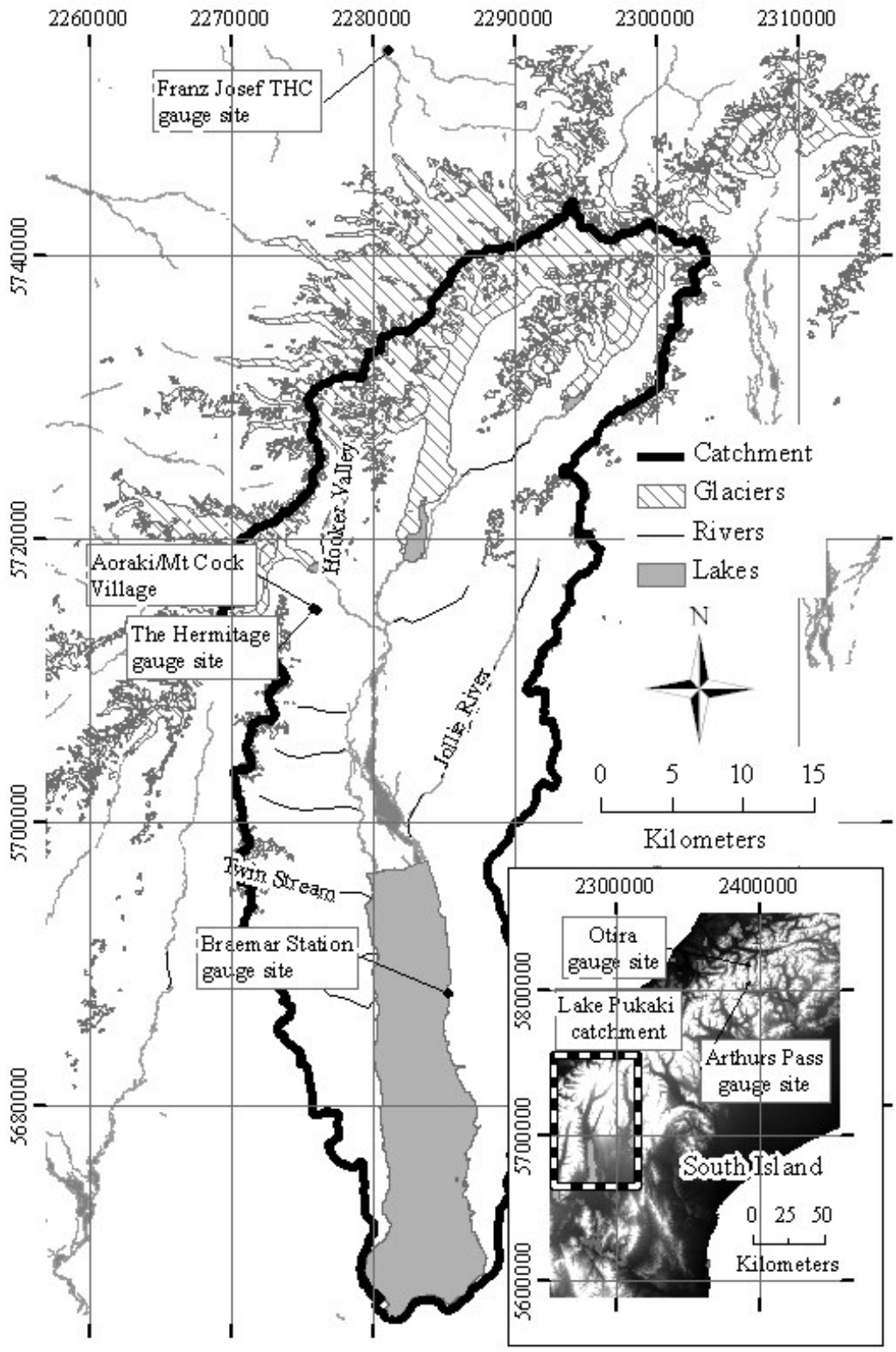

Figure 6-3. Locations of places mentioned in the text.

Site changes that are likely to have influenced the observations since 1928 were identified in chapter 3. These are 1934, 1937, and 1948. Prior to 1928, the hotel with which the rain gauge was associated, was rebuilt at a new site following flooding in early 1913 (Wilson, 1968). After this flooding the monthly record became intermittent until mid 1915 when it stopped completely (Fouhy, 2008). Not until July 1923 did the record start again, presumably at the site of the new hotel. This suggests a site change at 1923. The introduction of daily recording in 1928 also indicates a change of operation so is considered another possible site change. This leads to five known site changes that may have potentially affected the observed precipitation totals. Assessment of the effect of these site changes on the record has been carried out following the methods of Rhoades and Salinger (1993) and is described as follows: Logarithms (base 10) of monthly precipitation totals were obtained for the site of interest (The Hermitage) and for related neighbouring stations. As in chapter 3, three stations that are most likely to be in a similar climate zone to The Hermitage were identified: Otira, Arthurs Pass and Franz Josef THC (Figure 6-3). A series of differences between the log of monthly totals before and after a suspected site change was prepared. These differences were of like months to remove seasonal effects, and as long as possible without inclusion of a second suspected site change (either at The Hermitage, or at the neighbouring station). This was done for each site. If no site change had occurred, and there is no climatological trend, these series would be near random variables, normally distributed about zero. A new series is then generated from the sum of differences of the weighted neighbouring station difference series and The Hermitage difference series. The weighting is based on correlations of the log of 12 month offset monthly precipitation different series with neighbouring stations (see Figure 6-4) and is calculated as follows (Rhoades and Salinger, 1993):

$$w_i = \frac{\rho_i^4}{\sum_{j=1}^{n} \rho_j^4} \qquad \textbf{6-1}$$

Where:

w_i = weighting of site i and

ρ_i = correlation coefficient at site i.

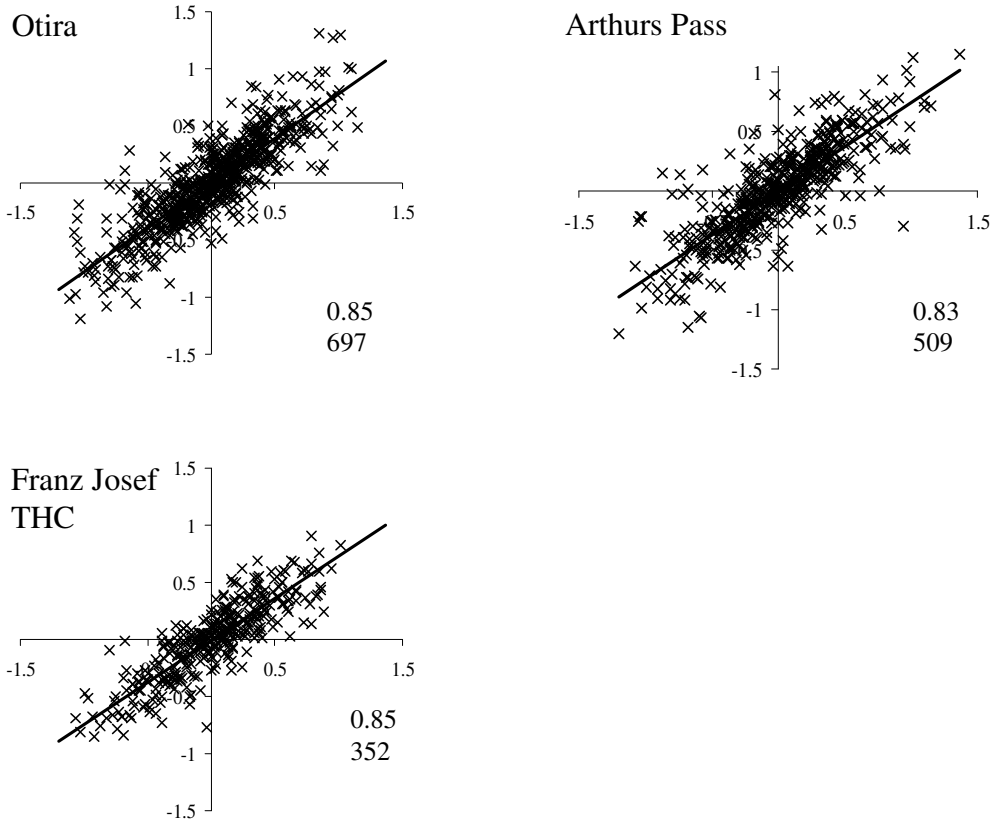

Figure 6-4. X-Y plots of the log of 12 month offset monthly precipitation difference series for The Hermitage against Otira, Arthurs Pass and Franz Josef THC. The two numbers in the lower right quadrant of each plot are the correlation coefficient (upper number) and the number of months in common between the series (lower number).

This weighting biases the influence of neighbouring stations towards those with the highest correlation. The weighted difference series is assumed to be a set of independent normally distributed random variables. The differencing effectively removes any climatological trends common to the sites, the assumption being that each of the sites responds in a similar manner to climatological forcing. Any statistically significant shift of this difference series is then attributed to the site change at The Hermitage. Statistical significance is determined by finding the 95 % confidence limits of the difference series average, and exponentiating these limits. If they encompass unity, then the shift is not significant at the 95 % level.
For identified significant shifts, the amount of shift was determined by the exponentiated average of the difference series.

For certain months, not all of the related stations had a recorded monthly total of precipitation, precluding their use in determining the weighted difference series and necessitating the use of different weightings. The weighting matrix for different related station combinations is shown in Table 6-1.

Table 6-1. Series weightings for different combinations of correlated stations.

	Otira	Arthurs Pass	Franz Josef THC
Otira	1	-	-
Otira and Arthurs Pass	0.53	0.47	-
All	0.35	0.31	0.34
Arthurs Pass	-	1	-
Arthurs Pass and Franz Josef THC	-	0.47	0.53
Franz Josef THC	-	-	1
Otira and Franz Josef THC	0.50	-	0.50

The weighted difference series is shown for each considered site change date in Figure 6-5. If the considered site change has no effect on the observations, then the weighted difference series should be a series of random variables normally distributed about zero. If the 95 % confidence limit of the mean of the difference series does not encompass zero then the site change is considered to have affected observations. If the difference is highly variable (as with the case for the first four difference series) the confidence limit also increases. If a trend is observed in the difference series, then it may be covering a period that includes an unknown second site change in any one of the stations. For the 1928 and perhaps 1914 site changes, this may have occurred. In both of these cases, the variability in the difference series precludes the statistically significant determination of a change in observation as a result of the site change. This is the case despite the fact that the (undocumented) move of the rain gauge with the building of the new hotel should have resulted in a reduced precipitation catch. Indeed the non-significant offset of the weighted difference indicate that prior to 1928 over 1.4 times the precipitation was observed compared to after 1928. Such an increase is greater than what would be expected with a move from the original hotel site to the current hotel site based on the average annual precipitation distribution estimated in Chapter 3. This result, combined with the high variability, indicates the quality of the record at that time was poor.

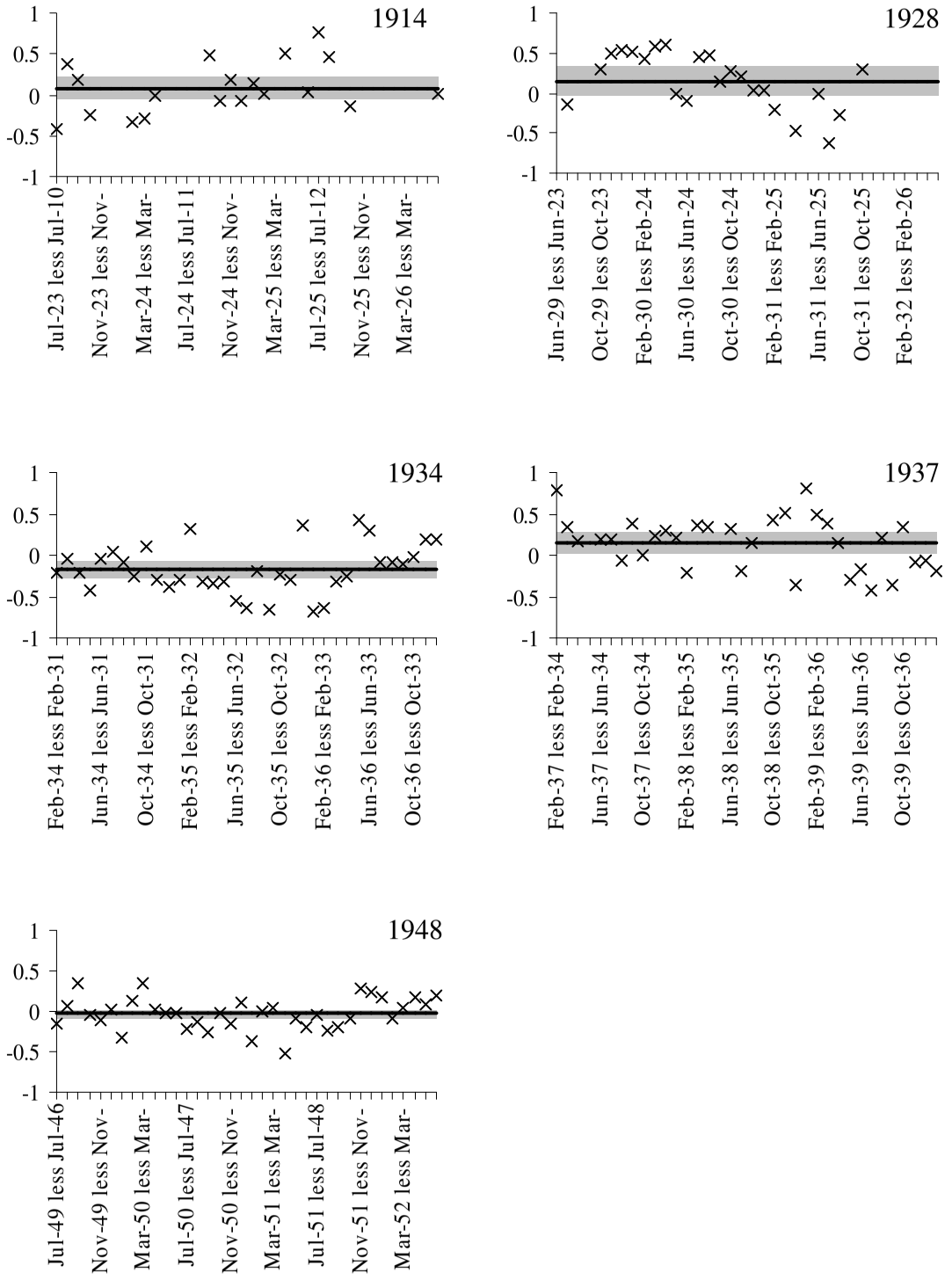

Figure 6-5. Weighted difference series across known site changes. X axis scale is log of monthly precipitation totals (in mm). The dark line is the mean of the differences. The grey band is the 95 % confidence interval. A significant site change effect is considered to occur when the 95 % confidence interval does not encompass zero.

The 1934 and 1937 site changes both show a significant shift in the difference series from a mean of zero indicating that in these cases the site change did affect the observations. The 1934 site change analysis indicates the pre-1934 observations were just 0.7 times those that were observed after 1934. The 1937 site change results indicate the pre-1937 observations were 1.4 times those observed after 1937. These two results indicate that between 1934 and 1937 the observations were generally being over reported. During this period the climate station was inspected twice by officials of the Meteorological Service leading to a recommendation to abandon the station (Fouhy, 2008) indicating that difficulties with observations were known to be occurring. Fortunately, the station was not abandoned, and the observations were improved. An assessment of the station's precipitation record, based on comparison with Otira by Salinger (1981) recommended that only the 1932-1933 and 1948-1965 records be used for analysis, but even then with caution. The shift in observations for the 1934-1937 period is shown in Figure 6-6.

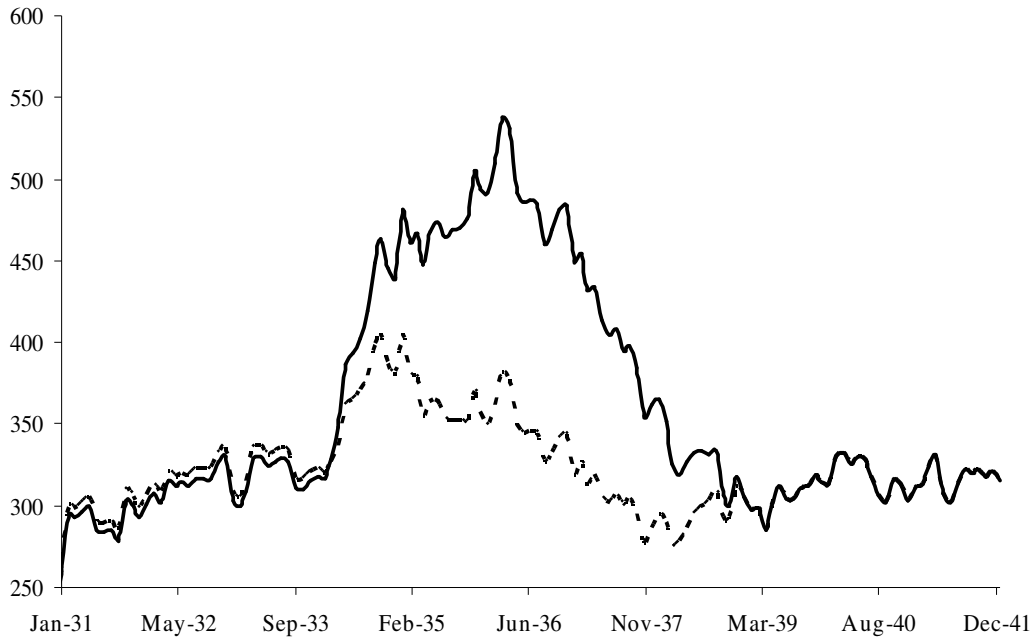

Figure 6-6. 36 month running mean of the log of monthly precipitation totals at The Hermitage from 1931 to 1950 as observed (solid line) and after correction (dotted line).

It is clear from this graph that the site change in 1937 did not occur on a single day, but occurred gradually over time. Such an effect is consistent with a change in the exposure of the precipitation gauge, especially through the growth of trees. Applying

the single correction factor to the period generates a series that appears to still be in error. In view of the variability of the early record, and the difficulty in correcting for the site changes between 1934 and 1937, attempts at correcting the record for site changes were abandoned leaving only the record after 1937 for assessment of climatological trends.

6.2.2 Braemar Station

Site history notes from the NIWA climate database indicate that there were site changes at Braemar in May 1928, May 1967, April 1969, some time shortly after May 1974, some time prior to March 1985 and in June 1989. In addition, throughout the history of the site, changes in exposure from growth of surrounding vegetation were noted. Nearby gauge sites used for homogeneity assessment were Tasman Downs, Guide Hill, Lake Pukaki No. 1, Lake Pukaki MWD, and Lake Tekapo. Monthly totals at Braemar had correlation coefficients of $r > 0.6$ against all of these sites. After comparison between Braemar and these nearby stations no site changes were found to cause a statistically significant shift in the monthly precipitation totals. This is likely to be a result of the much reduced horizontal precipitation gradient in the surrounding area as shown previously in Chapter 4, meaning that any shift in the gauge site has little effect on the gauge catch.

6.2.3 Long term trends

A review of trend analysis by Hirsch et al. (1991) finds parametric approaches the most powerful for identifying a monotonic trend where residuals are normally distributed random variables. The slope of the regression line provides an estimate of the trend magnitude, while the standard error of the residuals provides a measure of the significance. As was shown in Chapter 3, a log transform of monthly precipitation data leads to a near normal distribution enabling the use of this regression line approach. The variability of the residuals from the regression line (and hence the statistical significance of the regression slope) may be affected by seasonality in the precipitation record. De-seasoning of the time series is recommended by Hirsch et al. (1991) and is achieved here by differencing each month's precipitation with that observed the previous year (Rhoades and Salinger, 1993). Examples of using regression analysis for the estimation of precipitation trends may be found in Curtis et al. (1998), Schmidli and Frei (2005) and Lloyd (2009).

For all available monthly totals from January 1939 until February 2000, the difference of the log of the monthly total with the log of the monthly total one year before, was obtained. If there was no trend, then these would be near random variables, normally distributed about zero. In the presence of a trend, the mean of this series will be offset from zero. Statistical significance is attributed to the trend when the 95 % confidence limits of the mean do not encompass zero. The plot of The Hermitage and Braemar Station series with the mean and 95 % confidence limits is shown in Figure 6-7. No statistically significant temporal trend may be discerned from either.

To determine whether there has been long term seasonal trends, the analysis was repeated for individual months of the year. Once again, no significant trend was identified at the 0.95 % level for any month. This result is consistent with that which has been found for twenty one different precipitation stations throughout New Zealand for the 1920 to 1990 period (Salinger et al., 1992).

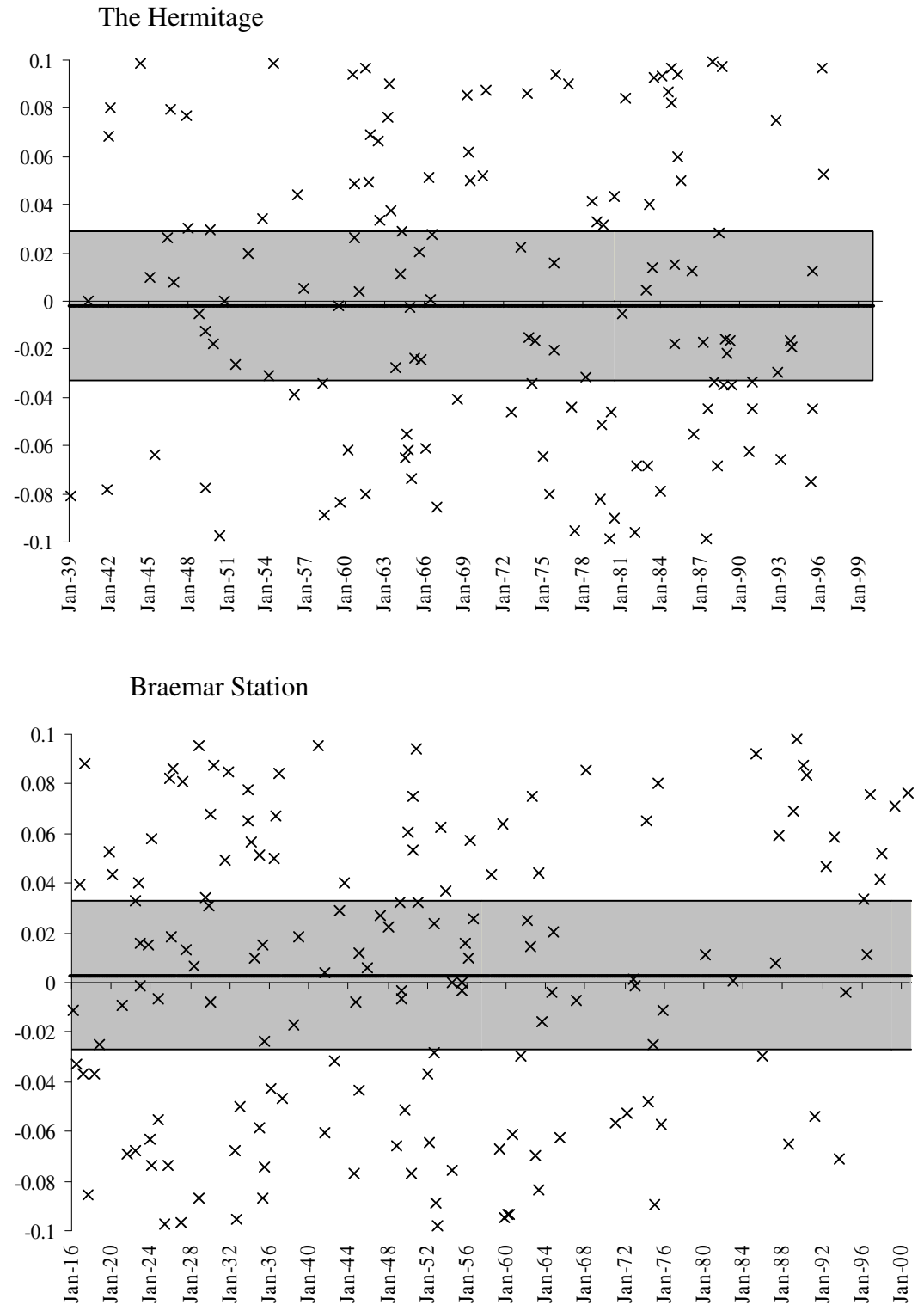

Figure 6-7. Plot of the difference of the log of monthly precipitation totals with the previous years logged monthly total. The grey shading represents the 95 % confidence interval around the dark line of the mean of the series.

6.2.4 Precipitation changes associated with the Interdecadal Pacific Oscillation

While no significant long term trend in The Hermitage or Braemar Station precipitation records is discernible, there may be shorter period changes associated with the Interdecadal Pacific Oscillation (IPO). To test for this, monthly precipitation data from 1950-1970 (within a negative phase of the IPO) was compared with 20 years of monthly data from 1980-2000 (within a positive phase) and with five years of data from 1939-1944 for The Hermitage, and 1924-1944 for Braemar Station (within an earlier positive phase). The periods selected were chosen to fall wholly within an IPO phase. Where possible, equal length periods have been used to keep variability resulting from sample sizes constant. Ideally the periods would be near the centre of their respective IPO phases. For the early period the record length prevents this. Testing for a climatic shift impact on precipitation is the same as testing for a site shift impact as was done above in section 6.2.1. The series of the difference of the log of the monthly totals for the period of interest from the average of the 1950-1970 monthly total logarithms was prepared. Then the null hypothesis that the difference of the period means from the 1950-1970 mean was zero was tested using the z statistic. A probability of less than 0.05 for the z statistic was considered statistically significant. The z statistic was found as follows:

$$z = \frac{\bar{x}_1 - \bar{x}_2}{\sqrt{\frac{{s_1}^2}{N_1} + \frac{{s_2}^2}{N_2}}} \qquad \textbf{6-2}$$

Where:

1 = the 1950 to 1970 series,

2 = the series being compared to the 1950 to 1970 series,

$\bar{x}$ = mean,

s = standard deviation,

N = number of items in the series.

Figure 6-8 shows the three periods together with 95 % confidence intervals. Table 6-2 shows the average monthly precipitation together with the annual average precipitation for the three IPO phases.

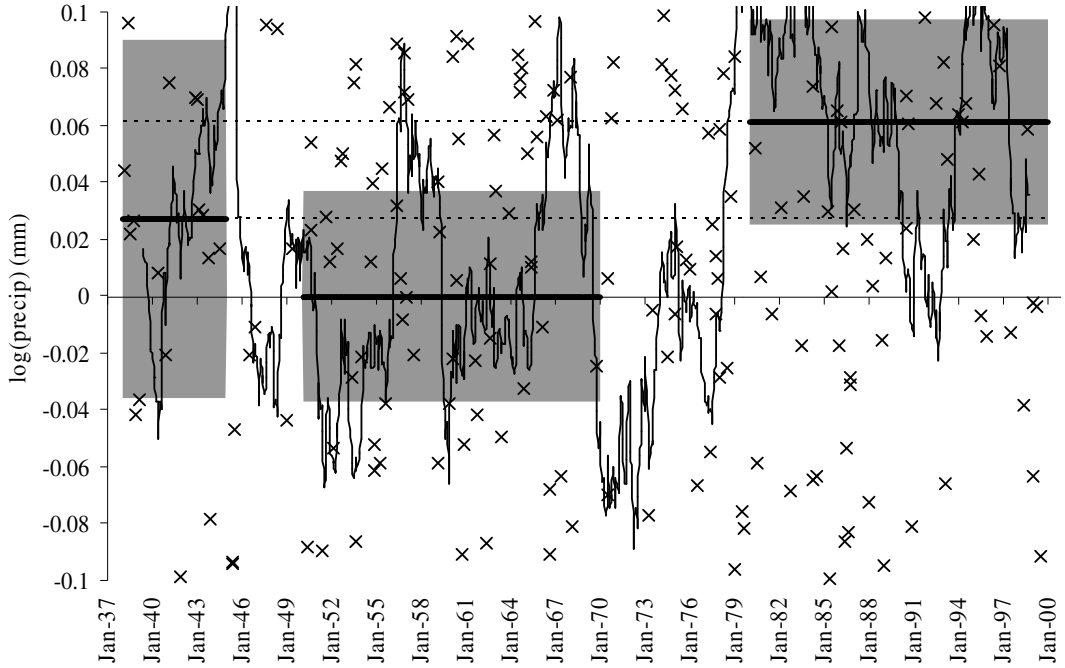

The Hermitage

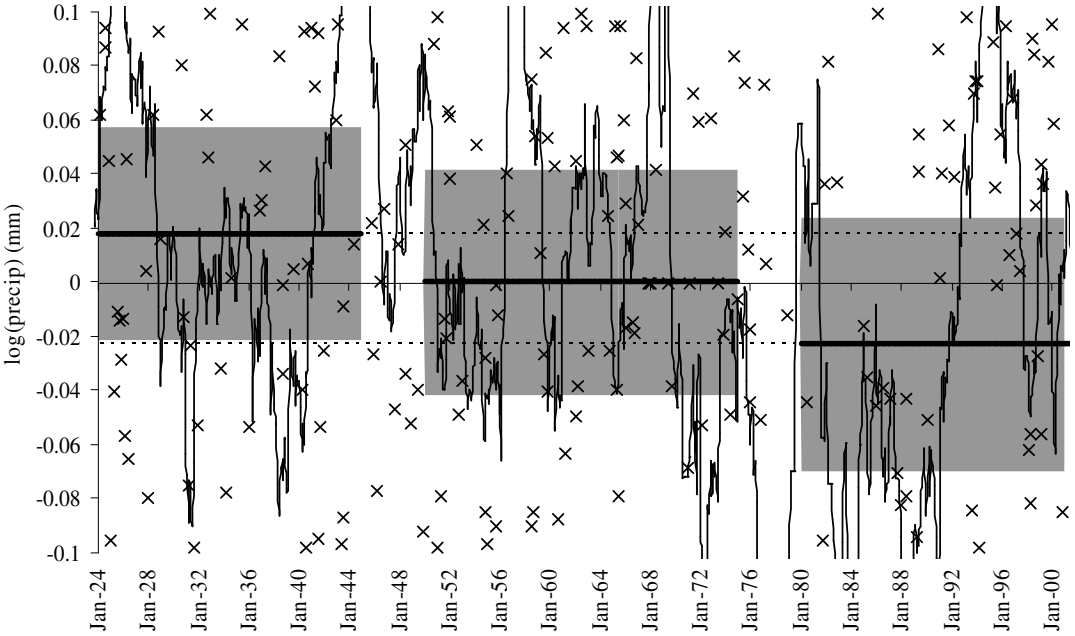

Braemar Station

Figure 6-8. Difference of the log of monthly precipitation totals and the mean of the log of the 1955-1970 monthly precipitation totals. The crosses are monthly totals less the mean of the 1955-1970 monthly totals. The banded lines are the 1939-1944, 1955-1970 and 1980-1995 means with shading representing the 95% confidence intervals. The varying line is the 3 year centred running mean. The dotted lines are extensions of the period means.

Table 6-2. Average monthly precipitation (mm) for different IPO periods. Bold indicates statistically different to the 1950-1970 values. Numbers in brackets are annual average values. Note that the time period used for the earliest IPO phase differed between the two gauge sites.

	1939-1944[*] 1924-1944[#]	1950-1970	1980-2000
[*]The Hermitage	287 (3444)	269 (3228)	**310 (3720)**
[#]Braemar Station	62 (744)	60 (720)	57 (684)

At The Hermitage on average there was 269 mm of total monthly precipitation in the period from 1950-1970. This increased to 310 mm for the 1980-2000 period, and 287 for the 1939-1944 period. The z statistic indicates the 1980-2000 period mean was statistically different from the 1950-1970 mean, but the 1939-1944 was not. The higher precipitation for the 1980-2000 period with respect the 1950-1970 period was consistent with increased rainfall observed in the South Island alpine region between the periods 1951-1975 and 1976-1994 (Salinger and Mullan, 1999) and with increased precipitation in the west of the South Island associated with the positive phase of the IPO (Salinger et al., 2001). It was also consistent with increased flood and low-flow magnitudes of South Island rivers draining the Southern Alps and increased rainfall magnitudes at Invercargill (290 km to the south south west, on the south coast) and Milford Sound (185 km to the south west and just 20 km from the west coat) (McKerchar and Henderson, 2003). The short series and precipitation variability of the 1939-1944 period precludes the conclusion that it was a relatively high precipitation period. For Braemar Station the 1950-1970 average precipitation of 60 mm decreased to 57 mm for the 1980-2000 period. This shift and that between the earlier 1924-1944 period and the 1950-1970 period are not statistically significant at the 95 % level so it cannot be concluded that the differences are not a result of simple inter-annual variation.

The effect of the IPO at a seasonal level was investigated through comparison of month-of-year series for each period. Table 6-3 shows the month-of-the-year period means. For The Hermitage, just two months returned a statistically significant increase, June and October. The October increase appears to be seasonally isolated with neither the September nor November 1980-2000 means greater than the 1950-1970 means. The July and August 1980-2000 means are higher than the respective 1950-1970 means suggesting that the IPO phase has an influence on winter precipitation. This result is also consistent with that found for the South Island Alpine

region (Salinger and Mullan, 1999) and for the south west of the South Island (Lorrey et al., 2007; Salinger et al., 2001) where winters were found to be relatively wetter but with little change in the spring and autumn. One difference to this previous work is that they also found the summers to be wetter. Similarly, the Franz Josef THC precipitation record has been found to have a statistically significant increase between the periods 1954-1974 and 1974-1994 for both the glacier ablation season (November to March) as well as the accumulation season (April to October) (Hooker and Fitzharris, 1999).

Table 6-3. Mean monthly totals for different IPO phases. Numbers in bold are significantly different from the 1950-1970 totals.

	Jan	Feb	Mar	Apr	May	Jun	Jul	Aug	Sep	Oct	Nov	Dec
The Hermitage												
1939 to 1944	383	351	319	445	256	284	165	216	300	249	275	264
1950 to 1970	316	276	291	309	302	203	197	232	253	280	330	292
1980 to 2000	385	236	379	316	305	**310**	241	276	253	**397**	311	373
Braemar Station												
1924 to 1944	81	49	53	71	**63**	59	51	74	69	66	66	58
1950 to 1970	71	54	49	54	88	54	60	65	68	61	64	61
1980 to 2000	47	43	61	49	**55**	68	62	68	59	75	58	58

A summertime increase in precipitation cannot be concluded from The Hermitage observations. This suggests that The Hermitage site (lee of the main divide of the Southern Alps) has a different seasonal response to the climate forcings associated with the IPO from that which has been observed at Franz Josef and the general climate region. This would indicate that caution needs to be taken when applying South Island West Coast region climate trends to the Lake Pukaki catchment. In terms of glacierization in the region, increased winter precipitation will lead to increased snow accumulation and positive glacier mass balances, consistent with the observed growth of the more rapid response glaciers in the region (Fitzharris et al., 2007; Kerr and Owens, 2008). For Braemar Station, May shows decreased precipitation during the +ve IPO phases compared to the –ve 1950-1970 phase. This change is in an opposite sense to that observed at The Hermitage indicating that the two sites are operating under different climate regimes. Consistent with the Braemar Station reduction in precipitation, Zheng and Thompson (2007) found reduced summer average precipitation day totals at Lake Tekapo associated with the 1977 IPO phase

change. In the Tekapo case, increased precipitation days led to an overall increase in summer precipitation. Of the rotated principle components prepared by Salinger and Mullan (1999) for New Zealand precipitation, the South Canterbury component would be the most likely region for Braemar Station. In their analysis they found the autumns to be wettest in the 1951-1975 period for this region, which may be related to the May variations observed here. They also found winters to be significantly wetter during the 1976-1994 period. This was not observed here though a non-significant increase in precipitation was. Interestingly Sallinger and Mullan (1999) did not find a significant decrease in precipitation for summer for the last phase of the IPO for this region. This suggests that, in a similar manner to The Hermitage, application of regionally observed climate differences to specific locations may not be valid.

6.2.5 Frequency trends

While no statistically significant trend in the magnitude of monthly precipitation has been found, no consideration has yet been made of the frequency of precipitation events, and in particular, the frequency of high precipitation events. Extreme precipitation events, as opposed to average conditions, apply stress to social and environmental systems. Recognising a trend or shift in the occurrence of extremes provides an indication that those social and environmental systems are under pressure and may lead to improved understanding and or management of them. Assessment of monthly magnitude trends cannot determine whether the change is a result of increased precipitation events or increased event magnitudes, or a combination of these. Nor can it discern whether changes are particular to certain event sizes or spread evenly across all events.

Trends in extreme rainfall have been explored for a variety of locations around the world including Europe (Tank and Können, 2003), Australia (Haylock and Nicholls, 2000), United States of America (Karl and Knight, 1998), India (Goswami et al., 2006), China (Wang and Zhou, 2005), Central and northern South America (Aguilar et al., 2005) and globally (Groisman et al., 1999) with two studies having investigated the New Zealand region (e.g. Manton et al., 2001; Salinger and Griffiths, 2001). In 1997, an international workshop on indices and indicators for climate extremes was held which recommended that for precipitation the minimum set of indicators to be used should be:

- The change in the magnitude of the 95th percentile for rain days

- The percentage of annual precipitation falling on days with more than the 95th percentile of precipitation (Nicholls and Murray, 1999).

Following these guidelines and adopting the indices used by the previous New Zealand studies led to the set of indices set out below being applied to The Hermitage 1939-2000 and Braemar Station 1924-2000 precipitation records:

- The frequency of days in each year with more than 1 mm of precipitation
- The frequency of days in each year with more than 2 mm of precipitation
- The 95th percentile of daily precipitation magnitude in each year.
- The 99th percentile of daily precipitation magnitude in each year.
- The frequency of days in each year with precipitation greater than the 1939-2000 95th percentile.
- The frequency of days in each year with precipitation greater than the 1939-2000 99th percentile
- The average magnitude in each year of daily precipitation greater than the 95th percentile
- The average magnitude in each year of daily precipitation greater than the 99th percentile
- The proportion of annual precipitation that fell on days greater than the 95th percentile
- The proportion of annual precipitation that fell on days greater than the 99th percentile

The percentiles were based on (i) all days, (ii) all days with more than 1 mm of precipitation, (iii) all days with more than 2 mm of precipitation. This led to 26 indices in total.

Initially long term trends were investigated. The difference between a year's index (logarithms were used for the magnitude indices) and the previous year's index provided a series, which, without trends, would be a random variable normally distributed about zero. A statistically significant trend was considered to be observed when the 95 % confidence limits of the mean of the difference series did not enclose zero. Appendix 4 provides tables of long term index trends. None of the indices were found to be statistically significant. Of the indices tested by Manton et al. (2001) the only significant trend for sites in the South Island was for an increase in the frequency of days exceeding the long term 99th percentile at Hokitika (110 km to the north of the

catchment on the windward side of the Southern Alps). Salinger and Griffiths (2001) found a significant decrease in the magnitude of precipitation greater than the 95th percentile at Lincoln (175 km to the east of the catchment, lee of the Southern Alps), with a decrease in days with more than the 95th percentile of rain at both Lincoln and Ashburton (110 km east of the catchment). These results could indicate that identified extreme index trend results are not widespread, that Braemar Station and The Hermitage are not in the same climate region as the sites considered by previous authors, or possibly that Braemar Station and The Hermitage are not representative of their respective climate regions. Table 6-4 shows a comparison of trends from around the world.

Table 6-4. Comparison of index trends from around the world. n/a indicates the index was not tested, plus and minus symbols indicate a statistically significant trend was observed and no entry indicates no statistically significant trend was observed.

Location	Period	Freq. of precip.	Intensity of precip.	Freq. of extremes	Intensity of extremes	Extreme precip. proportion of total	Citation
European Alps	1901 to 1994	n/a	n/a	+	n/a	n/a	(Frei and Schär, 2001)
Central and northern South America	1961 to 2000		+			+	(Aguilar et al., 2005)
SW, NW and E China	1961 to 2001	n/a	+	n/a	+	n/a	(Wang and Zhou, 2005)
Central, N and NE China	1961 to 2001	n/a	-	n/a	-	n/a	(Wang and Zhou, 2005)
Central India	1951 to 2000			+	+	+	(Goswami et al., 2006)
United States	1910 to 1996	+	+	+	+	+	(Karl and Knight, 1998)
E Australia	1910 to 1998	n/a	n/a			+	(Haylock and Nicholls, 2000)
SW Australia	1910 to 1998	n/a	n/a	-	-		(Haylock and Nicholls, 2000)
Europe	1946 to 1999	n/a	n/a		+		(Tank and Können, 2003)
Lincoln, New Zealand	1951 to 1998	n/a	n/a	-	-	n/a	(Salinger and Griffiths, 2001)
Marquesas Islands	1961 to 1998	+	n/a	+	+		(Manton et al., 2001)
Nan, Thailand	1961 to 1998	-	n/a			+	(Manton et al., 2001)

While the majority of statistically significant trends are for increasing precipitation, there are many significant decreasing, and non-significant trends observed. Regional trends are difficult to discern with nearby precipitation gauges often returning trends of an opposite sense (Frei and Schär, 2001; Manton et al., 2001). The period over which the trends were considered was also variable making intercomparisons difficult,

especially when temporal discontinuities were observed in the climate record. An example of the difficulty in interpreting single site trends occurred in the Marquesas Islands where a 50 % increase in mean annual precipitation occurred after 1976. This was initially interpreted as an observation-method induced change. Not until later comparison with neighbouring stations was it confirmed as a climate shift (Manton et al., 2001). Globally, extreme precipitation indices from 1951-2003 show poor spatial coherence with large areas of both positive and negative trends (Alexander et al., 2006). This spatial variability in index trends indicates the site specific nature of precipitation observations and that regional trends based on limited series should be treated with a great deal of caution.

With no clear long term trend determined in The Hermitage and Braemar Station precipitation records, it remains to investigate the possibility of index shifts associated with the IPO phase changes of 1944 (Braemar Station) and 1977 (Braemar Station and The Hermitage). For the magnitude series, the z statistic was used to determine if the 1980-2000 and 1924-1944 means were statistically different to the 1950-1970 means. For the frequency series the χ^2 statistic was used. A statistically significant shift in an index was considered to have occurred when the probability of the test statistic was less than 0.05. Table 6-5 shows the average number of rain days in a year for each period.

Table 6-5. Average number (percent of 365) of annual precipitation days for different IPO phases. Values in bold indicate the difference to the 1950-1970 period is statistically significant at the 0.95 level: italics indicates significance at the 0.9 level.

	The Hermitage		
	1924-1944	1950-1970	1980-2000
> 1 mm	-	146 (40 %)	**164 (45 %)**
> 2 mm	-	139 (38 %)	*146 (40 %)*
	Braemar Station		
> 1 mm	87 (24 %)	81 (22 %)	**70 (19 %)**
> 2 mm	75 (21 %)	72 (20 %)	**64 (18 %)**

For both The Hermitage and Braemar Station the +ve IPO periods returned statistically significant differences to the 1950-1970 –ve IPO period, but The Hermitage showed an increase in precipitation days, whereas Braemar Station showed a decrease in precipitation days. At Braemar Station no statistically significant difference was found between the earlier 1924-1944 +ve IPO period with the 1950-1970 period. This is of interest, as it suggests that it is not the IPO phase that is affecting the frequency of precipitation at Braemar Station. Analysis of the nearby

Tekapo precipitation record by Zheng and Thompson (2007) found a reduction in average daily precipitation, but an increase in annual precipitation total indicating an increase in precipitation day frequency between the 1950-1977 and 1978-1999 periods. Inspection of the Tekapo record confirmed a significant increase in precipitation frequency from the 1926-1944 period (the record began in 1926) to the 1950-1970 period, and another significant increase to the 1980-2000 period. This repeated increase would also suggest the change at Tekapo is not related to the IPO phase. Another nearby gauge site in a similar location with respect to the Southern Alps is Omarama, 40 km to the south west. This site showed no significant change in precipitation day frequency between the 1950-1970 period and the 1980-2000 period. The three different results for the three gauges indicate that the frequency response to the IPO phase is not consistent for these low precipitation locations. This may be a result of there being no relationship, or because other frequency modifying effects swamp the signal. One possible effect could be a change in gauge exposure, especially at Braemar Station where the gauge is located in a garden.

Following the IPO precipitation frequency change analysis, the extreme precipitation indices were explored. The change in the extreme precipitation indices for the different IPO periods at the Hermitage are shown in Table 6-6.

Table 6-6. Average extreme precipitation indices for The Hermitage for twenty year periods in different IPO phases. Values in bold indicate the difference to the 1950-1970 period is statistically significant at the 0.95 level: italics indicates significance at the 0.9 level.

Percentile	95th						99th					
Period	1950-1970			1980-2000			1950-1970			1980-2000		
Index	All	>1 mm	> 2 mm	All	>1 mm	> 2 mm	All	>1 mm	> 2 mm	All	>1 mm	> 2 mm
Percentiles (mm)	56	92	94	**66**	**101**	**105**	120	157	157	*134*	165	165
Frequency of upper percentile events (%)	4.6	1.9	1.8	**5.6**	**2.5**	**2.2**	1.0	0.4	0.4	1.1	0.5	0.5
Magnitude of high percentile events (mm)	98	136	136	**109**	143	143	166	193	193	**174**	198	198
Proportion of high percentile events to total (%)	2.5	3.6	3.6	2.5	*3.3*	3.3	4.4	5.1	5.1	*4.0*	**4.6**	**4.6**

Statistically significant increases in the index means were found for the 95th percentiles, the frequency of all days being greater than the long term 95th percentile, and for the magnitude of high percentile events when all rain days were considered.

The proportion of rain that fell on the high magnitude events compared to all rain reduced for the 1980-2000 period compared to the 1950-1970 period.
Peak value distributions may be characterised by the Gumbel distribution which enables estimation of extreme value probabilities. McKerchar and Henderson (2003) used a Gumbel frequency distribution of peak stream flows to demonstrate that the use of flow data from different IPO phases could result in different 1 in 100 year flood estimates being generated. In keeping with the standard indices, the 95th percentiles rather than the annual peak values, for The Hermitage, have been plotted against their annual exceedence probabilities on a Gumbel scale for the 1950-1970 period and the 1980-2000 period in Figure 6-9.

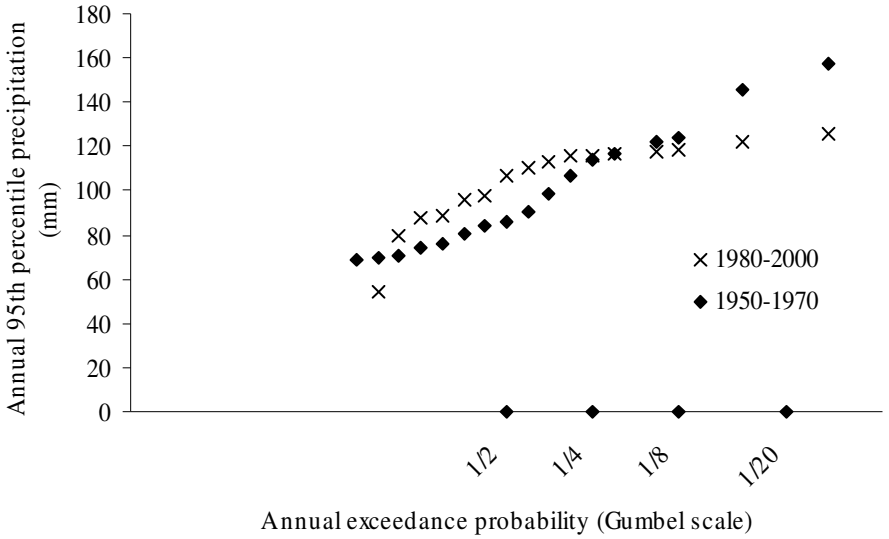

Figure 6-9. Annual 95th percentile precipitation frequency distribution for The Hermitage for 1950-1970 and 1980-2000.

This plot indicates that there has not been a linear shift in 95th percentiles, with the extreme years (less than ¼ exceedence probability) showing lower 95th percentiles for the positive IPO phase (1980-2000). The lack of significant change in the 99th percentiles supports this. The implication is that the IPO phase does not affect the very extreme events, which in turn indicates that extreme precipitation is not limited by circulation. It may be that duration is more important for the extreme events. Precipitation magnitude is known to be related to frontal intensity as well as wind speed (Chater and Sturman, 1998; Wratt et al., 2000). As circulation intensity increases so does wind speed, but the transit period of a front over a region reduces.

At some circulation intensity, the frontal transit period and the moist air advection will optimise the daily precipitation magnitude. Clarification of the limitations on extreme event magnitude processes would require the analysis of precipitation data at sub daily time steps, and would provide an interesting direction for future research. Table 6-7 shows that in general the Braemar 1950-1970 95th percentile indices were statistically significantly higher than for the +ve IPO phases before and after. The 99th percentile indices show a similar result but not as significant in general.

Table 6-7. Average extreme precipitation indices for Braemar Station for twenty year periods in different I.P.O. phases. Values in bold indicate the difference to the 1950-1970 period is statistically significant at the 0.95 level: italics indicates significance at the 0.9 level.

Percentile				95th					
Period	1924-1944			1950-1970			1980-2000		
Index	All	>1 mm	> 2 mm	All	>1 mm	> 2 mm	All	>1 mm	> 2 mm
Percentiles (mm)	15.4	**28.2**	**29.4**	16.5	31.2	32.4	**13.8**	**27.6**	**29.4**
Frequency of upper percentile events (%)	4.9	**1.1**	**0.9**	5.5	1.3	1.4	**4.1**	**1.0**	**0.8**
Magnitude of high percentile events	**25.2**	**39.4**	40.5	27.6	42.4	43.3	**21.5**	**31.5**	**40.0**
Proportion of high percentile events to total (%)	**0.028**	**0.044**	**0.045**	0.033	0.052	0.053	**0.026**	**0.039**	**0.039**
Percentile				99th					
Period	1924-1944			1924-1944			1924-1944		
Index	All	>1 mm	> 2 mm	All	>1 mm	> 2 mm	All	>1 mm	> 2 mm
Percentiles (mm)	**30.4**	45.8	45.9	33.1	48.2	48.2	**30.1**	*44.6*	*44.6*
Frequency of upper percentile events (%)	**0.9**	0.2	0.2	1.4	0.3	0.3	**0.8**	0.2	0.2
Magnitude of high percentile events	41.5	56.2	56.2	44.2	59.4	59.4	**33.4**	**43.4**	**53.9**
Proportion of high percentile events to total (%)	**0.047**	0.064	0.065	0.054	0.074	0.074	**0.041**	**0.054**	**0.055**

These changes indicate that at The Hermitage during the 1980-2000 period, compared to the earlier 1950-1970 period there were more precipitation events, more extreme precipitation events and the extreme events increased in magnitude. These changes are consistent with the findings of Salinger and Griffiths (2001) for Milford Sound, for which they found a significant shift in the frequency of days greater than the long term 95th percentile. In addition, McKerchar and Henderson (2003) found an increase

in frequency of high rainfall events at both Milford Sound and Invercargill. At Braemar Station a different picture emerges with a reduction in events and a reduction in frequency and magnitude of extreme events. The difference of the 1980-2000 and 1950-1970 precipitation distribution functions for The Hermitage and Braemar Station are shown in Figure 6-10. This clearly shows that for both sites it is the higher precipitation events that were most affected by the IPO phase change, but that the response is of an opposite sign for the two sites. At The Hermitage the precipitation increases while at Braemar Station the precipitation decreases.

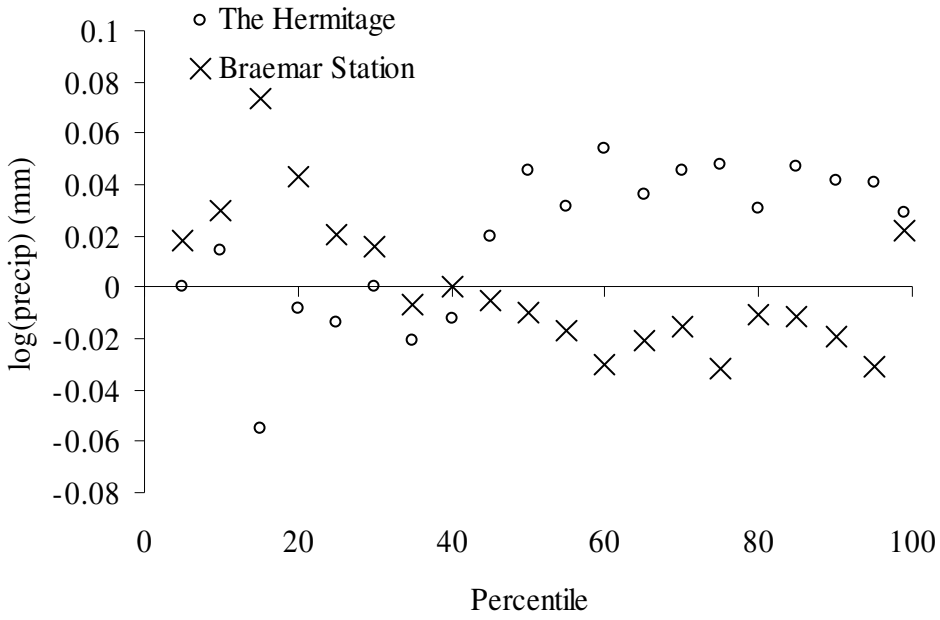

Figure 6-10. Difference of the log of the percentile magnitudes between the 1980 to 2000 period and the 1950-1970 period.

In comparing Lake Tekapo precipitation with Aoraki/Mt Cook precipitation Zheng and Thompson (2007) found the two locations had different responses to the IPO phase. They attributed this to the increased influence of westerly wind derived orographic precipitation at Aoraki/Mt Cook and increased influence of easterly storms on Tekapo. This may also explain the difference in response to the IPO phase of Aoraki/Mt Cook and Braemar Station.

6.2.6 Wind classes

The 50th percentile of daily precipitation magnitude at The Hermitage is different for different wind directions as shown in Chapter 4. A change in frequency of the different wind classes will therefore affect the precipitation. Given that daily

precipitation magnitudes and frequency have increased at The Hermitage between 1950-1970 (-ve IPO phase) and 1980-2000 (+ve IPO phase) and that the IPO modulates the strength of the Southern Oscillation (Power et al., 1999; Salinger et al., 2001), it is not unreasonable to expect that the precipitation changes may be attributable to changes in frequency of the wind classes. To this end, an assessment was made to find whether a statistically significant change in the frequency of wind classes may be observed for the different IPO phase periods. The wind class divisions derived in Chapter 4 were used to produce a daily series from the NCEP/NCAR 850 hPa wind direction average of reanalysis points 170E 42.5S and 170E 45S. An average wind direction was derived only for those days when the difference in wind direction at the two points was within 30^{o} of each other. Prior to the 1957-1958 International Geophysical Year there were very few observations taken in the Southern Ocean and Antarctic regions leading to this period of the reanalysis data being the least reliable, especially for the Southern Hemisphere (Kistler et al., 2001). For this reason the –ve IPO phase period used was from 1960- 1975, not 1950-1970 as was used for the precipitation analysis. The frequencies of each wind class for the 1960-1975 and the 1980-2000 periods were found. For each wind class a χ^2 test was made of the null hypothesis that the 1980-2000 frequency was the same as the 1960-1975 frequency. The 0.05 level was used to indicate a statistically significant difference. Of the five wind classes, the northerly, easterly and south westerly wind classes showed a statistically significant shift in their frequencies. The northerly and easterly both increased in frequencies between the 1960-1975 period and the 1980-2000 period, while the south westerly decreased in frequency. The northerly wind class increased by an average of two days, the easterly wind class increased on average by seven days and the south westerly decreased by an average of three days. By comparison, Lorrey et al. (2007) found no statistical change in circulation types over New Zealand between the 19 years prior to, and after, 1976/77. Lorrey et al.(2007) also found that there was no statistically significant seasonal change in circulation frequencies, but that at a monthly level, August did exhibit an increase in zonal circulation types and a decrease in blocking types. Although the changes in circulation frequencies were generally non-statistically significant, they still concluded that a frequency change had occurred and that this change partly explained observed precipitation changes. Salinger and Mullan (1999) found that west to south west circulation over New Zealand had become more “prevalent” during the 1976-

1994 period compared to 1951-1976. This may be interpreted as an increase in frequency, but in fact, the indices used were of circulation strength.

Can the observed precipitation changes be explained by these changes in wind class frequencies? If we assume that average northerly daily precipitation at The Hermitage (8.5 mm) falls on the extra northerly days and that previously these days had had average precipitation (12 mm), then there will be a reduction of 7 mm of precipitation. Similarly, for the seven extra easterly days, a change from average daily precipitation to easterly daily precipitation of 6 mm leads to an annual reduction of 42 mm. In the case of the three extra south westerly days, the change from average south westerly class precipitation of 14 mm leads to a reduction of 6 mm per year. Combined, these changes in wind class frequency indicate a total reduction in precipitation of 55 mm. At Braemar Station these wind class changes would lead to an increase of 1.4 mm. At both sites, the changes are counter to that which was observed, indicating that it is not the change in frequency of wind classes that has led to the change in observed precipitation. The problem remains to be explained of why there is increased precipitation at The Hermitage in the later IPO phase.

Lee side precipitation has been found to be correlated to wind speed in the New Zealand mountains (Chater and Sturman, 1998; Sinclair et al., 1997; Wratt et al., 2000). This may be explained by the process of increased hydrometeor drift and reduced barrier blocking of cross mountain winds (Sinclair et al., 1997). An analysis of monthly annual average wind magnitude for each of the classes shows a statistically significant increase in wind speed for all wind classes except northerly. The increase in the average wind speed for the north westerly, south westerly and south south westerly wind classes indicates an overall shift in the wind speed distribution for each wind class as shown in Figure 6-11. The Hermitage rain day distribution with respect to wind speed for each wind class, also shown in Figure 6-11, may then be used to estimate the number of extra rain days that occur as a result of the shift in the wind speed. Table 6-8 shows the results of applying the likelihood-of-precipitation to windspeed relationship to the changed windspeed frequency distribution for The Hermitage and Braemar Station, together with the changes actually observed. The estimated increase of 8 north west rain days is just one day different from that found from observations. For the other wind classes and for Braemar Station, the wind-speed change in precipitation estimation does not match the observed changes very well. This may be a result of the random error swamping

the estimated value, the wind speed to likelihood-of-precipitation relationship being variable in time, or from the wind speed not being the dominant control on precipitation likelihood.

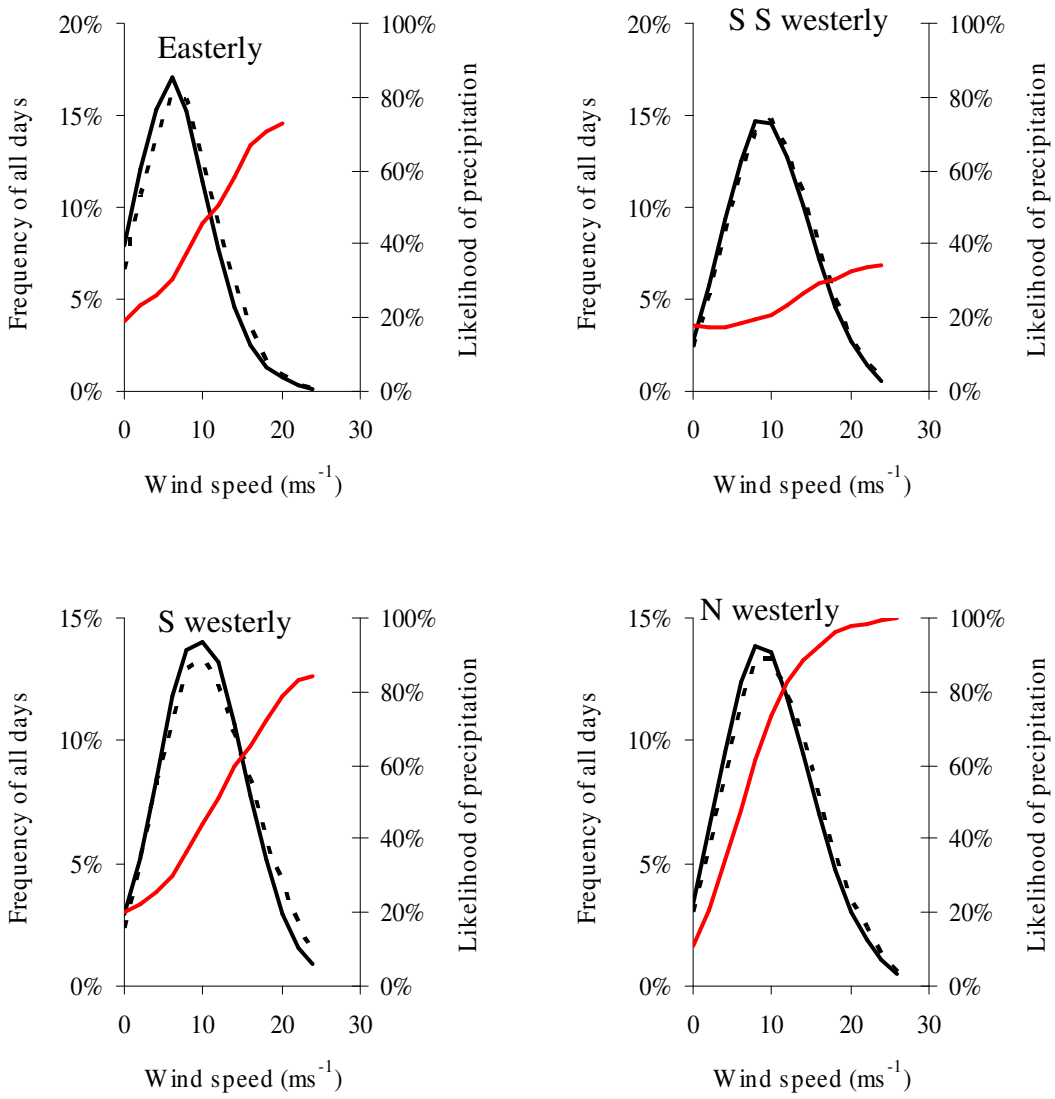

Figure 6-11. Wind classed frequency distributions of wind speeds (low pass filtered) for the 1960-1975 period (solid black lines) and the 1980-2000 period (dotted black lines), and likelihood of precipitation, (also low pass filtered), at The Hermitage (solid red lines) for different wind speeds for the 1960-2000 period.

All three of these factors are likely to play a part. The low numbers involved ensures that errors become increasingly important. For the less frequent wind classes and extreme wind speeds the number of precipitation observations in each class was often below ten ensuring random errors were relatively high. The physical explanation of wind speed being related to precipitation relies on the proximity of the precipitation

site to the orographic barrier. For wind classes other than north west at The Hermitage, and for all wind classes at Braemar Station the distance from the orographic barrier to the gauge site may be large enough that the relative importance of the increased spillover is reduced in relation to other precipitation controls so that it is no longer the principal control.

Table 6-8. Estimated change in precipitation days and precipitation magnitude between 1960-1975 and 1980-2000 based on the shift in the wind speed distribution for these two periods. The numbers in brackets are the changes actually observed.

	The Hermitage				
	E	SSW	SW	NW	Total
Extra rain days	9 (4)	1 (1)	6 (0)	8 (7)	24 (12)
Increased annual precipitation (mm)	111 (60)	7 (-8)	88 (-21)	464 (395)	670 (526)
	Braemar Station				
Extra rain days	4 (0)	0 (0)	3 (-3)	5 (1)	12
Increased annual precipitation (mm)	35 (1)	4 (0)	20 (-32)	61 (4)	120

The shift in the wind speed frequency distribution leads to not only increased precipitation days, but also to a general increase in precipitation magnitude. The average precipitation magnitude distribution at the Hermitage for different wind speeds is shown in Figure 6-12. The precipitation magnitude distributions may be combined with the number of extra days a year that rain is likely to fall given the shift in the wind speed distribution for each wind class to estimate the increased annual precipitation total as shown in Table 6-8. Once again, and for the same reasons, it is only the northwest wind classed precipitation at The Hermitage that the wind speed based estimate relates to the observed precipitation change.

Humidity, stability and temperature have also been correlated to lee precipitation magnitude in the Southern Alps (Chater and Sturman, 1998; Sinclair et al., 1997; Wratt et al., 2000). An assessment of humidity and stability was made through use of the NCEP/NCAR data for the single reanalysis point to the west of the Aoraki/Mt Cook region at 170E 42.5S. Following Wratt et al. (2000) the 850 hPa relative humidity parameter was used for humidity, and the 850 hPa less the 500 hPa equivalent potential temperature was used as an indication of stability. For the humidity, no long term trend was found, but a significant increase of 1.7 % was found between the 1960-1975 (65.4 ± 1 %) and the 1980-2000 (67.1 ± 0.7 %) periods. For stability, again no long term trend was identified, but a statistically significant

increase in stability of 0.002 K hPa^{-1} was found between the 1960 to 1975 period (-0.0497 ± 0.0009 K hPa^{-1}) and the 1980-2000 periods (-0.0514 ± 0.0006 K hPa^{-1}). No statistically significant shift in equivalent potential temperature was found for the 850 hPa or 500 hPa levels, though a non-statistically significant increase in the 500 hPa equivalent potential temperatures and decrease in the 850 hPa equivalent potential temperatures was found. These changes are shown in Table 6-9.

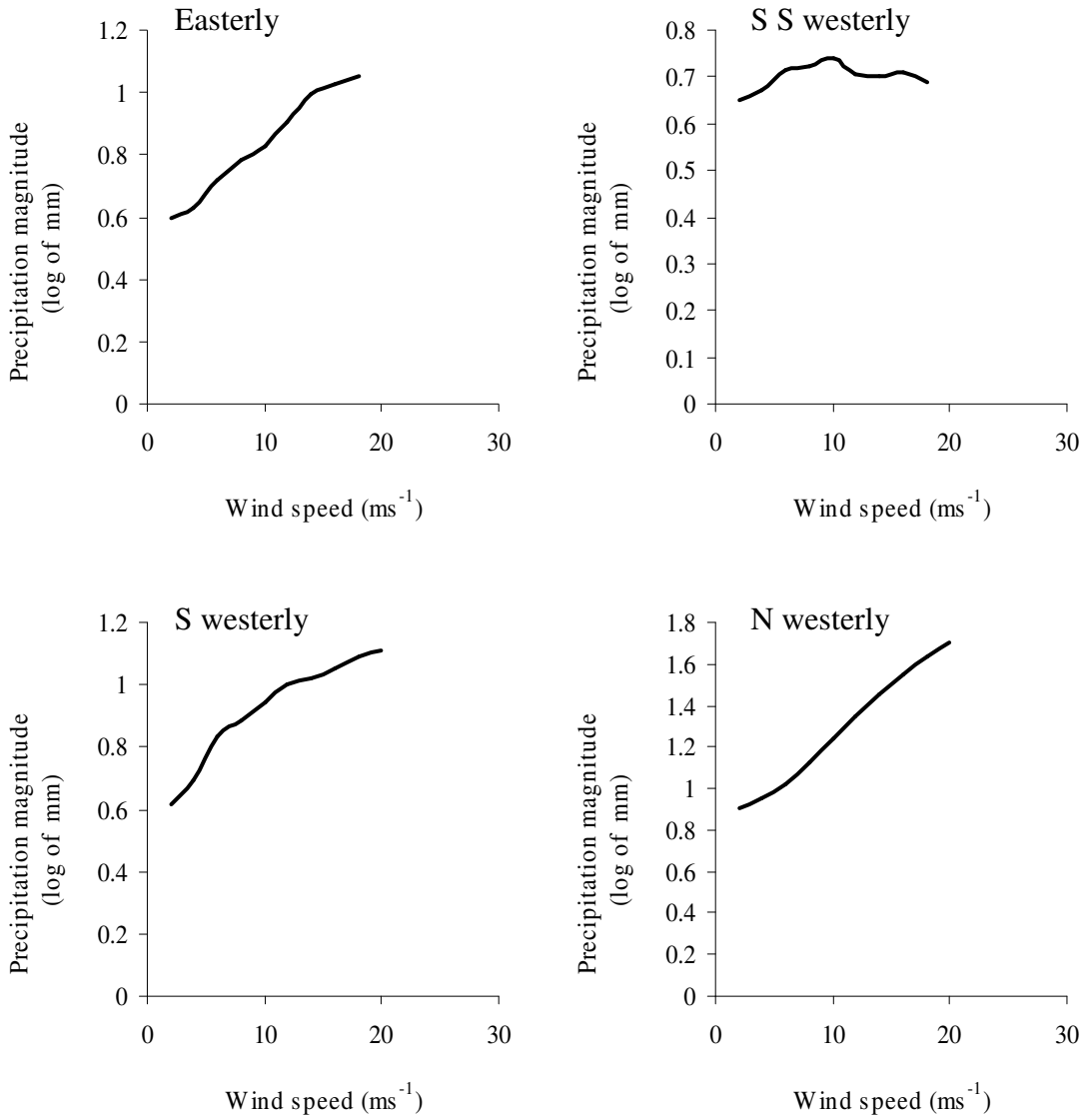

Figure 6-12. Wind classed magnitude of precipitation (low pass filtered) at The Hermitage for different wind speeds for 1960-2000.

Table 6-9. Wind classed average relative humidity and stability values

Wind direction	Period*	Wind speed (ms^{-1})	Days per year	Humidity (%)	Stability ($K\ hPa^{-1}$)
Northerly	All	9.7	19	75.3	-0.048
	-ve		17.7		-0.047
	+ve		20.6		-0.050
Easterly	All	8.1	49.2	68.9	-0.050
	-ve	7.6	44.4		
	+ve	8.4	51.8		
South south westerly	All	10.9	72.8	61.2	-0.052
	-ve	10.7			-0.051
	+ve	11.2			-0.052
South westerly	All	11.4	41.2	64.8	-0.051
	-ve	11.1	43.7	63.9	-0.050
	+ve	11.6	40.6	65.4	-0.052
North westerly	All	11.1	102.1	69.4	-0.051
	-ve	10.8			-0.049
	+ve	11.4			-0.051

*All = 1960 to 2000, -ve = 1960 to 1975, +ve = 1980 to 2000

The increase in humidity may be explained through the increased frequency of northerly sector winds, as the south west wind class was the only individual sector that showed a statistically significant increase in humidity. Interestingly all wind classes except easterly had an increase in stability. An increase in stability would tend to reduce precipitation, another reason why the wind speed derived precipitation increase was overestimated. An explanation for the increased stability is decreased sea surface temperatures. Decreased sea surface temperatures lead to reduced temperatures of the lower atmosphere, thereby increasing stability. An analysis of New Zealand sea surface temperatures by Folland and Salinger (1995) from 1873 to 1993 indicates that annual mean sea surface temperatures around New Zealand peaked shortly after 1970. Mean monthly sea surface temperatures (NOAA/ESRL, 2008) show the 1960 to 1975 average is 0.2 ^{o} C warmer than the 1980 to 2000 average. This reduction in sea surface temperatures may explain the increased stability and the over estimation of north westerly precipitation increase resulting from increased wind speed.

6.3 Discussion

Lack of a statistically significant long term trend in the precipitation record of The Hermitage and Braemar Station does not necessarily mean that there is no trend. It just means that if a trend exists, it cannot be discerned from the other natural variations. Globally, a general increasing trend in precipitation has been observed

over the last century (Dore, 2005) but are not statistically significant (Bates et al., 2008). This precipitation increase can be attributed to the rise in atmospheric moisture associated with increased temperatures (Trenberth, 1999). This physical explanation does not consider circulation changes associated with global warming, which can affect direction and strength of air flow. In many mountain regions, it is the change in air flow, as much as the increased moisture content, that impacts on precipitation. For instance, in explaining the observed increasing wintertime precipitation trend in the Swiss Alps, circulation change was considered the most likely cause, not just increased atmospheric moisture (Widmann and Schär, 1997). The temperature and humidity of an air mass dictates the elevation of the condensation level and the cloud base. In areas of orographic precipitation, the lower this level, the longer the uplift, and hence greater the time that is available to form hydrometeors and for precipitation to occur prior to the air mass passing beyond the associated mountains. This time factor indicates moisture flux rather than just moisture is the principal precipitation control in these locations. Consideration of moisture flux for estimating precipitation has been used successfully for many mountain regions of the world by Rasmussen and Conway (2004; 2005) and Rasmussen et al. (2007; 2001). Moisture flux may be considered a function of humidity and wind speed. It follows then, that a change in wind speed is just as capable of affecting orographic precipitation quantities as a change in atmospheric moisture. Indeed, in Sweden, the intensification of westerly flow has been identified as an explanation for the increased precipitation observed in some months of the year between 1890 and 1990 (Busuioc et al., 2001). Lee mountain precipitation has the additional link to wind speed through overcoming windward blocking and increased hydrometeor drift. Hydrometeor drift is affected by temperature as well as wind, but in a negative way. In warmer temperatures there are less frozen hydrometeors and so reduced drift. In terms of a lee side catchment, this may counter any precipitation increase caused by increased atmospheric moisture content. From these considerations the variation of wind speed, rather than temperature may become the principal precipitation controlling factor in some orographic precipitation environments. The Southern Alps is just such a location as has been confirmed by the correlation between wind speed and precipitation at Aoraki/Mt Cook being greater than the correlation to relative humidity (Wratt et al., 2000).

With specific relevance to lee precipitation, is the relationship of wind speed to windward blocking. Blocking occurs when the kinetic energy of the air mass cannot overcome the potential energy required to cross a mountain barrier. The non-dimensional term which provides an indication of this blocking limitation is the Blocking number (B) defined as:

$$B = Nh / U \qquad \textbf{6-3}$$

Where

N = Brunt-Vaisala frequency (s^{-1}),

h = the height of the barrier (m), and

U = the wind velocity (m s^{-1}).

Typical values for N and h for the Southern Alps have been given by Revell et al. (2002) as N = 0.01 s^{-1}, h = 2250 m. To overcome blocking, the wind velocity needs to be such that the Blocking number is less than two. This leads to the wind velocity needing to be greater than 11.25 m s^{-1}. If it is assumed that precipitation nearly always occurs at Aoraki/Mt Cook Village when there is no blocking, then this critical wind speed provides a threshold over which precipitation frequency is close to one. The precipitation to wind speed distribution at The Hermitage for north westerly conditions (Figure 6-11), shows that precipitation occurrence nearly always (>90 %) occurs for wind speeds greater than 15 m s^{-1}. This is higher than the value determined analytically but indicates that blocking is likely to be a significant contributing factor for the reduced precipitation occurrence at lower wind speeds.

The sensitivity of The Hermitage northwest precipitation to wind speed explains why the IPO variation results in the observed significant precipitation shift. The IPO modulation of SO led to a 0.6 m s^{-1} increase in 850 hPa north west mean wind speed between the 1950-1970 period and the 1980-2000 period, an increase of 5 %. The temperature increase required to increase the moisture content of the atmosphere by an equivalent amount may be found through using the Clausius-Clapyron equation:

$$\ln\left(\frac{e_{s1}}{e_{s2}}\right) = \frac{\Delta H_{vap}}{R}\left(\frac{1}{T_2} - \frac{1}{T_1}\right) \qquad \textbf{6-4}$$

Where:

e_s = saturation vapour pressure

ΔH_{vap} = enthalpy of evaporation of water = 40.7 kJ mol^{-1}

R = gas constant = 8.3145 J mol^{-1} K^{-1}

T = temperature in kelvin

If we assume an air temperature of 283 K (10 ^{o}C) then a temperature increase of 0.8 K is required to increase the saturated vapour pressure by an equivalent 5 %. For New Zealand a temperature increase of 0.7 ^{o}C has been observed from 1900 to 1990 (Folland and Salinger, 1995) and only a 0.14 ^{o}C temperature increase is determined from the NCEP/NCAR 850 hPa level temperatures at 170E 42.5S between 1960-1975 and 1980- 2000. This indicates that the wind speed variations are much more important than the temperature variations for affecting the moisture flux across the Southern Alps. This situation is similar to that considered to occur in the Patagonian Andes of South America (Schneider and Gies, 2004), an analogous region in terms of mountain height, proximity to the ocean, mountain axis orientation and southern latitude. This is considerably different to the mechanisms that were considered responsible for the modelled precipitation changes for lee catchments in North America under a global warming scenario (Diffenbaugh et al., 2005). In that study precipitation increases were explained by either increased atmospheric moisture-content, or increased leeside upslope flow, with no consideration of the impact of changed circulation.

The physical explanation of the importance of windspeed to orographic precipitation should hold true for all cross-mountain wind directions and yet no change in precipitation was observed for the south west and south south west wind classes. This is of interest as increased southwest flow has been related to the SO, and attributed as the explanation for increased glacier mass balances during the positive phase of the IPO (Fitzharris et al., 1997). The analysis here would indicate that while there may be strengthened south westerlies, in the lee of the main divide at least, they are not contributing to an increase in accumulation (though through temperature, they may reduce ablation). As mentioned earlier, this result may be explained through the greater distance that The Hermitage is from the south western orographic barrier. This situation is analogous to the greater distance Braemar Station is from the northwest wind orographic barrier. No wind speed relationship to precipitation magnitude is observed at Braemar, though a relationship to precipitation occurrence is apparent. The extension of wind speed to precipitation relationships to the lee of an orographic barrier appear to be very local to the barrier in question. For north west winds in the

upper Lake Pukaki catchment, the barrier is the main divide and the zone of influence extends to some location part way between Braemar Station and The Hermitage.

6.4 Conclusion

The long term precipitation records from The Hermitage (1939 to 2000) and Braemar Station (1914 to 2008) have been analysed for evidence of trends and multidecadal variations. In both cases no statistically significant long term trend was discernible. This is consistent with previous work for New Zealand (Salinger et al., 1992) and while it is not unique globally (Dore, 2005), it is counter to the general trend (Dai et al., 1997). Consideration of precipitation frequency, extreme precipitation magnitude and extreme precipitation frequency also found no long term trend at these two sites. Again this is not unusual, though in most extra-tropical regions at least, an increase in extreme precipitation magnitude has been identified and related to the global increase in greenhouse gasses (Groisman et al., 1999).

At the multidecadal level, a shift in precipitation magnitude and frequency was identified between the 1950-1970 period and 1980-2000 at The Hermitage. These periods were selected to coincide with different phases of the IPO. This IPO coincident variation is consistent with that found for general precipitation observed south west of the South Island of New Zealand (Salinger et al., 2001) and with increased flows in eastward draining catchments of the South Island with headwaters in the Southern Alps (McKerchar and Henderson, 2003). At Braemar Station, the precipitation was greater for the –ve phase of the IPO, an opposite response to The Hermitage and considered to be related to the reduced influence of westerly precipitation events at Braemar. Such spatial differences in IPO response are not unusual globally. The limited IPO cycles for which observations are available means that any relationships require a sound physical explanation to be convincing.

Wind speed and direction changes related to the last IPO switch have been identified showing that westerly winds do not increase in frequency, but do increase in strength. Relationships between wind speed, precipitation occurrence and precipitation magnitude have been used to determine if the change in westerly wind speed can explain the observed change in precipitation frequency and occurrence. Only for the north western wind sector and for precipitation at The Hermitage does wind speed derived precipitation change correspond to observed precipitation changes. This finding indicates the wind speed dependent processes of windward blocking and

hydrometeor drift combined with increased moisture flux are dominant controls for north west precipitation at The Hermitage.

The limited period of observations prevents determination of a clear relationship between precipitation and IPO phases. The physical link between wind speed and north westerly precipitation, in concert with the link between an enhanced SO with +ve IPO phases makes it reasonable to assert that the north westerly precipitation at The Hermitage is strongly IPO modulated. For the other wind directions and at Braemar Station, this conclusion cannot be made.

The hydrology of the Lake Pukaki catchment is predominantly controlled by the strength of the north westerly winds. While global warming scenarios indicate an increase in westerly wind strength in New Zealand (Mullan et al., 2008) the modulation of their strength through the IPO would tend towards reduced catchment precipitation during –ve phases. This may have particular relevance to the next twenty to thirty years with the increased likelihood of a switch to a negative IPO phase.

7 Conclusions

This thesis set out to improve the knowledge of the long term precipitation distribution in the Lake Pukaki catchment. This has been achieved through the preparation of the 1970-2000 average annual precipitation distribution utilising a larger (spatially and temporally), set of precipitation observation data than has previously been done for the region. The greater extent of the precipitation data used, the consideration of gauge undercatch, and the independent water balance validation, indicates that this is the highest quality average annual precipitation distribution yet prepared for the catchment. Another aim of this thesis was to identify climate-precipitation relationships. This has been achieved through the identification of precipitation distributions for five different wind direction classes. These distributions have, in turn, enabled a method of providing improved daily precipitation distribution estimates for the catchments, another thesis objective. These daily distributions were also independently validated, through providing improved lake inflow estimates. Identification of the temporal context of the average annual precipitation distribution was also an objective of this work. Through consideration of long term precipitation records, the described thirty year precipitation distribution has been identified to be susceptible to the multidecadal Pacific Ocean temperature fluctuations indexed by the IPO, with climate warming effects indistinguishable from natural inter annual variability. The final aim of this work was to contrast how the lake Pukaki catchment distribution contrasts to other regions of New Zealand and the world. In terms of New Zealand, while the precipitation magnitudes are not record-breaking, they appear to be very high for a catchment lee to the main divide. This indicates that the unique position of the catchment, in the wind shadow of a 3000 m glacierized orographic divide, results in different relative contributions of orographic precipitation processes to those observed elsewhere in the country. Globally, the precipitation distribution and synoptic climate relationships have no analogues in the northern hemisphere. The predominance of the near mono-directional moist air flow, in combination with the rapid orographic uplift being a rare combination. Some equatorial regions achieve the combination during seasonal monsoonal conditions, but are complicated by severe convective processes, which are rare in the Lake Pukaki catchment. The more mountainous mid latitude regions of the Northern Hemisphere either are much drier

(e.g. European Alps, Rockies), or have a much reduced air flow (e.g. Norway, British Columbia). The precipitation region of the world most like the Lake Pukaki catchment is in the Patagonian region of the Andes. In this area exist similar sized and oriented mountains, the same hemispheric moist air flow, and similar latitude to that within the Lake Pukaki catchment. Unfortunately, remoteness, and hence lack of observational data, prevents direct comparisons.

7.1 Mountain precipitation

Observations from around the world have shown that there is a complex interaction between terrain and precipitation. Terrain impacts on general precipitation generation processes, and is able to induce precipitation through forced uplift, where otherwise it would not occur. For this reason the spatial variation of horizontal precipitation fields is closely related to terrain complexity. The variety of terrain–precipitation processes possible, the increased variability in areas of complex terrain, and the generally low population density and poor access to mountainous regions has ensured that an understanding of how precipitation varies in these regions is limited. Transfer of findings from one region to another is problematic in that relative importance of terrain-precipitation relationships is region specific.

Modelling studies based on physics provide a path to a general theory of precipitation. Parameterisations of unresolved or poorly understood processes combined with constraints on input data resolution and processing power limit the applicability of these models. This is made worse by the paucity of calibration and validation data preventing optimisation of model formulations.

Localised hydrological understanding must therefore rely on in situ precipitation observations at a scale that captures the terrain induced variability and does not limit the particular application. Many observations at various scales and regions from throughout the world enable the broadening of the current mountain precipitation understanding. Precipitation distribution in the Southern Alps of New Zealand exhibits globally extreme characteristics providing valuable model validation case studies and insights into orographic precipitation limits.

7.2 Precipitation observations

Precipitation has been gauged in the Lake Pukaki catchment since 1905 at Aoraki/Mt Cook village. In addition, precipitation observations have been made at 58 gauges at

51 sites including 10 new gauges as part of this work. Assessment of site changes on record quality from the seven long term gauge sites identified only The Hermitage gauge record to be affected. This was considered a result of its positioning in a high magnitude and high horizontal precipitation gradient region. All other long term sites were in the lower catchment where precipitation magnitudes and gradients were low. The period for which the Hermitage record was considered reasonably free of site change effects was from 1948 to 2000.

Through relationships between gauge records, monthly precipitation totals for all gauge sites between 1971 and 2000 were prepared. This enabled long term average annual precipitation "normals" to be prepared for each site. Values ranged from 652 mm in the south east of the catchment to 10000 mm at the site furthest to the north west. Consideration of measurement error, undercatch and random error from correlation derived estimates led to the preparation of undercatch-corrected normals and error bounds for the normals. Undercatch error ranged from 50 mm per year near the outlet of Lake Pukaki where the gauge was close to the ground, there is little precipitation and it usually falls as rain, through to 2400 mm near the north western edge of the catchment where the gauge was 2 m high, snow is common in winter and precipitation magnitude is high. The error of the undercatch corrected normals (from measurement and correlation error) varied considerably. In the north west of the catchment the high precipitation and short observation period (1 year) led to an estimated error of 800 mm. At Braemar station in the south west of the catchment, the low rainfall and near complete thirty year record led to an error estimate of just 10 mm. The observed thirty year average annual totals and the undercatch-corrected totals were interpolated across the catchment using ordinary kriging to provide a precipitation distribution. These fields show a south east to north west gradient, though less severe than that depicted by the New Zealand Meteorological Service (NZMS) for the 1951 to 1980 average annual isohyet map (NZMS, 1985a). The difference is considered a result of the use of the objective kriging interpolation rather than the subjective method used by the NZMS, and the addition of the extra historic and new sites providing extra constraint to the interpolated field. The undercatch-corrected field ranged from 710 mm to 13200 mm, on average 17 % higher than the observed field, highlighting the significance of the undercatch assessment. The gradients and magnitudes determined are not extreme for New Zealand or other mountainous high precipitation regions of the world, but are greater than observations

from Northern Hemisphere mid-latitude mountain regions. Precipitation observations for regions within a few kilometres of the west of the catchment do not exist, so the location of the limit of the interpolated precipitation field is unknown. Identification of this limit is seen as crucial to understanding glaciological and hydrological processes in the region and requires urgent attention.

7.3 Wind classed precipitation distributions

As with many mountain locations around the world, the synoptic wind direction has a marked effect on the magnitude and distribution of precipitation in the Lake Pukaki catchment. The westerly wind is the most common and is the wind direction for which most precipitation falls in the catchment. Daily precipitation magnitudes increase as the synoptic wind direction moves north, and then drop off to very low levels for winds that come from the eastern side of the Southern Alps. Precipitation frequency and magnitude increase for wind directions from the south south west, steadily growing through the south west sector back to the common westerly direction. Wind-classed precipitation fields highlight these differences and also identify the gradient and extent. North westerly precipitation shows the greatest gradient and easterly the least. A general north west to south east gradient is apparent for all wind classes, but with a shift northward for the northerly class, and a shift southward for the south west and south south west wind classes. Precipitation occurring at Aoraki/ Mt Cook village during north westerly or northerly conditions indicates it is generally falling in upwind locations as well. This is not the case for the other wind directions. Precipitation falling at Tekapo generally means it is falling throughout the catchment for all wind classes. Preparation of wind classed precipitation distributions enables these wind-dependent characteristics to be accounted for when estimating daily precipitation fields. By describing the fields as ratios of the logs of precipitation at each location to that at a reference site, an estimate of precipitation at any location in the field may be determined from knowledge of the synoptic wind direction and the precipitation at the reference site. This provides a valuable tool for hydrological and meteorological applications where precipitation (or forecasts of precipitation) is only known at the reference site.
The almost monotonic precipitation-bearing wind direction observed for the Southern Alps in combination with the elevation and orientation of the mountains has a close analogue with that found in the Patagonian Andes, indicating that precipitation

process controls observed in the Lake Pukaki catchment are likely to be equally applicable in that region of the world.

7.4 Validation of precipitation distributions

Water balance derived estimates of areal average precipitation indicate that the gauge-based precipitation distribution is accurate within the estimated error. Relationships between stream flow event volumes and the synoptic wind direction occurring immediately prior, show a relationship that is similar to that found between precipitation and synoptic wind direction. This independent assessment confirms the validity of the relationships found. Application of wind-classed precipitation distributions for the derivation of daily precipitation fields in the Lake Pukaki catchment results in improved modelled lake inflows compared with not using the wind-classed distributions. An improvement was also found when modelling the Jollie Stream flows, and for the Hooker Stream, except during very high flows. This model output improvement is interpreted as validation of the wind-classed precipitation distributions.

7.5 Trends in precipitation

The precipitation record from two sites within the Lake Pukaki catchment shows no general trend from 1939 to 2000. The site located at Aoraki/Mt Cook village showed a shift to increased and more frequent precipitation between 1950-1970 and 1980-2000. These periods are during different phases of the Interdecadal Pacific Oscillation (IPO). This result is important for two reasons:

1. The atmospheric controls on precipitation vary with the phase of the IPO.
2. The 1970-2000 climate normals and precipitation distribution estimated for the Lake Pukaki catchment is biased to atmospheric conditions associated with the +ve phase of the IPO.

In the south east of the catchment, the response of precipitation frequency and magnitude was different to that observed at the village. This indicates that the catchment straddles at least two different precipitation climate regions with different controls on each.

The observed change in westerly synoptic flow strength with the IPO phase provides an explanation of the change in precipitation characteristics in the upper catchment. Increased flow leads to increased hydrometeor drift and decreased up-barrier

blocking, both effects leading to increased lee precipitation. This flow effect has a relatively much greater impact on precipitation than increased atmospheric moisture from temperature increase. Future precipitation magnitude and frequency will change in response to changes in circulation intensity rather than atmospheric warming. While global warming scenarios suggest increased circulation, the recent shift in the IPO phase to the negative could overwhelm this, leading to reduced precipitation in the catchment for the next 20 to 30 years.

7.6 Implications

This research demonstrates the ability to improve spatial precipitation distribution estimates through consideration of all available observations within a region and establishing relationships between observed precipitation magnitudes. A quantification of undercatch has also been made indicating that current New Zealand mountain average annual precipitation distributions are under-estimated by up to 20 %. While this relative value is low compared to that found in polar regions, the very high magnitude of precipitation received ensures it is a considerable amount in absolute terms. Such an offset indicates that applications using average annual precipitation distributions may be in considerable error. Where such applications are for flood management and engineering design, the undercatch omission will tend to reduce the safety margins.

The ability to improve daily precipitation estimates using wind-classed precipitation is conceivably possible for most regions of the world, but particularly in those locations where wind direction is a strong controller on precipitation processes. For mountain regions at least, this could lead to a step-change increase in daily spatial precipitation estimation quality.

This research has clearly demonstrated the ability of short term intensive precipitation observation campaigns in data sparse areas to improve spatial precipitation understanding. This provides a cost effective way of improving hydrological services in remote regions where long term sites are expensive to operate and difficult to locate on precipitation representative sites.

The relationships between Lake Pukaki precipitation and wind strength show that variations in the Interdecadal Pacific Oscillation, rather than global temperature change, is the most critical long term climate variation from a hydrological point of view in this region, and by extension to the South Island. Having said that, possible

process scenarios that lead to the high precipitation levels in the Lake Pukaki catchment, are temperature dependent. Generally, global warming scenarios consider the impact of temperature on the moisture holding capability of an air mass, and the change in circulation. A change in hydrometeor phase from ice to liquid could vastly change the distribution of precipitation in locations with orographic barriers close to the freezing level. This change in process is likely to have occurred in the past in association with glaciations. When freezing levels drop below (or rise above) mountain heights a significant change in distribution may occur. Such precipitation relocation is not generally assessed in current palaeo-climate reconstructions. This may be because precipitation distribution changes are not considered (e.g. Rother, 2006), or because the process scale commonly used for such reconstructions is too large for these effects to be resolved (e.g. Drost et al., 2007). Such a change under a warming climate could lead to a rapid de-glaciation of leeward regions, and possible increased glaciation of windward regions. Where hydrological or glaciological indicators have been used to infer mountain palaeoclimates, they may need re-interpretation under the consideration of the possibility of temperature driven precipitation redistribution. In a similar manner, assessments of the anticipated impacts of climate warming should include the consideration of potential re-distribution of precipitation.

7.7 Future research

The greatest limitation to understanding the distribution of precipitation in the Lake Pukaki catchment, and mountain regions generally is the lack of observations. As computer power and climate model sophistication increase, the validation of model output is increasingly difficult. The standard daily temporal scales of the historic precipitation record provides limited validation for models simulating processes that are rarely in a steady state for more than a few hours. In a similar way, the point observations traditionally used provide very little information for what is a fully spatial system. In terms of improving hydrological forecasting in mountain regions, a network of fully automatic precipitation gauges is required that are located in a hydrologically optimised manner, in concert with a radar network providing full coverage. In the Lake Pukaki catchment this could largely be achieved through installation of an up-valley facing radar located at the southern end of the lake, with precipitation gauges located at De La Beche Hut, in the upper Hooker Valley, at

Tasman Saddle Hut, at Glentanner station, and high on the Ben Ohau Mountains. The duplication of resources with three precipitation gauges within close vicinity of Aoraki/Mt Cook village, and the Rose Ridge climate station in effectively the same precipitation zone, is an inefficiency which could easily be resolved through cooperation of the different operating organisations.

As described in the introduction, the Southern Alps represent an ideal mountain precipitation laboratory. This laboratory should be utilised to improve precipitation models. Too often model validation studies are carried out on the European Alps or the North American Cascades, limiting the breadth of validation to generally low wind, gentle terrain and relatively dry conditions. True model testing requires the application of extreme conditions. These can be provided by the saturated, high wind, rapid uplift conditions of the Southern Alps virtually guaranteed at least once a week. More specifically, a precipitation climatology that is still poorly understood is in the upper Lake Pukaki catchment and the adjacent western flowing catchments. The continued difficulty in determining the precipitation in these regions should be a strong focus of research. The identified high precipitation regions in the lee of the main divide leaves a large question mark over the upper regions of these western catchments together with the processes that cause the high lee precipitation. Modelling points to the phase of the hydrometeors as being an important factor in this distribution and suggests the Lake Pukaki catchment is at risk of major precipitation regime changes under global warming scenarios as discussed in the previous section. Clarification of the distribution and underlying process may be addressed through short term observation campaigns together with modelling operations. An improved approach to that used for this research could be undertaken. Use of tipping bucket gauges with antifreeze reservoirs is considered the best current option. Wind speed and temperature should also be monitored at each gauge site to provide improved undercatch assessment. With full winter operation and short sampling periods, wind direction to precipitation distribution estimates could be vastly improved and temporal resolutions required for model validations generated. To assist with the undercatch correction, a reference site needs to be set up in New Zealand, preferably in a high wind, high precipitation, high elevation site. A full undercatch parameterisation for the variety of gauges used in New Zealand for a wide range of wind and temperature conditions could then be obtained.

With the future operation of the Global Precipitation Mission, regular (3-4 hour) 4 km horizontal resolution, 250 m vertical resolution precipitation rate measurements, to as low as 0.17 mm hr^{-1}, will become available (Hou, 2006). This will lead to an unprecedented improvement in mid-latitude precipitation observations, including mountain regions. Preparation of ground validation of this satellite based system to ensure that the full advantage may be made of its products is crucial. It is imperative that New Zealand becomes involved to calibrate high precipitation observations from mountain regions. The integration of these satellite observations into hydrological models will provide a quantum leap forward in mountain hydrological forecasting and process understanding.

8 References

Adam, J.C., Clark, E.A., Lettenmaier, D.P. and Wood, E.F., 2006. Correction of global precipitation products for orographic effects. Journal of Climate, 19(1): 15-38.

Adler, R.F., Kidd, C., Petty, G., Morisssey, M. and Goodman, M., 2001. Intercomparison of global precipitation products: The third precipitation intercomparison project (PIP-3). Bulletin of the American Meteorological Society, 82(7): 1377-1396.

Aguilar, E., Peterson, T.C., Obando, P.R., Frutos, R., Retana, J.A., Solera, M., Soley, J., García, I.G., Araujo, R.M., Santos, A.R., Valle, V.E., Brunet, M., Aguilar, L., Álvarez, L., Bautista, M., Castañón, C., Herrera, L., Ruano, E., Sinay, J.J., Sa´nchez, E., Oviedo, G.I.H., Obed, F., Salgado, J.E., Vázquez, J.L., Baca, M., Gutiérrez, M., Centella, C., Espinosa, J., Martínez, D., Olmedo, B., Espinoza, C.E.O., Núñez, R., Haylock, M., Benavides, H. and Mayorga, R., 2005. Changes in precipitation and temperature extremes in Central America and northern South America, 1961–2003. Journal of Geophysical Research, 110(D23107): 15.

Ahrens, B., 2006. Distance in spatial interpolation of daily rain gauge data. Hydrological and Earth System Sciences, 10: 197-208.

Aldridge, R., 1976. The measurement of rainfall at ground level. Journal of Hydrology (NZ), 15(1): 35-40.

Alexander, L.V., Zhang, X., Peterson, T.C., Caesar, J., Gleason, B., Tank, A.M.G.K., Haylock, M., Collins, D., Trewin, B., Rahimzadeh, F., Tagipour, A., Kumar, K.R., Revadekar, J., Griffiths, G., Vincent, L., Stephenson, D.B., Burn, J., Aguilar, E., Brunet, M., Taylor, M., New, M., Zhai, P., Rusticucci, M. and Vazquez-Aguirre, J.L., 2006. Global observed changes in daily climate extremes of temperature and precipitation. Journal of Geophysical Research, 111(D05109).

Allen, S., Owens, I.F. and Sirguey, P., 2008. Satellite remote sensing procedures for glacial terrain analyses and hazard assessment in the Aoraki Mount Cook region, New Zealand. New Zealand Journal of Geology and Geophysics, 51: 73-87.

Allerup, P., Madsen, H. and Vejen, F., 1997. A comprehensive model for correcting point precipitation. Nordic Hydrology, 28: 1-20.

Allis, J.A., Harris, B. and Sharp, A.L., 1963. A comparison of five rain-gage installations. Journal of Geophysical Research, 68(16): 4723-4729.

Anders, A.M., Roe, G.H., Durran, D.R. and Minder, J.R., 2007. Small-scale spatial gradients in climatological precipitation on the Olympic Peninsula. Journal of Hydrometeorology, 8: 1068-1081.

Anderson, B., 2004. The response of Ka Roimata O Hine Hukatere/Franz Josef Glacier to climate change. Ph.D. Thesis, University of Canterbury, Christchurch.

Anderton, P.W., 1974. Estimation of snow storage and melt in the catchment of Lake Pukaki, New Zealand Hydrological Society Symposium Proceedings, Dunedin.

Anderton, P.W., 1975. Tasman Glacier 1971-73. Report no. 33, Ministry of Works and Development.

Archer, A.C., 1970. Studies of snow characteristics in the north-eastern Ben Ohau Mountains, New Zealand. Journal of Hydrology (NZ), 9(1): 4-21.

Archer, A.C. and Collett, G.I., 1970. Climatopes of the sub-alpine and alpine zones of the nort-east Ben Ohau Range, New Zealand. In: R.J. Johnston and J.M. Soons (Editors), Proceedings of the 6th New Zealand Geographical Society conference. New Zealand Geographical Society, Christchurch, pp. 216-226.

Archer, A.C., Simpson, M.J.A. and Macmillan, B.H., 1973. Soils and vegetation of the lateral moraine at Malte Brun, Mount Cook region, New Zealand. New Zealand Journal of Botany, 11: 23-48.

Austin, J.M., 1939. Comparison of rain-gauges at Apia. The New Zealand Journal of Science and Technology, 21(1B): 52B - 56B.

Baldwin, M.P., 2001. Annular modes in global daily surface pressure. Geophysical Research Letters, 28: 4115-4118.

Banta, R.M., 1990. The role of mountain flows in making clouds. In: W. Blumen (Editor), Atmospheric processes over complex terrain. Meteorological Monographs. American Meteorological Society, Boston, pp. 229-283.

Bardossy, A. and Plate, E.J., 1992. Space-time model for daily rainfall using atmospheric circulation patterns. Water Resources Research, 28(5): 1247-1259.

Barringer, J.R.F., 2003. National digital elevation model version 2. Information In Formation, 13: 3.

Barros, A.P. and Lettenmaier, D.P., 1993. Dynamic modeling of the spatial distribution of precipitation in remote mountainous areas. Monthly Weather Review, 121: 1195-1214.

Barry, R.G., 1978. Aspects of the precipitation characteristics of the New Guinea mountains. The Journal of Tropical Geography, 47: 13-30.

Barry, R.G., 1992. Mountain weather and climate. Routledge, London, 402 pp.

Barstad, I., Grabowski, W.W. and Smolarkiewicz, P.K., 2007. Characteristics of large-scale orographic precipitation: Evaluation of linear model in idealized problems. Journal of Hydrology, 340: 78-90.

Basist, A., Bell, G.D. and Meentemeyer, V., 1994. Statistical relationships between topography and precipitation patterns. Journal of Climate, 7: 1305-1315.

Bates, B.C., Kundzewicz, Z.W., Wu, S. and J.P. Palutikof (Editors), 2008. Climate change and water. Technical paper VI of the Intergovernmental Panel on Climate Change. IPCC Secretariat, Geneva, 210 pp.

Beck, C., Greiser, J. and Rudolf, B., 2004. A new monthly precipitation climatology for the global land areas for the period 1951 to 2000. In, Climate Status Report. German Weather Service, Offenbach, pp. 181-190.

Belfort Instrument, 2008. Precipitation, high capacity precipitation gauge: Model 6071. http://www.digiwx.com/content/precipitation_m6071.cfm. Accessed: 7-10-2008

Benoit, R., Desgagné, M., Pellerin, P., Pellerin, S. and Chartier, Y., 1997. The Canadian MC2: A semi-lagrangian, semi-implicit wideband atmospheric model suited for finescale process studies and simulation. Monthly Weather Review, 125: 2382-2415.

Berezovskaya, S., 2006. Development of bias-corrected precipitation dataset and climatology for the Arctic regions. http://www.uaf.edu/water/faculty/yang/bcp/photos.htm. Accessed: 7-10-2008

Berger, A., 1988. Milankovich theory and climate. Reviews of Geophysics, 26(4): 624-657.

Berthier, E., Arnaud, Y., Vincent, C. and Remy, F., 2006. Biases of SRTM in high-mountain areas: Implications for the monitoring of glacier volume changes. Geophysical Research Letters, 33(L08502).

Beven, K., 1989. Changing Ideas in hydrology - the case of physically based models. Journal of Hydrology, 105: 157-172.

Biswas, A.K., 1967. Development of rain gauges. Journal of the Irrigation and Drainage Division. Proceedings of the American Society of Civil Engineers: 99-124.

Bormann, N. and Marks, C.J., 1999. Mesoscale rainfall forecasts over New Zealand during SALPEX96: Characterization and sensitivity studies. Monthly Weather Review, 127: 2880-2893.

Bowden, D.T., 1994. Application of a snowmelt-runoff model to the Lake Pukaki basin, Mount Cook. M.Sc. Thesis, University of Canterbury, Christchurch.

Braham Jr, R.R., 1960. Roots of orographic cumuli. Journal of Meteorology, 17: 214-226.

Brown, L.J. and Weeber, J.H., 2002. Groundwaters of the Canterbury region. Report No. R00/10, Environment Canterbury, Christchurch.

Browning, K.A., 1980. Chapter 3. Structure, mechanism and prediction of orographically enhanced rain in Britain. In, Orographic effects in planetary flows. GARP publications series. World Meteorological Organization, International Council of Scientific Unions, Geneva, pp. 85-114.

Buishand, T.A. and Brandsma, T., 1999. Dependence of precipitation on temperature at Florence and Livorno (Italy). Climate Research, 12: 53-63.

Burns, J.I., 1953. Small-scale topographic effects on precipitation distribution in San Dimas experimental forest. Transactions, American Geophysical Union, 34(5): 761-768.

Busuioc, A., Chen, D. and Hellström, C., 2001. Temporal and spatial variability of precipitation in Sweden and its link with the large-scale atmospheric circulation. Tellus A, 53(3): 348-367.

California DWR, 2008. California cooperative snow surveys. http://cdec.water.ca.gov/snow/info/snow_pillow.html. Accessed: 7-10-2008

Campbell Scientific Inc., 2004. CS705 Precipitation adapter. Campbell Scientific Inc, Logan, Utah, 16 pp.

Campbell Scientific Inc., 2008. SR50 Sonic ranging sensor. http://www.campbellsci.ca/Catalogue/SR50A_Man.pdf. Accessed: 7-10-2008

Carabajal, C.C. and Harding, D.J., 2005. ICESat validation of SRTM C-band digital elevation models. Geophysical Research Letters, 32(L22S01).

Chater, A. and Sturman, A., 1998. Atmospheric conditions influencing the spillover of rainfall to lee of the Southern Alps, New Zealand. International Journal of Climatology, 18: 77-92.

Chen, M., Xie, P., Janowiak, J. and Arkin, P.A., 2002. Global land precipitation: A 50-yr monthly analysis based on gauge observations. Journal of Hydrometeorology, 3: 249-266.

Chen, W.Y., 1982. Assessment of Southern Oscillation sea-level pressure indices. Monthly Weather Review, 110(7): 800-807.

Chinn, T.J., 1979. How wet is the wettest of the wet West Coast? New Zealand Alpine Journal, 32: 85-88.

Chinn, T.J., 2001. Distribution of the glacial water resources of New Zealand. Journal of Hydrology (NZ), 40(2): 139-187.

Choularton, T.W. and Perry, S.J., 1986. A model of the orographic enhancement of snowfall by the seeder-feeder mechanism. Quarterly Journal of the Royal Meteorological Society, 112: 335-345.

Clare, G.R., Fitzharris, B., Chinn, T.J. and Salinger, M., 2002. Interannual variation in end-of-summer snowlines of the Southern Alps of New Zealand, and relationships with Southern Hemisphere atmospheric circulations and sea surface temperature patterns. International Journal of Climatology, 22: 107-120.

Clausen, B. and Biggs, B., 2000. Flow variables for ecological studies in temperate streams: groupings based on covariance. Journal of Hydrology, 237: 184-197.

Coates, G., 2002. The rise and fall of the Southern Alps. Canterbury University Press, Christchurch.

Colle, B.A., 2004. Sensitivity of orographic precipitation to changing ambient conditions and terrain geometries: An idealized modeling perspective. Journal of Atmospheric Sciences, 61: 588-606.

Cotton, C.A., Pielke Sr., R.A., Walko, R.L., Liston, G.E., Tremback, C.J., Jiang, H., McAnelly, R.L., Harrington, J.Y., Nicholls, M.E., Carrio, G.G. and McFadden, J.P., 2003. RAMS 2001: Current status and future directions. Meteorology and Atmospheric Physics, 82: 5-29.

Cox, S.C. and Barrell, D.J.A., 2007. Geology of the Aoraki area. GNS Science, Lower Hutt, N.Z., 71 p, 1 map pp.

Cox, S.C., Ferris, B.G. and Allen, S.K., In preparation. Vampire rock avalanches, Aoraki/Mount Cook National Park. 2008/10, Geological and Nuclear Sciences., Wellington.

Cruetin, J.D. and Obled, C., 1982. Objective analysis and mapping techniques for rainfall fields: an objective comparison. Water Resources Research, 18(2): 413-431.

Curtis, J., Wendler, G., Stone, R., and Dutton, E., 1998. Precipitation decrease in the western arctic, with special emphasis on Barrow and Barter Island, Alaska. International. Journal of Climatology, 18: 1687-1707.

Cutler, E.S., 2002. High elevation seasonal snow melt at the Tasman Glacier neve, Southern Alps, NZ. M.Sc. Thesis, University of Otago, Dunedin.

Dai, A., Fung, I.Y. and Del Genio, A.D., 1997. Surface observed global land precipitation variations during 1900-88. Journal of Climate, 10(11): 2943-2962.

Daly, C., 2006. Guidelines for assessing the suitability of spatial climate data sets. International Journal of Climatology, 26(6): 707-721.

Daly, C., Neilson, R.P. and Philips, D.L., 1994. A statistical-topographical model for mapping climatological precipitation over mountain terrain. Journal of Applied Meteorology, 33: 140-158.

Daly, C. and Taylor, G., 2000. United States Average Annual Precipitation, 1961-1990. Spatial Climate Analysis Service, Oregon State University; USDA - NRCS National Water and Climate Center, Portland, Oregon; USDA - NRCS National Cartography and Geospatial Center, Fort Worth,Texas.

de Vries, M.E. and Olafsson, H., 2003. Distribution of precipitation in a mesoscale mountain range - The Reykjanes experiment (REX). In, Geophysical Research Abstracts. European Geophysical Society.

Dettinger, M.D. and Diaz, H.F., 2000. Global characteristics of stream flow seasonality and variability. Journal of Hydrometeorology, 1: 289-310.

Diffenbaugh, N.S., Pal, J.S., Trapp, R.J. and Giorgi, F., 2005. Fine-scale processes regulate the response of extreme events to global change. Proceedings of the National Academey of Sciences of the United States of America, 102(44): 15774-15778.

Disdromet Ltd., 2004. Disdromet Ltd. homepage. http://www.distromet.com/. Accessed: 4th October 2008

Dore, M.H.I., 2005. Climate change and changes in global precipitation patterns: What do we know? Environment International, 31(8): 1167-1181.

Drost, F., Renwick, J., Bhaskran, B., Oliver, H. and McGregor, J., 2007. Simulation of New Zealand's climate using a high-resolution nested regional climate model. International Journal of climatology, 27: 1153-1169.

Duncan, M., 1987. River hydrology and sediment transport. In: A.B. Viner (Editor), Inland waters of New Zealand. DSIR, Wellington, pp. 113-137.

Duncan, M. and Woods, R., 2004. Flow regimes. In: J. Harding, M.P. Mosley, C.P. Pearson and B. Sorrell (Editors), Freshwaters of New Zealand. New Zealand Hydrological Society Inc., New Zealand Limnological Society Inc., Christchurch, pp. 7.1-7.14.

Eder, G., Sivapalan, M. and Nachtnebel, H.P., 2003. Modelling water balances in an alpine catchment through exploitation of emergent properties over changing time scales. Hydrological Processes, 17(11): 2125-2149.

Environment Canada, 2008. Nipher snow gauge. http://www.on.ec.gc.ca/skywatchers/ontario/wx_office_tour. Accessed: 7-10-2008

Farr, T.G., Rosen, P.A., Caro, E., Crippen, R., Duren, R., Hensley, S., Kobrick, M., Paller, M., Rodriguez, E., Roth, L., Seal, D., Shaffer, S., Shimada, J., Umland, J., Werner, M., Oskin, M., Burbank, D. and Alsdorf, D., 2007. The shuttle radar topography mission. Reviews of Geophysics, 45: 33.

Fassnacht, S.R., 2004. Estimating alter-shielded gauge snowfall undercatch, snowpack sublimation, and blowing snow transport at six sites in the coterminous USA. Hydrological Processes, 18: 3481-3492.

Fenwick, J., 2008. Raingauge types. Personal communication to: T. Kerr, Christchurch.

Fitzharris, B., 1992. The 1992 electricity crisis and the role of climate and hydrology. New Zealand Geographer, 48(2): 79-83.

Fitzharris, B., Chinn, T.J. and Lamont, G.N., 1997. Glacier balance fluctuations and atmospheric circulation patterns over the Southern Alps, New Zealand. International Journal of Climatology, 17: 745-763.

Fitzharris, B., Clare, G.R. and Renwick, J., 2007. Teleconnections between Andean and New Zealand glaciers. Global and Planetary Change, 59(1-4): 159-174.

Fitzharris, B. and Garr, C.E., 1995. Simulation of past variability in seasonal snow in the Southern Alps, New Zealand. Annals of Glaciology, 21: 377-382.

Flowers, G.E., 2008. Subglacial modulation of the hydrograph from glacierized basins. Hydrological Processes, 22(19): 3903-3918.

Folland, C.K., 2008. Interdecadal Pacific Oscillation time series. http://www.iges.org/c20c/IPO_v2.doc. Accessed: August 2008

Folland, C.K. and Salinger, J.M., 1995. Surface temperature trends and variations in New Zealand and the surrounding ocean, 1871-1993. International Journal of Climatology, 15: 1195-1218.

Fouhy, E., 2008. The Hermitage 1901 - 1970 monthly precipitation totals. Personal communication to: T. Kerr, Christchurch.

Fountain, A.G. and Tangborn, W.V., 1985. The effects of glaciers on streamflow variations. Water Resources Research, 21(4): 579-586.

Frei, C. and Schär, C., 1998. A precipitation climatology of the Alps from high-resolution rain-gauge observations. International Journal of Climatology, 18: 873-900.

Frei, C. and Schär, C., 2001. Detection probability trends in rare events: theory and application to heavy precipitation in the alpine region. Journal of Climate, 14: 1568-1584.

Fuhrer, O. and Schär, C., 2005. Embedded cellular convection in moist flow past topography. Journal of Atmospheric Sciences, 62(8): 2810-2828.

Fujiyoshi, Y., Kondo, H., Inoue, J. and Yamada, T., 1987. Characteristics of precipitation and vertical structure of air temperature in northern Patagonia. Bulletin of Glacier Research, 4: 15-23.

Funatsu, B.M., Gan, M.A. and Caetano, E., 2004. A case study of orographic cyclogenesis over South America. Atmosfera: 91-113.

Garen, D.C., 1995. Estimation of spatially distributed values of daily precipitation in mountainous areas, Canadian Water Resources Association conference, Vancouver, pp. 237-242.

Givone, C. and Meignien, X., 1990. Influence of topography on spatial distribution of rain, Hydrology of mountainous areas. IAHS, Czechoslovakia, pp. 57-65.

Global Water, ND. WL400 Water level sensor. http://www.globalw.com/downloads/WL400/WL400B.pdf. Accessed: 7-10-2008

Golubev, V.S., Groisman, P.Y. and Quayle, R.G., 1992. An evaluation of the United States standard 8-in. nonrecording raingage at the Valdai Polygon, Russia. Journal of Atmospheric and Oceanic Technology, 49: 624 - 629.

Goodison, B.E., 1978. Accuracy of Canadian snow gage measurements. Journal of applied meteorology, 17: 1542-1548.

Goodison, B.E., Ferguson, H.L. and McKay, G.A., 1981. Measurement and data analysis. In: D.M. Gray and D.M. Male (Editors), Handbook of snow. Principles, processes, and applications. Pergamon Press, Willowdale.

Goodison, B.E., Sevruk, B. and Klemm, S., 1989. WMO solid precipitation measurement intercomparison: objectives, methodology, analysis. In: J.W. Delleur (Editor), Atmospheric Deposition. International Association of Hydrological Sciences, Baltimore, pp. 57-64.

Goodison, B.E., Turner, V.R. and Metcalfe, J.R., 1983. A nipher-type shield for recording precipitation gauges, 5th Symposium, Meteorological Observation and Instrumentation. American Meteorological Society Toronto.

Gordon, N.D., 1986. The Southern Oscillation and New Zealand weather. Monthly Weather Review, 114: 371-387.

Goswami, B.N., Venugopal, V., Sengupta, D., Madhusoodanan, M.S. and Xavier, P.K., 2006. Increasing trend of extreme rain events over India in a warming environment. Science, 314(5804): 1442-1445.

Gray, W.R. and Austin, G.L., 1993. Rainfall estimation by radar for the Otaki catchment: the OPERA pilot study. Journal of Hydrology (NZ), 31(2): 91-110.

Gray, W.R. and Seed, A., 1997. Radar observations of orographic enhancement in New Zealand. In: B.j. Benedito and O. Massambani (Editors), Weather Radar Technology for Water Resources Management. UNESCO, IHP-UNESCO, IRTCUD, Sao Paulo.

Green, M.J., 1970. Effects of exposure on the catch of rain gauges. Journal of Hydrology (NZ), 9(2): 55-70.

Grell, G.A., Dudhia, J. and Stauffer, D.R., 1995. A description of the fifth-generation Penn State/NCAR mesoscale model (MM5). NCAR/TN-398+STR, Mesoscale and microscale meteorology division, National Center for Atmospheric Research, Boulder.

Griffiths, G.A. and McSaveney, M.J., 1983a. Distribution of mean annual precipitation across some steepland regions of New Zealand. New Zealand Journal of Science, 26: 197-209.

Griffiths, G.A. and McSaveney, M.J., 1983b. Hydrology of a basin with extreme rainfalls- Cropp River, New Zealand. New Zealand Journal of Science, 26: 293-306.

Griffiths, G.M., 2006. Changes in New Zealand daily rainfall extremes 1930 - 2004. Weather and Climate, 27: 3-44.

Groisman, P.Y., Karl, T.R., Easterling, D.R., Knight, R.W., Jamason, P.F., Hennessy, K.J., Suppiah, R., Page, C.M., Wibig, J., Fortuniak, K., Razuvaev, V.N., Douglas, A., Førland, E. and Zhai, P.-M., 1999. Changes in the probability of heavy precipitation: important indicators of climatic change. Climatic Change, 42: 243-283.

Groisman, P.Y. and Legates, D.R., 1994. The accuracy of United States precipitation data. Bulletin of the American Meteorological Society, 75(3): 215-227.

Gurtz, J., Baltensweiler, A. and Lang, H., 1999. Spatially distributed hydrotope-based modelling of evapotranspiration and runoff in mountainous basins. Hydrological Processes, 13(17): 2751-2768.

Guttman, N.B., 1989. Statistical descriptors of climate. Bulletin of the American Meteorological Society, 70(6): 602 - 607.

Gysi, H., 1998. Orographic influence on the distribution of accumulated rainfall with different wind directions. Atmospheric Research, 47-48: 615-633.

Habib, E., Krajewski, W.F. and Kruger, A., 2001. Sampling errors of tipping-bucket rain gauge measurements. Journal of Hydrological Engineering, 6(2): 159-166.

Haiden, T., 2008. Parameterization of elevation effects in short-duration precipitation analysis, 13th Conference on Mountain Meteorology. American Meteorological Society, Whistler.

Haines, A.T., Finlayson, B.L. and McMahon, T.A., 1988. A global classification of river regimes. Applied Geography, 8: 255-272.

Halstead, I., 1994. Rain gauge field book. National Institute of Water and Atmospheric Research Ltd., Tekapo.

Halstead, I., 2008a. Calibration accuracy of tipping bucket precipitation gauges. Personal communication to: T. Kerr, Tekapo.

Halstead, I., 2008b. NIWA stream flow errors. Personal communication to: T. Kerr, Tekapo.

Halstead, I., Tuck, E. and Curry, B., 2003. Waitaki catchment snow report 2002/03 season. WGG2002-23, NIWA.

Hanson, C.L., 1989. Precipitation catch measured by the Wyoming shield and the dual-gage system. Water Resources Research, 25(1): 159-164.

Hanson, C.L., Johnson, G.L. and Rango, A., 1999. Comparison of precipitation catch between nine measureing systems. Journal of Hydrological Engineering, 4(1): 70-75.

Hanson, C.L., Pierson, F.B. and Johnson, G.L., 2004. Dual-gauge system for measuring precipitation: historical development and use. Journal of Hydrological Engineering, 9(5): 350-359.

Hay, L.E., 1991. Simulation of precipitation by weather type analysis. Water Resources Research, 27(4): 493-501.

Haylock, M. and Nicholls, N., 2000. Trends in extreme rainfall indices for an updated high quality data set for Australia, 1910-1998. International Journal of Climatology, 20(13): 1533-1541.

Henderson, R.D., Ibbitt, R. and McKerchar, A.I., 2003. Reliability of linear regression for estimation of mean annual low flow: a Monte Carlo approach. Journal of Hydrology (NZ), 42(1): 75-95.

Henderson, R.D. and Thompson, S.M., 1999. Extreme rainfalls in the Southern Alps of New Zealand. Journal of Hydrology (NZ), 38(2): 309-330.

Hewitson, B.C. and Crane, R.G., 2005. Gridded area-averaged daily precipitation via conditional interpolation. Journal of Climate, 18(1): 41-57.

Heyworth, M.R. and Sealy, J.R., 1980. Introduction to statistics. Longman Paul Ltd., Auckland.

Hill, F.F., 1983. The use of average annual rainfall to derive estimates of orographic enhancement of frontal rain over England and Wales for different wind directions. Journal of Climatology, 3: 113-129.

Hill, H.W., 1961. Northwesterley rains in Canterbury. 136, New Zealand Meteorological Service, Wellington.

Hirsch, R. M., Alexander, R. B., Smith, R. A., 1991. Selection of methods for the detection and estimation of trends in water quality. Water Resources Research, 27(5): 803-813.

Hobbs, P.V., Easter, R.C. and Fraser, A.B., 1973. A theoretical study of the flow of air and fallout of solid precipitation over mountainous terrain: Part II. Microphysics. Journal of Atmospheric Sciences, 30: 813-823.

Hobbs, P.V., Houze JR, R.A. and Matejka, T.J., 1975. The dynamical and microphysical structure of an occluded frontal system and its modification by orography. Journal of Atmospheric Sciences, 32: 1542-1562.

Hochstein, M.P., Watson, M.I., Malengeau, B., Nobes, D.C. and Owens, I.F., 1998. Rapid melting of the terminal section of the Hooker Glacier (Mt Cook National Park, New Zealand). N.Z. Journal of Geology and Geophysics, 41: 203-218.

Hodur, R.M., 1997. The Naval Research Laboratory's Coupled Ocean/Atmosphere Mesoscale Prediction System (COAMPS). Monthly Weather Review, 125: 1414-1430.

Hofierka, J., Parajka, J., Mitasova, H. and Mitas, L., 2002. Multivariate interpolation of precipitation using regularized spline with tension. Transactions in GIS, 6(2): 135-150.

Hooker, B.L. and Fitzharris, B., 1999. The correlation between climatic parameters and the retreat and advance of Franz Josef Glacier, New Zealand. Global and Planetary Change, 22: 39-48.

Horrell, G.A., 1990. Map of mean annual rainfall, South Westland, New Zealand. R90/16, Canterbury Regional Council, Christchurch.

Horrell, G.A., 2006. Personal Communication. Personal communication to: T. Kerr, Christchurch.

Hou, A., 2006. The global precipitation measurement (GPM) mission: an overview, 2006 EUMETSAT Meteorological Satellite Conference, Helsinki.

Houze Jr., R.A., 1993. Section 12.4.2 Upslope Condensation. In, Cloud Dynamics. International Geophysics Series. Academic Press, San Diego, pp. 531-534.

Hovind, E.L., 1965. Precipitation distribution around a windy mountain peak. Journal of Geophysical Research, 70(14): 3271-3278.

Huffman, G.J., Adler, R.F., Arkin, P., Chang, A., Ferraro, R., Gruber, A., Janowiak, J., McNab, A., Rudolf, B. and Schneider, U., 1997. The Global Precipitation Climatology Project (GPCP) Combined Precipitation Dataset. Bulletin of the American Meteorological Society, 78: 5-20.

Hutchinson, P.D., 1990. Regression estimation of low flow in New Zealand. Publication No. 22, Hydrology Centre, DSIR Marine and Freshwater, Christchurch.

Ibbitt, R., McKerchar, A.I. and Woods, R., 2004. Catchments, streamflow and the use of models. In: J. Harding, M.P. Mosley, C.P. Pearson and B. Sorrell (Editors), Freshwaters of New Zealand. New Zealand Hydrological Society Inc., New Zealand Limnological Society Inc., Christchurch.

Inoue, J., Kondo, H., Fujiyoshi, Y., Yamada, T., Fukami, H. and Nakajima, C., 1987. Summer climate of the Northern Patagonia Icefield. Bulletin of Glacier Research, 4: 7-14.

Jakeman, A.J. and Hornberger, G.M., 1992. How much complexity is warranted in a rainfall-runoff model? Water Resources Research, 29(8): 2637-2649.

James, J.W., 1964. The effect of wind on precipitation catch over a small hill. Journal of Geophysical Research, 69(12): 2521-2524.

Jansson, A., Tveito, O.E., Pirinen, P. and Scharling, M., 2007. NORDGRID -a preliminary investigation on the potential for creation of a joint Nordic gridded climate dataset. no. 03/2007 Climate, Norwegian Meteorological Institute, Blindern.

Johansson, B. and Chen, D., 2003. The influence of wind and topography on precipitation distribution in Sweden: Statistical analysis and modelling. International Journal of Climatology, 23: 1523-1535.

Johansson, B. and Chen, D., 2005. Estimation of areal precipitation for runoff modelling using wind data: a case study in Sweden. Climate Research, 29: 53-61.

Kääb, A., 2005. Remote sensing of mountain glaciers and permafrost creep. Geographisches Institut der Universität Zürich, Zürich, 264 pp.

Kalnay, E., Kanamitsu, M., Kistler, R., Collins, W., Deaven, D., Gandin, L., Iredell, M., Saha, S., White, G., Woollen, J., Zhu, Y., Leetmaa, A., Reynolds, R., Chelliah, M., Ebisuzaki, W., Higgins, W., Janowiak, J., Mo, K.C., Ropelewski, C., Wang, J., Jenne, R. and Joseph, D., 1996. The NCEP/NCAR 40-year reanalysis project. Bulletin of the American Meteorological Society, 77(3): 437-471.

Karl, T.R. and Knight, R.W., 1998. Secular trends of precipitation amount, frequency, and intensity in the United States. Bulletin of the American Meteorological Society, 79(2): 231-241.

Keefer, G., 2006. Hagerstown weather station history. http://i4weather.net/stationhistory.html. Accessed: 7-10-2008

Kerr, T., 2005. Snow storage modelling in the Lake Pukaki catchment, New Zealand: An investigation of enhancements to the SnowSim model. M.Sc. Thesis, University of Canterbury, Christchurch.

Kerr, T. and Owens, I.F., 2008. Ghiacciai e cambiamenti climatici durante l'ultimo secolo nella regione Aoraki/Mt Cook, Nuova Zelanda (Glaciers and climate change over the last century in the Aoraki/Mt Cook region, New Zealand). Terra Glacialis, Speciale 2008: 15pp.

Kidson, D.E., 1929. South Island New Zealand mean annual rainfall for period 1891-1925. Department of Scientific and Industrial Research, Wellington.

Kidson, J.W., 2000. An analysis of New Zealand synoptic types and their use in defining weather regimes. International Journal of Climatology, 20: 299-316.

Kirchner, J.W., 2008. Catchments as simple dynamical systems: catchment characterization, rainfall-runoff modeling, and doing hydrology backwards. Water Resources Research, In Press.

Kirkbride, M.P., 1995. Relationships between temperature and ablation on the Tasman Glacier, Mount Cook National Park, New Zealand. New Zealand Journal of Geology and Geophysics, 38: 17-27.

Kirkbride, M.P. and Warren, C.R., 1999. Tasman Glacier, New Zealand: 20th-century thinning and predicted calving retreat. Global and Planetary Change, 22: 11-28.

Kirshbaum, D.J., Bryan, G.H. and Rotunno, R., 2007. The triggering of orographic rainbands by small-scale topography. Journal of Atmospheric Sciences, 64(5): 1530-1549.

Kistler, R., Kalnay, E., Collins, W., Saha, S., White, G., Woollen, J., Chelliah, M., Ebisuzaki, W., Kanamitsu, M., Kousky, V., Dool, H.v.d., Jenne, R. and Fiorino, M., 2001. The NCEP-NCAR 50 year reanalysis: monthly means CD-ROM and documentation. Bulletin of the American Meteorological Society, 82(2): 247-267.

Koschmieder, H., 1934. Methods and results of definite rain measurements. Monthly Weather Review, 62: 5-7.

Krause, P., Boyle, D.P. and Bäse, F., 2005. Comparison of different efficiency criteria for hydrological model assessment. Advances in Geosciences, 5: 89-97.

Larson, L.W. and Peck, E.L., 1974. Accuracy of precipitation measurements for hydrological modeling. Water Resources Research, 10(4): 857-863.

Leathwick, J.R., Morgan, F., Wilson, G., Rutledge, D., McLeod, M. and Johnston, K., 2003. Land environments of New Zealand: A technical guide. David Bateman Ltd., Auckland, 237 pp.

Leathwick, J.R., Wilson, G. and Stephens, R.T.T., 1998. Climate surfaces for New Zealand, revised 2002. Lc9798/126, Manaki Whenua - Landcare Research, Hamilton.

Lee, T.J., Pielke, R.A., Kessler, R.C. and Weaver, J., 1989. Influence of cold pools down-stream of mountain barriers on downslope winds and flushing. Monthly Weather Review, 117: 2041-2058.

Legates, D.R. and DeLiberty, L., 1993. Precipitation measurement biases in the United States. Water Resources Research, 29(5): 855-861.

Legates, D.R. and Willmott, C.J., 1990. Mean seasonal and spatial variability in gauge-corrected, global precipitation. International Journal of Climatology, 10: 111-127.

Lidén, R. and Harlin, J., 2000. Analysis of conceptual rainfall-runoff modelling performance in different climates. Journal of Hydrology, 238: 231-247.

Lindström, G., Johansson, B., Persson, M. and Gardelin, M., 1997. Development and test of the distributed HBV-96 hydrological model. Journal of Hydrology, 201: 272-288.

Linsley, R.K., 1958. Correlation of rainfall intensity and topography in northern California. Transactions, American Geophysical Union, 39(1): 15 - 18.

LINZ, 2007. New Zealand geodesy 2003-2006. Office of the Surveyor General. Land Information New Zealand.

Lloyd, P. 2009. On the determination of trends in rainfall. *Water SA*. 35(3): 237-244.

Lorrey, A., Fowler, A.M. and Salinger, J.M., 2007. Regional climate regime classification as a qualitative tool for interpreting multi-proxy palaeoclimate data spatial patterns: A New Zealand case study. Palaeogeography, palaeoclimatology, palaeoecology, 253: 407-433.

Loukas, A. and Quick, M., 1996. Spatial and temporal distribution of storm precipitation in southwestern British Columbia. Journal of Hydrology, 174: 37-56.

Madgetech, 2008. Rain 110. www.madgetech.com/dynamic_site/view_product.php?itemnumber=RAIN110. Accessed: 7-10-2008

Mamassis, N. and Koutsoyiannis, D., 1996. Influence of astmospheric circulation types on space-time distribution of intense rainfall. Journal of Geophysical Research, 101(D21): 26267-26276.

Manton, M.J., Della-Marta, P.M., Haylock, M.R., Hennessy, K.J., Nicholls, N., Chambers, L.E., Collins, D.A., Daw, G., Finet, A., Gunawan, D., Inape, K., Isobe, H., Kestin, T.S., Lefale, P., Leyu, C.H., Lwini, T., Maitrepierre, L., Ouprasitwong, N., Page, C.M., Pahalad, J., Plummer, N., Salinger, M.J., Suppiah, R., Tran, V.L., Trewin, B., Tibig, I. and Yee, D., 2001. Trends in extreme daily rainfall and temperature in Southeast Asia and the South Pacific: 1961-1998. International Journal of Climatology, 21: 269-284.

Mantua, N.J. and Hare, S.R., 2002. The Pacific Decadal Oscillation. Journal of Oceanography, 58: 35-44.

Mantua, N.J., Hare, S.R., Zhang, Y., M.Wallace, J. and Francis, R.C., 1997. A Pacific interdecadal climate oscillation with impacts on salmon production. Bulletin of the American Meteorological Society, 78: 1069-1079.

Marshall, G.J., 2003. Trends in the Southern Annular Mode from observations and reanalyses. Journal of Climate, 16(24): 4134-4143.

Mass, C., 1981. Topographically forced convergence in western Washington State. Monthly Weather Review, 109: 1335-1347.

McAlevey, B., 1998. A distributed seasonal snow model for New Zealand. M.Sc. Thesis, University of Otago, Dunedin.

McCauley, M. and Sturman, A., 1999. A study of orographic blocking and barrier wind development upstream of the Southern Alps, New Zealand. Meteorology and Atmospheric Physics, 70: 121-131.

McGinley, J., 1982. A diagnosis of alpine lee cyclogenesis. Monthly Weather Review, 110: 1271-1287.

McGowan, H.A. and Sturman, A.P., 1996a. Climatic indicators of monthly and seasonal inflows into an alpine lake, Lake Pukaki, New Zealand. In: D.H.

Braddock (Editor), Prospects and needs for climate forecasting. Miscellaneous series. The Royal Society of New Zealand, Wellington, pp. 57-62.

McGowan, H.A. and Sturman, A.P., 1996b. A hydrometeorological approach to the forecasting of inflows to alpine lakes. Physical Geography, 17(6): 513-533.

McGowan, H.A. and Sturman, A.P., 1996c. Short- and medium-term trends in the hydrometeorology of the central southern alps, New Zealand. International Journal of climatology, 16: 1267-1279.

McKerchar, A.I. and Henderson, R.D., 2003. Shifts in flood and low-flow regimes in New Zealand due to interdecadal climate variations / Variations dans les régimes de crue et de basses aux en Nouvelle-Zélande dues à des variations climatiques inter-décennales. Hydrological Sciences Journal, 48(4): 637-654.

McKerchar, A.I. and Pearson, C.P., 1989. Flood frequency in New Zealand. Publication No. 20, Hydrology Centre, Division of Water Sciences, Department of Scientific and Industrial Research, Christchurch.

McKerchar, A.I. and Pearson, C.P., 1997. Quality of long flow records for New Zealand rivers. Journal of Hydrology (NZ), 36(2): 15-41.

McKerchar, A.I., Pearson, C.P. and Fitzharris, B., 1998. Dependency of summer lake inflows and precipitation on spring SOI. Journal of Hydrology, 205: 66-80.

McKerchar, A.I., Pearson, C.P. and Moss, M.E., 1996. Prediction of summer inflows to lakes in the Southern Alps, New Zealand, using the spring Southern Oscillation Index. Journal of Hydrology, 184: 175-187.

McMillan, H., Freer, J., Pappenberger, F., Krueger, T. and Clark, M., 2008. How good are our flow measurements during floods?, 2008 NZHS and MSNZ joint annual conference "Extremes", Shantytown, West Coast.

McNulty, D., n.d. North westerly precipitation ratios. unpublished. Copy available for viewing at Alpine Guides, Aoraki/Mt Cook, Mt Cook.

McSaveney, M.J., 1979. An effective antifreeze for storage raingauges. Journal of Hydrology (NZ), 18(1): 52-54.

McSaveney, M.J., Chinn, T.J., Horrell, G.A. and Longson, C.K., 1978. The measured distribution of precipitation across the Southern Alps, Ministry of Works and Development, Christchurch.

McSaveney, M.J. and Davies, T.R.H., 2005. Engineering for debris flows in New Zealand. In: M. Jakob and O. Hungr (Editors), Debris-flow hazards and related phenomena. Praxis. Springer, Berlin, pp. 635-658.

Measurement Resources, 2006. Level sensor 2001. http://www.measurement-resources.com.au/downloads/datasheets/levels_datasheet/1001.pdf. Accessed: 7-10-2008

MeteoSwiss, 2005. Normwerte 1961-90 der Niederschlagssumme. Accessed: 17 April 2008

Micovic, Z. and Quick, M.C., 1999. A rainfall and snowmelt runoff modelling approach to flow estimation at ungauged sites in British Columbia. Journal of Hydrology, 226: 101-120.

Milewska, E.J., Hopkinson, R.F. and Niitsoo, A., 2005. Evaluation of geo-referenced grids of 1961 - 1990 Canadian temperature and precipitation normals. Atmosphere-Ocean, 43(1): 49-75.

Minder, J.R., Durrana, D.R., Roeb, G.H. and Andersc, A.M., 2008. The climatology of small-scale orographic precipitation over the Olympic mountains: Patterns and processes. Quarterly Journal of the Royal Meteorological Society, 134(633): 817-839.

Mink, J.F., 1960. Distribution pattern of rainfall in the leeward mountains, Oahu, Hawaii. Journal of Geophysical Research, 65(9): 2869-2876.

Mitchell, T.D. and Jones, P.D., 2005. An improved method of constructing a database of monthly climate observations and associated high-resolution grids. International Journal of Climatology, 25: 693-712.

Mohr, M. and Tveito, O.E., 2008. Daily temperature and precipitation maps with 1 km resolution derived from Norwegian weather observations, 17th Conference on Applied Climatology. American Meteorological Society, Whistler.

Montenari, A., 2004. An attempt to quantify uncertainty in observed river flows: effect on parameterization and performance evaluation of rainfall-runoff models, 2004 AGU Fall Meeting, San Francisco.

Mullan, B., Wratt, D., Dean, S., Hollis, M., Allan, S., Williams, T. and Kenny, G., 2008. Climate change effects and impacts assessment: A guidance manual for local government in New Zealand. Ministry for the Environment Wellington, 167 pp.

Nash, J.E. and Sutcliffe, J.V., 1970. River flow forecasting through conceptual models part 1 - A discussion of principles. Journal of Hydrology, 10(3): 282-290.

Ndiaye, O., Goddard, L. and Ward, M.N., 2008. Using regional wind fields to improve general circulation model forecasts of July-September Sahel rainfall. International Journal of Climatology, Early view: pp 14.

Neale, S., 1996. Measuring and modelling snow melt in a New Zealand alpine environment. M.Sc. Thesis, University of Otago, Dunedin.

Neale, S.M. and Fitzharris, B., 1997. Energy balance and synoptic climatology of a melting snowpack in the Southern Alps, New Zealand. International Journal of Climatology, 17: 1595-1609.

Neff, E.L., 1977. How much rain does a rain gage gage? Journal of Hydrology, 35: 213-220.

New, M., Lister, D., Hulme, M. and Makin, I., 2002. A high-resolution data set of surface climate over global land areas. Climate Research, 21: 1-25.

New Zealand., 1857. New Zealand gazette, No. 26 (Sept. 23, 1857)-. Govt. Printer, Wellington.

Nicholls, N. and Murray, W., 1999. Workshop on indices and indicators for climate extremes: Ashville, NC, USA, 3-6 June 1997 breakout group B: Precipitation. Climatic Change, 42: 23-29.

Nicholson, S.E., Yin, X. and Ba, M.B., 2000. On the feasibility of using a lake water balance model to infer rainfall: an example from Lake Victoria. Hydrological Sciences Journal, 45(1).

Niemczynowicz, J., 1989. Altitude effect on summer precipitation measured in Swedish mountains, The seventh northern research basins symposium/workshop, Llulissat.

NIWA, 2008. The National Climate Database. http://cliflo.niwa.co.nz/. Accessed:

NOAA/ESRL, 2008. Kaplan SST V2. http://www.cdc.noaa.gov/. Accessed: 27 September 2008

NWS, 2006. Rainfall gages. http://www.wrh.noaa.gov/sgx/cpm/rainfall.php?wfo=sgx. Accessed: 7-10-2008

NZMS, 1966. Summaries of climatological observations at New Zealand stations to 1960. New Zealand Meteorological Service Miscelaneous publication 122. New Zealand Meteorological Service, Wellington.

NZMS, 1973. Rainfall normals for New Zealand, 1941 to 1970 : stations in New Zealand and outlying islands, including the Cook Group, Pitcairn Island, Niue Island and Western Samoa. New Zealand Meteorological Service

Miscelaneous publication 145. New Zealand Meteorological Service, Wellington, [N.Z.].

NZMS, 1975a. Average annual rainfall (mm) 1941-70. New Zealand Meteorological Service, Wellington.

NZMS, 1975b. Supplement one to Rainfall normals for New Zealand, 1941 to 1970 : stations in New Zealand and outlying islands, including the Cook Group, Pitcairn Island, Niue Island and Western Samoa. New Zealand Meteorological Service Miscelaneous publication 145 Supplement No.1. New Zealand Meteorological Service, Wellington.

NZMS, 1985a. New Zealand Annual Rainfall: Normals 1951-1980, New Zealand Meteorological Service, Wellington, N.Z.

NZMS, 1985b. Rainfall normals for New Zealand, 1951 to 1980 : stations in New Zealand, the Cook Group, Pitcairn Island, Kiribati, Tonga, Tuvalu, Fiji, and Western Samoa. New Zealand Meteorological Service. New Zealand Meteorological Service, Wellington, 36 pp.

NZMS, 2008. Maps and rain radar. http://metservice.co.nz/default/index.php?alias=allnzrainradar. Accessed: 8-10-2008

Panziera, L. and Germann, U., 2008. Orographic forcing and doppler winds, the key for nowcasting heavy precipitation in the mountains, 13th Conference on Mountain Meteorology. American Meteorological Society, Whistler, Canada.

Pearson, C.P., 1995. Regional frequency analysis of low flows in New Zealand rivers. Journal of Hydrology (NZ), 33(2): 94-122.

Perrin, C., Michel, C. and Andréassian, V., 2003. Improvement of a parsimonious model for streamflow simulation. Journal of Hydrology, 279: 275-289.

Peterson, T.C., Easterling, D.R., Vose, R.S. and Eischeid, J.K., 1993. The Global Historical Climatology Network Precipitation data, United States, pp. 7.

Peterson, T.C., Easterling, D.R., Karl, T.R., Groisman, P., Nicholls, N., Plummer, N., Torok, S., Auer, I., Boehm, R., Gullett, D., Vincent, L., Heino, R., Tuomenvirta, H., Mestre, O., Szentimrey, T., Salinger, J., Forland, E.J., Hanssen-Bauer, I., Alexandersson, H., Jones, P., Parker, D., 1998. Homogeneity adjustments of in situ atmospheric climate data: a review. International Journal of Climatology, 18: 1493-1517.

Pielke, R.A., Cotton, W.R., Walko, R.L., Tremback, C.J., Lyons, W.A., Grasso, L.D., Nicholls, M.E., Moran, M.D., Wesley, D.A., Lee, T.J. and Copeland, J.H., 1992. A comprehensive meteorological modeling system RAMS. Meteorology and Atmospheric Physics, 49: 69-91.

Poff, N.L., Olden, j.D., Pepin, D.M. and Bledsoe, B.P., 2006. Placing global stream flow variability in geographic and geomorphic contexts. River Research and Applications, 22(2): 149-166.

Power, S., Casey, T., Folland, C., Colman, A. and Mehta, V., 1999. Inter-decadal modulation of the impact of ENSO on Australia. Climate Dynamics, 15: 319-324.

Prowse, T.D. and Owens, I.F., 1982. Energy balance over melting snow, Craigeburn Range. Journal of Hydrology (NZ), 21 no2: 133-147.

Prowse, T.D. and Owens, I.F., 1984. Characteristics of snowfalls, snow metamorphism, and snowpack structure with implications for avalanching, Craigeburn Range, New Zealand. Arctic and Alpine Research, 16(1): 107-118.

Purdie, J., 1996. Ice loss at the terminus of the Tasman Glacier. M.Sc. Thesis, University of Otago, Dunedin.

Purdie, J. and Fitzharris, B., 1999. Processes and rates of ice loss at the terminus of Tasman Glacier, New Zealand. Global and Planetary Change, 22: 79-91.

Purdy, J.C. and Austin, G.L., 2003. The role of synoptic cloud in orographic rainfall in the Southern Alps of New Zealand. Meteorological Applications, 10: 355-365.

Purdy, J.C., Austin, G.L., Seed, A.W. and Cluckie, I.D., 2005. Radar evidence of orographic enhancement due to the seeder feeder mechanism. Meteorological Applications, 12: 199-206.

Putkonen, J., 2004. Continuous Snow and Rain Data at 500 to 4400 m Altitude near Annapurna, Nepal, 1999-2001. Arctic, Antarctic, and Alpine Research, 36(2): 244-248.

Rasmussen, L.A. and Conway, H., 2004. Climate and glacier variability in western North America. Journal of Climate, 17: 1804-1815.

Rasmussen, L.A. and Conway, H., 2005. Influence of upper-air conditions on glaciers in Scandinavia. Annals of glaciology, 42: 402-407.

Rasmussen, L.A., Conway, H. and C.F., R., 2007. Influence of upper air conditions on the Patagonia icefields. Global and Planetary Change, 59(203-216): 14.

Rasmussen, L.A., Conway, H. and Hayes, P.S., 2000. The accumulation regime of Blue Glacier, U.S.A., 1914-96. Journal of Glaciology, 46(153): 326-334.

Rasmussen, L.A., Conway, H. and Hayes, P.S., 2001. Estimating Olympic Peninsula precipitation from upper air wind and humidity. Journal of Geophysical Research, 106(D2): 1493-1501.

Rasmusson, E.M. and Carpenter, T.H., 1982. Variations in tropical sea surface temperature and surface wind fields associated with the Southern Oscillation / El Ninö. Monthly Weather Review, 110(5): 354-384.

Rechard, P.A. and Larson, L.W., 1971. The use of snow fences for shielding precipitation gages. In: J.N. Washichek (Editor), 39th Annual meeting, Western Snow Conference, Billings, Montana.

Reinking, R.F., Snider, j.B. and Coen, J.L., 2000. Influences of storm-embedded orographic gravity waves on cloud liquid water and precipitation. Journal of Applied Meteorology, 39: 733-759.

Renwick, J. and Thompson, D., 2006. The Southern Annualar mode and New Zealand climate. Water and Atmosphere, 14(2): 24-25.

Revell, M.J., Copeland, J.H., Larsen, H.R. and Wratt, D.S., 2002. Barrier jets around the Southern Alps of New Zealand and their potential to enhance alpine rainfall. Atmospheric Research, 61: 277-298.

Rhoades, D.A. and Salinger, M., 1993. Adjustment of temperature and rainfall records for site changes. International Journal of climatology, 13: 899-913.

Robichaud, A.J. and Austin, G.L., 1988. On the modelling of warm orographic rain by the seeder-feeder mechanism. Quarterly Journal of the Royal Meteorological Society, 114: 967-988.

Rodriguez-Puebla, C., Encinas, A.H. and Sáenz, J., 2001. Winter precipitation over the Iberian peninsula and its relationship to circulation indices. Hydrolocial and Earth System Sciences, 5(2): 233-244.

Roe, G.H. and Baker, M.B., 2006. Microphysical and geometrical controls on the pattern of orographic precipitation. Journal of the Atmospheric Sciences, 63: 861-880.

Rögnvaldsson, Ó., Bao, J.-w. and Ólafsson, H., 2007. Sensitivity simulations of orographic precipitation with MM5 and comparison with observations in Iceland during the Reykjanes Experiment. Meteorologische Zeitschrift, 16(1): 87-98.

Röhl, K., 2005. Terminus disintegration of debris-covered, lake-calving glaciers. PhD. Thesis, University of Otago, Dunedin, 434 pp.

Rother, H., 2006. Late Pleistocene Glacial Geology of the Hope-Waiau Valley System in North Canterbury, New Zealand, University of Canterbury, Christchurch, 320 pp.

Ruddell, A.R., 1995. Recent glacier and climate change in the New Zealand Alps. Ph.D. Thesis, University of Melbourne, Melbourne.

Ryan, A.P., 1987. The climate and weather of Canterbury (including Aorangi). New Zealand Meteorological Service, Wellington.

Salinger, M.J., 1979. Climatic regions of New Zealand based on cluster techniques. New Zealand Statistician, 14: 26-34.

Salinger, M.J., 1980. New Zealand climate: I. Precipitation patterns. Monthly Weather Review, 108: 1892-1904.

Salinger, M.J., 1981. New Zealand climate: the instrumental record. Ph.D. Thesis, Victoria University of Wellington, Wellington.

Salinger, M.J., Basher, R.E., Fitzharris, B., Hay, J.E., Jones, P.D., MacVeigh, J.P. and Schmidely-Leleu, I., 1995. Climate trends in the South-West Pacific. International Journal of Climatology, 15: 285-302.

Salinger, M.J. and Griffiths, G.M., 2001. Trends in New Zealand daily temperature and rainfall extremes. International Journal of Climatology, 21: 1437-1452.

Salinger, M.J., Heine, M.J. and Burrows, C.J., 1983. Variations of the Stocking (Te Wae Wae) Glacier, Mount Cook and climatic relationships. New Zealand Journal of Science, 26: 321-338.

Salinger, M.J., McGann, R., Coutts, L., Collen, B. and Fouhy, E., 1992. South Pacific historical climate network. Rainfall trends in New Zealand and outlying islands, 1920 - 1990, New Zealand Meteorological Service, Wellington.

Salinger, M.J. and Mullan, A.B., 1999. New Zealand climate: temperature and precipitation variations and their links with atmospheric circulation 1930-1994. International Journal of Climatology, 19: 1049-1071.

Salinger, M.J., Renwick, J. and Mullan, A.B., 2001. Interdecadal pacific oscillation and South Pacific climate. International Journal of Climatology, 21: 1705-1721.

Sanson, J. and Gray, W.R., 2002. The optimization and calibration of a rain intensity gauge. Journal of Atmospheric and Oceanic Technology, 19: 3-20.

Sarker, R.P., 1966. A dynamical model of orographic rainfall. Monthly Weather Review, 94(9): 555-572.

Schaefli, B. and Gupta, H.V., 2007. Do Nash values have value? Hydrological Processes, 21: 2075-2080.

Schär, C. and Frei, C., 2005. Orographic precipitation and climate change. In: U.M. Huber, H.K.M. Bugmann and M.A. Reasoner (Editors), Global change and mountain regions. Springer, Dordrecht, pp. 255-266.

Schär, C., Frei, C., Lüthi, D. and Davies, H.C., 1996. Surrogate climate-change scenarios for regional climate models. Geophysical Research Letters, 23(6): 669-672.

Schmidli, J. and Frei, C., 2005. Trends of heavy precipitation and wet and dry spells in Switzerland during the 20th century. International Journal of Climatology, 25: 753-771.

Schneider, C. and Gies, D., 2004. Effects of El Ninö–Southern Oscillation on southernmost South America precipitation at 53 °S revealed from NCEP–NCAR reanalyses and weather station data. International Journal of Climatology, 24: 1057-1076.

Schneider, C., Glaser, M., Kilian, R., Santana, A., Butorovic, N. and Casassa, G., 2003. Weather observations across the Southern Andes at 53^{o}S. Physical Geography, 24(2): 97-119.

Segond, M., Wheater, H.S. and Onof, C., 2007. The significance of spatial rainfall representation for flood runoff estimation: A numerical evaluation based on the Lee catchment, UK. Journal of Hydrology, 347(1-2): 116-131.

Seko, K., 1987. Seasonal variation of altitudinal dependence of precipitation in Langtang Valley, Nepal Himalayas. Bulletin of Glacier Research, 5: 41-47.

Serra, Y.L., A'Hearn, P., Freitag, H.P. and McPhaden, M.J., 2001. ATLAS self-siphoning rain gauge error estimates. Journal of Atmospheric and Oceanic Technology, 18: 1989-2002.

Sevruk, B., 1985. Correction of precipitation measurements: Swiss experience, Workshop on the correction of precipitation measurements, Zurich.

Sevruk, B. and Cvila, B., 2005. Error sources of precipitation measurements using electronic weight systems. Atmospheric Research, 77: 39-47.

Sevruk, B. and Mieglitz, K., 2002. The effect of topography, season and weather situation on daily precipitation gradients in 60 Swiss valleys. Water Science and Technology, 45(2): 41-48.

Sevruk, B. and Nevenic, M., 1998. The geography and topography effects on the areal pattern of precipitation in a small prealpine basin. Water Science and Technology, 37(11): 163-170.

Sharples, J.J., Hutchinson, M.F. and Jellett, D.R., 2005. On the horizontal scale of elevation dependence of Australian monthly precipitation. Journal of Applied Meteorology, 44(12): 1850-1865.

Shen, S., Dzikowski, P., Li, G. and Griffith, D., 2001. Interpolation of 1961–97 daily temperature and precipitation data onto Alberta polygons of ecodistrict and soil landscapes of Canada. Journal of Applied Meteorology, 40: 2162-2177.

Sheridan, M., 1995. Dam dwellers - end of an era - living with hydro-electricity development in the Waitaki Valley and MacKenzie Country. Sheridan Press, Twizel.

Simpson, J.J., Hufford, G.L., Fleming, M.D., Berg, J.S. and Ashton, J.B., 2002. Long-term climate patterns in Alaskan surface temperature and precipitation and their biological consequences. Geoscience and Remote Sensing, IEEE Transactions on, 40(5): 1164-1184.

Sinclair, M.R., 1993. A diagnostic study of the extratropical precipitation resulting from tropical cyclone Bola. Monthly Weather Review, 121: 2690-2707.

Sinclair, M.R., 1994. A diagnostic model for estimating orographic precipitation. Journal of Applied Meteorology, 33: 1163-1175.

Sinclair, M.R., Wratt, D.S., Henderson, R.D. and Gray, W.R., 1997. Factors affecting the distribution and spillover of precipitation in the Southern Alps of New Zealand - A case study. Journal of Applied Meteorology, 36: 428-442.

Singh, P. and Kumar, N., 1997. Effect of orography on precipitation in the western Himalayan region. Journal of Hydrology, 199: 183-206.

Sitron, 2006. Sitron Capacitive level sensors. http://www.sitron.com/level_c_sc404.htm. Accessed: 7-10-2008

Skamarock, W.C., Klemp, J.B., Dudhia, J., Gill, D.O., Barker, D.M., Wang, W. and Powers, J.G., 2005. A Description of the Advanced Research WRF Version 2. NCAR/TN–468+STR, National Centre for Atmospheric Research, Boulder.

Skermer, N.A., Rawlings, G.E. and Hurley, A.J., 2002. Debris flow defences at Aoraki Mount Cook Village, New Zealand. Quarterly Journal of Engineering Geology and Hydrogeology, 35: 19-24.

Smith, R.B., 1979. The influence of mountains on the atmosphere. Advances in Geophysics, 21: 87-230.

Smith, R.B., 2003. A linear upslope-time-delay model for orographic precipitation. Journal of Hydrology, 282: 2-9.

Smith, R.B., 2006. Progress on the theory of orographic precipitation. Geological Society of America Special Paper 398: 16.

Smith, R.B., Jiang, Q., Fearon, M., Tabary, P., Dorninger, M., Doyle, J. and Benoit, R., 2003. Orographic precipitation and air mass transformation: An alpine example. Quarterly Journal of the Royal Meteorological Society, 129: 433-454.

Steiner, M., Bousquet, O., Houze JR, R.A. and Smull, B.F., 2003. Airflow within major alpine river valleys under heavy rainfall. Quarterly Journal of the Royal Meteorological Society, 129: 411-431.

Stickley, A.R., 1940. An evaluation of the Bergeron-Findeisen precipitation theory. Monthly Weather Review, 68(10): 272-280.

Stow, C.D., Bradley, S.G., Farrington, K.E., Dirks, K.N. and Gray, W.R., 1998. A Rain Gauge for the Measurement of Finescale Temporal Variations. Journal of Atmospheric and Oceanic Technology, 15: 127-135.

Stozzi, T., Wegmuller, U., Wiesmann, A. and Werner, C., 2003. Validation of the X-SAR SRTM DEM for ERS and JERS SAR geocoding and 2-pass differential interferometry in alpine regions, IGARSS '03. IEEE, Toulouse, France.

Stueffer, M., Rott, H. and Skvarca, P., 2007. Glaciar Perito Moreno, Patagonia: climate sensitivities and glacier characteristics preceding the 2003/04 and 2005/06 damming events. Journal of Glaciology, 53(180): 3-16.

Sturges, D.L., 1984. Comparison of precipitation as measured in gages protected by a modified alter shield, wyoming shield, and stand of trees. In: B.A. Shafer (Editor), 52nd Annual meeting. Western Snow Conference, Sun Valley, Idaho.

Sturges, D.L., 1986. Precipitation measured by dual gauges, wyoming-shielded gages, and in a forest opening. In: D.L. Kane (Editor), Cold Regions Hydrology Symposium. American Water Resources Association, Bethseda, Maryland.

Sturman, A. and Wanner, H., 2001. A comparative review of the weather and climate of the Southern Alps of New Zealand and the European Alps. Mountain Research and Development, 21(4): 359-369.

Suggate, R.P. (Editor), 1978. The Geology of New Zealand, 1. E.C.Keating, Wellington.

Sweeney, J.C. and O'Hare, G.P., 1992. Geographical variations in precipitation yields and circulation types in Britain and Ireland. Transactions of the Institute of British Geographers, 17(4): 448-463.

Tabler, R.D., Berg, N.H., Trabant, D.C., Santeford, H.S. and Rechard, P.A., 1990. Measurement and evaluation of winter precipitation. In: W.L. Ryan and R.D. Crissman (Editors), Cold regions hydrology and hydraulics : a state of the practice report. Technical Council on Cold Regions Engineering monograph. American Society of Civil Engineers, New York, pp. 9-38.

Tait, A., Henderson, R.D., Turner, R. and Zheng, X., 2006. Thin plate smoothing spline interpolation of daily rainfall for New Zealand using a climatological rainfall surface. International Journal of Climatology, 26: 2097-2115.

Tait, A. and Turner, R., 2005. Generating multiyear gridded daily rainfall over New Zealand. Journal of Applied Meteorology, 44(9): 1315-1323.

Tan, B.Q. and O'Connor, K.M., 1996. Application of an empirical infiltration equation in the SMAR conceptual model. Journal of Hydrology, 185: 275-295.

Tani, M., 1996. An approach to annual water balance for small mountainous catchments with wide spatial distributions of rainfall and snow water equivalent. Journal of Hydrology, 183(3-4): 205-225.

Tank, A.M.G.K. and Können, G.P., 2003. Trends in indices of daily temperature and precipitation extremes in Europe 1946-99. Journal of Climate, 16: 3665-3680.

Thies Clima, 2005. Precipitation. http://www.thiesclima.com/disdrometer.htm. Accessed: 7-10-2008

Thompson, C.S., Sinclair, M.R. and Gray, W.R., 1997. Estimating Long-term annual precipitation in a mountainous region from a diagnostic model. International Journal of Climatology, 17: 997-1007.

Thompson, S.M., 1997. Snow storage estimation for hydro-electricity catchments from monitored rainfall and river flow, NIWA, Wellington.

Thompson, S.M., 2002. River discharge from mountains with frequent rain. Journal of Hydrology (NZ), 41(2): 125-144.

Thompson, S.M. and Adams, J.E., 1979. Suspended load in some major rivers of New Zealand. In: D.L. Murray and P. Ackroyd (Editors), Physical Hydrology. New Zealand Experience. New Zealand Hydrological Society.

Tomlinson, A. and Sansom, J., 1994. Rainfall normals for New Zealand 1961 - 1990, NIWA, Wellington.

Trenberth, K.E., 1999. Conceptual framework for changes of extremes of the hydrological cycle with climate change. Climatic Change, 42(1): 327-339.

Ummenhofer, C.C. and England, M.H., 2007. Interannual extremes in New Zealand precipitation linked to modes of Southern Hemisphere climate variability. Journal of Climate, 20: 5418-5440.

Verbunt, M., Gurtz, J., Jasper, K., Lang, H., Warmerdam, P. and Zappa, M., 2003. The hydrological role of snow and glaciers in alpine river basins and their distributed modeling. Journal of Hydrology, 282(1-4): 36-55.

Wallace, S.J., 2001. Mapping glacial landforms in the Pukaki and Tekapo lake basins. P.G.Dip.Sc. Thesis, University of Otago, Dunedin.

Wang, Y. and Zhou, L., 2005. Observed trends in extreme precipitation events in China during 1961–2001 and the associated changes in large-scale circulation. Geophysical Research Letters, 32(L09797): 4.

Warnick, C.C., 1953. Experiments with windshields for precipitation gages. Transactions, American Geophysical Union, 34(3): 379-388.

Weiler, M., McGlynn, B.L., McGuire, K.J. and McDonnell, J.J., 2003. How does rainfall become runoff? A combined tracer and runoff transfer function approach. Water Resources Research, 39(11): 1315.

Weingartner, R. and Pearson, C.P., 2001. A comparison of the hydrology of the Swiss Alps and the Southern Alps of New Zealand. Mountain Research and Development, 21(4): 370-381.

Weston, K.J. and Roy, M.G., 1994. The directional-dependence of the enhancement of rainfall over complex orography. Meteorological Applications, 1: 267-275.

Whitehouse, I.E., 1982. Erosion on Sebastapol, Mt Cook, New Zealand, in the last 85 years. New Zealand Geographer, 38(2): 77-80.

Whitehouse, I.E., 1988. Geomorphology of the central Southern Alps, New Zealand: the interaction of plate collision and atmospheric circulation. Zeitschrift fur Geomorphologie. Supplementband, 69: 105-116.

Widmann, M. and Schär, C., 1997. A principal component and long-term trend analysis of daily precipitation in Switzerland. International Journal of Climatology, 17(12): 1333-1356.

Wigley, H., 1979. The Mount Cook way - the first fifty years of the Mount Cook Company. Collins, Auckland.

Willmott, C.J. and Matsuura, K., 2001. Terrestrial air temperature and precipitation: monthly and annual time series (1950-1999)(version 1.02). Accessed: 18-2-2008

Wilson, H.D., 1976. Vegetation of Mount Cook National Park, New Zealand. National Parks Authority Scientific Series No. 1. Department of Lands and Survey, Wellington.

Wilson, J., 1968. Aorangi the story of Mt Cook. Whitcomb and Tombs Ltd, Christchurch.

Wilson, J.W. and Atwater, M.A., 1972. Storm rainfall variability over Connecticut. Journal of Geophysical Research, 77(21): 3950-3956.

WMO, 1983. Guide to climatological practices. Secretariat of the World Meteorological Organization, Geneva.

WMO, 1986. Intercomparison of models of snowmelt runoff, WMO-No.646. 23, World Meteorological Organization, Geneva.

WMO, 2008. World weather/climate extremes archive http://wmo.asu.edu/#continental. Accessed: 18th October 2008

Woods, R., Hendrikx, J. and Tait, A., 2006. Estimating mean flow of New Zealand rivers. Journal of Hydrology (NZ), 45(2): 95-110.

Wratt, D.S., Revell, M.J., Sinclair, M.R., Gray, W.R., Henderson, R.D. and Chater, A.M., 2000. Relationships between air mass properties and mesoscale rainfall in New Zealand's Southern Alps. Atmospheric Research, 52: 261-282.

Wratt, D.S., Ridley, R.N., Sinclair, M.R., Larsen, H., Thompson, S.M., Henderson, R.D., Austin, G.L., Bradley, S.G., Auer, A., Sturman, A.P., Owens, I.F., Fitzharris, B., Ryan, B.F. and Gayet, J.-F., 1996. The New Zealand Southern Alps experiment. Bulletin of the American Meteorological Society, 77(4): 683-692.

Xie, P. and Arkin, P., 1996. Analysis of global monthly precipitation using gauge observations, satellite estimates, and numerical predictions. Journal of Climate, 9(4): 840-858.

Xu, C.Y. and Singh, V.P., 1998. A review on monthly water balance models for water resoure investigations. Water Resources Management, 12: 31-50.

Yang, D., Goodison, B.E., Ishida, S. and Benson, C.S., 1998. Adjustment of daily precipitation data at 10 climate stations in Alaska: Application of World Meteorological Organization intercomparison results. Water Resources Research, 34(2): 241-256.

Yang, D., Goodison, B.E. and Metcalfe, J.R., 1995. Accuracy of Tretyakov precipitation gauge: result of WMO intercomparison. Hydrological Processes, 9: 877-895.

Yang, D., Goodison, B.E., Metcalfe, J.R., Louie, P., Leavesley, G., Emerson, D., Hanson, C.L., Golubev, V.S., Elomaa, E., Gunther, T., Pangburn, T., Kang, E. and Milkovic, J., 1999a. Quantification of precipitation measurement discontinuity induced by wind shields on national gauges. Water Resources Research, 35(2): 491-508.

Yang, D., Ishida, S., Goodison, B.E. and Gunther, T., 1999b. Bias correction of daily precipitation measurements for Greenland. Journal of Geophysical Research, 104(D6): 6171-6181.

Zängl, G., 2004. The sensitivity of simulated orographic precipitation to model components other than cloud microphysics. Quarterly Journal of the Royal Meteorological Society, 130: 1857-1875.

Zängl, G., 2005. The impact of lee-side stratification on the spatial distribution of orographic precipitation. Quarterly Journal of the Royal Meteorological Society, 131: 1075-1091.

Zängl, G., 2008. The temperature dependence of small-scale orographic precipitation enhancement. Quarterly Journal of the Royal Meteorological Society, 134(634): 1167-1181.

Zängl, G., Aulehner, D., Wastl, C. and Pfeiffer, A., 2008. Small-scale precipitation variability in the Alps: Climatology in comparison with semi-idealized numerical simulations. Quarterly Journal of the Royal Meteorological Society, 134(636): 1865-1880.

Zheng, Z. and Thompson, C.S., 2007. Simulation of precipitation in the upper Waitaki catchment, New Zealand, and its relation to the Interdecadal Pacific Oscillation: Interannual and intraseasonal variability. Journal of Hydrology, 339: 105-117.

A1. Appendix 1: Manual measurements from new precipitation gauges.

List of tables in this appendix

Table A1-1. Manual measurements for Ball Shelter precipitation gauge.

Date	Dist. from rim (mm)	Precip. since last time (mm)	Total (mm)	Notes
15/11/2005 17:27	1835	0	0	Gauge installed
15/11/2005 17:56	1768	0	0	An extra 1.5 l of water was added so as to cover the bottom of the sensor cable.
16/11/2005 10:19	1760	8	8	
18/11/2005 06:17	1759	1	9	
15/12/2005 07:27	1620	139	148	
18/01/2006 13:58	1062	558	706	
15/02/2006 08:34	1007	55	761	
16/03/2006 09:08	853	154	915	Gauge emptied
16/03/2006 09:36	1794	0	915	After emptying.
11/04/2006 09:45	1505	289	1204	Evidence of Kea visiting the gauge.
16/05/2006 09:20	1204	301	1505	1.5 cm of snow on the ground. Kea damage. Gauge emptied
16/05/2006 10:32	1803	0	1505	After emptying
23/06/2006 14:22	1250	553	2058	60 cm of snow on the ground. Contents largely frozen. Gauge emptied
23/06/2006 16:00	1758	0	2058	After emptying
25/07/2006 15:30	1640	118	2176	50-60 cm of snow on the ground
11/08/2006 16:56	1545	95	2271	30-40 cm of snow on the ground
14/09/2006 10:40	1301	244	2515	No snow. Gauge emptied.
14/09/2006 10:55	1780	0	2515	After emptying
17/10/2006 08:20	1341	439	2954	2 cm of snow on the ground. Gauge emptied
17/10/2006 08:41	1756	0	2954	After emptying
1/12/2006 18:10	726	1030	3984	Gauge emptied.
1/12/2006 18:21	1758	0	3984	After emptying
16/01/2007 08:39	1094	664	4648	2 possums in the gauge. Gauge emptied.
16/01/2007 08:55	1787	0	4648	After emptying
27/02/2007 08:42	1579	208	4856	Gauge emptied.
27/02/2007 08:52	1565	0	4856	After emptying
3/04/2007 14:16	1247	318	5174	Gauge removed.

Table A1-2. Manual measurements for De La Beche precipitation gauge.

Date	Dist. from rim (mm)	Precip. since last time (mm)	Total (mm)	Notes
16/11/2005 17:28	1800	0	0	Gauge installed.
17/11/2005 06:44	1795	5	5	
18/01/2006 19:41	27	1768	1773	Gauge overfull, gauge emptied
18/01/2006 19:55	1768	0	1773	After emptying
15/02/2006 06:45	1528	240	2013	
16/03/2006 17:00	908	620	2633	Gauge emptied
16/03/2006 17:32	1814	0	2633	After emptying
11/04/2006 18:08	1050	764	3397	10 cm of snow on the ground, gauge emptied
11/04/2006 18:50	1878	0	3397	After emptying
12/04/2006 07:41	1869	0	3397	
12/04/2006 07:44	1769	0	3397	After adding antifreeze
16/05/2006 20:30	951	818	4215	30 cm of snow on the ground. Ice in the gauge. Gauge partially emptied
16/05/2006 21:01	1000	0	4215	Emptying problematic as a result of ice in the gauge
17/05/2006 07:45	908	0	4215	After adding antifreeze
5/07/2006 18:30	27	881	5096	Gauge overfull
25/07/2006 08:30	1744	0	5096	160 cm of snow on the ground
10/08/2006 16:42	1520	224	5320	120 cm of snow on the ground
13/09/2006 16:20	756	764	6084	90 cm of snow, gauge emptied
13/09/2006 16:41	1710	0	6084	After emptying
17/10/2006 15:52	361	1349	7433	10-15 cm of snow on the ground, gauge emptied
17/10/2006 16:11	1784	0	7433	After emptying
30/11/2006 20:30	10	1774	9207	10-15 cm of new snow on the ground, gauge overfull, gauge emptied
30/11/2006 20:52	1790	0	9207	After emptying
16/01/2007 17:26	872	918	10125	Gauge emptied
16/01/2007 17:37	1688	0	10125	After emptying
27/02/2007 18:38	1200	488	10613	Gauge emptied
27/02/2007 16:45	1707	0	10613	After emptying
2/04/2007 20:24	864	843	11456	Gauge removed

Table A1-3. Manual measurements for Jollie precipitation gauge.

Date	Dist. from rim (mm)	Precip. since last time (mm)	Total (mm)	Notes
15/12/2005 18:20	2141	0	0	Gauge installed.
9/01/2006 09:50	2032	109	109	Clear sky.
9/01/2006 10:13	2025	0	109	Logger fitted. Change in level from previous reading is due to the sensor cable (and weight) being immersed in the water inside the gauge.
14/02/2006 12:07	1928	97	206	
18/03/2006 12:45	1894	34	240	Gauge emptied.
18/03/2006 12:57	2037	0	240	After emptying.
15/05/2006 12:18	1765	272	512	
15/05/2006 12:43	1683	0	512	After adding 2 l of antifreeze.
26/07/2006 11:43	1305	460	972	20 cm of snow on the ground, gauge emptied.
26/07/2006 12:00	2022	0	972	After emptying.
16/09/2006 12:07	1865	157	1129	No snow on the ground.
28/11/2006 11:33	1280	585	1714	Gauge emptied.
28/11/2006 11:39	1956	0	1714	After emptying.
2/03/2007 13:04	1696	260	1974	Gauge emptied.
2/03/2007 13:14	1873	0	1974	After emptying.
5/04/2007 13:53	1777	96	2070	Gauge removed.

Table A1-4. Manual measurements for Murchison precipitation gauge.

Date	Dist. from rim (mm)	Precip. since last time (mm)	Total (mm)	Notes
17/02/2006 12:00	2032	0	0	Gauge installed.
19/03/2006 12:04	1989	43	43	Gauge emptied
19/03/2006 00:00	2027	0	43	After emptying.
13/04/2006 12:39	1854	173	216	.
24/06/2006 11:30	1260	?	?	40-50 cm of snow on the ground, contents frozen.
24/06/2006 11:33	1145	0	810	After adding antifreeze
4/07/2006 13:00	1805			50-60 cm of snow on the ground, gauge leaking.
17/07/2006 10:46	2000			30 cm of snow on the ground. Leak repaired.
17/08/2006 09:37	1917	130	940	20 cm of snow on the ground
26/11/2006 11:43	951	966	1906	Gauge emptied.
26/11/2006 12:00	2000	0	1906	After emptying.
18/01/2007 08:32	1720	280	2186	Clear and calm
1/04/2007 14:00	1530	190	2376	Gauge removed.

Table A1-5. Manual measurements for Rudolf precipitation gauge.

Date	Dist. from rim (mm)	Precip. since last time (mm)	Total (mm)	Notes
15/02/2006 16:00	2005	0	0	Gauge installed
17/03/2006 09:45	2014		0	This measurement was taken after repairing a leak.
12/04/2006 09:36	1239	775	775	50 cm of snow around the gauge. Gauge emptied.
12/04/2006 10:27	1444	0	775	After emptying
16/05/2006 17:28	550	894	1669	35 cm of snow on the ground. A lot of ice in the gauge, gauge emptied.
16/05/2006 17:46	2020	0	1669	Still some ice in the gauge after emptying
6/07/2006 09:45	400	1620	3289	170 cm snow on the ground
18/10/2006 10:26	1979	0	3289	2 m of snow on the ground
1/12/2006 08:32	80	1899	5188	50 cm of snow on the ground, gauge overfull
1/12/2006 09:00	1935	0	5188	After emptying
17/01/2007 08:01	1710	225	5413	Gauge leaking
17/01/2007 08:36	1930	0	5413	After emptying.
28/02/2007 08:33	1385	545	5958	Gauge emptied.
28/02/2007 08:41	1651	0	5958	After emptying.
2/04/2007 17:30	814	837	6795	Gauge removed.

Table A1-6. Manual measurements for East Hooker precipitation gauge.

Date	Dist. from rim (mm)	Precip. since last time (mm)	Total (mm)	Notes
14/12/2005 12:15	2052	0	0	Gauge installed.
16/01/2006 15:28	909	1143	1143	Gauge emptied.
16/01/2006 16:06	1951	0	1143	After emptying.
9/02/2006 10:40	1838	113	1256	
15/03/2006 15:40	1139	699	1955	Gauge emptied.
15/03/2006 16:30	2023	0	1955	After emptying.
10/04/2006 12:00	1448	575	2530	10 cm of snow on the ground.
13/05/2006 16:45	938	510	3040	Gauge emptied.
13/05/2006 17:05	1811	0	3040	After emptying.
22/06/2006 13:32	700	1111	4151	80 cm of snow on the ground, gauge frozen.
22/06/2006 13:50	617	0	4151	After adding antifreeze.
16/07/2006 10:40	416	201	4352	90 cm of snow on the ground. Gauge emptied.
16/07/2006 11:17	1915	0	4352	After emptying.
16/08/2006 11:21	1550	365	4717	130 cm of snow on the ground.
16/08/2006 11:25	1415	0	4717	After adding antifreeze.
15/09/2006 10:40	358	1057	5774	1 m of snow on the ground. Gauge emptied.
15/09/2006 11:04	1888	0	5774	After emptying.
16/10/2006 15:19	522	1366	7140	5 cm of snow on the ground, gauge emptied.
16/10/2006 15:44	1886	0	7140	After emptying.
27/11/2006 15:25	160	1726	8866	Gauge emptied.
27/11/2006 15:36	1950	0	8866	After emptying.
12/01/2007 15:32	1006	944	9810	Gauge emptied.
12/01/2007 15:40	1950	0	9810	After emptying.
1/03/2007 11:44	1354	596	10406	Gauge emptied.
1/03/2007 11:57	1941	0	10406	After emptying.
4/04/2007 15:16	1252	689	11095	Gauge removed.

Table A1-7. Manual measurements for Mueller precipitation gauge.

Date	Dist. from rim (mm)	Precip. since last time (mm)	Total (mm)	Notes
14/12/2005 14:24	1971	0	0	Gauge installed.
17/01/2006 12:21	1099	872	872	.
13/02/2006 15:14	917	182	1054	Gauge emptied.
13/02/2006 15:36	1948	0	1054	After emptying
20/03/2006 10:18	1328	620	1674	Gauge emptied.
20/03/2006 11:15	1980	0	1674	After emptying
14/04/2006 10:45	1532	448	2122	5-10 cm of snow on the ground.
18/05/2006 11:51	2175	?		10-20 cm of snow on the ground. Gauge leaking.
18/05/2006 12:26	1951	0	2122	After repairing leak.
15/07/2006 12:35	835	1116	3238	90 cm of snow on the ground. Gauge emptied.
15/07/2006 13:23	1941	0	3238	After emptying.
15/08/2006 13:06	1710	231	3469	140 cm of snow on the ground. Gauge emptied.
15/08/2006 13:12	1545	0	3469	After emptying.
17/09/2006 09:38	1021	524	3993	70 cm of snow on the ground. Gauge emptied.
17/09/2006 09:55	1770	0	3993	After emptying.
20/10/2006 08:30	896	874	4867	No snow. Gauge emptied.
20/10/2006 08:41	1896	0	4867	After emptying.
27/11/2006 07:50	88	>1808	6675	Gauge overfull. Gauge emptied.
27/11/2006 08:07	1975	0	6675	After emptying.
15/01/2007 15:40	1020	955	7630	Gauge emptied.
15/01/2007 15:47	1910	0	7630	After emptying.
26/02/2007 15:38	1526	384	8014	Gauge emptied.
26/02/2007 15:48	1850	0	8014	After emptying.
4/04/2007 08:15	1220	630	8644	Gauge removed.

Table A1-8. Manual measurements for Stocking precipitation gauge.

Date	Dist. from rim (mm)	Precip. since last time (mm)	Total (mm)	Notes
13/12/2005 15:40	1975	0	0	Gauge installed
10/01/2006 11:17	1426	549	549	
17/01/2006 16:37	1288	138	687	
15/02/2006 00:00	1188	100	787	
20/03/2006 15:32	885	303	1090	Gauge emptied.
20/03/2006 16:09	2002	0	1090	After emptying.
10/04/2006 16:00	1660	342	1432	
17/05/2006 19:14	1317	343	1775	3 cm of snow on the ground.
19/06/2006 14:49	652	665	2440	20-30 cm of snow on the ground. Gauge emptied.
19/06/2006 15:04	1968	0	2448	Ice around the inside of the gauge, but liquid down the centre.
16/07/2006 14:56	1774	194	2634	10 cm of snow on the ground, contents liquid
16/08/2006 14:45	1595	179	2813	Less than 5 cm of patchy snow on the ground.
14/09/2006 17:05	1279	316	3129	No snow on the ground.
19/10/2006 09:44	515	764	3893	Gauge emptied.
19/10/2006 10:00	1750	0	3893	After emptying.
25/11/2006 12:10	794	956	4849	Gauge emptied.
25/11/2006 12:30	1930	0	4849	After emptying.
14/01/2007 08:22	1230	700	5549	Gauge emptied.
14/01/2007 08:30	1788	0	5549	After emptying.
1/03/2007 15:53	1580	208	5757	Gauge emptied.
1/03/2007 16:00	1888	0	5757	After emptying.
31/03/2007 14:40	1509	379	6136	Gauge removed.

Table A1-9. Manual measurements for Aoraki precipitation gauge.

Date	Dist. from rim (mm)	Precip. since last time (mm)	Total (mm)	Notes
18/01/2006 11:51	2100	0	0	Gauge installed.
17/02/2006 16:31	2040	60	60	
20/03/2006 17:33	1812	228	288	Gauge emptied.
20/03/2006 17:38	2028	0	288	After emptying
10/04/2006 17:30	1798	230	518	
18/05/2006 16:21	1545	253	771	
19/06/2006 16:50	1070	?	?	20 cm of snow on the ground. Snow in the gauge.
3/07/2006 11:07	1085	460	1231	Gauge emptied.
3/07/2006 11:12	1986	0	1231	After emptying
17/07/2006 14:39	1868	118	1349	
17/08/2006 12:48	1750	118	1467	
15/09/2006 15:31	1546	204	1671	
20/10/2006 12:24	1026	520	2191	Gauge emptied.
20/10/2006 12:29	2008	0	2191	After emptying
1/12/2006 19:50	1122	886	3077	Gauge emptied.
1/12/2006 19:55	1828	0	3077	After emptying
18/01/2007 15:00	1544	284	3361	Gauge emptied.
18/01/2007 15:05	1931	0	3361	After emptying
1/03/2007 17:17	1774	157	3518	Gauge emptied.
1/03/2007 17:22	1663	0	3518	After emptying
3/04/2007 16:48	1391	272	3790	Gauge removed.

Table A1-10. Manual measurements for Tasman precipitation gauge.

Date	Dist. from rim (mm)	Precip. since last time (mm)	Total (mm)	Notes
16/02/2006 10:03	1982	0	0	Gauge installed.
17/03/2006 12:59	1800	?	0	Gauge on a severe angle. Gauge emptied and straightened.
17/03/2006 13:44	2044	0	0	After emptying and straightening.
11/04/2006 15:45	1548	496	496	5-10 cm of snow on the ground.
17/05/2006 10:00	1026	522	1018	Ice in gauge. Gauge emptied.
17/05/2006 10:30	2015	0	1018	After emptying.
5/07/2006 10:15	2050	?	1018	Gauge leaking.
25/07/2006 11:47	1933	?	1485	50 cm of snow on the ground. Leak repaired.
10/08/2006 11:16	1844	89	1574	40 cm of snow on the ground.
13/09/2006 13:09	1615	229	1803	25 cm of snow on the ground.
17/10/2006 13:32	1140	475	2278	No snow. Gauge emptied.
17/10/2006 13:52	1934	0	2278	After emptying,
1/12/2006 13:00	2050	0	2278	Gauge fallen over, logger not working, 10 cm of new snow on the ground. After straightening.
16/01/2007 14:44	1468	582	2860	Gauge emptied.
16/01/2007 15:07	1905	0	2860	After emptying.
27/02/2007 16:05	1595	310	3170	Gauge emptied.
27/02/2007 16:11	1875	0	3170	After emptying.
2/04/2007 17:17	1392	483	3653	Gauge removed.

A2. Appendix 2: Daily precipitation regressions

This appendix contains three tables of the numbers of days used for the regression analysis between the logs of the precipitation at gauge sites and reference sites. There is one table for each reference site.

Following these tables, scatter plots of the log of daily precipitation (+ 1 mm) at each site (y axis) and each reference site (x axis) for the five different wind classes are provided. In each case the x and y axis have been offset by 1, with the trend line optimised to pass through the origin. Figure captions indicate the station pairs. Each plot provides the equation of the trend line and the wind-class direction.

List of tables in this appendix

List of figures in this appendix

Table A2-1. Number of days of regression between gauge sites and observations taken at Aoraki.Mt Cook Village. Missing values indicate less than 5 observations.

Site	Map index	NW	N	E	SSW	SW
Malte Brun Hut	2	83	19	21	19	31
Rose Ridge	3	154	31	43	38	62
Ball Hut	4	292	47	55	42	57
Hooker Hut	5	147	14	26	31	46
Mt Cook-ECAN to Hermitage	13	732	125	173	155	172
Mt Cook-ECAN to EWS	13	523	88	133	131	174
Hooker Rd. Bridge	14	489	83	116	105	152
Hooker Flat	15	425	69	68	81	122
Sealey Village	25	132	17	21	27	42
Jollie Hut	34	1489	230	406	298	284
Glentanner	36	127	24	16	23	35
The Rest	37	413	72	65	70	91
Braemar Station	39	1784	274	427	324	361
Guide Hill	40	1283	205	305	188	196
Tasman Downs	41	1139	190	308	205	203
Lake Pukaki No. 1	42	627	97	142	104	146
Lake Pukaki MWD	43	626	105	163	93	129
Ball Shelter	K4	37	6	7		7
De La Beche	K3	28				10
Jollie Stream	K9	24	9	9	5	
Murchison	K5	36	10	7		7
Rudolf Glacier	K2	17				5
East Hooker	K6	26	5	5		5
Mueller Glacier	K8	24		6		7
Stocking Stream	K7	27	5			8
Tasman Glacier	K1	14	6	5		5

Table A2-2. Number of days of regression between gauge sites and observations taken at Tekapo. Missing values indicate less than 5 observations.

Site	Map index	NW	N	E	SSW	SW
Malte Brun Hut	2	40	12	18	0	9
Rose Ridge	3	61	16	23	10	14
Ball Hut Gauge	4	142	25	33	17	17
Hooker Hut	5	69	6	15	8	18
Mt Cook-ECAN to Tekapo AS	13	677	122	171	123	97
Mt Cook-ECAN to Tekapo EWS	13	146	29	49	31	33
Mt Cook EWS to Tekapo EWS	13	101	18	42	71	35
Hermitage to Tekapo AS	12	1831	286	504	319	326
Hooker Rd. Bridge	14	534	94	131	96	74
Hooker Flat	15	231	36	47	29	51
Sealey Village	25	86	7	12	11	20
Jollie Hut	34	1929	891	158	276	170
Glentanner	36	86	17	13	8	16
The Rest	37	286	46	62	37	52
Braemar Station	39	1392	214	370	224	212
Guide Hill	40	829	151	256	135	119
Tasman Downs	41	842	150	245	149	122
Lake Pukaki No. 1	42	522	72	142	73	107
Lake Pukaki MWD	43	518	82	135	68	97
Ball Shelter	K4	20				
De La Beche	K3	13				
Jollie Stream	K9	18	7	5		
Murchison	K5	23	6			
Rudolf Glacier	K2	9				
East Hooker	K6	12				
Mueller Glacier	K8	12		5		
Stocking Stream	K7	10				
Tasman Glacier	K1	9				

Table A2-3. No. of days of regression between gauge sites and observations taken at Franz Josef. Missing values indicate less than 5 observations.

Site	Map index	NW	N	E	SSW	SW
Malte Brun Hut	2	105	23	18	28	38
Rose Ridge	3	133	28	16	28	57
Ball Hut Gauge	4	306	49	32	42	67
Hooker Hut	5	170	19	18	33	58
Mt Cook ECAN	13	298	55	37	123	115
Hermitage to Franz Josef Manual	13	1347	252	222	302	366
Hermitage to Franz Josef THC	12	2141	312	235	402	614
Hooker Rd. Bridge	14	275	49	33	49	115
Hooker Flat	15	442	73	44	39	103
Sealey Village	25	135	15	16	71	134
Jollie Hut	34	1247	921	162	23	41
Glentanner	36	129	27	11	151	200
The Rest	37	438	71	42	21	30
Braemar Station	39	1066	150	119	65	92
Guide Hill	40	510	55	44	172	252
Tasman Downs	41	384	44	37	44	82
Lake Pukaki No. 1	42	657	103	81	40	68
Lake Pukaki MWD	43	570	93	84	110	159
Ball Shelter	K4	39	7		70	117
De La Beche	K3	33				7
Jollie Stream	K9	24	10	6		10
Murchison	K5	38	12	6	5	
Rudolf Glacier	K2	19				9
East Hooker	K6	28	6			5
Mueller Glacier	K8	25	5			5
Stocking Stream	K7	29	5			7
Tasman Glacier	K1	17	6			9

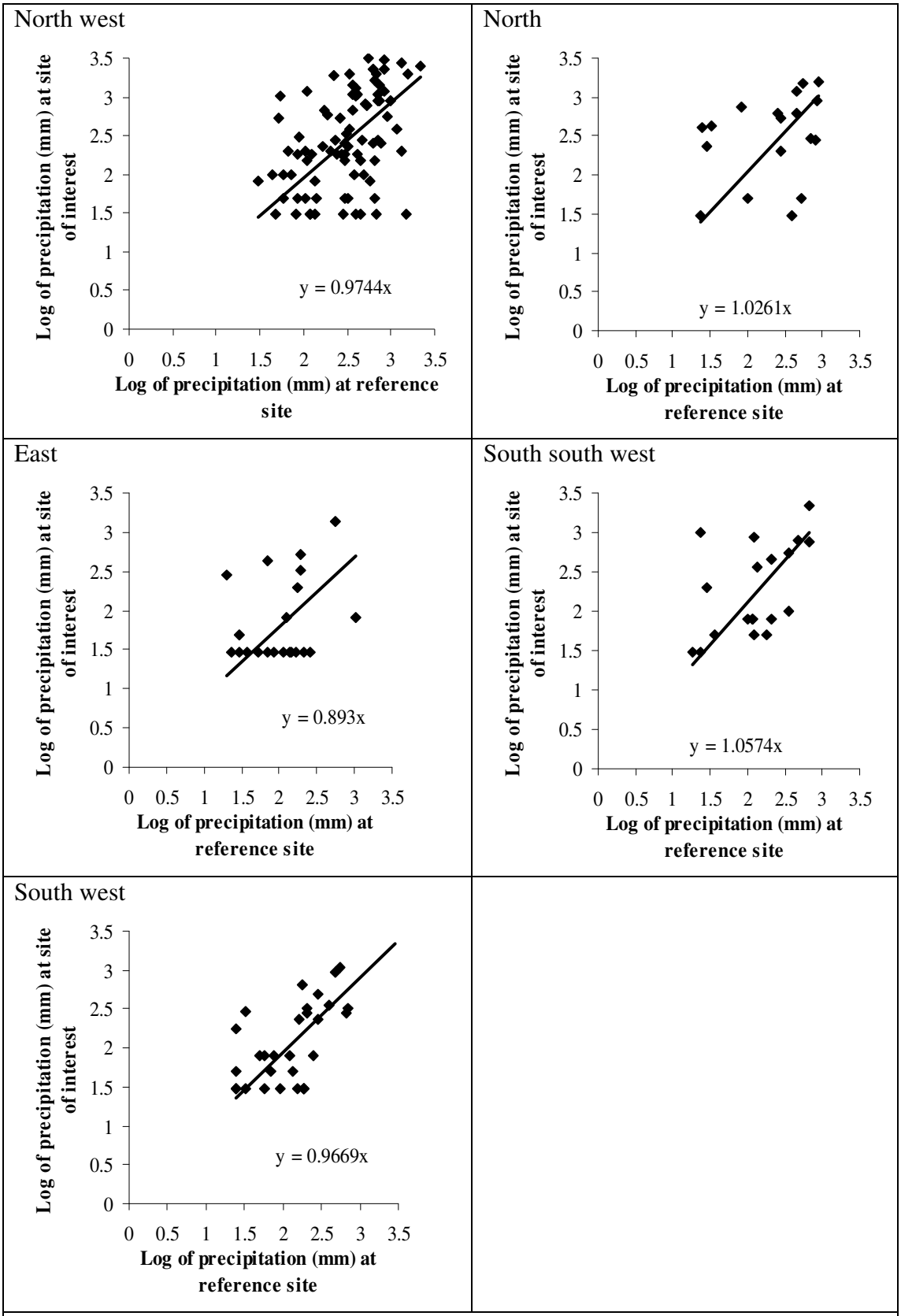

Figure A2-1. Malte Brun Hut (y axis) against The Hermitage (x axis) for different wind classes.

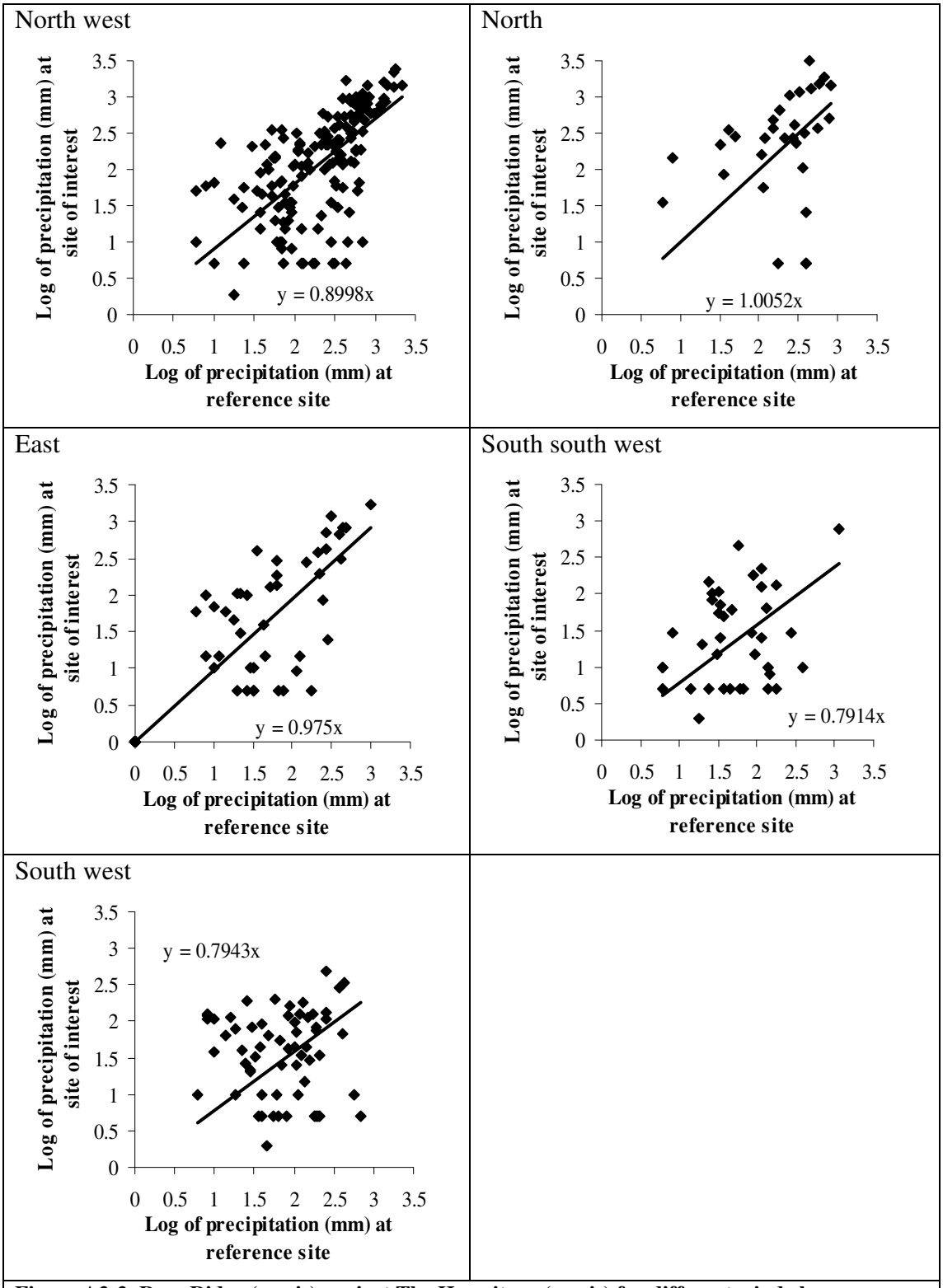

Figure A2-2. Rose Ridge (y axis) against The Hermitage (x axis) for different wind classes.

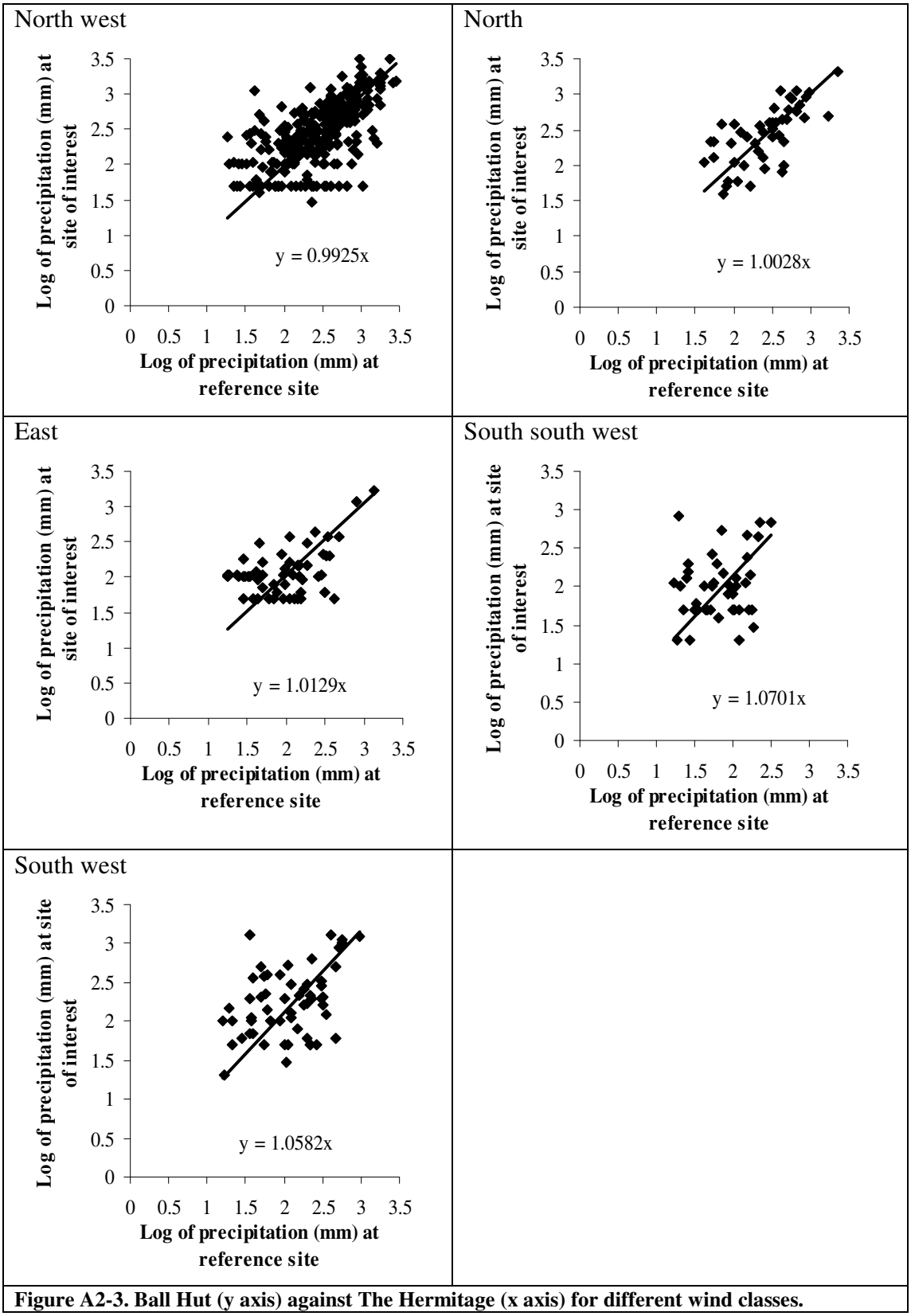

Figure A2-3. Ball Hut (y axis) against The Hermitage (x axis) for different wind classes.

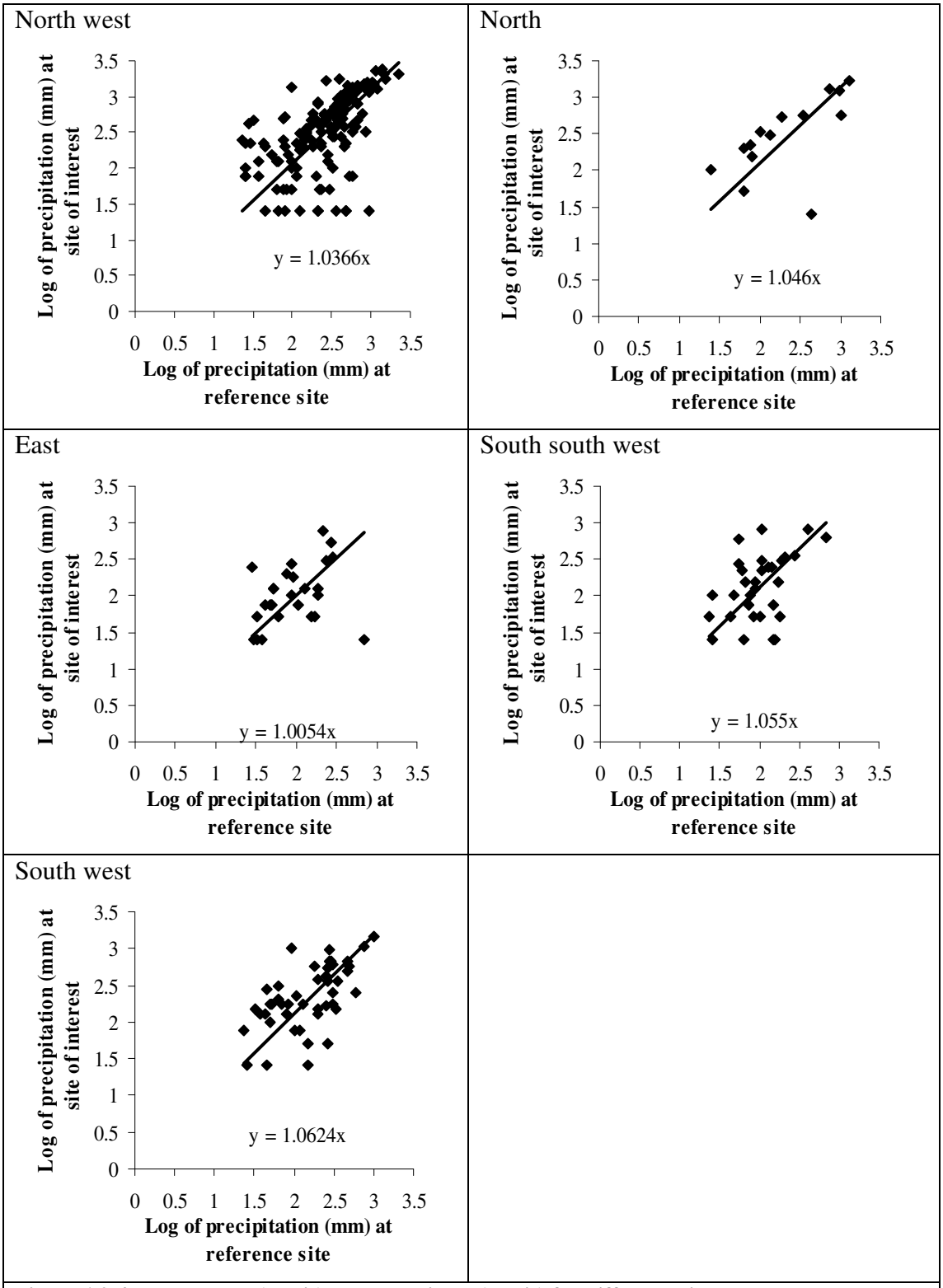

Figure A2-4. Hooker Hut (y axis) The Hermitage (x axis) for different wind classes.

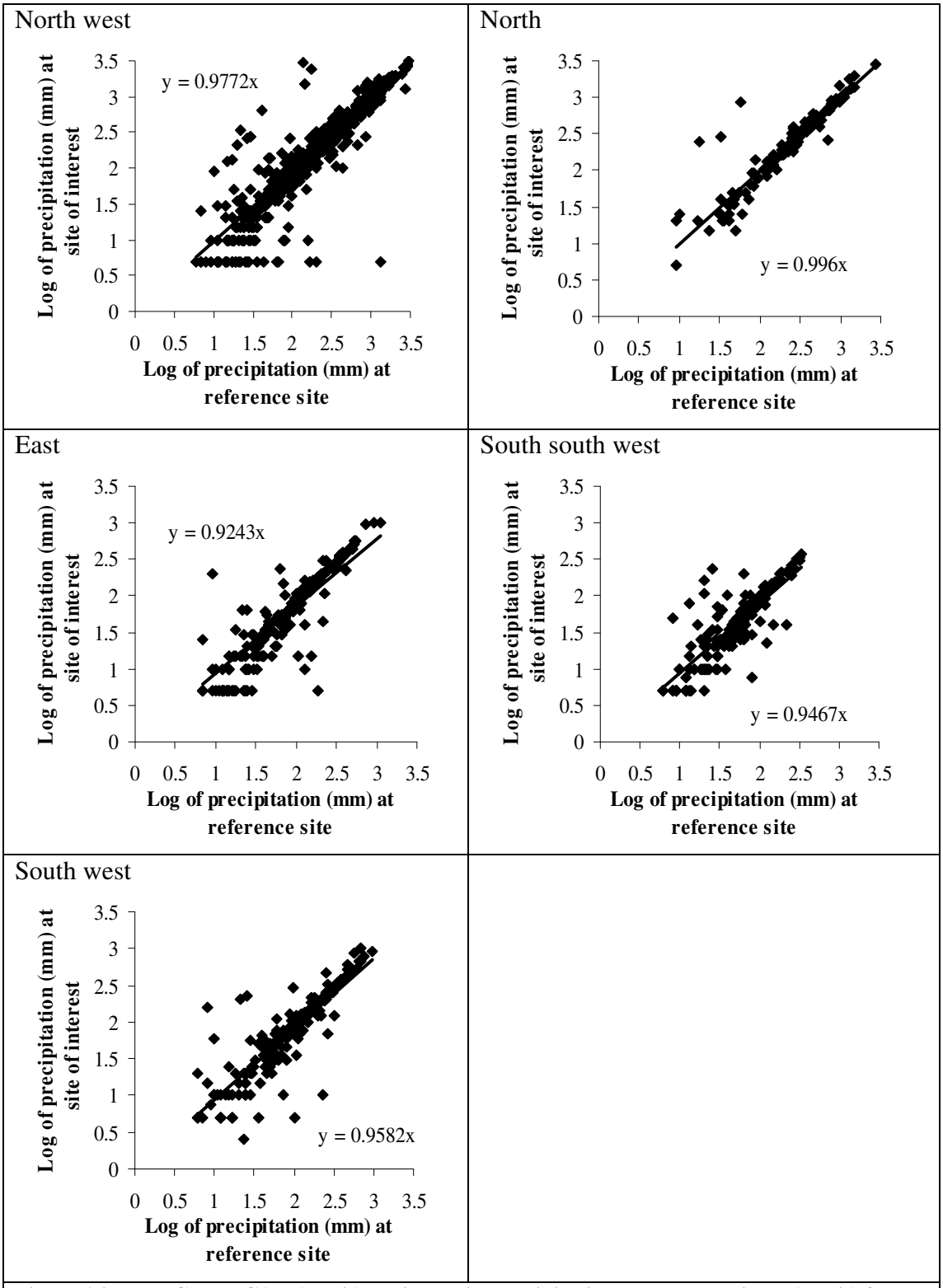

Figure A2-5. Mt Cook ECAN (y axis) against daily precipitation at The Hermitage (x axis) for different wind classes.

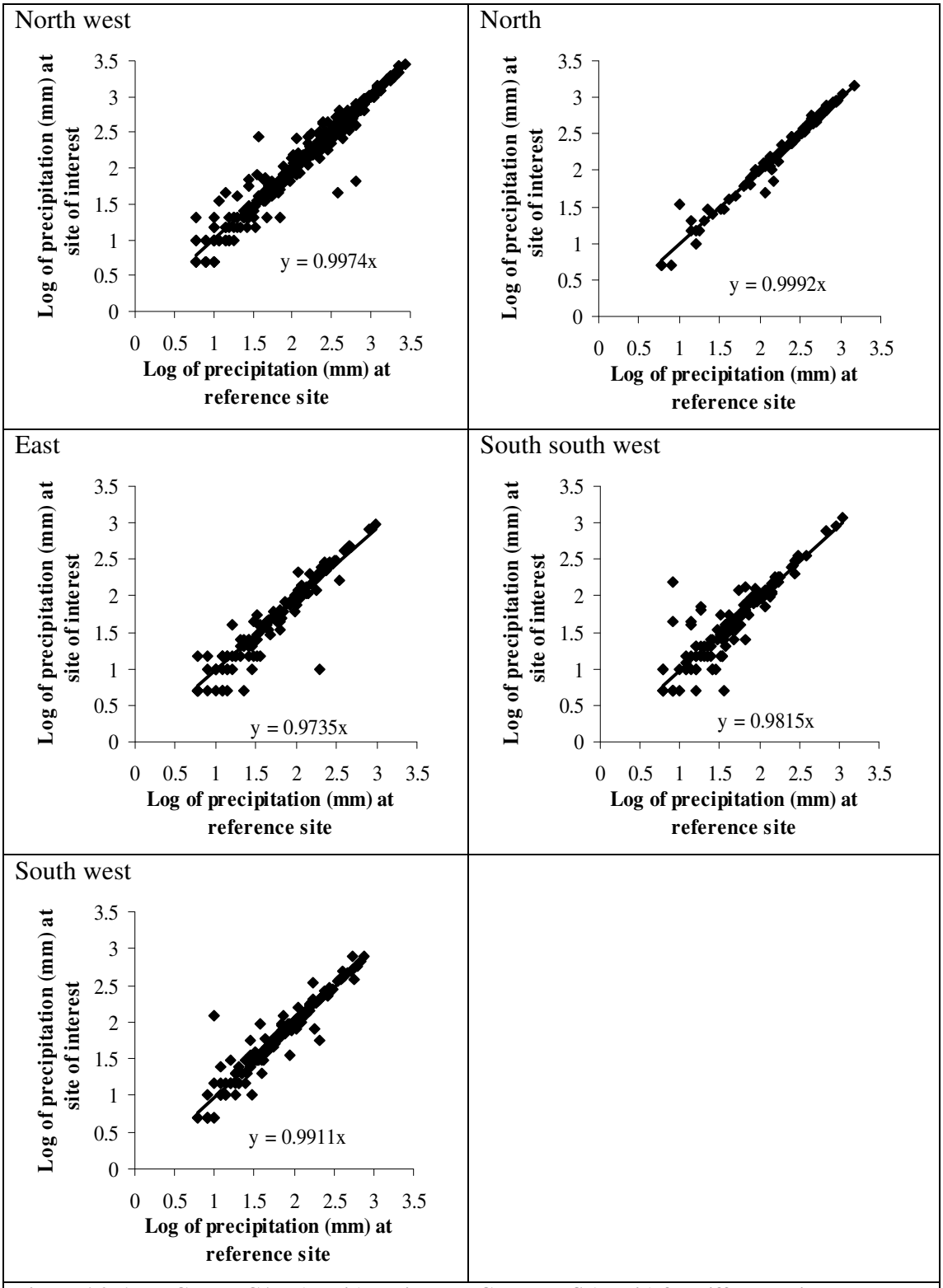

Figure A2-6. Mt Cook-ECAN (y axis) against Mt Cook-EWS (x axis) for different wind classes.

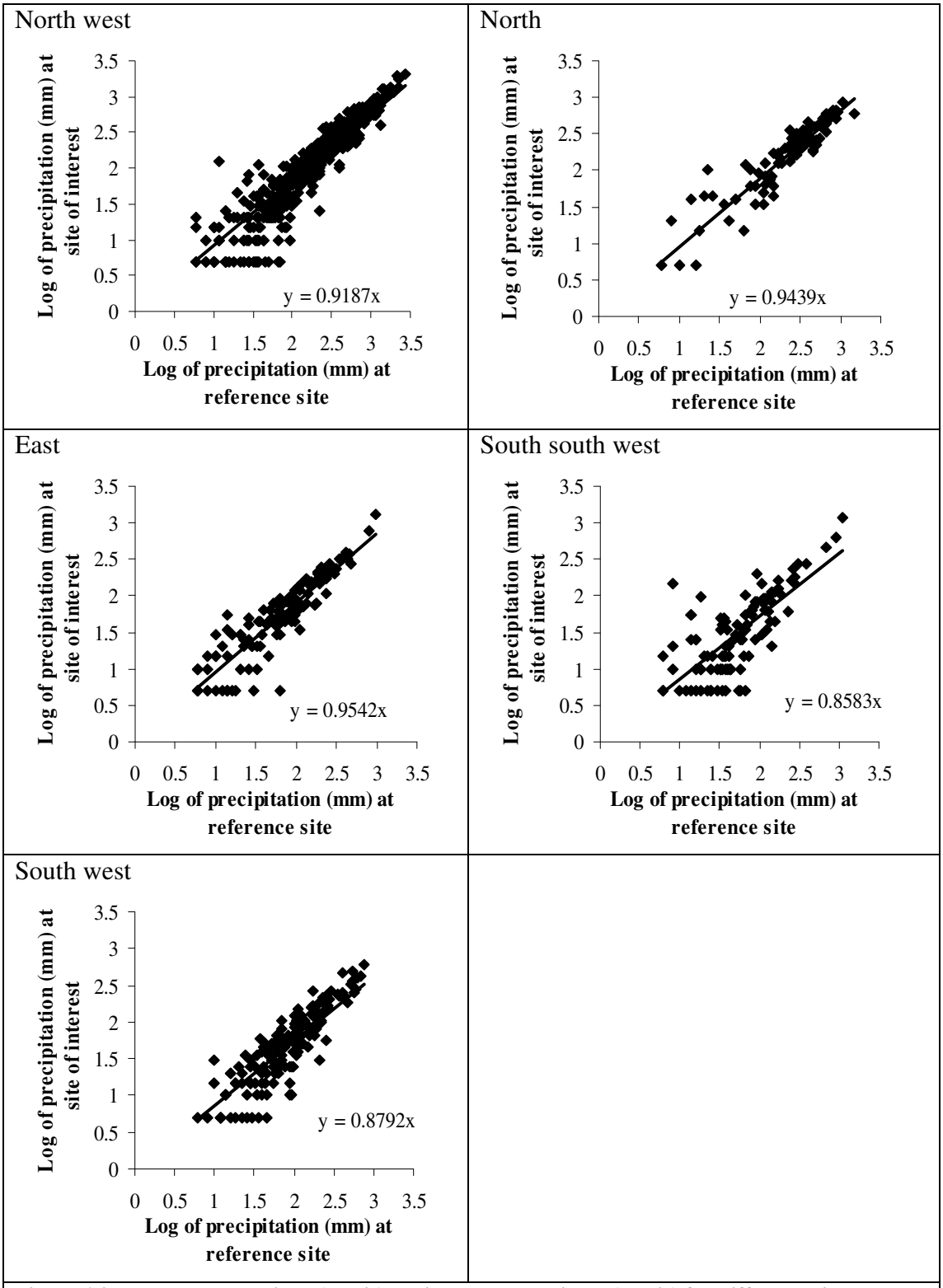

Figure A2-7. Hooker Rd Bridge (y axis) against The Hermitage (x axis) for different wind classes.

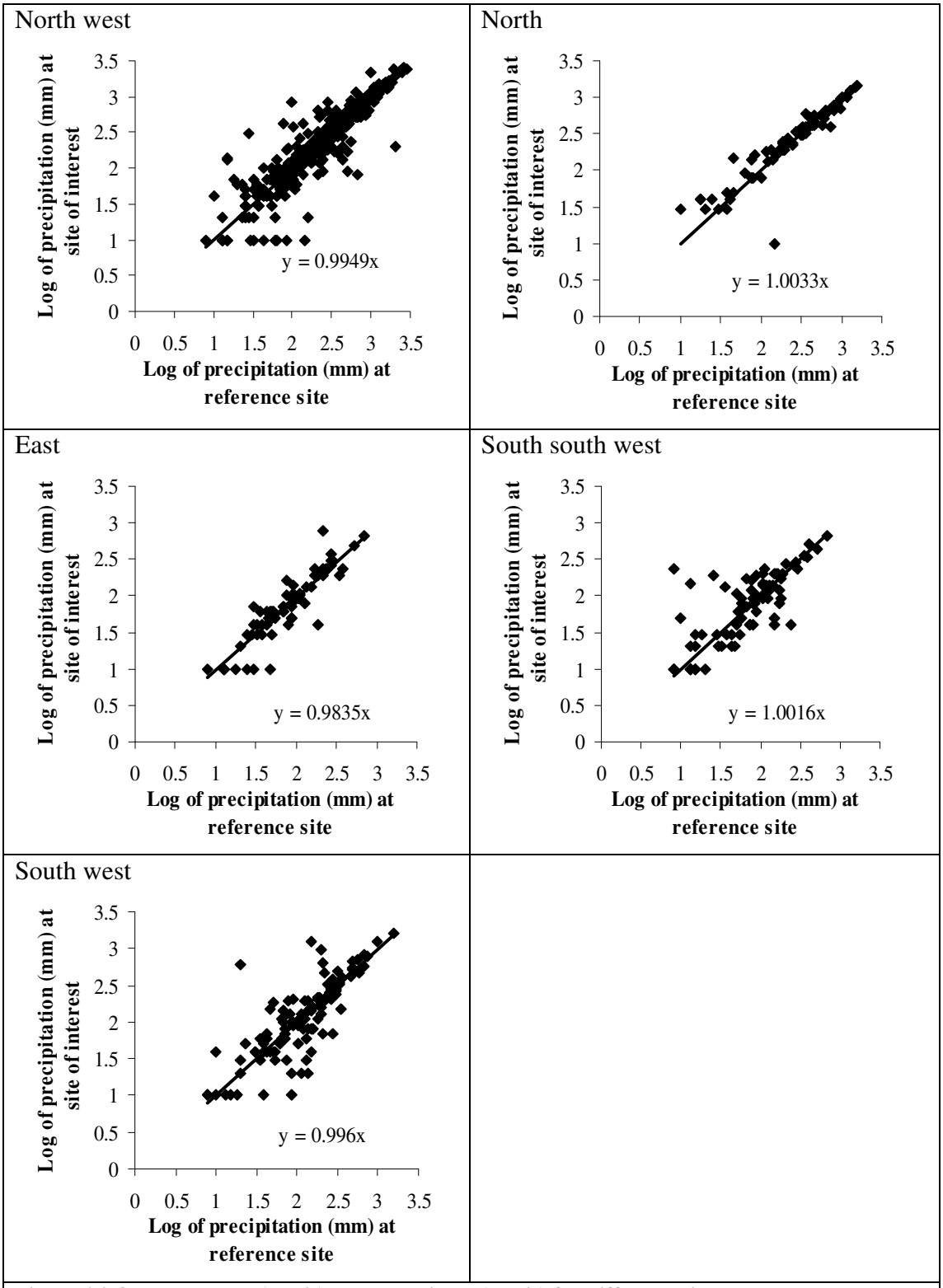

Figure A2-8. Hooker Flat (y axis) The Hermitage (x axis) for different wind classes.

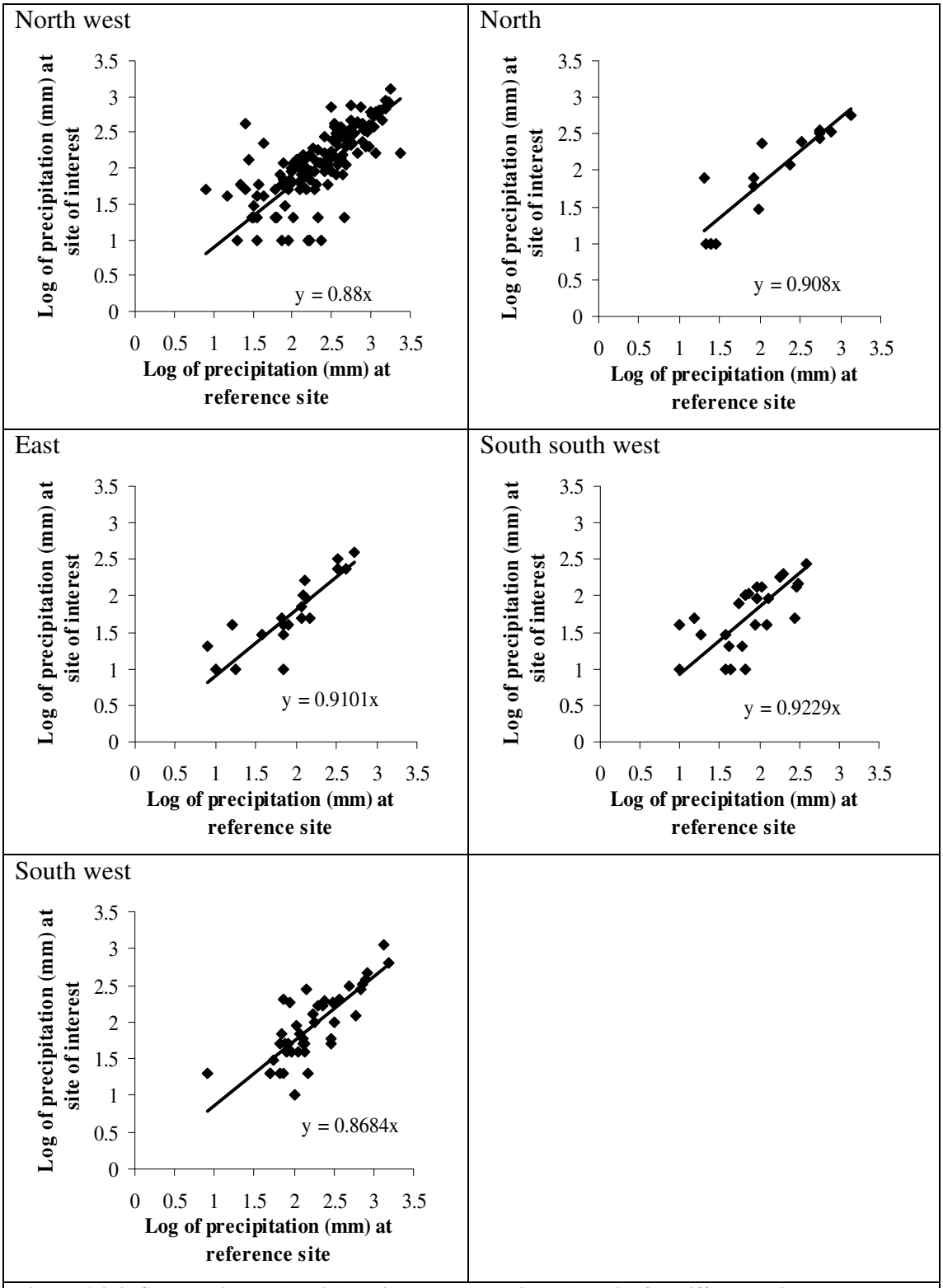

Figure A2-9. Sealey Village (y axis) against The Hermitage (x axis) for different wind classes.

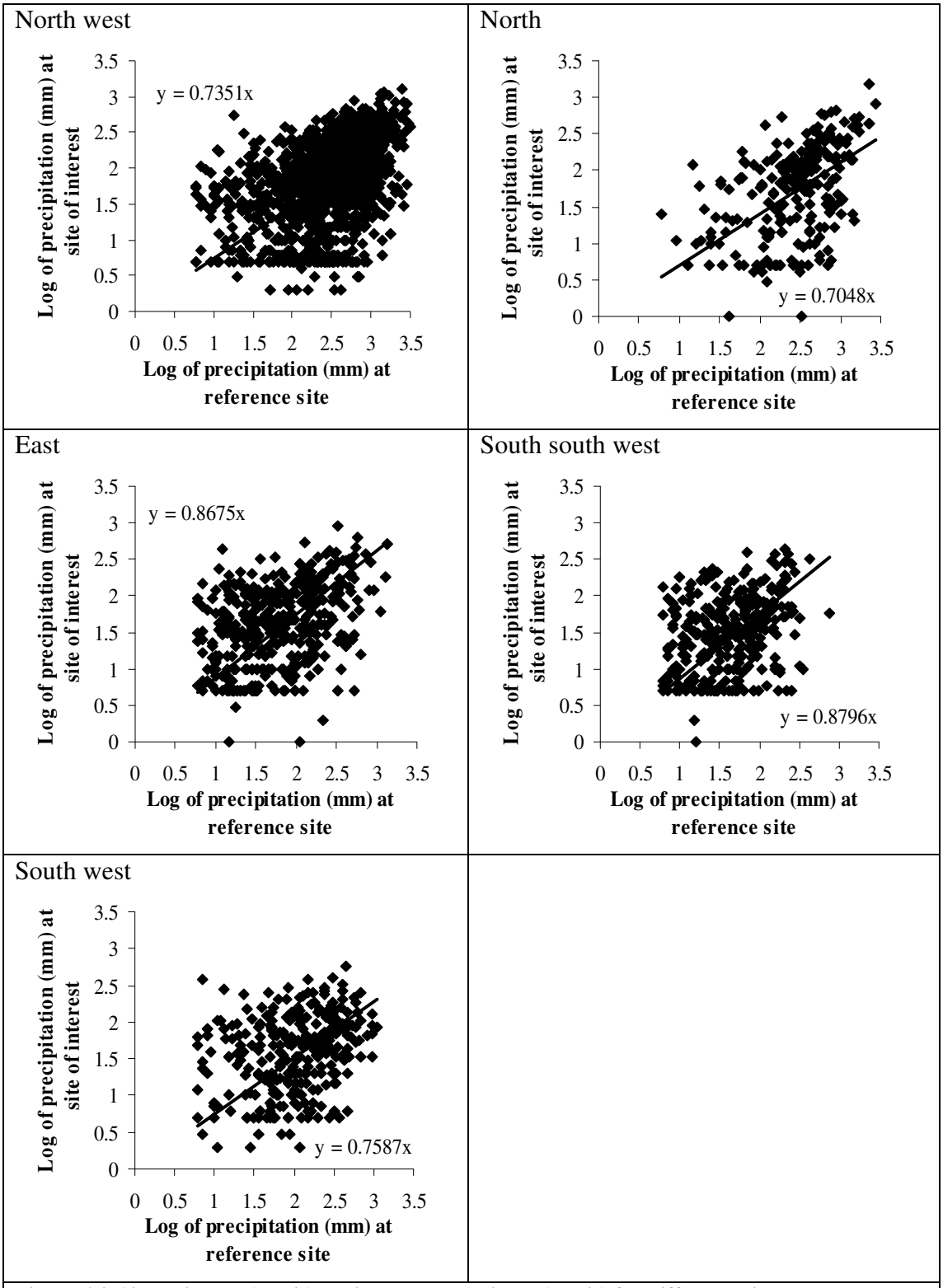

Figure A2-10. Jollie Hut (y axis) against The Hermitage (x axis) for different wind classes.

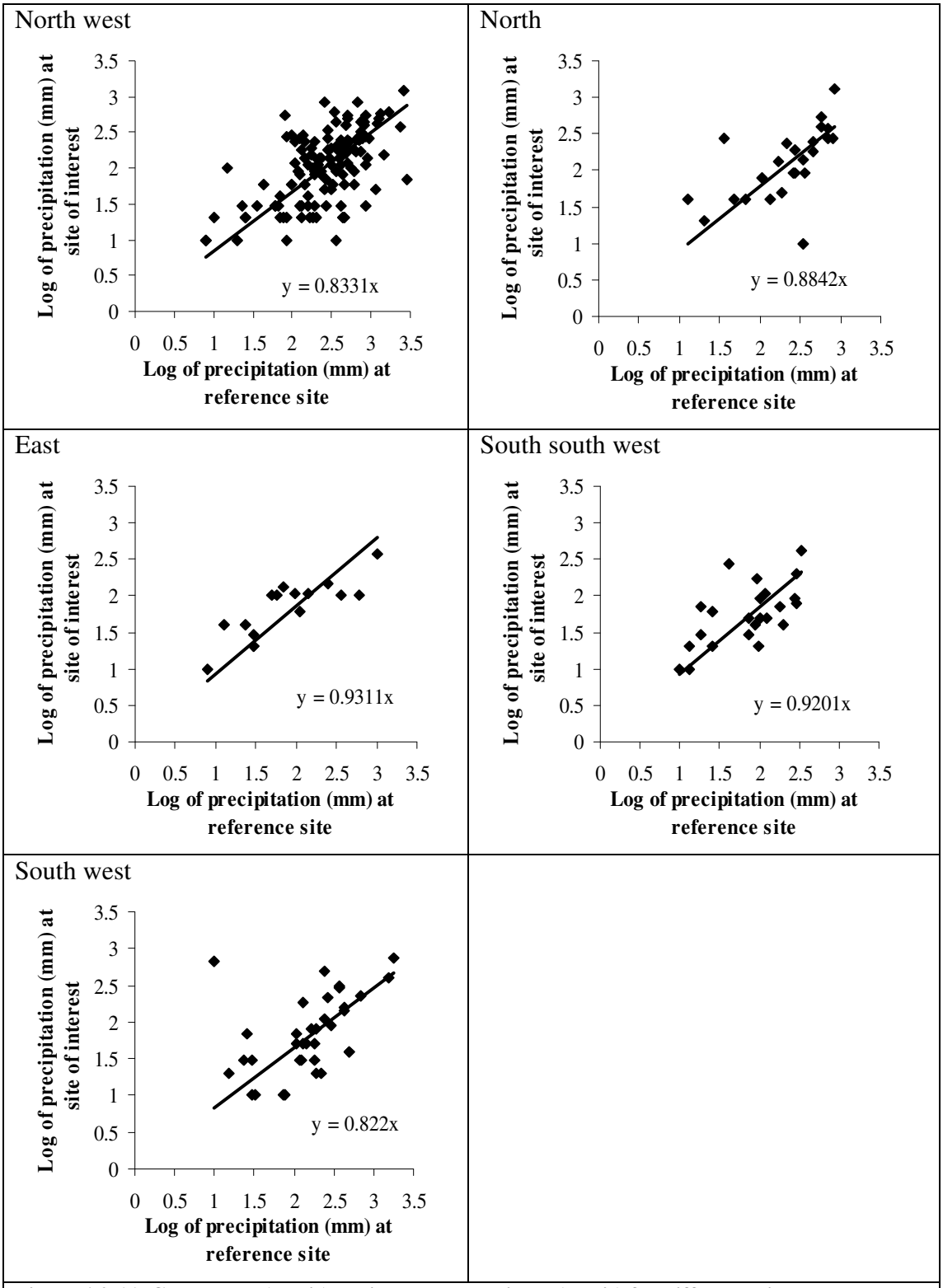

Figure A2-11. Glentanner (y axis) against The Hermitage (x axis) for different wind classes.

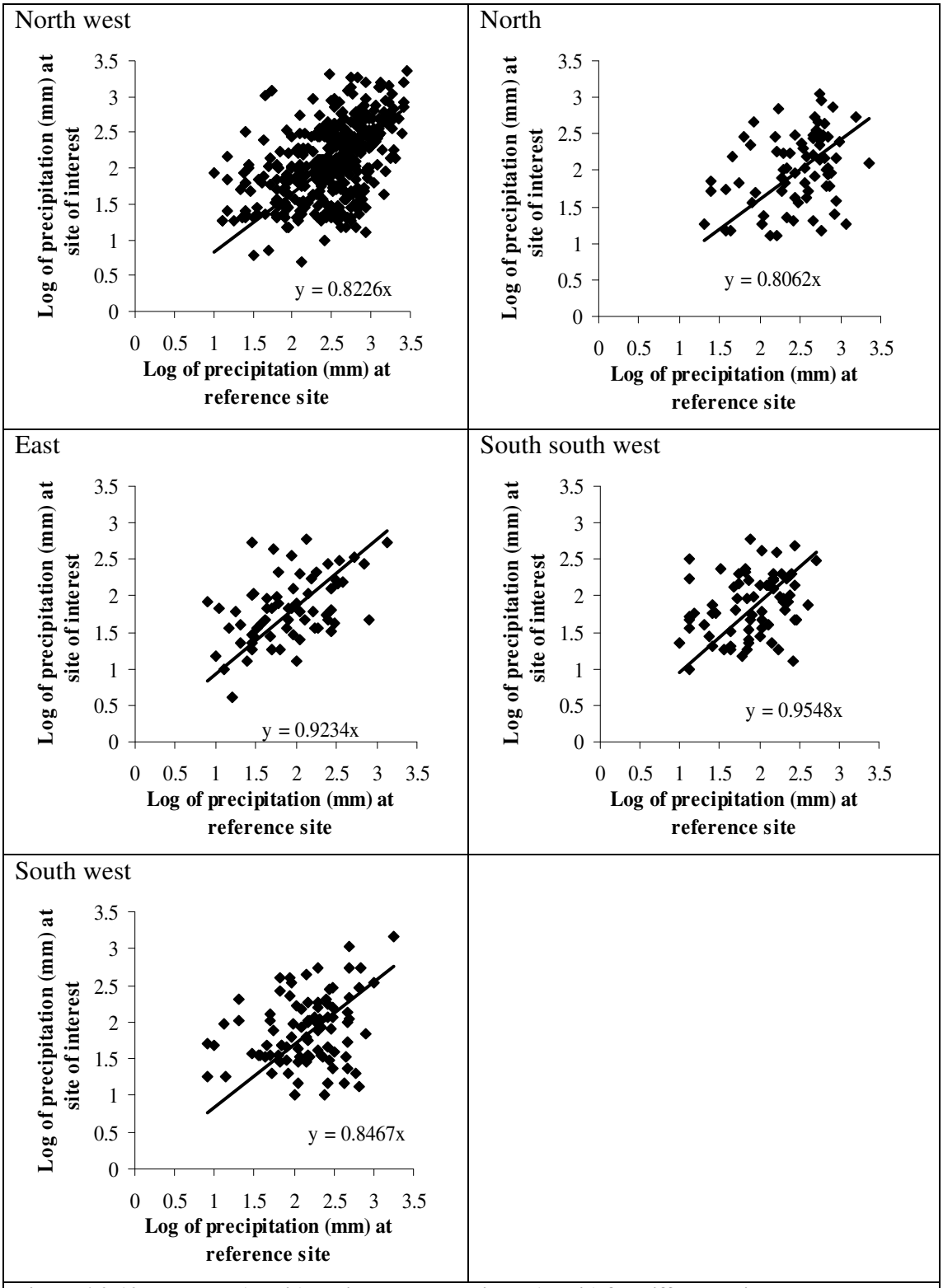

Figure A2-12. The Rest (y axis) against The Hermitage (x axis) for different wind classes.

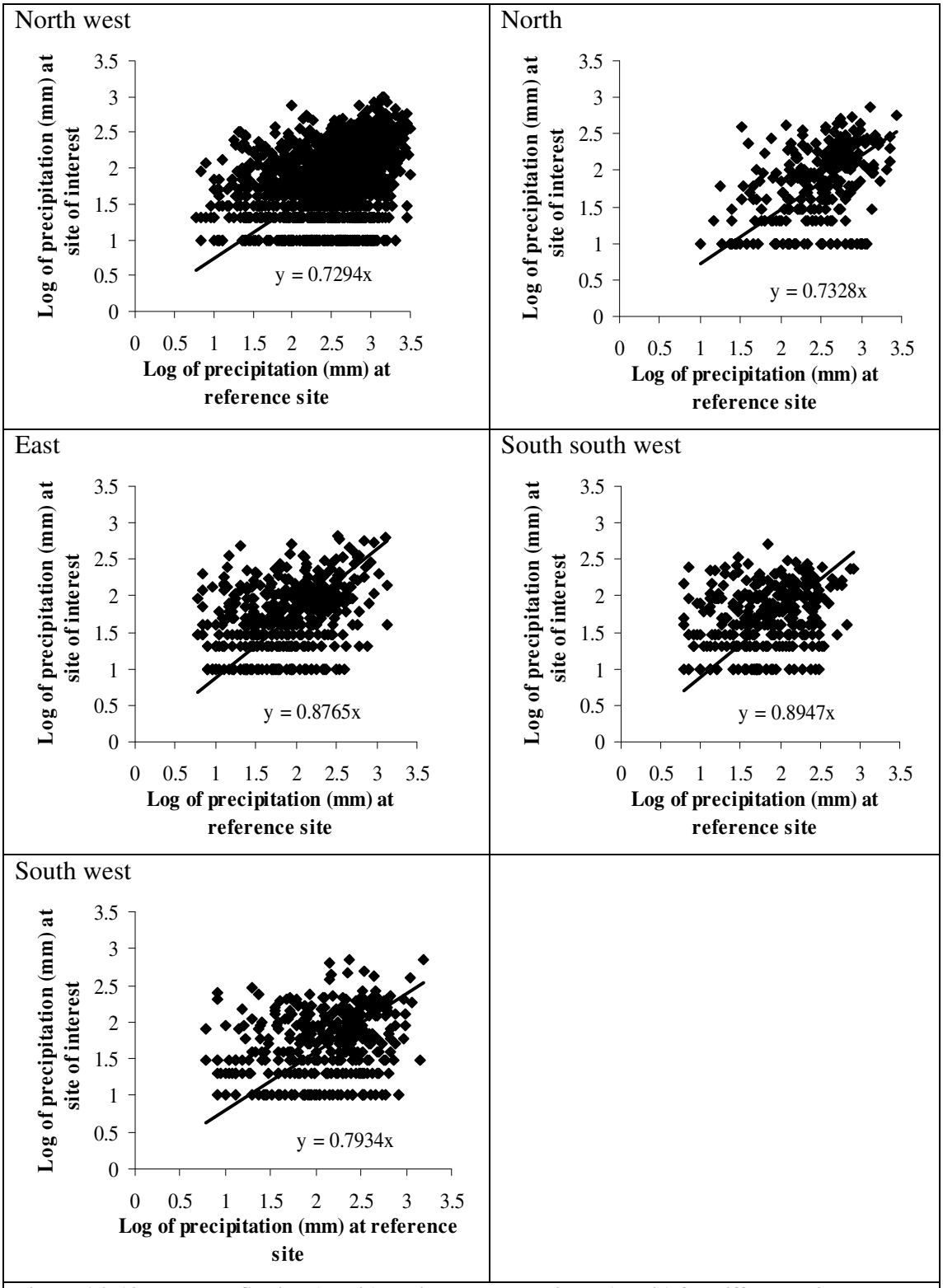

Figure A2-13. Braemar Station (y axis) against The Hermitage (x axis) for different wind classes.

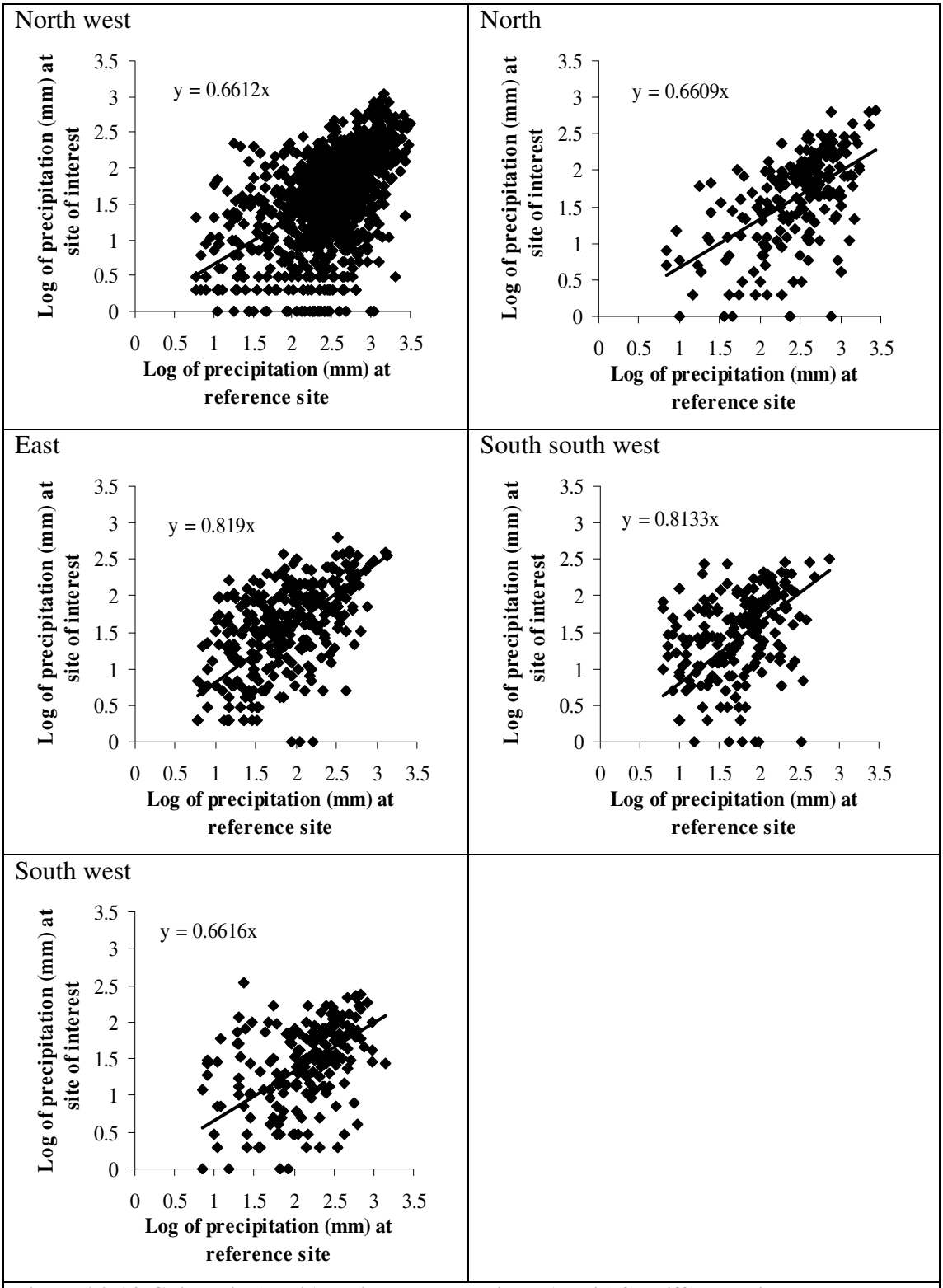

Figure A2-14. Guide Hill (y axis) against The Hermitage (x axis) for different wind classes.

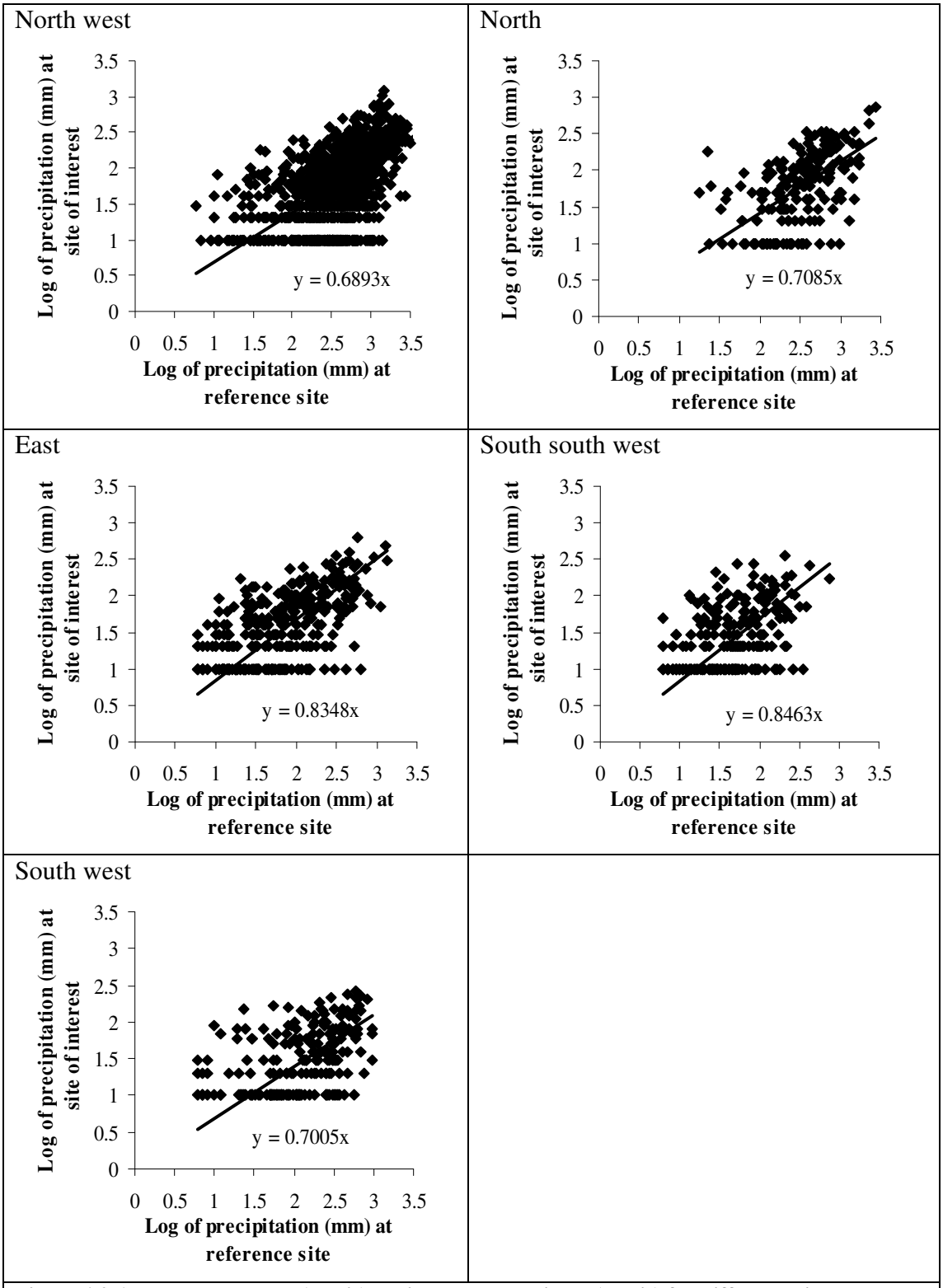

Figure A2-15. Tasman Downs (y axis) against The Hermitage (x axis) for different wind classes.

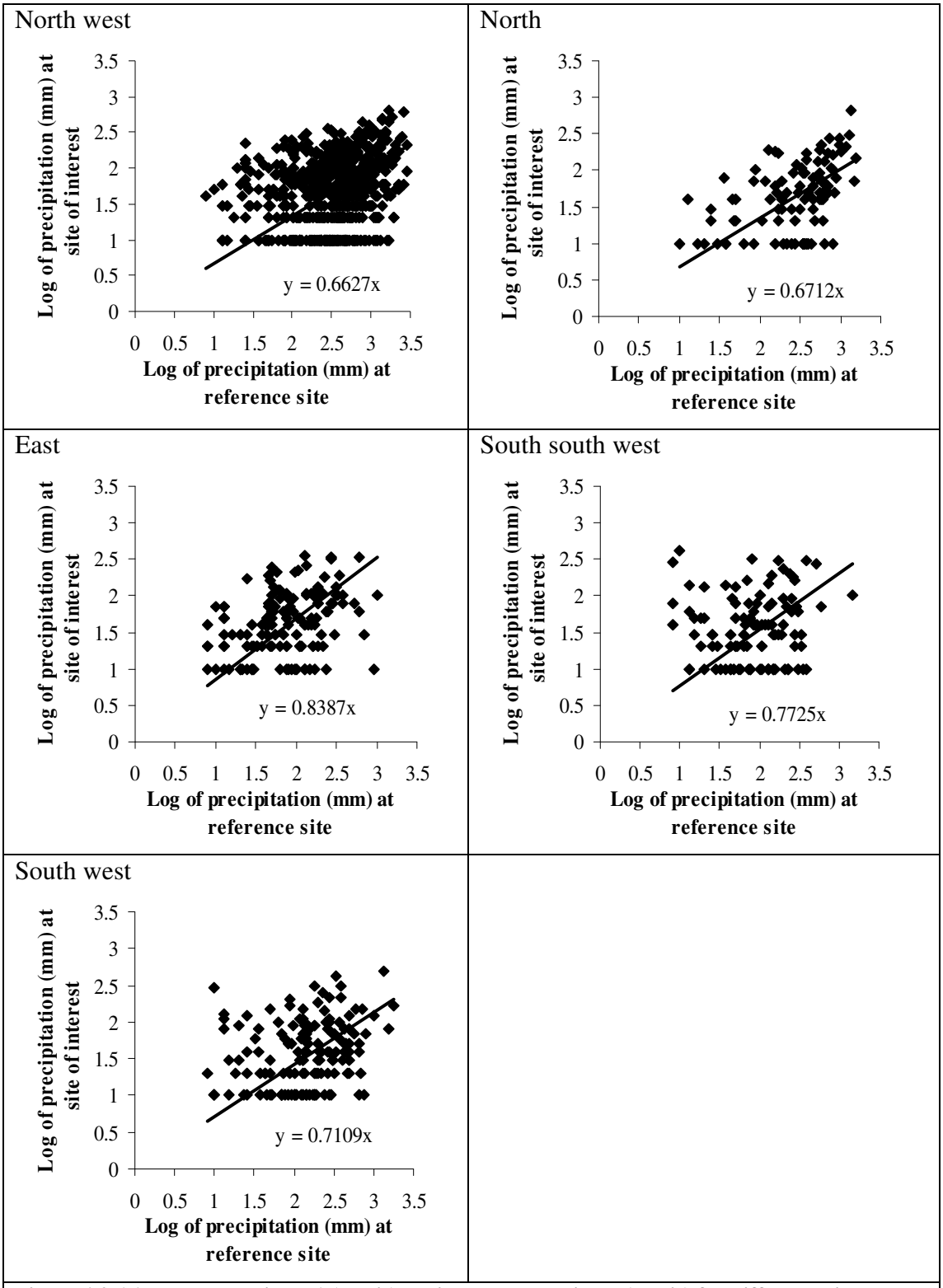

Figure A2-16. Lake Pukaki No. 1 (y axis) against The Hermitage (x axis) for different wind classes.

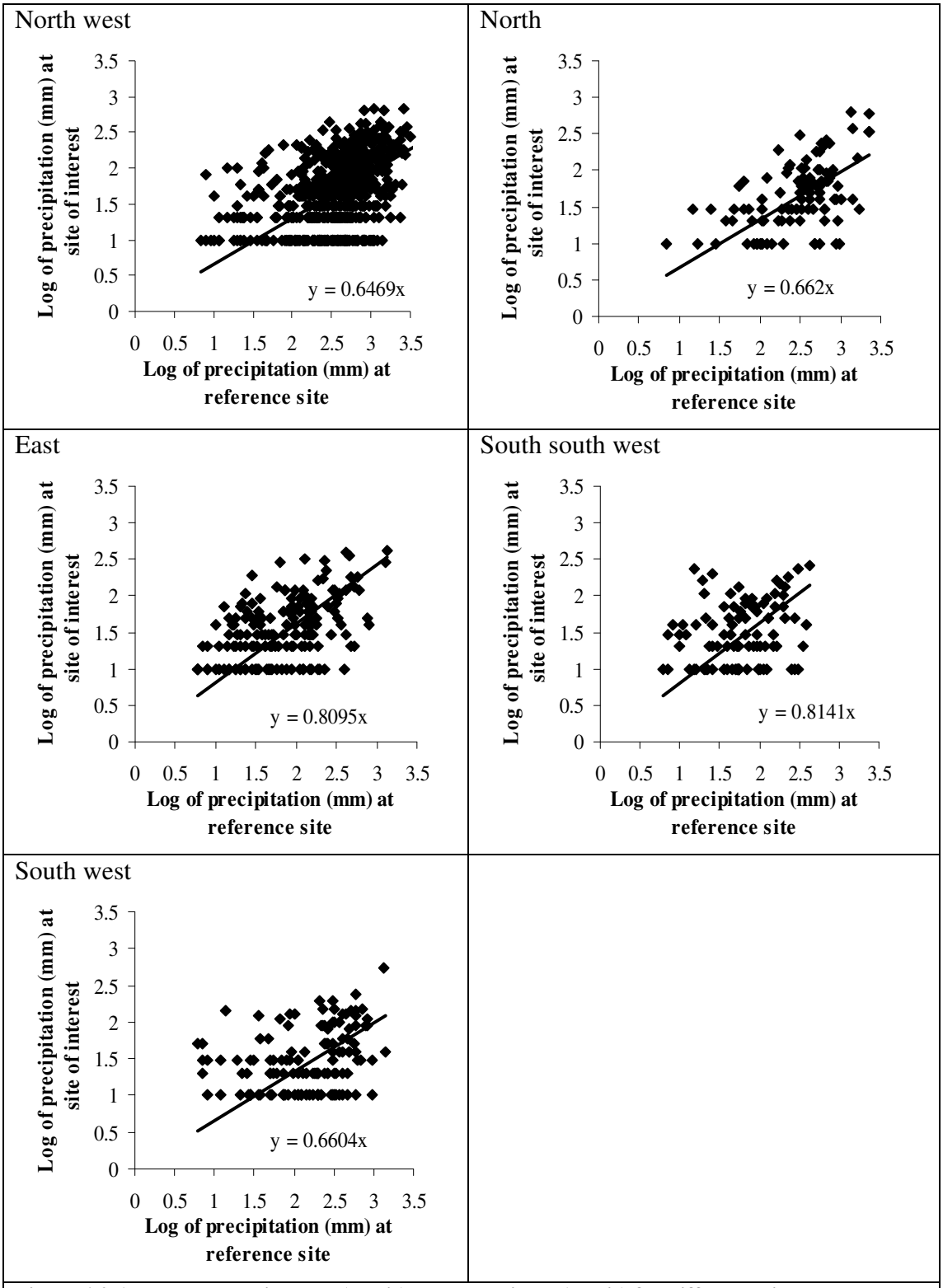

Figure A2-17. Lake Pukaki MWD (y axis) The Hermitage (x axis) for different wind classes.

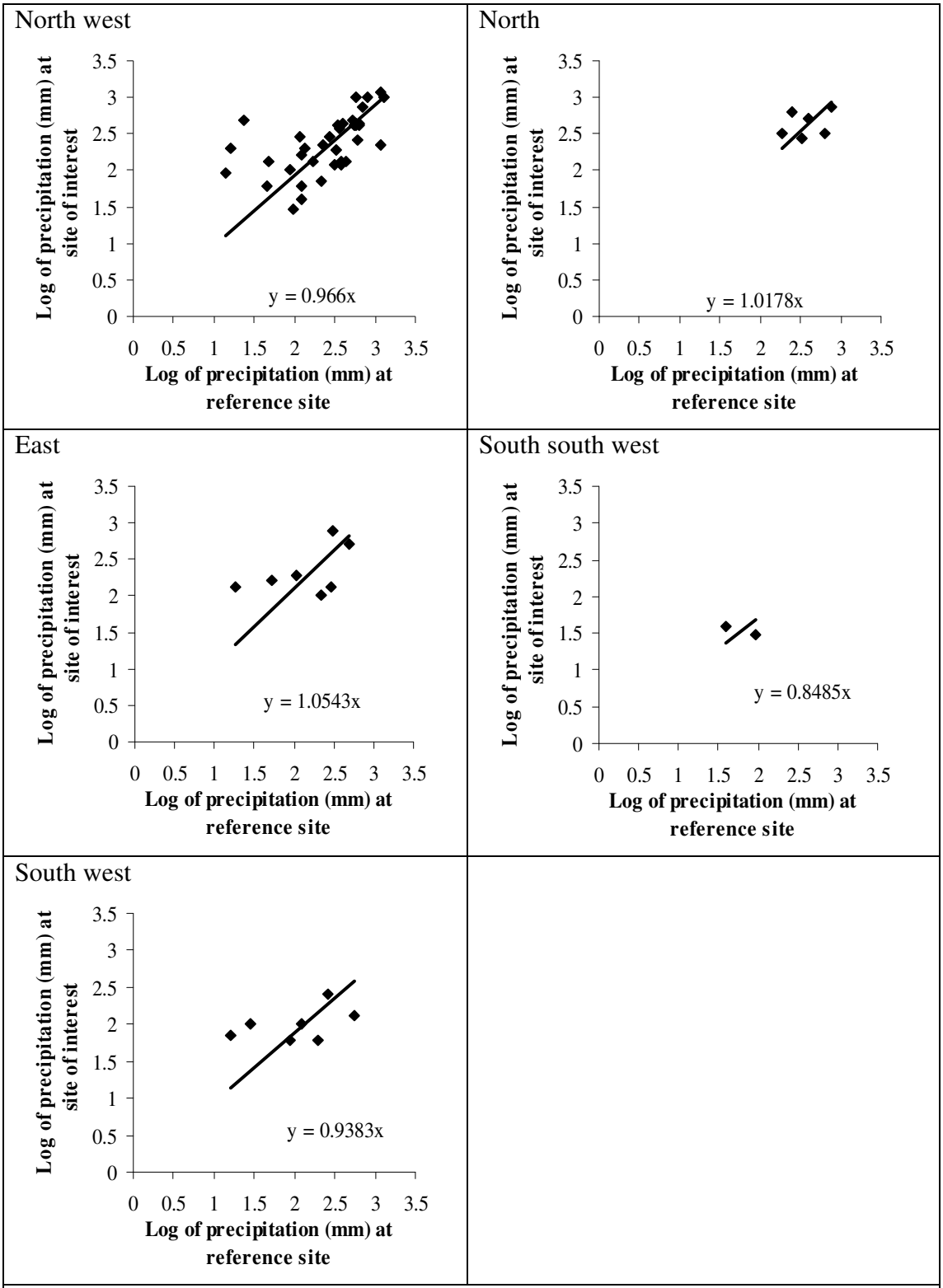

Figure A2-18. Ball Shelter (y axis) against Mt Cook-EWS (x axis) for different wind classes.

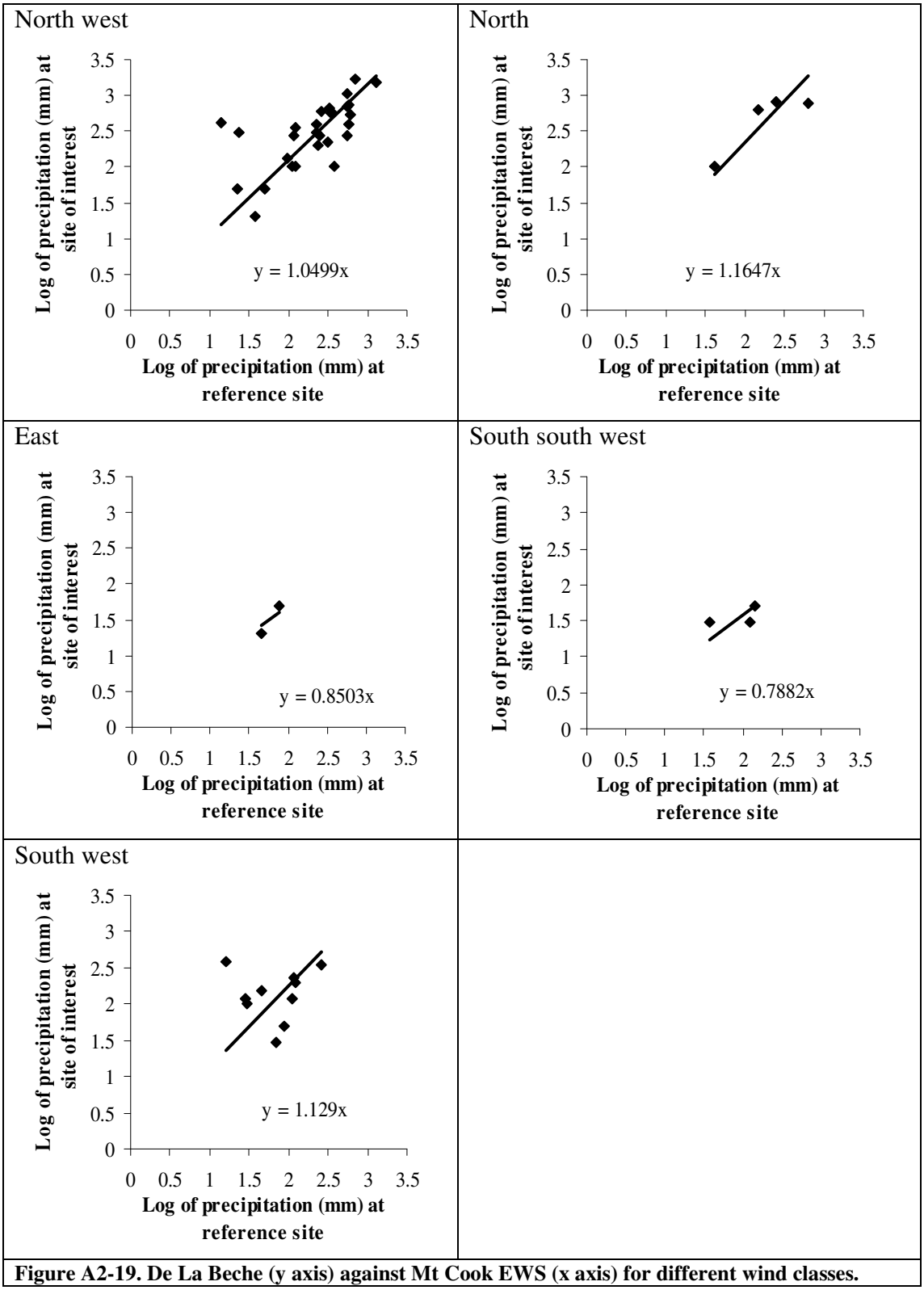

Figure A2-19. De La Beche (y axis) against Mt Cook EWS (x axis) for different wind classes.

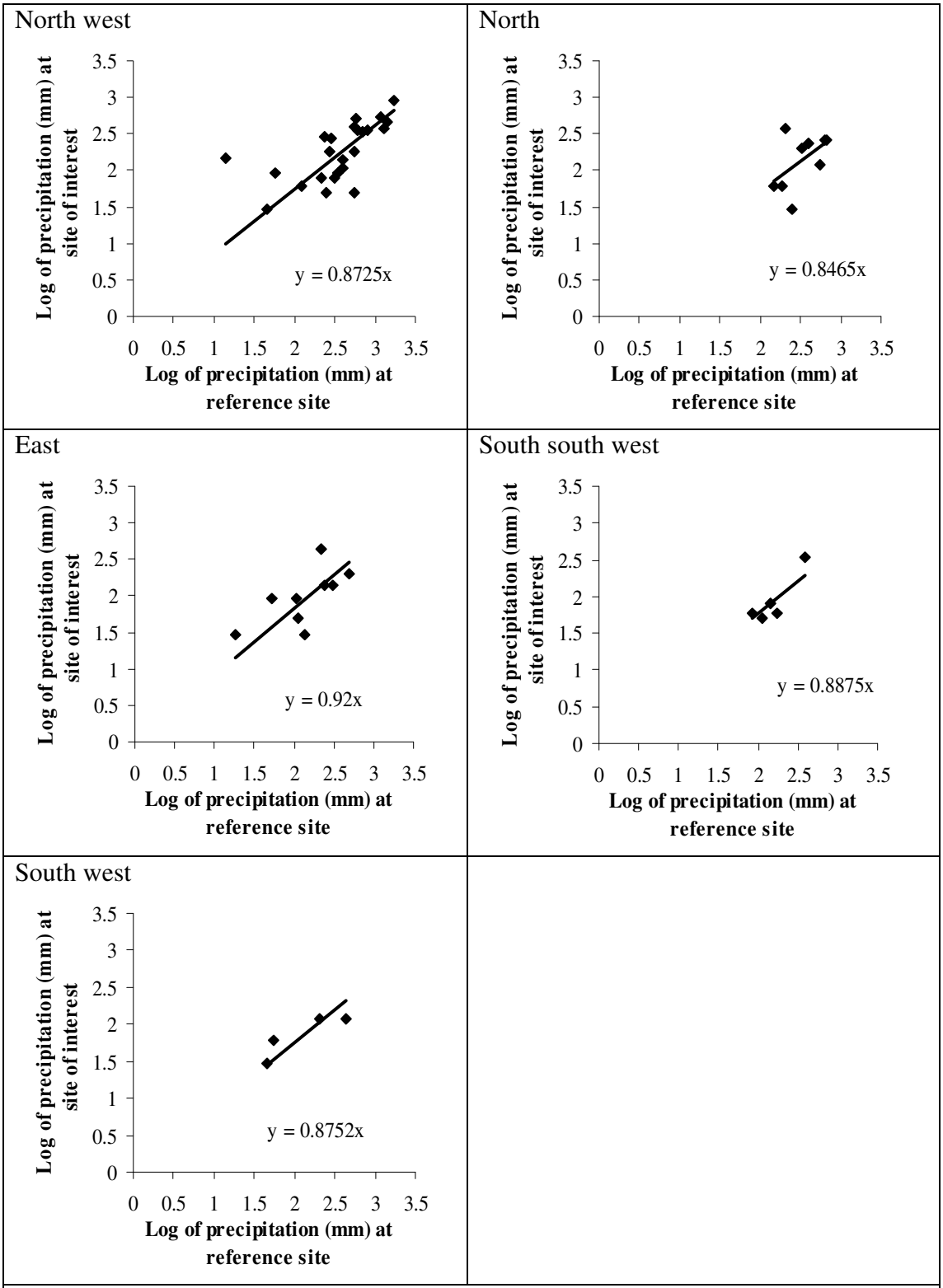

Figure A2-20. Jollie Stream (y axis) against Mt Cook EWS (x axis) for different wind classes.

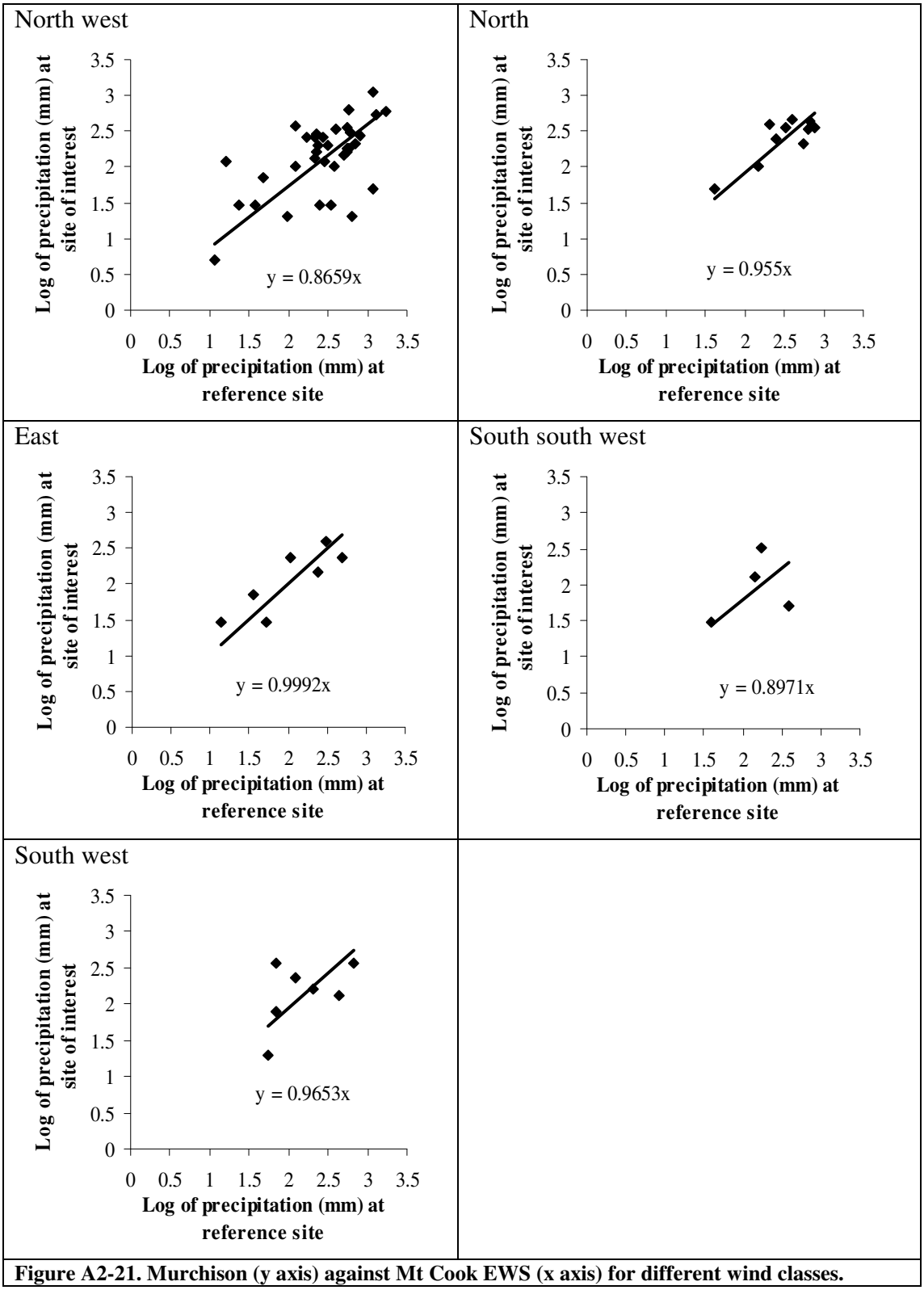

Figure A2-21. Murchison (y axis) against Mt Cook EWS (x axis) for different wind classes.

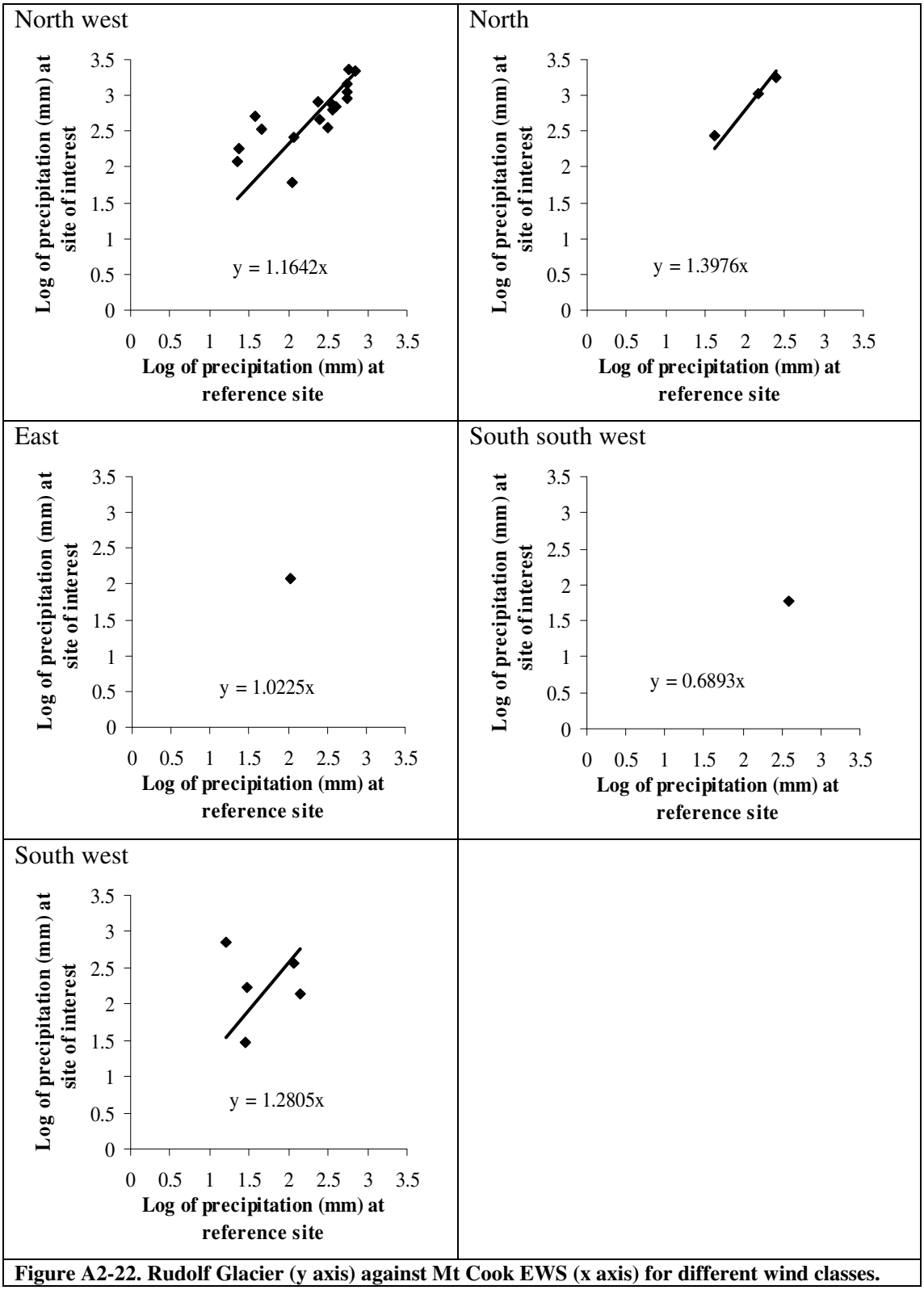

Figure A2-22. Rudolf Glacier (y axis) against Mt Cook EWS (x axis) for different wind classes.

North west

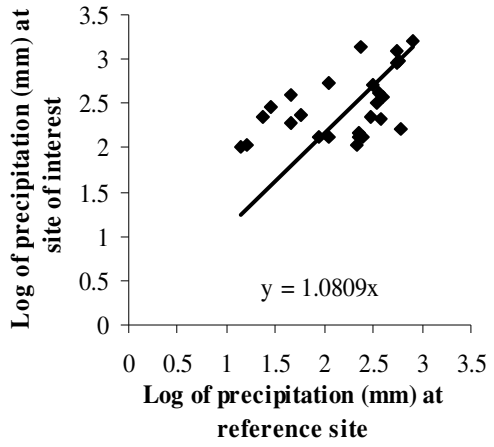

North

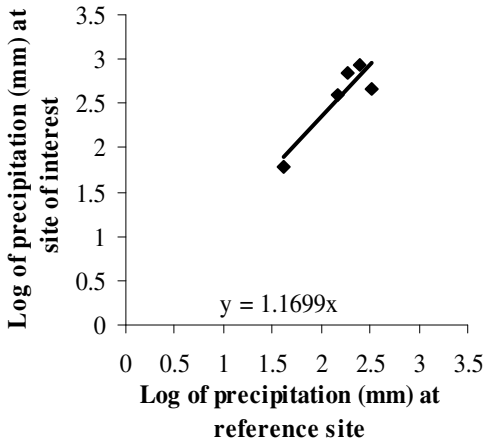

East

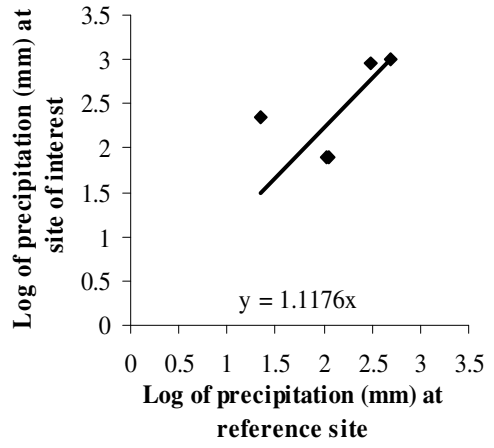

South south west –*no observations*

South west

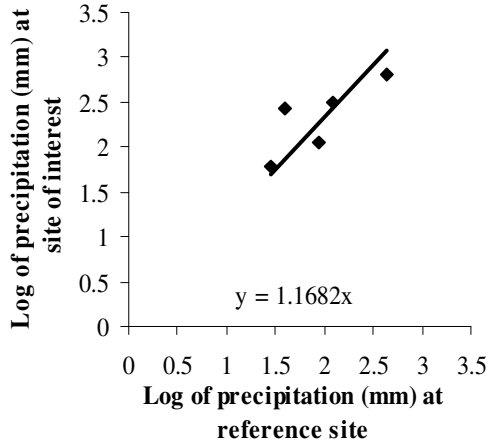

Figure A2-23. East Hooker 1 (y axis) against Mt Cook EWS (x axis) for different wind classes.

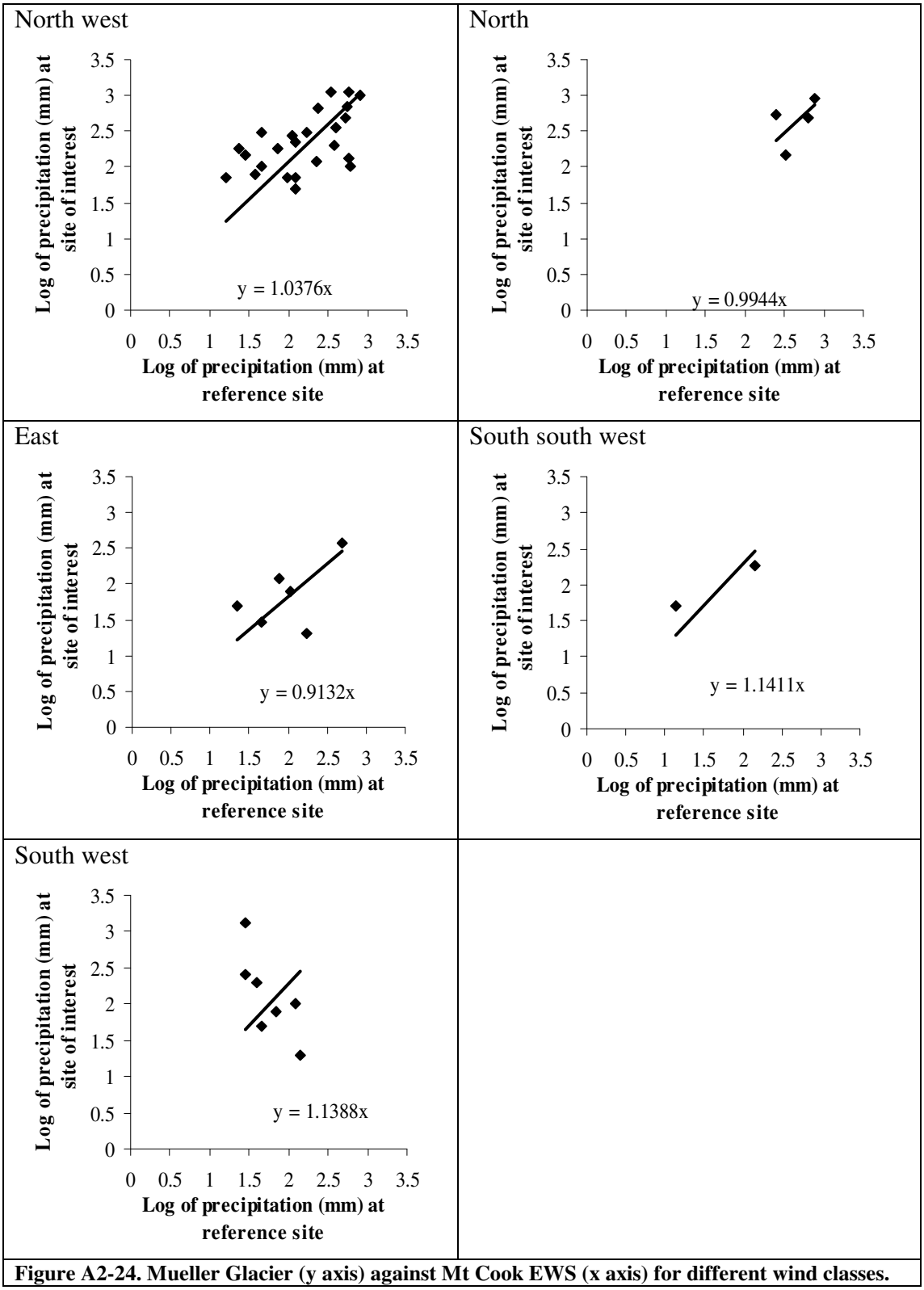

Figure A2-24. Mueller Glacier (y axis) against Mt Cook EWS (x axis) for different wind classes.

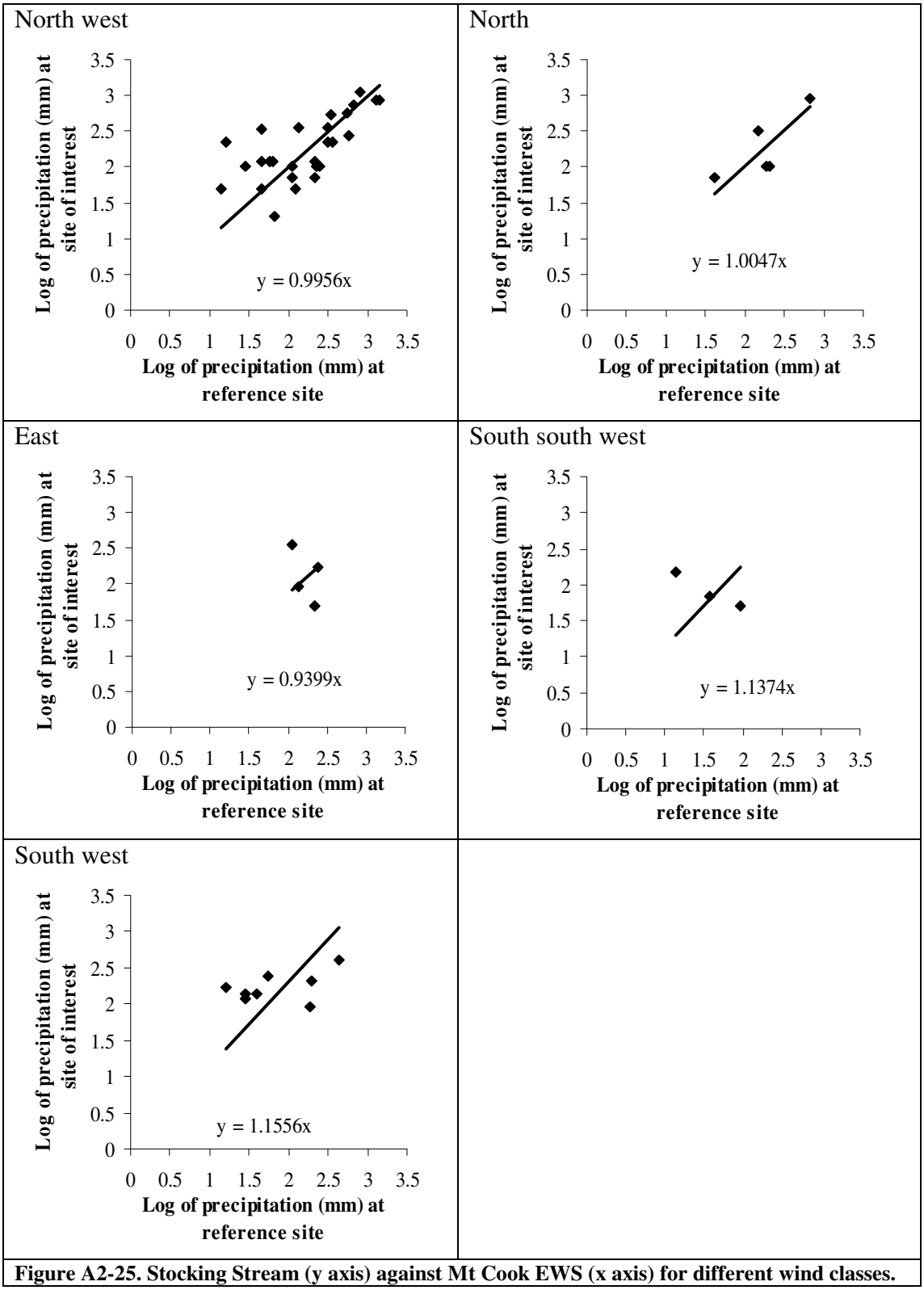

Figure A2-25. Stocking Stream (y axis) against Mt Cook EWS (x axis) for different wind classes.

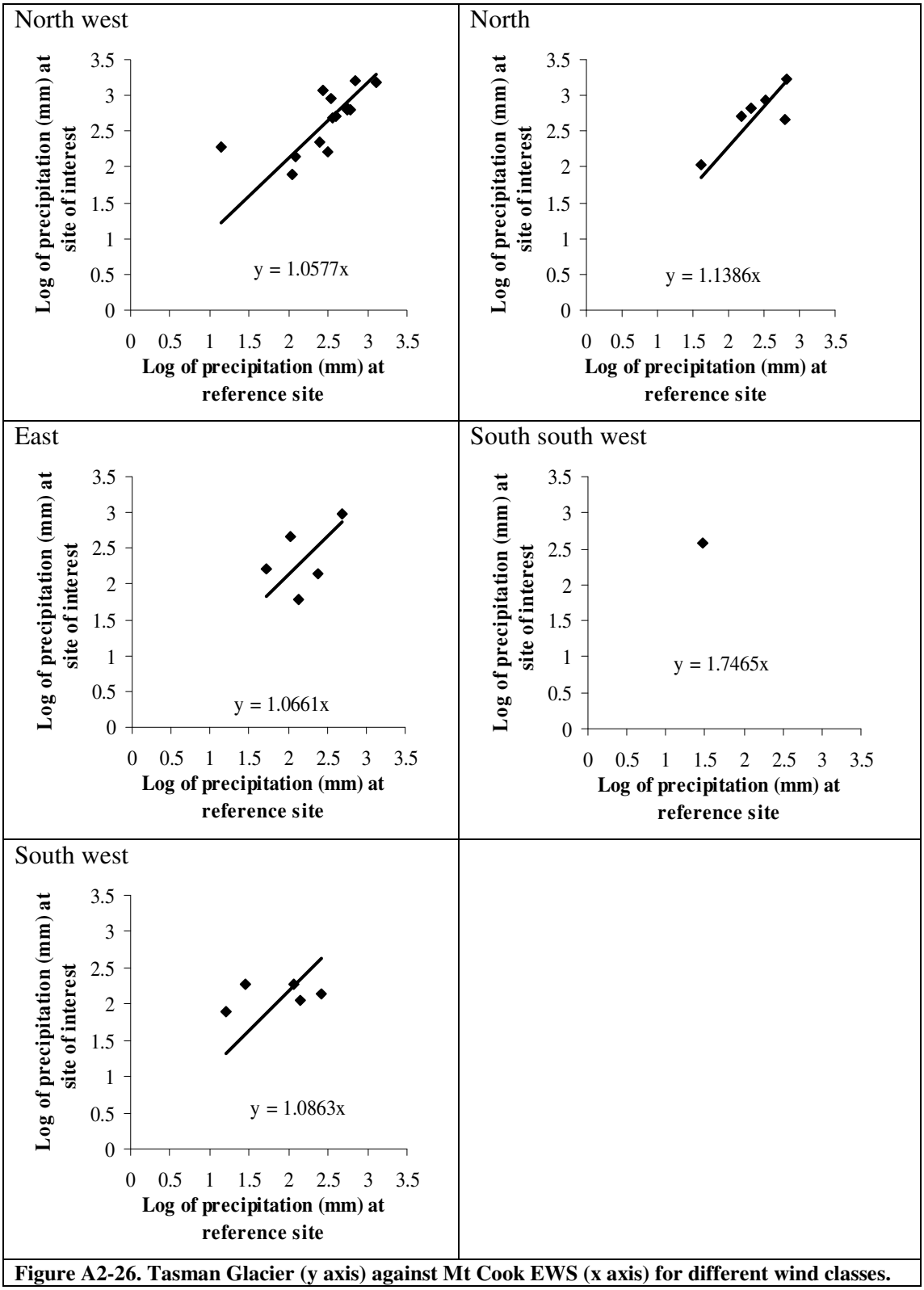

Figure A2-26. Tasman Glacier (y axis) against Mt Cook EWS (x axis) for different wind classes.

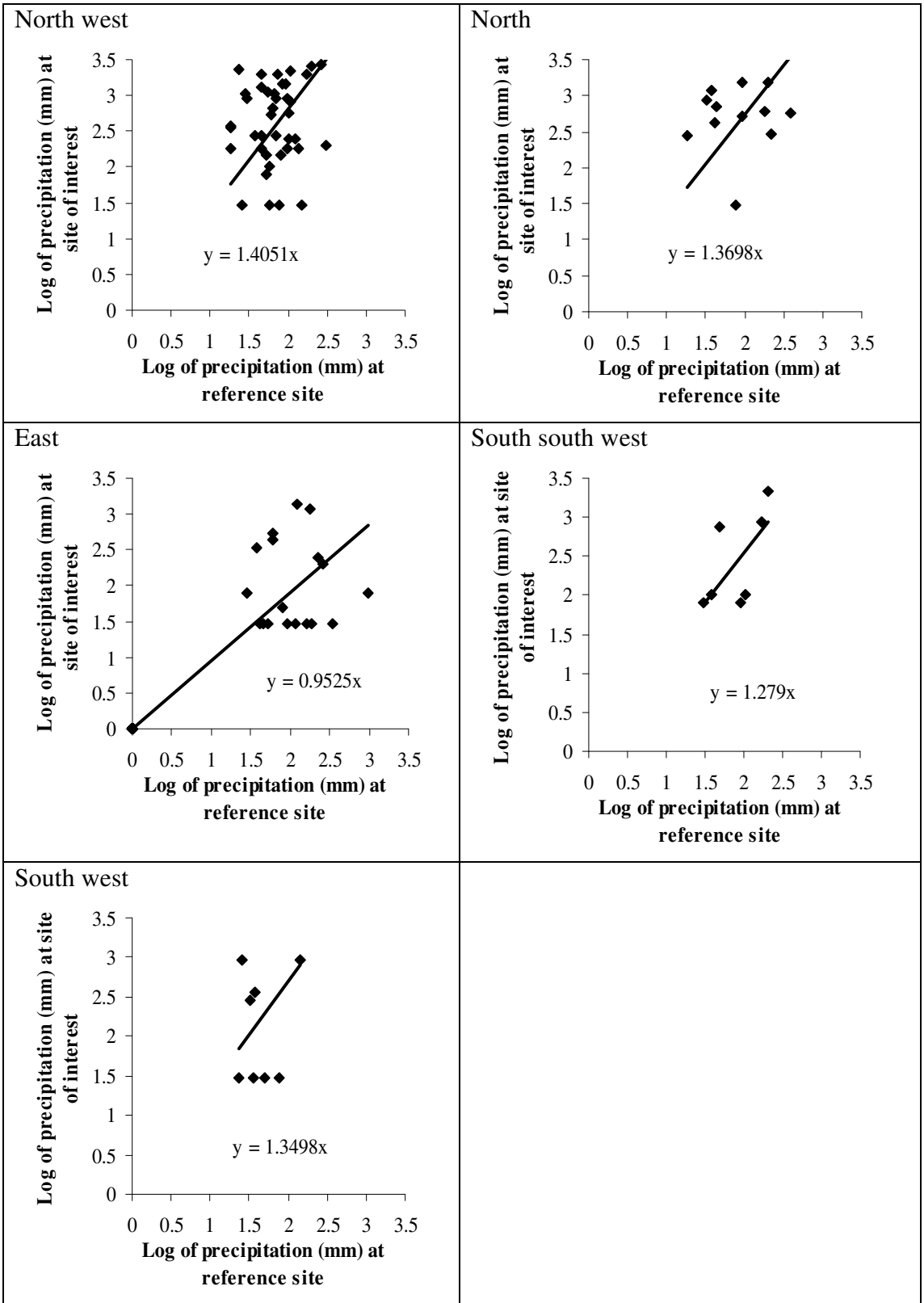

Figure A2-27. Malte Brun Hut (y axis) against Tekapo AS (x axis) for different wind classes.

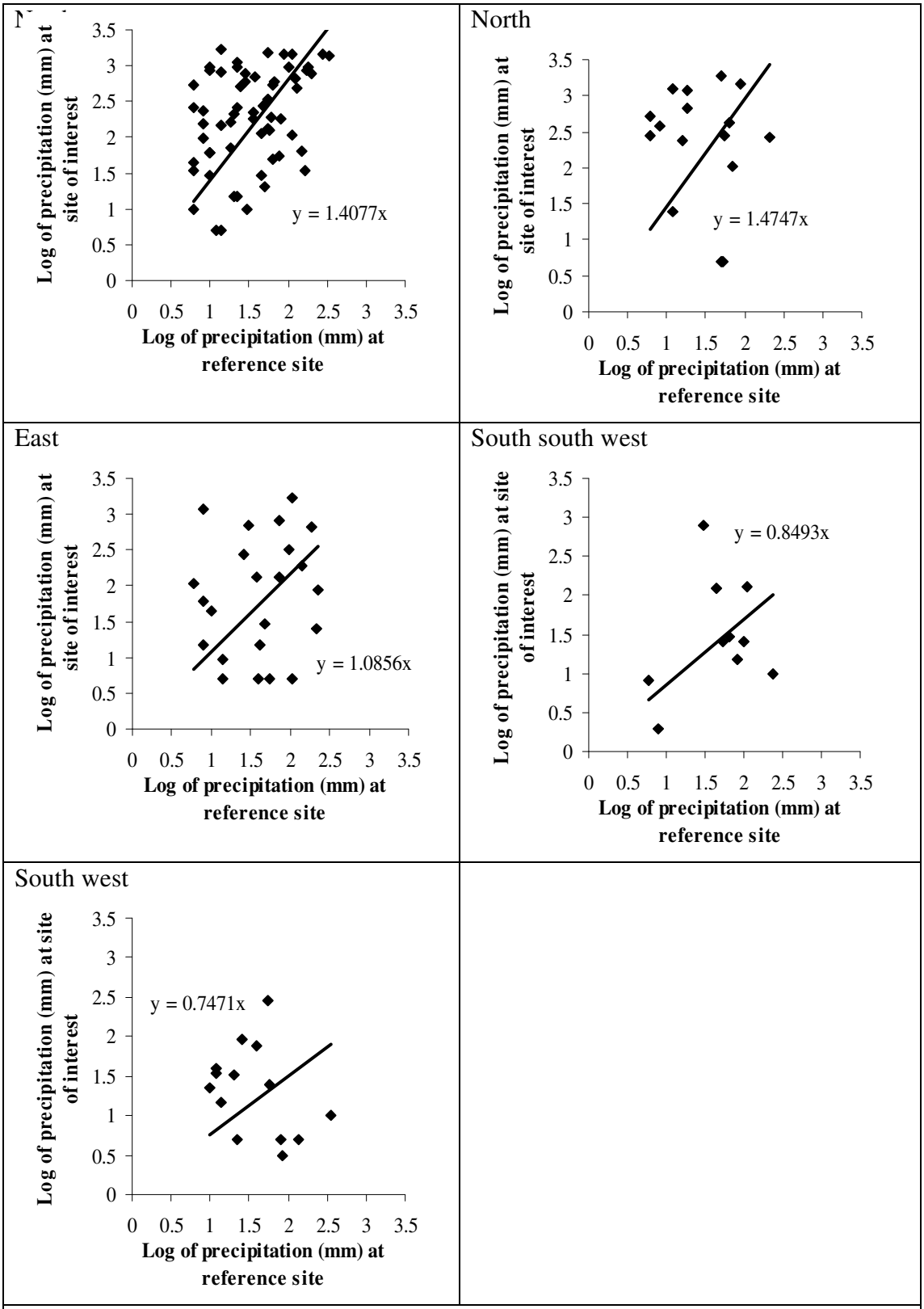

Figure A2-28. Rose Ridge (y axis) against Tekapo EWS (x axis) for different wind classes.

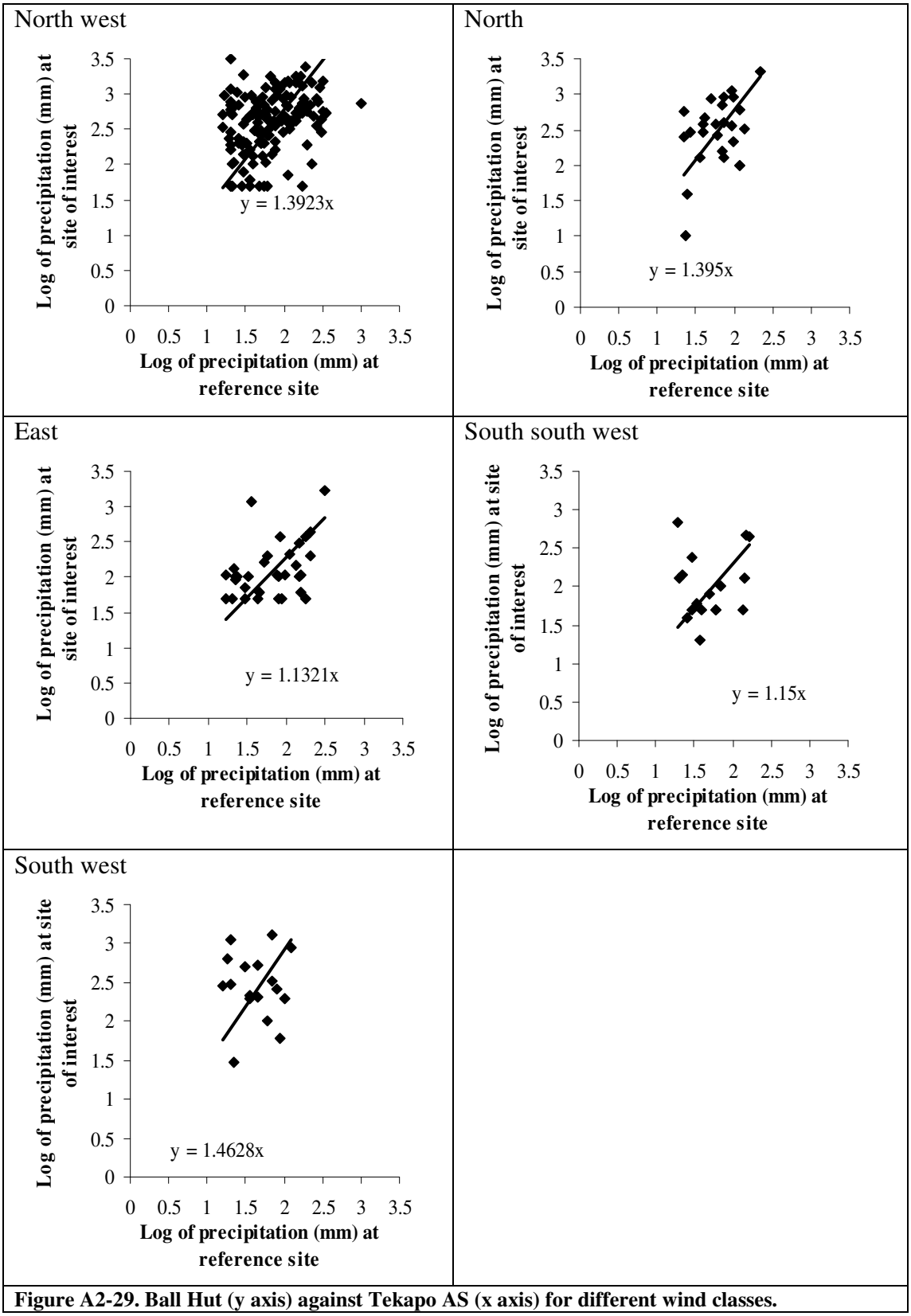

Figure A2-29. Ball Hut (y axis) against Tekapo AS (x axis) for different wind classes.

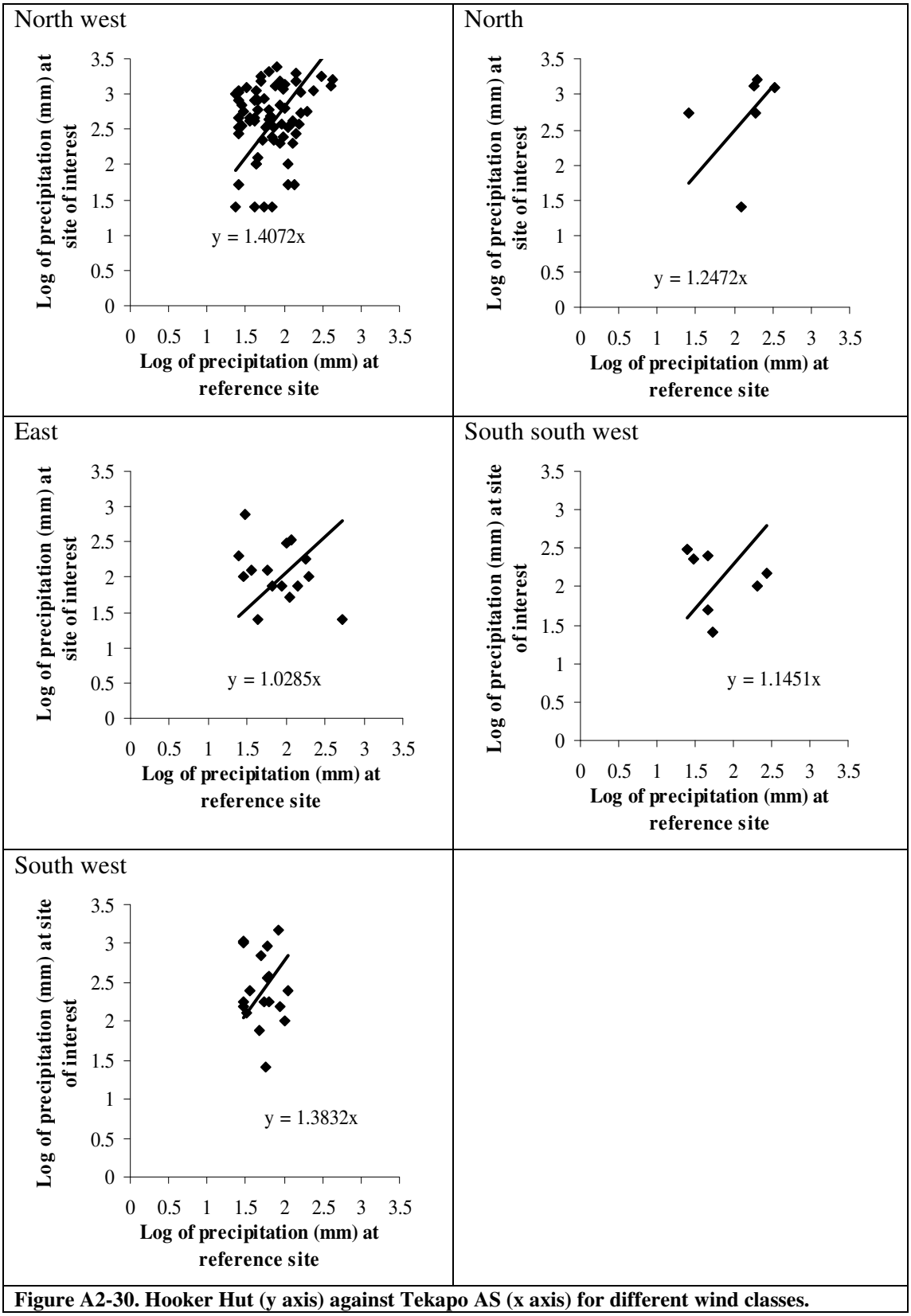

Figure A2-30. Hooker Hut (y axis) against Tekapo AS (x axis) for different wind classes.

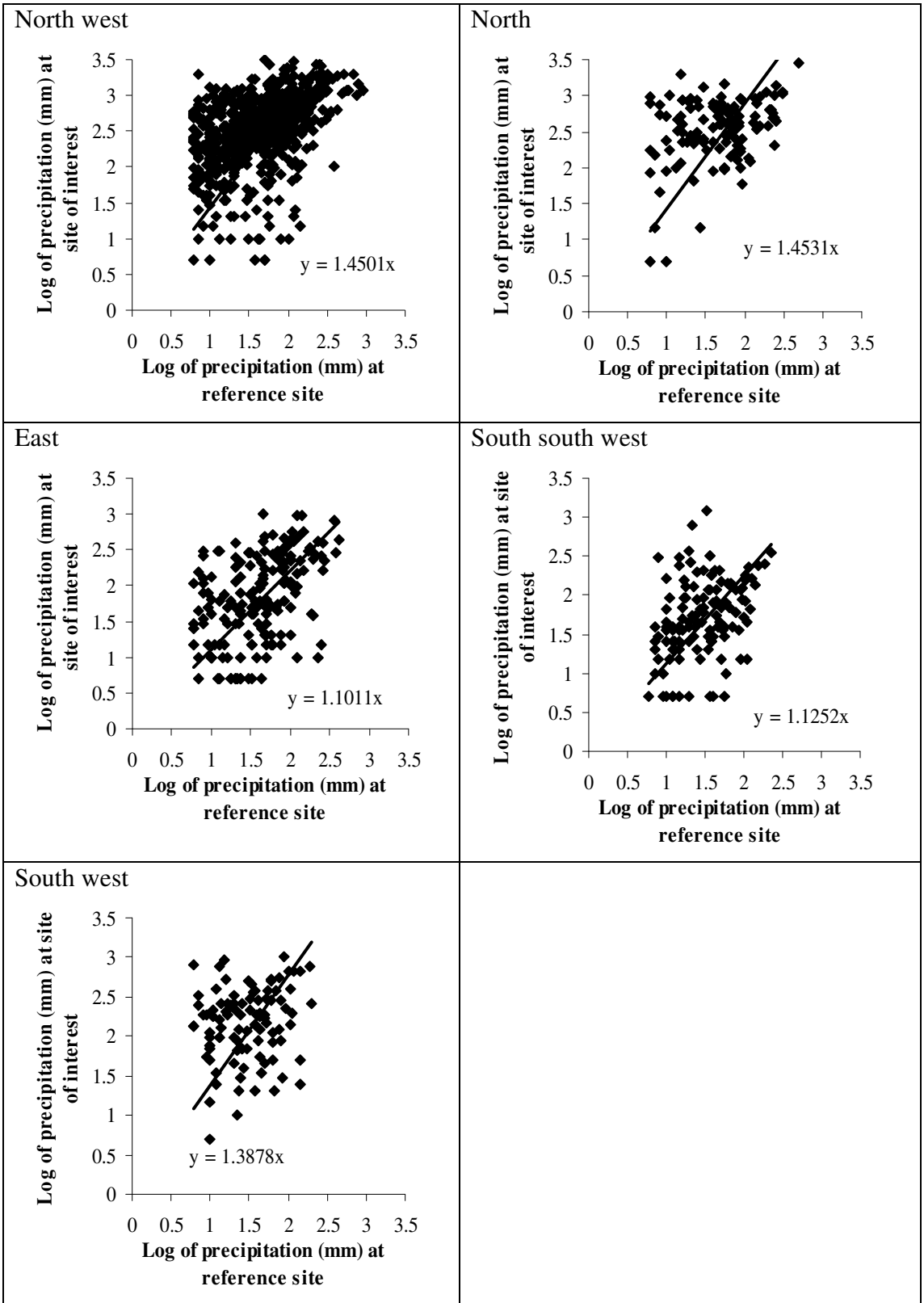

Figure A2-31. Mt Cook ECAN (y axis) against Tekapo AS (x axis) for different wind classes.

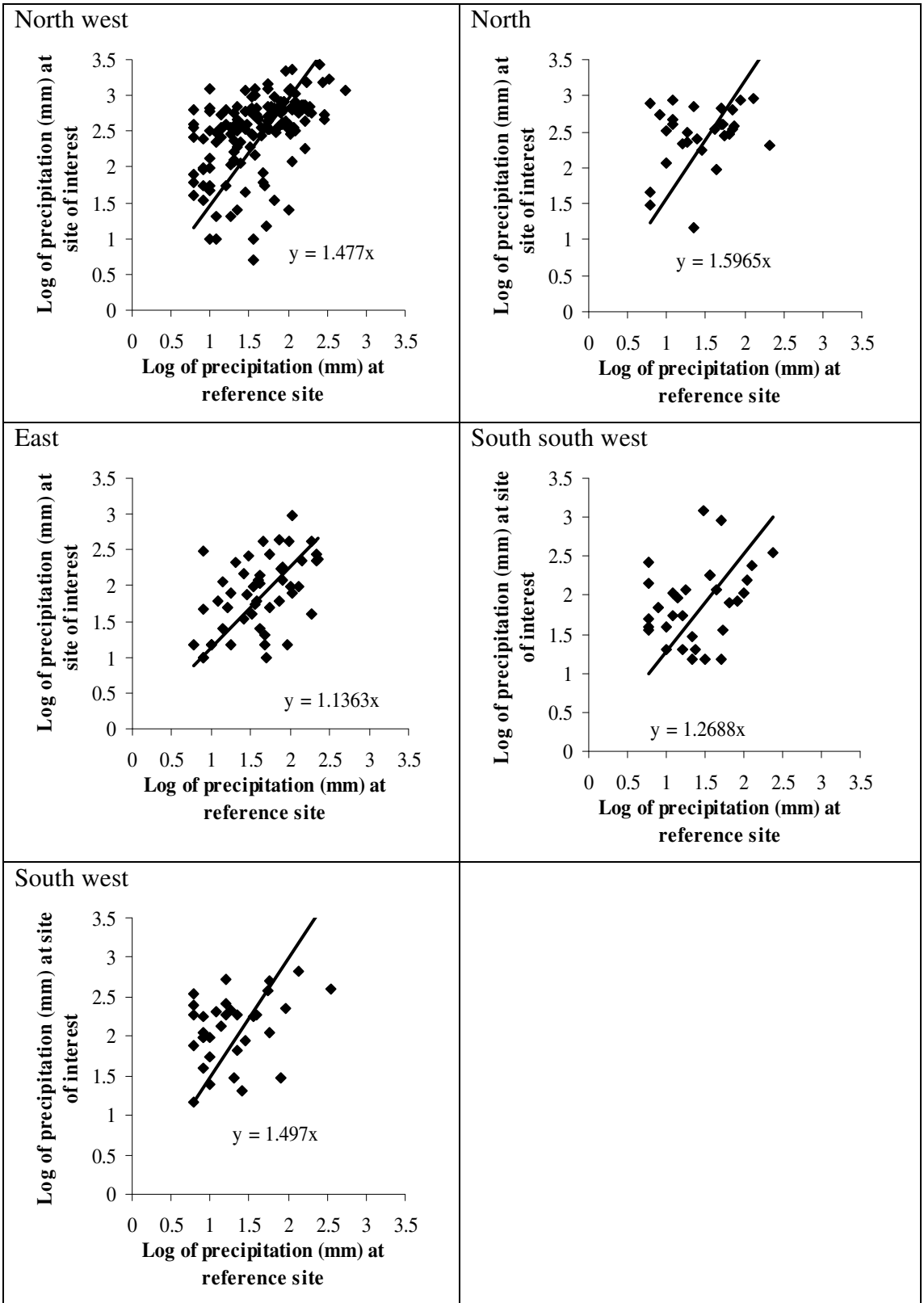

Figure A2-32. Mt Cook ECAN (y axis) against Tekapo EWS (x axis) for different wind classes.

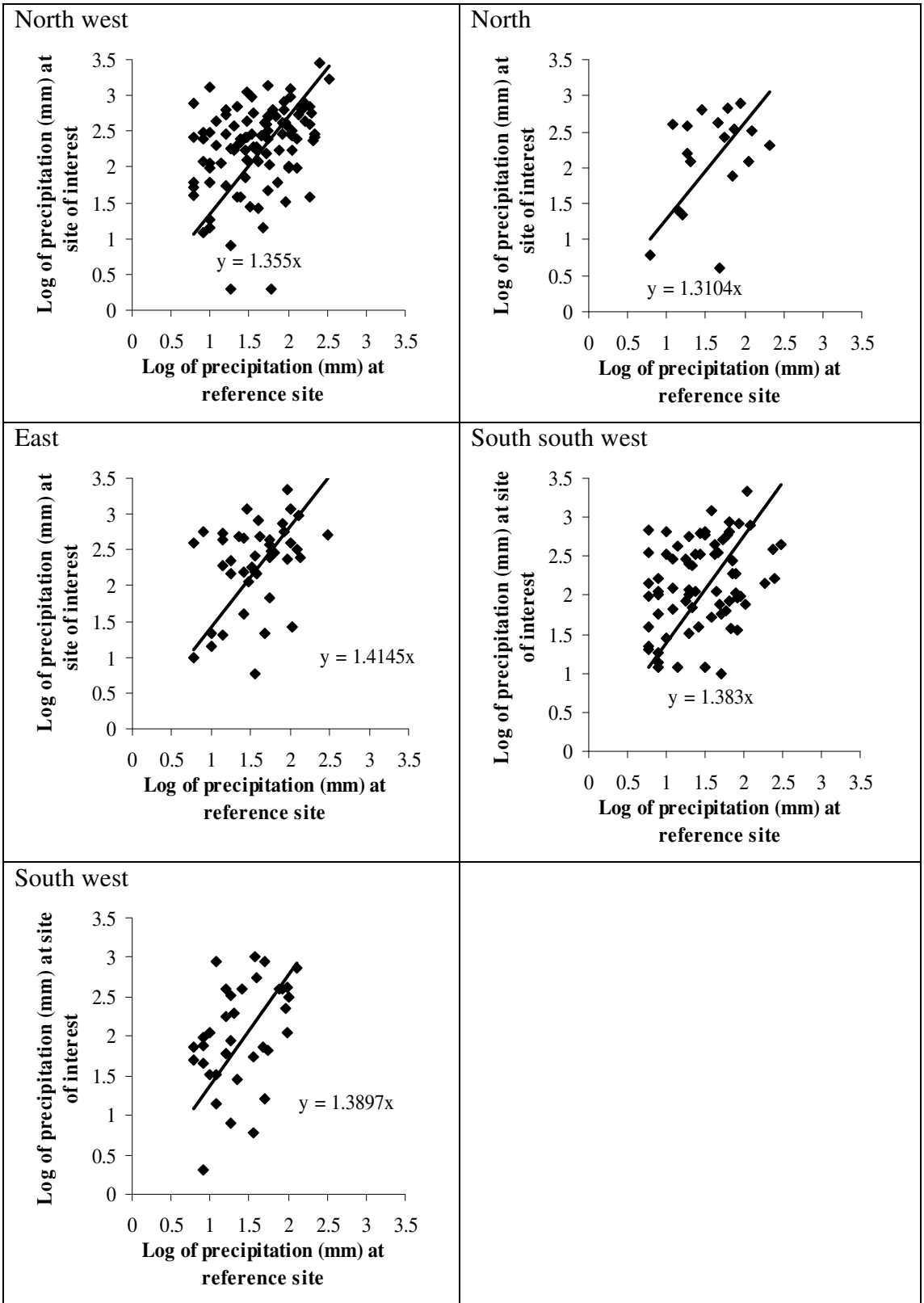

Figure A2-33. Mt Cook EWS (y axis) against Tekapo EWS (x axis) for different wind classes.

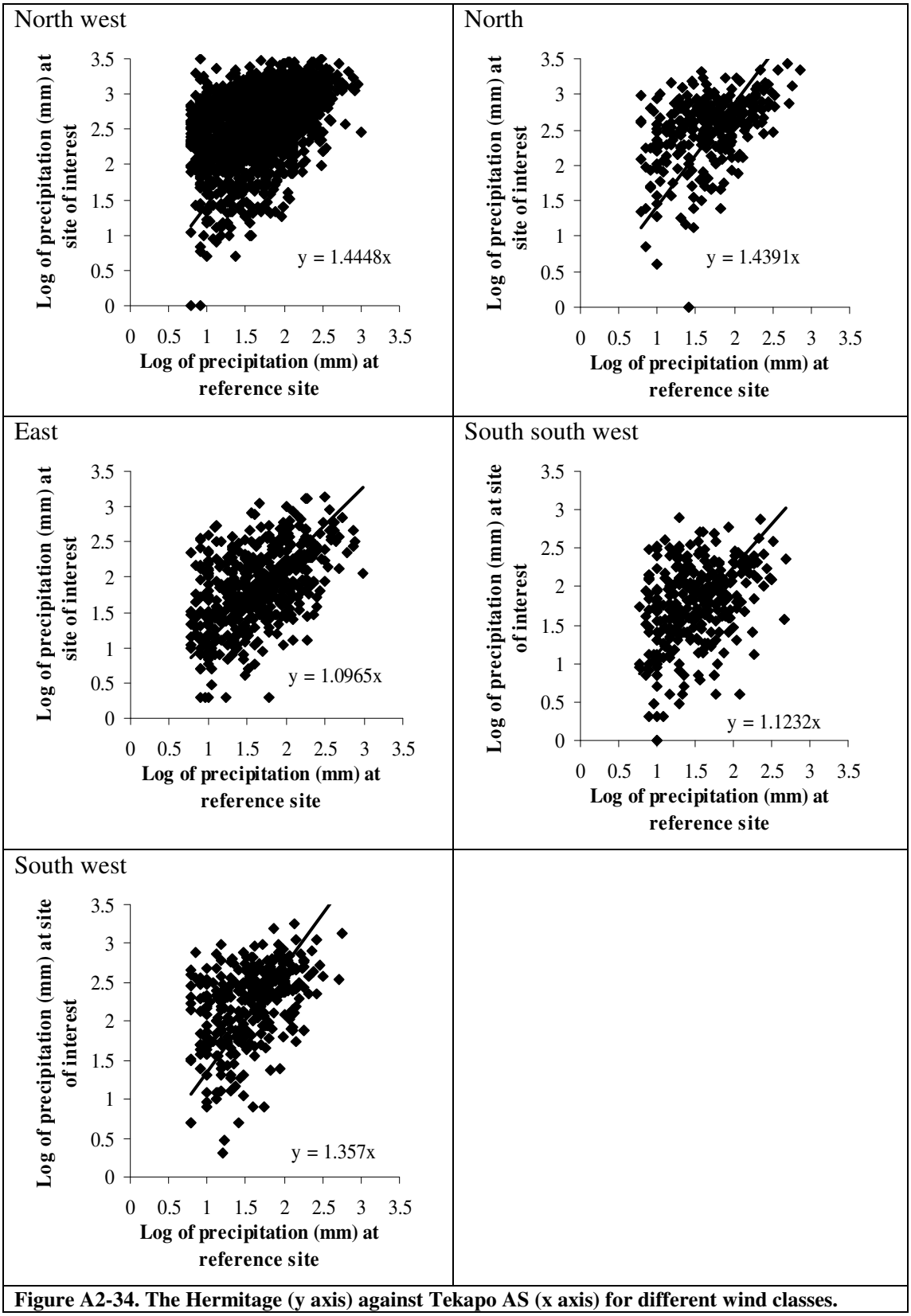

Figure A2-34. The Hermitage (y axis) against Tekapo AS (x axis) for different wind classes.

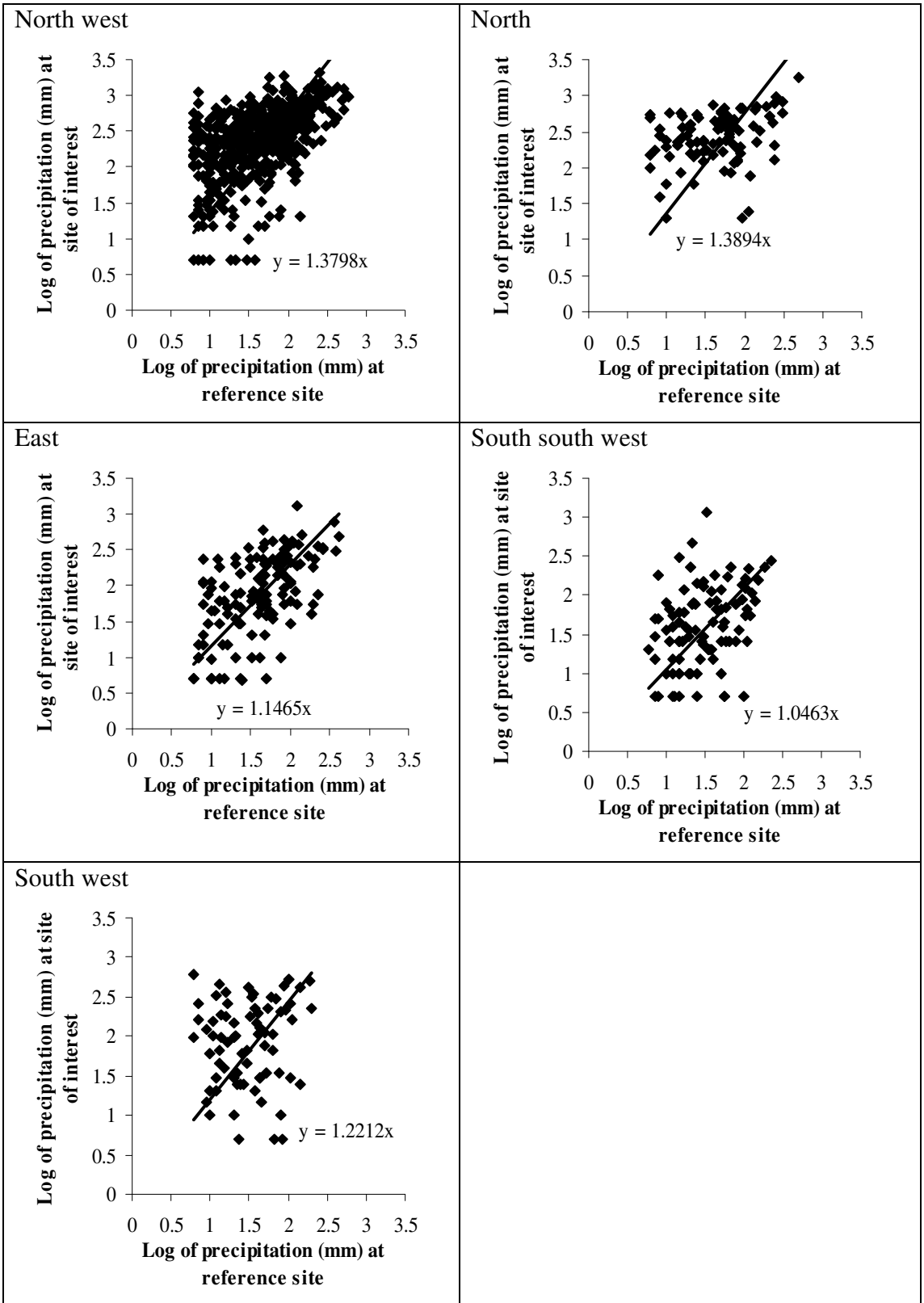

Figure A2-35. Hooker Rd Bridge (y axis) against Tekapo AS (x axis) for different wind classes.

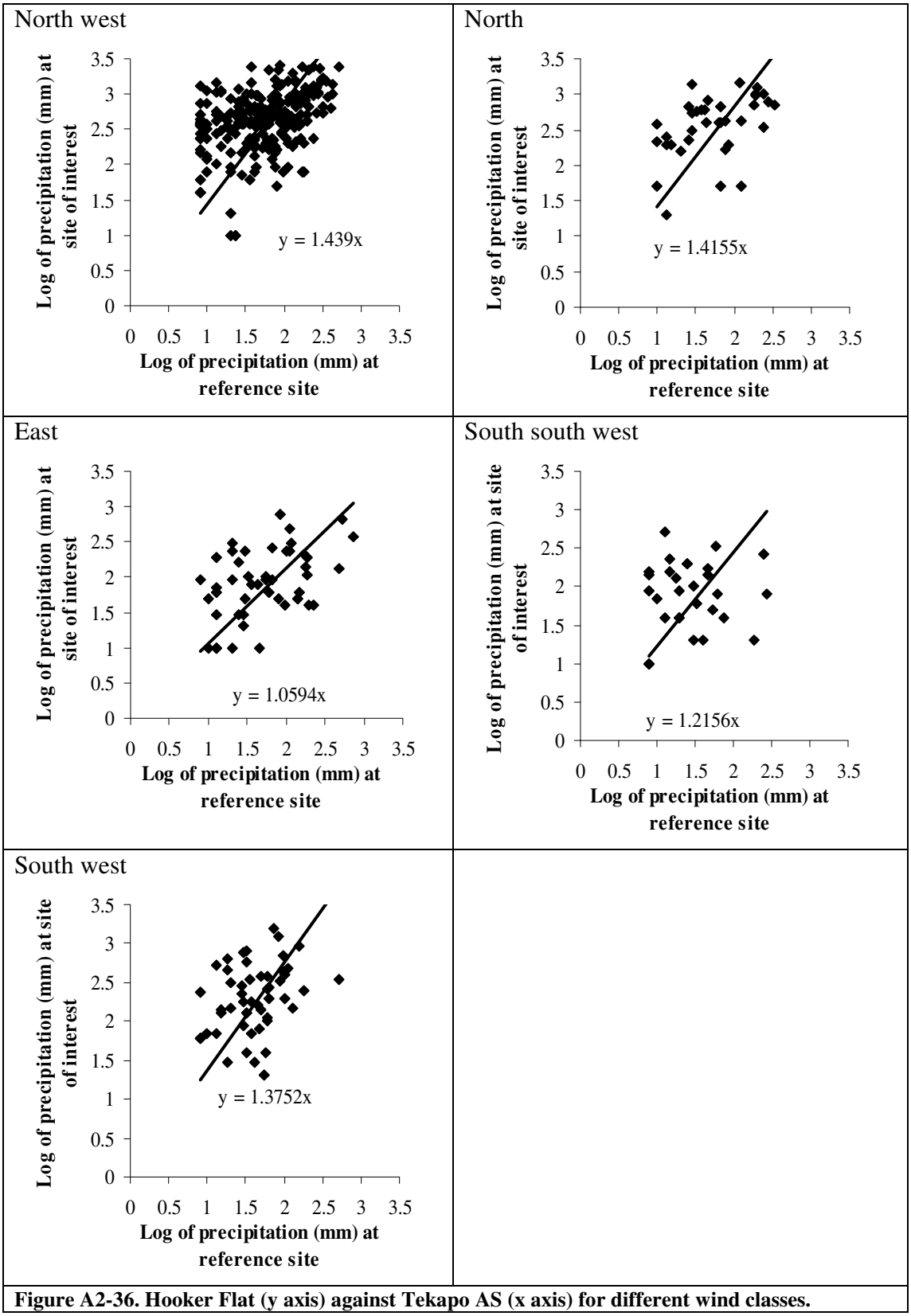

Figure A2-36. Hooker Flat (y axis) against Tekapo AS (x axis) for different wind classes.

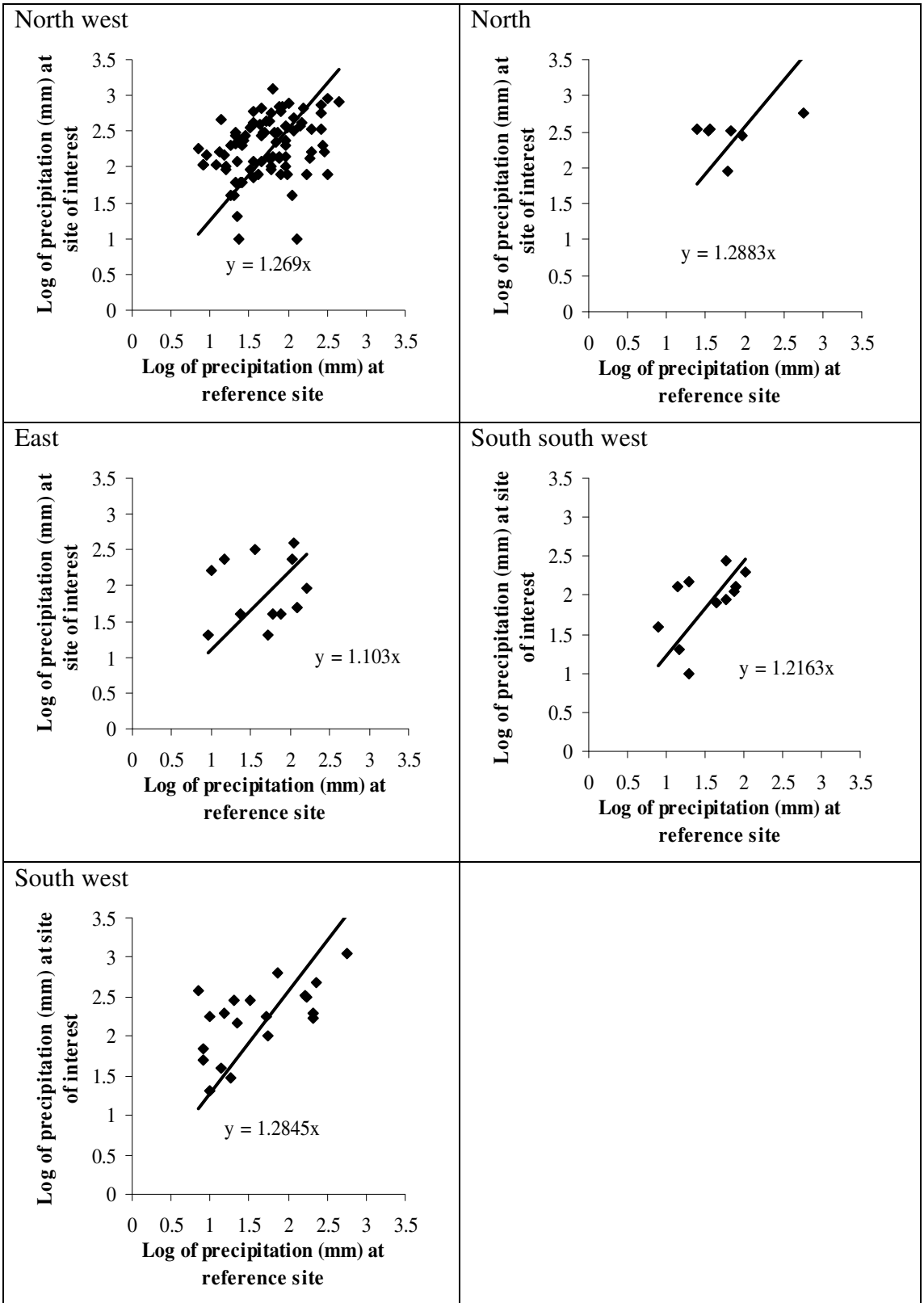

Figure A2-37. Sealey Village (y axis) against Tekapo AS (x axis) for different wind classes.

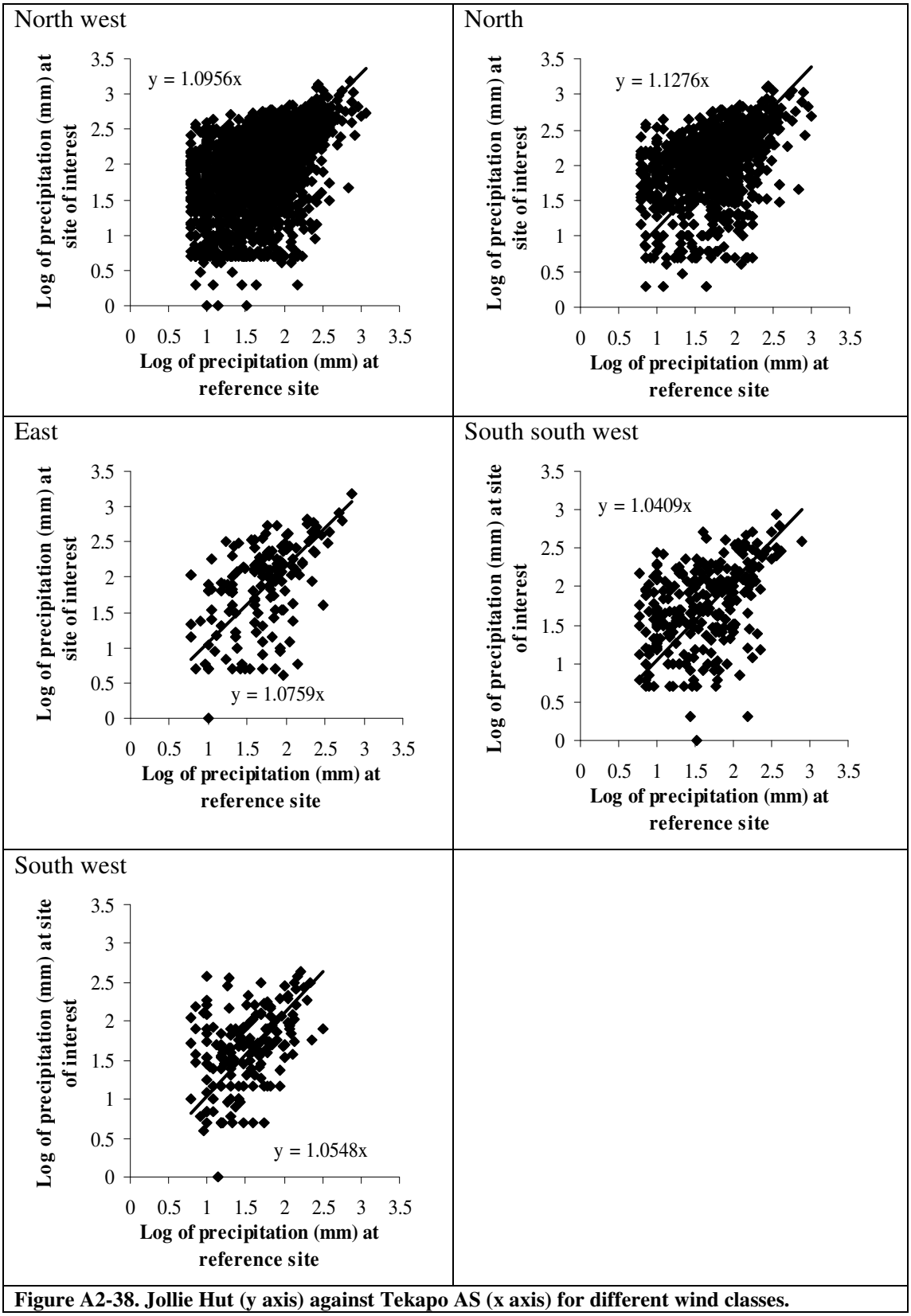

Figure A2-38. Jollie Hut (y axis) against Tekapo AS (x axis) for different wind classes.

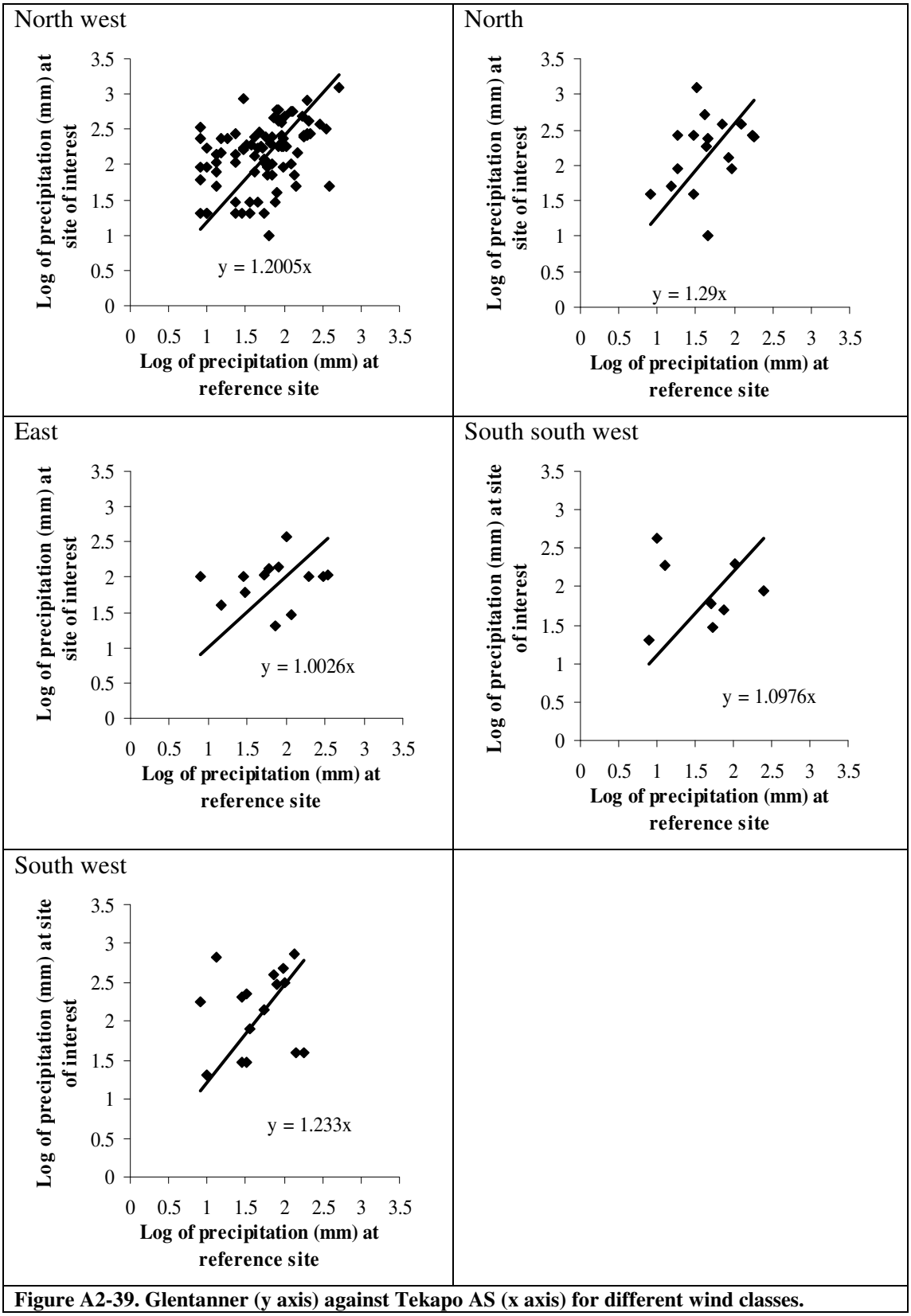

Figure A2-39. Glentanner (y axis) against Tekapo AS (x axis) for different wind classes.

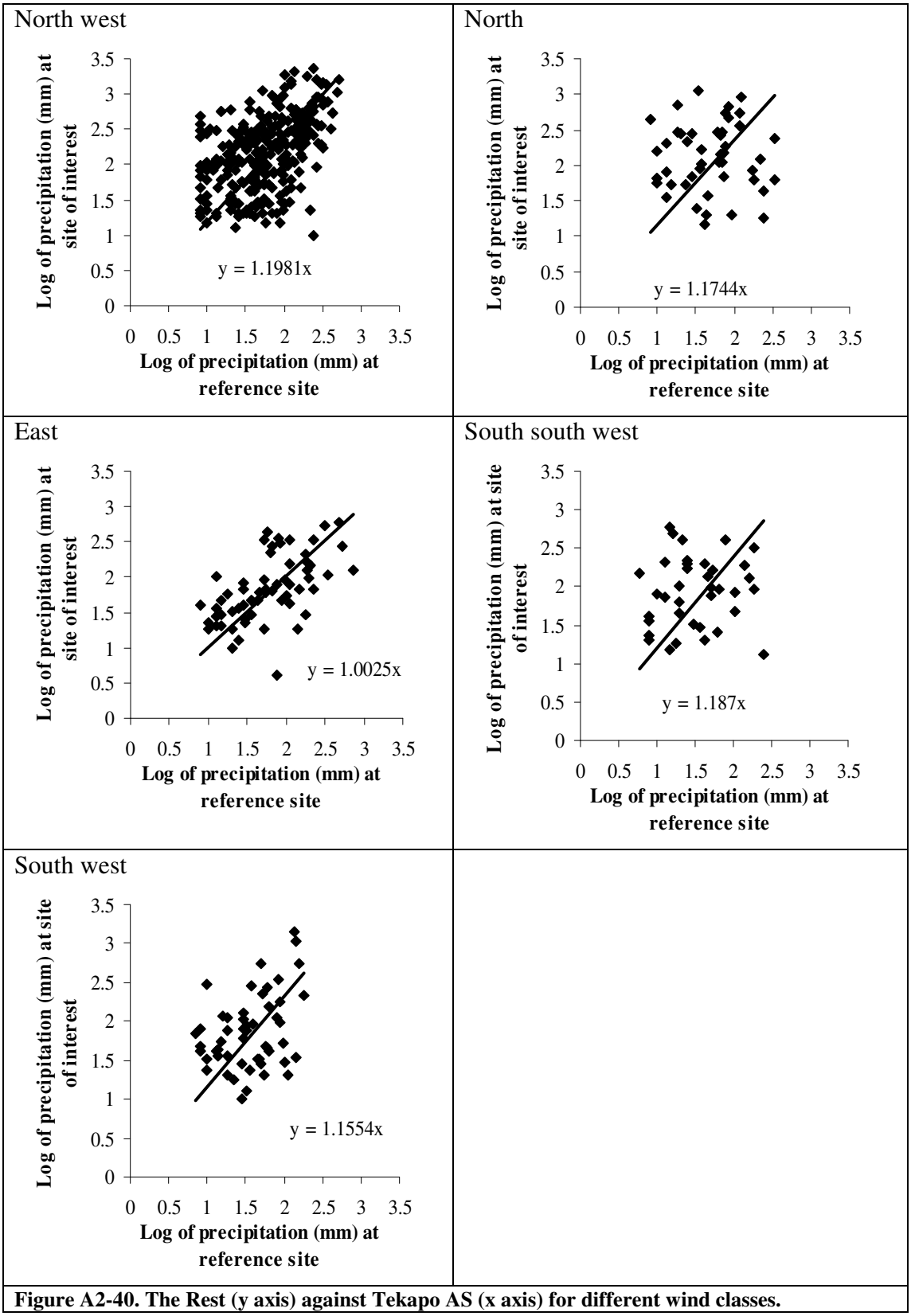

Figure A2-40. The Rest (y axis) against Tekapo AS (x axis) for different wind classes.

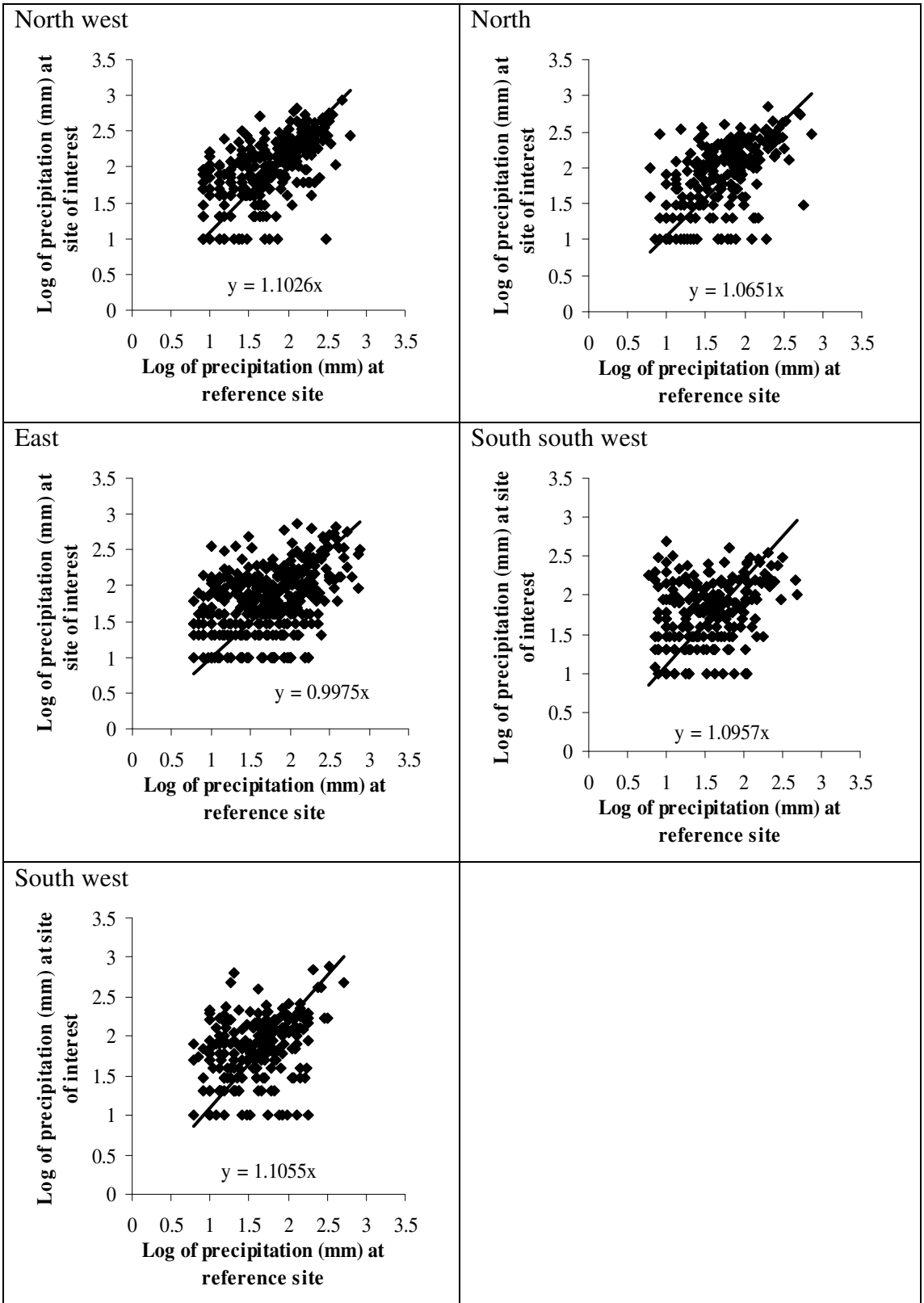

Figure A2-41. Braemar Station (y axis) against daily precipitation at Tekapo AS (x axis) for different wind classes.

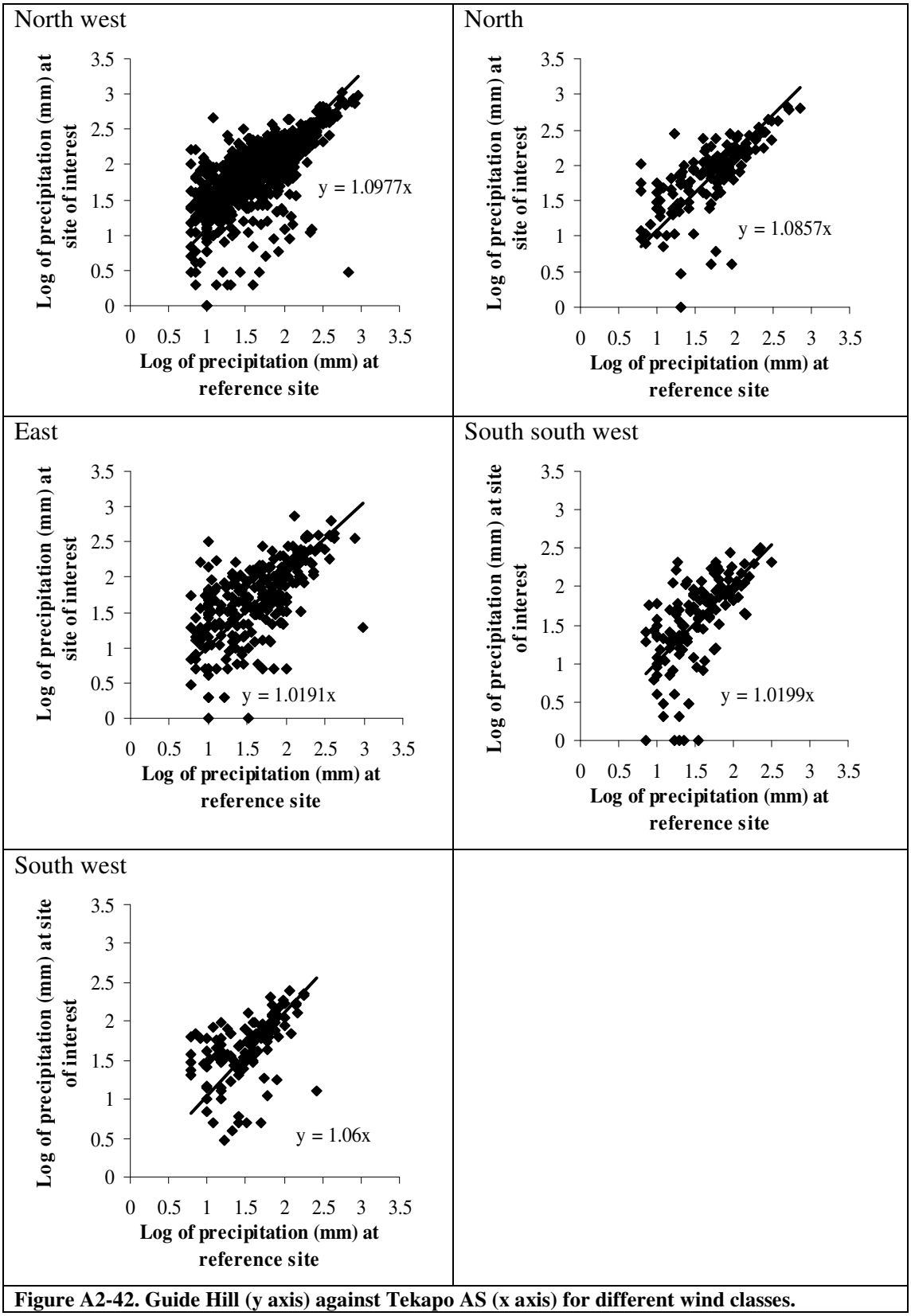

Figure A2-42. Guide Hill (y axis) against Tekapo AS (x axis) for different wind classes.

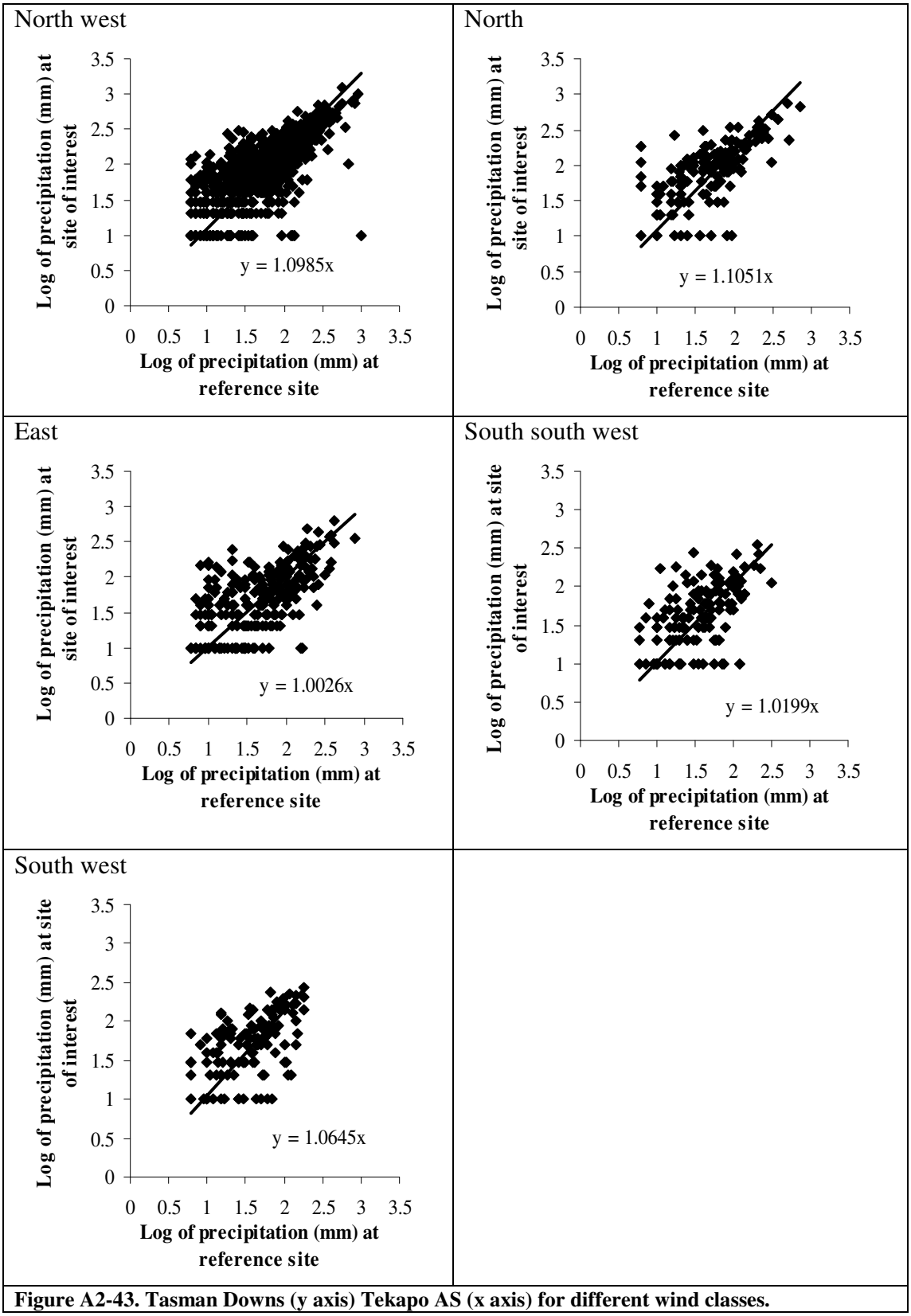

Figure A2-43. Tasman Downs (y axis) Tekapo AS (x axis) for different wind classes.

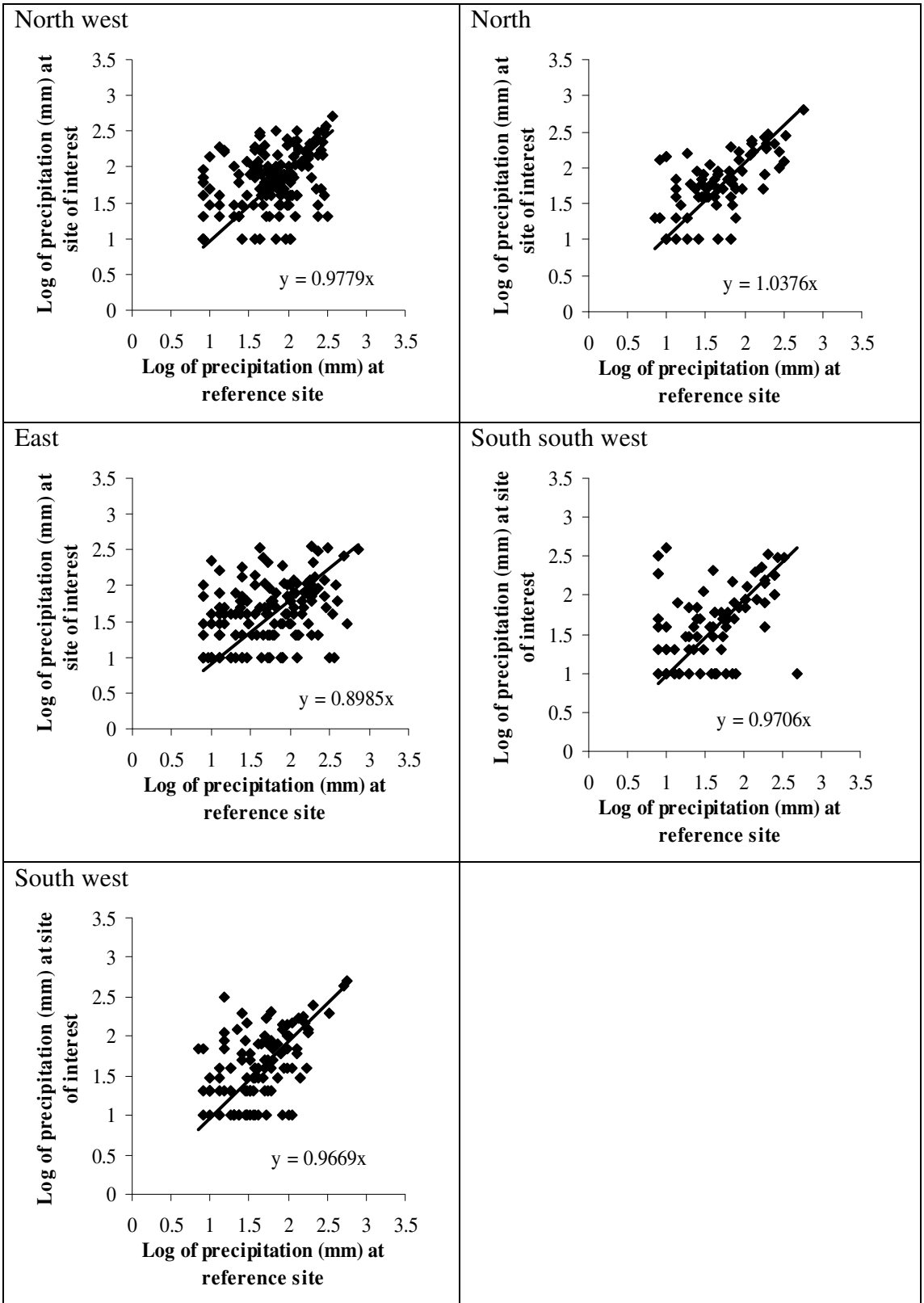

Figure A2-44. Lake Pukaki No. 1 (y axis) against Tekapo AS (x axis) for different wind classes.

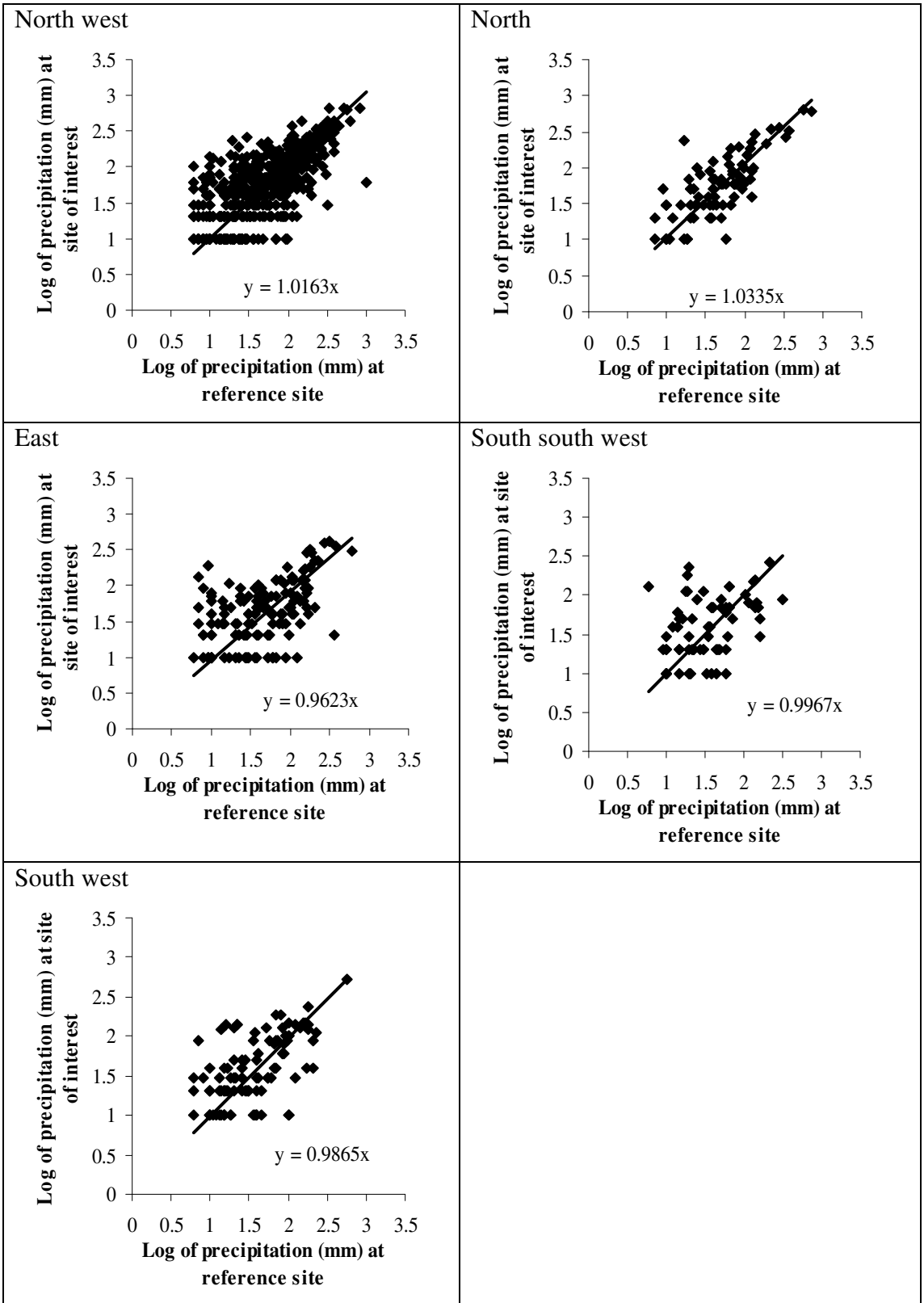

Figure A2-45. Lake Pukaki MWD (y axis) against Tekapo AS (x axis) for different wind classes.

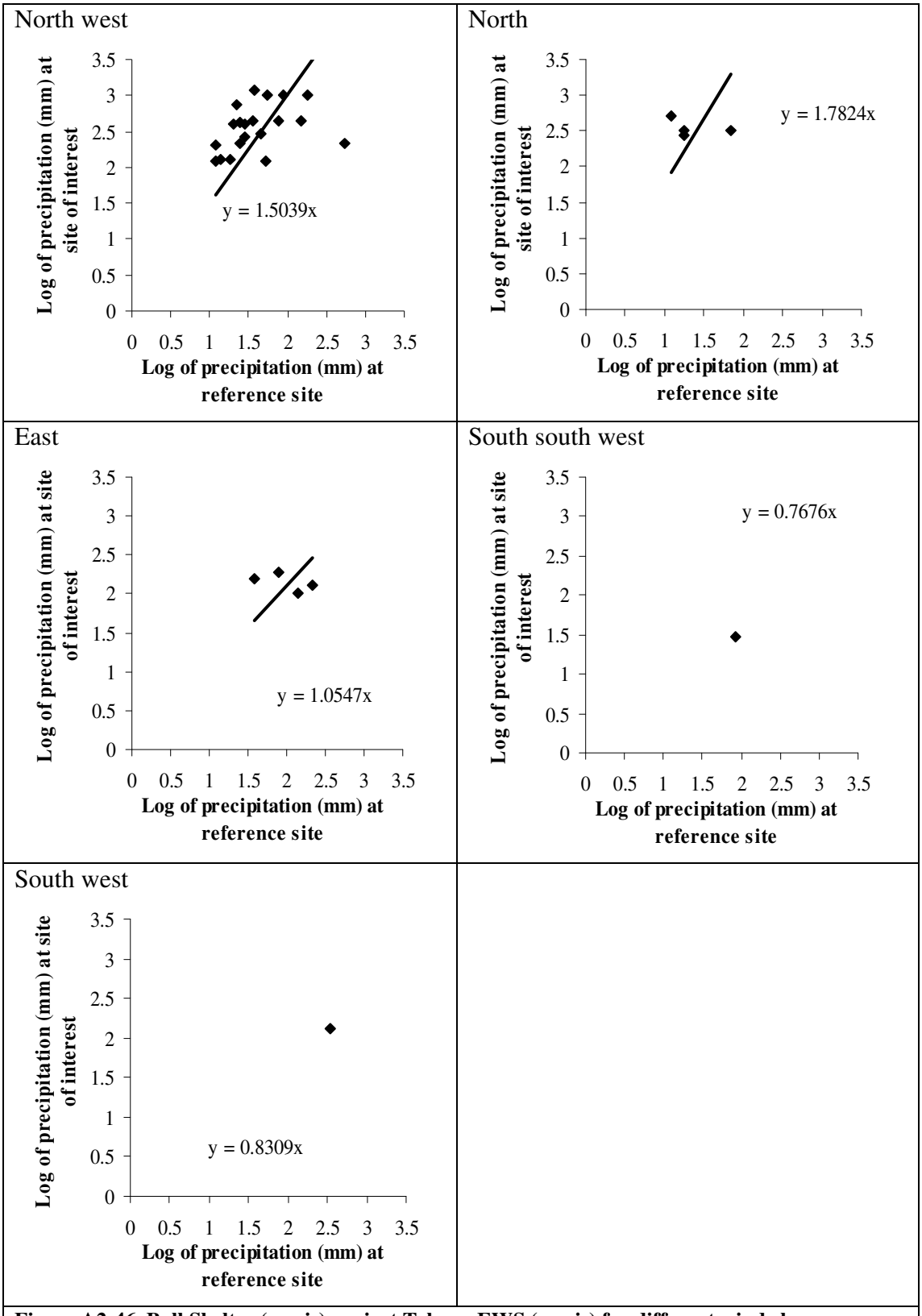

Figure A2-46. Ball Shelter (y axis) against Tekapo EWS (x axis) for different wind classes.

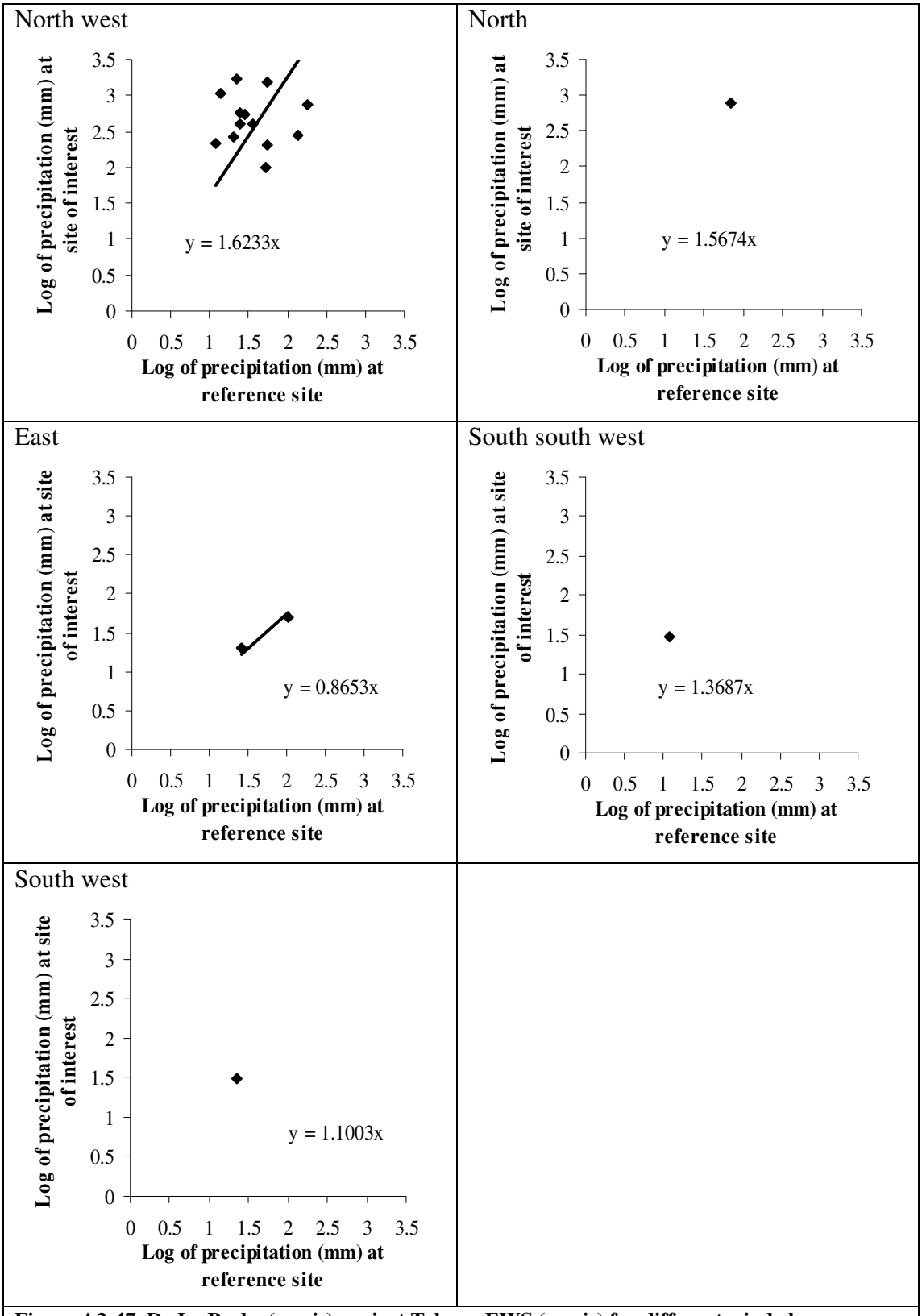

Figure A2-47. De La Beche (y axis) against Tekapo EWS (x axis) for different wind classes.

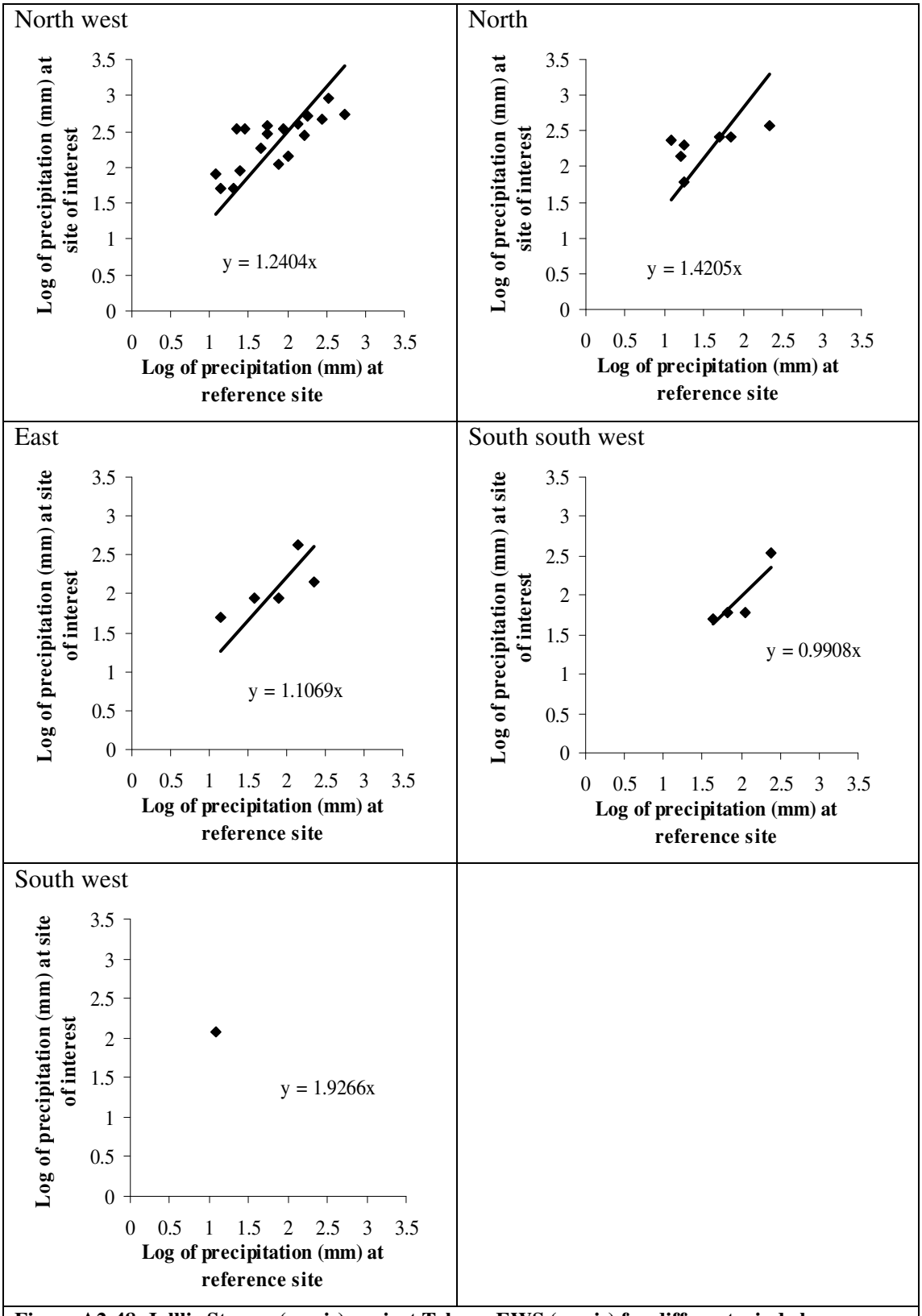

Figure A2-48. Jolllie Stream (y axis) against Tekapo EWS (x axis) for different wind classes.

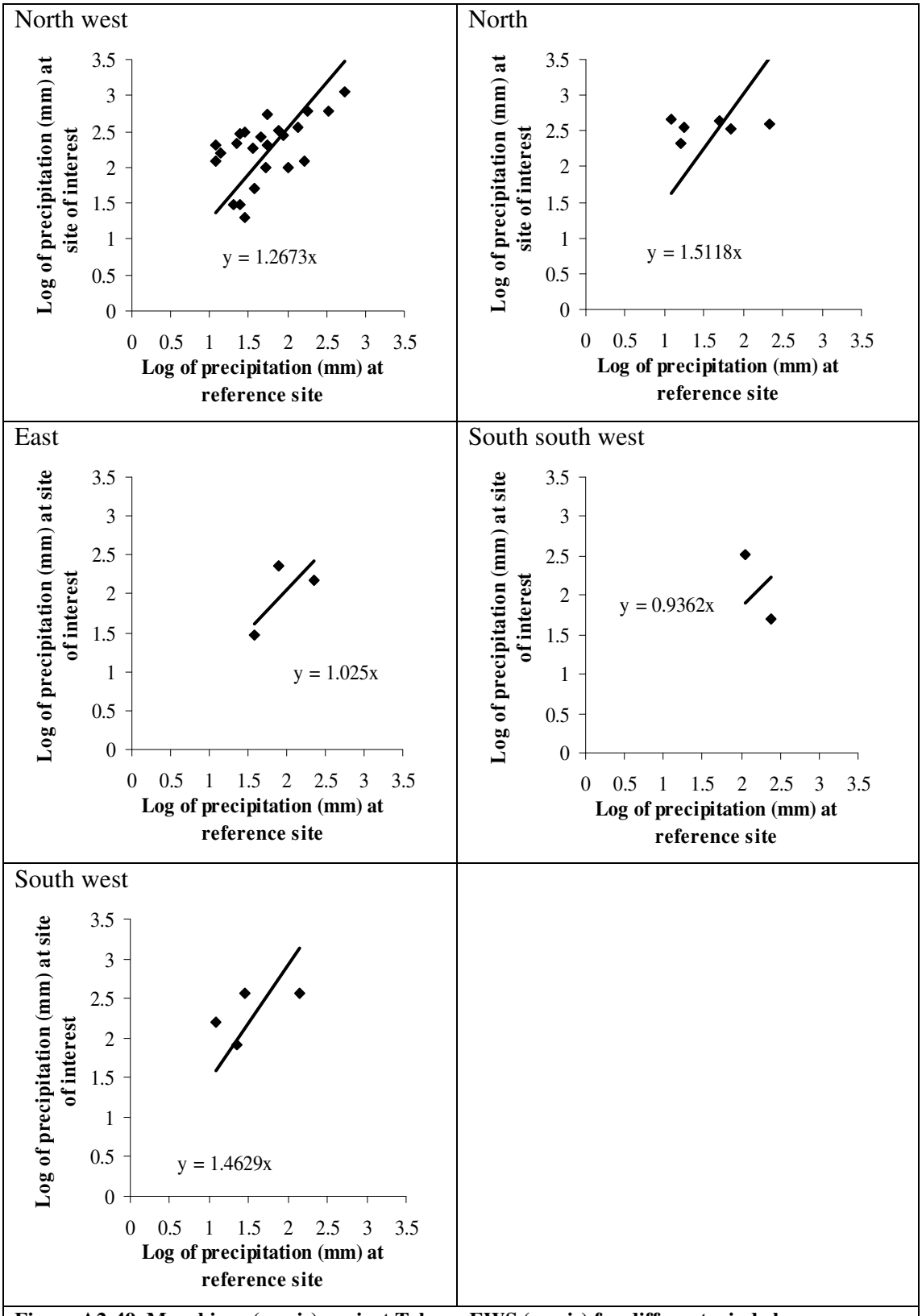

Figure A2-49. Murchison (y axis) against Tekapo EWS (x axis) for different wind classes.

North west

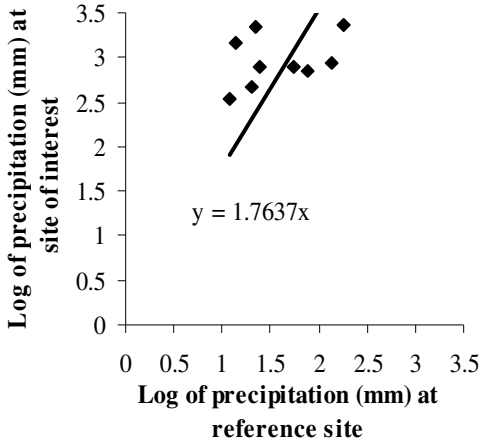

North

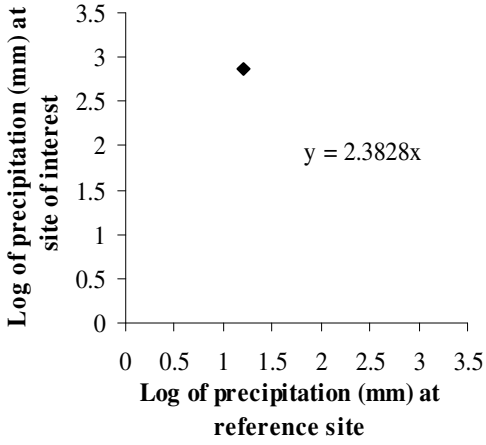

East

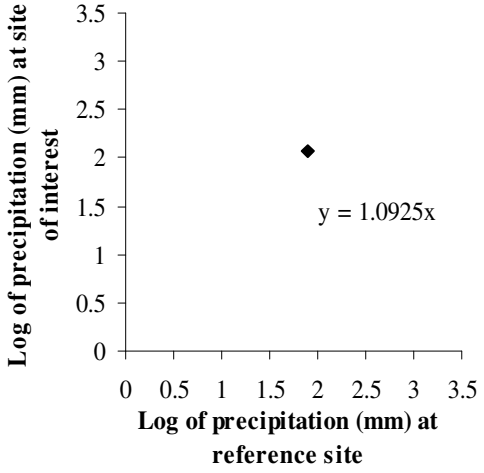

South south west

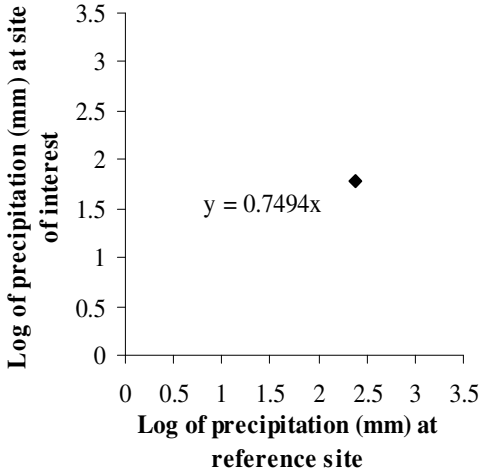

South west – *no observations*

Figure A2-50. Rudolf Glacier (y axis) against Tekapo EWS (x axis) for different wind classes.

North west

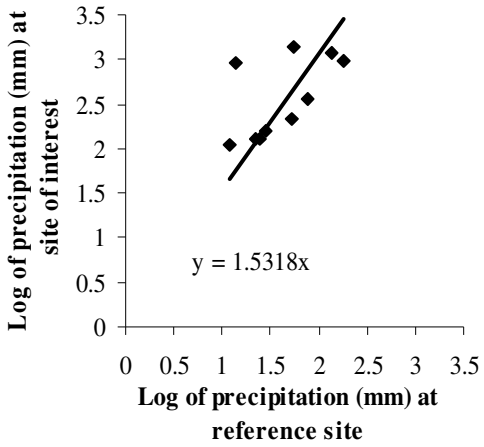

North

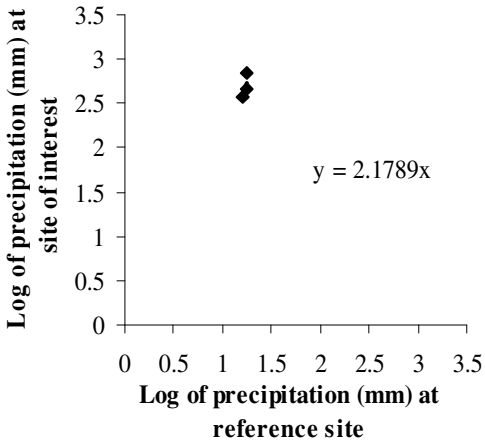

East

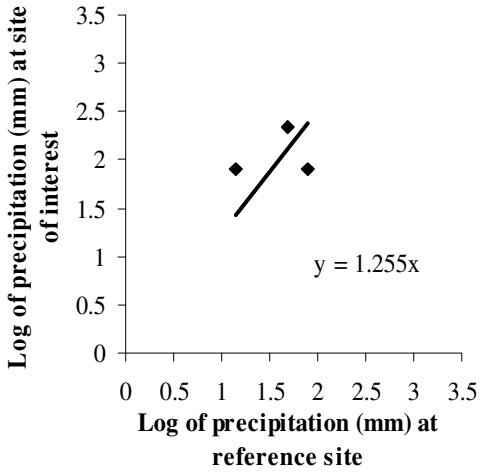

South south west – *no observations*

South west – *no observations*

Figure A2-51. East Hooker (y axis) against Tekapo EWS (x axis) for different wind classes.

North west

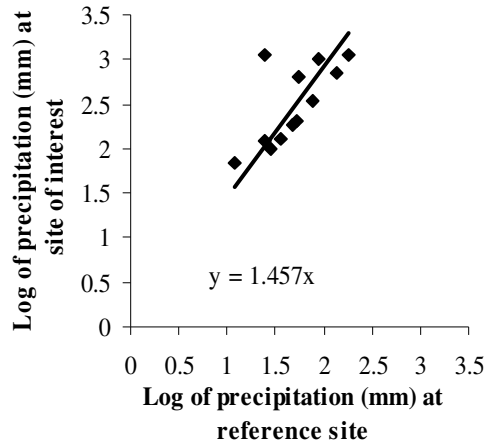

North

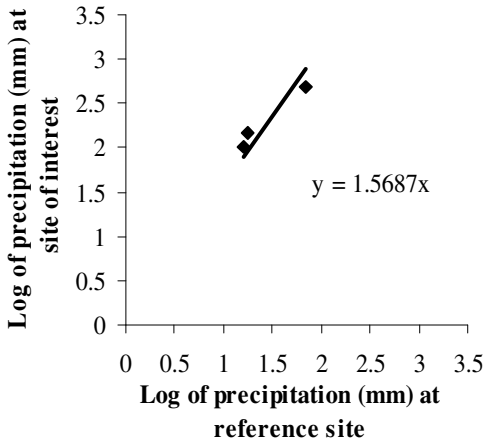

East

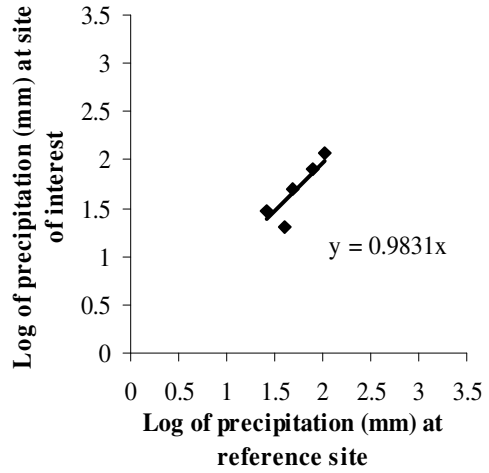

South south west – *no observation*

South west

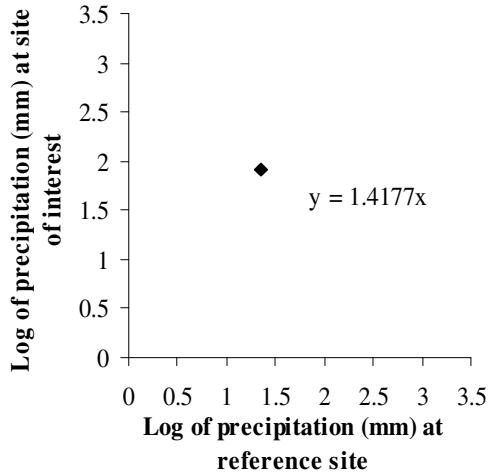

Figure A2-52. Mueller Glacier (y axis) against Tekapo EWS (x axis) for different wind classes.

North west

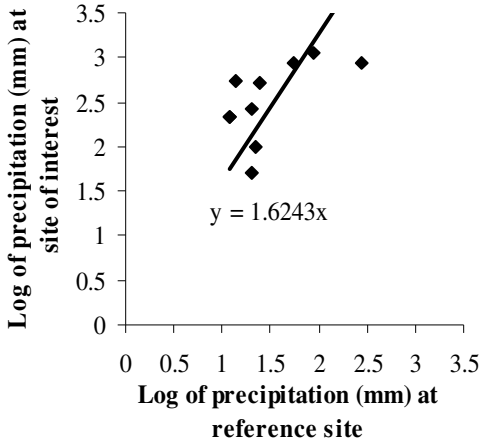

North

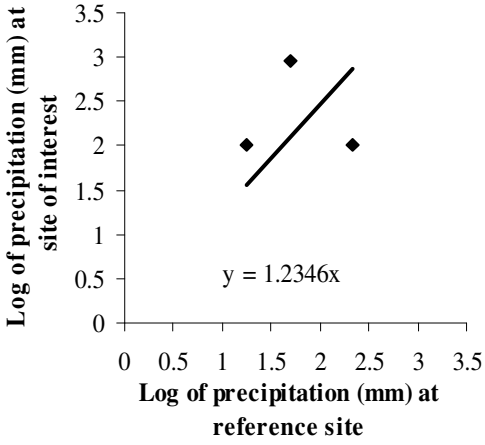

East

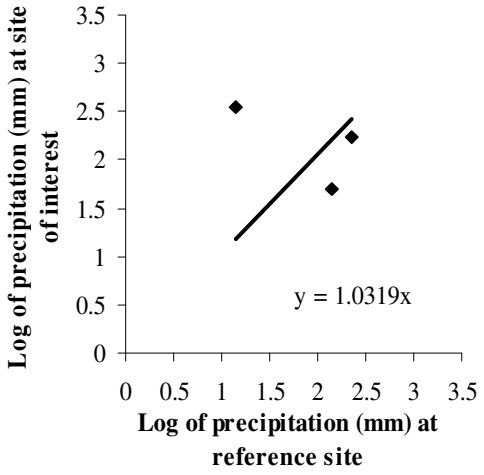

South south west

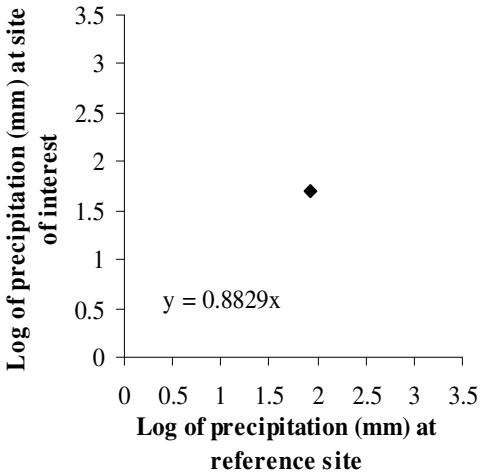

South west – *no observations*

Figure A2-53. Stocking Stream (y axis) against Tekapo EWS (x axis) for different wind classes.

North west

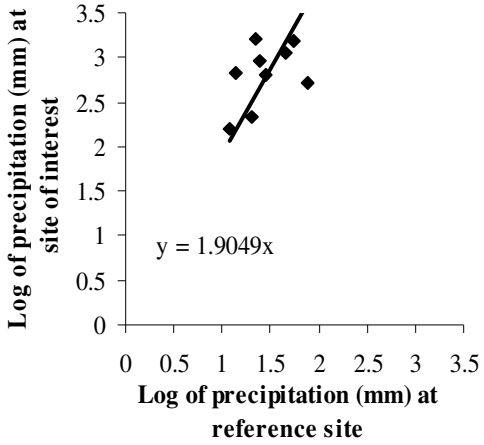

North

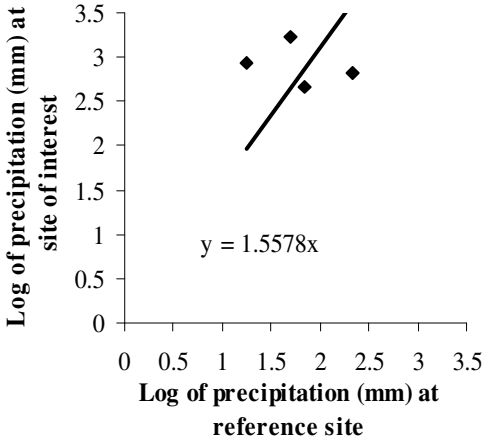

East

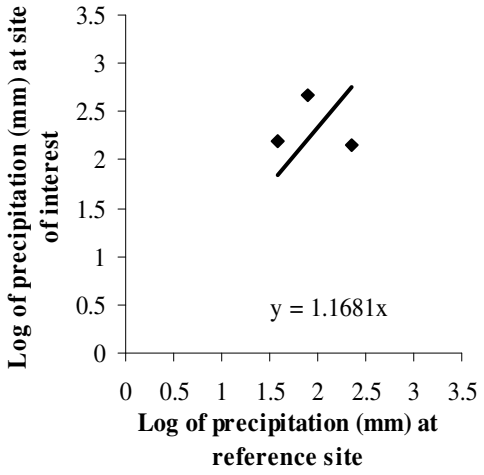

South south west

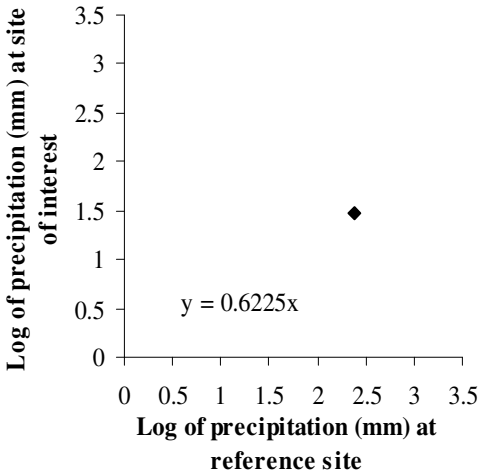

South west – *no observations*

Figure A2-54. Tasman Glacier (y axis) against Tekapo EWS (x axis) for different wind classes.

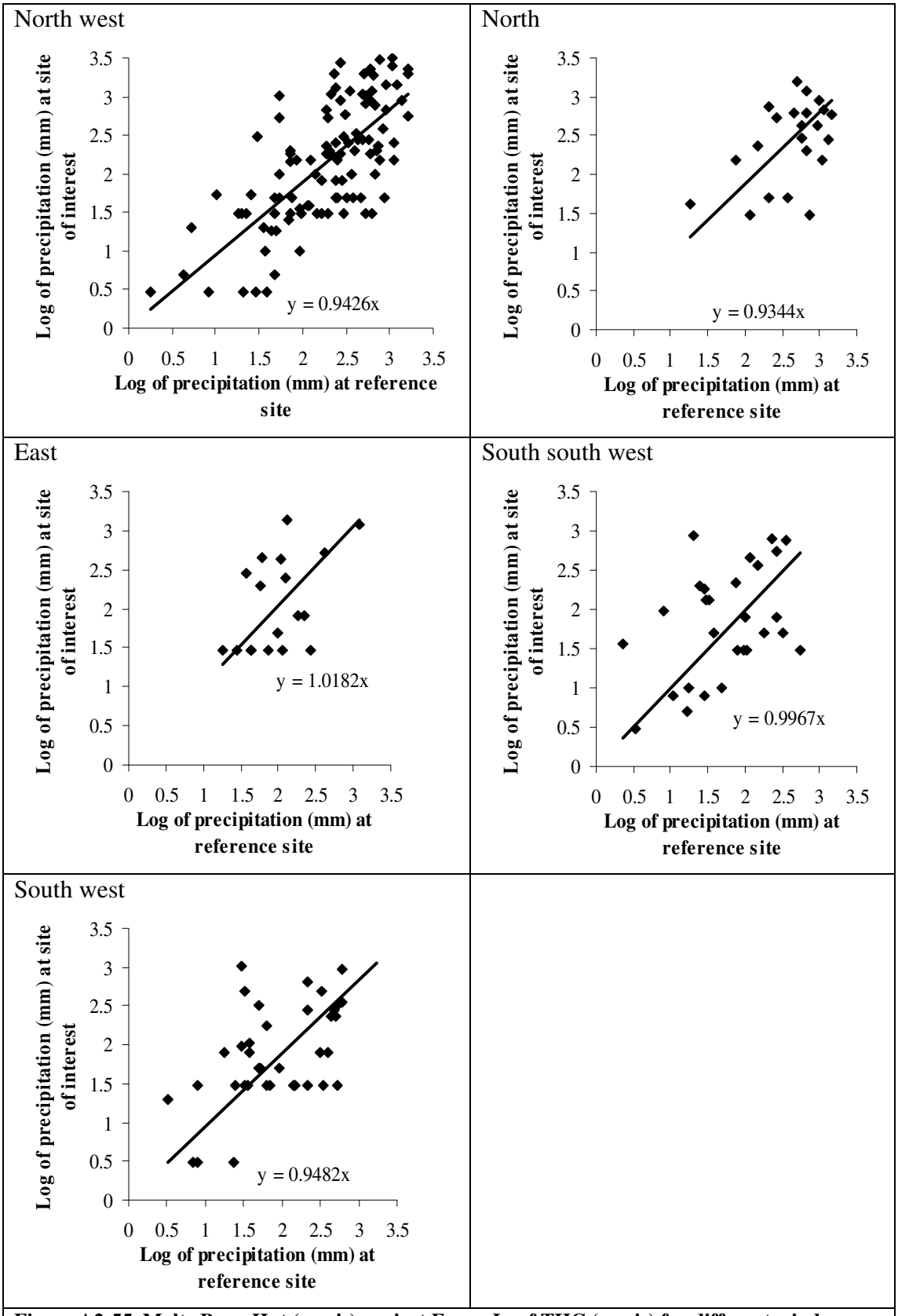

Figure A2-55. Malte Brun Hut (y axis) against Franz Josef THC (x axis) for different wind classes.

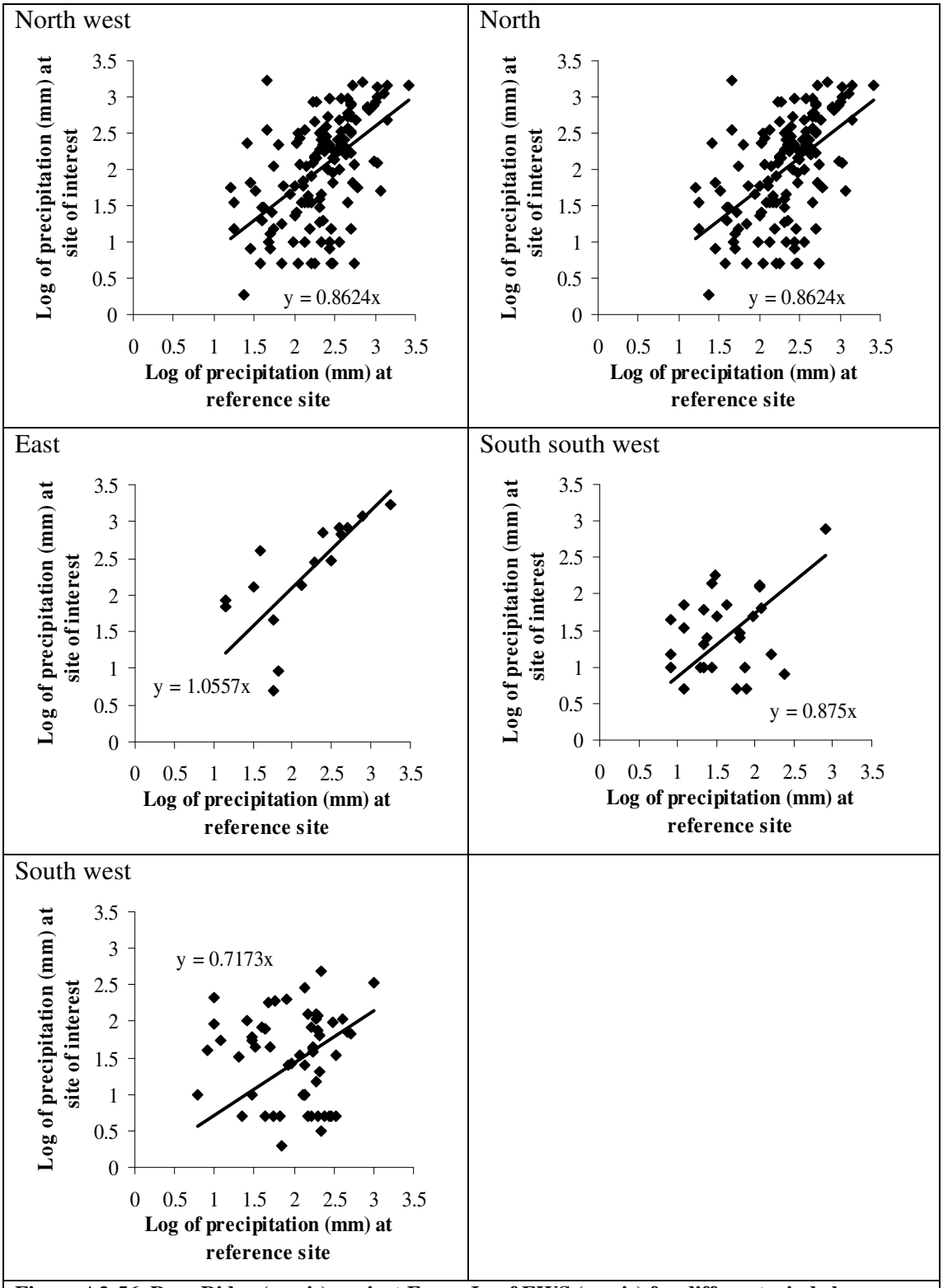

Figure A2-56. Rose Ridge (y axis) against Franz Josef EWS (x axis) for different wind classes.

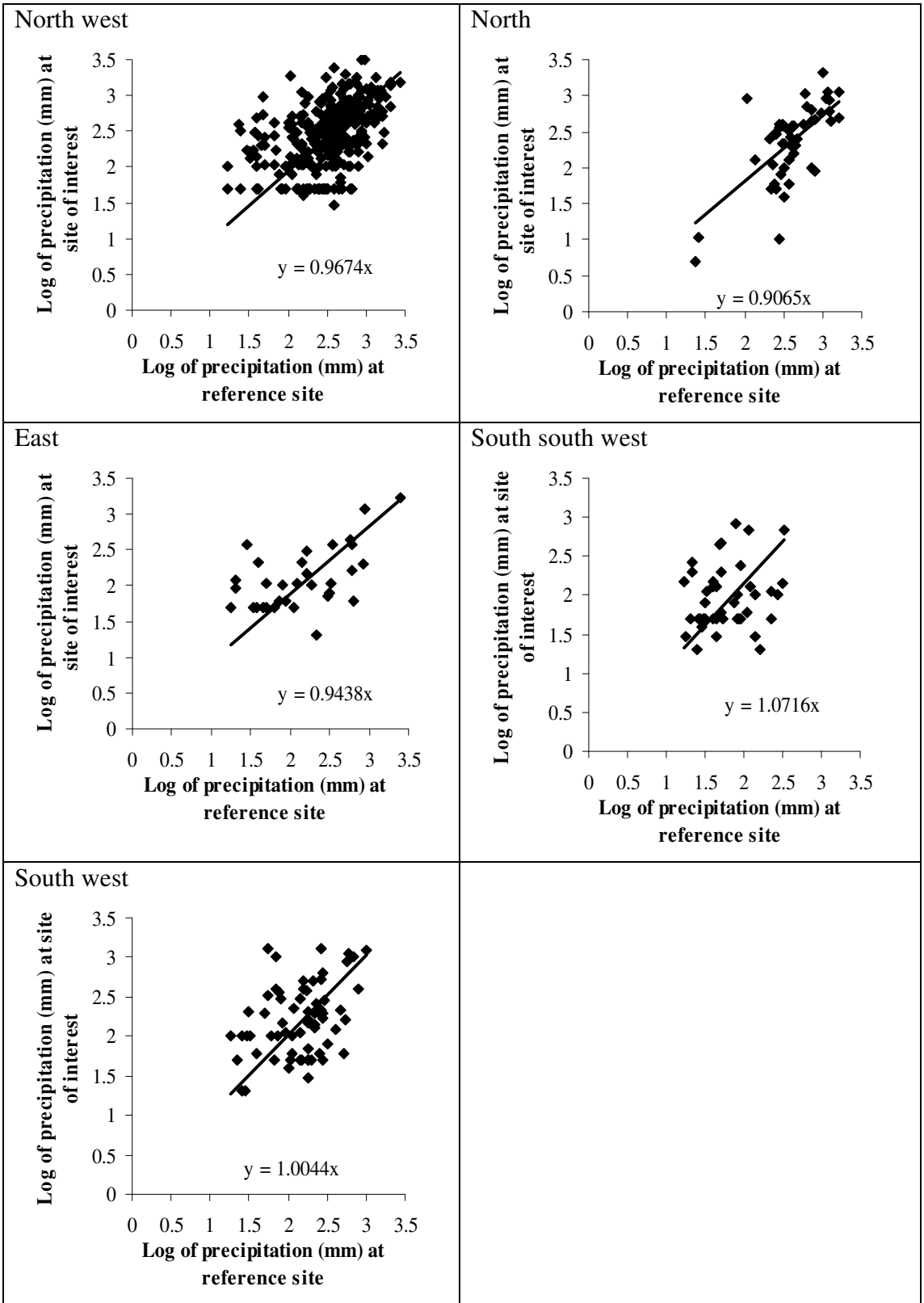

Figure A2-57. Ball Hut (y axis) against Franz Josef THC (x axis) for different wind classes.

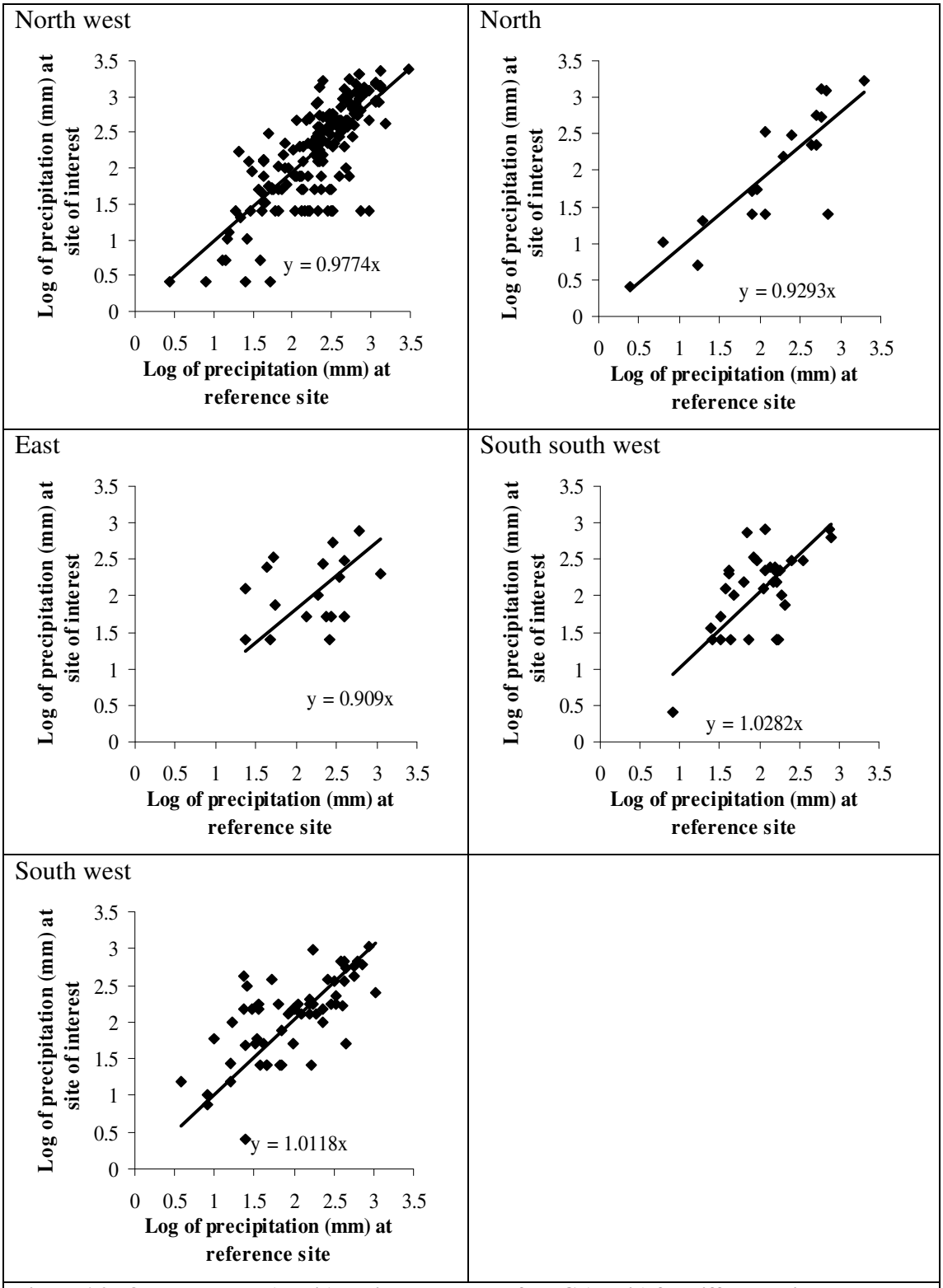

Figure A2-58. Hooker Hut (y axis) against Franz Josef THC (x axis) for different wind classes.

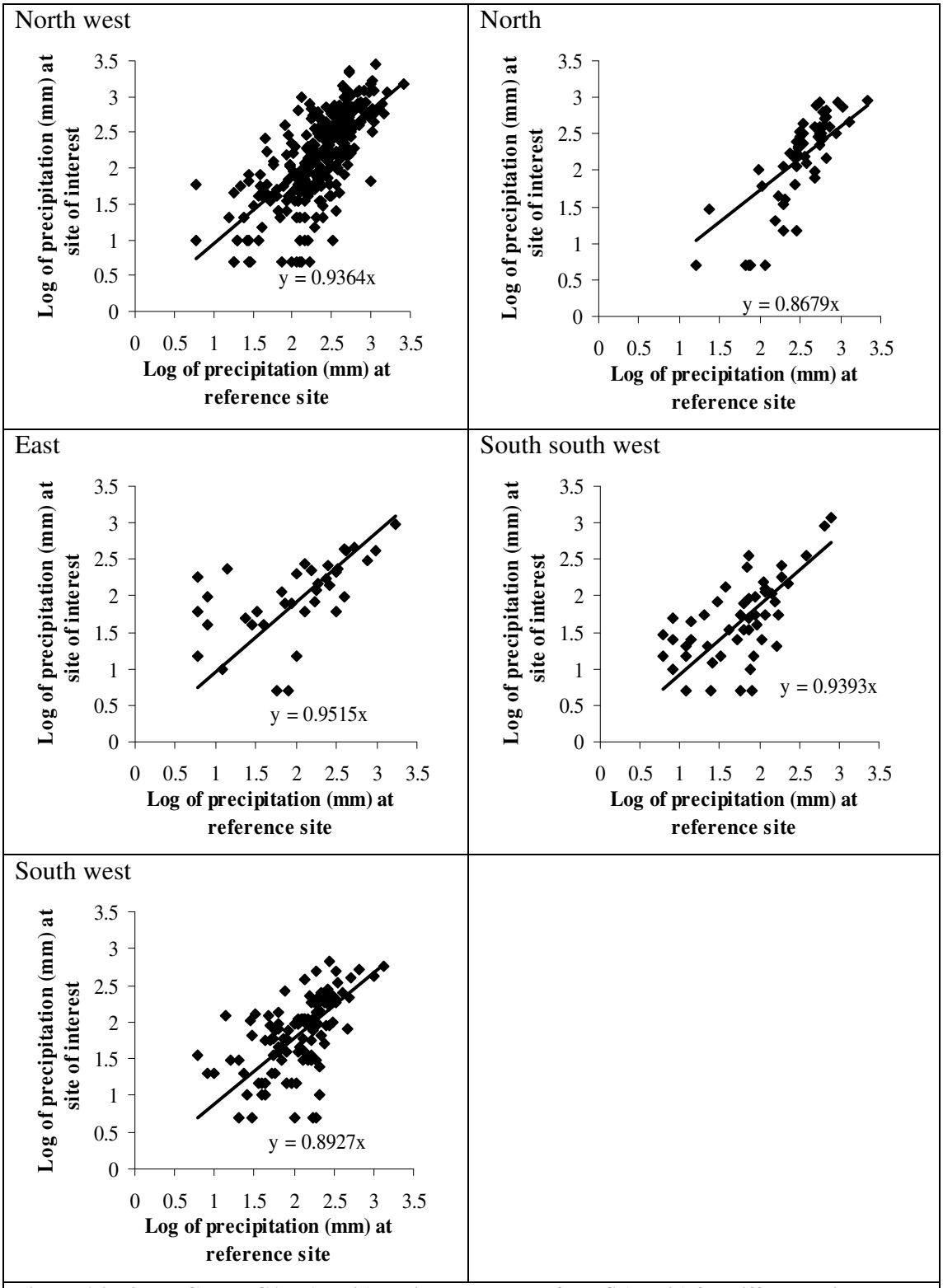

Figure A2-59. Mt Cook ECAN (y axis) against Franz Josef EWS (x axis) for different wind classes.

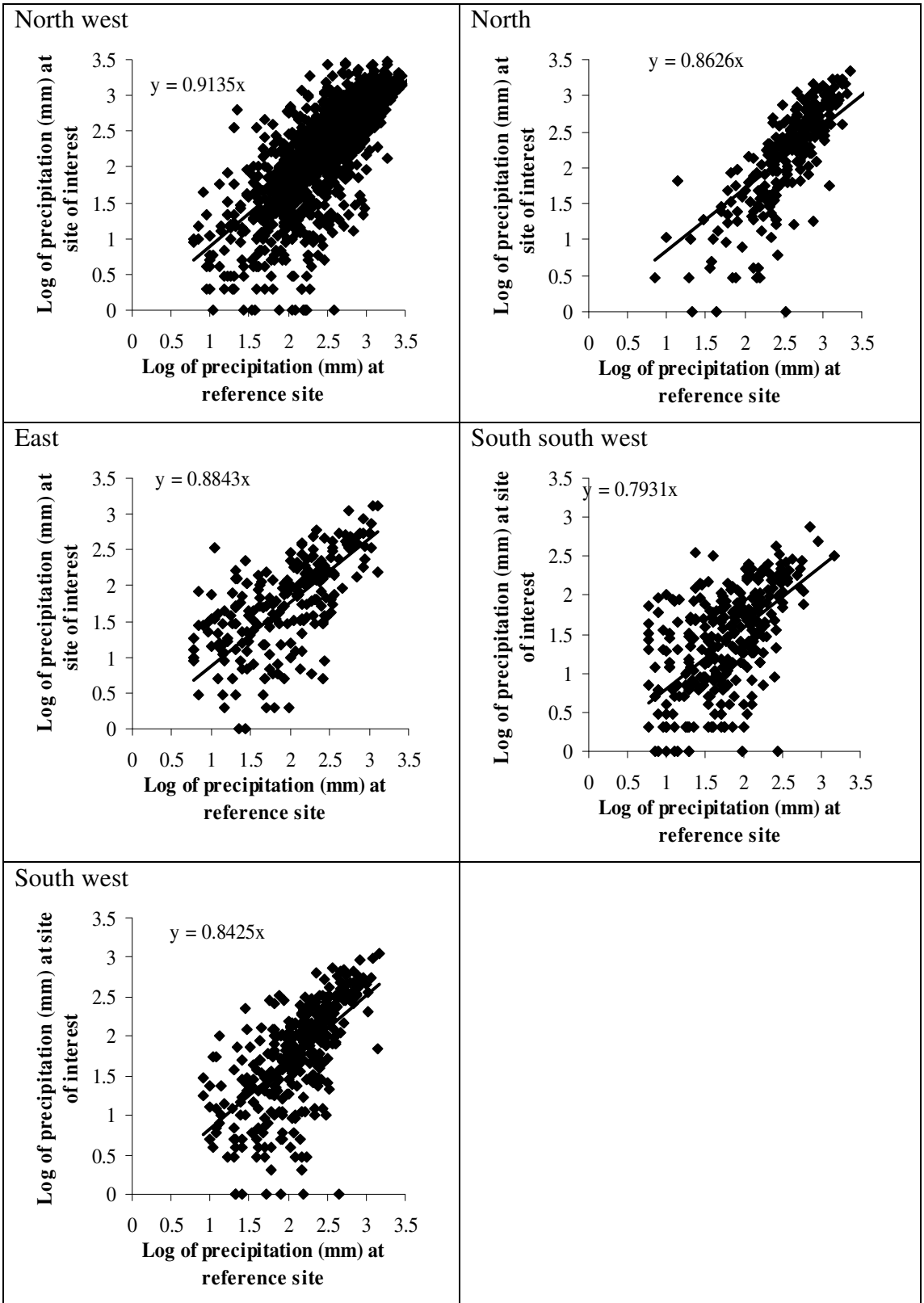

Figure A2-60. The Hermitage (y axis) against Franz Josef Manual (x axis) for different wind classes.

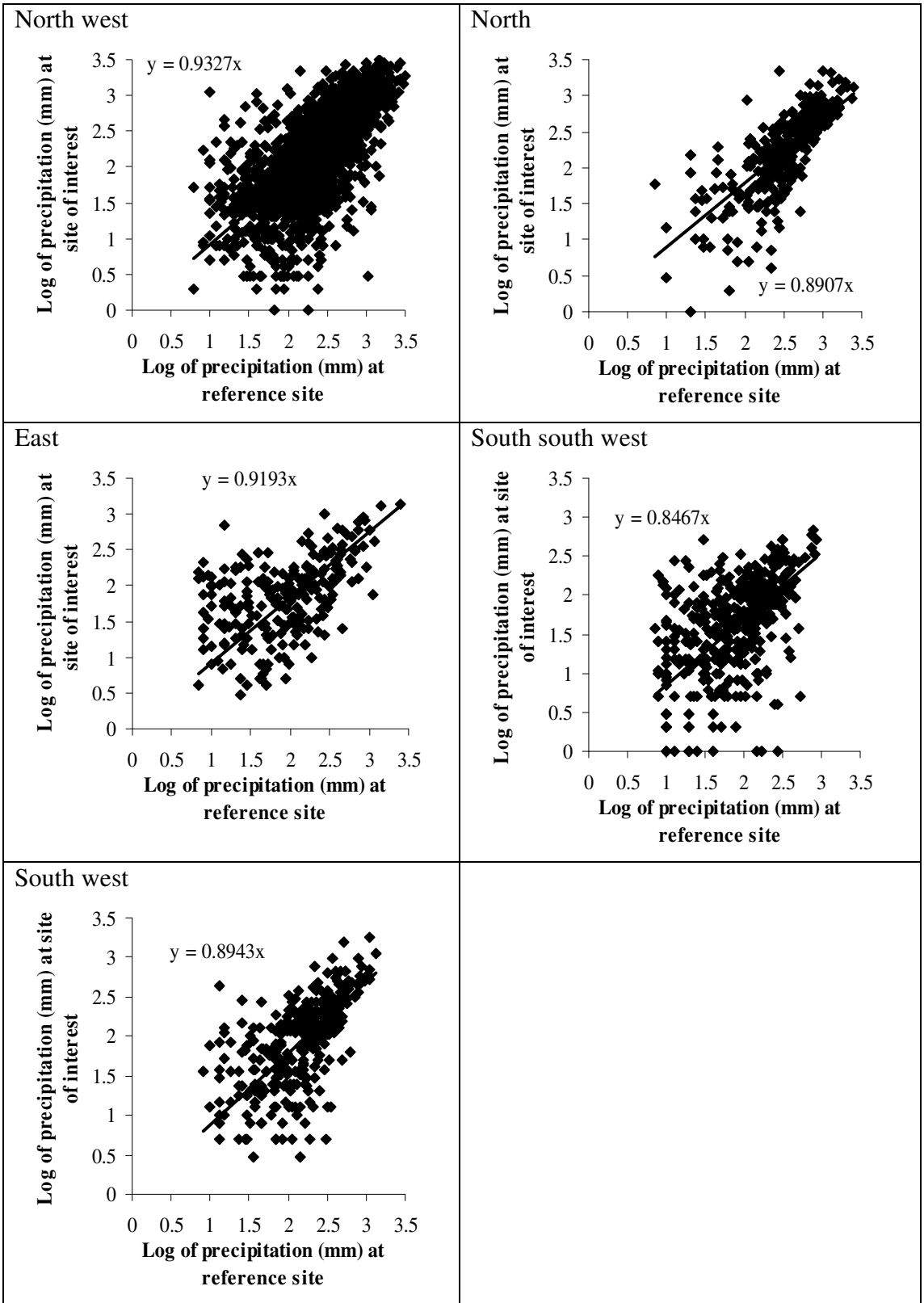

Figure A2-61. The Hermitage (y axis) against Franz Josef THC (x axis) for different wind classes.

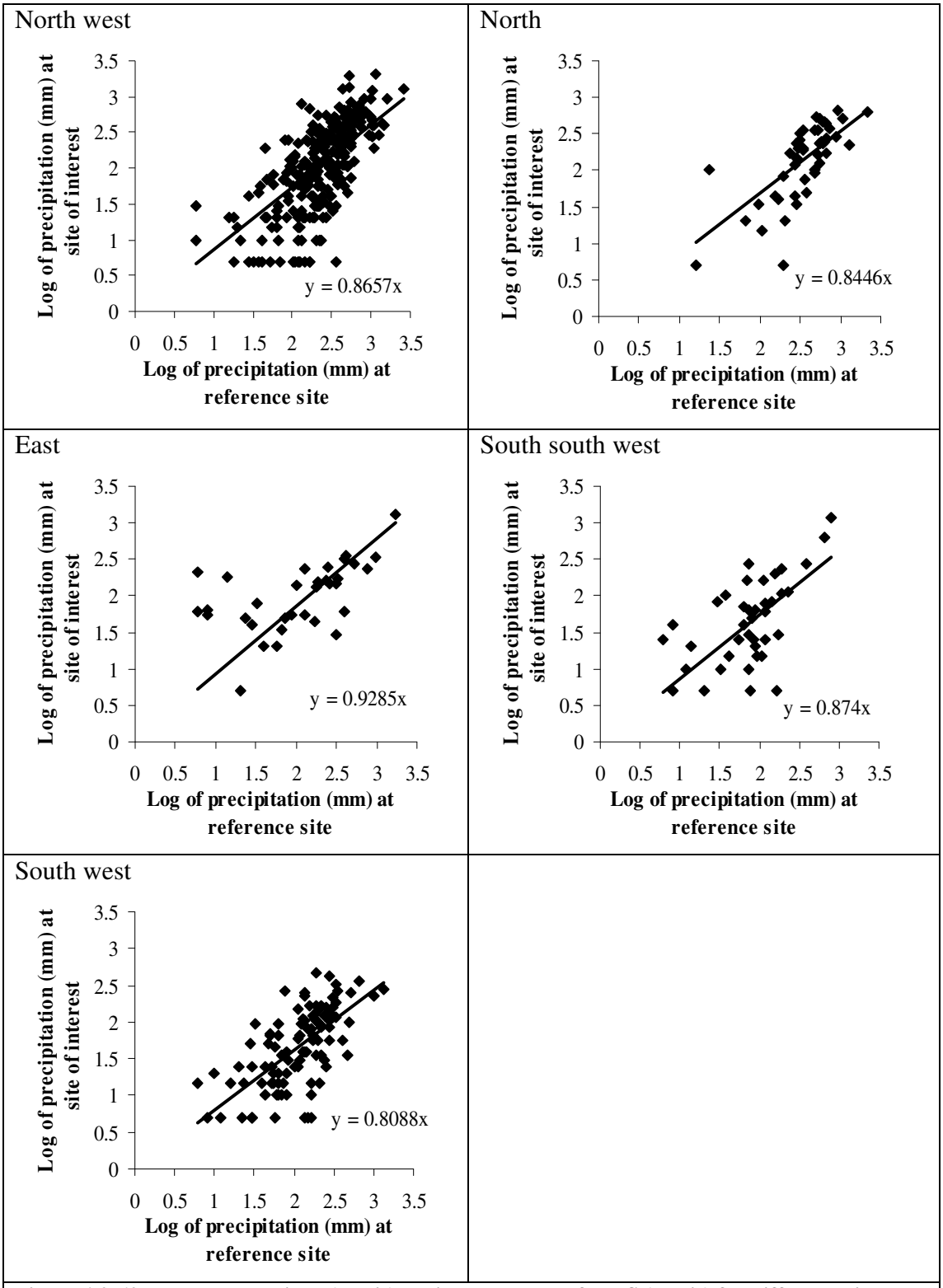

Figure A2-62. Hooker Rd Bridge (y axis) against Franz Josef EWS (x axis) for different wind classes.

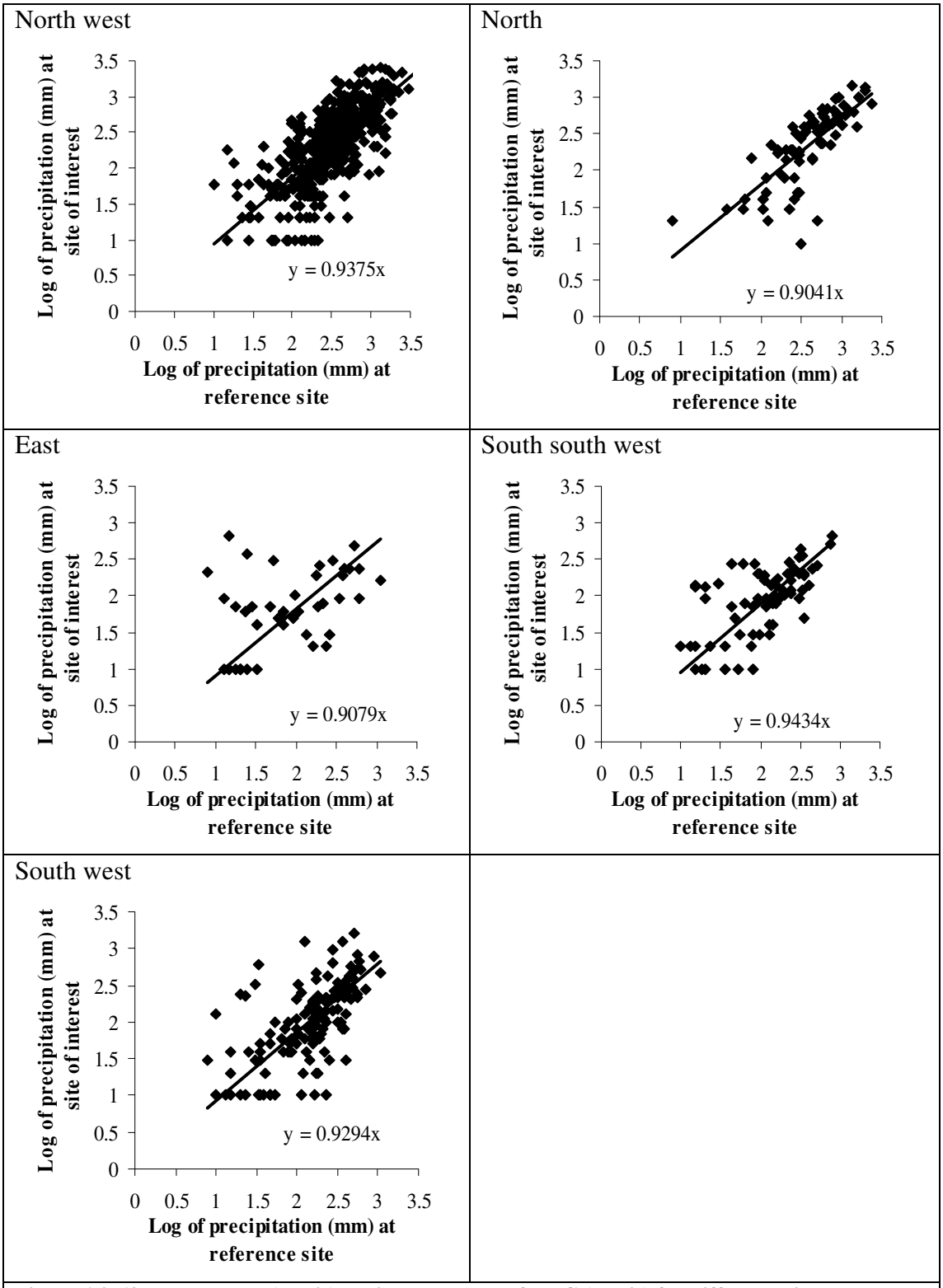

Figure A2-63. Hooker Flat (y axis) against Franz Josef THC (x axis) for different wind classes.

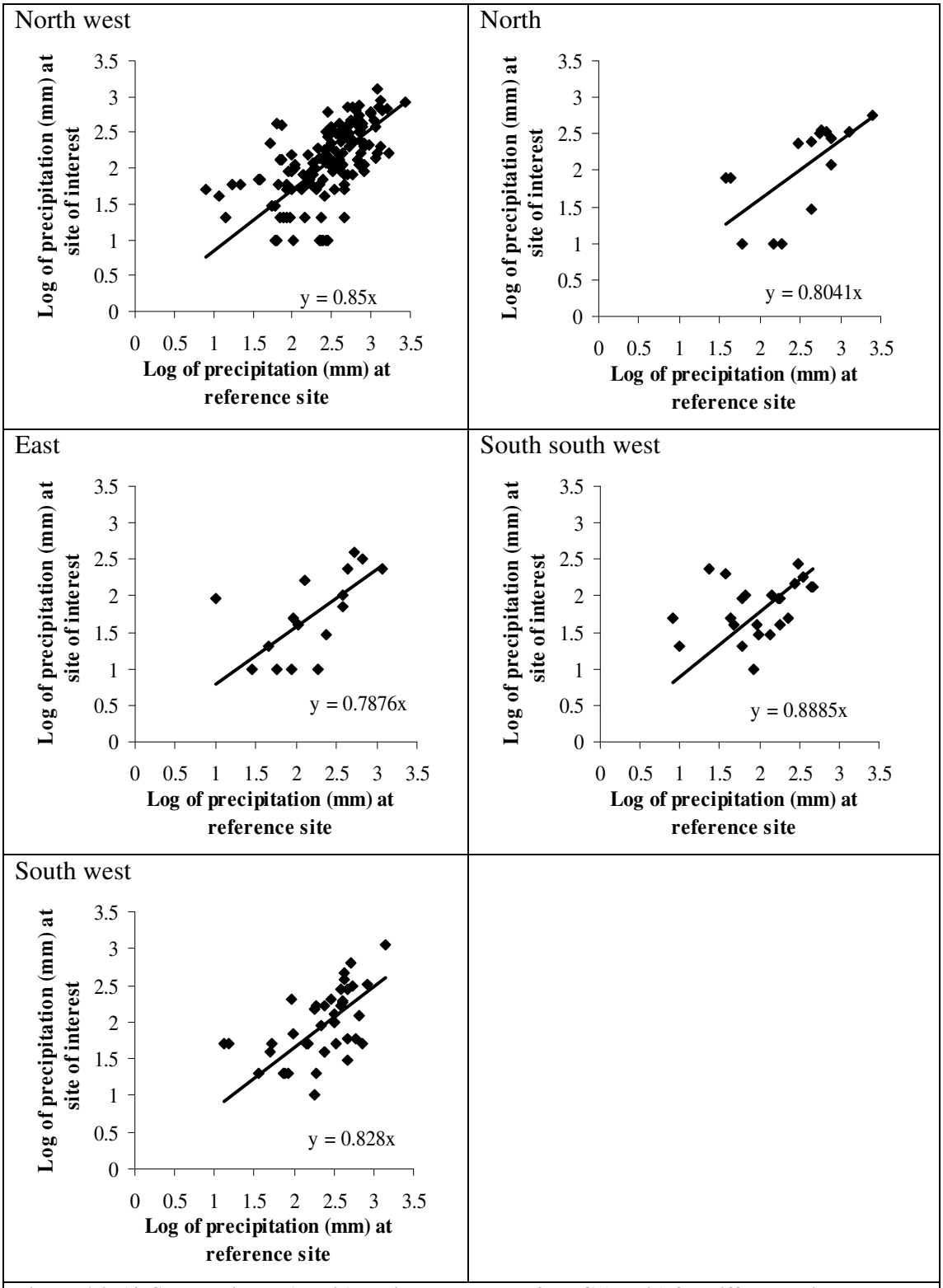

Figure A2-64. Sealey Village (y axis) against Franz Josef THC (x axis) for different wind classes.

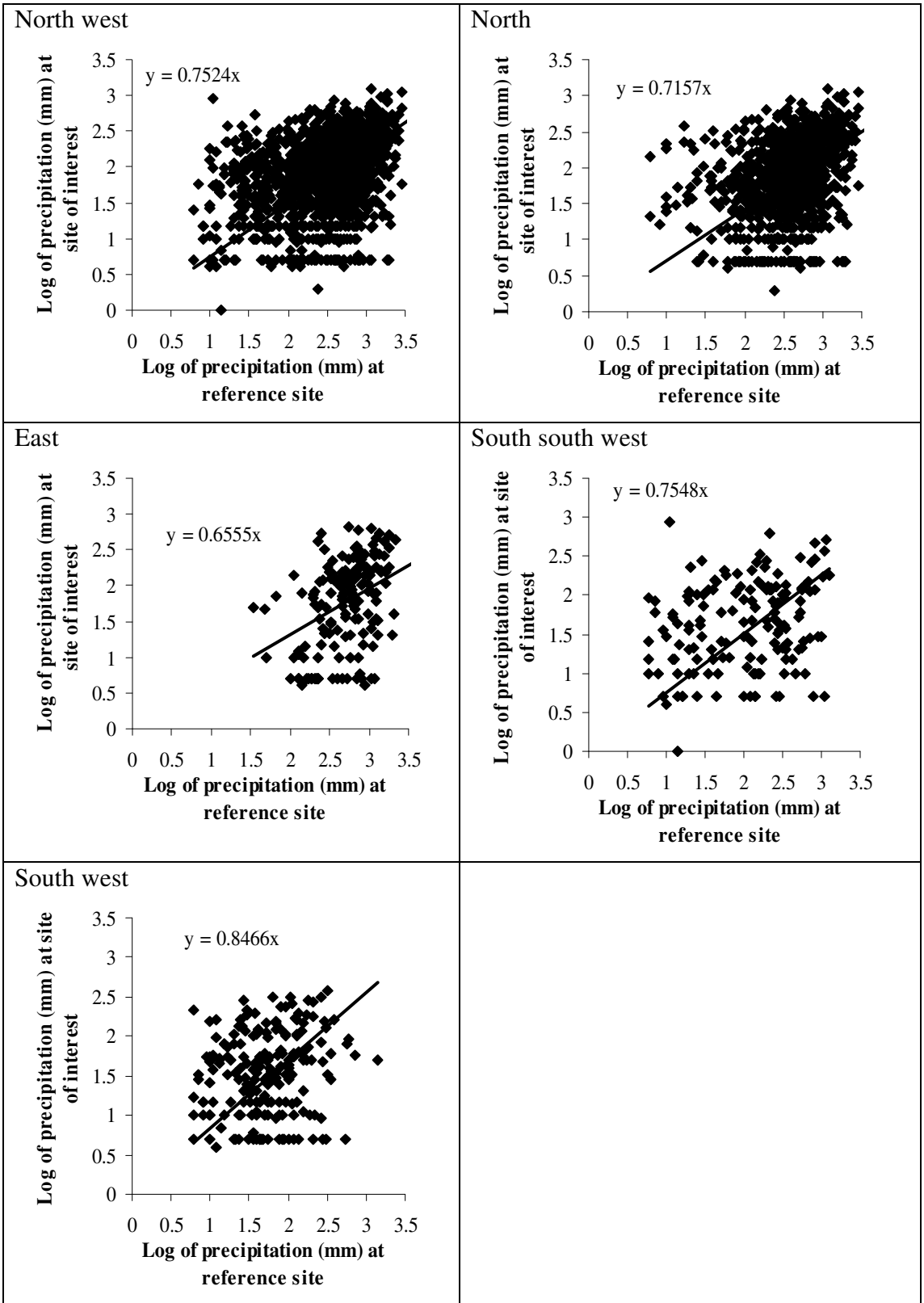

Figure A2-65. Jollie Hut (y axis) against Franz Josef Manual (x axis) for different wind classes.

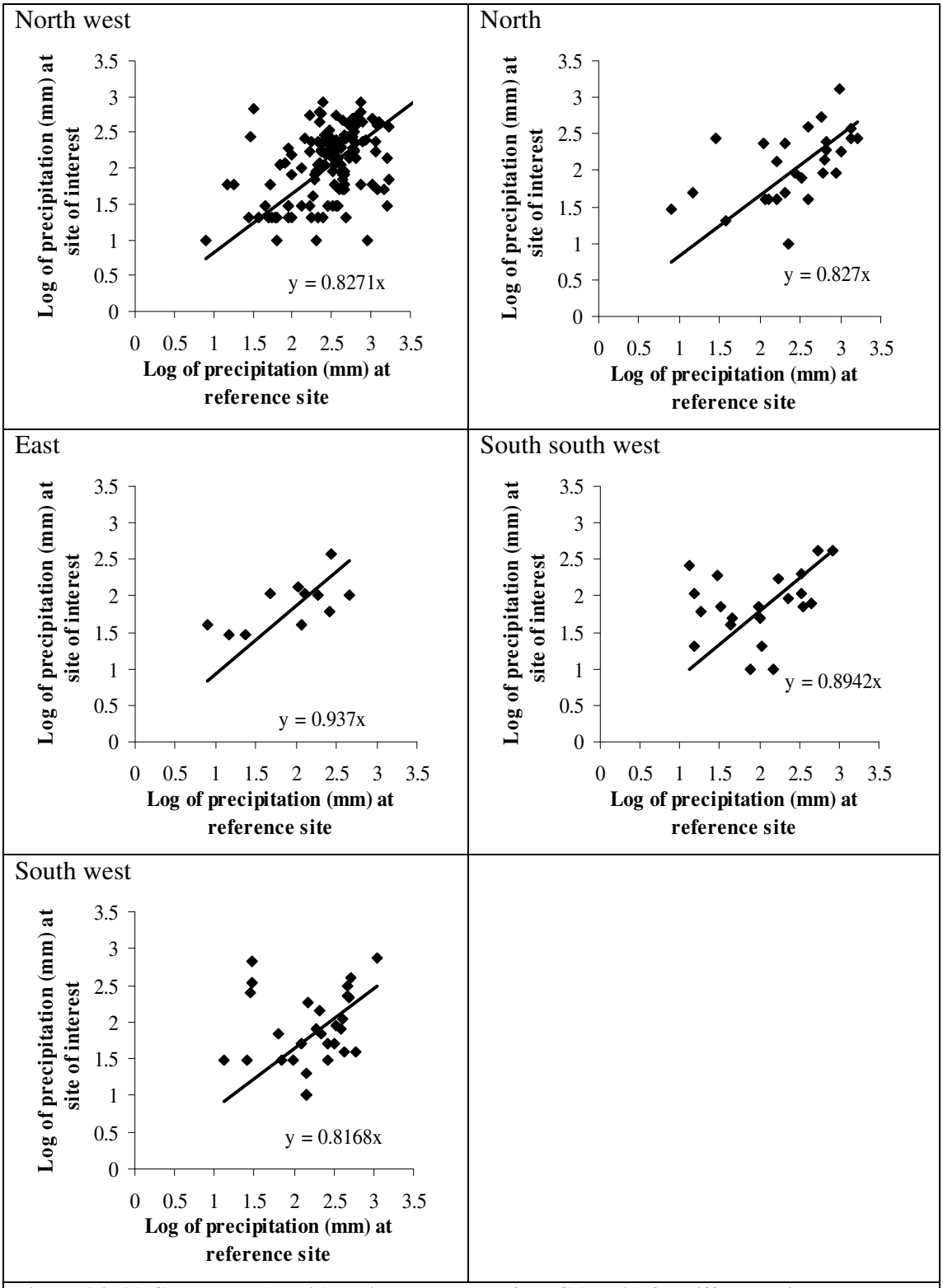

Figure A2-66. Glentanner (y axis) against Franz Josef THC (x axis) for different wind classes.

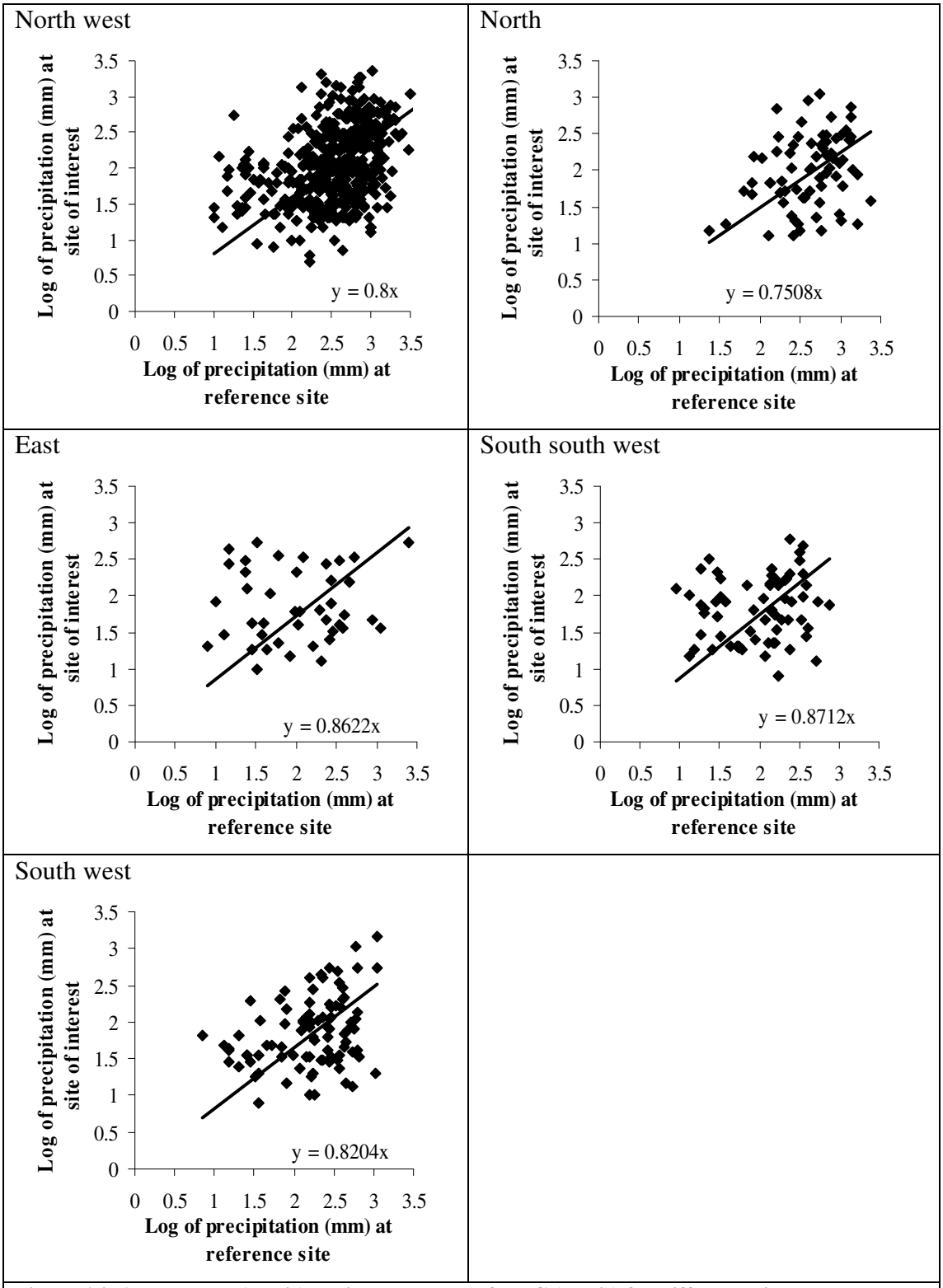

Figure A2-67. The Rest (y axis) against Franz Josef THC (x axis) for different wind classes.

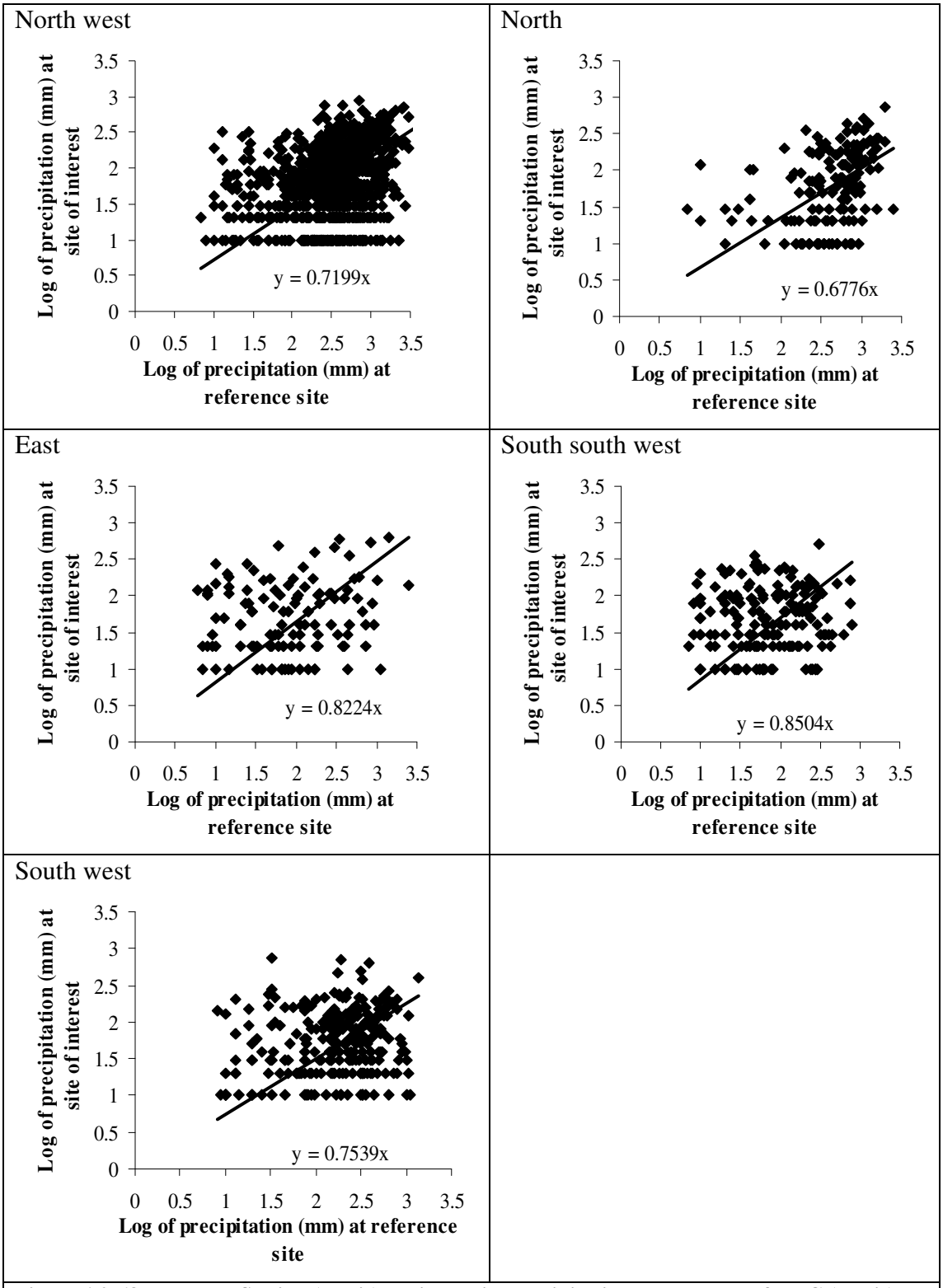

Figure A2-68. Braemar Station (y axis) against daily precipitation at Franz Josef THC (x axis) for different wind classes.

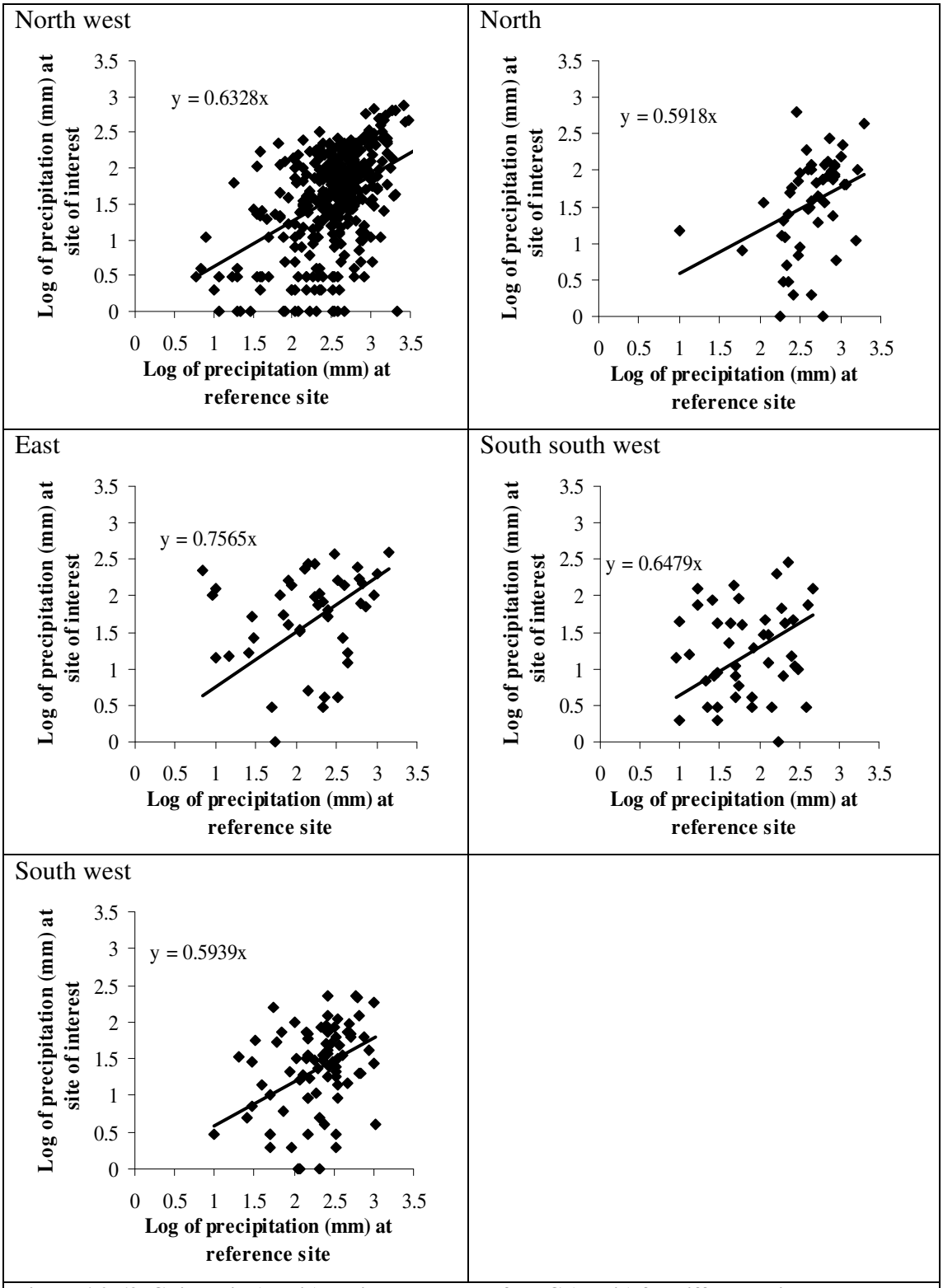

Figure A2-69. Guide Hill (y axis) against Franz Josef THC (x axis) for different wind classes.

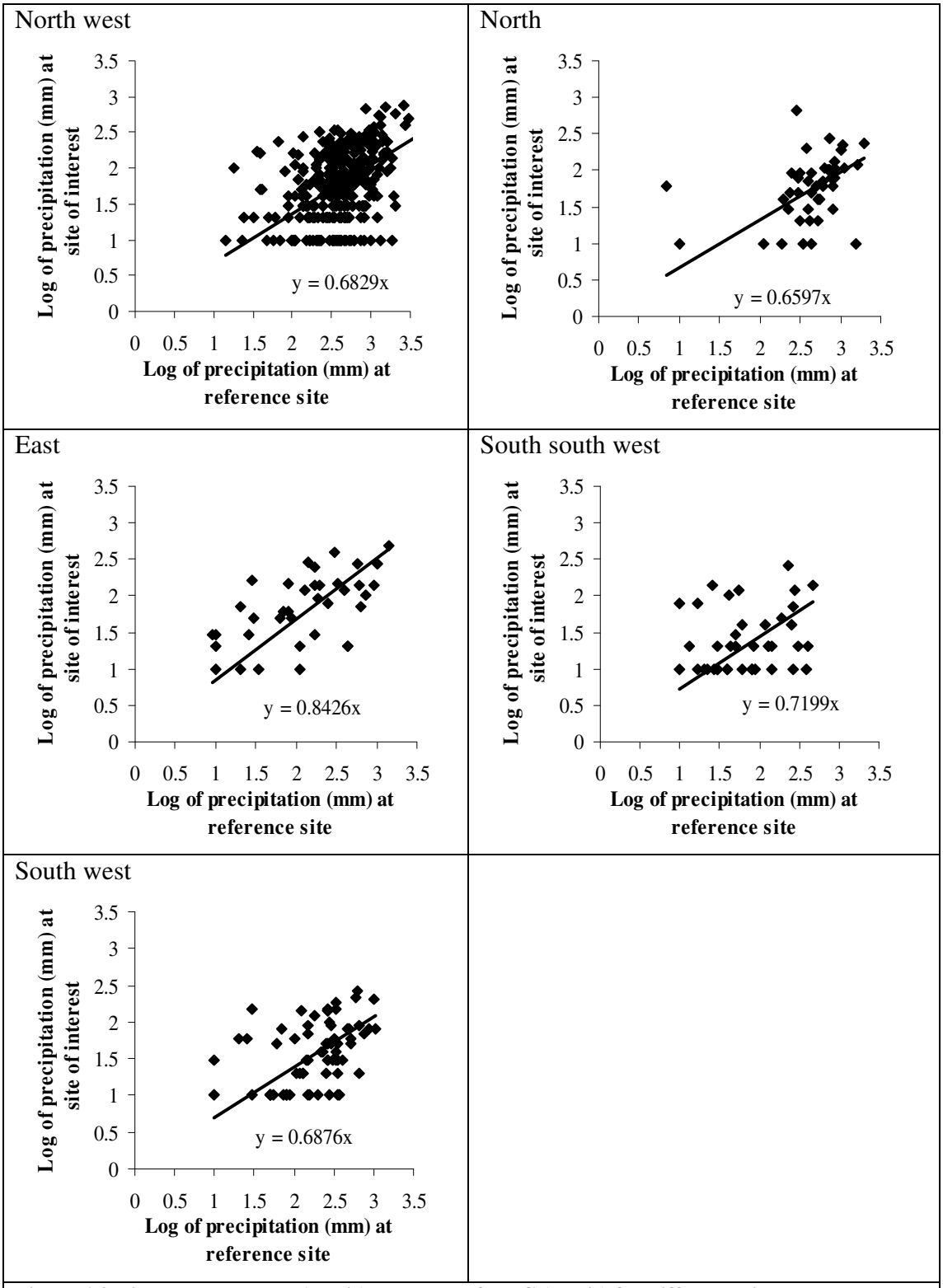

Figure A2-70. Tasman Downs (y axis) Franz Josef THC (x axis) for different wind classes.

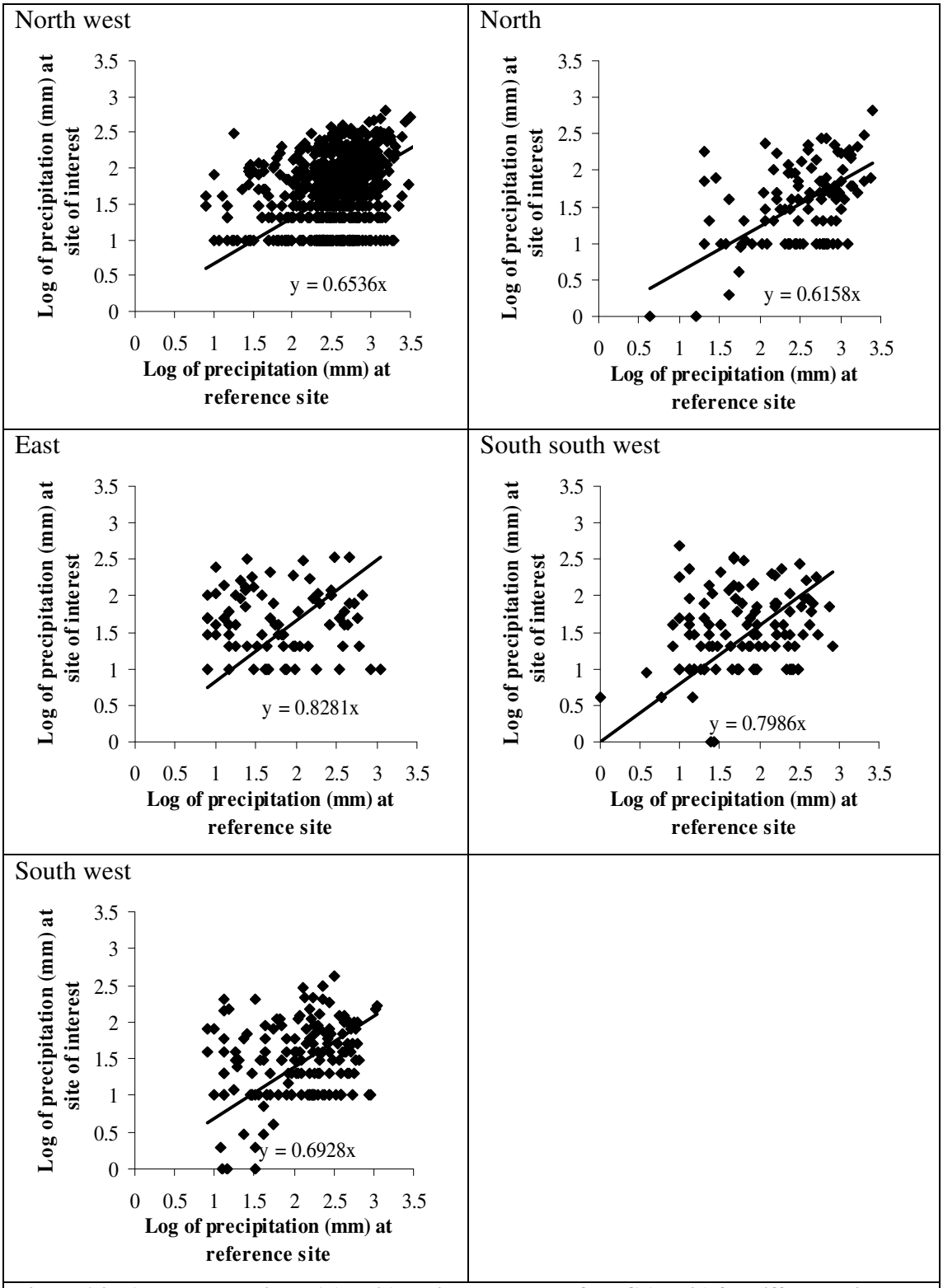

Figure A2-71. Lake Pukaki No. 1 (y axis) against Franz Josef THC (x axis) for different wind classes.

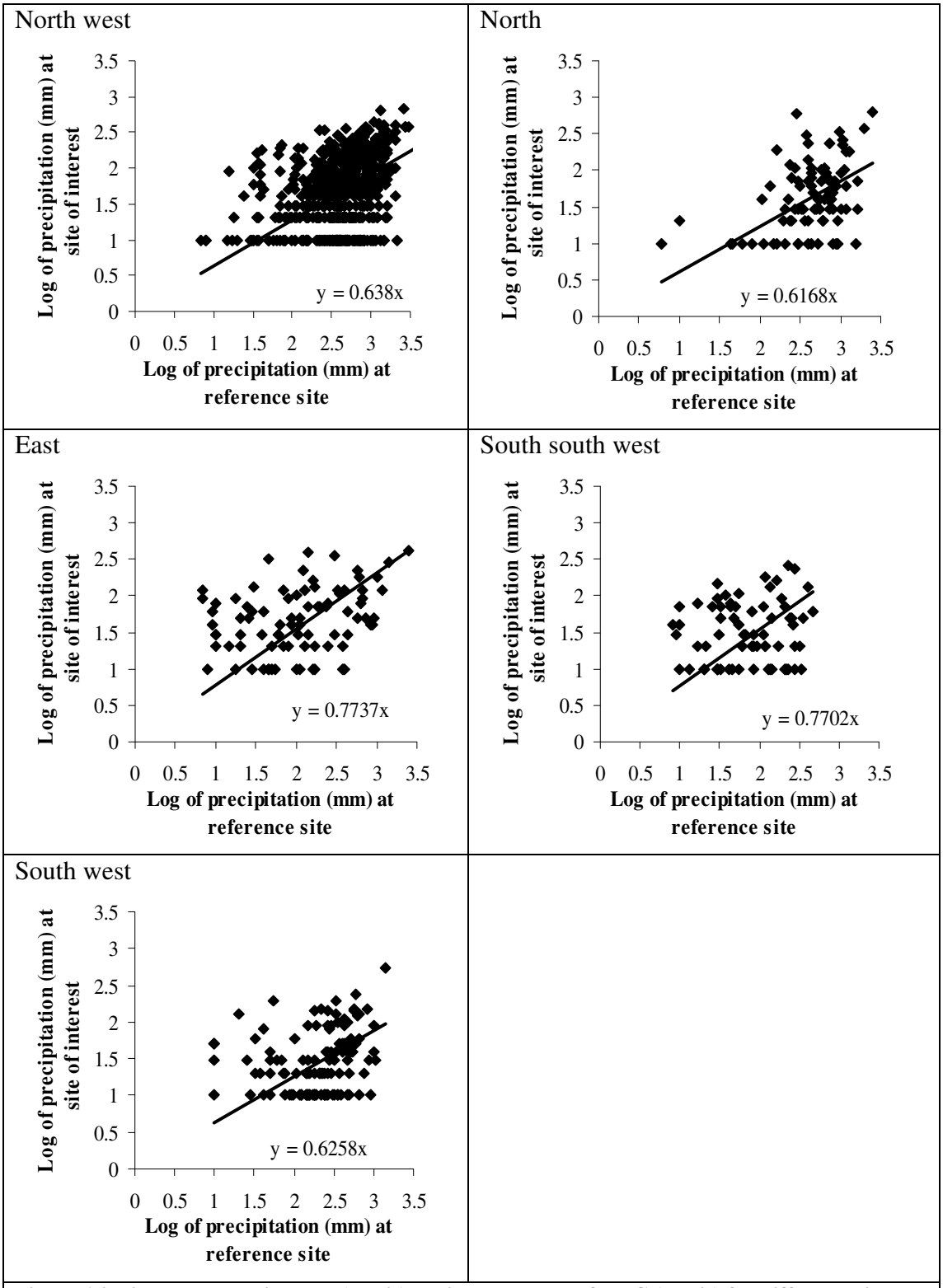

Figure A2-72. Lake Pukaki MWD (y axis) against Franz Josef THC (x axis) for different wind classes.

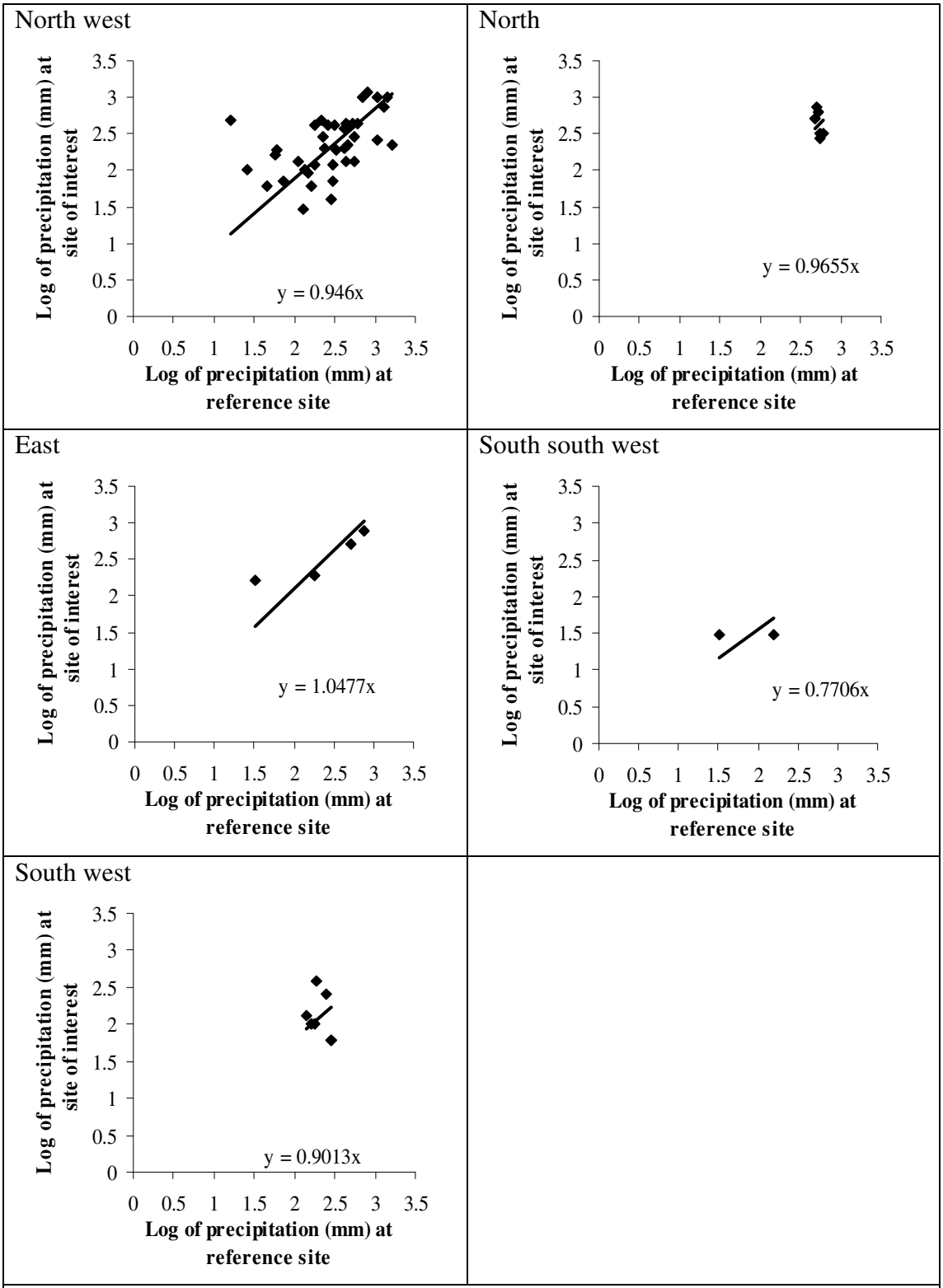

Figure A2-73. Ball Shelter (y axis) against Franz Josef EWS (x axis) for different wind classes.

North west

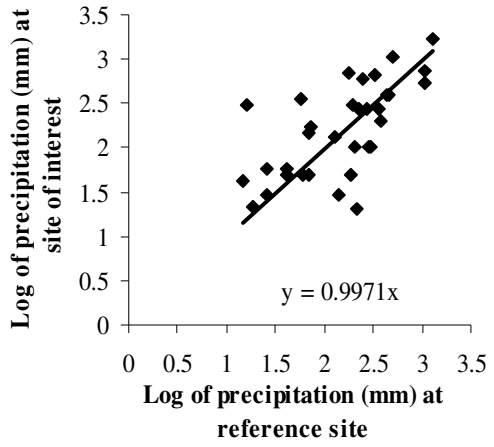

North

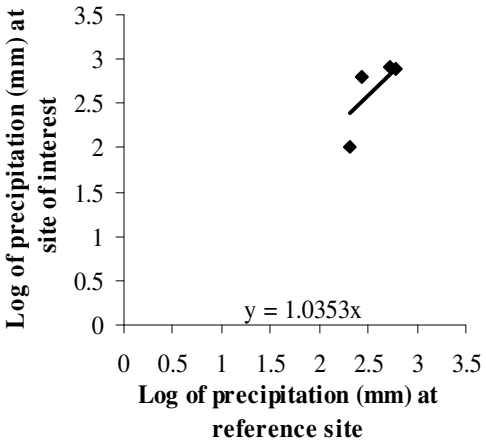

East – *no observations*

South south west

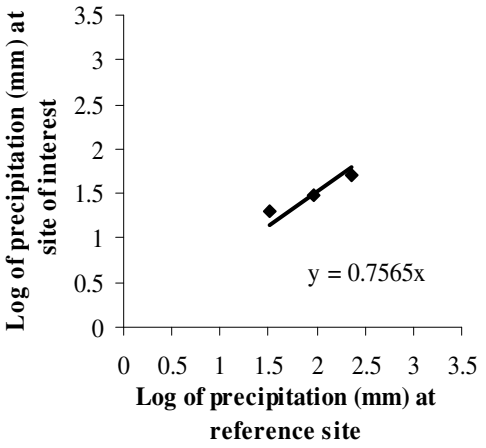

South west

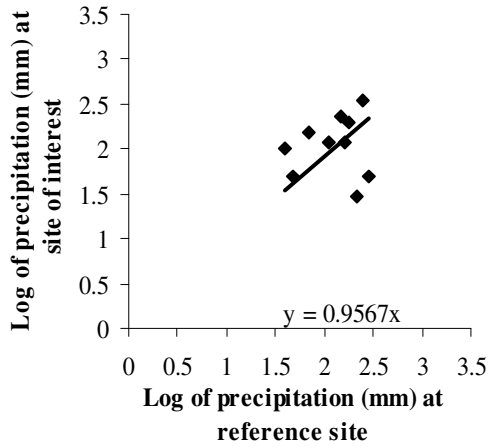

Figure A2-74. De La Beche (y axis) against Franz Josef EWS (x axis) for different wind classes.

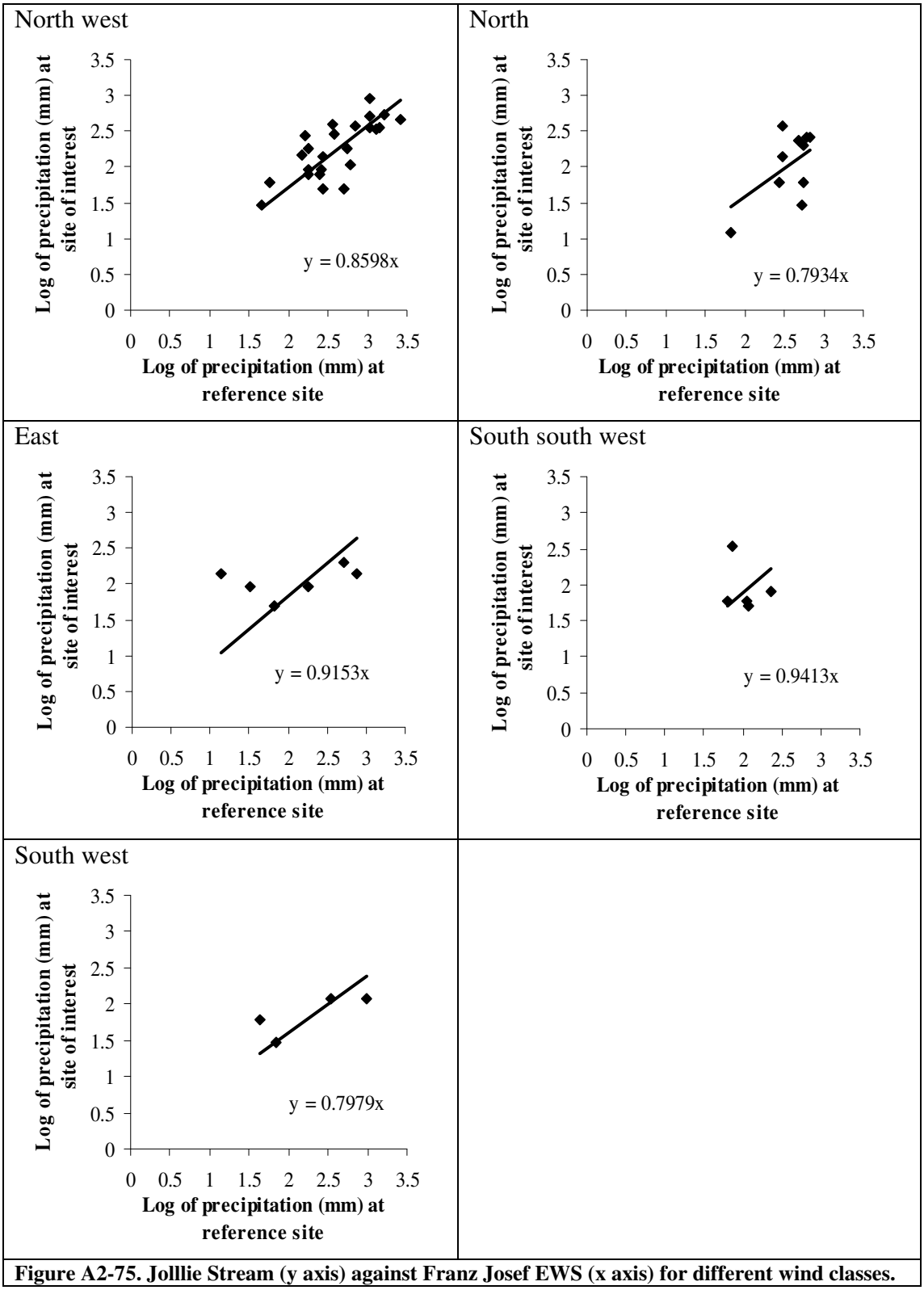

Figure A2-75. Jolllie Stream (y axis) against Franz Josef EWS (x axis) for different wind classes.

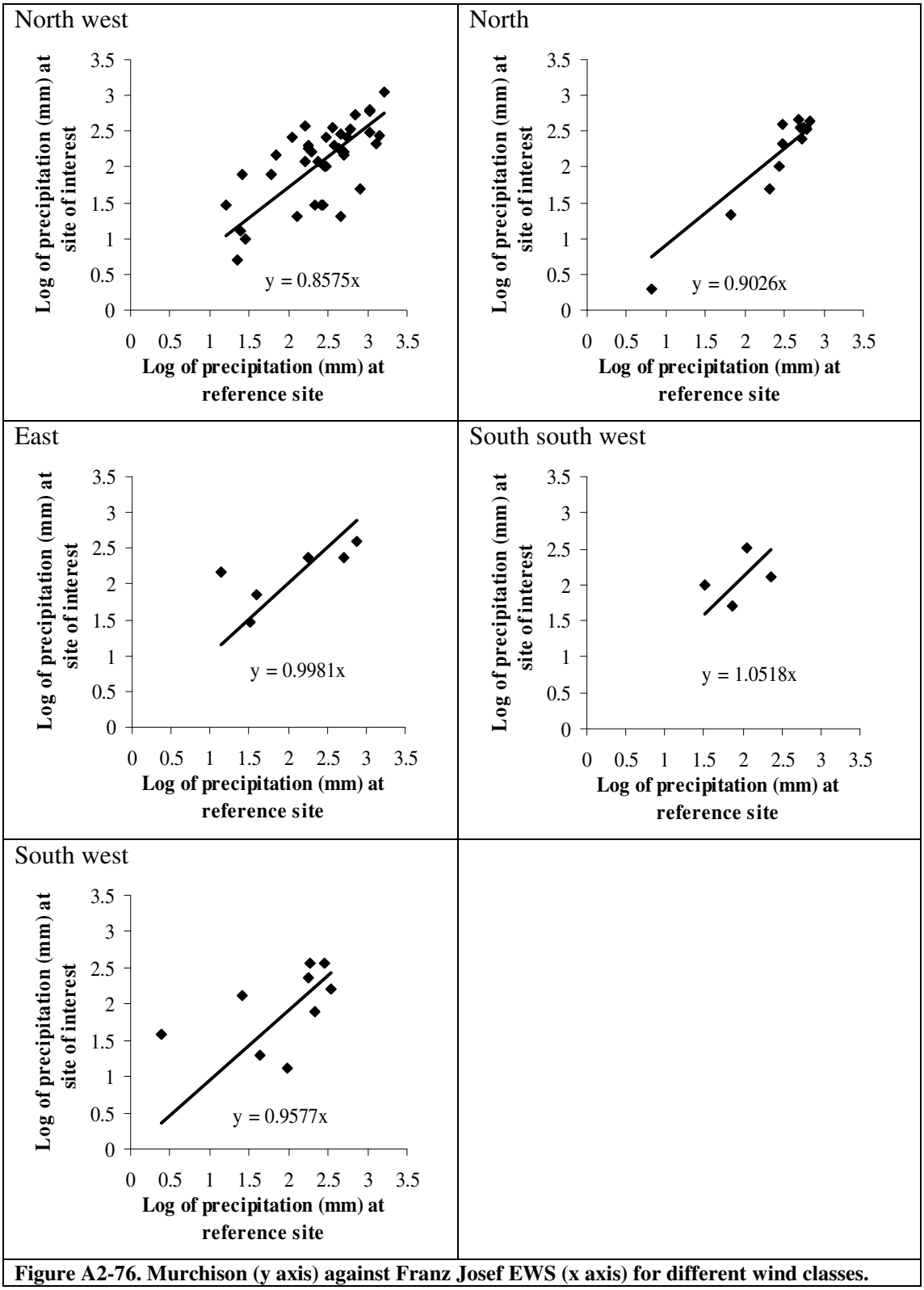

Figure A2-76. Murchison (y axis) against Franz Josef EWS (x axis) for different wind classes.

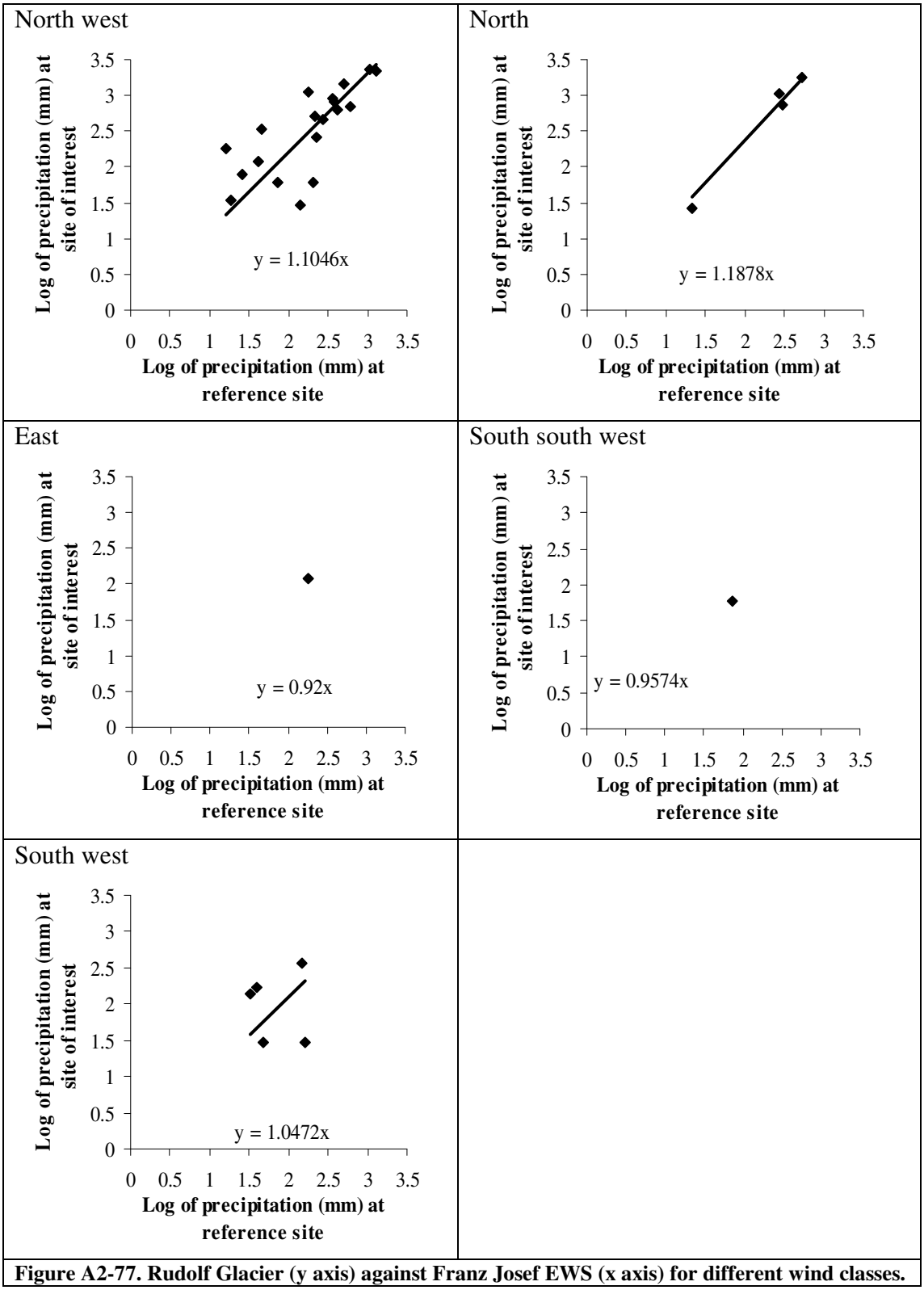

Figure A2-77. Rudolf Glacier (y axis) against Franz Josef EWS (x axis) for different wind classes.

North west

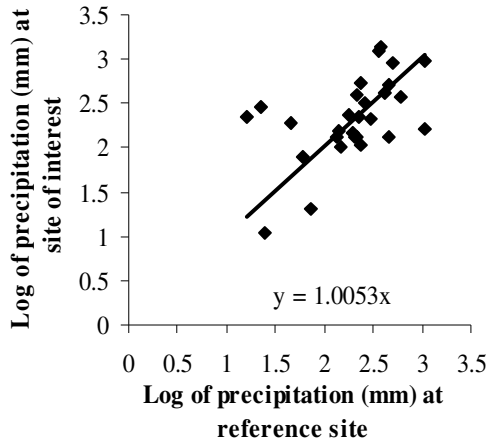

North

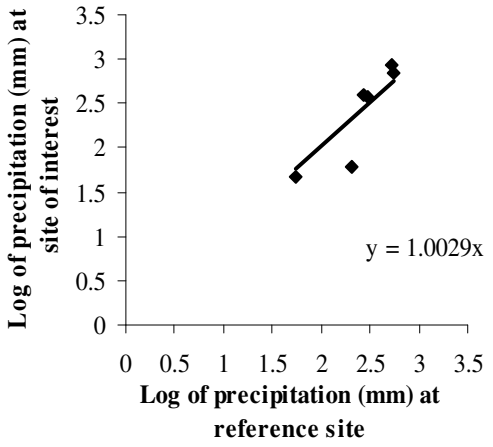

East

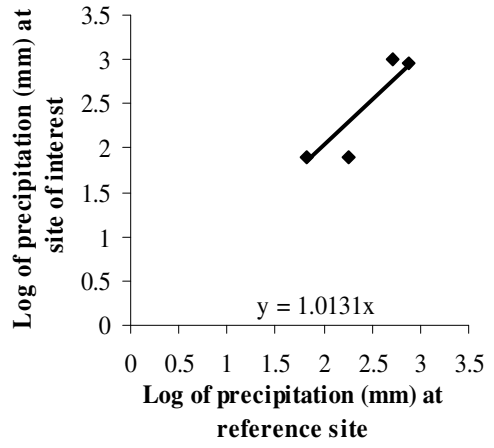

South south west – *no observations*

South west

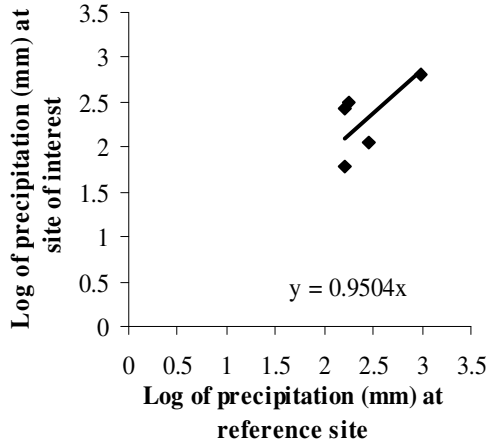

Figure A2-78. East Hooker (y axis) against Franz Josef EWS (x axis) for different wind classes.

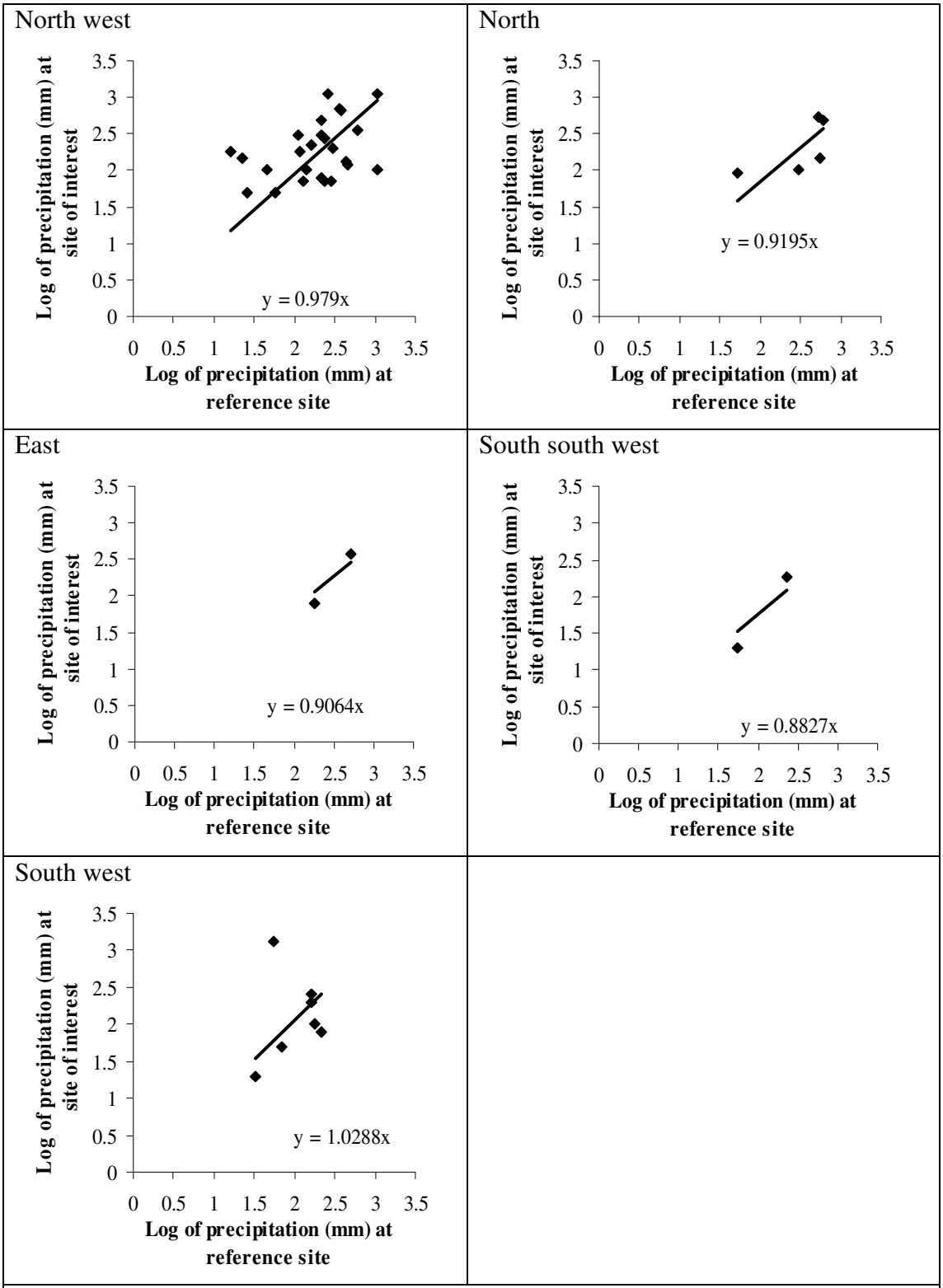

Figure A2-79. Mueller Glacier (y axis) against Franz Josef EWS (x axis) for different wind classes.

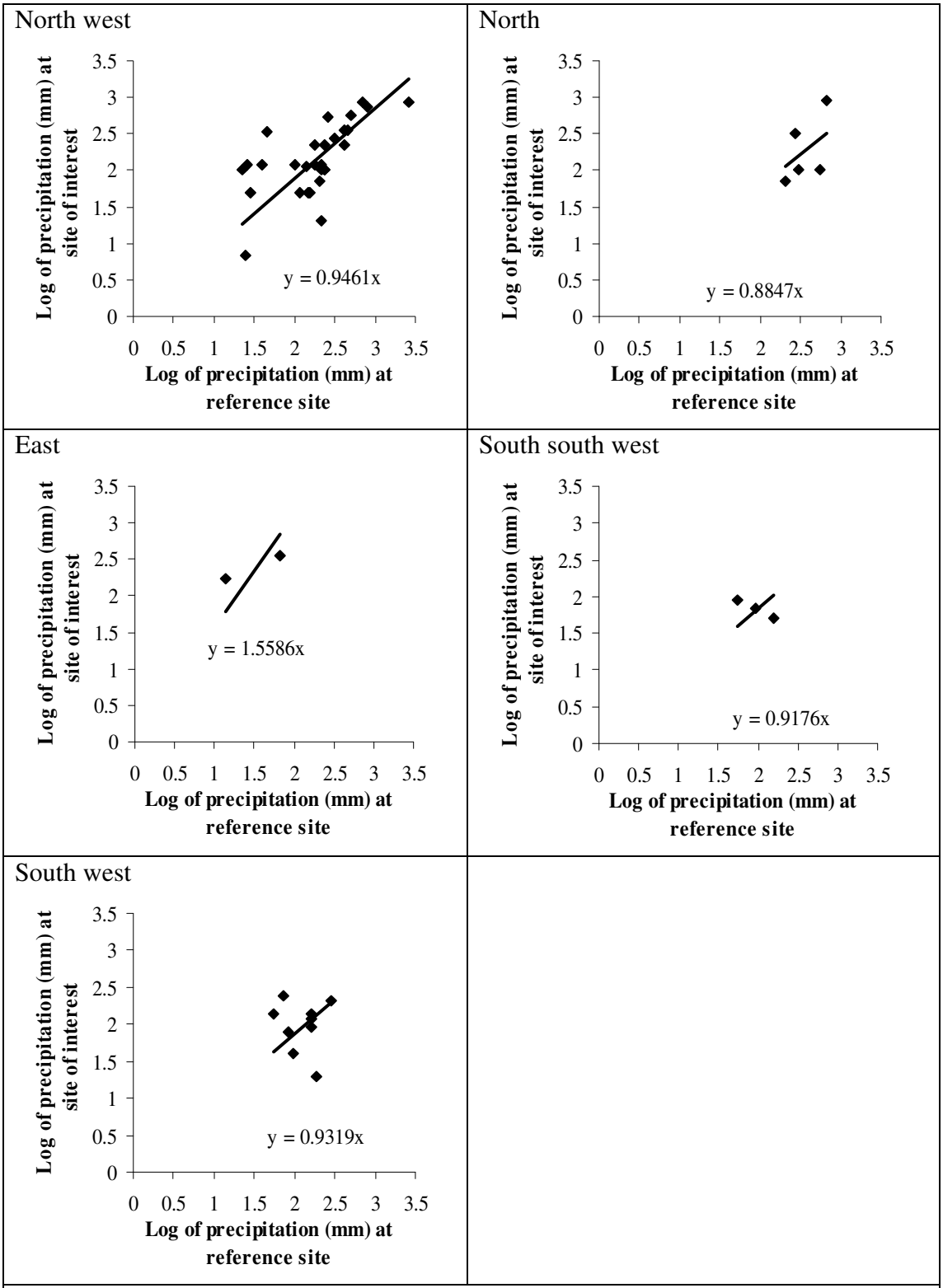

Figure A2-80. Stocking Stream (y axis) against Franz Josef EWS (x axis) for different wind classes.

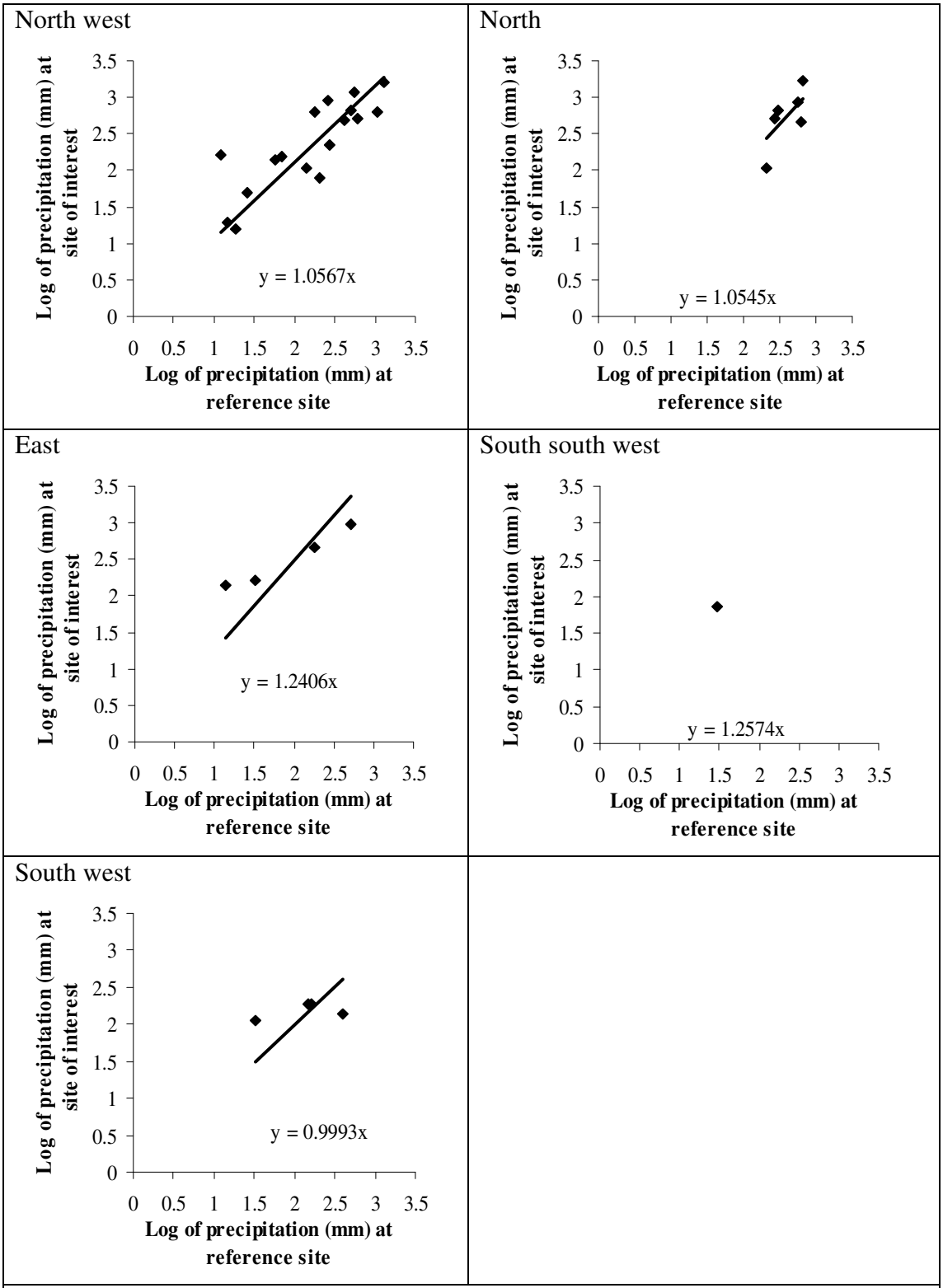

Figure A2-81. Tasman Glacier (y axis) against Franz Josef EWS (x axis) for different wind classes.

A3. Appendix 3: SnowSim-Pukaki model output

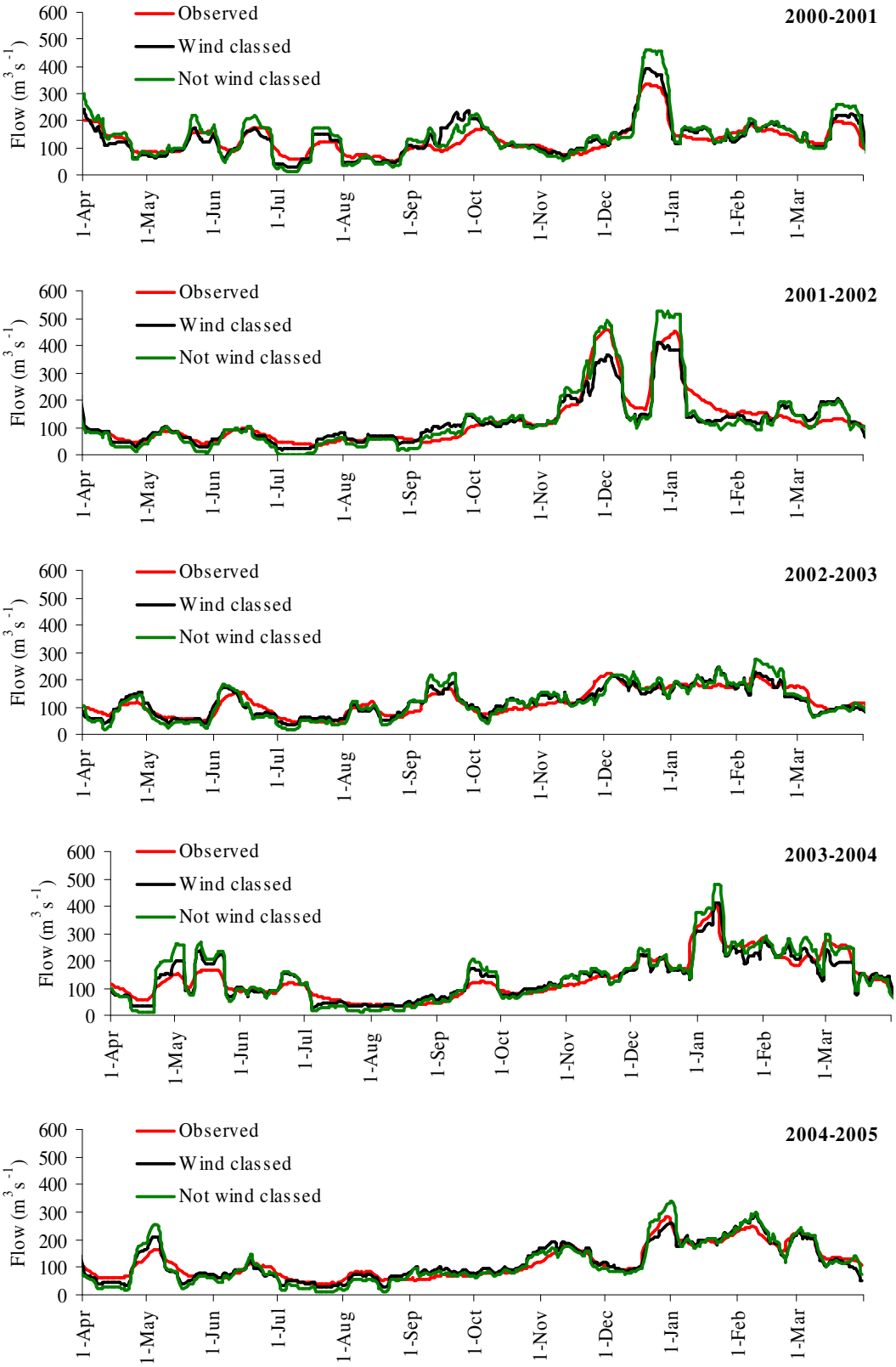

Figure A3-1. 14 day running average of SnowSim-Pukaki modelled daily Lake Pukaki catchment liquid water output with and without wind classed precipitation distribution compared to

observed flow.

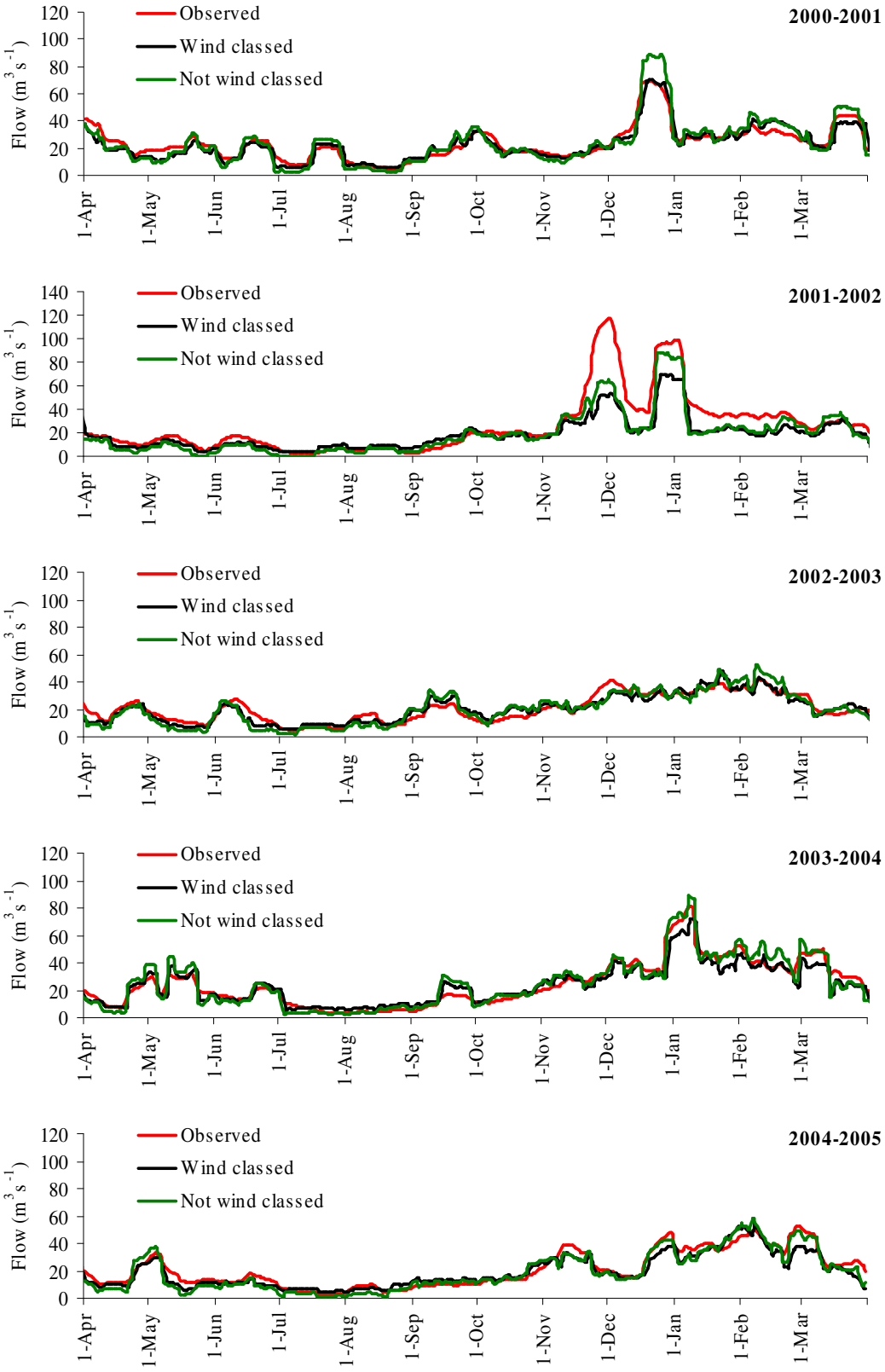

Figure A3-2. 14 day running average of SnowSim-Pukaki modelled daily Hooker catchment liquid water output with and without wind classed precipitation distribution compared to observed flow.

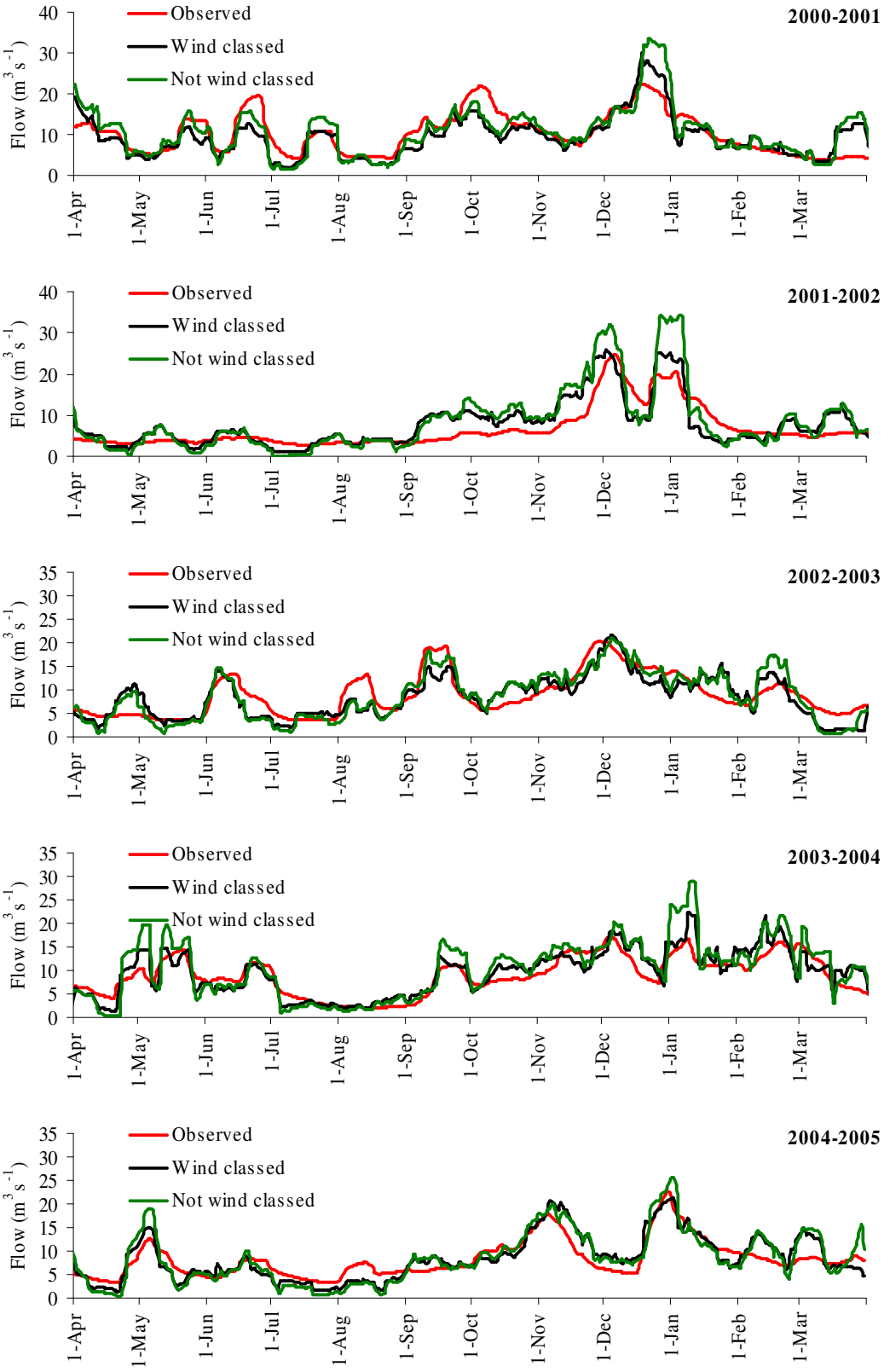

Figure A3-3. 14 day running average of SnowSim-Pukaki modelled daily Jollie catchment liquid water output with and without wind classed precipitation distribution compared to observed flow.

A4. Appendix 4: Index Trend statistics

Table A4-1. The Hermitage precipitation gauge frequency and extreme trends over the 1937 to 2000 period. Note that no trends were found to be statistically significant at the 0.05 level.

	>1 mm	>2mm
Frequency of rain days trend (% per decade)	-0.008	-0.009

Percentile	95th			99th		
Index	All	>1 mm	>2 mm	All	>1 mm	>2 mm
extreme percentile trend (mm per decade)	0.000	-0.013	-0.013	-0.005	0.012	0.010
extreme frequency trend (days per decade)	-0.231	-0.607	-0.760	0.305	0.152	0.152
extreme precipitation magnitude trend (mm per decade)	-0.001	-0.001	-0.001	0.007	0.007	0.007
trend of the relative frequency of extreme precipitation (% per decade)	0.000	0.001	0.001	0.002	0.002	0.002

Table A4-2. Braemar precipitation gauge frequency and extreme trends over the 1924 to 2000 period. Note that no trends were found to be statistically significant at the 0.05 level

	>1 mm	>2mm
Frequency of rain days trend (% per decade)	-1.102	-1.338

Percentile	95th			99th		
Index	All	>1 mm	>2 mm	All	>1 mm	>2 mm
extreme percentile trend (mm per decade)	-0.016	0.004	0.001	-0.001	0.003	0.002
extreme frequency trend (days per decade)	-0.260	0.268	0.268	0.268	-0.133	-0.133
extreme precipitation magnitude trend (mm per decade)	-0.042	-0.022	-0.005	-0.033	-0.033	-0.020
trend of the relative frequency of extreme precipitation (% per decade)	0.016	0.057	0.065	0.075	0.221	0.235